THE DESIGN OF HIGH PRESSURE PLANT AND THE PROPERTIES OF FLUIDS AT HIGH PRESSURES

THE DESIGN OF HIGH PRESSURE PLANT AND THE PROPERTIES OF FLUIDS AT HIGH PRESSURES

BY

DUDLEY M. NEWITT

M.C., D.Sc., PH.D.

ASSISTANT PROFESSOR OF CHEMICAL TECHNOLOGY
IMPERIAL COLLEGE OF SCIENCE AND
TECHNOLOGY

OXFORD
AT THE CLARENDON PRESS
1940

OXFORD UNIVERSITY PRESS
AMEN HOUSE, E.C. 4
LONDON EDINBURGH GLASGOW NEW YORK
TORONTO MELBOURNE CAPETOWN BOMBAY
CALCUTTA MADRAS
HUMPHREY MILFORD
PUBLISHER TO THE UNIVERSITY

PRINTED IN GREAT BRITAIN

PREFACE

In preparing this book an attempt has been made to survey briefly the specific effects of pressure upon physical processes taking place in liquid and gaseous systems. It will be found that nearly all the characteristic properties of a fluid come under review, and the ground to be covered is, therefore, extensive, and some selection and condensation have been necessary.

In view of the rather specialized nature of the subject it has been thought advisable to emphasize the experimental aspect and to devote several chapters to the design of high-pressure plant and equipment and to the methods of measuring high pressures. The calculations of the stresses and strains set up in the walls of pressure vessels are dealt with fully and it is hoped that sufficient detail has been given to enable any one with the necessary basic scientific training to embark upon high-pressure work with a reasonable degree of security.

There follows an account of the pressure-volume-temperature relationships of gases and a discussion of the equation of state problem. A review of recent compressibility work is given together with a summary of data relating to the volumetric behaviour of the more important gases and their binary mixtures.

A chapter upon the liquefaction of gases has been contributed by my colleague Dr. M. Ruhemann.

The use of enthalpy-entropy and temperature-entropy diagrams in the design of compressors and of gas circulating pumps is described. The concluding part of the book deals with the dielectric properties and refractivity of gases and with the viscosity and compressibility of pure liquids and of aqueous solutions of salts, alkalis, and acids.

Numerous tables of data are given in the text and in Appendixes.

The reader will find that, in spite of much progress in the last few years, there is still a serious lack of fundamental data of all kinds relating to condensed systems. For this reason, and in order further to stimulate interest in this important field, particular attention has been paid throughout to the description of apparatus and experimental methods. Much of the contents of the book is taken from original papers published during the past few years, but

frequent quotations are given from the earlier classical papers on the subject, and every care has been taken to present both old and new viewpoints in their proper perspective.

In conclusion it is a pleasant duty to express my thanks to the many workers both in Europe and America who have accorded me permission to make the fullest use of their publications. I am particularly indebted to Professors P. Bridgman, F. G. Keyes, A. Michels, I. Masson, and to Drs. Beattie, Bartlett, and Dr. and Mrs. Deming, whose work constitutes such a valuable contribution to this branch of Physics.

Acknowledgements are also due to the Councils of the Royal Society, the American Chemical Society, the American Academy of Arts and Sciences, the Faraday Society, Messrs. Longmans, Green & Co., Ltd., and to Messrs. John Wiley & Sons, Inc. (Fig. 77) for permission to reproduce illustrations from their *Proceedings* and publications.

D. M. N.

IMPERIAL COLLEGE OF SCIENCE
AND TECHNOLOGY, LONDON

CONTENTS

PART I

THE DESIGN OF HIGH-PRESSURE PLANT AND THE MEASUREMENT OF HIGH PRESSURES

PART II

THE PROPERTIES OF FLUIDS AT HIGH PRESSURES

LIST OF PLATES

PART I

THE DESIGN OF HIGH-PRESSURE PLANT AND THE MEASUREMENT OF HIGH PRESSURES

I

THE PROPERTIES OF MATERIALS USED IN THE CONSTRUCTION OF HIGH-PRESSURE PLANT AND EQUIPMENT

IT is proposed in this and the succeeding two chapters to describe the various methods by which cylindrical vessels may be constructed to withstand high internal pressure, and to indicate the theoretical basis for computing the magnitudes of the stresses and strains set up in their walls both as the result of the method of construction and of the imposed working pressure.

Although, in general, the stresses concerned will not exceed those corresponding with the tensile and compressive elastic limits of the material, in some instances 'over-stressing' as a factor in construction will have to be considered; and it is necessary, therefore, to have some knowledge of the behaviour of materials over a wide range of conditions, including those in which permanent deformation and even rupture may occur. At present, the cause of elastic failure is not known, and the mathematical theory of elasticity is confined to the limits within which Hooke's law is obeyed; but from empirical results in the regions of 'slip' and 'yield' it is possible to modify the physical properties of a material in a known manner and to make use of such residual effects as 'self-hooping' in cylinder construction.

The elementary requirements of a material to withstand the complicated system of stresses due to high pressures are (*a*) high elasticity and (*b*) a degree of plasticity which finds expression in the terms ductility, malleability, and toughness, and which enables high stresses to be sustained without danger of sudden fracture or fragmentation. The data upon which these properties are assessed are provided by the standard tensile, extension, bending, hardness, and impact tests familiar to engineers. The tensile and extension values give a measure of the elasticity, and the bending, hardness, and impact values a measure of the plasticity; the results taken as a

whole enable an estimate to be made of the safe working stress in the material under test.

The selection of a suitable material is, however, governed by a number of additional factors of which the more important are the size of the projected plant, the working temperature, and the nature of the process for which the plant is required. Considerations of cost also make it expedient to employ, where possible, commercial products which are readily obtainable in the form of forgings, rolled bars of various section, and seamless tubes.

A brief description of some of the more important materials available is given below.

The Low and High Carbon Steels

Under this head are included those steels containing up to about 1 per cent. of carbon, 0·5–1 per cent. of manganese, and traces of silicon, sulphur, and phosphorus. The best-known representative of the low carbon steels is mild steel. This material, made by the acid or basic open-hearth process, has a moderate tensile strength at room temperatures, and good ductile properties. It is used extensively in the construction of gas-containers, air-receivers, pipe-lines, and commercial cylinders for the storage of liquefiable gases. The chemical composition and physical properties of the steel recommended by the Gas Cylinders Research Committee (Fourth Report) for the latter purpose, are as follows:

Chemical Composition:

Carbon	0·2–0·25 per cent.
Manganese	0·45–0·75 per cent.
Silicon	not to exceed 0·2 per cent.
Sulphur	not to exceed 0·045 per cent.
Phosphorus	not to exceed 0·045 per cent.
Iron	the remainder.

Physical Properties, after heating to between 860° and 890° C. and cooling in still air:

(*a*) The yield-point (i.e. the point at which the extension of the test-piece increases without increase of load) should be not less than 17 tons per sq. inch.

(*b*) The ultimate stress should be between 28 and 33 tons per sq. inch.

(*c*) The elongation of the test-piece should be not less than 15 per cent.

By increasing the carbon content there is a progressive increase in tensile strength accompanied, however, by a decrease in ductility; and the high carbon steels, even after careful and consistent heat treatment are liable to unexpected variations in plasticity which are

not always revealed by the usual mechanical tests. For this reason they have been largely replaced in recent years by nickel- and nickel-chromium steels.

It should be mentioned, however, that a 0·4 per cent. carbon steel has been recommended by the Gas Cylinders Research Committee (First Report, 1921) for the manufacture of commercial cylinders for the 'permanent' gases, and experience now extending over upwards of fifteen years has shown it to be quite satisfactory for this purpose. The chemical composition and physical properties of the steel in question are specified as follows:

Chemical Composition:

Carbon . . .	0·43–0·48 per cent.
Manganese . . .	0·50–0·90 per cent.
Silicon . . .	not to exceed 0·30 per cent.
Sulphur . . .	not to exceed 0·045 per cent.
Phosphorus . . .	not to exceed 0·045 per cent.
Iron	the remainder.

Physical Properties, after heating to between 820° and 850° C. and cooling in still air:

(*a*) The yield-point should be not less than 20 tons per sq. inch.

(*b*) The ultimate stress should be not less than 40 tons per sq. inch.

(*c*) The elongation should be not less than 14 per cent.

The carbon steels readily oxidize on heating in air and tend to undergo structural changes when maintained for long periods above 400° C.

Nickel-, Nickel-Chromium, and Nickel-Chromium-Molybdenum Steels

Steels containing varying small percentages of nickel or of nickel and chromium have a much better combination and range of elastic and plastic properties than have the high carbon steels; in particular, the regularity with which the results of heat treatment can be reproduced and the absence of 'mass-effect', even in large forgings in which the rate of cooling is comparatively slow, are qualities which recommend them for pressure work.

The effect of the addition of nickel to a steel is to improve the tensile properties, each 1 per cent. up to about 5 per cent. giving rise to an increase of 4,000 to 6,000 lb. per sq. inch, approximately, over that of the corresponding carbon steel. The addition of chromium increases the strength and hardness of the steel without materially increasing its brittleness; it tends, however, to increase the susceptibility to brittleness on prolonged heating at high temperatures, in which respect it differs from nickel.

The use of nickel and chromium together results in a general improvement in physical properties; the nickel appears to strengthen and toughen the ferrite matrix of the steel whilst the chromium tends to toughen the carbide (cementite and pearlite) constituents. The relative quantities added should be so adjusted that the increased susceptibility to brittleness on prolonged heating due to the chromium, is balanced by an opposite effect due to the nickel; the optimum ratio is found to be Ni:Cr = 2·5:1.

The commercial 'high' and 'low' grades of nickel-chromium steel contain approximately 3·5 and 1·5 per cent. of nickel and 1·5 and 0·6 per cent. of chromium, respectively, the effect of the higher proportions being to improve the plastic properties without very much altering the tensile strength.

On prolonged heating at temperatures between 250° and 500° C. nickel-chromium steels are liable to a form of embrittlement known as 'temper-brittleness', the effect of which is to diminish sensibly the ductility of the metal as measured by the ordinary impact tests. The magnitude of the change in a typical instance may be seen from the following data in which a 3·38:0·6 Ni-Cr steel is compared with a 3 per cent. nickel steel:

Composition, %				*Heat treatment*	*Embrittling treatment*	*Impact test, ft.-lb.*	
C	Mn	Ni	Cr			*before*	*after*
0·25	0·48	3·05	0·03	Normalized at 800°–850° C.	Maintained at 450° C. for 100 hours	25, 27,	16, 17,
0·28	0·65	3·38	0·60	Oil-hardened at 830° C.; tempered at 650° C.		54, 56	7, 9

Nickel-Chromium-Molybdenum Steels

The addition of molybdenum to a nickel-chromium steel is found to eliminate the susceptibility to temper-brittleness and to counteract the softening produced by tempering. The change in properties with increase in molybdenum content is progressive but the optimum effect is obtained by the addition of not more than about 0·5 per cent.

The chemical composition and physical properties of a typical steel of this class are given in Table 1 [1].

The data in Table 1 relate to small forgings and are the results of short-time tests carried out at room temperatures; it must be emphasized that they give little indication as to the behaviour of the material at high temperatures.

TABLE 1

Chemical Composition: C = 0·27, Ni = 2·55, Cr = 0·68, Mo = 0·62, and Mn = 0·57 per cent.

Heat treatment			*Physical properties*						
	Tempered								
Oil-hardened from, °C.	*Temp., °C.*	*Time, hrs.*	*Elastic limit, tons/sq. in.*	*Yield-point, tons/sq. in.*	*Max. load, tons/sq. in.*	*Elongation, %*	*Reduction of area, %*	*Average Brinell hardness number*	*Average Izod impact figure, ft.-lb.*
900	600	2	55	62·6	67·1	19	58	326	38
900	650	2	44	50·0	56·1	24	67	273	55
900	670	2	41	45·0	52·0	25	57	249	60
900	700	2	23	36·4	53·0	24	58	244	60

Average modulus of elasticity = 13,000 tons per sq. inch.

To harden nickel-chromium-molybdenum steels they should be heated to between 830° and 850° C. and, after soaking, quenched in oil. They should be withdrawn from the quenching bath after a time depending on the mass and, for most purposes, should be immediately tempered by heating to between 550° and 650° C., the actual temperature being determined by the ultimate tensile strength and other physical properties desired. To avoid distortion, cooling from the tempering temperature should take place in the furnace. A big increase in tensile strength, accompanied, however, by a loss in ductility, may be obtained by hardening and immediately tempering at a low temperature in the region of 200° C., preferably in an oil bath.

A detailed account has been given by F. E. Smith (*Proc. Inst. Mech. Eng.* **133**, 139 (1936)) of the treatment of large forgings used in the Billingham Plant of Messrs. Imperial Chemical Industries, Ltd., for the production of petrol by the hydrogenation of bituminous coal at high pressures, from which the following passages are taken:

'The manufacture of the steel and of the forgings is inspected at all stages, and in collaboration with the steel-makers a report is prepared covering the melting of the steel and the casting of the ingot. After the core has been removed, the ends of the hollow billet or ingot are sulphur-printed in order to ensure that the top and bottom croppage has been adequate and also to ensure that the hole made by the removal of the core has been sufficient to remove all the central weakness present in the original ingot; in addition, any laps, surface cracks, &c., are also removed. The latest developments in the production of such large hollow vessels tend towards a method of forging whereby the original ingot is not allowed to become cold until a considerable amount of

forging has been done on it and the first opportunity to carry out sulphur printing and inspection occurs when most of the forging has been done.

'After all forging has been completed the forging is rough-machined and is heat-treated; from the users' point of view, it is most important that the heat treatment should be absolutely correct, since the resistance of the vessel to hydrogen attack and general service conditions can be appreciably diminished by any errors in temperature control during the treatment.

'After heat-treatment, and before final machining, test-pieces are marked out and stamped at each end of the forging. Tensile, bend, and impact test specimens are taken from various parts of the wall thickness in a transverse direction relative to the main direction of hot working. The broken test-pieces are sectioned and examined microscopically as a further check on the heat treatment and on its uniformity.

'In addition to these tests, certain parts of the forging may be macro-etched to ensure that the material is free from undue segregation.

'After final machining is complete the vessel is assembled for hydraulic test. This consists in bringing the complete assembly up to a pressure of $1\frac{1}{2}$ times the working pressure and taking measurements of the circumferential and longitudinal strains and of the volumetric stretch, as the pressure is increased to a maximum and then decreased to zero. Pressure-deflexion curves are plotted and these should show, of course, that the forging has undergone no permanent set during the test.

'The complete record of each forging thus obtained is not only a safeguard against accidents, but enables the special features of each vessel to be correlated, giving the best possible guidance with regard to the use of vessels in particular duties and showing whether service conditions are affecting the forging in any way.'

The Effect of Overstrain on the Properties of Steel

For some purposes it is necessary to overstrain steels and to make use of the residual stresses set up as the result of the permanent deformation due to the overstrain. If a load-extension test is made on a sample of high tensile steel by a recording apparatus which applies the load continuously and magnifies the extension some 100-fold, a diagram similar to that reproduced in Fig. 1 is obtained. The tensile 'limit of proportionality' or 'elastic limit' is given by OE', the 'slip' range by EA, the true 'yield' range by AB, and the 'semi-plastic' and 'plastic' ranges by BC and CG, respectively. It will be noted that, in the yield range, there is an increase of extension without a corresponding increase of load and the stress-strain release to no load after overstrain (CD) is nearly elastic; OD measures the permanent set produced by the overtensioning load OC'. A diagram similar in all respects to Fig. 1 is obtained if a compressive instead of a tensile stress is employed.

By using a pull-push recorder the behaviour of a specimen when subjected to a tensile followed by a compressive stress can be studied.

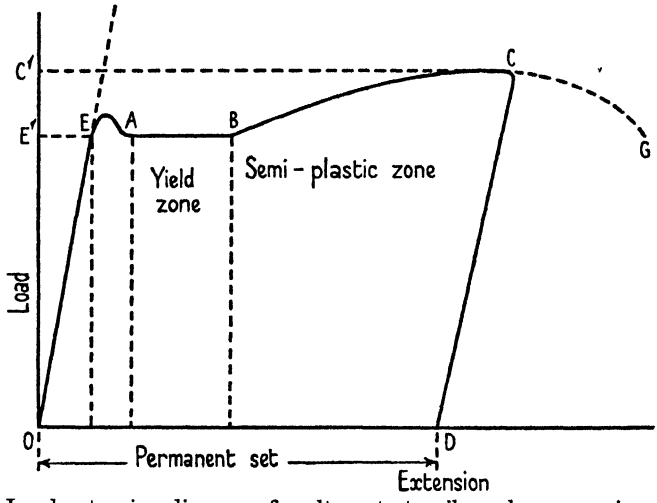

FIG. 1. Load-extension diagrams for alternate tensile and compressive stresses.

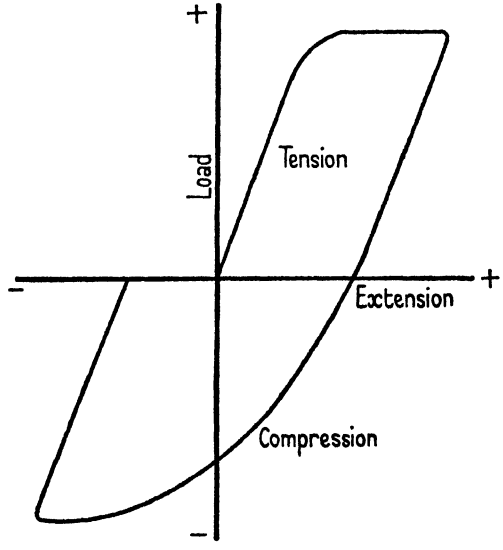

FIG. 2. Load-extension diagrams for high tensile steel.

The diagram in Fig. 2, which relates to a typical high tensile steel, indicates that when stressed beyond its elastic limit, it has practically no compressive elasticity and no compressive yield; it is also evident that the permanent set may have either a positive or a negative value

according to the relative magnitudes of the applied stresses. In general, high tensile steels have the same elastic limits in tension and in compression and the phenomena of slip and yield are very similar; the modulus of elasticity has also the same value in tension and compression and is unaltered by overstressing.

To take a specific example [2] we may consider the behaviour of a nickel-chromium-molybdenum steel of the following chemical composition, when subjected to overstrain: carbon = 0·23, silicon = 0·11, manganese = 0·57, phosphorus = 0·03, sulphur = 0·03, nickel = 2·46, chromium = 0·68, and molybdenum = 0·62 per cent.

Test-pieces were cut from a forging of the steel, oil-hardened at 830° C., tempered at 550° C., and quenched in water. The original tensile properties of the specimen were as follows:

Elastic limit	39·5 tons per sq. inch.
Yield-point	43·3 „ „
Stress at maximum load	52·8 „ „
Elongation	14·8 per cent.
Reduction of area	57·8 „
Average modulus of elasticity	13,100 tons per sq. inch.

On applying a tensile stress sufficient to overstrain the metal and cause a permanent set of about 3 per cent., its resultant tensile properties were:

	Overtension		*Resultant properties*					
Specimen	*Stress, tons/sq. in.*	*Permanent set, %*	*Elastic limit, tons/sq. in.*	*Yield-point, tons/sq. in.*	*Stress at max. load, tons/sq. in.*	*Elongation, %*	*Reduction of area, %*	*Average modulus of elasticity, tons/sq. in.*
1	46·0	2·70	5·1	..	..	..	..	13,100
2	46·0	3·55	..	49·3	51·8	11·3	52·5	..

The effect of the overtension is to lower the original elastic limit and to increase the original yield.

The elastic properties of the overstressed metal can be largely restored by a subsequent *low-temperature heat treatment.* Thus, on heating a number of overstrained specimens of the above steel for one hour at 200° C., their resultant properties were found to be modified as shown in Table 2.

TABLE 2

The Effect of Overstressing a Nickel-Chromium-Molybdenum Steel followed by Low-temperature Heat Treatment

	Overtension		*Resultant properties after heat treatment*					
Specimen	*Stress, tons/sq. in.*	*Permanent set, %*	*Elastic limit, tons/sq. in.*	*Yield-point, tons/sq. in.*	*Stress at max. load, tons/sq. in.*	*Elongation, %*	*Reduction of area, %*	*Average modulus of elasticity, tons/sq. in.*
3	43·0	0·58	43·7	45·5	..	..	..	13,100
4	43·0	1·06	..	47·9	51·1	12·8	57·8	..
5	48·0	4·47	49·8	54·9	..	..	..	13,100
6	48·0	5·36	..	56·6	57·1	5·2	49·5	..
7	49·9	6·90	52·4	57·5	..	..	..	13,100
8	49·3	7·02	..	..	60·1	..	52·2	..

The above data show that the original elastic limit has been increased to at least the value of the overtensioning stress, whilst both the original tensile yield and the stress at maximum load have been increased; the percentage elongation, on the other hand, has been reduced. The effect of overtensioning followed by heat treatment at 200° C. upon the plasticity of the metal is shown by the following comparative Izod impact test figures:

Overtensioning stress, tons/sq. in.	*Average Izod impact figures, ft.-lb.*
0	64·2
44·3	40·3
46·0	36·3
48·0	29·7
50·0	25·8

In a similar way a low-temperature heat treatment of an overcompressed steel restores its tensile elasticity, although not to its original value.

According to Macrae [2] the optimum temperature for the low-temperature heat treatment of an overstressed steel varies with the type of steel (see table on p. 10).

A knowledge of the behaviour of steels on overstressing is necessary in the construction of cylinders by the 'auto-frettage' process, and the method by which the resultant stresses and strains are calculated, will be described in Chapter III.

Material	*Composition, %*	*Optimum temperature for a low-temperature treatment of 1 hour, ° C.*
Mild steel	C = 0·2	200
High carbon steel	C = 0·3–0·4	250
Cast steel	C = 0·26 Mn = 1·28	375
Nickel steel	C = 0·36 Ni = 3·72	250
Nickel-chromium steel	C = 0·25 Ni = 3·75 Cr = 0·55	330
Nickel-chromium-molybdenum-steel	C = 0·23 Ni = 2·46 Cr = 0·68 Mn = 0·57 Mo = 0·62	400

The Effect of Heat upon the Properties of Carbon and Alloy Steels

The results of short-time mechanical tests indicate that, in general, the elastic properties of metals are adversely affected, and the plastic properties are improved, by increase of temperature. Thus, mild steel which has a moderately high tensile strength (an ultimate stress of about 30 tons per sq. inch) and a high ductility at room temperature, tends to become brittle at liquid air temperature and to lose most of its elastic strength when heated to about 500° C. The change in properties on heating is often accompanied by a change in structure; in carbon steels, for example, there is a tendency to spheroidization of the cementite on prolonged heating above 400° C., and many stainless steels lose their corrosion-resisting properties and undergo a coarsening of grain in the temperature range 500°–850° C. [3].

All metals exhibit the phenomenon of 'creep' at sufficiently high temperatures and their strength, as indicated by tensile tests, depends upon the time they are under stress, varying from a maximum value approximately equal to the ultimate strength as given by the normal rate of loading, for short periods, to a minimum value approximately equal to the limiting creep stress, for long periods. The limiting creep stress curve may, therefore, be considered as the true ultimate strength curve where high temperatures of long duration are concerned.

The 'pearlite' steels, which include all the commercial structural steels, have very low limiting creep stresses at temperatures above 450° C., and lose practically the whole of their elastic strength above 600° C. The addition of nickel does little to improve their creep properties, but chromium has a definite beneficial effect and when present to the extent of about 5 per cent., combined with 0·5 per cent. of molybdenum, in a low carbon steel, the resultant material has over twice the strength of the corresponding carbon steel at 540° C.

The 'martensitic' chromium steels containing from 12 to 14 per cent. of chromium have excellent corrosion resisting properties and a comparatively high creep strength, but their ductility is low and they show a tendency to grain coarsening on prolonged exposure to high temperatures. They may be hardened and tempered, and are therefore useful for the construction of valve parts and the like.

The best refractory metals are the 'austenitic' stainless steels containing varying high percentages of nickel and chromium together with, in some instances, smaller percentages of tungsten. These alloys possess relatively high limiting creep stresses up to 600°, satisfactory resistance to oxidation up to 900° C., and stability of structure at high temperatures [4].

The data contained in Table 3 show the stresses necessary to produce a uniform rate of creep in various types of steel, at temperatures between 350° and 600° C. [3].

TABLE 3

Stresses necessary to produce a Uniform Rate of Creep at Various Temperatures

	Chemical composition, %							*Stress in lb. per sq. in. to give a rate of creep of 0·000001 in. per in. per day at the following temperatures, °C.*			
Material	C	Ni	Cr	Mo	V	Si	W	*350°*	*450°*	*550°*	*600°*
Mild steel	0·20	..	..	..	..	..	..	22,500	14,500	4,500	..
Ni-Cr steel	0·30	3·8	0·95	..	..	..	..	31,000	9,000	1,000	..
Ni-Cr-Mo steel	0·28	3·5	0·87	0·24	..	..	..	56,000	33,500	2,000	..
Cr-V steel	0·35	..	1·13	..	0·15	..	..	85,000	22,500	2,000	..
Cr-Si steel	0·61	..	8·32	..	..	2·62	..	53,500	25,500	4,500	..
martensitic steel	0·27	..	14·00	..	..	..	..	49,000	27,000	4,500	..
austenitic steel	0·16	8·0	18·00	..	..	..	0·6	..	14,500	6,500	4,500

It will be of interest to consider, in a little more detail, the behaviour of a typical heat-resisting steel at high temperatures, and for this purpose we have selected a material having the following chemical composition:

Carbon	0·46 per cent.	Chromium	14·00 per cent.
Silicon	1·20 „ „	Tungsten	3·59 „ „
Manganese	1·09 „ „	Sulphur	0·028 „ „
Nickel	26·50 „ „	Phosphorus	0·026 „ „

Short- and long-time tensile tests upon this material gave the results summarized in Table 4 [5].

TABLE 4. *Tensile Properties of a Nickel-Chromium-Tungsten Steel at High Temperatures*

	Short-time tensile tests			
Temperature, ° C.	*Ultimate stress, tons/sq. in.*	*Elongation, %*	*Reduction of area, %*	*Estimated limiting creep stress, tons/sq. in.*
15	45·8	33·5	42·5	..
500	40·9	27·0	33·0	..
600	34·7	22·0	29·0	11·0
700	25·1	21·0	28·0	6·0
800	17·3	39·0	43·0	2·0

A set of strain-time curves for various stress values at 700° C. are reproduced in Fig. 3. It will be seen that for stresses above 7 tons per sq. inch the rate of creep increases with time, and the curves terminate abruptly with the fracture of the test-piece. The rate of creep for a stress of 7 tons per sq. inch, on the other hand, is very nearly constant, and the conditions correspond closely with those for the limiting creep stress.

The best method of applying such data to design is still open to question. The limiting creep stress is a somewhat indefinite quantity depending, amongst other factors, upon the sensitivity of the measuring apparatus and upon the condition of the sample in respect of heat treatment; and it is frequently necessary to employ in practice much higher working stresses. The problem then becomes one of estimating the maximum rate of creep that will give no more than a certain permissible deformation during the lifetime of the part concerned.

It must also be borne in mind, when designing pressure plant, that we have to deal with a complex system of stresses which may give

rise to creep conditions differing from those due to a simple axial tensile stress. In the case of a cylindrical vessel subjected to an internal hydrostatic pressure, for example, it has been shown that the resultant creep resembles that given by a tube under torsion, and hence data based upon creep due to simple shear would be a

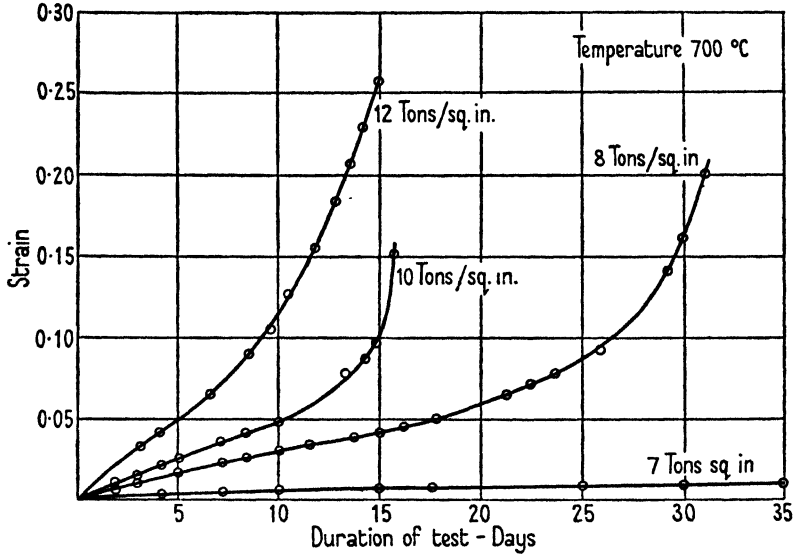

FIG. 3. Creep stresses of a typical heat-resisting steel.

more reliable guide than those based upon tension [6]. This aspect of design will be dealt with more fully in Chapter III.

In order to avoid making the prolonged and tedious observations necessary in evaluating the true limiting creep stress, various 'accelerated' creep tests have been proposed; but since, by their nature, they take no account of the slow structural changes which are known to occur when steel is subjected to the combined action of heat and stress over long periods, the results must be used with some caution [3].

The Effect of Low Temperatures on the Properties of Metals

In a number of high-pressure processes it is necessary to maintain certain parts of the plant at liquid air temperature (−180° C.) and for design purposes we must know how the mechanical properties of the materials used in its construction vary with reduction of

temperature. It is possible to generalize to some extent; the tensile strength and yield-point of most metals rise progressively with lowering of the temperature whilst the elongation, reduction of area, and impact values fall. With low carbon steels, for example, the ultimate strength is nearly doubled on cooling from room temperature to −180° C. and the impact value is reduced to about 1/20 of its original value; that is to say, the steel becomes hard and brittle at liquid air temperature.

The results of tests on the mechanical properties of five typical steels at temperatures between 15° and −180° C. are given in Table 5 [7].

TABLE 5. *The Effect of Low Temperatures upon the Mechanical Properties of some Ferrous Metals*

Composition of metal, %	*Temperature*, ° C.	*Ultimate stress*, tons/sq. in.	*Yield-point*, tons/sq. in.	*Elongation*, %	*Reduction of area*, %	*Impact value*, ft.-lb.	*Impact value after warming to room temperature*, ft.-lb.
Armco iron:	+ 15	20·4	..	27·9	73·2	78·0 (b)	83·0
C = 0·035	− 20	24·0	13·7	42·0	75·0		
Mn = 0·02	− 50	26·5	18·8	43·0	74·0		
S = 0·016	− 70	27·5	19·4	37·5	72·0	4·0 (b)	
P = 0·003	−100	29·8	25·5	26·5	70·0		
	−120	34·4	29·8	17·0	68·0		
	−180	50·0	..	nil	nil	1·5 (b)	
'Vibrac' steel:	+ 15	68·0	61·5	14·0	65·0	57·5 (b)	60·6
C = 0·33 Si = 0·16	− 21	69·0	62·9	15·6	64·0		
Mn = 0·64 S = 0·012	− 60	73·2	64·0	14·0	63·0		
Ni = 2·54 P = 0·035	− 67	72·8	65·0	15·6	62·0	53·0	
Cr = 0·67	− 96	76·1	66·6	16·4	61·0		
Mo = 0·64	−180	90·0	82·0	17·0	63·0	22·0 (b)	
Low carbon steel	+ 15	29·6	24·4	29·7	71·8	94·0	91·0
	− 65	36·0	30·2	33·6	70·3	49·0	
	−180	54·2	..	26·5	55·0	3·0 (b)	
Austenitic steel:	+ 15	41·4	16·5	54·0	74·0	114·0	107·5
C = 0·11	− 20	51·0	19·0	62·5	73·0		
Ni = 10·05	− 60	61·1	22·2	61·0	74·0	117·5	
Cr = 18·3	− 96	69·0	24·0	46·1	70·0		
	−116	80·0	32·5	48·5	63·0	107·5	
	−180	99·5	33·3	45·7	55·0	100·0	
'Anka' steel:	−180	109·3	37·5	38·0	52·0	75·0	
C = 0·11							
Ni = 10·1							
Cr = 15·8							

(b) indicates that the specimen was broken in the machine.

Armco iron, which is a very pure form of iron, shows a large increase in ultimate strength with reduction of temperature, but its ductility decreases and at —180° C. it has practically no resistance to impact. The low carbon steel behaves in the same way save that it retains its ductility down to —65° C.

The nickel-chromium-molybdenum steel (Vibrac) shows an increase of ultimate strength of about 30 per cent. and a considerable increase in extension. The impact strength remains fairly constant down to about —100° C. after which it diminishes fairly rapidly. The austenitic steels increase in tensile strength and retain nearly the whole of their impact strength on cooling to —180° C. Even after prolonged soaking at liquid air temperature their ductile properties show little change.

Amongst the non-ferrous metals copper, nickel, and aluminium retain their tensile and impact strength unimpaired down to —180° C., and the same may be said of copper-nickel alloys, 70–30 brass, and nickel-silver. The data in Table 6 show the small variation in mechanical properties between 15° and —180° C. [8].

The Action of Gases upon Metals

In many high-pressure processes gases are in direct contact with the metal walls of containers, often at elevated temperatures, and it is necessary to know something of the effects produced by them on the mechanical properties of the metal as the result of any adsorption, diffusion, or solution that may take place.

Adsorption is of two kinds, the one a purely physical reversible process in which the gas, in molecular form, is held on the surface by the field of force due to unsaturated atoms of the metal lattice, and the other an irreversible process with respect to temperature, in which the gas is dissociated and its atoms are linked directly to the metal atoms in the surface; the first type is usually known as physical adsorption and the second as chemisorption or activated adsorption.

Physical adsorption is a low-temperature process in which equilibrium is reached very quickly; it is mainly a property of the surface, and, at saturation, all gases are adsorbed to approximately the same extent. The effect of pressure is to increase the amount of gas adsorbed until a layer one molecule thick has been formed, after which no further adsorption takes place. Chemisorption, on the

TABLE 6. *The Mechanical Properties of Various Non-Ferrous Metals and Alloys at Low Temperatures.* (*Colbeck and MacGillivray*)

Material	*Temperature,* ° *C.*	*Ultimate strength, tons/sq. in.*	*Elongation on 2 in., %*	*Reduction in area, %*	*Impact test, ft.-lb.*
Annealed copper (Cu = 99·985%)	+ 15	14·0	48·0	76·5	43·0
	− 10	14·3	40·2	78·0	..
	− 40	15·1	47·0	77·0	45·0
	− 80	17·2	47·0	74·0	44·0
	−120	18·4	44·6	70·0	44·5
	−180	22·7	57·6	77·0	50·0
Nickel:	+ 15	29·25	42·4	78·0	89·0
Ni = 99·7	− 10	31·10	44·4	75·5	..
Mg = 0·26	− 40	32·0	45·0	71·5	90·5
Co = 0·14	− 80	34·1	43·4	73·0	92·0
Si = 0·23	−120	36·0	44·7	77·0	93·0
Fe = 0·10	−180	43·7	53·2	74·5	98·5
S = < 0·005					
Aluminium:	+ 15	4·38	35·9	90·4	19·0
Si = 0·054	− 10	5·10	35·9	90·4	..
Fe = 0·07	− 40	5·20	39·8	91·8	19·0
	− 80	5·30	37·9	91·5	20·0
	−120	6·30	39·5	90·2	21·0
	−180	9·30	43·8	87·0	27·0
Brass 70/30:	+ 15	22·8	49·4	77·0	65·5
Cu = 69·56	− 10	23·7	48·5	77·0	..
Fe = 0·10	− 40	24·4	57·7	77·0	66·0
Zn = 30·50	− 80	25·5	59·5	79·0	69·0
	−120	27·3	54·7	77·5	70·5
	−180	32·8	74·6	73·0	78·5
Aluminium-bronze:	+ 15	34·5	26·0	29·0	24·0
	− 10	34·4	32·8	30·0	..
Cu = 91·1	− 40	35·6	34·8	36·0	24·0
Fe = 0·056	− 80	36·9	30·9	30·0	23·5
Mn = 0·44	−120	39·3	32·4	31·0	21·0
Zn = 1·02	−180	42·9	28·5	30·0	20·5
P = 0·018					
Al = 7·31					

other hand, is a relatively slow process, and over a certain range of temperature adsorption increases with increase of temperature; it is moreover a specific property of certain metal-gas systems and does not occur at all with gases which have no chemical valencies, as for example argon. In regard to the effect of gases on metals chemisorption is of importance in that it is the prelude to diffusion and solution.

Diffusion. There is strong evidence that diffusion is preceded by the dissociation of adsorbed layers of gas, the atoms penetrating the

metal lattice and not travelling by way of the boundary surfaces between the metal crystals. Like chemisorption it is a specific process and only occurs to an appreciable extent between metals and gases that have some chemical affinity. Thus, for example, nitrogen will diffuse readily through iron with which it can form a nitride but not through copper.

The rate of diffusion (D) depends on temperature in accordance with the relation

$$D = ae^{-q/T}$$

and is directly proportional to the square root of the pressure at high pressure.

Smithells and Ransley [9] have shown that the rate of diffusion may become independent of the pressure if chemical combination between the gas and metal takes place at the surface, and they quote as a typical instance the system nickel-oxygen. At 900° C. the diffusion of oxygen through nickel becomes independent of pressure at about 0·25 mm. Above this pressure a layer of nickel oxide becomes visible and increases in thickness owing to the fact that the rate of passage of oxygen through the oxide layer is greater than the rate of diffusion through the metal.

Although lattice diffusion is normal for gas-metal systems, there is evidence that in certain circumstances diffusion may take place along grain boundaries. This is peculiarly the case at very high pressures and P. W. Bridgman records that in some of his experiments, hydrogen at a pressure of 9,000 kg./sq. cm. escaped through the walls of a steel cylinder, 2 inches external diameter and ¼ inch bore, with explosive violence, although the metal showed no evidence of fracture or fissuring [10].

Mention may also be made of the diffusion of compound gases. When pure iron is heated in carbon monoxide at temperatures above 850° C. carbon diffuses into the metal, the rate of diffusion decreasing as the carbon content of the steel is increased. Similarly, when steel is heated in ammonia, nitrogen diffuses into the metal; but if the surface of the steel is oxidized, nitrogen is no longer adsorbed and diffusion ceases.

Solubility. Under this head is included the absorption of gas by the metal with the formation of a definite compound and a uniform distribution of the gas in an atomic state through the metal lattice. The equilibrium conditions in such a gas-metal system are dependent

on temperature, pressure, and the presence of other phases and are subject to the phase rule.

In all cases of simple solution the amount of gas absorbed is proportional to the square root of the pressure and increases with increase of temperature according to the equation

$$s = ce^{-E_s/2kT},$$

where c is a constant and E_s is the heat of solution. When these

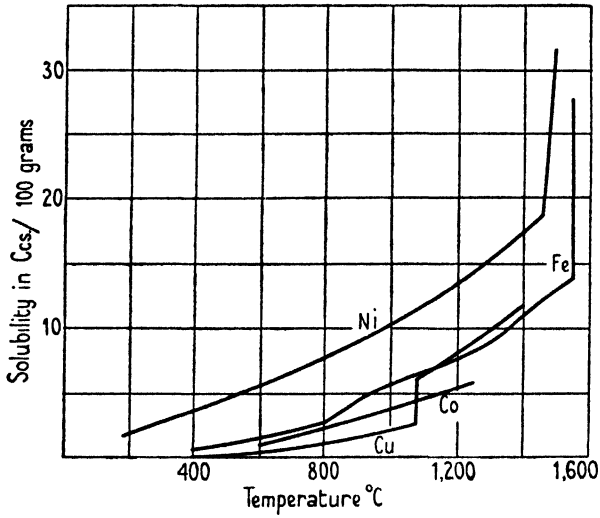

FIG. 4. Solubility of hydrogen in metals.

relations are found not to hold, there is usually evidence of the formation of a third phase.

The most interesting case both from a theoretical and practical aspect is that of hydrogen. Hydrogen is absorbed by a very large number of metals forming true solutions or definite hydrides. Metals in which it goes into solution include: iron, nickel, cobalt, copper, molybdenum, and aluminium. In these metals solution is a reversible process, the solubility increasing abruptly at the melting-point. Solution is usually accompanied by a slight increase in volume, but there is very little change in the mechanical properties of the metal. An idea of the extent of the solubility at various temperatures is given by the curves in Fig. 4.

Metals which form definite hydrides include palladium, thorium, titanium, vanadium, and the rare earth metals. In the initial stages of absorption these metals form true solutions, but with large amounts

of gas combination occurs although the process is still reversible. Usually absorption takes place very rapidly between 300° and 500° C., the lattice structure undergoes a rearrangement and the metal tends to become less ductile. At higher temperatures the hydrides are decomposed and gas is given off. The original ductility of the metal is sometimes, although not always, restored by heating *in vacuo*.

The data in Table 7 give the absorption of hydrogen by metals of this class at a number of temperatures.

TABLE 7. *Absorption of Hydrogen by Metals forming Hydrides* [9]

	Absorption of H_2 *in c.c. per 100 gm. of metal*			
Temp., °C.	*Palladium*	*Thorium*	*Titanium*	*Vanadium*
20	..	12,500	40,300	15,000
300	330	10,700	40,000	6,000
500	190	9,100	35,400	1,840
700	170	8,450	22,000	640
1,000	155	2,600	6,500	240

The Effect of Hydrogen on Steel

All steels are acted upon by hydrogen to a greater or less extent; in the initial stages the gas is absorbed and the metal becomes embrittled; in the later stages the hydrogen combines chemically with the carbon in the steel, fissures develop, and there is a loss of tensile strength and ductility. The rate of decarburization depends upon the composition and structure of the steel and upon temperature and pressure. Mild steel, for example, may be attacked at as low a temperature as 200° C. Mild steel converters have been used at the Fuel Research Station at Greenwich for the hydrogenation of coal and a number of failures have occurred due to the decarburization and intergranular weakening of the metal by hydrogen [11]; in one instance, for example, a converter working at 480° C. and a pressure of 200 atmospheres failed after 700 hours. The hydrogen content of the steel was in some cases as high as 14 vols. of gas to 1 vol. of metal. The four photomicrographs in Plate 1 show the effect of the hydrogen in decarburizing the steel and producing intergranular cracks.

Low nickel- and the 3·5:1·5 nickel-chromium steels resist attack rather better than mild steel, but tend to develop fissures when subject to a hydrogen pressure of 250 atmospheres at about 300° C. The addition of chromium to a carbon steel increases the resistance

to attack, and when present to the extent of 6 per cent. the steel may safely be used at 250 atmospheres and about 450° C.

The chromium-nickel austenitic (stainless) steels absorb large quantities of hydrogen and suffer loss of ductility but they do not undergo decarburization by the gas at 250 atmospheres and 450° C. [12]. One of the most resistant alloys has the composition: chromium = 12, nickel = 60, and tungsten = 2·5 per cent., and this material has been used in the construction of catalyst tubes for the Claude synthesis of ammonia at 1,000 atmospheres and 550° C. with successful results.

The Effect of Hydrogen on Copper and its Alloys

It will be seen from Fig. 4 that the solubility of hydrogen in copper is not very large but increases considerably at the melting-point. When copper is heated in hydrogen at 300 atmospheres and 450° C. for long periods it loses the greater part of its tensile strength, and monel metal and brass are similarly affected. The data in regard to these materials, however, is very limited and further work is required before the conditions under which they may safely be used in contact with hydrogen at high pressures can be defined.

Nitrogen

Generally speaking, nitrogen is dissolved by and diffuses into those metals which are known to form nitrides, giving rise to a change in the lattice structure and causing embrittlement. It produces, in steel, austenitic and martensitic structures analogous to those produced by carbon, and the extreme hardness of the nitrides is made use of industrially to form resistant surfaces by the 'nitriding' process.

Carbon Monoxide

Very little data is available in regard to the action of this gas upon steel. It is known that when iron and nickel are heated *in vacuo* carbon monoxide is evolved, but there is evidence that it originates from reaction between dissolved oxides and carbides in the metal. Carbon monoxide combines chemically with iron, nickel, and certain other metals forming carbonyls which are usually low-boiling liquids or vapours. Pressure favours the reaction and in the case of iron it appears to be catalysed by water vapour. Mild steel cylinders in which the gas is stored at room temperature and at

Normal microstructure of the steel. *White*: Ferrite. *Shaded*: Pearlite.

Completely decarburized region, extending to a depth of $\frac{5}{8}$ inch from the inner surface of the converter.

Intergranular Cracks in decarburized region.

Complete disintegration of the inner surface.

PHOTOMICROGRAPHS OF A RUPTURED MILD STEEL BERGIUS CONVERTER

Previously reproduced by A. T. Barber and A. H. Taylor in the Proceedings of the Institution of Mechanical Engineers, vol. 128.

120 atmospheres pressure are found to contain relatively large quantities of the carbonyl (probably ferro-penta-carbonyl) which collects in the bottom of the cylinder as a dark-brown liquid. The gas may be freed from carbonyl by passing it over activated charcoal or through a heated tube containing refractory material; the decomposition temperature of ferro-penta-carbonyl at 1 atmosphere being about 180° C. Alloy steels are also attacked by carbon monoxide, and for this reason high-pressure plant for handling it is frequently lined with copper.

Oxygen

By reason of its chemical reactivity oxygen is soluble in most metals although its solubility is rather difficult to determine, as an oxide phase appears as soon as saturation is reached. The oxidation of certain metals occurs to a large extent along the grain boundaries and may result in fissuring.

The Effect of Mercury on Steel

Mercury at high pressures attacks steel, and numerous cases of failure attributable to its action are to be found in the literature [13].

Bridgman has found that the maximum pressure of mercury that steel will support is 6,000 kg./cm.^{2}, the destructive action being due to a combination of an opening of the pores of the steel by the mercury and the formation of an amalgam between the mercury and the clean surface of the steel in the pores. There is no action between the steel and the mercury unless the pores are opened, and hence, when the steel is subjected to a uniform pressure on all sides mercury has no deleterious action on it.

REFERENCES

1. Research Department, Woolwich, Report No. 67, 1926.
2. MACRAE, *Overstrain in Metals*, H.M. Stationery Office, 1930.
3. *Symposium on Effect of Temperature on the Properties of Metals*, Am. Soc. Mech. Eng. and Am. Soc. for Testing Materials, 1931.
4. 'Special Alloy Steels as applied to Chemical Engineering', *J. Soc. Chem. Ind.* **51**, 502 and 527.
5. Dept. of Sci. and Ind. Research, Special Report No. 15, 1929.
6. R. W. BAILEY, *Engineering*, **129**, 265, 327, 772, 785, and 818 (1930).
7. COLBECK, MACGILLIVRAY, and MANNING, *Trans. Inst. Chem. Eng.*, p. 89 (1933).
8. COLBECK and MACGILLIVRAY, *Trans. Inst. Chem. Eng.*, p. 107 (1933).

9. *Gases and Metals*, C. J. Smithells (Chapman & Hall, Ltd., 1937).
10. BRIDGMAN, *Proc. Am. Acad.* **59**, 173 (1924).
11. BARBER and TAYLOR, 'High-Pressure Plant for Experimental Hydrogenation Processes', *Proc. I. Mech. E.*, 1934.
12. INGLIS and ANDREWS, *Proc. Iron and Steel Inst.*, 1933.
13. AMAGAT, *Ann. Chim. et Phys.* **29** (1893); CAILLETET, COLARDEAN, and RIVIÈRE, *Compt. Rend.* **130**, 1585 (1903); BRIDGMAN, *Proc. Am. Acad.* **46**, 325 (1911).

II

CYLINDERS FOR THE STORAGE AND TRANSPORT OF 'PERMANENT' AND 'LIQUEFIABLE' GASES

GAS cylinders are so widely used nowadays both in the laboratory and workshop that some knowledge of their construction, the methods employed in testing them, and the precautions which should be observed in their use, is desirable. Every year a number of accidents happen which are attributable to lack of care in handling or storing the cylinders and not to any defect in material or construction.

In Great Britain the manufacture and testing of gas cylinders for trade purposes is based upon the recommendations of the Gas Cylinders Research Committee of the Department of Scientific and Industrial Research, which has issued four reports (published by H.M. Stationery Office), namely:

First Report (1921), *Cylinders for Permanent Gases*—now out of print.
Summary of Recommendations contained in the First Report (1928).
Second Report (1926), *Periodical Heat Treatment of Gas Cylinders.*
Third Report (1929), *Alloy Steel Light Cylinders.*
Fourth Report (1929), *Cylinders for Liquefiable Gases.*

Specifications based upon these reports have been issued by the British Standards Institution, as follows:

No. 399—1930: *'High Carbon' Steel Cylinders for the Storage and Transport of the 'Permanent' Gases.*
No. 400—1931: *'Low Carbon' Steel Cylinders for the Storage and Transport of 'Permanent' Gases.*
No. 401—1931: *Steel Cylinders for the Storage and Transport of 'Liquefiable' Gases.*†
No. 341—1931: *Valve Fittings for Compressed Gas Cylinders.*
No. 349—1933: *Identification Colours for Gas Cylinders.*

The materials used in the construction of such cylinders have been selected chiefly on the basis of their mechanical properties, availability, ease of manufacture, and cost. For the permanent gases which are used for medical, aeronautical, and mine rescue work, weight is also an important factor.

In the First Report of the Committee the question of weight reduction was fully considered, and it was recommended that a 0·45

† By liquefiable gases is meant gases which have relatively high critical temperatures, and which are generally reduced to the liquid phase by the pressures used in charging them into the cylinders.

per cent. carbon steel should be permitted as an alternative to the 0·25 per cent. mild steel which had hitherto been almost universally employed in cylinder construction. By the use of this material it was possible to raise the permissible working stress from 8 to 10 tons per sq. inch, and thus to effect a reduction in weight of the order of 20 per cent. Particulars of the limits of chemical composition and mechanical properties of this steel are given in the preceding chapter.

In the Third Report an account is given of tests made on a number of experimental cylinders constructed of duralumin, a 3 per cent. nickel steel, a nickel-chromium, and a nickel-chromium-molybdenum steel. Whilst all these steels have properties superior to mild steel and to the high carbon steel recommended in the First Report, considerable difficulties were experienced in manufacture, particularly in the 'necking' operation. The Report recommends as the result of numerous tests that in special cases where it is highly important to have very light, small cylinders a nickel-chromium-molybdenum steel should be used for the storage and transport of the 'permanent' gases. The steel should have the following chemical composition and mechanical properties:

Chemical Composition:

Nickel	2·5 per cent.	Carbon	0·3 per cent.
Chromium	0·6 „	Silicon	0·15 „
Molybdenum	0·6 „	Sulphur	0·04 „ (max.)
Manganese	0·6 „	Phosphorus	0·03 „ (max.)

the balance being iron.

Mechanical Properties:

Ultimate tensile strength	55 to 65 tons per sq. inch.
Yield stress	not less than 45 tons per sq. inch.
Elongation	not less than 18 per cent. on 2-in. gauge length.

A working stress of 25 tons per sq. inch may safely be adopted with this material thereby effecting a reduction in weight of about one-third over the low carbon steel.

High Carbon Steel Cylinders for 'Permanent' Gases

These cylinders should be either solid drawn or made from seamless steel tube, and the ends should not be welded on, nor should metal be added in the process of closing. The minimum thickness of wall is calculated from the formula

$$t = \frac{pD}{2f+p},$$

where p = maximum working pressure in lb. per sq. inch,
f = 22,400 lb. per sq. inch,
D = external diameter in inches.

Tensile and impact tests should be carried out on material cut from one finished cylinder in every batch. In addition one cylinder from each batch should be subjected to a flattening test and every finished cylinder should be tested hydraulically to a pressure of 3,000 lb. per sq. inch. The permanent stretch shown by the latter test should not exceed 10 per cent. of the total stretch under the proof pressure. For a full description of these tests reference should be made to the First Report.

Steel Cylinders for Liquefiable Gases

The physical properties of the gases coming within this classification differ so widely that some subdivision is necessary. The generally accepted values of the boiling-point, critical temperature, and critical pressure of the more important amongst them are given in Table 8.

TABLE 8. *Critical Temperature, Critical Pressure, and Boiling-point of Various Liquefiable Gases*

Gas	*Boiling-point, 760 mm., °C.*	*Critical temperature, °C.*	*Critical pressure, Atms.*
1. Sulphur dioxide	− 10·8	157·2	77·7
2. Ammonia	− 33·5	132·4	111·5
3. Chlorine	− 33·6	144·0	76·1
4. Methyl chloride	− 24·1	143·1	65·8
5. Ethyl chloride	+ 12·5	187·2	52·0
6. Hydrocyanic acid	+ 26·1	183·5	52·3
7. Phosgene	+ 8·2 (756 mm.)	182·0	56·0
8. Carbon dioxide	− 78·2	31·1	73·0
9. Nitrous oxide	− 89·8	36·5	71·7
10. Ethylene	−102·7	9·7	50·9

It will be seen that Nos. 5, 6, and 7 have boiling-points above 0° C. and hence are in the liquid state at atmospheric pressure in cold weather, whilst Nos. 8, 9, and 10 have comparatively low critical temperatures and may, in exceptional circumstances, be entirely in the gaseous phase at high pressures.

The principal points which have to be considered in connexion with the design of cylinders for the liquefiable gases are:

1. The maximum temperature to which the contents are likely

to rise in temperate and tropical climates. An examination of the extreme shade temperatures in various latitudes indicates that 65° C. in tropical and 45° C. in temperate climates may be taken as the maxima likely to be attained under ordinary working conditions.

2. The maximum quantity of gas which may be placed in the cylinder without any possibility of the internal pressure becoming excessive at the maximum temperature. This quantity is fixed by the permissible 'filling ratio' which will be defined later.

3. The method of determining the thickness of the cylinder wall so that it will withstand not only the stresses due to the internal pressure but also mechanical shocks to which it may be subjected in handling.

4. The most suitable material for the construction of the cylinders and valves.

5. The methods of manufacture and testing of cylinders.

Filling Ratios. The filling ratio is defined as the weight in lb. of gas permitted for each lb. weight of water capacity of the cylinder. In determining the ratio account must be taken of the thermal expansion and compressibility of the liquid phase. Liquefied gases have, in all cases, a high coefficient of thermal expansion, and unless a sufficient amount of free space is left in filling, it is possible that, as the result of rise of temperature, the cylinder may subsequently become completely filled with liquid and dangerous pressures may develop.

For the sake of convenience in classification the liquefiable gases are divided into two groups, the one containing those gases having critical temperatures which are never reached under atmospheric conditions (Table 8, Nos. 1–7), and the other containing the gases having critical temperatures within the range of ordinary atmospheric temperature (Nos. 8–10). The filling ratios recommended for the gases in the two groups are given in Table 9.

Group I. Special precautions are necessary in storing hydrocyanic acid under pressure to prevent polymerization. The pure concentrated acid is stable, but decomposes and polymerizes under the influence of alkali and iron with a considerable evolution of heat. The effect of the iron may be removed by the addition of 0·1 per cent. of concentrated sulphuric acid or acetic acid so that the storage of concentrated hydrocyanic acid (98 per cent. and over) with 0·1 per cent. of sulphuric or acetic acid in steel containers or tinplate canisters

TABLE 9. *Filling Ratios recommended, Percentage Free Space available, and Working Pressure in Cylinder at the assumed Maximum Temperature*

Gas	*Temperate climates, 45° C.*			*Tropical climates, 65° C.*		
	Filling ratio	*Percentage free space at 45° C.*	*Working (gauge) pressure, lb./sq. in.*	*Filling ratio*	*Percentage free space at 65° C.*	*Working (gauge) pressure, lb./sq. in.*
Group I:						
Sulphur dioxide	1·25	4·5	87	1·19	4·5	160
Chlorine	1·25	6·3	174	1·19	6·0	283
Ammonia	0·54	5·4	241	0·51	5·0	412
Methly chloride	0·83	5·0	130	0·79	4·6	211
Hydrocyanic acid	0·60	8·6	12	0·57	8·9	32
Ethyl chloride	0·82	4·4	29	0·79	4·3	60
Phosgene	1·25	5·7	53	1·19	6·6	95
Group II:						
Carbon dioxide	0·75	..	1,800	0·667	..	1,800
Nitrous oxide	0·75	..	1,800	0·667	..	1,800
Ethylene	0·325	..	1,800	0·270	..	1,800

may be regarded as being free from danger. Any absorbent material used must not be alkaline or otherwise basic.

Gases belonging to this group have high critical temperatures, and there is a very rapid increase of pressure with rise of temperature when a cylinder becomes full of the liquefied gas. Thus, a cylinder charged with sulphur dioxide to a filling ratio of 1·31, would become completely filled with liquid at a temperature of 44·6° C., and the internal pressure would be 100 lb./sq. inch; on increasing the filling ratio to 1·32 the cylinder would be completely filled with liquid at 41·2° C., the pressure being 90 lb./sq. inch, and on allowing the temperature to rise to 44·6° C. the pressure would increase to 650 lb./sq. inch.

Group II. The three gases of this group have low critical temperatures and the internal pressures in cylinders containing them is relatively high, even at low atmospheric temperatures. The point at which a cylinder becomes completely filled with liquefied gas is not sharply defined, even for high filling ratios. Furthermore, the presence of small percentages of other gases is sufficient to cause internal pressures which are greatly in excess of those which would be anticipated on the basis of the behaviour of the pure gas; it has been found, for example, that in the case of carbon dioxide of purity

96 per cent (the remainder being probably air), the internal pressure in a cylinder when the filling ratio was 0·75 and the temperature 45° C., was 2,740 lb./sq. inch, or 525 lb./sq. inch greater than would be given by the pure gas under the same conditions of filling and temperature.

It is necessary that the filling should be carefully carried out since a small excess has an appreciable effect on the maximum pressure. The Gas Cylinders Research Committee therefore recommend that:

(1) The purity of the gases should be

(*a*) carbon dioxide	. not less than	99	per cent.
(*b*) nitrous oxide . .	„	97	„
(*c*) ethylene . .	„	98	„

(2) the capacity of each individual cylinder should be carefully ascertained, and

(3) the accuracy of filling by weight, based upon the true capacity, should be within 1·8 per cent.

Calculation of the Dimensions of Cylinders for Liquefiable Gases

The containers at present in use for the storage and transport of liquefiable gases may be divided into two classes, namely: (1) cylinders of wrought iron or steel (lap-welded or seamless) closed at one end and fitted with a valve at the other end. The wrought iron and lap-welded steel cylinders are being replaced by the seamless steel cylinders, to which alone, therefore, this class may be regarded as restricted, and (2) containers made up of steel plates welded together and sometimes mounted to form a wagon tank.

The formulae given below for calculating the thickness of the cylinder wall are intended to refer to class (1) but they may also be used as the basis for the design of the larger containers constructed of welded steel plates, due allowance being made for man-holes and the mechanical shocks and 'surging' incidental to road and rail transport.

The formula $t = pD/(2f+p)$ determines the thickness of the wall of a cylinder in terms of the outside diameter D, the internal pressure p, and a maximum allowable working stress f in the cylinder wall. It assumes that the internal pressure is large relative to any external forces likely to act upon the cylinder in the course of normal handling. In the case of the permanent gases where the usual working pressure is 1,800 lb./sq. inch, this assumption is justified. With the liquefiable

gases the maximum working pressure is, for the pure gases, the saturation vapour pressure; and as will be seen from Table 9, it is usually quite low. A cylinder designed on the basis of the above formula for any of the gases of Group I would therefore be quite unsuitable for ordinary storage or transport purposes, and another method based upon an assumed value for the internal pressure has to be employed.

The Gas Cylinders Research Committee (Fourth Report) make the following recommendations:

'The thickness of the cylinder wall should not be less than the value of t (in inches) as given by the following formulae:

(a) when the working pressure is 1,500 lb./sq. in. or over,

$$t = pD/(2f+p); \tag{2.1}$$

(b) when the working pressure is 500 lb./sq. in. or less,

$$t = \frac{pD}{4f}\left[1+\sqrt{\left(1+\frac{633f}{p^2D}\right)}\right]; \tag{2.2}$$

(c) when the working pressure is between 500 and 1,500 lb./sq. in.,

$$t = t_3+(t_2-t_3)\left(\frac{p}{1000}-0{\cdot}5\right), \tag{2.3}$$

where p = the maximum internal working gauge pressure, lb. per sq. in. (see Table 9),

D = external diameter in inches,

f = 17,920 lb./sq. in.,

t_2 = value of t in formula (2.1), taking p as 1,500 lb./sq. in.,

t_3 = value of t in formula (2.2), taking p as 500 lb./sq. in.

The cylinders should be made of a low carbon steel, particulars of which are given in Chapter I, and alloy steels should not be used.

The Committee also make a number of special recommendations of which the following may be noted:

1. The water capacity of each individual cylinder should be carefully ascertained and, by using the appropriate filling ratio, the true gas capacity determined.

2. The proof pressure applied in the hydraulic stretch test should be the value of p calculated from the formula $p = 2ft/(D-t)$, with the appropriate values for D and t and a value for f of 33,600 lb./sq. inch.

3. Care should be taken to ensure that the gas is freed from

moisture and the accuracy of the charge should be determined by weighing.

4. Hydrocyanic acid should not be stored in cylinders for more than six months; it should have a purity of not less than 98 per cent., and it should be stabilized to prevent polymerization.

5. The valves of carbon dioxide cylinders may be fitted with a safety device. In the case of cylinders for use in the tropics, the device provided should be a softened copper safety disk so arranged as to burst at a pressure of between 2,600 and 2,850 lb./sq. inch. In temperate climates the alternative of a spindle carrying a vulcanite disk to form a gas-tight joint with the valve seat may be adopted.

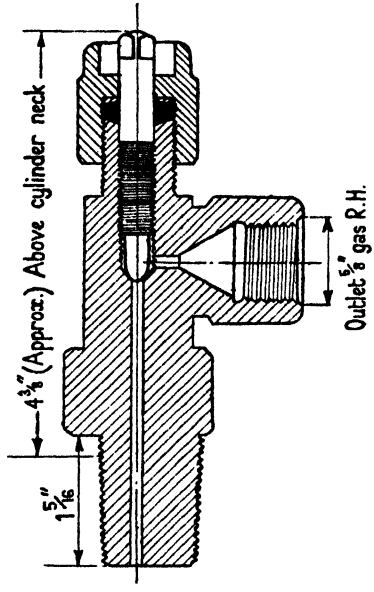

Fig. 5. Gas cylinder valve.

Cylinder Valves

The type of valve commonly fitted to commercial gas cylinders is illustrated in section in Fig. 5. The body is made of bronze or steel, the spindle of steel, and the packing of leather. Particulars of the materials used in the construction of the valve bodies for various gases, the details of the screw threads on the outlet, and the dimensions of the spindle end to accommodate the cylinder key, are given in Tables 10 A and B.

The valves are provided with stems screwing into the cylinders, $1\frac{1}{8}$ inches long ($\pm\frac{1}{64}$ in.) for stems of 1 in. diameter, and 1 inch long ($\pm\frac{1}{64}$ in.) for stems 0·715 in. diameter. The stems are given a taper of 1 in 8 on the diameter measured at the small end, and are screwed (right-handed) for the whole of their length. The threads are of standard Whitworth form (55°) cut at right angles to the taper with 14 T.P.I. measured along the taper. Cylinders and valve stems for nitrous oxide, sulphur dioxide, ethylene, helium, and neon, and for small cylinders of other gases may be screwed parallel if desired.

The valves of cylinders exceeding 4 inches in external diameter should be protected either (*a*) by means of a stout metal cap or metal

TABLE 10 A. *Details of Cylinder Valves*†

1		2	3	4	5
Gas		*Material of valve*	*Screw thread of outlet*		*Spindle, square inch*
Name	*Symbol*				
Acetylene[1]	C_2H_2	Bronze	Internal	Left-handed B.S.P. $\frac{3}{4}$ in., 14 T.P.I.	$\frac{5}{32}$
Air		Bronze	Internal	Right-handed B.S.P. $\frac{3}{4}$ in., 14 T.P.I.	$\frac{5}{32}$
Ammonia	NH_3	Steel	External	Right-handed B.S.P. $\frac{3}{4}$ in., 14 T.P.I.	$\frac{3}{8}$
Argon	A	Bronze	Internal	Right-handed B.S.P. $\frac{3}{4}$ in., 14 T.P.I.	$\frac{5}{32}$
Carbon dioxide	CO_2	Bronze	External	Right-handed. Full dia. 0·860, + 0, − 0·007 B.S.W., 14 T.P.I.	..
Carbon monoxide	CO	Bronze	Internal	Left-handed B.S.P. $\frac{3}{4}$ in., 14 T.P.I.	$\frac{5}{32}$
Chlorine	Cl	Steel	External	Right-handed B.S.P. $\frac{3}{4}$ in., 14 T.P.I.	$\frac{3}{8}$
Coal gas		Bronze	Internal	Left-handed B.S.P. $\frac{3}{4}$ in., 14 T.P.I.	$\frac{5}{32}$
Ethyl chloride (inflammable and non-inflammable grades)	C_2H_5Cl	Steel or Bronze	External	Left-handed B.S.P. $\frac{3}{4}$ in., 14 T.P.I.	$\frac{3}{8}$
Ethylene (large cylinders)	C_2H_4	Bronze	Internal	Left-handed B.S.P. $\frac{3}{4}$ in., 14 T.P.I.	$\frac{5}{32}$
Hellium (large cylinder)	He	Bronze	Internal	Right-handed B.S.P. $\frac{3}{4}$ in., 14 T.P.I.	$\frac{5}{32}$
Hydrogen	H	Bronze	Internal	Left-handed B.S.P. $\frac{3}{4}$ in., 14 T.P.I.	$\frac{5}{32}$
Methane	CH_4	Bronze	Internal	Left-handed B.S.P. $\frac{3}{4}$ in., 14 T.P.I.	$\frac{5}{32}$
Methyl bromide	CH_3Br	Steel or Bronze	External	Right-handed B.S.P. $\frac{3}{4}$ in , 14 T.P.I.	$\frac{3}{8}$
Methyl chloride (inflammable and non-inflammable grades)	CH_3Cl	Steel or Bronze	External	Left-handed B.S.P. $\frac{3}{4}$ in , 14 T.P.I.	$\frac{3}{8}$
Neon (large cylinders)	Ne	Bronze	Internal	Right-handed B.S.P. $\frac{3}{4}$ in., 14 T.P.I.	$\frac{5}{32}$
Nitrogen	N	Bronze	Internal	Right-handed B.S.P. $\frac{3}{4}$ in., 14 T.P.I.	$\frac{5}{32}$
Nitrous oxide	N_2O	Bronze	External	Right-handed B.S.W. $\frac{11}{16}$ in., 20 T.P.I.	$\frac{11}{32}$
Oxygen	O	Bronze	Internal	Right-handed B.S P. $\frac{3}{4}$ in., 14 T.P.I.	$\frac{5}{32}$
Phosgene	$COCl_2$	Steel	External	Right-handed B S.P. $\frac{3}{4}$ in., 14 T.P.I.	$\frac{3}{8}$
Sulphur dioxide	SO_2	Steel or bronze	External	Right-handed B.S.P. $\frac{3}{4}$ in., 14 T.P.I.	$\frac{3}{8}$

[1] Excluding small cylinder and cylinders for special purposes.

TABLE 10 B. *Alternative Valves for use with Cylinders of 25 lb. Water Capacity and under*†

1	2	3	4	5
Gas	*Material of valve*	*Screw thread of outlet*		*Spindle, square in.*
Chlorine	Steel	External	Right-handed B.S.P. $\frac{3}{8}$ in., 19 T.P.I.	$\frac{5}{32}$
Ethyl chloride (inflammable and non-inflammable grades)	Steel or bronze	External	Left-handed B.S.P. $\frac{1}{4}$ in., 19 T.P.I.	$\frac{5}{32}$
Methyl bromide	Steel or bronze	External	Right-handed B.S.P. $\frac{1}{4}$ in., 19 T.P.I.	$\frac{5}{32}$
Methyl chloride (inflammable and non-inflammable grades)	Steel or bronze	External	Left-handed B.S.P. $\frac{1}{4}$ in., 19 T.P.I.	$\frac{5}{32}$
Phosgene	Steel	External	Right-handed B.S.P. $\frac{3}{8}$ in., 19 T.P.I.	$\frac{5}{32}$
Sulphur dioxide	Steel or bronze	External	Right-handed B.S.P. $\frac{1}{4}$ in., 19 T.P.I.	$\frac{5}{32}$

† From British Standards Institution, Specification No. 341—1931.

casing securely attached to the cylinder body and provided with adequate vent holes, or (*b*) by so designing the cylinder that the valve lies wholly inside an extension of the cylinder body which completely and suitably protects it from injury through impact.

Valves should be tested from time to time, and should a leak be discovered at the seating, the cylinder should be emptied and the valve seating cleaned and remade if necessary; no attempt should

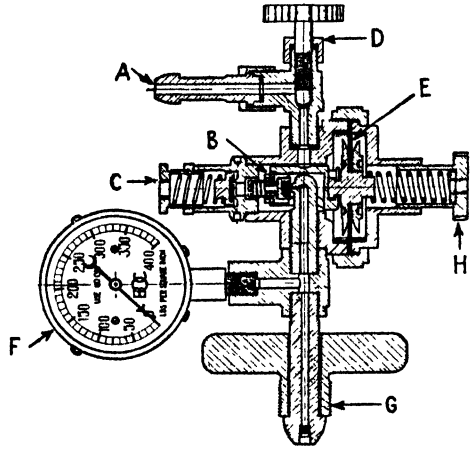

Fig. 6. Gas Regulator.

A. Outlet connexion. *B*. Special valve seat—proof against ignition risk; also incorporates patent non-return device. *C*. Safety valve—preventing accumulation of pressure inside body. *D*. Outlet valve. *E*. Special reinforced diaphragm. *F*. High-pressure gauge indicating contents of cylinder. *G*. Fly-nut and nipple for inserting regulator in valve socket. *H*. Pressure adjusting screw. A cutting regulator is similar, but an outlet pressure gauge is provided between the outlet connexion *A* and the safety valve *C*.

be made to correct a leak by forcing the spindle on to the seating. A leak at the valve packing will only be evident when the valve is open, and can usually be remedied by tightening the gland nut.

No oil or grease in any form should be used inside or outside the valve fitting.

Gas Reducing Valves

In order to obtain a steady supply of gas at atmospheric pressure from a gas cylinder a reducing valve must be employed. The commercial type supplied by the British Oxygen Co. is shown in section in Fig. 6.

In this valve high-pressure gas from the cylinder passes through a fine jet at *B* into an expansion chamber which is normally closed

Cylinder U.H. 12. Normalized at 830° to 850° C. Nominal Thickness 0·26″.
Pressure at Elastic Limit—297 Atmospheres. Bursting Pressure 504 Atmospheres.

Cylinder U.H. 2. Annealed at 650° C. Nominal Thickness 0·26″.
Pressure at Elastic Limit—221 Atmospheres. Bursting Pressure—446 Atmospheres.

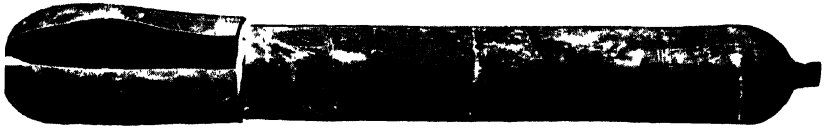

Cylinder U.H. 15. Not Heat Treated. Nominal Thickness 0·26″.
Pressure at Elastic Limit—312 Atmospheres. Bursting Pressure—574 Atmospheres.

Cylinder U.H. 1. Normalized at 820° to 850° C. Nominal Thickness 0·232″.
Pressure at Elastic Limit—252 Atmospheres. Bursting Pressure—440 Atmospheres.

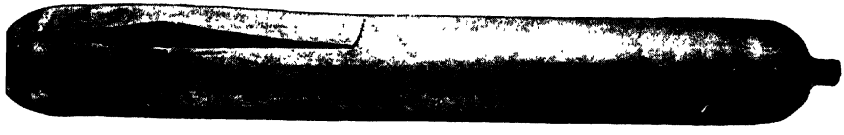

Cylinder U.H. 7. Annealed at 650° C. Nominal Thickness 0·232″.
Pressure at Elastic Limit—236 Atmospheres. Bursting Pressure—419 Atmospheres.

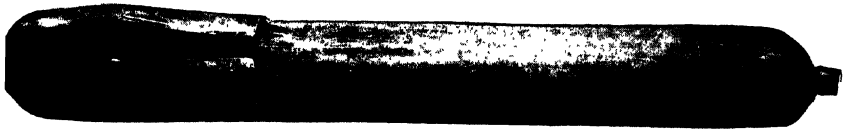

Cylinder U.H. 19. Not Heat Treated. Nominal Thickness 0·232″.
Pressure at Elastic Limit—267 Atmospheres. Bursting Pressure—494 Atmospheres.

The Carbon-Contents of the Steels from which the Cylinders were made ranged between 0·374 and 0·506 per cent.

GAS CYLINDERS BURST UNDER HYDRAULIC PRESSURE

(From First Report Gas Cylinders Research Committee, by permission of the Controller of H.M. Stationery Office.)

by the valve *D*. The pressure in the expansion chamber is regulated by means of a spring *H*, acting upon a reinforced leather diaphragm *E*, which forms one side of the expansion chamber. When the pressure rises above the amount required to give the desired rate of flow the diaphragm moves outward and a flat plate attached to it comes in contact with the jet *B* and cuts off the gas supply. With the cylinder valve full open the rate of gas flow is adjusted by means of the valve *D*. A spring-loaded safety valve at *C* prevents an accumulation of pressure inside the expansion chamber.

The Markings on Gas Cylinders

Cylinders are usually permanently marked with (*a*) the makers and owners identification marks, (*b*) the date of the last hydraulic test, (*c*) a mark indicating the specification to which the cylinder was constructed, and (*d*) in the case of cylinders for liquefiable gases, the internal pressure required for the hydraulic test and the tare and gross weights. In addition the valve should be marked with the name or chemical symbol of the gas contained in the cylinder.

Identification Colours of Cylinders

In order to avoid mistakes in identification all cylinders should be painted according to a distinctive scheme so that the colours are indicative of their contents. A specification for identification colours has been published by the British Standards Institution (Specification No. 349—1932). It provides for identification colours for the gases most commonly in use, the underlying principle of the scheme being that yellow should represent toxic or poisonous gases, and red or maroon inflammable gases.

In accordance with the specification the cylinders should be entirely covered with a coat of paint of the colour specified in Tables 11 and 12. In addition, a distinguishing colour band should be painted round the neck of each cylinder adjacent to the valve fitting, wide enough to occupy half the portion of the cylinder between the junction of the hemispherical and cylindrical portions and the neck. Particulars of the colours of the bands for different gases are also given in Tables 11 and 12.

For cylinders for medical purposes, the name or chemical symbol of the gas should be stencilled or painted on or near the shoulder of the cylinder. For gases other than those provided for in these tables

TABLE 11.† *British Standard Identification Colours for Gas Cylinders, excluding Cylinders for Medical Purposes*

Gas		*Ground colour of cylinder*		*Colour of bands*	
Name	*Symbol*	*Nominal*	*British Standard Colour No.*	*Nominal*	*British Standard Colour No.*
Acetylene	C_2H_2	Maroon	41	None	..
Air	..	Grey	30	None	..
Ammonia	NH_3	Black	..	Red and Yellow‡	37 and 56
Argon	A	Blue	3	None	..
Carbon dioxide for temperate use	CO_2	Black	..	None	..
Carbon dioxide, for tropical and marine use	CO_2	Black	..	White or aluminium paint	..
Carbon monoxide	CO	Red	37	Yellow	56
Chlorine	Cl	Yellow	56	None	..
Chlorine, cylinders fitted with internal dip-pipes	Cl	Yellow	56	Black	..
Ethyl chloride, inflammable	C_2H_5Cl	Grey	30	Red	37
Ethyl chloride, non-inflammable	C_2H_5Cl	Grey	30	None	..
Ethylene	C_2H_4	Mauve	..	Red	37
Ethylene oxide	C_2H_4O	Mauve	..	Red and Yellow‡	37 and 56
Freon (dichlordifluormethane)	CCl_2F_2	Parti-coloured: bottom end grey, neck end mauve	30 (grey)	..	..
Helium	He	Medium brown	11	None	..
Hydrocyanic acid	..	Blue	3	Yellow	56
Hydrogen	H	Red	37	None	..
Methane	CH_4	Red	37	None	..
Methyl bromide	CH_3Br	Blue	3	Black	..
Methyl chloride, inflammable	CH_3Cl	Green	25	Red	37
Methyl chloride, non-inflammable	CH_3Cl	Green	25	None	..
Neon	Ne	Medium brown	11	Black	..
Nitrogen	N	Dark grey	32	Black	..
Oxygen	O	Black	..	None	..
Phosgene	$COCl_2$	Black	..	Blue and Yellow‡	3 and 56
Sulphur dioxide	SO_2	Green	25	Yellow	56

† From British Standards Institution, Specification No. 349—1932.

‡ The red or blue band should be placed adjacent to the valve fitting and the yellow band between that and the ground colour of the cylinder.

TABLE 12. *British Standard Identification Colours for Gas Cylinders for Medical Purposes*

Gas		*Ground colour of cylinder*		*Colour of bands*	
Name	*Symbol*	*Nominal*	*British Standard Colour No.*	*Nominal*	*British Standard Colour No.*
Carbon dioxide (for inhalation)	CO_2	Green with black bottom	25	..	..
Carbon dioxide with internal tube (for snow making)	CO_2	Green	25	..	..
Ethyl chloride	C_2H_5Cl	As Table 11	..	..	..
Ethylene	C_2H_4	As Table 11	..	..	..
Nitrous oxide	N_2O	Black	..	..	..
Oxygen	O	Black	..	White	..
Oxygen and CO_2 mixture	..	Black	..	Green with white neck	25

The British Standard Colours referred to are contained in the British Standard Schedule of Colours for Ready-Mixed Paints (No. 381).

the cylinders should be specially labelled indicating the nature of the contents.

Periodic Tests and Examination

Every cylinder when ready to be put into service and at intervals of two years thereafter should be subjected to a hydraulic stretch test, preferably by the 'water-jacket' method. In this method the cylinder is enclosed in a vessel filled with water and fitted with a gauge-glass projecting from its upper cover. The changes in volume of the cylinder on applying and after the removal of the internal hydraulic pressure are measured by the changes in level of the water in the gauge-glass. The proof pressure to be applied in the case of cylinders for the permanent gases is 3,000 lb./sq. inch. For cylinders for the liquefiable gases the proof pressure should be the value of p calculated from the formula $p = 2ft/(D-t)$, where $f = 33{,}600$ lb./sq. inch. The permanent stretch shown by the test should not exceed 10 per cent. of the temporary stretch under the proof pressure.

The periodical re-heat treatment of carbon steel gas cylinders which have not been obviously damaged, serves no useful purpose and is not recommended.

Corrosion and Chemical Action

There is no evidence that cylinders containing any of the gases referred to in Table 9 suffer from internal corrosion provided the gases and cylinder are free from moisture. It should be noted, however, that when compressing gases into a cylinder water may easily be introduced unless special provision is made for drying the gas. Moist air and oxygen will oxidize steel, and moist carbon monoxide at high pressures will readily combine with iron to give iron carbonyl. There is some evidence that the attack by carbon monoxide may be local, but as far as the writer is aware no instances of cylinder failure due to this cause have been reported.

Accidents involving or attributable to Gas Cylinders

The reports of H.M. Inspectors of Explosives contain the details of numerous accidents in which gas cylinders are involved; and as many of these are directly attributable to the improper use of cylinders, some account of the precautions which should be adopted may be given.

By following the recommendations of the Gas Cylinders Research

Committee in regard to the marking and colouring of cylinders and to the design of valves, there is very little danger that a cylinder containing a combustible gas could be mistaken for one containing a non-combustible gas. There are many instances, however, in which oxygen has been mistaken for air with disastrous consequences, and the following extract from the 61st Annual Report of H.M. Inspectors of Explosives (1936), will serve to illustrate the nature of the hazard:

'The dangers of the use of oil or grease in connexion with oxygen are well known and every oxygen cylinder has a label on which is written the warning 'It is dangerous to use oil or grease'. Two accidents have been reported to us which were due to the use of compressed oxygen by mistake instead of compressed air.

'The first of these occurred in a factory where an oil-purifying plant is in use. By mistake a cylinder of oxygen was used instead of compressed air. As the oil in the plant had previously been heated to a temperature of 500° F. it is not surprising that an explosion occurred when oxygen was admitted. Four men were injured.

'In the second accident fuel-storage tanks were being tested. Again it was a case of compressed oxygen being used by mistake instead of compressed air. A workman then entered the tank carrying a lighted candle and there was a violent "combustion" and the man was severely burned.'

In this connexion it should be borne in mind that the sudden introduction of compressed oxygen into a closed system containing oil or other combustible is always fraught with danger, and a number of cases have been recorded in which pressure gauges containing traces of oil have been destroyed by explosion when oxygen was introduced.

Gas cylinders are liable to burst when their internal pressure is increased beyond a certain amount as the result of (*a*) external heating, (*b*) the exothermic decomposition or polymerization of their contents (e.g. acetylene, hydrocyanic acid), and (*c*) the transmission of a shock wave to the cylinder through the connexion pipe leading from an enclosed system in which an explosion or detonation has occurred.

The Nature of Cylinder Bursts

When a steady and gradually increasing hydraulic pressure is applied to a gas cylinder filled with liquid the stresses in the cylinder wall increase until the elastic limit of the material is reached; on further increase of pressure the cylinder becomes permanently stretched and eventually the walls rupture and allow the liquid to escape. Failure occurs by shear and the walls are generally split

CYLINDER BURST DUE TO A GAS EXPLOSION

open in a longitudinal direction from the end farthest removed from the valve; fragmentation does not normally take place. The photographs reproduced in Plate 2 are taken from the First Report of the Gas Cylinders Research Committee and show the effects of actual bursts on a number of cylinders tested at the National Physical Laboratory. Reference to the details given on the plate show that, for the ordinary type of cylinder, the elastic limit is reached when the internal pressure is in the neighbourhood of 250 atmospheres and that a burst is liable to occur when the internal pressure exceeds some 400 atmospheres at room temperature.

A cylinder may also burst as the result of having its wall pierced by a flying fragment of metal or other hard substance. The National Physical Laboratory have carried out extensive firing tests in which light alloy steel cylinders were charged with oxygen to a pressure of 120 atmospheres and armour piercing bullets were fired at them. In some cases the bullet pierced both walls of the cylinder without further damage although the cylinder itself was projected a considerable distance. In others, the cylinder burst, the walls opened out, and the shattered metal was thrown a distance of some 40 yards. No tests were reported on the high carbon steel cylinders, but, in view of the mechanical properties of the metal, it is not improbable that in similar circumstances a burst might sometimes occur.

Plate 3 shows the effect of an explosion of a mixture of carbon monoxide and oxygen which had accidentally been filled into a gas cylinder to a pressure of about 100 atmospheres. The explosion was caused by opening the cylinder suddenly to a reducing valve, when the rise of temperature as the gas was adiabatically compressed into the valve was sufficient to cause ignition. No fragmentation occurred.

Many instances of cylinder bursts due to fire have been reported and have frequently resulted in serious damage and loss of life. When a cylinder is in contact with burning material or is heated by radiation from a fire, the pressure of its contents may rise above the permissible limit. At the same time, if the temperature exceeds 350° C. or thereabouts, the steel walls of the cylinder will lose strength and rupture may occur. If the heating should happen to be local and confined to the upper part of the cylinder, the soldered joint or the lead capsule at the valve may fuse, releasing the gas comparatively slowly and thus relieving the stresses in the cylinder wall. When a burst occurs at full pressure, there is usually a loud

report or explosion and the suddenly released gas sets up a shock wave which, travelling outwards at high velocity in all directions, may cause serious damage to movable objects or light structures encountered in its path. Furthermore, if the gas is combustible it may, by diffusion into the atmosphere, form an explosive mixture.

It is evident, therefore, that charged gas cylinders must always be regarded as a potential source of danger and they should, where possible, be stored in a fire-proof room or in a separate building.

III

THE STRESSES AND STRAINS IN THE WALLS OF CYLINDERS SUBJECTED TO INTERNAL AND EXTERNAL PRESSURES

WHEN an internal and/or an external pressure is applied to a hollow cylinder, a system of stresses is set up in the walls which gives rise to temporary or permanent strains according as the stresses are smaller or greater than those corresponding with the elastic limits of the material of which the cylinder is constructed. The principal stresses in question are a radial compressive stress, P, a tensile hoop

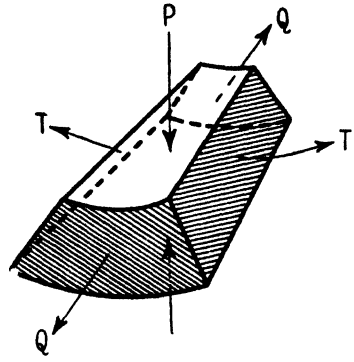

Fig. 7. The three principal stresses in the wall of a cylinder subjected to internal pressure.

stress, T, and a longitudinal stress, Q (Fig. 7). Both P and T vary with distance from the axis of the cylinder, whilst Q, which is usually small in comparison with the other two, is assumed to act uniformly over the cross-section of the walls. The stresses P and T acting at right angles to one another produce a shear stress, the maximum value of which is equal to one-half their algebraic difference and is set up in a plane at 45° to their directions. We may, therefore, write

$$\text{Maximum shear stress} = \tfrac{1}{2}\{T-(-P)\}$$
$$= \tfrac{1}{2}(T+P).$$

This maximum shear stress is equivalent to a simple stress, S, of magnitude $(T+P)$, and it will be shown later that, according to one criterion, elastic failure of the cylinder may be assumed to occur when S exceeds the stress at the elastic limit of the material as determined by the usual tensile test.

The distribution of the stresses P and T in the walls of the cylinder when the elastic limit of the material is not exceeded is approximately as shown in Fig. 8. If the internal pressure is progressively increased, the annular layers of metal will pass in turn through the various states defined in Fig. 1 (p. 7), i.e. the elastic, slip, yield, and semi-plastic ranges; and when the pressure is such that the inner layers

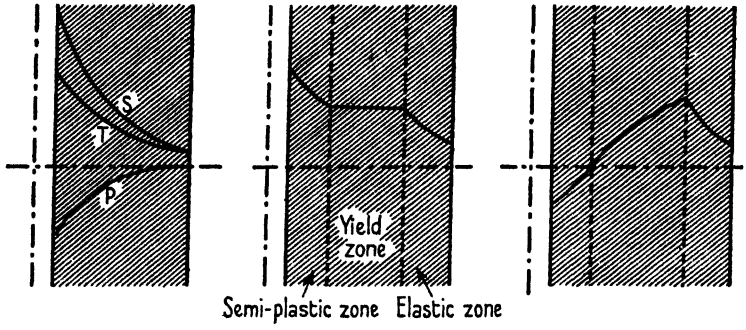

Fig. 8. Fig. 9. Fig. 10.

Fig. 8 Variation of stresses in the walls of a cylinder stressed within the elastic limit.

Fig. 9. Variation of hoop-stresses in the walls of a cylinder stressed beyond the elastic limit.

Fig. 10. Residual stresses in the walls of a cylinder due to overstressing.

are stressed within the semi-plastic range, the tensile stresses in the walls will be as shown in Fig. 9, and will give rise to strains tending to increase the cylinder diameter; permanent strains will be set up in the semi-plastic and yield zones and, on release of the internal pressure, will resist the contraction of the outer layers in the elastic zone. There will therefore be a residual system of stresses in the walls, the inner layers being in compression and the outer layers in tension (Fig. 10). From the results given in Table 2 (p. 9) it will be clear that the original elastic properties of the metal have been considerably modified by overtension and overcompression, and to stabilize the cylinder so that it will behave elastically on repeated applications of pressure up to the original overstressing pressure, a low-temperature heat treatment will be necessary.

The process by which a cylinder is overstressed and subsequently rendered elastic is known as 'auto-frettage', and the method of calculating the auto-frettage pressure necessary to give specified residual stresses in the walls will be described later. It may be mentioned here, however, that too great a degree of overtension

tends to destroy those ductile qualities measured by the 'impact' test, and for practical purposes 2·5 per cent. strain of the bore layer under load may be considered as the extreme upper limit for satisfactory results.

Stresses in a Steel Cylinder subjected to Internal and External Pressures

The method of calculating the magnitude of the stresses P and T at any point in the walls of a thick-walled cylinder is as follows:

Let P_0 = the radial pressure per unit area acting on the inner wall of the cylinder,

P_1 = the radial pressure acting on the external wall of the cylinder,

R_0 and R_1 = the internal and external radii of the cylinder, respectively,

R and $(R+dR)$ the internal and external radii of an elementary cylinder, and

P and $P+dP$ = the radial pressures on the inner and outer surfaces of the elementary cylinder.

For unit axial length the pressure tending to burst the elementary cylinder across any diameter is $2PR-2(P+dP)(R+dR)$, and this is balanced by a tensile stress $2T\,dR$, so that

$$2PR-2(P+dP)(R+dR) = 2T\,dR;$$

or, neglecting the products of small quantities,

$$P\,dR+R\,dP+T\,dR = 0;$$

and in the limit

$$P+R\frac{dP}{dR}+T = 0, \tag{3.1}$$

or,

$$\frac{d(RP)}{dR}+T = 0.$$

It is now necessary to assume that the strain parallel to the axis of the cylinder is constant and uniformly distributed so that a plane cross-section of the cylinder perpendicular to the axis will remain undistorted on application of pressure, and the longitudinal stress will be uniformly distributed over the cross-section.

The longitudinal strain e_Q is given by

$$e_Q = \frac{1}{E}(Q+\sigma P-\sigma T),$$

where E = modulus of elasticity and σ = Poisson's ratio; hence $T-P$ is constant.

Let $T-P = 2a$. From (3.1)

$$\frac{d(RP)}{dR} = -T, \qquad \frac{PdR}{dR}+\frac{RdP}{dR} = -T,$$

or,
$$P+T = -R\frac{dP}{dR};$$

and since
$$T-P = 2a,$$

$$2P = -R\frac{dP}{dR}-2a, \qquad 2(P+a) = -R\frac{dP}{dR}, \qquad \frac{dP}{P+a} = \frac{-2dR}{R},$$

and,
$$\log_e(P+a) = \log_e bR^{-2},$$

where b is a constant of integration. Therefore

$$P+a = \frac{b}{R^2}, \qquad P = \frac{b}{R^2}-a, \tag{3.2}$$

and
$$T = \frac{b}{R^2}+a, \tag{3.3}$$

where a and b depend upon the radii of the cylinder.

From (3.2) and (3.3)
$$P+T = \frac{2b}{R^2}; \tag{3.4}$$

that is, the sum of the radial pressure and the hoop tension at any point in the cylinder walls varies inversely as the square of the distance from the axis.

The constants a and b may be calculated from (3.2) by substituting known values for P and R.

Thus
$$P_0 = \frac{b}{R_0^2}-a$$

and
$$P_1 = \frac{b}{R_1^2}-a,$$

from which
$$a = \frac{P_0R_0^2-P_1R_1^2}{R_1^2-R_0^2},$$

and
$$b = \frac{R_1^2R_0^2(P_0-P_1)}{R_1^2-R_0^2}.$$

From the values of a and b so ascertained the formulae in Table 13 are derived.

TABLE 13. *Distribution of Stresses in the Walls of a Thick Cylinder subjected to Internal and/or External Pressure*

Value of radial pressure and hoop tension at radius	*Cylinder subjected to internal pressure P_0 and external pressure P_1*	*Cylinder subjected to internal pressure P_0 alone*	*Cylinder subjected to external pressure P_1 alone*
R_0	$T_0 = \frac{P_0 R_0^2 - P_1 R_1^2}{R_1^2 - R_0^2} + \frac{R_1^2(P_0 - P_1)}{R_1^2 - R_0^2}$	$T_0 = P_0 \frac{R_1^2 + R_0^2}{R_1^2 - R_0^2}$	$T_0 = -\frac{2P_1 R_1^2}{R_1^2 - R_0^2}$
R	$P = \left(\frac{R_0^2 R_1^2}{R^2} \times \frac{P_0 - P_1}{R_1^2 - R_0^2}\right) - \frac{P_0 R_0^2 - P_1 R_1^2}{R_1^2 - R_0^2}$	$P = \frac{P_0 R_0^2}{R^2} \times \frac{R_1^2 - R^2}{R_1^2 - R_0^2}$	$P = \frac{P_1 R_1^2}{R^2} \times \frac{R^2 - R_0^2}{R_1^2 - R_0^2}$
	$T = \left(\frac{R_0^2 R_1^2}{R^2} \times \frac{P_0 - P_1}{R_1^2 - R_0^2}\right) + \frac{P_0 R_0^2 - P_1 R_1^2}{R_1^2 - R_0^2}$	$T = \frac{P_0 R_0^2}{R^2} \times \frac{R_1^2 + R^2}{R_1^2 - R_0^2}$	$-T = \frac{P_1 R_1^2}{R^2} \times \frac{R^2 + R_0^2}{R_1^2 - R_0^2}$
R_1	$T_1 = \frac{P_0 R_0^2 - P_1 R_1^2}{R_1^2 - R_0^2} + \frac{R_0^2(P_0 - P_1)}{R_1^2 - R_0^2}$	$T_1 = \frac{2P_0 R_0^2}{R_1^2 - R_0^2}$	$-T_1 = P_1 \frac{R_1^2 + R_0^2}{R_1^2 - R_0^2}$
Note:—	$T_0 - P_0 = T \quad P = T_1 - P_1$	$P_1 = 0$ $T_0 - P_0 = \frac{2P_0 R_0^2}{R_1^2 - R_0^2} = T_1$ and $T_0 = T_1 + P_0$	The hoop stress is a compressive stress

For a cylinder with closed ends there will be a longitudinal stress, Q, due to the load acting on the ends, which may be assumed to be uniformly distributed over the cross-section of the walls. The total pressure on the ends is $\pi R_0^2 P_0$ distributed over an area $\pi(R_1^2 - R_0^2)$.

Hence
$$Q = \frac{\pi R_0^2 P_0}{\pi(R_1^2 - R_0^2)} = \frac{P_0 R_0^2}{R_1^2 - R_0^2}. \tag{3.5}$$

For a cylinder with open ends $Q = 0$.

Strains in a Cylinder subjected to Internal and External Pressures

When a cube (Fig. 11) is subjected to three principal stresses P, T, and Q, the strains set up in the direction of the stresses are

$$e_P = -\frac{1}{E}(P + \sigma T + \sigma Q),$$

$$e_T = \frac{1}{E}(T + \sigma P - \sigma Q),$$

and
$$e_Q = \frac{1}{E}(Q - \sigma T + \sigma P).$$

The above relations applied to a cylinder with open ends (i.e. $Q = 0$) enable the expansion of the cylinder due to an internal pressure to

be calculated. Thus, for example, the total increase in circumference at a radius R is given by $2\pi R \times e_T$ and the increase of radius by $R \times e_T$. The unit expansion (or strain) of the radius R is therefore e_T or

$$\frac{\delta R}{R} = \frac{1}{E}(T+\sigma P).$$

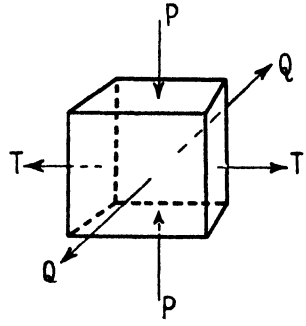

Fig. 11. The strains resulting from the action of three stresses at right angles to one another.

Expressed in terms of the stresses at the bore

$$\frac{\delta R}{R} = \frac{P_0 R_0^2}{R^2 E}\left\{\frac{(1+\sigma)R_1^2+(1-\sigma)R^2}{R_1^2-R_0^2}\right\}, \tag{3.6}$$

and

$$\delta R = \frac{P_0 R_0^2}{RE}\left\{\frac{(1+\sigma)R_1^2+(1-\sigma)R^2}{R_1^2-R_0^2}\right\}.$$

Similarly,

$$\delta R_0 = \frac{R_0 P_0}{E}\left\{\frac{(1+\sigma)R_1^2+(1-\sigma)R_0^2}{R_1^2-R_0^2}\right\}, \tag{3.7}$$

and

$$\delta R_1 = \frac{2P_0 R_1 R_0^2}{E(R_1^2-R_0^2)}. \tag{3.8}$$

The strain in a longitudinal direction, $\delta L/L$, is given by

$$e_Q = \frac{1}{E}(Q-\sigma T+\sigma P),$$

and since in an open cylinder $Q = 0$,

$$\frac{\delta L}{L} = \frac{-\sigma}{E}(T-P) = -\frac{2P_0 R_0^2 \sigma}{E(R_1^2-R_0^2)}. \tag{3.9}$$

It should be noted that $\delta L/L$ is a compressive strain so that the effect of an internal pressure upon a cylinder with open ends is to shorten it.

In the case of a cylinder with closed ends, if L is its length and δL

the extension in length due to an internal pressure P_0, then the strain e_Q is given by $\delta L/L$. Also

$$e_Q = \frac{1}{E}(Q-\sigma T+\sigma P),$$

$$= \frac{Q}{E}-\frac{\sigma}{E}(T-P). \tag{3.10}$$

Since $T-P$ is a constant, (3.5) and (3.10) give

$$\frac{\delta L}{L} = \frac{P_0 R_0^2}{(R_1^2-R_0^2)E} - \frac{\sigma}{E} \times \frac{2P_0 R_0^2}{(R_1^2-R_0^2)}$$

$$= \frac{P_0 R_0^2}{E(R_1^2-R_0^2)} \times (1-2\sigma). \tag{3.11}$$

As Poisson's ratio for steel is always less than 0·5, $\delta L/L$ will always be positive.

The Effect of the Stress Q on a plane at right angles to the axis of the Cylinder

The value of the principal stress Q is given by (3.5). It will produce equal strains in the direction of the radial pressure P and the hoop tension T of magnitude

$$= -\frac{\sigma Q}{E} = -\frac{\sigma P_0 R_0^2}{E(R_1^2-R_0^2)}. \tag{3.12}$$

Now the strain in the direction of hoop tension in a cylinder with open ends is given by (3.6), and the resultant strain at any radius R will therefore be the algebraic sum of the strain given by (3.6) and (3.12), that is:

Resultant Strain at R:

$$\frac{\delta R}{R} = \frac{P_0 R_0^2}{R^2 E}\left\{\frac{(1+\sigma)R_1^2+(1-\sigma)R^2}{R_1^2-R_0^2}\right\} - \frac{\sigma P_0 R_0^2}{E(R_1^2-R_0^2)},$$

$$= \frac{P_0 R_0^2}{E}\left\{\frac{(1+\sigma)R_1^2+(1-2\sigma)R^2}{R^2(R_1^2-R_0^2)}\right\}. \tag{3.13}$$

Resultant Strain at R_0:

$$\frac{\delta R_0}{R_0} = \frac{P_0}{E}\left\{\frac{(1+\sigma)R_1^2+(1-2\sigma)R_0^2}{R_1^2-R_0^2}\right\}. \tag{3.14}$$

Resultant Strain at R_1:

$$\frac{\delta R_1}{R_1} = \frac{P_0 R_0^2}{E}\frac{(2-\sigma)}{(R_1^2-R_0^2)}. \tag{3.15}$$

The expansion δR at any radius can be obtained by multiplying the strain as given by (3.13), (3.14), or (3.15) by the radius.

It is evident from the above that the magnitude of the expansion of a cylinder due to internal pressure will vary according as it has open or closed ends; it is assumed, however, that although the effect of closed ends is to lessen the strains in the hoop tension and radial compression directions, the stresses in these directions are unaltered

Strains due to the Equivalent Simple Stress S

The hypothetical strain $\delta r/r$ due to the stress S is given by

$$\frac{\delta r}{r} = \frac{S}{E} = \frac{T+P}{E}, \tag{3.16}$$

whilst the actual strain $\dfrac{\delta R}{R} = \dfrac{T+\sigma P}{E}$.

The value of the hypothetical strains at radii R_0, R, and R_1 are as follows:

$$\frac{\delta r_0}{r_0} = \frac{S_0}{E} = \frac{S_1 R_1^2}{E R_0^2}, \tag{3.17}$$

$$\frac{\delta r}{r} = \frac{S}{E} = \frac{S_0 R_0^2}{E R^2}, \tag{3.18}$$

and

$$\frac{\delta r_1}{r_1} = \frac{S_1}{E} = \frac{S_0 R_0^2}{E R_1^2}. \tag{3.19}$$

The Criterion of Elastic Failure

As the pressure P is progressively increased both T and Q increase until at the elastic limit of the cylinder the maximum principal stress, the maximum shear stress, the maximum strain, and the strain energy reach certain critical values. Any further increase of P will then cause elastic failure of the material with resultant 'permanent set' or rupture. From the practical point of view it is necessary to ascertain the relation between the value of P at the elastic limit, and some property which can conveniently be measured by the application of a uniaxial stress to a representative test-piece of the material from which the vessel is made.

Of the various theories put forward to account for elastic failure only four need be specifically mentioned. According to these theories failure will occur when either (1) the maximum principal stress equals the stress at the elastic limit under simple tension, (2) the maximum strain equals the strain at the elastic limit under simple tension,

(3) the maximum shear stress reaches a critical value, and (4) the strain energy per unit volume reaches a critical value.

None of these theories is able adequately to account for all the facts associated with the complex system of stresses found in hydraulic plant, but if attention is confined to thick-walled cylinders the Maximum Shear Stress and the Strain Energy theories are found, by experiment, to give the most accurate results.

The methods of calculating the principal stresses and strains have been described and it is now proposed to compare the results of experiments on cylinder failures with the predictions of theory.

The following diagrammatic representation will be found useful [1].

Maximum Stress Theory (Fig. 12)

Let P and T be the principal stresses in a two-dimensional stress system and assume that each stress may be either compressive or tensile, the latter being taken as positive.

If the elastic limits of the material in simple tension and compression are F and F', then according to the Maximum Stress theory (1) the material will reach its elastic limit when the ordinates of the point P, T pass outside the area $ABCD$; for most steels $F = F'$.

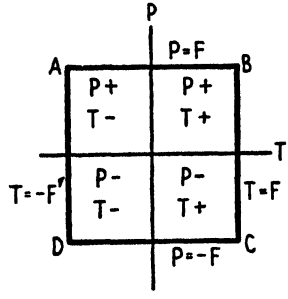

Fig. 12. Diagram illustrating Maximum Stress theory.

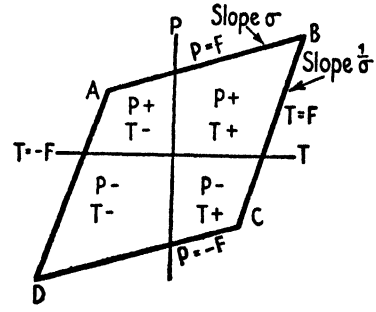

Fig. 13. Diagram illustrating Maximum Strain theory.

Maximum Strain Theory (Fig. 13)

The strains due to P and T are

$$e_P = -\frac{1}{E}(P+\sigma T)$$

and

$$e_T = \frac{1}{E}(T+\sigma P),$$

and according to the Maximum Strain theory (2) the elastic limit will be reached when either of these equals F/E. That is,

$$P+\sigma T = F, \qquad (3.20)$$
$$T+\sigma P = F,$$

and the ordinates of the point P, T pass out of the parallelogram $ABCD$.

Maximum Shear Stress Theory (Fig. 14)

When the principal stresses are of opposite sign the maximum shear stress is equal to one-half the algebraic difference of P and T and, according to the Maximum Shear Stress theory, the elastic limit will be passed when $P-T$ or $T-P = F$, that is, when the ordinates of P, T pass outside the area $ABCD$.

If P and T have the same sign the greatest shearing stress is $\frac{1}{2}P$ or $\frac{1}{2}T$, according to which is greater, and the ordinates of P, T will pass outside the area $BHCOAID$ when the material passes the elastic limit. In the case of a cylinder, the planes on which the maximum shearing stress exists will be parallel to the axis and inclined at 45° to the radius at every point.

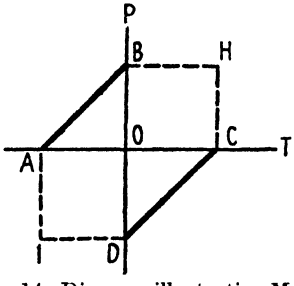

Fig. 14. Diagram illustrating Maximum Shear Stress theory.

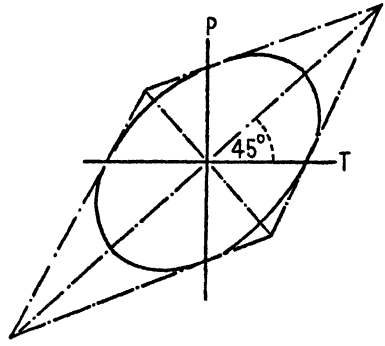

Fig. 15. Diagram illustrating Strain Energy theory.

The Strain Energy Theory (Fig. 15)

The strain energy per unit volume in a two-dimensional stress system is

$$\frac{1}{2E}(P^2+T^2-2\sigma PT),$$

and the strain energy at the elastic limit in pure tension is $F^2/2E$. Hence

$$P^2+T^2-2\sigma PT = F^2,$$

which is the equation of an ellipse with axes inclined at 45° to the coordinate axes. If the elastic limit and modulus of elasticity for

the material is the same in tension and compression this ellipse marks the boundary at which elastic failure will occur.

The slope of the tangent at $T = 0$ is σ and at $P = 0$ is $1/\sigma$ and hence the ellipse is contained in the parallelogram given by the Maximum Strain theory.

It may be remarked here that the Strain Energy theory gives a continuous change in the values of both principal stresses as they pass through negative and positive values whilst the Maximum Shear Stress theory indicates that if the magnitude of one of the principal stresses changes continuously from a small positive to a small negative value there will be a discontinuity in the value of the other stress.

If we turn now to the formulae summarized in Table 13 it is possible to calculate, on the basis of the various theories, the maximum permissible internal pressure a cylinder, made from a steel having a known elastic limit, is capable of withstanding. Let the elastic limit of the material in simple tension be called F. Then according to:

1. *The Maximum Principal Stress Theory* the elastic limit of the cylinder will be reached when $T = F$ and

$$\frac{P_0}{F} = \frac{R_1^2 - R_0^2}{R_1^2 + R_0^2}, \tag{3.21}$$

2. *The Maximum Strain Theory*

$$\frac{P_0}{F} = \frac{4(R_1^2 - R_0^2)}{5R_1^2 + 3R_0^2}, \tag{3.22}$$

where $\sigma = 0{\cdot}25$;

3. *The Maximum Shear Stress Theory* the elastic limit will be reached when $P + T = F$ and

$$\frac{P_0}{F} = \frac{R_1^2 - R_0^2}{2R_1^2}; \tag{3.23}$$

4. *The Strain Energy Theory.* In this case

$$P_0^2 + T_0^2 + 2\sigma P_0 T_0 = F^2$$

and

$$\frac{P_0}{F} = \frac{R_1^2 - R_0^2}{R_0^2\sqrt{\{2(1+\sigma)(R_1/R_0)^4 + 2(1-\sigma)\}}}, \tag{3.24}$$

or, if $\sigma = 0{\cdot}25$,

$$\frac{P_0}{F} = \frac{2(R_1^2 - R_0^2)}{\sqrt{(10R_1^4 + 6R_0^4)}}. \tag{3.25}$$

The results of bursting tests made on thick-walled cylinders have shown that in the case of brittle materials such as cast iron the Maximum Principal Stress theory applies within the limits of experi-

mental error, whilst for ductile material such as high tensile steels the Maximum Shear Stress and the Strain Energy theories hold more closely.

Thus reference may be made to an investigation by Cook and Robertson [2] into the strength of thick hollow cylinders of cast iron and mild steel and to similar data by Macrae [3] upon cylinders of high tensile steel, which serve to illustrate the extent of the agreement between theory and practice.

The tubes employed by Cooke and Robertson were of the form shown in section in Fig. 16 and, in the case of cast iron, were turned and bored from a solid casting, whilst those of mild steel were made from solid shafting $2\frac{1}{4}$ in. in diameter, one end being left solid.

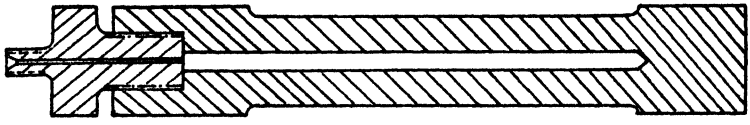

Fig. 16. Cylinder employed by Cook and Robertson.

Cast Iron

With this material rupture occurs approximately at the elastic limit. The data for tubes in which the ratio of the external to internal diameter varied from 1·30 to 2·96 are summarized in Table 14.

In the calculated results the tensile strength of the material is that obtained from specimens cut from the walls of the ruptured cylinder; the calculated bursting pressure and values of P/F are based upon the Maximum Principal Stress theory, equation (3.21).

TABLE 14. *Results of Tests on Cast Iron Cylinders. (Cook and Robertson)*

External diameter D_1, *inch*	*Internal diameter* D_0, *inch*	$\frac{D_1}{D_0}$	*Tensile strength* (F), *lb./sq. in.*	*Bursting pressure* (P) *lb./sq. in.*	*Calculated bursting pressure, lb./sq. in.*	*Observed* $\frac{P}{F}$	*Calculated* $\frac{P}{F}$
1·133	0·873	1·30	18,600	5,060	4,760	0·272	0·256
1·420	0·923	1·54	24,500	9,520	9,950	0·388	0·406
1·390	0·755	1·83	23,550	13,000	12,710	0·552	0·540
1·710	0·922	1·85	26,900	14,550	14,800	0·540	0·550
1·561	0·793	1·97	24,200	15,100	14,300	0·623	0·590
1·475	0·750	1·97	24,750	16,460	14,600	0·665	0·590
1·516	0·635	2·40	26,700	19,250	18,800	0·720	0·704
1·870	0·630	2·96	21,700	17,410	17,300	0·802	0·796

The results show that for this material the Maximum Principal Stress theory gives results in satisfactory agreement with the experimental data.

Mild Steel

In the case of mild steel the yield pressure in the cylinder was determined by measuring the elastic extension on the external surface. Whilst all the stresses are below the elastic limit the elastic extension of every part of the cylinder is directly proportional to the internal pressure, but when yield takes place at the internal surface there is a redistribution of stresses and if the diametral extensions are plotted against the pressures, a deviation from the straight line is at this point observed.

The results of a number of experiments in which the ratio of the diameters D_1/D_0 was increased from 1·35 to 3·65 are contained in Table 15.

TABLE 15. *Results of Tests on Mild Steel Cylinders*

Ratio of external to internal diameter	*Stress at yield in simple tension (F), lb./sq. in.*	*Yield pressure in cylinder (P), lb./sq. in.*	*Experimental value of* $\frac{P}{F}$	*Calculated values of P/F according to*			
				Max. Princ. Stress theory	*Max. Princ. Strain theory†*	*Max. Shear Stress theory*	*Max. Strain Energy theory*
1·35	35,300	9,700	0·275	0·291	0·295	0·225	0·262
1·53	35,300	12,000	0·340	0·402	0·393	0·287	0·344
1·58	35,300	12,500	0·354	0·430	0·415	0·300	0·363
1·58	35,300	12,500	0·354	0·430	0·415	0·300	0·363
1·74	35,300	14,700	0·416	0·506	0·475	0·336	0·411
1·77	35,300	14,400	0·407	0·515	0·483	0·340	0·417
1·79	35,300	15,400	0·436	0·525	0·490	0·344	0·422
1·79	35,300	15,200	0·430	0·525	0·490	0·344	0·422
1·79	35,300	15,400	0·436	0·525	0·490	0·344	0·422
1·79	35,300	14,600	0·413	0·525	0·490	0·344	0·422
1·86	34,000	13,600	0·400	0·554	0·511	0·356	0·449
1·97	34,000	14,100	0·415	0·590	0·539	0·372	0·460
2·19	36,860	18,090	0·490	0·655	0·583	0·395	0·494
2·19	36,860	18,090	0·490	0·655	0·583	0·395	0·494
2·45	36,860	18,740	0·508	0·713	0·625	0·416	0·522
2·66	36,860	20,150	0·546	0·752	0·649	0·429	0·539
2·88	36,860	20,300	0·550	0·784	0·672	0·439	0·553
3·05	36,860	20,200	0·547	0·806	0·684	0·446	0·562
3·26	36,860	21,700	0·588	0·827	0·697	0·452	0·571
3·65	36,860	21,800	0·591	0·860	0·718	0·467	0·583

† Calculated from $\frac{P}{F} = \frac{4(R_1^2 - R_0^2)}{5R_1^2 + 2R_0^2}$.

On comparing the experimental values of P/F with those calculated from (3.21) to (3.25) it will be seen that the Strain Energy theory gives the closest approximation to the experimental figures.

It must be borne in mind that whilst in the actual experiments there are three principal stresses at the internal surface of the cylinder, account has only been taken in the calculations of the radial and hoop stresses P and T, and there is therefore a possibility that the longitudinal stress Q may exert an influence on the elastic limit as determined by the other two. That it does so, however, is very improbable since the proportional difference between the experimental and calculated values of P/F does not vary with increase of D_1/D_0 although the value of Q diminishes.

End Effects

In the above experiments the cylinders employed had one solid end, the effect of which might be to increase the pressure at which the internal layers of the cylinder commence to yield; to test this point the yield pressures of four cylinders having the same external and internal diameters, but of varying lengths, were determined with the results recorded in Table 16.

TABLE 16. *Influence of the Length of Cylinder upon the Yield Pressure*

Internal diameter of cylinders = $\frac{5}{8}$ inch
External „ „ „ = $1\frac{1}{8}$ inch.

Length, inches	*Yield pressure, lb./sq. in.*
2·00	15,400
4·25	15,250
6·75	15,400
9·00	14,700

The close agreement in the values of the yield pressure makes it evident that the end effect can only extend a very short distance.

High Tensile Steels

The results obtained with nickel steel, nickel-chromium, and nickel-chromium-molybdenum steels of the composition given on p. 10 are summarized in Table 17. The tubes employed had all an internal diameter D_0 of 3 inches, the external diameter D_1 varying from 6 to 7·5 inches.

TABLE 17. *Results of Tests on High Tensile Steel Cylinders* [3]

Class of steel	$\frac{D_1}{D_0}$	*Tensile elastic limit (F), tons/sq. in.*	*Bore pressure (P) at which bore was stressed to (F), tons/sq. in.*	*P/F*	*P/F Calculated according to*			
					Max. Princ. Stress theory	*Max. Princ. Strain theory*	*Max. Shear Stress theory*	*Max. Strain Energy theory*
Nickel steel	2·15	28·08	11·48	0·409	0·644	0·577	0·392	0·488
,, ,,	2·15	28·94	11·50	0·397	0·644	0·577	0·392	0·488
,, ,,	2·50	21·31	9·00	0·422	0·724	0·631	0·420	0·527
,, ,,	2·50	28·80	12·10	0·420	0 724	0 631	0 420	0·527
Nickel-chromium steel	2 00	29·57	11·93	0·404	0·600	0·546	0·375	0·466
Nickel-chromium-molybdenum steel	2·00	37·62	14·10	0·374	0·600	0·546	0 375	0·466
,, ,,	2·00	33·44	12·68	0·379	0·600	0·546	0·375	0·466
,, ,,	2·00	32·45	12·10	0·373	0·600	0·546	0·375	0·466

It is evident from the above data that in the case of high tensile steels the Maximum Shear Stress theory gives the closest approach to the experimental results; in all calculations involving these steels it will therefore be employed.

Stresses set up in the walls of a Simple Cylinder according to the Maximum Shear Stress Theory

The method of calculating the values of the radial and hoop stresses P and T at any point in the wall of a simple cylinder has been described and the formulae connecting P, T, and the dimensions of the cylinder are summarized in Table 13.

According to the Maximum Shear Stress theory elastic failure of the cylinder will take place for a certain value of the maximum shear stress produced by the two principal stresses P and T. The maximum shear stress is equal to half their algebraic difference and is set up on a plane inclined at 45° to their direction of action.

Thus the maximum shear stress $= \frac{1}{2}(T-[-P])$,

$$= \tfrac{1}{2}(T+P).$$

It is equivalent to a simple stress S of magnitude $T+P$, which, according to the theory, is the determining stress in the cylinder.

Thus if F is the elastic limit in tension of the material of which the cylinder is constructed, the elastic limit of the cylinder will be reached when

$$T_0+P_0 = F = S_0,$$

or,

$$P_0\left(\frac{R_1^2+R_0^2}{R_1^2-R_0^2}+1\right) = F;$$

and the internal pressure P_0 required so to stress the cylinder will be given by

$$P_0 = \frac{F}{2}\left(1-\frac{R_0^2}{R_1^2}\right); \tag{3.26}$$

the tensile elastic limit will be reached at any radius R when

$$P = \frac{F}{2}\left(1-\frac{R^2}{R_1^2}\right).$$

The simple stress at any point in the wall is calculated as follows:

Let S_0, S, and S_1 be the equivalent simple stresses at the internal radius R_0, any radius R, and the external radius R_1, respectively, then:

TABLE 18

At radius R_1	*At radius* R	*At radius* R_0
$S_1 = T_1+P_1$	$S = S_0\frac{R_0^2}{R^2} = S_1\frac{R_1^2}{R^2}$	$P_0 = \frac{S_0-S_1}{2}$
and since $P_1 = 0$		
$S_1 = T_1$	$P = \frac{S-S_1}{2}$ (3.30)	$P_0 = \frac{S_0}{2}\left(1-\frac{R_0^2}{R_1^2}\right)$ (3.31)
$= \frac{2P_0R_0^2}{R_1^2-R_0^2}$		
$\therefore S_1 = S_0-2P_0 = T_1$ (3.27)		$S_0 = S_1\frac{R_1^2}{R_0^2} = S\frac{R^2}{R_0^2}$ (3.32)
Also since $P_0 = \frac{S_0-S_1}{2}$		
$P_0 = \frac{S_0}{2}\left(1-\frac{R_0^2}{R_1^2}\right)$ (3.28)		
and $S_1 = S_0\frac{R_0^2}{R_1^2}$ (3.29)		

In Fig. 17 the distribution of the stresses in the wall is shown graphically. It will be seen from the figure that $T_0 = T_1+P_0$, the P and T curves being symmetrically situated with respect to OP_1 and the horizontal line drawn through T_1.

Limitations of Strength in a Simple Cylinder

According to the Maximum Shear Stress theory the limit of strength in a simple cylinder will be reached when the equivalent simple stress S_0 at the bore attains the value of the stress F at the elastic limit in simple tension; the internal pressure will then be

$$P_0 = \frac{F}{2}\left(1-\frac{R_0^2}{R_1^2}\right).$$

It can be seen from this equation that the maximum value of P_0 will be $0{\cdot}5F$. For most purposes, however, a cylinder in which the wall thickness is equal to the diameter (i.e. $R_1 = 3R_0$ and $P_0 = 0{\cdot}444F$) may be regarded as giving the limit of strength for this type of vessel.

Reference to Fig. 17 will show that even when the bore of the cylinder is stressed to the elastic limit (i.e. $S_0 = F$) the outer layers of metal are supporting only a comparatively small stress. Thus the area OS_0UP_1 may be taken as a measure of the total strength of the cylinder wall, and $OS_0T_1P_1$ the strength that can be utilized in a simple cylindrical vessel.

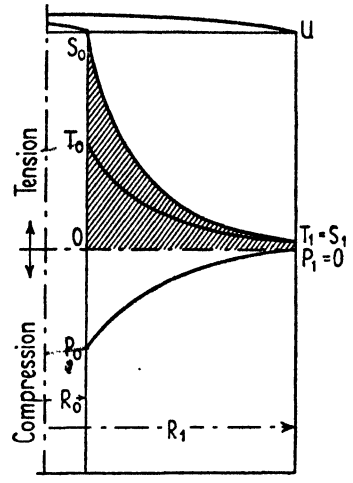

Fig. 17. Distribution of hoop stress, radial stress, and equivalent simple stress in a cylinder.

To utilize the strength of the metal to better advantage various types of compound cylinders have been developed, and it is now proposed to indicate briefly the theory underlying their design and the methods used in calculating the stresses set up in their walls.

Compound Cylinders built by Shrinkage

I. The Duplex Cylinder

In this type of cylinder two tubes are taken of such dimensions that before shrinkage the inner diameter of the outer tube is smaller than the outer diameter of the inner tube by a predetermined amount V, called the 'shrinkage'. The outer tube is heated uniformly until it has expanded sufficiently to contain the inner tube, which is then placed in position so as to form a compound cylinder. On cooling, the contraction of the outer tube is resisted by the compressive elasticity of the inner tube and the resultant effect is as though an internal pressure was applied to the former and an external pressure to the latter. Provided the tubes have been accurately machined and the heating and cooling have been uniform, the pressure is radial and acts on both tubes at the surface of contact. The diameter of contact will differ from the original diameter of the two tubes by a small amount which, for most purposes, may be neglected.

In the compound cylinder, therefore, the inner tube is initially in a state of compression and the outer one in tension, and on applying an internal pressure the resultant hoop stresses in the former will be less and in the latter will be greater than in the corresponding zones of a simple cylinder of the same over-all dimensions; in other words, there will be a more uniform distribution of stresses in the walls of the compound cylinder.

The Initial Stresses due to Shrinkage

Let D_0, D_2, and D_4 = the internal, contact, and external diameters of the compound cylinder,
V = shrinkage,
T_2 = hoop stress in inner tube at surface of contact,
P_2 = radial ,, ,, ,, ,,
S_2 = equivalent simple stress ,, ,,
T_0 = hoop stress at bore of inner tube,
P_0 = radial ,, ,, ,,
S_0 = equivalent simple stress ,,
T'_2 and S'_2 = the hoop and equivalent simple stresses at the bore of the outer tube,
P_4, T_4, and S_4 = the radial, hoop, and equivalent simple stresses at the outer surface of the compound cylinder,
P_1, T_1, S_1 / P_3, T_3, S_3 = the corresponding stresses at intermediate diameters D_1 and D_3.

In calculating the initial stresses the first step is to determine P_2. The shrinkage V is known from the dimensions of the two tubes before shrinkage and is equal to the sum of the amounts by which the outer diameter of the inner tube and the inner diameter of the outer tube contract and expand, respectively. The inner diameter of the outer tube is strained by an amount $(T'_2+\sigma P_2)/E$ and has expanded by $(D_2/E)(T'_2+\sigma P_2)$. Similarly, the outer diameter of the inner tube has contracted by an amount equal to $(D_2/E)(T_2-\sigma P_2)$.

Therefore,
$$V = \frac{(T'_2+T_2)D_2}{E},$$

and
$$T'_2+T_2 = \frac{VE}{D_2}. \tag{3.33}$$

This quantity is termed the 'shrinkage force'.

From the equations summarized in Table 13

$$T'_2 = P_2\frac{D_4^2+D_2^2}{D_4^2-D_2^2}, \tag{3.34}$$

$$-T_2 = P_2\frac{D_2^2+D_0^2}{D_2^2-D_0^2}, \tag{3.35}$$

and hence $$\frac{VE}{D_2} = P_2\left\{\frac{D_4^2+D_2^2}{D_4^2-D_2^2}+\frac{D_2^2+D_0^2}{D_2^2-D_0^2}\right\},$$

and $$P_2 = \frac{VE}{D_2\left\{\frac{D_4^2+D_2^2}{D_4^2-D_2^2}+\frac{D_2^2+D_0^2}{D_2^2-D_0^2}\right\}}. \qquad (3.36)$$

In (3.36) all the quantities on the right-hand side are known and hence P_2 can be determined.

From a knowledge of P_2 and the dimensions of the cylinder the stresses in the walls can be calculated from the equations in Table 13. The results are summarized on p. 58 (Table 19).

The contractions and expansions due to shrinkage are as follows:

Outer Tube

(1) The expansion δD_3 of a diameter D_3 due to shrinkage is given by

$$\delta D_3 = \frac{(T_3+\sigma P_3)D_3}{E}.$$

(2) Expansion at D_4:

$$\delta D_4 = \frac{T_4 \times D_4}{E}.$$

Inner Tube

(3) Contraction δD_1 at a diameter D_1:

$$\delta D_1 = \frac{(T_1-\sigma P_1)D_1}{E}.$$

(4) Contraction at D_0:

$$\delta D_0 = \frac{T_0 \times D_0}{E}.$$

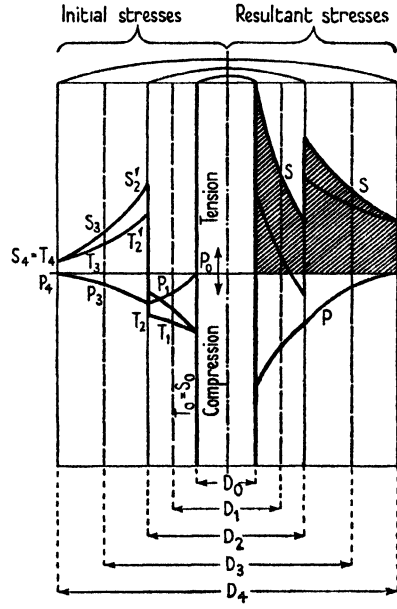

FIG. 18. Initial and resultant stresses in a compound cylinder (duplex).

The stresses in the walls of the compound cylinder due to an internal pressure alone are calculated as for a simple cylinder by the equations in Tables 13 and 18; and the resultant stresses due to shrinkage plus internal pressure are obtained by summation. In Fig. 18 the distribution of stresses in such a cylinder, before and after the application of an internal pressure, are shown graphically.

In a similar way the resultant strains are obtained by summation of the strains due to shrinkage and to the applied internal pressure.

TABLE 19. *Equations for Calculating the Initial Stresses in a Duplex Compound Cylinder*

	Inner tube			*Outer tube*		
Stress	D_0	D_1	D_2	D_2	D_3	D_4
P	$P_0 = 0$	$P_1 = \dfrac{P_2 D_2^2 (D_1^2 - D_0^2)}{D_1^2 (D_2^2 - D_0^2)}$	$P_2 = \dfrac{VE}{D_2\left\{\dfrac{D_4^2+D_2^2}{D_4^2-D_2^2} + \dfrac{D_2^2+D_0^2}{D_2^2-D_0^2}\right\}}$	P_2 as in previous column	$P_3 = \dfrac{P_2 D_2^2}{D_3^2}\dfrac{D_4^2-D_3^2}{D_4^2-D_2^2}$	$P_4 = 0$
T	$T_0 = -T_2 - P_2$	$-T_1 = \dfrac{P_2 D_2^2}{D_1^2}\dfrac{D_1^2+D_0^2}{D_2^2-D_0^2}$	$-T_2 = P_2 \dfrac{D_2^2+D_0^2}{D_2^2-D_0^2}$	$T_2' = \dfrac{P_2(D_4^2+D_2^2)}{D_4^2-D_2^2}$	$T_3 = \dfrac{P_2 D_2^2}{D_3^2}\dfrac{D_4^2+D_3^2}{D_4^2-D_2^2}$	$T_4 = T_2' - P_2$
S	$S_0 = -T_0 + P_0$	$S_1 = -T_1 + P_1$	$S_2 = -T_2 + P_2$	$S_2' = T_2' + P_2$	$S_3 = T_3 + P_3$	$S_4 = T_4$
	$= -T_0$	$= -\dfrac{2P_2 D_2^2 D_0^2}{D_1^2(D_2^2 - D_0^2)}$	$= -\dfrac{2P_2 D_0^2}{D_2^2 - D_0^2}$	$= \dfrac{2P_2 D_4^2}{D_4^2 - D_2^2}$	$= \dfrac{2P_2 D_4^2 D_2^2}{D_3^2(D_4^2 - D_2^2)}$	$= S_2' - 2P_2$
	$= -\dfrac{2P_2 D_2^2}{D_2^2 - D_0^2}$					

II. The Triplex Cylinder

In this case the resultant stresses due to the combined shrinkage are calculated on the assumption that the two inner tubes are first shrunk together, and that the outer cylinder is shrunk on to a simple cylinder of the same dimensions as the duplex cylinder. The stresses due to the two separate shrinkage operations are then summed algebraically. The distribution of the initial stresses and the resultant stresses due to shrinkage and to an internal pressure are shown graphically in Fig. 19.

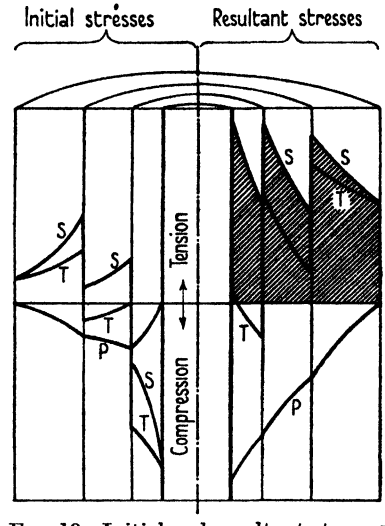

FIG. 19. Initial and resultant stresses in a compound cylinder (triplex).

Shrinkage. In the design of compound cylinders by shrinkage it can be shown that the most suitable arrangement is that in which the diameters are in geometric progression.

The actual shrinkage must be such that the initial and resultant stresses do not exceed the stresses at the elastic limit of the material, and due regard must be paid to the temperature to which the outer tube must be raised to give the necessary expansion for building the compound cylinder.

III. Wire- or Ribbon-wound Cylinders

In this method of construction initial compressive stresses are set up in a tube by winding it with steel wire or ribbon at high tension. The wire may be wound at constant tension or the tension may be varied in such a way that on the application of a predetermined bore pressure the stresses in the wire coils are uniform throughout.

The winding process sets up radial and hoop stresses in both the tube and wire, and the winding tensions, being at right angles to the radius, act as hoop tensions. It is assumed in the calculations given below that the winding acts as a homogeneous tube.

Let R_0, R_1, and R_2 = the internal and external radii of the tube and of the wire-winding respectively (Fig. 20),

P_0 and T_0 = initial stresses,

P_1 and T_1 = stresses due to an internal pressure P, and
T = winding tensile stress in the wire at a radius R.
The resultant stresses will be P_0+P_1 and T_0+T_1.

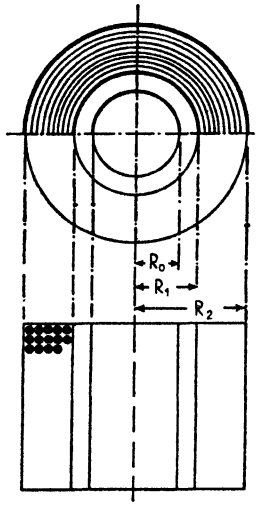

FIG. 20. Section through a wire-wound cylinder.

The general equation for equilibrium is given by (3.1), namely,

$$P_0+R\frac{dP_0}{dR}+T_0 = 0,$$

or
$$\frac{d(RP_0)}{dR}+T_0 = 0. \qquad (3.37)$$

At a radius R in the winding P_0 will represent the radial pressure due to all the layers of wire between R and the external radius R_2. These outer layers will reduce the hoop stress in the wire between R and R_1, and if the tube is assumed to be homogeneous between R_0 and R and under an external pressure P_0, the diminution of hoop tensile stress will be

$$P_0\frac{R^2+R_0^2}{R^2-R_0^2},$$

hence
$$T_0 = T-P_0\frac{R^2+R_0^2}{R^2-R_0^2}. \qquad (3.38)$$

This equation gives the hoop tensile stress due to winding at any radius R.

Method (1). *Stresses in the Wire to be constant on the Application of a given Internal Pressure.* If F is the elastic limit in simple tension of the material of which the tube is constructed, then by this method

$$P_0+T_0+P_1+T_1 \leqslant F.$$

From the equation to a simple cylinder (Table 13)

$$P_1+T_1 = \frac{2PR_0^2R_2^2}{R^2(R_2^2-R_0^2)},$$

and within the winding

$$P_1+T_1+P_0+T_0 = F;$$

hence
$$P_0+T_0 = F-\frac{2PR_0^2R_2^2}{R^2(R_2^2-R_0^2)}, \qquad (3.39)$$

and from (3.38)

$$P_0+T-\frac{P_0(R^2+R_0^2)}{R^2-R_0^2} = F-\frac{2PR_0^2R_2^2}{R^2(R_2^2-R_0^2)},$$

and
$$T = F-\frac{2PR_0^2R_2^2}{R^2(R_2^2-R_0^2)}+\frac{P_0(R^2+R_0^2)}{R^2-R_0^2}-P_0. \qquad (3.40)$$

From (3.37) and (3.39),

$$\frac{dP_0}{dR} = \frac{2PR_2^2}{R_2^2-R_0^2}\frac{R_0^2}{R^3} - \frac{F}{R},$$

and

$$P_0 = \frac{2PR_2^2}{R_2^2-R_0^2}\frac{R_0^2}{2R^2} - F\log_e R + A,$$

where A is a constant.

Now when $R = R_2$, $P_0 = 0$, and

$$A = -\frac{2PR_2^2}{R_2^2-R_0^2}\frac{R_0^2}{2R_2^2} + F\log_e R_2.$$

Therefore

$$P_0 = \frac{2PR_2^2}{R_2^2-R_0^2}\frac{R_0^2}{2}\left(\frac{1}{R^2} - \frac{1}{R_2^2}\right) + F\log_e \frac{R_2}{R}. \tag{3.41}$$

Let P_2 be the value of P_0 at the outer radius R_1 of the tube, then

$$P_2 = \frac{2PR_2^2}{R_2^2-R_0^2}\frac{R_0^2}{2}\left(\frac{1}{R_2^2} - \frac{1}{R_1^2}\right) + F\log_e \frac{R_2}{R_1}. \tag{3.42}$$

From (3.40), (3.41), and (3.42) the tension T in the wire at any radius can be calculated and also the stresses in the tube due to the winding. Thus at the bore of the tube ($R = R_0$) there will be a hoop stress due to the external pressure P_2 of magnitude

$$\frac{-2P_2R_1^2}{R_1^2-R_0^2}.$$

Also the equivalent simple stress at the bore due to the internal pressure P is

$$\frac{2PR_2^2}{R_2^2-R_0^2},$$

and the resultant equivalent simple stress is

$$\frac{2PR_2^2}{R_2^2-R_0^2} - \frac{2P_2R_1^2}{R_1^2-R_0^2}.$$

This stress has to equal F. That is,

$$P_2 = \frac{R_1^2-R_0^2}{2R_1^2}\left\{\frac{2PR_2^2}{R_2^2-R_0^2} - F\right\}.$$

Substituting this value in (3.42),

$$\log_e \frac{R_2}{R_1} = \frac{P}{F} - \frac{R_1^2-R_0^2}{2R_1^2}. \tag{3.43}$$

From (3.40) and (3.41), eliminating P_0,

$$T = F\left[1 + \frac{2R_0^2}{R^2-R_0^2}\log_e \frac{R_2}{R}\right] - \frac{2PR_0^2}{R^2-R_0^2}. \tag{3.44}$$

Putting $R = R_1$, $\quad T = F\left(1-\frac{R_0^2}{R_1^2}\right)$;

and $R = R_2$, $\quad T = F-\frac{2PR_0^2}{R_2^2-R_0^2}$.

Method (2). *Wire-winding at Constant Tension T.* From (3.38)

$$T_0 = T-P_0\frac{R^2+R_0^2}{R^2-R_0^2},$$

where T_0 and P_0 are the initial hoop and radial stresses in the winding at radius R. Also

$$P_0+R\frac{dP_0}{dR} = -T_0 = \frac{P_0(R^2+R_0^2)}{R^2-R_0^2}-T,$$

and

$$\frac{dP_0}{dR}+P_0\left\{\frac{-2R_0^2}{(R^2-R_0^2)R}\right\} = -\frac{T}{R}.$$

Multiply by the integration factor $R^2/(R^2-R_0^2)$.

Then

$$\frac{R^2P_0}{R^2-R_0^2} = -\tfrac{1}{2}T\log_e(R^2-R_0^2)+A,$$

where A is the integration constant.

When $R = R_2$, $P_0 = 0$ and

$$A = \tfrac{1}{2}T\log_e(R_2^2-R_0^2).$$

Substituting the value of A,

$$P_0 = \frac{(R^2-R_0^2)T}{2R^2}\log_e\frac{R_2^2-R_0^2}{R^2-R_0^2}, \tag{3.45}$$

and from (3.38)

$$T_0 = T\left[1-\frac{R^2+R_0^2}{2R^2}\log_e\frac{R_2^2-R_0^2}{R^2-R_0^2}\right]. \tag{3.46}$$

From (3.45) and (3.46) the initial stresses in the winding are calculated. These produce at the surface of the tube a pressure P_2 given by

$$P_2 = \frac{(R_1^2-R_0^2)T}{2R_1^2}\log_e\frac{R_2^2-R_0^2}{R_1^2-R_0^2}.$$

At the bore of the tube $P = 0$. The stresses in the tube due to winding and to an internal pressure can therefore be calculated from the equations in Table 13.

Equation (3.46) shows that the stress T due to winding alone decreases from the outside; the stress due to an internal pressure in the tube, on the other hand, increases in the direction of the bore so

that the resultant hoop stress in the winding is fairly constant. The initial and resultant stresses for compound cylinders constructed by this method are shown graphically in Fig. 21.

It will be evident that various combinations of wire-winding and shrinkage are possible in building up a compound cylinder. Thus a duplex or triplex tube may be wire-wound, and the wire winding may be protected by a steel jacket which may also be shrunk on so as to exert a compressive stress. In all cases the distributions of stresses are calculated by summing the separate stresses due to shrinkage and winding as determined by the methods already given.

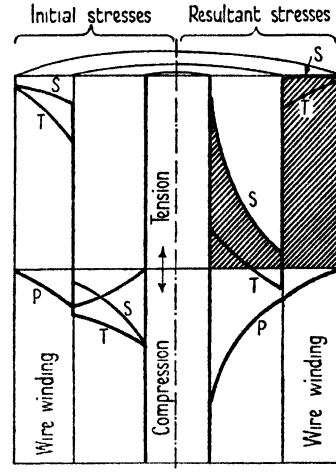

FIG. 21. Initial and resultant stresses in a wire-wound cylinder.

IV. Auto-frettaged Cylinders

In order to manufacture a cylinder by the auto-frettage process it is necessary to be able to calculate the pressure that must be applied in order to produce the desired

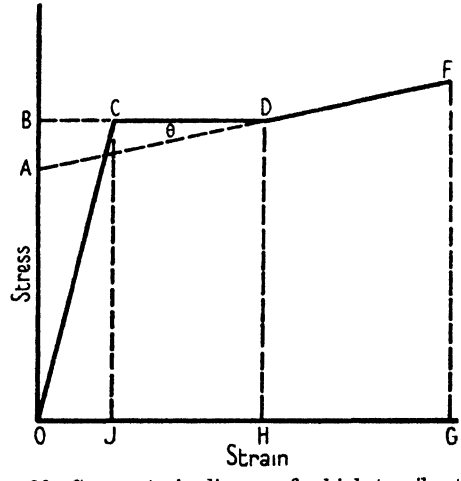

FIG. 22. Stress-strain diagram for high-tensile steel.

degree of overtension. This requires a knowledge of the stress-strain relationship of the particular steel used as given by a diagram such as that shown in Fig. 22.

The constants relating to this diagram for various classes of steel, as given by Macrae [3], are summarized in Table 20; it should be noted that for any particular class of steel they are, within limits, independent of the heat treatment.

TABLE 20. *Stress-Strain Relationships of Various Classes of Steels*

(For composition of steels see p. 10.)

Class	*Strain OH*	*Strain OG*	*Yield stress Y, tons/sq. in.*	$\frac{OA}{OB}$	*AB*
Mild steel	0·0082	0·025	12·75	0·8275	2·20
High carbon steel	0·0057	0·025	22·20	0·8636	3·00
Cast steel	0·0169	0·025	25·12	0·7253	6·90
Nickel steel	0·0083	0·025	31·80	0·9049	3·02
Nickel-chromium steel	0·0075	0·025	32·41	0·9285	2·32
Nickel-chromium-molybdenum steel	0·004	0·025	37·56	0·9702	1·12

Note: $AB = \left(1 - \frac{OA}{OB}\right) Y = Z$; OG = the strain at the end of the semi-plastic range.

It is also necessary to have available for each class of steel a compression chart such as that shown in Fig. 23 giving over-compression curves after different stages of overtension.

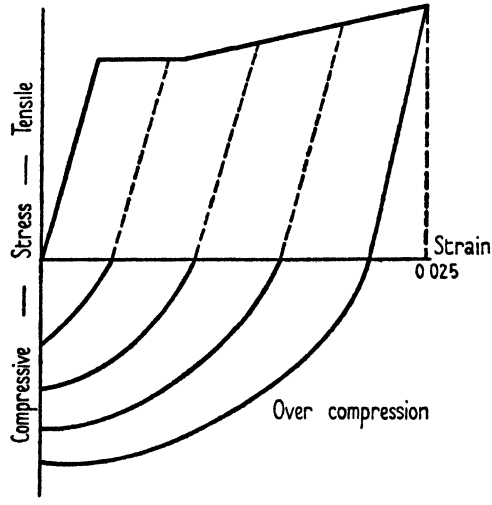

FIG. 23. Compression load-extension curves following overtension.

The Expansion of the Cylinder due to the Auto-frettage Pressure. The following treatment is due to A. E. Macrae (loc. cit.):

In Fig. 24 the radial pressures and equivalent simple stresses, in the walls of a cylinder overstressed so that the inner layers of the walls are in the semi-plastic zone and the outer layers in the elastic zone, are shown graphically. The equivalent simple stresses in the cylinder correspond with the stresses shown in the stress-strain diagram, Fig. 25, and the equivalent simple strains in the cylinder ($\delta D/D$) can be read off from the diagram.

The value of $\delta D/D$ at any diameter D, stressed elastically, is given by

$$\frac{\delta D}{D} = \frac{S}{E} = \frac{T+P}{E} = \frac{S_0 D_0^2}{E D^2}.$$

At D_0, the internal diameter,

$$\frac{\delta D_0}{D_0} = \frac{S_0}{E} = \frac{S_1 D_1^2}{E D_0^2},$$

and at D_3, the external diameter,

$$\frac{\delta D_3}{D_3} = \frac{S_3}{E} = \frac{S_0 D_0^2}{E D_3^2}.$$

The equivalent simple strains therefore vary inversely as the square of the diameters in a cylinder stressed to within the elastic limit and the same relation is found to apply to an overtensioned cylinder. It must be borne in mind that these are hypothetical strains which would be produced in a test-piece by the stress $S = T+P$ and are not strains actually present in the cylinder.

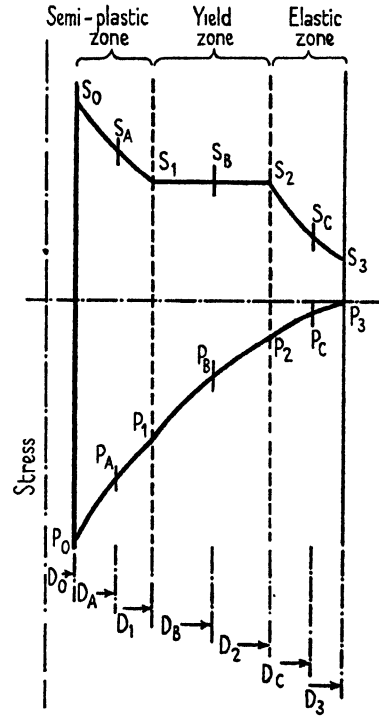

FIG. 24. Stresses due to auto-frettage pressure.

Now when a cylinder is overstressed it is found that on releasing the pressure, elastic unit expansions of magnitude $(T+\sigma P)/E$ are released and there remains a residual unit expansion $\delta d/d$. The unit expansion under pressure, at a diameter D, is therefore given by $\frac{\delta d}{d} + \frac{T+\sigma P}{E}$, where T and P are the hoop and radial stresses at D due to a bore pressure P_0, when the cylinder is considered to behave

elastically. But the strain dD/D in a test-piece subjected to an over-tensioning stress $T+P$ is equal to $\frac{\delta d}{d}+\frac{T+P}{E}$, and hence

$$\text{the unit expansion under pressure} = \frac{\delta D}{D} - \frac{(1-\sigma)P}{E}.$$

Expressing P in terms of the bore pressure P_0, the actual strain or unit expansion at any diameter D, when the bore pressure is acting, is given by

$$\frac{\delta D}{D} - \frac{(1-\sigma)}{E}\frac{P_0 D_0^2}{D^2} \times \frac{(D_3^2-D^2)}{(D_3^2-D_0^2)}, \tag{3.47}$$

and this quantity multiplied by D gives the expansion at the diameter D when the bore pressure is acting.

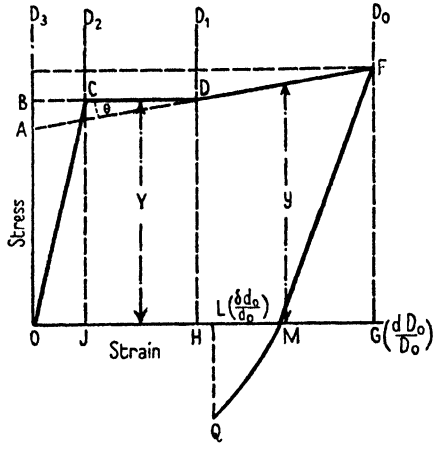

FIG. 25. Stress-strain diagram of bore layer on application and release of auto-frettage pressure.

At the bore diameter ($D = D_0$) the expansion of the bore under pressure P_0 is, from (3.47),

$$= D_0\left\{\frac{\delta D_0}{D_0} - \frac{(1-\sigma)P_0}{E}\right\} \tag{3.48}$$

and at the external surface ($D = D_3$) the expansion of the diameter is δD_3.

Referring to Fig. 24 the diameters D_1 and D_2 separate the yield zone from the semi-plastic zone on the one hand and the elastic zone on the other; and P_1 and P_2 are the radial pressures and S_1 and S_2 the equivalent simple stresses at these diameters, respectively.

The Elastic Zone. The stress-strain relationship in this zone is linear and at any diameter D,

$$\frac{S}{\delta D/D} = E$$

and corresponds with an internal pressure P_2 acting on the bore diameter D_2.

The Yield Zone. In this zone $S_2 = S_1 = Y$, and it is necessary to derive equations for determining the values of the boundary diameters D_1 and D_2.

The Semi-plastic Zone. Referring to Fig. 25, it is necessary to determine the relation between any stress y and the corresponding strain between diameters D_0 and D_1.

(i) It will be seen from Fig. 25 that the strain at diameter $D_2 = Y/E$. Therefore the strain at diameter $D_1 = OH = \frac{Y}{E}\frac{D_2^2}{D_1^2}$, and

$$\frac{D_2}{D_1} = \sqrt{\left(OH \times \frac{E}{Y}\right)}.$$

(ii) From Fig. 25, $$\frac{\text{Strain at } D_0}{\text{Strain at } D_1} = \frac{OG}{OH} = \frac{D_1^2}{D^2},$$

and $$\frac{D_1}{D_0} = \sqrt{\left(\frac{OG}{OH}\right)}.$$

(iii) It is found by experiment that for any particular class of steel both the angle θ (Fig. 25) and the strain OH are constant. The stress y at any point in the semi-plastic range may therefore be calculated from

$$y = Y + \frac{AB}{BD}\frac{\delta D}{D} - AB. \tag{3.49}$$

The constants for various classes of steel are given in Table 21.

TABLE 21. *Auto-frettage Constants for Various Steels (see Fig. 25)*

(For composition of steels see p. 10.)

Class of steel	*Strain OH*	*Strain OG*	$\sqrt{OH}$	$\sqrt{\left(\frac{OG}{OH}\right)} = \frac{D_1}{D_2}$	AB	$\tan\theta = \frac{AB}{OH}$	E
Mild steel . . .	0·0082	0·025	0·09055	1·746	2·20	268	13,000
High carbon steel .	0·0057	0·025	0·07551	2·094	3·00	526	13,000
Cast steel . . .	0·0169	0·025	0·1300	1·216	6·90	408	12,770
Nickel steel . .	0·0083	0·025	0·0911	1·736	3·02	364	12,600
Nickel-chromium steel	0·0075	0·025	0·0866	1·826	2·32	309	13,300
Nickel-chromium-molybdenum steel .	0·004	0·025	0·06325	2·500	1·12	280	13,100

From a knowledge of the above constants the stresses and strains due to the auto-frettage pressure in the three zones may be calculated.

In the elastic zone the equations given in Table 13 may be used; in the yield and semi-plastic zones it is necessary to derive the equations from the fundamental relation:

$$D\frac{dP}{dD} + P + T = 0.$$

In the 'yield' zone at any diameter D_B the following relations hold:

(i) $D_B\,d(P_B) + P_B\,d(D_B) + T_B\,d(D_B) = 0$,

(ii) $T_B + P_B = Y$,

and it can be shown that

$$d(P_B)+Y\frac{d(D_B)}{D_B}=0.$$

On integrating and substituting for the constant of integration,

$$P_1 = P_2+2{\cdot}3026Y\log_{10}\frac{D_2}{D_1}, \tag{3.50}$$

and since $P_2 = \frac{1}{2}Y\left(1-\frac{D_2^2}{D_3^2}\right)$,

$$P_1 = Y\left(2{\cdot}3026\log_{10}\frac{D_2}{D_1}-\frac{D_2^2}{2D_3^2}+0{\cdot}5\right), \tag{3.51}$$

and at any diameter D_B,

$$P_B = Y\left(2{\cdot}3026\log_{10}\frac{D_2}{D_B}-\frac{D_2^2}{2D_3^2}+0{\cdot}5\right). \tag{3.52}$$

In the 'semi-plastic' zone

(i) $D_A\,d(P_A)+P_A\,d(D_A)+T_A\,d(D_A)=0$,

(ii) $T_A+P_A=y_A$,

(iii) $y_A = Y+\frac{AB}{BD}\frac{\delta D_A}{D_A}-AB$,

(iv) $\frac{\delta D_A}{D_A}=\frac{k}{D_A^2}$,

and (v) $k = D_1\delta D_1 = D_0\delta D_0$.

From these equations together with (3.49) it can be shown that

$$d(P_A)+Y\frac{d(D_A)}{D_A}+\frac{AB}{BD}\frac{k\,d(D_A)}{D_A^3}-AB\frac{d(D_A)}{D_A}=0.$$

On integrating and simplifying,

$$P_0 = P_1+2{\cdot}3026(Y-AB)\log_{10}\frac{D_1}{D_0}-0{\cdot}5(y_1-y_0). \tag{3.53}$$

At diameter D_1, $y_1 = Y$; also $y_0 = S_0$; on substituting these values and simplifying,

$$P_0 = 2{\cdot}3026\left(Y\log_{10}\frac{D_2}{D_0}-AB\log_{10}\frac{D_1}{D_0}\right)-Y\frac{D_2^2}{2D_3^2}+0{\cdot}5\left\{Y+AB\left(\frac{D_1^2}{D_0^2}-1\right)\right\} \tag{3.54}$$

and $$P_A = 2{\cdot}3026\left(Y\log_{10}\frac{D_2}{D_A}-AB\log_{10}\frac{D_1}{D_A}\right)-Y\frac{D_2^2}{2D_3^2}+$$
$$+0{\cdot}5\left\{Y+AB\left(\frac{D_1^2}{D_A^2}-1\right)\right\}. \tag{3.55}$$

On removal of the auto-frettage pressure the return to no-load is elastic and subsequently compressive stresses are set up as shown in Fig. 25. The magnitude of these stresses may be determined from a set of curves similar to those in Fig. 23 provided the strains set up by the auto-frettage pressure and the permanent set on releasing the pressure are known.

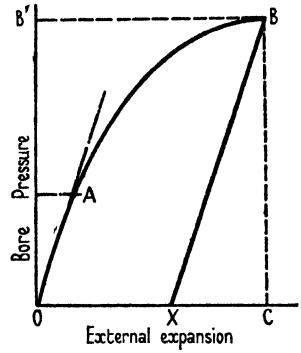

Fig. 26. External expansion of cylinder subjected to internal pressure.

The first step is to construct a curve showing the relation between the bore pressure and the exterior expansion of the cylinder, the expansion being directly measured or calculated by the method already indicated. In Fig. 26 OA represents the elastic expansion and AB the overtension of the cylinder up to the auto-frettage pressure OB'. By drawing BX parallel to OA the residual expansion of the exterior, OX, is obtained. Thus, for example, referring to Fig. 24, S_3 can be calculated from the equation

$$S_3 = \frac{2P_2D_2^2}{D_3^2 - D_2^2},$$

and the exterior expansion δD_3 is then given by

$$\delta D_3 = \frac{S_3}{E} D_3.$$

On releasing the auto-frettage pressure the residual strains are:

$\frac{\delta d_3}{d_3}$ at the exterior diameter D_3,

$\frac{\delta d}{d}$ at any diameter D,

and $\frac{\delta d_0}{d_0}$ at the bore D_0.

Since
$$\frac{\delta d_3}{d_3} = \frac{\delta d}{d}\frac{D^2}{D_3^2} = \frac{\delta d_0}{d_0}\frac{D_0^2}{D_3^2},$$

the residual expansion at any diameter can be calculated provided the corresponding value at the bore or the external diameter is known. Both these latter quantities can be obtained by direct measurement.

Referring to Fig. 25:

(i) At the bore, $OL = \dfrac{\delta d_0}{d_0}$, (ii) At any diameter D_A,

$MG = \dfrac{S_0}{E}$, $OG = \dfrac{\delta D_A}{D_A}$,

$OG = \dfrac{\delta D_0}{D_0}$, $OL = \dfrac{\delta d_A}{d_A}$,

and $OM = \dfrac{\delta D_0}{D_0} - \dfrac{S_0}{E}$. and $OM = \dfrac{\delta D_A}{D_A} - \dfrac{S_A}{E}$.

Finally, to determine the residual compressive stress QL (Fig. 25), the value of OM enables the compressive stress-strain curve MQ to be identified with the corresponding curve in Fig. 23 for the class of steel used; and the intersection of the ordinate LQ, where $OL = \delta d_0/d_0$, with the curve gives the compressive stress in the bore layer.

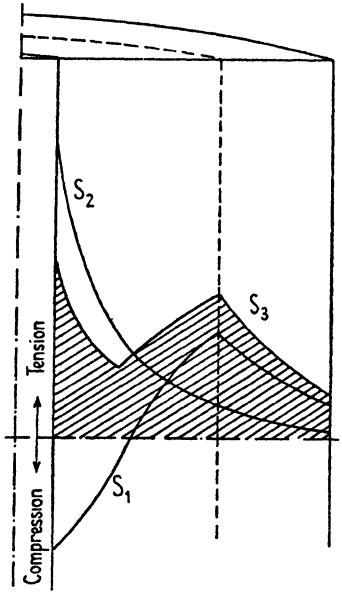

FIG. 27. Initial and resultant equivalent simple stresses in an auto-frettaged cylinder.

In a similar way the compressive stress at any intermediate diameter can be determined.

The formulae for the stresses and strains set up on the first application and release of the auto-frettage pressure are summarized in Table 22.

As an example of the distribution of stresses in the walls of an auto-frettaged cylinder before and on the application of an internal pressure the three curves S_1, S_2, and S_3 in Fig. 27 give the equivalent simple stresses, (i) initially (S_1), (ii) due to an internal pressure of 28·7 tons per sq. inch alone (S_2), and (iii) the resultant of S_1 and S_2 (S_3), for a cylinder of nickel-chromium-molybdenum steel, 1·25 inches internal and 6 inches external diameter. It will be seen that the result of auto-frettage is to give a fairly even distribution of stresses in the walls resembling that obtained with a duplex cylinder (cf. Fig. 18).

TABLE 22. *Formulae for Calculating the Stresses and Strains set up on the Application and Release of an Auto-frettage Pressure P_0*

Stresses in the elastic zone	*Stresses in the yield zone*	*Stresses in the semi-plastic zone*
$P_3 = 0$	$P_1 = Y\left(2{\cdot}3026\log_{10}\frac{D_2}{D_1} - \frac{D_2^2}{2D_3^2} + 0{\cdot}5\right)$	$P_0 = 2{\cdot}3026\left(Y\log_{10}\frac{D_2}{D_0} - AB\log_{10}\frac{D_1}{D_0}\right) - Y\frac{D_2^2}{2D_3^2} + 0{\cdot}5\left\{Y + AB\left(\frac{D_1^2}{D_0^2} - 1\right)\right\}$
$P_C = \frac{S_C}{2}\left(1 - \frac{D_0^2}{D_3^2}\right) = \frac{S_C - S_3}{2}$	$P_B = Y\left(2{\cdot}3026\log_{10}\frac{D_2}{D_B} - \frac{D_2^2}{2D_3^2} + 0{\cdot}5\right)$	$P_A = 2{\cdot}3026\left(Y\log_{10}\frac{D_2}{D_A} - AB\log_{10}\frac{D_1}{D_A}\right) - Y\frac{D_2^2}{2D_3^2} + 0{\cdot}5\left\{Y + AB\left(\frac{D_1^2}{D_A^2} - 1\right)\right\}$
$P_2 = \frac{S_2}{2}\left(1 - \frac{D_2^2}{D_3^2}\right)$		
$S_3 = S_2 - 2P_2 = \frac{2P_2D_2^2}{D_3^2 - D_2^2}$	$\left.\begin{matrix} S_1 \\ S_B \\ S_2 \end{matrix}\right\} = Y$	$S_0 = Y - \frac{AB}{BD}\frac{dD_0}{D_0} - AB$ $S_A = Y + \frac{AB}{BD}\frac{dD_A}{D_A} - AB$
$S_2 = 2P_2\left(\frac{D_3^2}{D_3^2 - D_2^2}\right)$		
$S_C = \frac{S_2D_2^2}{D_C^2}$		

Expansions under auto-frettage pressure P_0	*Residual expansion on release of auto-frettage pressure*
At D_3; $\delta D_3 = \frac{S_3D_3}{E}$	At D_3; $\delta d_3 = \frac{s_3 \times D_3}{E}$
At D; $\delta D = \left\{\frac{\delta D}{D} - \frac{(1-\sigma)}{E}\frac{P_0D_0^2}{D^2}\left(\frac{D_3^2 - D^2}{D_3^2 - D_0^2}\right)\right\}D$	At D; $\delta d = \left(\frac{s_3}{E} \times \frac{D_3^2}{D^2}\right)D$
At D_0; $\delta D_0 = \left\{\frac{\delta D_0}{D_0} - \frac{(1-\sigma)P_0}{E}\right\}D_0$	At D_0; $\frac{\delta d_3}{\delta d_0} = \frac{D_0}{D_3}$, $\frac{\delta d_2}{\delta d_3} = \frac{D_3}{D_2}$, etc. $\frac{\delta d_3}{d_3}\Big/\frac{\delta d_0}{d_0} = \frac{D_0^2}{D_3^2}$, etc.

The Heat Treatment of the Auto-frettaged Cylinder. Experiments carried out with test-pieces have shown that overtension lowers the tensile elastic limit of steel and reduces the compressive elastic limit practically to zero; a subsequent low-temperature treatment, however, restores and in some instances improves the elastic properties. Thus steel overtensioned in the 'yield' range and subjected to a low-temperature treatment while under 'no-load' or lowered tensile load will have a new tensile elastic limit equal to, at least, the value of the overtensioning stress; the new compressive elastic limit, however, decreases as the tensile limit increases.

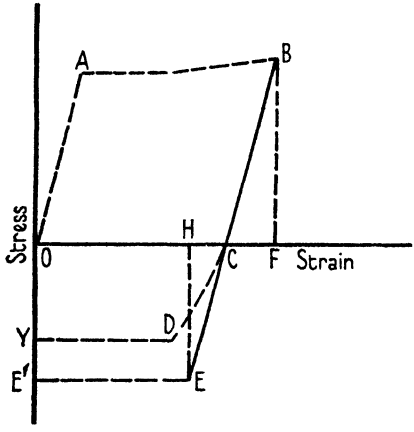

FIG. 28. Combined overtension and overcompression on application and release of auto-frettage pressure.

Repeated 'overtensions' and 'combined overtensions and overcompressions', followed in each case by suitable low-temperature treatments, will produce progressively increased tensile and reduced compressive elastic limits.

It has also been found that in the case of high-tensile steels, provided the compression at the bore after the first auto-frettage does not exceed 15·0 tons per sq. inch, one low-temperature treatment ensures that the cylinder is elastic for a bore pressure equal to the auto-frettage pressure. This is shown by the diagram in Fig. 28; *OABCD* is the stress-strain relationship for the combined overtension and overcompression at the bore layers. After one low-temperature heat treatment the cylinder is elastic up to the original compressive elastic limit *E* and a reapplication of pressure up to the original auto-frettage pressure will stress the bore layers elastically along the line *ECB*, *HF* being the new strain range.

If the residual compressive stress in the bore layer of a high-tensile steel cylinder exceeds 15·0 tons per sq. inch, one low-temperature treatment does not restore the tensile elastic properties but produces a new compressive elastic limit for a range of stresses equal to *OE'* (Fig. 29). Reapplication and release of the auto-frettage pressure will set up a second cycle of combined overtension and

overcompression as indicated by the line *EKLN*, and a second low-temperature treatment will set up new tensile and compressive elastic limits. On a third application of the auto-frettage pressure the bore layers will behave elastically, the stress-strain relationship being given by the line *MLK*.

The optimum temperatures for the low-temperature treatments of the various classes of steel are given on p. 10. In the case of thick-walled cylinders the rate of heating must be uniform and slow (several hours) and the temperature once reached must be maintained for from 1 to 2 hours.

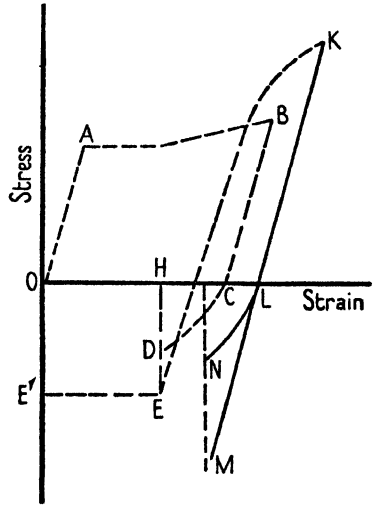

FIG. 29. Combined overtension and overcompression after two auto-frettage treatments.

A Comparison of the Various Types of Construction

In the design of compound cylinders the underlying principle in all cases is the utilization of the compressive as well as the tensile strength of the metal in such a manner that, on the application of an internal pressure, there will result a more even distribution of stresses in the walls than would be obtained with a simple cylinder; for a given internal pressure, therefore, it is possible to effect a considerable saving in weight by using a compound cylinder.

The choice of the particular type of construction for the compound cylinder depends largely upon the size of plant and the purpose for which it is to be used. Thus, for example, the very accurate machining required in preparing the individual tubes for shrinking sets a limit to the size of cylinder that can economically be constructed by this method. Wire-winding, on the other hand, can be applied to vessels of any size and affords a ready and simple means of regulating the stress distribution throughout the walls. Generally speaking, however, the auto-frettage process is best adapted to the construction of cylinders of moderate size for carrying out chemical reactions at high pressures and temperatures, particularly in cases where the

working conditions involve fluctuations in temperature giving rise to momentary large temperature gradients in the walls.

The Temperature Factor in the Design of High-pressure Vessels

It has been shown in Chapter I that the apparent strength of steel at high temperatures depends upon the time it is under stress and varies from a maximum value, approximately equal to the ultimate strength—given by the normal rate of loading, for short periods, to a minimum value approximately equal to the limiting 'creep' stress, for long periods. The limiting creep-stress curve may be considered as being the true ultimate-strength curve where high temperatures of long duration are concerned, and in such cases a suitable factor of safety must be employed in design to ensure that the working stresses are not too far removed from the limiting creep stress at the working temperature.

It must also be borne in mind that the limiting creep stress gives rise to a certain amount of initial creep and permanent deformation, although for most purposes these effects are so small as to be negligible.

Stresses due to a Temperature Gradient in the Cylinder Walls

Comparatively large temperature gradients may be set up in the walls of pressure vessels as the result of applied heat or heat liberated by exothermic reactions proceeding within the vessel; and since their effect is to set up stresses which, in conjunction with those due to the working pressure, may be of sufficient magnitude to cause elastic failure, it is necessary in certain circumstances to make adequate provision for their possible occurrence.

The evaluation of such stresses is based upon the assumption that the rate of flow of heat is constant so that the temperature t at any radius R within the walls is given by the equation

$$t = \frac{t_0 \log_e(R/R_1) + t_1 \log_e(R_0/R)}{\log_e(R_0/R_1)}, \tag{3.56}$$

where t_0 and t_1 are the temperatures at the internal and external radii, R_0 and R_1, respectively.

If α is the coefficient of linear expansion of the metal, the expansion strains at the radius R are αt in all directions, and if x is the radial displacement of a point originally at a distance R from the axis of

the cylinder due to stresses in the walls and to temperature expansion the total strains will be: radial $= dx/dR$, circumferential $= x/R$, and longitudinal $= L$.

The difference between the total strains and the expansion strains give the strains due to the temperature stresses. If P_T, T_T, and Q_T are the radial, circumferential, and longitudinal temperature stresses, then

$$\frac{dx}{dR}-\alpha t = \frac{1}{E}\{P_T-\sigma(T_T+Q_T)\},$$

$$\frac{x}{R}-\alpha t = \frac{1}{E}\{T_T-\sigma(P_T+Q_T)\}, \tag{3.57}$$

and

$$L-\alpha t = \frac{1}{E}\{Q_T-\sigma(P_T+T_T)\}.$$

Combining these equations with the fundamental equation

$$P-T+R\frac{dP}{dR} = 0,$$

the following values for the temperature stresses at any radius R are obtained:

$$P_T = \frac{E}{2(1-\sigma)}\left\{\frac{t_1 R_1^2-t_0 R_0^2+(R_0^2 R_1^2/R^2)(t_0-t_1)}{R_1^2-R_0^2}-t\right\}, \tag{3.58}$$

$$T_T = \frac{E}{2(1-\sigma)}\left\{\frac{t_1 R_1^2-t_0 R_0^2-(R_0^2 R_1^2/R^2)(t_0-t_1)}{R_1^2-R_0^2}-\frac{t_0-t_1}{\log_e(R_0/R_1)}-t\right\}, \tag{3.59}$$

$$Q_T = \frac{E\alpha}{(1-\sigma)}\left\{\frac{t_1 R_1^2-t_0 R_0^2}{R_1^2-R_0^2}-\frac{t_0-t_1}{2\log_e(R_0/R_1)}-t\right\}. \tag{3.60}$$

The magnitude of these stresses for even moderate temperature gradients is quite considerable. Thus, for example, for a cylinder of internal diameter 1·25 inches and external diameter 6 inches, the stresses set up by a temperature gradient of 235° C, due on the one hand to internal and on the other to external heating, are as given in Table 23. The distribution of stresses in the cylinder walls are shown by means of the curves in Fig. 30.

Attention may be drawn to the following important features of these results:

1. A temperature gradient due to internal heating sets up compressive stresses in the inner layers of the cylinder walls which reduce the tensile stresses due to an internal pressure. The cylinder therefore

TABLE 23. *Stresses due to a Temperature Gradient in a Cylinder*

Reference diameters	Internal heating				External heating			
	Temp., °C.	Tons per sq. in.			Temp., °C.	Tons per sq. in.		
		P	T	Q		P	T	Q
1·25	250·0	0	−44·4	−44·4	15·0	0	44·4	44·4
3·0	118·8	−9·35	− 0·95	− 9·27	146·2	9·35	0·96	10·47
4·0	75·72	−6·18	7·07	0·92	189·2	6·18	− 7·07	− 0·91
5·0	42·33	−2·95	11·94	9·60	222·7	2·94	−11·94	− 9·62
6·0	15·0	0	16·69	16·70	250·0	0	−16·69	−16·70

Coefficient of linear expansion of metal — 0·000013.

becomes stronger provided always that its mechanical properties do not suffer appreciably by reason of the increased temperature.

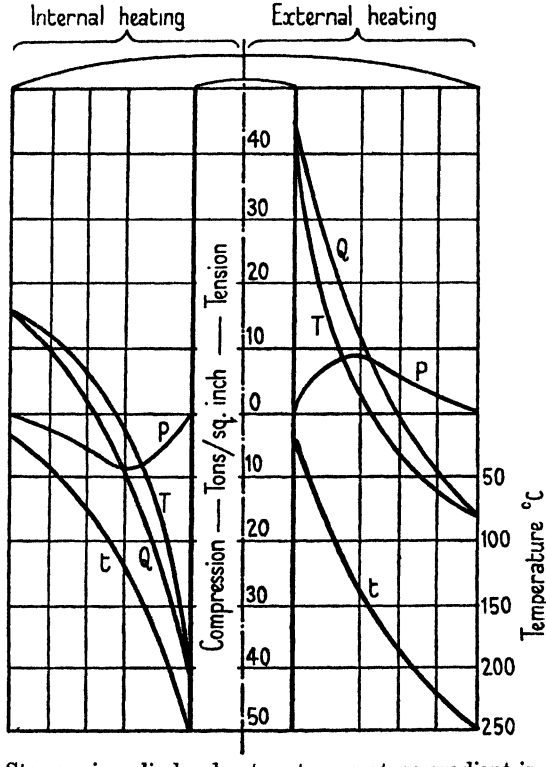

FIG. 30. Stresses in cylinder due to a temperature gradient in the walls.

2. A temperature gradient due to external heating sets up tensile stresses in the inner layers and compressive stresses in the outer layers of the cylinder walls; it therefore tends to weaken the cylinder.

It is interesting to note, however, that provided a sufficiently high gradient could be produced it would be possible to overtension the inner layers of the cylinder and thus produce the same combination of residual stresses as are obtained by auto-frettage.

3. The longitudinal temperature stresses vary with distance from the axis of the cylinder.

4. There are zones in the cylinder wall at which the longitudinal and circumferential temperature stresses are zero. The radial temperature stress is zero at the inner and outer walls of the cylinder and passes through a maximum in the zone in which the circumferential stress is zero.

BIBLIOGRAPHY

1. CASE, *Strength of Materials*. Edward Arnold & Co., 1925.
2. COOK and ROBERTSON, *Engineering*, 15 Dec. 1911, p. 787.
3. MACRAE, *Overstrain of Metals*. H.M. Stationery Office, 1930.

IV

THE DESIGN OF PLANT

APART from gauges, compressors, gas cylinders, and capillary copper and steel tubing there is very little standard pressure equipment that can be purchased ready-made, and it is usually necessary specially to design reaction vessels, pumps, valves, and the like for the specific purpose required and to have them made by skilled and reliable mechanics. For their successful operation it is essential to observe certain fundamental principles in the design, to select the appropriate materials for the construction of the various parts, and to ensure that both the material and the workmanship are of the highest quality. It is proposed, therefore, to illustrate by a few typical examples the various types of vessels and auxiliary parts used in small-scale and semi-scale experimental work, directing attention to certain details which experience has shown are of importance in connexion with their construction and maintenance.

The Obturation of Pressure Joints

Joints are almost invariably made along a circular ring of contact between two metal parts held together by some suitable coupling device such as a clamp or a set of bolts or studs. It has been estimated that in order to bring two metal surfaces into the intimate contact necessary to ensure a pressure-tight joint a proximity of about 10^{-6} inch is required; this figure cannot be approached by ordinary machining methods, or even by grinding, and it is therefore necessary to force the two surfaces together until local overstraining occurs in the area of contact and the plastic flow of the metal causes the surfaces to mate together. One of the fundamental principles in the design of a pressure joint is that there should be a high intensity of contact pressure produced by a relatively small coupling force.

The problem of calculating the stresses set up when two bodies are pressed together has been worked out by Hertz [1] and an approximate solution has been given by Andrews [2]. For our purpose we shall adopt a simple criterion of a successful joint suggested by W. R. D. Manning [3], namely, that 'it will continue to hold satisfactorily as long as the pressure between the jointing faces remains greater than the pressure to be resisted', we may

calculate quite simply the minimum force (F) necessary to retain tightness.

Let d be the internal diameter of the ring of contact and y its mean width; then, by definition,

$$F = P \times (\text{area of the ring of contact})$$

$$= P \times \tfrac{1}{4}\pi(d+2y)^2,$$

where P is the internal pressure.

For a plain steel to steel joint it is usually found that a force greater than that calculated from this equation has to be employed to obtain the initial plastic flow at the contact surfaces, and hence both d and y should be kept as small as possible. The minimum diameter of the ring of contact is fixed by the dimensions of the joint, and although the criterion we have adopted places no restriction on the width y, practical considerations enable a minimum value to be fixed without difficulty.

There are many types of metal to metal joints all of which, if properly designed, are capable of withstanding pressures up to about 1,000 atmospheres, but not much higher; a number of them are shown in section in Fig. 31. Fig. 31 (*a*) is a joint which has been successfully used on a semi-scale Bergius converter, $7\frac{7}{8}$ inches in internal diameter, working at a pressure of 200 atmospheres; (*b*) has been used to make a joint between a screwed plug, $1\frac{1}{2}$ inches in diameter, and a bomb for withstanding gaseous explosions at initial pressures of 200 atmospheres, and (*c*) has been used in connexion with a copper-lined catalyst tube, 3 inches in internal diameter, for the synthesis of methanol from water-gas. In constructing these joints it is important to ensure that all tool marks are removed from the seatings and during use both surfaces must be kept scrupulously clean.

Another method by which intimate contact between two steel surfaces may be obtained without unduly increasing the coupling force is to interpose a washer made of some softer metal such as copper, bronze, aluminium, or mild steel. A typical example is the joint *à escalier* described by Amagat [4] and shown in section in Fig. 32. It will be noted that the design is such as to afford adequate sideways support to the washer and thus to prevent lateral flow. This joint is frequently used in autoclaves, hydraulic cylinders, and

other containers, and for pressures up to several hundred atmospheres it is both convenient and effective.

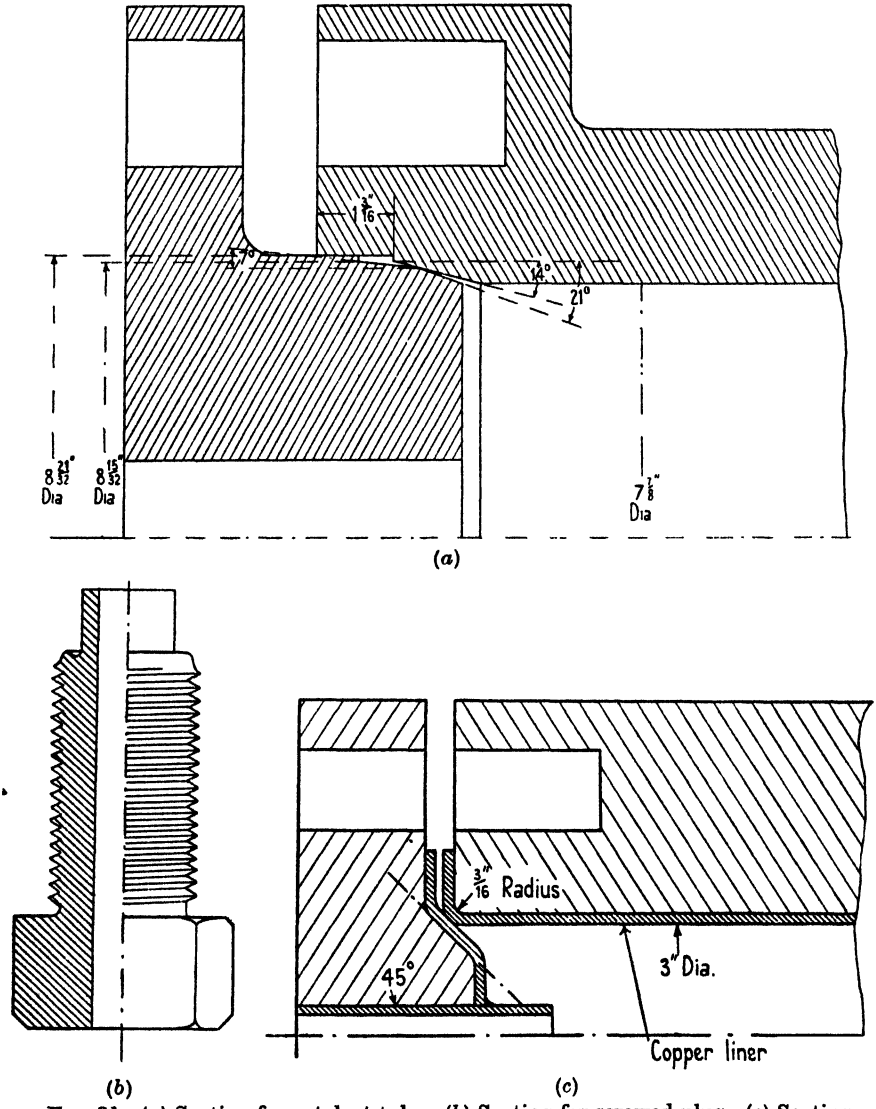

FIG. 31. (*a*) Seating for catalyst tube. (*b*) Seating for screwed plug. (*c*) Seating for lined tube.

In the joints so far described the necessary pressure is applied by means of studs or bolts which have to withstand not only the axial tensile stresses due to the internal pressure but also the initial

stresses due to tightening. The resultant load may be anything between the sum of these two stresses as a maximum and the greater of the two as a minimum. For vessels of large diameter (two feet or more) designed for pressures of several hundred atmospheres, it is not possible to accommodate sufficient bolts or studs to take the load on any reasonable pitch circle and hence these joints cannot be used.

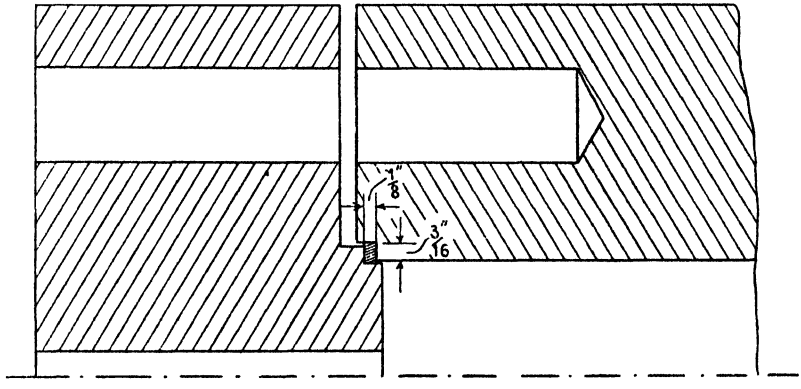

FIG. 32. Amagat's joint.

Self-tightening Joints

In this type of joint the maximum coupling force is that required to give the initial plastic flow at the area of contact, the contact pressure automatically increasing with increase of the internal pressure. The principle employed is that of incorporating in the joint a partially unsupported ring of metal, the shape and section of which is such that it makes complete circles of contact with the two members to be joined. On applying an internal pressure the ring tends to expand elastically and to be forced into more intimate contact with the seatings; and since the internal pressure is acting on a much larger area than the balancing external pressure, the contact pressure will always be greater than the internal pressure.

Self-tightening joints, in one form or another, are used in nearly all apparatus working at pressures of upwards of 1,000 atmospheres, in large-scale plant for pressures of upwards of about 300 atmospheres, and for a variety of other purposes which will be indicated later. Fig. 33 is known as a lens-ring joint and is perhaps the simplest self-tightening joint to construct and the most convenient for small-scale plant. It consists of a lens-shaped ring, usually made of

hardened nickel steel, seating between two conical surfaces, the joint being so designed that the ring receives no lateral (radial) support. The radius of curvature of the lenticular surfaces should be proportional to the internal radius of the ring, the best ratio for the two radii in the case of a high carbon steel ring and a seating angle of 30° being about 2 : 1. The example illustrated was used to obturate a screwed plug, $1\frac{1}{2}$ inches in diameter, in a cylindrical vessel designed to withstand 5,000 atmospheres internal pressure.

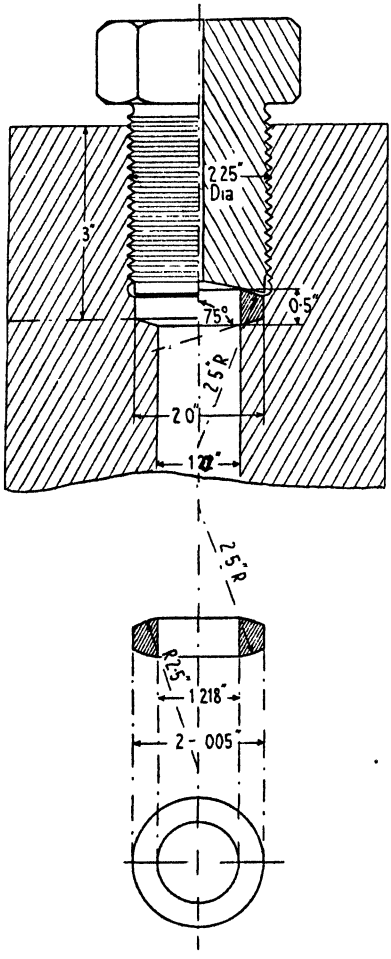

FIG. 33. Lens-ring joint.

For lens-ring joints of large diameter (several feet or more) greater elasticity is given to the ring by making the internal surface concave, as shown in Fig. 35.

In the lens-ring joint there is an axial component of the contact force, the magnitude of which depends upon the angle of the conical seating. By making the seatings parallel with the axis of the joint, as in Fig. 34, the axial component is eliminated, the pressure on the seatings acts in a purely radial direction, and the self-tightening property becomes fully effective. The ring used with this seating (known as a wave ring) has two crests which are slightly greater in diameter than the sockets forming the seatings, so that the initial contact pressure round the joint is made by driving the ring into the sockets [3]; the construction calls for high-grade work and accurate finishing, the degree of interference ranging from 1 in 2,000 to 1 in 10,000.

An enlarged section of a wave-ring joint is shown in Fig. 34. In calculating the dimensions of the joint an empirical relationship is

used; it has been found from experience that for rings of diameter between $1\frac{1}{2}$ inches and 6 inches diameter, if Y is the tensile yield stress of the metal, P the internal pressure (in the same units), and d the bore of the ring, then overstrain of the joint will occur if the greatest thickness of the ring y' is less than $Pd/6Y$. In practice,

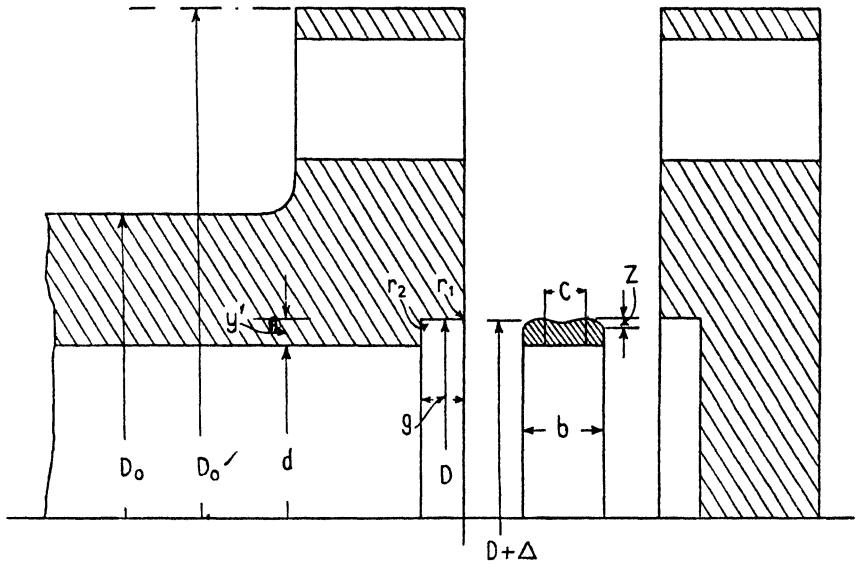

Dimension	*Recommended size*
b	3 to $5y'$
g	$1{\cdot}01 \times b/2$
C	$0{\cdot}6 \times b$
Z	$\frac{1}{10}$ to $\frac{1}{5} \times b$
Δ	$0{\cdot}0002$ to $0{\cdot}0005 \times d$
r_1	$\frac{1}{10}$ to $\frac{1}{5} \times y'$
r_2	$\frac{1}{3}$ to $\frac{1}{4} \times y'$

$$D_0'/D = D_0/d$$

FIG. 34. Wave-ring joint.

therefore, y', which is also the depth of the socket, is chosen to lie between $Pd/2Y$ and $Pd/5Y$. For pressures below about 30 atmospheres this relation leads to a ring that is too thin for practical use and in such cases it may be stiffened up as desired. Having determined the value of y', the remaining dimensions of the joint may be taken from the table below Fig. 34. It should be noted that the thickness of wall at the joint must be sufficient to ensure that the elastic expansion of the sockets shall be less than that of the ring.

In order to avoid damaging the surfaces of the wave ring when

making the joint the sockets should be provided with a 'lead' or radius at the mouth (r_1) and the ring should be coated with a suitable lubricant or 'flashed' with copper. The force to be held by the coupling, which may be of any of the usual forms, is given by $P \times (d+2y')^2$. An important advantage of the wave-ring joint is that an appreciable amount of yield at the coupling may take place without a leak developing.

Coupling Devices

In making joints of large diameter to withstand pressures of several hundred atmospheres the coupling devices are liable to become very heavy and costly, and it has already been pointed out that flanged joints connected by bolts or studs are impracticable for diameters of several feet and pressures of 300 atmospheres or more. The alternative is to employ some form of clamp so designed that the hoop stresses necessary to give the required contact pressure are kept small.

The Vickers-Anderson Coupling [5]. In this coupling, one form of which is shown in section in Fig. 35, the two parts are held together by means of a clamp which usually consists of three segments bolted together, and the joint is obturated by means of a plain washer or a lens ring. The contact pressure is obtained by machining a shoulder, with an external conical face, on each of the two parts of the joint, and clamping them together with the three-segmented ring which is recessed with corresponding conical surfaces. The angle of the cones should be less than the angle of friction of the metal.

When an ordinary or a hollow lens ring such as is shown in the figure is employed, the joint becomes self-tightening; and since the bolts closing the clamp are required only to give the initial contact pressure and not to take any effective load, a considerable reduction in the weight of the coupling may be effected. This joint has been used successfully for converters, 5 feet in internal diameter, used in the hydrogenation of coal at a pressure of 250 atmospheres.

Bridgman's Joint

Bridgman makes use of the self-tightening principle in rather a different way to the lens-ring type of joint. Thus, for example, to obturate a small moving piston he employs a piston head and packing of the form in Fig. 36 (*a*). The head *A* made of hardened steel is an easy fit in the cylinder and is turned down on the inner side to

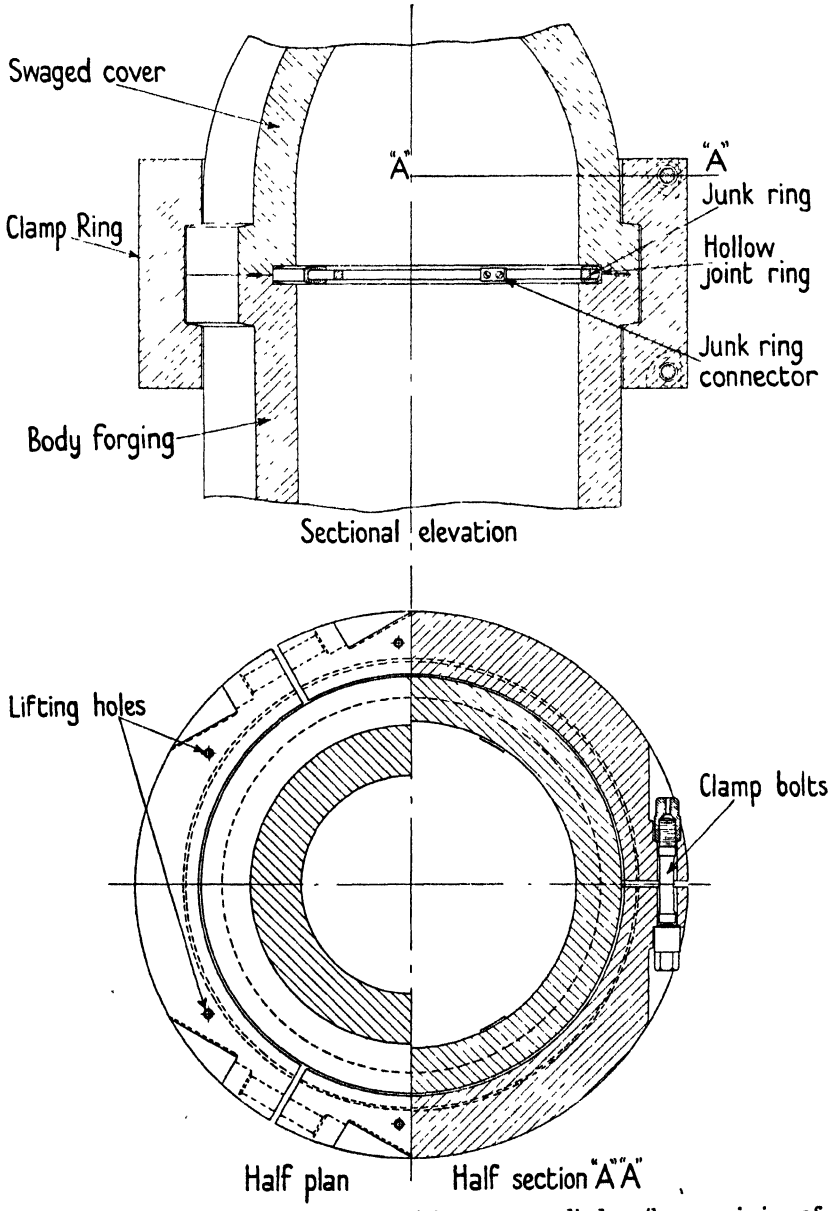

FIG. 35. Vickers-Anderson joint for high-pressure cylinders (by permission of Imperial Chemical Industries, Ltd.).

accommodate a $\frac{1}{16}$ inch thick copper washer B, a soft rubber packing washer C, $\frac{1}{8}$ inch thick, and a second copper washer D. The washers are held in position and compressed by a hardened steel ring E which rests on the piston. The pressure acting over the full area of the head A is transmitted to the smaller area of the rubber washer which thereby becomes self-tightening. This device is satisfactory at pressures up to about 10,000 atmospheres, but at higher pressures the rubber washer tends to 'pinch off' the steel stem of the head and frequent replacements are necessary.

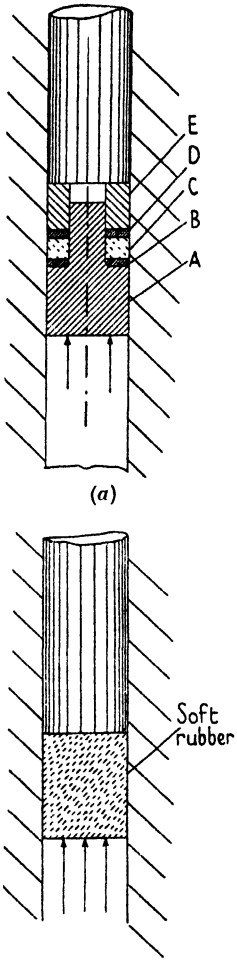

FIG. 36. (a) Bridgman packing. (b) Poulter packing.

A much simpler device has been adopted by Poulter, who employs a soft rubber bung, as shown in Fig. 36 (*b*), to obturate the piston. Provided a good quality rubber, containing only a small amount of filler, is used this joint is satisfactory up to pressures of 20,000 atmospheres. It cannot, however, be used at high temperatures and it is usually necessary to renew the packing for each experiment.

Screw Threads

In designing bolts and nuts, connectors, and screwed plugs of various kinds for use at high pressure the theory underlying the design of screw threads should be borne in mind.

The greatest load on a screwed plug or bolt is generally in the direction of its axis, and is supported by the reaction between the surface of the thread on the plug or bolt and that in contact with it on the nut. If R (Fig. 37) is the reaction at a point A on the surface of the thread on a bolt (i.e. the normal pressure between the bolt and nut at that point), it may be resolved into two forces, the one, L, parallel to the axis of the bolt and representing that portion of the load carried by the surface of the thread at A, and the other, M, acting at right angles to the axis and tending to burst the nut. For a given load both R and M will increase with the angle θ of the

thread; and since the friction between two surfaces is proportional to the normal pressure between them, it will also increase with θ.

If we consider a square thread with the load acting at right angles to the surface, the reaction R will be very nearly equal to the load and the friction will be a minimum. There will be no radial component and therefore no bursting action on the nut. Since, however,

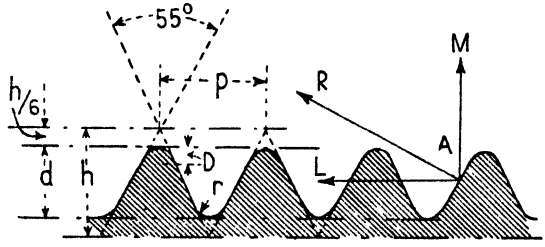

Dimensions of Whitworth thread

$d = \frac{2}{3}h$
p = pitch
h = angular depth = 0·960495p
$h/6$ = shortening
r = radius at apex = 0·137329p
D = depth of rounding = 0·073917p

FIG. 37. Standard Whitworth thread.

the shearing action of the load has to be supported by the material at the root of the thread a V-shaped thread will be almost double as strong as a square thread of the same core diameter. A buttress thread combines the advantages of both V and square threads, provided the load acts on the perpendicular face of the thread, and it may with advantage be employed for screw-rams and other mechanisms in which it is desirable to reduce the friction to a minimum. An example of its application may be seen in Fig. 45.

It is both customary and convenient to employ standard threads whenever possible; for plugs and fittings up to about 1 inch diameter, for example, a British Standard Pipe Thread can be recommended, whilst for larger diameters a somewhat coarser thread of the Whitworth type is preferable. Thus, for a plug of, say, 2 inches diameter a Whitworth thread of 6 T.P.I. would be easier to keep clean and less liable to seize than a Standard Pipe Thread having 11 T.P.I.

In calculating the holding strength of a screwed plug we may take the safe strength as being one-half the shear strength of the material if solid, or we may base the calculation on the area at the core diameter provided the length of thread is not less than the diameter of the plug. The manner in which a screw thread fails under stress depends upon the properties of the metal from which it is cut; for hard brittle material failure is by shear near the root of the thread; for ductile material the thread fails as a cantilever. In bolts and studs there is a tendency for stress concentration to occur at the end

of the thread and it is good practice to clear away the metal at this point to the core diameter.

The hexagon heads of screwed plugs, bolts, and nuts should be made of standard size and standard spanners should be used for tightening. In calculating the stresses due to the load an additional

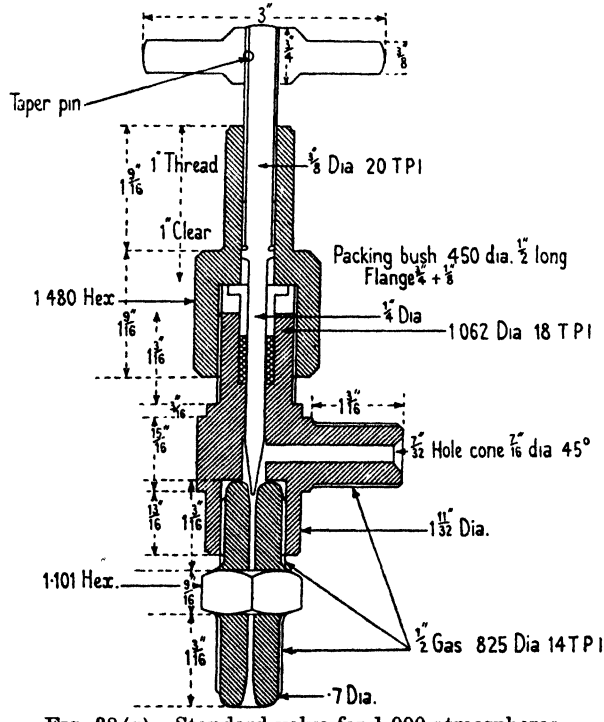

FIG. 38 (*a*). Standard valve for 1,000 atmospheres.

50 per cent. may then be added for tightening up in the case of diameters up to 1½ inches and 25 per cent. for larger diameters.

Screw threads are particularly liable to seize under conditions in which creep takes place, that is, when subjected to a combination of high stress and high temperature. This tendency may be reduced by using ground threads, by making the two parts of different quality steel and by using a suitable lubricant. A small hole drilled in the nut will enable paraffin to be forced into the threads should a seizure occur.

Valves. The valves used on commercial gas cylinders are incapable of fine adjustment and are in other respects unsuitable for incorporation in high-pressure systems. The chief requirements of

a high-pressure valve for general purposes are ease of operation and fine adjustment, but the following points in design are of importance in connexion with their construction and maintenance: (1) the design should be such as to utilize, as far as possible, standard sections of bar or rod; (2) the seatings should be readily accessible for cleaning and remaking; (3) the holding threads on the spindle should be well clear of the packing and should, preferably, be above it; (4) the packing should be accessible for renewal; and (5) the spindle end should be provided with a guide. Fine adjustment is best obtained by using a fine thread on the spindle and by allowing an appropriate angle between the spindle end and the conical seating.

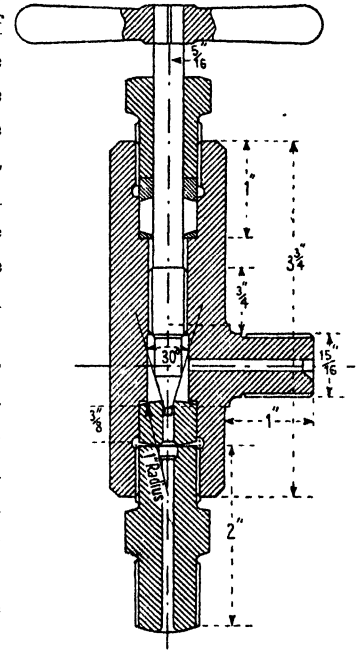

FIG. 38 (*b*). Valve with lens-ring seating.

Two designs of valve suitable for work up to 1,000 atmospheres and conforming to most of the above requirements are illustrated in Fig. 38 (*a*) and (*b*). The constructional details and dimensions are indicated on the drawings. It will be seen that valve (*b*) utilizes a lens ring for the dual purpose of making the seating and of obturating the connecting plug at the base. A suitable valve packing material for most purposes is asbestos string softened with a mixture of grease and graphite; leather washers cut to size and softened in tallow may also be used.

It may be noted in passing that considerable difficulty is experienced in obtaining any form of packing which will remain tight against a hydrostatic pressure of mercury. Amagat alludes to the difficulty in the following words [4]: 'Il ne faut pas, du reste, perdre de vue que tel joint qui tient parfaitement l'eau, l'huile ou la glycérine sous de très fortes pressions laisse passer le mercure sous des pressions bien moins considérables'; and other workers have confirmed this observation. To overcome this difficulty it is usually possible to introduce into the system an oil-mercury liquid piston

device similar to that described on p. 101, so that the packing material comes in contact with oil only.

When a valve has to be maintained fully open for long periods heavy demands are made on the packing and leaks are likely to

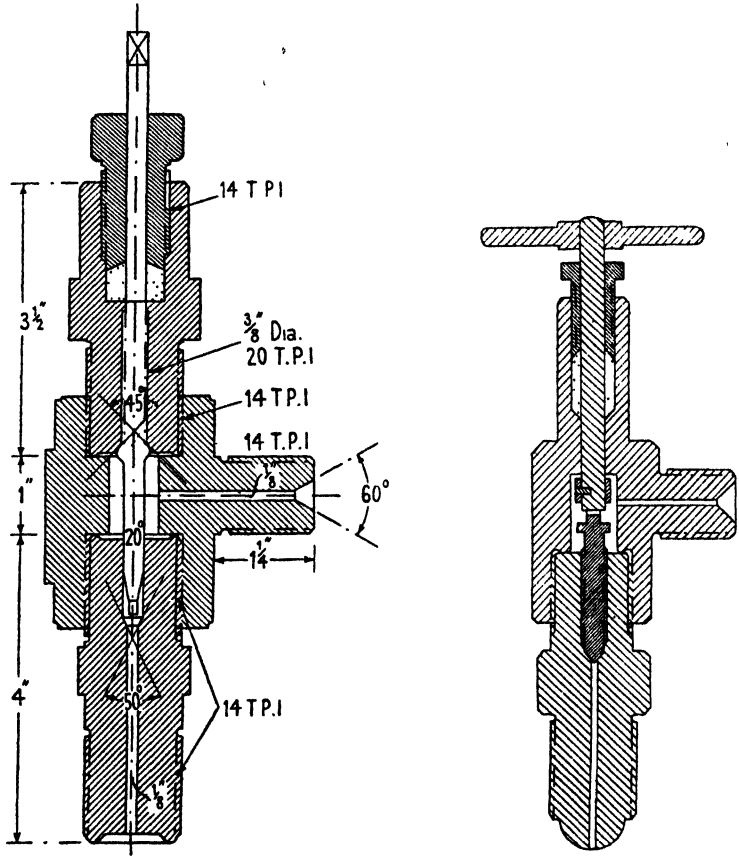

(*c*) (*d*)

FIG. 38. (*c*) Double-seating valve. (*d*) Valve with removable head.

develop. In such circumstances it is advisable to employ the type shown in Fig. 38 (*c*); this valve is provided with a double seat which allows the packing to be completely isolated from the fluid.

Another type of valve which has certain special applications is shown in Fig. 38 (*d*). The design is such that when the valve is closed, the upper part of the spindle together with the packing gland and nut can be removed. It is particularly useful in cases where the weight of a pressure vessel has to be reduced to a minimum or where

it is required to maintain a very accurate temperature control by completely immersing the vessel in a thermostat.

Pipe-lines and Fittings

Pipe-lines of small diameter are usually made of cold-drawn, seamless, copper, mild steel, or high-tensile steel tubing which is supplied by the makers in lengths up to about 15 feet. The safe wall-thickness of such tubing may be calculated by the method described in Chapter III, but for most purposes it is sufficient, in the case of copper or steel, to make the ratio of wall-thickness to bore equal to 0·5 for pressures up to 300 atmospheres and 1·0 for pressures between 300 and 1,000 atmospheres.

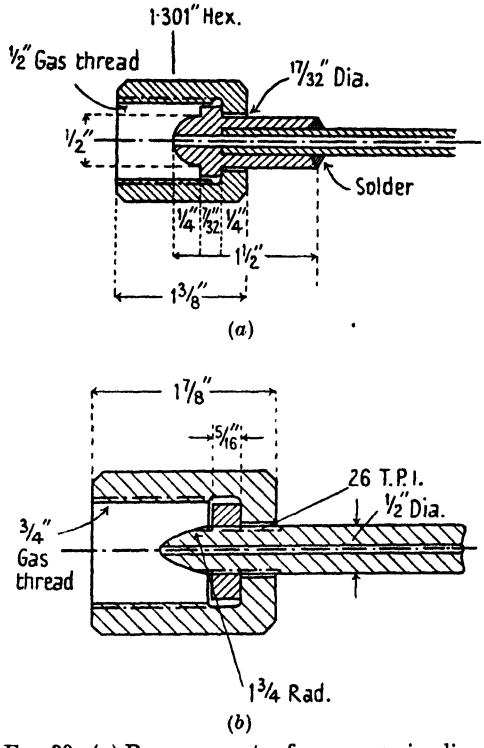

FIG. 39. (*a*) Brass connector for copper pipe-line. (*b*) Steel connector.

The design of couplings and connexions depends upon the material of the tubing and on the working pressure. For copper capillary tubing which is quite flexible, a convenient form of connexion is that shown in Fig. 39 (*a*); the tube is soft-soldered or brazed into a brass nipple, and the joint is made on a conical seating by tightening the union nut. For steel tubing which is stiff and difficult to bend by hand, a similar type of connexion may be used, but it is advisable to cut the tube to length and to screw on the nipple, using a fine thread (e.g. 26 T.P.I. for a ⅜ inch external diameter tube), and silver-solder it in position.

Soldered joints cannot safely be used at pressures above about 1,000 atmospheres and should be replaced by the type of fitting shown in Fig. 39 (*b*). The tubing is accurately cut to length and

conical seatings are turned on the ends; it is then bent to shape and the joint made by a screwed collar and union nut.

A great deal of inconvenience will be avoided if all pipe-line fittings are standardized, using, say, $\frac{1}{2}$ inch or 1 inch British Standard Pipe Threads and the correct size hexagon nuts.

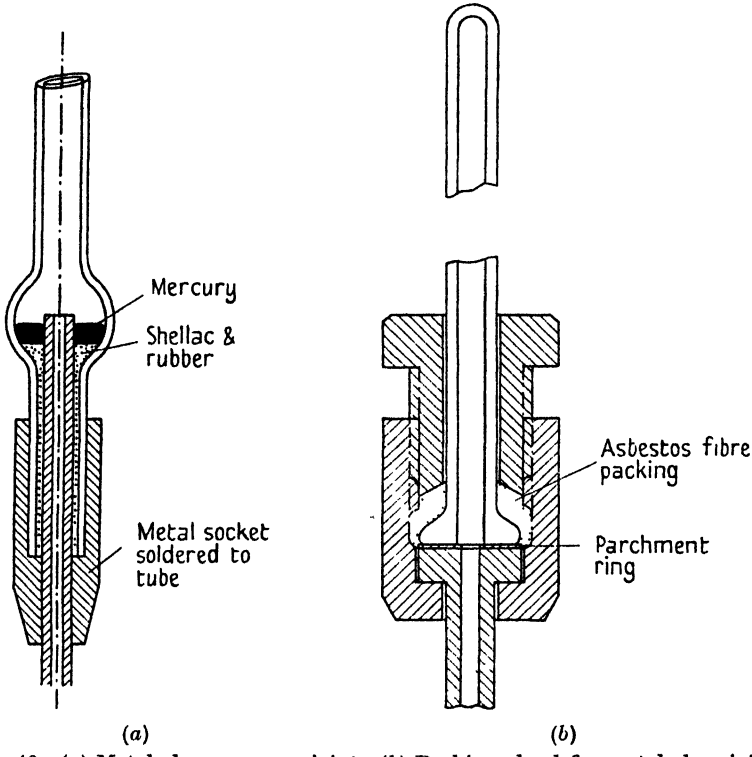

FIG. 40. (*a*) Metal-glass pressure joint. (*b*) Packing gland for metal-glass joint.

The Use of Glass and Transparent Quartz

Glass and quartz, if properly annealed and suitably supported, are capable of withstanding much higher stresses than is generally supposed. Thus Onnes and Braak [6] report experiments with capillary glass tubing in which internal pressures of 1,000 atmospheres were sometimes reached, and much higher pressures have been successfully withstood by flat glass windows.

Onnes and Braak, employing ordinary Thuringen glass, carefully annealed and connected to the metal part of the pressure apparatus by the fitting shown in Fig. 40 (*a*), carried out a series of measure-

ments on the bursting pressures of tubes of varying bore and wall-thickness, the results of which are summarized in Table 24.

TABLE 24. *Bursting Pressures of Glass Tubes*

Series	*No.*	*External diameter (D), mm.*	*Internal diameter (d), mm.*	*Ratio D/d*	*Bursting pressure, atmospheres*
a	1	9·3	3·5	2·66	340
	3	8·7	4·2	2·07	230
	5	9·2	3·0	3·07	380
	7	10·4	4·0	2·60	240
	9	17·6	5·0	3·52	290
b	11	6·8	1·00	6·80	420
	13	6·5	0·35	18·57	500
	17	5·8	0·46	12·61	1,200
	21	6·6	1·00	6·60	660
	23	6·4	1·35	4·74	520
c	25	3·8	2·42	1·57	283
	26	6·4	4·78	1·34	221
	28	7·4	5·11	1·45	179

The successful use of glass tubes at high pressures depends largely on the care taken in making the pressure joint and on the absence of strains in the glass. An alternative form of joint which permits of a certain degree of flexibility is shown in Fig. 40 (*b*) which is self-explanatory.

One of the earliest recorded uses of a glass window at high pressures is contained in a paper by Amagat published in 1893 [7]. The window which consisted of a cylinder 1 cm. in diameter and 2 cm. thick was housed in a steel plug and fixed by means of marine glue. A better method of making the joint is shown in Fig. 41 (*a*). The window, in the form of a truncated cone 1 inch thick and 1 inch in diameter with a taper of $\frac{1}{16}$ inch per inch, is ground into a steel plug with fine emery and is held in position by means of a collar. Pressure acting on the larger end of the window forces it into closer contact with the seating and ensures a gas-tight joint. This type of fitting is suitable for pressures up to about 500 atmospheres.

T. C. Poulter has developed a simple and elegant method of obturating a flat window against pressures of upwards of 10,000 atmospheres [8]. The window, which must be of good quality optical glass with accurately ground flat parallel faces, is mounted in contact with a hardened steel ring which must also have optically ground faces. No packing material of any sort is employed, but during

assembly the window may be held in place by a small quantity of liquid balsam.

A typical mounting for a window 11 mm. in diameter with an aperture of 6 mm. is shown in Fig. 41 (*b*). It will be seen that a hydraulic pressure acts on one face and on the sides of the window.

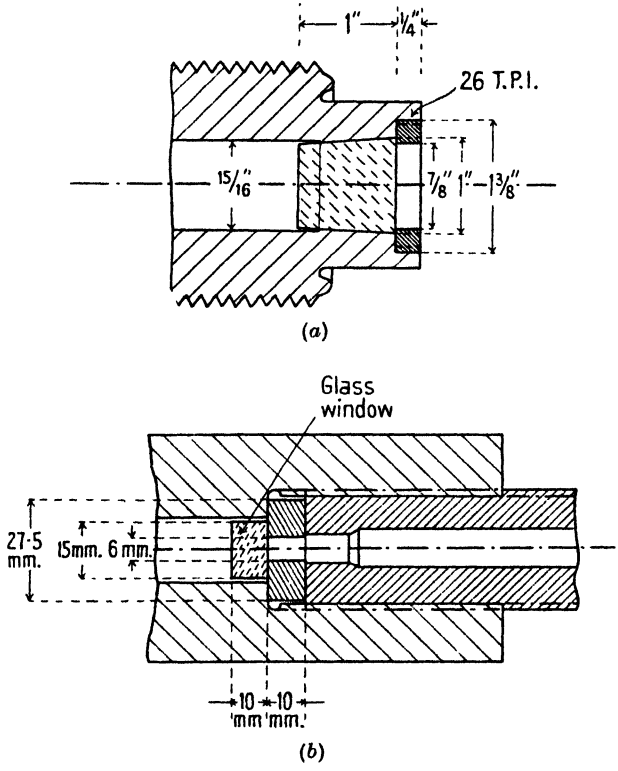

FIG. 41. (*a*) Conical window fitting. (*b*) Flat window fitting.

When a window mounted in this fashion begins to fail, the first sign is the flaking of a thin layer of glass from the unsupported area at the aperture of the steel leaving a rough surface. Poulter finds that a glass window will withstand very much higher pressures if oil or glycerine is used to transmit the pressure than if water, alcohol, or ether is the transmitting medium. Windows surrounded by the latter liquids will frequently break on lowering the pressure even though they have previously withstood much greater pressures. It appears as though the liquids actually penetrate into the glass and subsequently expand on release of pressure.

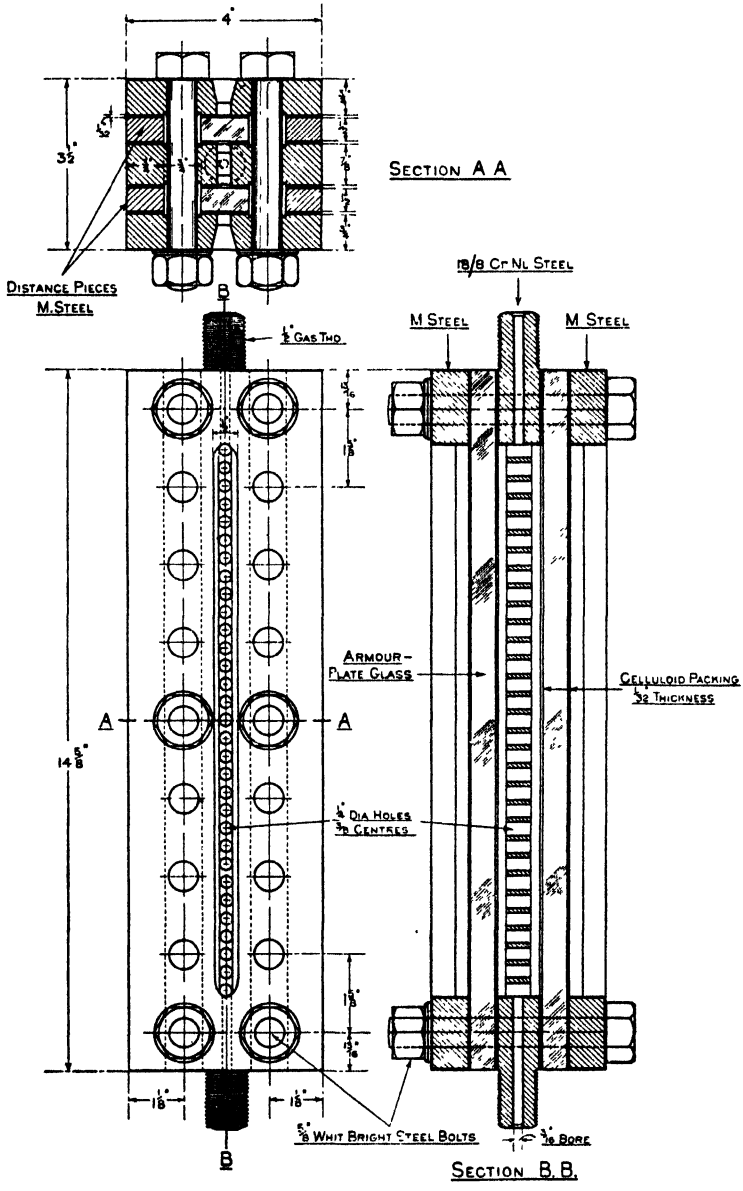

Fig. 41 (c). High-pressure sight gauge.

Liquid-level Indicators

No entirely satisfactory means of accurately measuring small changes in liquid level in high-pressure systems has yet been evolved, but methods based upon the change in electrical resistance of a wire, the movement of a balanced U-tube, and direct visual observation are practicable if not very convenient.

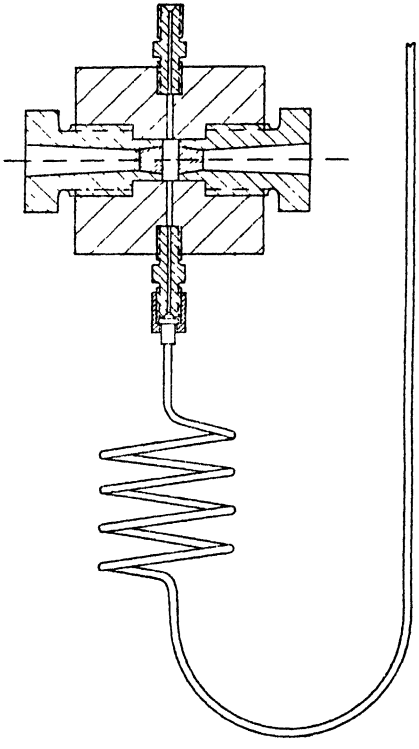

Fig. 41 (*d*). Liquid-level indicator.

The ordinary standard gauge glass, if properly mounted, will withstand pressures of the order of 150 atmospheres, but with continuous use the tube undergoes fatigue and eventually fractures. An improved design in which the tube is replaced by two flat strips of glass, $\frac{3}{8}$ inch to $\frac{1}{2}$ inch thick, held by steel straps, has been described by Newitt and Sen [9] and by Barber, Taylor, King, and Fraser Shaw of the Fuel Research Station [10]. In this method considerable care is necessary to prevent unbalanced stresses being set up in the glass during assembly. Armour-plate glass is employed and the glass and metal surface on which it rests must be true to within 2/1000 inch. In the Fuel Research Station model, shown in section in Fig. 41 (*c*) a celluloid packing is inserted between the glass and metal and distance pieces and ties are used to take up the bending load. When all precautions are taken pressures up to about 300 atmospheres may be successfully withstood.

For higher pressures the design shown in Fig. 41 (*d*) has proved quite serviceable. The windows are conical in shape, have an aperture of 1 inch diameter, and are mounted in steel plugs which screw into the body of the indicator. Connexion with the pressure system is made through a copper capillary tube bent into the

form of a coil of suitable radius. The liquid surface is kept within the aperture of the window by raising or lowering the indicator which is mounted on a vertical column. One important advantage of this arrangement is that the windows may readily be removed for cleaning.

Insulated Connexions

Fig. 42 (*a*) shows in section a screwed plug fitted with a central insulated steel rod, of the type usually employed in high-pressure

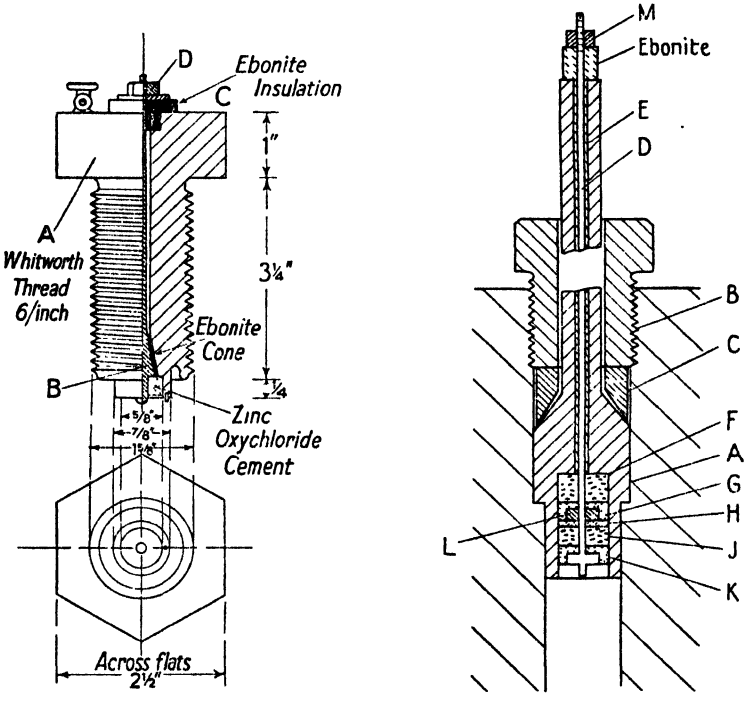

(*a*) (*b*)

FIG. 42. (*a*) Insulated plug. (*b*) Insulated plug (Bridgman).

work. The insulator consists of a hollow cone made of ebonite, ivory, or porcelain, which fits closely into the plug and is held in position by the steel rod *B*. Ebonite insulators, 2–3 mm. thick, are turned to shape on a lathe and a pressure-tight joint is made by assembling the plug, heating to about 100° C., and drawing the cone into intimate contact with its housing by tightening the nut *D* on the end of the steel rod. Porcelain insulators are usually made not more

than 1 mm. thick and must be carefully ground so that they make accurate surface contact with the plug and central steel rod. The angle of the cone in both cases should be about 6°. Ebonite insulators may be used up to pressures of about 1,000 atmospheres at room temperatures, and porcelain up to 3,000 atmospheres, or even higher.

For pressures beyond 3,000 atmospheres, however, the conical type of insulation has not proved entirely satisfactory, and Bridgman has developed a design of insulated plug based upon the self-tightening principle which is both easier to construct and more reliable in operation [11].

Fig. 42 (*b*) shows, in section, a Bridgman plug, as modified by Adams [12]. The outer body of the plug *A* is made of nickel-chromium steel, hardened in oil; it is obturated by means of the screwed plug *B* and the conical washer *C*, the latter being made of soft steel and cut to an angle slightly more acute than that of the conical surface of the body. The central steel rod *D* has its upper end insulated by a thin glass tube *E* and its lower end by a 6-mm. thick ring of limestone *F*, 3 mm. of talc *G*, a 1-mm. thick soft rubber washer *H*, a second ring of limestone *J*, and finally a 3-mm. thick layer of talc *K*. A hardened steel disk *L* prevents the rubber blowing out past the limestone.

The insulating properties of the plug are improved if all parts are dipped in paraffin, heated to about 130°, and are then assembled before the paraffin has solidified. The initial tightness of the packing is effected by 'pulling up' on the nut *M*. In using this plug care must be taken on releasing the pressure to ensure that the rod *D* is not subjected to over-tension by the friction of the washers.

Compressors and Hydraulic Pumps

As compressors are in the nature of standard equipment it is not proposed to consider their design in detail. There are, however, one or two points in their construction to which attention may be drawn.

Multi-stage compressors are so designed that the total work of compression is equally divided between the stages. In calculating the work in the higher stages it is necessary to employ an accurate equation of state for the gas and to know the variation of its specific heats both with temperature and pressure. As gases differ considerably among themselves in respect of their pressure-volume-tempera-

ture relationships it is evident that the efficiency of the compressor will vary with the particular gas undergoing compression.

Compressors should be fitted with a gas filter on the inlet side and an efficient oil-separator on the outlet side. The packing gland should be situated on the pressure side to ensure that any leak will be outwards, and each stage should be provided with an efficient safety valve. All valves should be mounted in separate screwed plugs so that they can be removed for cleaning and repair without dismantling the cylinder.

The methods of calculating the work required for compression and the pressure and temperature distributions in multi-stage compressors are described in Chapter XV.

Oxygen should on no account be compressed in oil-lubricated compressors.

Hand-operated hydraulic pumps are capable of giving a pressure of 1,500 atmospheres, or if provided with an auxiliary screw plunger, a pressure of 5,000 atmospheres. In the pump shown in section in Fig. 43 (*a*) the piston P is $\frac{7}{8}$ inch in diameter and is obturated by S.E.A. packing rings. During the suction stroke oil enters the cylinder from a reservoir, through the inlet valve V and during the compression stroke it is forced through the outlet valve O to the chamber D. The pressure in D is stepped up to the final pressure by screwing in the $\frac{1}{2}$-inch diameter plunger R. The screw consists of a 1-inch standard Whitworth thread and is operated by a wheel. The back pressure is taken up by the two thrust bearings B, B.

When required to compress gas the pump should be used in conjunction with a liquid-piston device, one form of which is illustrated in Fig. 43 (*b*), whereby direct contact between the oil and gas is obviated. The liquid-piston consists of a column of mercury contained in a steel U-tube AB. One limb of the tube A is connected by way of the valve V_1 with the pressure side of the hydraulic pump and through the valve V_2 with the oil reservoir of the pump. The other limb is connected through the valve V_3 with a gas storage cylinder and through V_4 with the apparatus into which it is desired to compress the gas. The permissible upper limit for the level of mercury in either limb is indicated by contacts made through the insulated leads L_1 and L_2. In using the apparatus gas from the storage cylinder at a pressure of several hundred atmospheres is admitted through the valve V_3 to the limb B, oil being run out at the

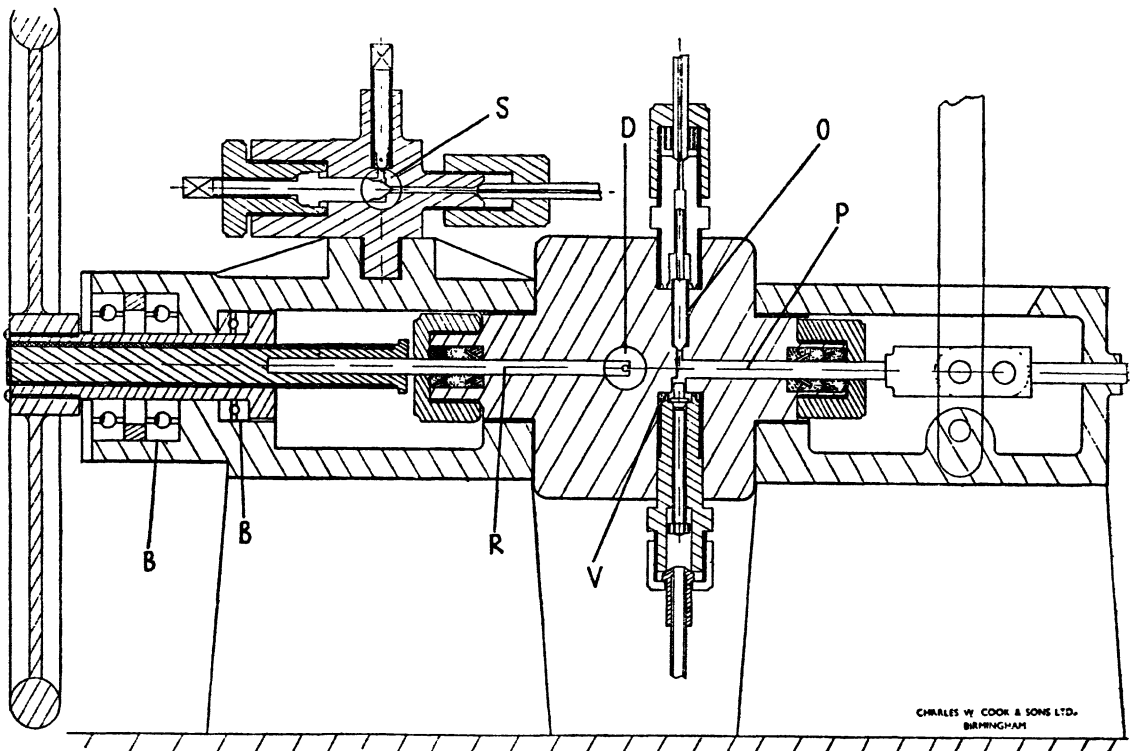

FIG. 43 (*a*). Hand-operated hydraulic pump with screw plunger.

valve V_2 until the mercury level in A reaches the contact L_1. V_3 and V_2 are then closed and oil is pumped in through V_1 until the gas in B has been compressed to the desired pressure or until mercury

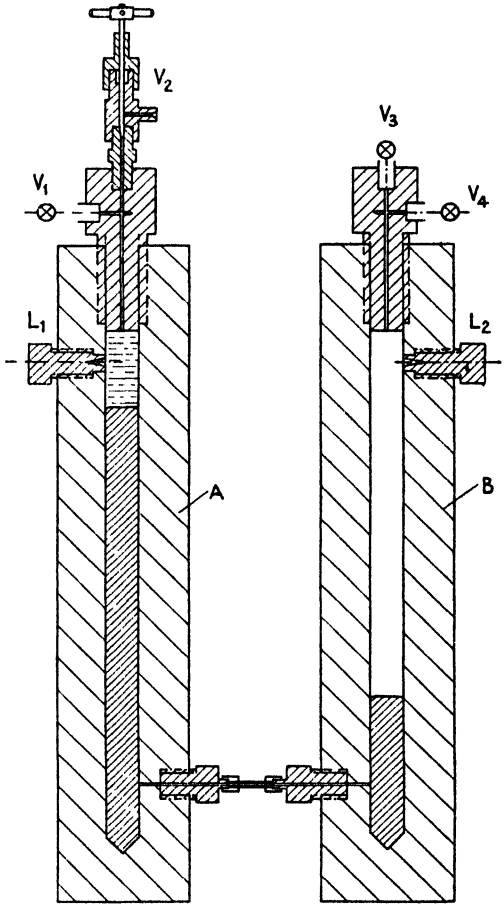

FIG. 43(*b*). Liquid-piston pump.

makes contact with L_2. V_1 is then closed and the gas admitted to the apparatus through V_4.

An Experimental Apparatus for studying Liquid-phase Reactions at Pressures up to 5,000 Atmospheres

The design of the apparatus, which is shown in section in Fig. 44, is such that a pressure of 1,000 atmospheres, developed by means of an auxiliary hand-operated hydraulic pump of conventional design,

is stepped-up to 5,000 atmospheres by an intensifier which forms an integral part of the reaction vessel.

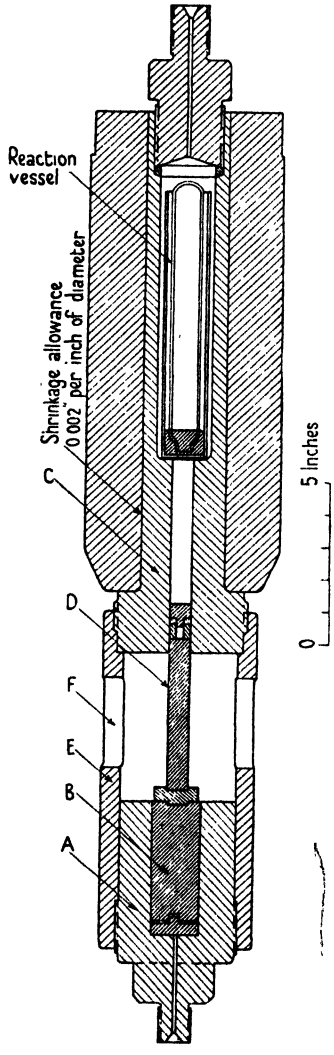

FIG. 44. Pressure vessel for 5,000 atmospheres.

The low-pressure side of the intensifier consists of a simple cylinder *A* and piston *B*, and the high-pressure side of a compound cylinder *C* and piston *D*. The two cylinders are held together against the thrust of the pistons and are alined by the steel sleeve *E* which is provided with sight holes *F* through which the pistons may be observed. The diameters of the pistons are 1·5 and 0·6 inches, respectively, giving the intensifier a theoretical ratio of 6·25 or an actual ratio of about 5·3. The pistons are obturated by soft rubber washers held in position by movable heads as shown in Fig. 36 (*a*).

The upper part of cylinder *C* is enlarged to 1·25 inches internal diameter and serves as the reaction vessel; the reactants, contained in a glass tube over mercury, are placed therein and the remaining space is completely filled with liquid paraffin or other liquid suitable for transmitting the pressure.

The two cylinders are constructed of a nickel-chromium-molybdenum steel, particulars of which will be found in Chapter I. The reaction chamber, which is 6 inches in external diameter, is made up of two cylinders shrunk together, the diameter of contact being 2·75 inches and the shrinkage allowance 0·002 inch per inch of diameter. The stresses in the walls of this vessel before and during the application of the working pressure are given in Table 25.

The plug closing the reaction chamber is obturated by a lens ring, details of which are given in Fig. 33.

TABLE 25. *Stresses in a Compound Cylinder due to Shrinkage and Internal Pressure*

Stresses, tons per sq. in.		*Inner cylinder Diameters, in.*			*Outer cylinder Diameters, in.*		
		1·25	2	2·75	2·75	4	6
Shrinkage	Radial stress (P_1)	0	6·70	8·72	8·72	2·90	0
	Hoop stress (T_1)	−21·98	−15·27	−13·26	13·35	7·71	4·63
	Equivalent simple stress (S_1)	−21·98	− 8·57	− 4·54	22·07	10·61	4·63
Initial pressure	Radial stress (P)	39·22	14·21	6·68	6·68	2·22	0
	Hoop stress (T)	42·76	17·76	10·22	10·22	5·77	3·54
	Equivalent simple stress (S)	81·98	31·97	16·90	16·90	7·99	3·54
Resultant	Radial stress (P_R)	39·22	20·91	15·40	15·40	5·12	0
	Hoop stress (T_R)	20·78	2·49	− 3·04	23·57	13·48	8·17
	Equivalent simple stress (S_R)	60·00	23·40	12·36	38·97	18·60	8·17

The two pistons are constructed of 'race' steel and are ground and lapped into their respective cylinders.

To calibrate the apparatus the high-pressure cylinder is connected to a free-piston gauge and the low-pressure cylinder to a standard Bourdon gauge; pressure is then applied to the latter by means of the hydraulic pump and corresponding readings are taken of the pressures in the two cylinders both for rising and falling pressures. Having ascertained in this way the actual ratio of the intensifier, it is usually sufficient in practice to record the pressure on the low-pressure side.

The connexions from the hydraulic pump to the intensifier are made of solid-drawn high-tensile steel tubing having an internal diameter of $\frac{1}{8}$ inch and a wall-thickness of $\frac{3}{16}$ inch. The pipe-lines are connected to the apparatus by means of a collar and nut as shown in Fig. 39 (*b*).

With this apparatus a pressure of 5,000 atmospheres may be developed in the course of a few minutes and may be maintained for several days without measurable loss.

Injection Pumps

In using liquid-piston pumps, free-piston gauges, and other apparatus in which liquids are being subjected to high pressures, it is frequently necessary to inject oil or other liquid against the

working pressure. For this purpose a simple injection pump without valves is extremely useful.

Fig. 45 (*a*) shows such a pump designed by Professor F. Keyes for use in measuring accurately the compressibility of water up to pressures of about 300 atmospheres. The method consists in connecting the pump to a vessel of known volume containing the water and increasing the pressure by forcing the piston inwards. The diminution in volume due to the compressibility is given by the volume swept out by the piston. The pump consists of a steel cylinder *C* into which fits a piston *P* made of selected drill steel rod. The packing is made up of a number of hard rubber rings *R* fitting closely the piston and enclosing some softer material. Keyes employs fine woven cotton sheeting cut on the bias in strips about 2 to 3 cm. in width and passed repeatedly through purified ceresin wax at a temperature of 110° until no further air bubbles appear; it is allowed to drain and when cool is wrapped tightly around the piston. The packing is held in place and compressed by the steel ring *S* and the gland nut *N*. The piston has a clearance of between 0·05 and 0·1 mm. in the cylinder and about 0·5 mm. in the gland nut.

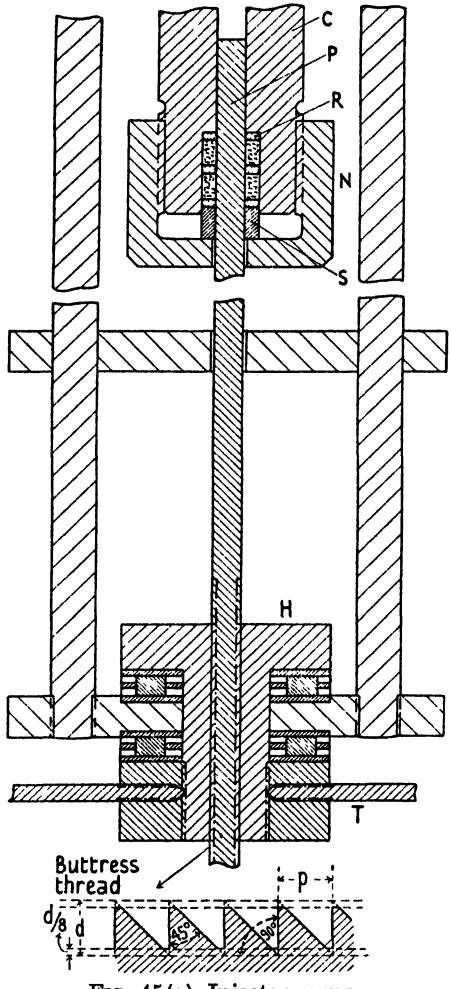

Fig. 45 (*a*). Injector pump.

A convenient size of piston is $\frac{7}{8}$ inch diameter. The threaded part is usually made separately and joined to the piston proper by turning a one-degree taper for about 5 cm. on one end of the latter and making

it a shrink fit into a corresponding socket in the threaded member. To minimize friction a buttress thread is employed for the screw and the nut H is made of bronze. Two roller thrust bearings are used to take the back thrust on the nut, and the nut is rotated by four spokes screwed into the locking member T.

Safety Devices

In the operation of high-pressure processes the possibility of the failure of any part of the main plant or auxiliary fittings is an important consideration and provision should be made in the design and lay-out for localizing the effects of such failure and for the protection of workers. It should also be borne in mind that whilst the accident hazard is always present, it is much increased in cases where exothermic processes are involved or where inflammable material is being handled.

The usual cause of failure in high-pressure plant is due to the setting up of abnormal stresses as the result of (1) the self-acceleration of highly exothermic reactions with the consequent sudden increase in pressure, (2) the explosion of combustible mixtures by the heat liberated from localized reactions on catalysts, or on some active surface in the reaction zone, or by adiabatic compression, and (3) the occurrence of exothermic reactions due to impurities introduced with the reactants or present in the plant. In addition corrosion, fatigue, and temperature 'creep' may give rise to dangerous conditions.

It is, therefore, advisable to incorporate in the plant some device for releasing the pressure when it exceeds a certain predetermined value.

Safety Valves and Bursting Disks. Although the ultimate purpose of both safety valves and bursting disks is the same, namely, to release pressure, they have somewhat different fields of application; the former are best fitted to deal with a gradual rise of pressure such as would result from faulty temperature control, whilst the latter are to be preferred where there is a likelihood of explosion and sudden release of pressure is desirable or imperative.

Safety valves of the spring-loaded type designed for high pressures suffer from the defect that they do not re-seat satisfactorily. They should, therefore, be set to the maximum permissible pressure and should, where possible, be mounted in a by-pass in such a way that they may be isolated from the main plant for resetting.

Bursting disks are intended, not to maintain the working pressure below a fixed maximum, but to reduce it suddenly by allowing the contents of the plant to escape to the atmosphere. They should, therefore, be incorporated in the main apparatus, near the reaction zone, have an effective aperture large enough to deal with the contents of the whole pressure system, and be provided with a large

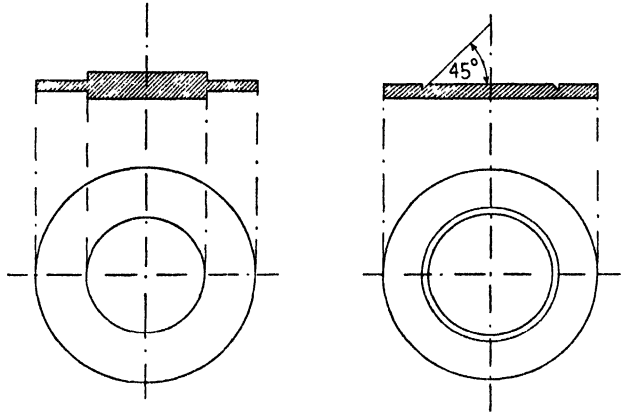

FIG. 45(*b*). Bursting disks.

capacity lead-off to the open air. To fulfil their purpose adequately they must be of sufficient strength to withstand the working pressure for long periods without fatigue and must function without appreciable 'lag'. The design should be such as to produce a concentration of stress in a narrow ring of metal of approximately the effective diameter of the disk. Two types are shown in section in Fig. 45 (*b*).

It must be emphasized that neither safety valve nor bursting disk will protect a plant from the disruptive action of a detonation set up within it. It is usually possible, however, so to arrange reaction vessels and pipe-lines that the chances of a detonation are minimized, even though the contents may become ignited. Thus, for example, long straight runs of pipe-line should be avoided and buffer chambers, packed with conducting material, should be incorporated in strategic positions.

Protective Screens. One of the dangers arising from the failure of a pressure vessel is due to fragmentation. For this reason it is sometimes desirable to surround parts of the plant with steel plate screens or rope mantlets. In explosive works mantlets, woven of good manilla rope of the form and dimensions shown in Fig. 45 (c) are

hung from supports in such a way as to swing freely under the impact of high-velocity projectiles. Mild steel plates are effective against small fragments and, provided they are rigidly mounted, serve also to deflect explosion and shock waves.

In arranging protective screens the importance of having ready access to all parts of the plant must be kept in mind; it is indeed

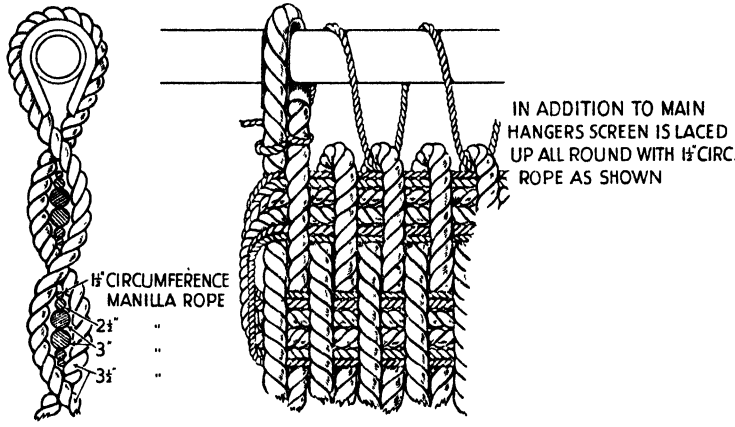

FIG. 45(c). Rope mantlet.

sometimes best to avoid their use altogether and to locate the plant in a separate room with remote controls. The practice of relegating pressure apparatus to a dark corner of the laboratory where space is restricted is not to be recommended.

Precautions to be observed in the use of gas cylinders and pressure gauges are dealt with in Chapters II and V, respectively.

The Proof and Periodic Testing of Pressure Vessels

The proof testing of a pressure vessel may be carried out by applying to it a steady pressure in excess of the working pressure but not sufficiently high to strain the walls beyond their elastic limit. The pressure should be maintained for at least 1 hour and, on its release, the vessel should exhibit no permanent extension of any part. Immediately after the test the vessel should undergo a final stabilizing heat treatment by maintaining it for 1 hour at a temperature of 200° C. in the case of mild steel, and at 400° C. in the case of high tensile steels.

The above test should be repeated at periodic, but not too frequent, intervals and should always be followed by a stabilizing treatment.

For vessels having to withstand high temperatures as well as high pressures an additional precautionary measure is to determine periodically the Brinnell hardness at a number of points on the sides and ends.

The onset of failure is usually, although not invariably, betrayed by signs which suggest that the material is undergoing some change in mechanical properties. Thus, for example, any permanent change in dimensions, the persistent recurrence of leaks, the seizing of screw threads, and local corrosion are indications that all is not well and call for an immediate examination of the vessel both inside and out. Certain types of failure, such as that due to the action of hydrogen and that caused by fatigue, give little warning, and constant vigilance and the strict observance of safety regulations are necessary to avoid serious accidents.

BIBLIOGRAPHY AND REFERENCES

1. LOVE, *Elasticity*, p. 194. Cambridge University Press, 1927.
2. ANDREWS, *Proc. Phys. Soc.* **43**, 1 (1931).
3. MANNING, Conference on Jointing and Packing, Soc. Chem. Ind. (Chemical Engineering Group), 1937.
4. AMAGAT, *Ann. de Chim. et de Phys.* **19**, 350 (1880).
5. SMITH, *Proc. Inst. Mech. Eng.* **133**, 139 (1936).
6. ONNES and BRAAK, Comm. Univ. of Leiden, No. 166.
7. AMAGAT, *Ann. de Chim. et de Phys.* (6), **29**, 90 (1893).
8. POULTER, *Phys. Rev.* **40**, 860 (1932).
9. NEWITT and SEN, *Trans. Inst. Chem. Eng.* **10**, 22 (1932).
10. KING and FRASER SHAW, Chem. Eng. Congress of the World Power Conference (1936).
11. BRIDGMAN, *Proc. Am. Acad. Arts and Sci.* **49**, 627 (1914).
12. ADAMS, *J. Am. Chem. Soc.* **53**, 3769 (1931).

V

THE MEASUREMENT OF HIGH PRESSURES

THE pressure p exerted by an ideal gas on the surface of its container is given, in terms of the kinetic theory, by the equation

$$p = \frac{\frac{1}{3}mnu^2}{v}, \tag{5.1}$$

where n is the number of molecules contained in a volume v of gas, u is their mean speed, and m their mass. (5.1) may be written

$$p = \frac{2}{3}\frac{n}{v}(\tfrac{1}{2}mu^2), \tag{5.2}$$

from which it is seen that the pressure of an ideal gas is equal to two-thirds of the kinetic energy of translation of the molecules per unit volume. Eq. (5.2) shows that the pressure of a gas may be increased by increasing the ratio n/v or by increasing the kinetic energy of translation, i.e. the temperature.

The dimensions of pressure are given by (5.1), which may be written in the dimensional form

$$p = \frac{ML}{T^2}\frac{1}{L^2}, \tag{5.3}$$

and the units of pressure will therefore be those of a force per unit area or the product of a mass and its acceleration. In the C.G.S. system the internationally accepted unit of pressure is 1 dyne per sq. cm., called the barye.† A more convenient unit for high-pressure work is 10^6 dynes per sq. cm., known as the bar.

The *normal atmosphere* is defined as the pressure exerted by a vertical column of liquid (mercury), 76 cm. long, of density 13·5951 gm. per c.c., the acceleration of gravity being 980·665 cm. sec.$^{-2}$

Conversion factors for the various pressure units in common use are given in Table 26 (p. 110).

Pressure gauges may be classified as primary (absolute) and secondary gauges according as they measure directly a force or weight balancing the pressure or some secondary effect, such as the elastic deformation of a spring, which is a function of the pressure. They may be further subdivided according to the scheme on p. 111.

† Recommendation of the International Congress of Physicists, Pasco (1900).

TABLE 26. *Conversion Factors for Pressure Units*

($g = 980{\cdot}665$ cm. sec.$^{-2}$)

Unit	*Barye (dynes per sq. cm.)*	*Bar*	*Gm. wt. per cm.²*	*Kg. wt. per m.²*	*Normal atmosphere*
Barye (dynes per sq. cm.)	1	10^{-6}	$1{\cdot}01972\times10^{-3}$	$1{\cdot}01972\times10^{-2}$	$9{\cdot}86923\times10^{-7}$
Bar	10^{6}	1	$1{\cdot}01972\times10^{3}$	$1{\cdot}01972\times10^{4}$	0·986923
Gm. wt. per cm.²	980·665	$9{\cdot}80665\times10^{-4}$	1	10	$9{\cdot}67841\times10^{-4}$
Kg. wt. per m.²	98·0665	$9{\cdot}80665\times10^{-5}$	10^{-1}	1	$9{\cdot}67841\times10^{-5}$
Normal atmosphere	$1{\cdot}01325\times10^{6}$	1·01325	$1{\cdot}03323\times10^{4}$	$1{\cdot}03323\times10^{5}$	1
Cm. of mercury at 0° C.	$1{\cdot}33322\times10^{4}$	$1{\cdot}33322\times10^{-2}$	13·5951	$1{\cdot}35951\times10^{2}$	$1{\cdot}31579\times10^{-2}$
Inches of mercury at 0° C.	$3{\cdot}38639\times10^{4}$	$3{\cdot}38639\times10^{-2}$	34·5316	$3{\cdot}45316\times10^{2}$	$3{\cdot}34211\times10^{-2}$
Cm. of water at 4° C.	$9{\cdot}80638\times10^{2}$	$9{\cdot}80638\times10^{-4}$	0·999972	9·99972	$9{\cdot}67814\times10^{-4}$
Inches of water at 4° C.	$2{\cdot}49082\times10^{3}$	$2{\cdot}49082\times10^{-3}$	2·53993	25·3993	$2{\cdot}45825\times10^{-3}$
Lb. wt. per in.²	$6{\cdot}8947\times10^{4}$	$6{\cdot}8947\times10^{-2}$	70·3064	$7{\cdot}03064\times10^{2}$	$6{\cdot}80454\times10^{-2}$
Ton (2,240 lb.) wt. per in.²	$1{\cdot}5444\times10^{8}$	$1{\cdot}5444\times10^{2}$	$1{\cdot}57485\times10^{5}$	$1{\cdot}57485\times10^{6}$	152·420

Unit	*Cm. of mercury at 0° C.*	*Inches of mercury at 0° C.*	*Cm. of water at 4° C.*	*Inches of water at 4° C.*	*Lb. wt. per in.²*	*Ton (2,240 lb.) wt. per in.²*
Barye (dynes per sq. cm.)	$7{\cdot}50064\times10^{-5}$	$2{\cdot}95300\times10^{-5}$	$1{\cdot}01974\times10^{-3}$	$4{\cdot}0147\times10^{-4}$	$1{\cdot}45039\times10^{-5}$	$6{\cdot}47501\times10^{-9}$
Bar	75·0064	29·5300	$1{\cdot}01974\times10^{3}$	401·474	14·5039	$6{\cdot}47501\times10^{-3}$
Gm. wt. per cm.²	$7{\cdot}35561\times10^{-2}$	$2{\cdot}89590\times10^{-2}$	1·00003	0·393712	$1{\cdot}42235\times10^{-2}$	$6{\cdot}34981\times10^{-6}$
Kg. wt. per m.²	$7{\cdot}35561\times10^{-3}$	$2{\cdot}89590\times10^{-3}$	0·100003	$3{\cdot}93712\times10^{-2}$	$1{\cdot}42235\times10^{-3}$	$6{\cdot}34981\times10^{-7}$
Normal atmosphere	76·0002	29·9212	$1{\cdot}03326\times10^{3}$	$4{\cdot}06794\times10^{2}$	14·6961	$6{\cdot}56080\times10^{-3}$
Cm. of mercury at 0° C.	1	0·393700	13·5954	5·35253	0·193369	$8{\cdot}63261\times10^{-5}$
Inches of mercury at 0° C.	2·54001	1	34·5325	13·5955	0·491158	$2{\cdot}19269\times10^{-4}$
Cm. of water at 4° C.	$7{\cdot}35541\times10^{-2}$	$2{\cdot}89582\times10^{-2}$	1	0·393701	$1{\cdot}42231\times10^{-2}$	$6{\cdot}34964\times10^{-6}$
Inches of water at 4° C.	0·186827	$7{\cdot}35538\times10^{-2}$	2·54000	1	$3{\cdot}61266\times10^{-2}$	$1{\cdot}61281\times10^{-5}$
Lb. wt. per in.²	5·17147	2·03600	70·3083	27·6804	1	$4{\cdot}46433\times10^{-4}$
Ton (2,240 lb.) wt. per in.²	$1{\cdot}15840\times10^{4}$	$4{\cdot}56061\times10^{3}$	$1{\cdot}57489\times10^{5}$	$6{\cdot}20037\times10^{4}$	$2{\cdot}23998\times10^{3}$	1

Primary (absolute) Gauges

Open and closed mercury columns and columns of reduced height	Free-piston gauges

Secondary Gauges

Elastic deformation of a metal tube (e.g. Bourdon gauge, Petaval gauge).	Compressibility of a pure liquid.	Some effect due to work done on the molecules of a substance (e.g. refractive index, electrical resistance, piezoelectric effect).
Inelastic deformation of a metal (e.g. crusher gauge).	Vapour-pressure of a pure liquid.	

Primary Gauges

For all accurate pressure work some form of primary gauge must be available, either for the direct measurement of pressure or for calibrating a secondary gauge. For general purposes the free-piston gauge is the most convenient, but for the highest accuracy it is usually necessary to resort to a mercury column in order to determine the constants of the free-piston gauge.

The Mercury Column Gauge

All the earlier accurate measurements of high pressure were made with open mercury column gauges which were erected against the wall of a building or in the shaft of a well or mine. The column used by Amagat in his preliminary determination of the compressibility of nitrogen was over 900 feet long and was installed in the shaft of the Verpilleux mine at Méons near Saint-Étienne [1], the compressibility apparatus being placed in a disused gallery near the foot of the shaft. Shorter columns, reading up to about 30 atmospheres, are still frequently employed by gauge makers for calibrating steam-gauges.

The use of this type of gauge is by no means free from difficulties; all parts of the column must be accessible and this involves the provision of numerous joints and valves for inserting observation tubes at various levels, and some form of lift for the observer. Corrections are necessary for changes in the density of the mercury due to pressure and temperature variations.

To obviate the cost and difficulty of erecting long columns H. Kammerlingh Onnes has employed a principle, first suggested by Richards in 1845, to construct an *open gauge of reduced height* [2]. The gauge consists of a number of mercury-in-glass columns connected

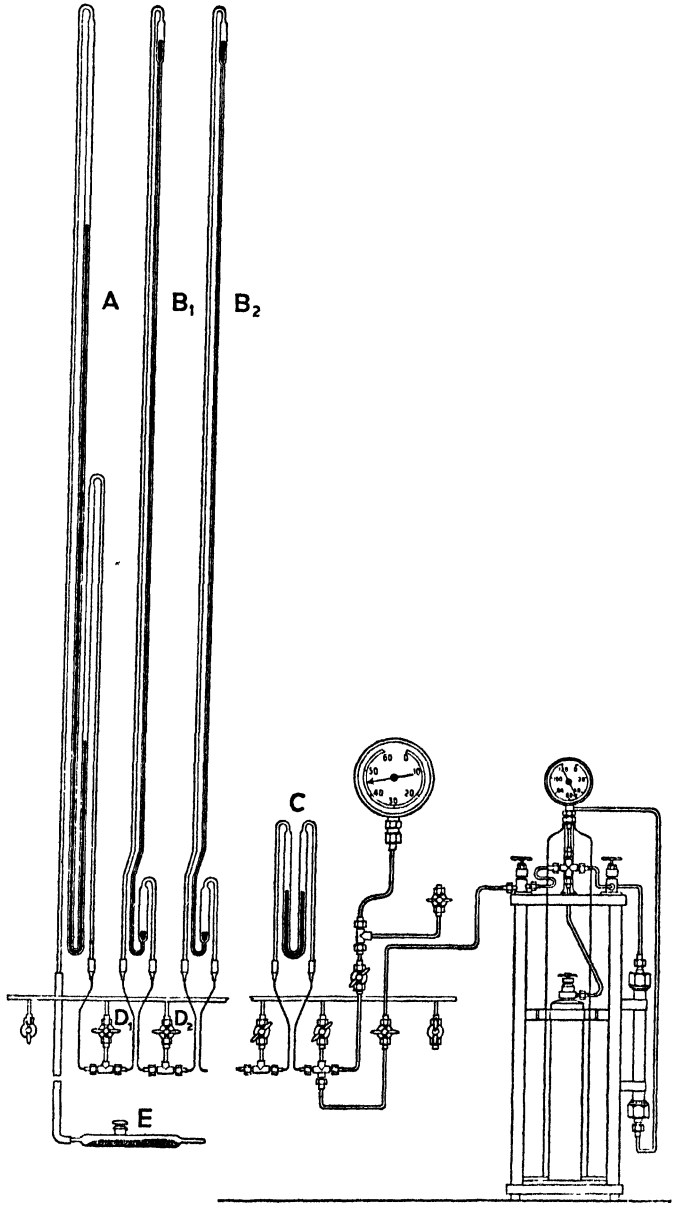

FIG. 46. Open-column gauge of reduced height.

in series as shown in Fig. 46. The pressure to be measured is applied to the right-hand arm of the first column, C, and is balanced by a gas pressure applied above the mercury in the left-hand arm. This pressure in turn is measured by transferring it to the second column, B_2, where it causes the mercury to rise under an excess of pressure, which is measured by the third column, B_1, etc. The extreme left-hand column, A, is open to the atmosphere and serves to measure fractions of an atmosphere.

In the gauge erected at Leiden the maximum pressure that can be measured is 60 atmospheres, there being 15 columns each 3·14 metres long, in series. Pressure is applied to the column through the metal valves D_1, D_2, etc., by means of compressed hydrogen or air, a suitable correction being made for the difference in pressure of the compressed gas at the lower mercury meniscus in one column and at the upper meniscus in the neighbouring one. The practical pressure limit for a gauge of this type, constructed in glass, is about 100 atmospheres, but by constructing all parts in steel and using an electrical device for locating the position of the mercury levels, a very much higher range of pressures could be measured. It is evident from the above description, however, that the accurate measurement of a high pressure involves the integration of a large number of separate readings and the errors of observation are multiplied.

A more convenient form of mercury column gauge will be described in connexion with the calibration of free-piston gauges.

The Free-piston Gauge or Pressure Balance

In 1893 Amagat published the last of his classical papers on the compressibility of fluids [3], in which he stated:

'Quand j'ai entrepris ces recherches, il n'existait aucun instrument permettant de mesurer avec certitude des pressions supérieures aux limites dans lesquelles on avait pu comparer avec un manomètre à air libre les appareils à indications empiriques que tout le monde connaît; les manomètres à gaz présentent, dans la pratique, de graves inconvénients; il ne pouvait du reste être employé que jusqu'à vers 430 atmosphères, limite supérieure des déterminations que j'ai faites en 1878, avec un manomètre à air libre dans les puits Verpilleux.'

In 1880 his contemporary Louis Cailletet had described a primary gauge [4], which resembles in all essential respects the free-piston gauges used to-day, in the following words:

'Le manomètre que j'emploie en ce moment, et qui permet de mesurer des pressions de 1500 atm. avec une approximation suffisante, est construit

d'après un principe qui est dû à M. Marcel Deprez. Lorsque l'on comprime de l'eau sous un piston parfaitement cylindrique et ajusté dans une cavité pratiquée dans une masse métallique, de telle façon que l'espace annulaire compris entre la pièce fixe et le piston soit très petit, l'eau ne s'échappera qu'avec une grande lenteur par cet étroit passage. Avec cet appareil, qui ne supporte aucun frottement, il sera possible, en chargeant de poids la soupape, de peser les pressions qui tendront à la soulever. L'appareil que j'ai construit se compose d'un cube d'acier fondu de $0^{m},20$ de côté, dans lequel est creusé

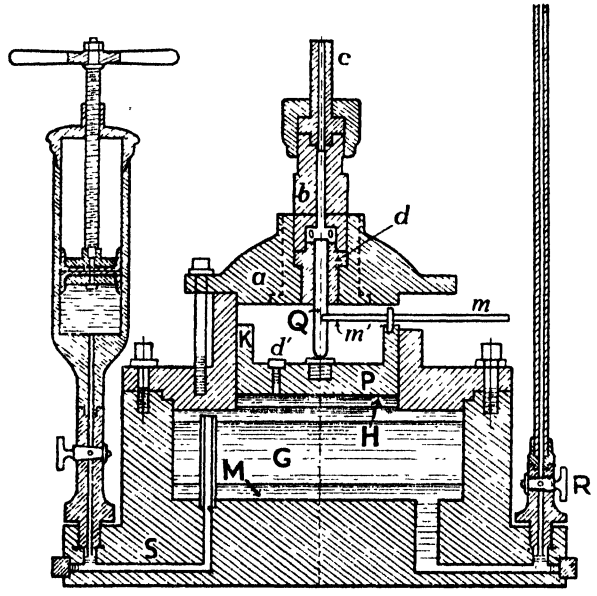

FIG. 47. Amagat's pressure balance.

un cylindre qui reçoit le piston également en acier et ajusté avec une telle précision que la largeur de l'espace annulaire compris entre eux est inférieur à 1/200 de millimètre. Un levier très mobile, monté sur des axes, peut recevoir à une de ses extrémités des poids qui exercent ainsi sur la soupape des pressions exactement connues.

'J'ai placé au-dessous du piston une membrane de baudruche, dont la résistance à la flexion est assez petite pour être négligée et qui présente l'avantage de supprimer l'écoulement de l'eau autour de la soupape. J'ai pu m'assurer en outre que les indications fournies par cet appareil sont exactes à 1/200 environ.'

In 1883 Amagat adopted a similar form of gauge, a diagram of which is reproduced in Fig. 47. The design is a little more elaborate than that of Cailletet in that there are two pistons Q and P. The pressure to be measured acts upon the smaller piston Q and is transmitted by way of the larger piston to the liquid in the chamber

G, where it is measured by means of the open mercury column R. Amagat employed two large pistons of 6 cm. and 12 cm. diameter, respectively, and a number of small pistons of varying diameter, the smallest being 0·5527 cm. In a series of experiments in which pressures up to 3,000 atmospheres were attained, a combination of pistons was used which gave a maximum height of 5·20 metres of mercury in the column R.

The Theory of the Free-piston Gauge. In its simplest form this gauge consists of a hard steel cylindrical piston ground and lapped to fit the lapped hole in a hard steel cylinder, no packing of any sort being employed. The pressure to be measured is transmitted, usually by means of a suitable liquid such as a mineral oil, to one end of the piston and is balanced by weights acting on the opposite end.

Under ideal conditions the pressure P would be given in terms of the balancing weights W, the weight of the piston w and its cross-sectional area a, and the atmospheric pressure p, by the relation

$$P = (W+w)/a+p. \tag{5.4}$$

In practice it is necessary to take into account the slow leak of liquid past the piston which exerts a frictional force tending to raise the piston, and the distortion of the cylinder and piston under the system of stresses set up by the hydrostatic pressure. If both cylinder and piston are assumed to be perfectly cylindrical and the annular space between them to be so narrow that the frictional effect of the escaping liquid is equally divided between them, then we may apply the usual hydrodynamical equation for the steady motion of a cylindrical shell of incompressible fluid moving upwards in the direction of the z-axis, namely

$$\frac{\mu}{r}\frac{\partial}{\partial r}\left(r\frac{\partial v}{\partial r}\right) = \frac{\partial p}{\partial z} = \text{constant}, \tag{5.5}$$

where μ is the coefficient of viscosity of the liquid, v the velocity along the direction of the z-axis, p the pressure per unit area, and r the radius of the cylinder. If a and b are the radii of the cylinder and piston, respectively, and if no 'slip' occurs at the solid boundaries, $\partial v/\partial r$ may be assumed to be zero, and integration of (5.5) gives

$$\mu\frac{\partial v}{\partial r} = \frac{a-b}{2}\frac{\partial p}{\partial z}\frac{a+b}{r}.$$

Since a and b are approximately equal, $(a+b)/r$ may be taken as 2,

and the total force on the cylindrical surface F, parallel to the axes, becomes

$$F = \pi a(a-b)\frac{\partial p}{\partial z}l = \pi a(a-b)(p_1-p_0), \tag{5.6}$$

where l is the length of the cylinder. The force due to the oil leak is therefore independent of the viscosity of the oil and of the rapidity of the leak and is an invariable fraction of the pressure measured. Its effect is to increase the effective diameter of the piston to the mean of the diameters of the piston and cylinder [5].

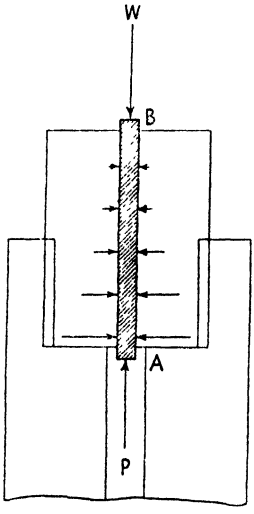

FIG. 48. Forces acting on piston of pressure balance.

The distortion of the cylinder and piston is the result of stress systems set up by the hydrostatic pressure and the balancing weights. On the piston there is an axial thrust produced by the pressure P and the weights W (Fig. 48), acting in opposite directions, which is uniform throughout the length of the piston. In addition, there is a variable compressive stress normal to the curved surface, equal in magnitude to the hydrostatic pressure at the lower end A and to 1 atmosphere at the upper end B. On the cylinder there is a variable internal hydrostatic pressure equal in magnitude to, and distributed in the same way as, the compressive stress on the piston. The tendency of these compressive stresses is to open up the cylinder at its lower end and to reduce the sectional area of the piston.

The increase in the internal radius of a cylinder δR due to an internal pressure p is given by the equation

$$\delta R = \frac{R_0 p}{E}\left\{\frac{(1+\sigma)R_1^2+(1-\sigma)R_0^2}{R_1^2-R_0^2}\right\}, \tag{5.7}$$

where R_0 and R_1 are the internal and external radii, respectively. The diminution in radius of the piston due to the same pressure p is $pk/3$, where k is the coefficient of compressibility of steel.

It is evident from the above that distortion due to hydrostatic pressure will change the effective area of the piston by an amount increasing in percentage value with the pressure; and the assumption that the effective area of the piston is the mean of the cross-sectional

areas of piston and cylinder and is independent of the pressure must be used with caution where moderate pressures are concerned, and is certainly not valid at very high pressures.

The change in the diameter of the piston with change in temperature is usually of sufficient magnitude to necessitate a correction.

Eq. (5.4) may, therefore, be modified to give

$$P = (W+w)/sa+p, \tag{5.8}$$

where s is a function of pressure and temperature and sa may be designated the effective area of the piston.

The most satisfactory means of determining sa is by comparing the readings of the gauge with those of a mercury column over the required pressure range. A very convenient method of carrying out the calibration has been developed by Holborn and Schultze [6] and requires the use of two free-piston gauges having pistons of approximately the same diameter and a closed mercury-in-steel column of moderate length (about 900 cm.). The gauges are connected, alternately, with the top and bottom of the column and comparative readings are taken in steps fixed by the length of the column. The column described below and illustrated in Fig. 49 is essentially that used at the Reichsanstalt, modified in some of its details by Keyes and Davey [5].

The column A consists of a steel tube 875 cm. long, of 1 cm. bore and a wall-thickness of 0·476 cm. The lower end screws into the steel block B and makes connexion with the short column K. Mercury can be pumped into the two columns by means of a hydraulic pump connected to the block at L, and a fine adjustment of the mercury levels can be made by means of the piston injector I. The level of mercury in the two columns is indicated by electrical contact with two insulated needles at R_1 and R_2, respectively. The needles are connected with an electrical device consisting of a relay operating on 0·002 amp. used to connect the circuit to a 4-volt flash-light bulb which gives visual indications when contact is made or broken at the mercury-oil junction. For sharp contact it is essential that as small a current as possible pass between the needle and mercury, as otherwise emulsification of the mercury in the oil takes place.

The top of the column A is connected to one or other of the two free-piston gauges G_8 and G_9 by way of the tube C (0·7 cm. bore), which is filled with oil of known density and compressibility. The

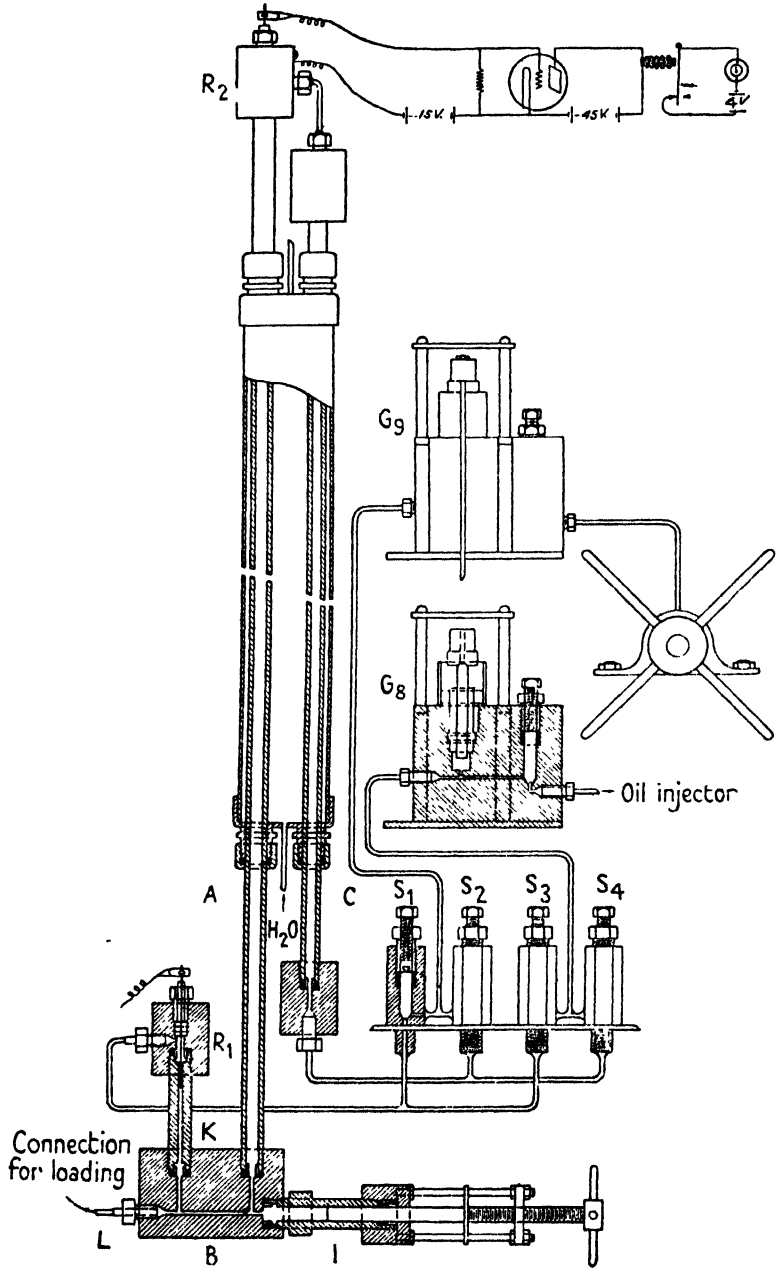

FIG. 49. Mercury-in-steel column for calibrating gauges.

valves S_{1-4} enable either of the two gauges to be connected to the top or bottom of the column at will.

Both the mercury and connecting-oil column are enclosed in a water jacket which is constructed of a 7·5 cm. diameter brass tube, well lagged. The water in the jacket is circulated in a closed circuit by means of a pump and its temperature is indicated by a number of thermometers disposed along the length of the jacket.

In order to reduce the observed length of mercury column to pressure units (force per unit area) the temperature, dilatation, and compressibility of the mercury must be known. A correction is also necessary for the stretch of the column due to the internal pressure, and for the thermal expansion of the steel.

For the purpose of checking, periodically, the constants of a free-piston gauge it is convenient to have available some suitable reference pressure, and O. Bridgeman has suggested the vapour pressure of liquid carbon dioxide at 0° C. Such a liquid-vapour system has the advantage that temperature is the only independent variable. The gas may readily be obtained in a high state of purity, and equilibrium is easy to establish and reproduce.

The following are selected values of the vapour pressure of carbon dioxide at 0° in international millimetres of mercury:

Source	*Vapour pressure, mm.* Hg
Kuenen and Robson, *Phil. Mag.* (6), **3**, 149 (1902	$26{\cdot}10 \times 10^3$
Jenkins and Pye, *Phil. Trans.*, A, **213**, 67 (1914)	$26{\cdot}30 \times 10^3$
Keyes and Kenney, *Am. Soc. Refrig. Eng.* **3**, 4 (1917)	$26{\cdot}05 \times 10^3$
Meyers and Van Dusen, *Refrig. Eng.* **17**, 180 (1926)	$26{\cdot}13 \times 10^3$

Bridgeman (*J. Am. Chem. Soc.* **49**, 1174 (1927)) has made a very accurate redetermination of the constant, and finds, as the average of thirty independent measurements made with four different free-piston gauges, the value $26144{\cdot}7 \pm 1{\cdot}0$ international mm. of mercury ($g = 980{\cdot}665$), which is equivalent to $34{\cdot}4009 \pm 0{\cdot}0013$ atmospheres, The constants of the gauges were determined by comparison with a 9-metre mercury-in-steel column.

The Design of the Free-piston Gauge. To reduce the frictional force between the piston and cylinder, both must be truly cylindrical

and the width of the annular space between them must lie within comparatively small limits [7]. If the space is too narrow, the oil film between piston and cylinder will be discontinuous, and if too wide the piston will wander and its axis will no longer coincide with that of the cylinder. The question of fit is a difficult one and experience is probably the best guide to the permissible tolerance. It has been suggested that a practical test of the suitability of a piston is to apply a potential difference to the piston and cylinder, when, on rotating or oscillating the former, the insulation due to the oil film should be maintained.

When taking a pressure reading the piston should be rotated or oscillated to facilitate its axial movement and to maintain it in a central position within the cylinder. A certain critical speed seems to be necessary to reduce the friction between the piston and cylinder to a minimum, but opinion is divided as to whether a rotary or oscillatory movement is preferable [6, 7].

The constant of the gauge may be defined as the weight in grams which enables the piston at a given temperature to support a pressure equivalent to 1 mm. of mercury at 0° C., and is given by the expression

$$C = \frac{10g}{\pi d^2/4 \times \rho \times g_s}, \tag{5.9}$$

where g and g_s are the values of the gravitational constants, international (= 980·665) and at the place in question, respectively, ρ is the density of mercury in c.c. per gm. at 0° C., and d is the effective diameter of the piston in cm. The temperature correction for the constant is as follows:

$$C_{t_2} = C_{t_1}\{1+2{\cdot}2\times 10^{-5}(t_1-t_2)\}.$$

Piston-cylinder combinations are found to undergo an ageing effect which necessitates a redetermination of the constant at periodic intervals.

The simplest form of free-piston gauge and one that is quite satisfactory up to pressures of about 1,500 atmospheres is illustrated in Fig. 50 [8]. Referring to the inset, C and F are the piston and cylinder, respectively, fitting into the gauge block O and held in position by the nut G; the joint between the cylinder and block is obturated by an annealed aluminium gasket.

The weights are carried on a scale-pan attached to the cross-bar D which is supported on the piston through the intermediary of a

ball-bearing B. The isometric drawing shows the arrangement for oscillating the piston at 30 oscillations per minute. E is a metal bar, clamped to the piston and engaging with the hardened steel rollers P, by means of which the necessary movement is given. The

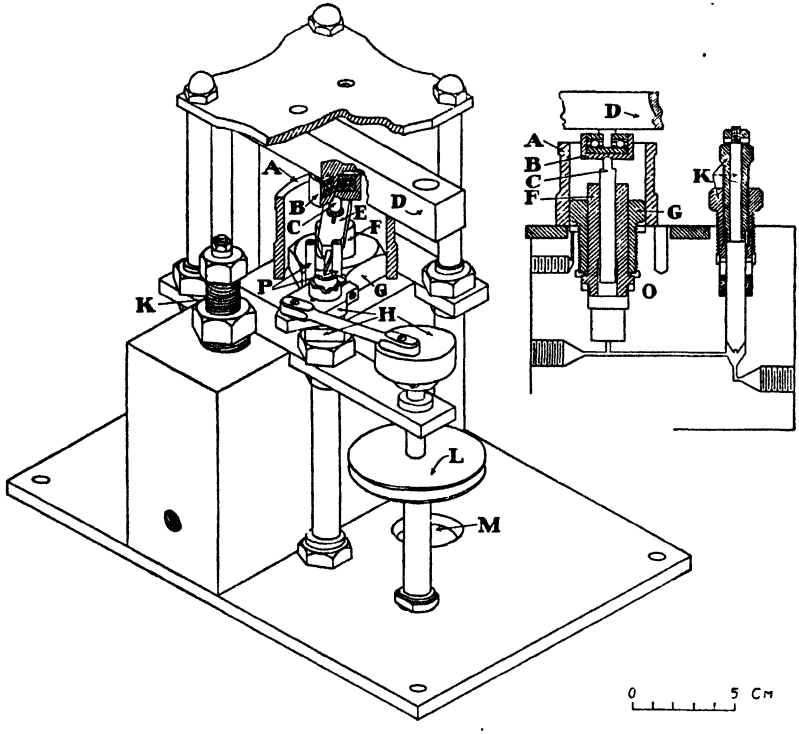

FIG. 50. Pressure balance showing the mechanism for oscillating the piston.

holes M in the base plate permit the passage of the suspension rods of the scale-pan.

This form of balance is used in the Research Laboratory of Physical Chemistry in the Massachusetts Institute of Technology, and the illustration given is reproduced from a paper by Professor F. G. Keyes [8]. In covering a pressure range from a few atmospheres to 1,200 atmospheres a relatively uniform sensitivity is obtained by employing four separate piston-cylinder combinations, so designed that they fit into the same gauge block. The accuracy obtained is of the order of 1 part in 40,000 up to 150 atmospheres and 1 part in 10,000 between 500 and 1,000 atmospheres.

For the highest accuracy it is necessary to know all the liquid levels within the apparatus before the pressure actually exerted upon the piston can be evaluated. It is also convenient and in some cases necessary to have an oil-injection pump connected with the balance so that the oil lost by leakage can be replaced.

The main disadvantages of this simple form of balance are the difficulty of supporting the heavy weights required to balance high pressures and the increase in the percentage errors with pressure due to the deformation of the piston and the acceleration of the oil-leak. Bridgman [9] has endeavoured to overcome these defects by using pistons of very small diameter and by so arranging the cylinder that it is subjected externally to the full hydrostatic pressure over its entire length. The design of a gauge constructed on this principle and working up to a pressure of 13,000 kg./cm.^{2} is shown in Fig. 51. The cylinder C is made of hardened nickel steel and is obturated by a soft steel cone, D, to which pressure is applied by means of a screwed plug E. The piston A is $\frac{1}{16}$ inch in diameter and is provided with an extension B which supports the weight carrier.

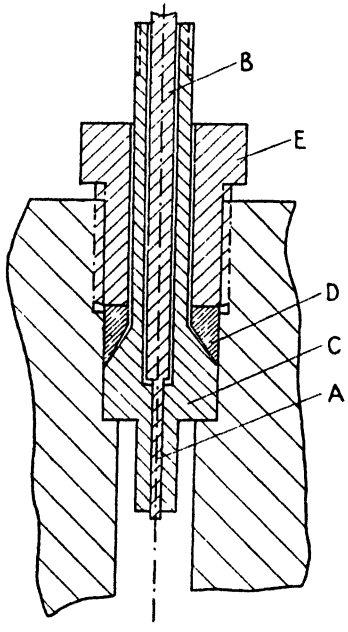

FIG. 51. Bridgman's pressure balance.

The effect of this arrangement is practically to eliminate the expansion of the cylinder at its lower end since the internal and external hydrostatic pressures balance one another. At the upper end, on the other hand, the external pressure acting on the cylinder is the full hydrostatic pressure whilst internally the pressure is only about 1 atmosphere. The cylinder, therefore, tends to contract in this region and may eventually shrink on to the piston. The correction for the deformation of the piston is small and at 13,000 kg./cm.^{2} does not exceed 0·23 per cent. Bridgman estimates that, employing all precautions, the gauge is capable of an accuracy of 0·1 per cent. at the highest pressure. It may be mentioned that at the pressures

for which this gauge is designed most organic liquids including mineral oils become very viscous and may even solidify at room temperatures. In order to transmit the pressure to the piston, Bridgman therefore employs a mixture of equal parts of glycerine and water, to which is added sufficient glucose to make a rather thick syrup.

The Differential Piston Gauge

A modified form of Amagat's original free-piston gauge has been developed at the National Physical Laboratory [10], and has recently been further improved and refined by A. Michels [11]. It will be recalled that Amagat made use of two pistons differing in sectional area, to step-down the pressure so that it could conveniently be measured by means of an open mercury column of moderate height. In the modern form the two pistons are replaced by a single differential piston, the effective area of which is the difference between the cross-sectional areas of the two parts.

The advantage of this type of gauge over the simple free-piston gauge lies in the much smaller weight necessary to balance a given pressure. It is, however, more difficult to construct and the frictional effects due to imperfect alinement of piston and cylinder are apt to be large.

Plate 4 is taken from a photograph of Michels's gauge and illustrates the method of supporting the balancing weights and the arrangement for giving a uniform rotary movement to the piston.

The Bourdon Gauge

Of the secondary gauges employed in high-pressure work this type is so widely used that some knowledge of its construction and properties is desirable.

The elastic element of the Bourdon gauge is a bronze or steel tube of elliptical section, closed at one end and bent to the arc of a circle; when the open end is held rigid the stresses set up in the tube on the application of an internal hydrostatic pressure are such as to cause the tube partially to straighten out and the free end to move through a distance proportional to the pressure. The movement is magnified by mechanical means and is indicated by a pointer moving over a calibrated dial.

For high pressures the tubes are constructed from bars of steel by first drilling them to the requisite diameter and then turning on the

outside to ensure an even thickness of wall. The ends are threaded and are provided with seatings which serve to make the metal-to-metal joints with the body and end-piece of the gauge, severally. The part between the screwed ends is flattened and, finally, the whole tube is annealed to eliminate any induced stresses, and hardened. The dimensions of the tubes employed for various pressure ranges are given in Table 27.

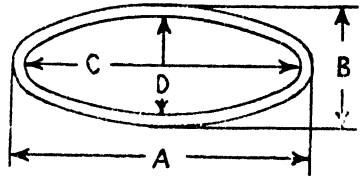

TABLE 27. *Dimensions of Bourdon Tubes*

Gauge dial, inches	*Pressure, lb./sq. in.*	*A, mm.*	*B, mm.*	*C, mm.*	*D, mm.*	*Overall length of tube, mm.*
4	1,000	13·9	6·5	11·8	5·0	120
	2,000	12·7	5 6	11·1	4·9	120
	3,000	12·4	6·5	10·5	4·6	120
	5,000	13 8	6·7	11·5	4·4	120
	4 tons	13·4	7·0	10·1	3·7	120
5	800	13·0	5·9	11·4	4·3	150
	2,000	13·3	6·5	12·3	4·5	150
	3,000	12·4	7·4	10·0	5·0	150
	4 tons	11·7	7·3	9·0	4·6	150
6	1,000	16·2	8·7	14·2	6·7	180
	2,000	17·2	8·9	14·0	6·6	180
	3,000	16·3	8·0	13·7	5.4	180
	8 tons	10·8	7·3	6·5	3·0	180

The internal mechanism of the gauge is shown in Plate 4. The open end of the tube is screwed into a forged steel central boss, the bottom flange of which forms a support for the casing, and its upper part for the magnifying mechanism. The other end of the tube is closed by a screw cap which is connected by means of a link with one arm of a pivoted quadrant; the other arm of the quadrant consists of a toothed segment gearing with the teeth of a pinion placed in the centre of the dial and on which the pointer is fixed. The small amount of 'back-lash' in the gearing is taken up by a fine hair-spring, one end of which is attached to the pinion and the other to a fixed point of the mechanism. Accuracy in manufacture and adjustment of the mechanism are necessary to reduce the lag to a minimum and

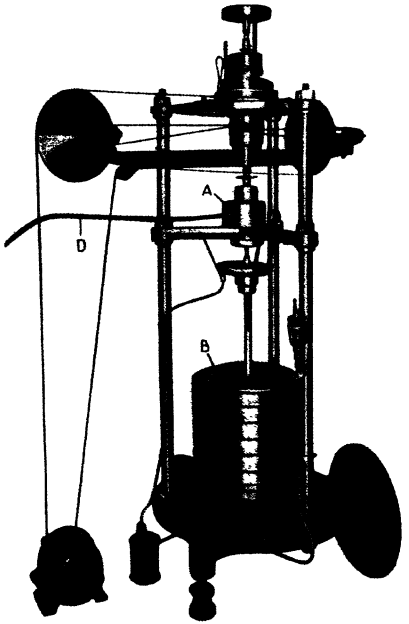

DIFFERENTIAL PISTON GAUGE

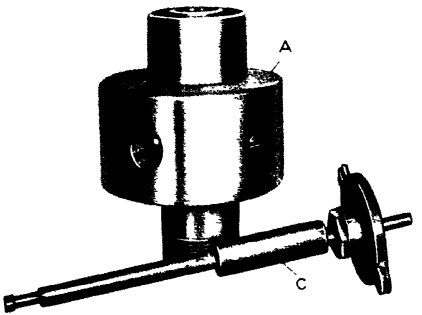

DETAIL OF DIFFERENTIAL PISTON AND CYLINDER

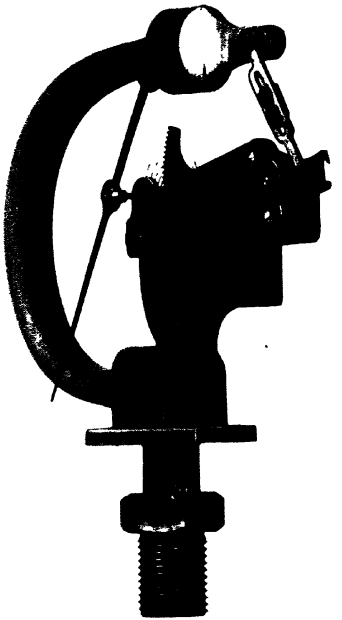

INTERNAL MECHANISM OF BOURDON GAUGE

PLATE 4

to ensure freedom of movement. For accurate work the magnifying mechanism may be dispensed with and the movement of the tube measured directly by means of a cathetometer.

Bourdon gauges are made with dials from 4 to 12 inches in diameter. As supplied by the makers, the zero mark usually corresponds to 1 atmosphere and a metal stop fixed in the dial plate serves to support the pointer in the zero position. When the gauge forms part of a system that has to be evacuated, the stop should be removed, as otherwise the needle will be forced on to it and be either bent or twisted on its axis. In this connexion it may be mentioned that the pointer is a forced fit on its axis and a special tool is required to remove it; no attempt should be made to alter its setting by manual twisting.

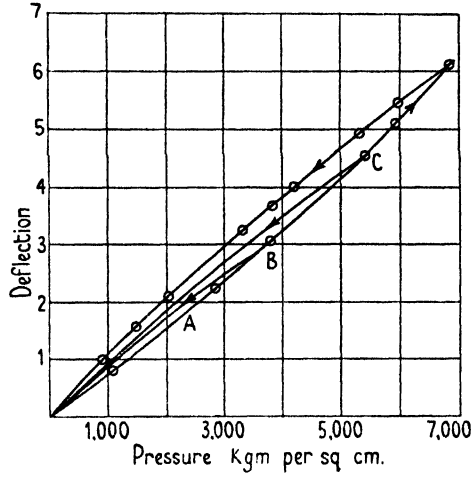

FIG. 52. Hysteresis effect with Bourdon gauge.

The extreme range of a Bourdon gauge is about 5,000 atmospheres, but above 2,000 atmospheres hysteresis effects come into prominence and special precautions have to be taken to avoid introducing large errors from this cause. Frequent calibrations against a primary gauge for both rising and falling pressures are necessary and the gauge should never be used for long periods at pressures of upwards of three-quarters of the nominal maximum pressure. When all precautions are taken the readings of a 50-atmosphere gauge will be correct to about 0·02 atmosphere, a 250-atmosphere gauge to 0·1 atmosphere, and a 1,000-atmosphere gauge to 0·5 atmosphere.

Fig. 52 shows the effect of applying four cycles of pressure to a Bourdon gauge from zero by steps to a maximum pressure of about 7,000 kg./cm.^{2} From O to A there is no appreciable difference between the readings for rising and falling pressure; at B hysteresis effects begin to appear, whilst at the highest pressure, they are very pronounced, the departure from linearity in the loop being about 40 per cent. [12].

Precautions in the use of the Bourdon Gauge. The commercial pattern of gauge has a metal dial and a brass dust-proof casing. In the event of a sudden failure of the tube there is therefore always the danger of the dial and its glass cover being shattered and causing damage. To minimize this hazard the back of the gauge is provided with a safety flap held in position by a light spring, or the back itself is made of very light gauge metal which will easily tear and so prevent any high pressure being developed in the casing. To enable these safety devices to work, the gauge must be mounted in such a way that the back is unsupported, and it is good practice to fix it high up so that in the event of a fracture flying fragments are not likely to cause personal injury to the observer.

High-pressure gas should never be suddenly released into a gauge as the adiabatic compression of the gas may give rise to a substantial increase in temperature. A number of instances are on record in which explosive mixtures of gases have become ignited through this cause and serious damage has resulted. A throttling device is therefore frequently fitted to gauges to prevent a sudden inrush of gas. In gauges for use with oxygen it is essential to have the gauge and all connexions entirely free from oil.

The Manganin Resistance Gauge

The suggestion that pressure might be measured in terms of the change of electrical resistance of a wire with pressure was made by Lisell [13], who found that the resistance of manganin (an alloy of approximate composition: copper = 80 to 84 per cent., manganese = 4 to 15 per cent., nickel = up to 12 per cent., and iron = difference) increased linearly with pressure up to 3,000 kg./cm.^{2} and that its temperature coefficient of resistance was so low that no special precautions were necessary in maintaining constancy of temperature.

Bridgman has redetermined the pressure coefficient of resistance [9] and finds the linear relationship holds to 10,000 kg./cm.^{2}, there being no measurable hysteresis or elastic after-effects. He has subsequently employed it in the construction of a secondary gauge for the measurement of hydrostatic pressures (by extrapolation) up to 21,000 kg./cm.^{2} The gauge consists essentially of a coil of double silk-covered manganin wire 0·005 in. in diameter and about 5 metres

long, giving a resistance of about 120 ohms. The wire is doubled and wound non-inductively on itself into a coreless toroid of about 1 cm. diameter. After winding the coil is seasoned by exposure to a temperature of 140° C. for from 6 to 10 hours. The best transmitting liquid to employ is petroleum ether. A gauge constructed in this way should have a long life provided changes of pressure are made slowly. In measuring the resistance added accuracy is obtained by introducing a second compensating coil in the thermostat with the pressure vessel.

The compactness of the manganin gauge renders it particularly well adapted to high-pressure work, although the variation in the properties of the alloy obtained from different sources necessitates the calibration of the coils against a primary gauge.

Gauges for Measuring and Recording Rapid Changes of Pressure

The time period, θ, of a pressure gauge may be expressed in terms of the weight of its elastic element, W, and the force, A, required to produce unit displacement in it, by the relation

$$\theta = 2\pi\sqrt{\frac{W}{Ag}}.$$

In practice there is a minimum value to W and a maximum value to A, since the gauge must possess sufficient mechanical strength to withstand the stresses set up by the sudden changes in pressure, and the movement of the elastic element, due to the action of the pressure, must be sufficiently large to be measured with accuracy. In order to obtain a smooth pressure-time record free from vibration the time period θ must be small in comparison with the time intervals to be measured, and hence the ratio W/A must be kept as small as possible; that is to say, the elastic element or spring must be relatively rigid.

Fig. 53 shows, in half-section, a Petavel gauge designed for recording continuously the rapid changes of pressure during solid and gaseous explosions in closed vessels [14]. The whole instrument is massively constructed and consists of a heavy steel body, B, screwed into the reaction vessel and containing the elastic element and other auxiliary fittings. The pressure to be measured acts on the exposed end of a solid steel piston, A, fitting closely into the gauge body, and is transmitted to a stiff steel tubular spring S, the far end of

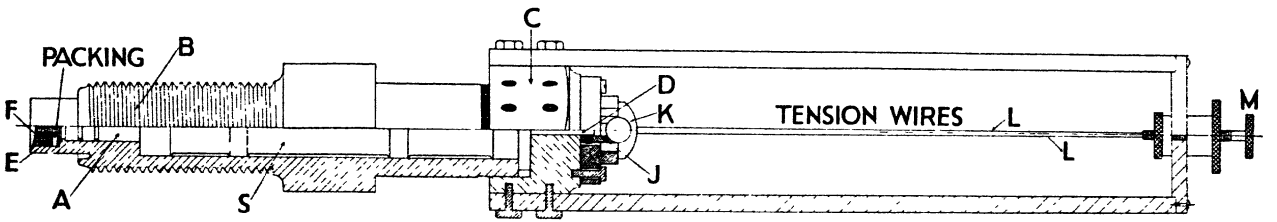

(*a*)

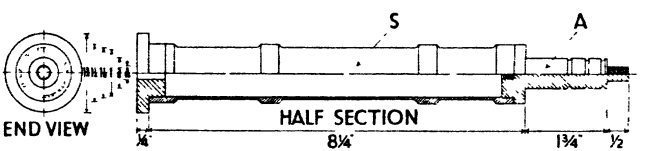

(*b*)

FIG. 53. Petavel recording manometer.

which is held rigid by means of the nut C. The contraction of the spring allows the piston to move forward a small distance, and the movement is transferred to an optical lever device situated on C by means of a steel rod D screwed into the end of the piston and passing axially through the spring. The movement of the beam of light reflected from the mirror K is photographed on a rotating drum camera, time intervals being recorded by means of a tuning-fork interrupting the beam. The dimensions of the piston and spring for a pressure range of 50 to 500 atmospheres are shown in the figure (inset).

In the use of this type of gauge considerable care is necessary to minimize friction between the moving parts of the magnifying mechanism and between the piston and cylinder. Frequent calibrations should be made by static or dynamic methods [15] against a primary gauge, and the sensitivity should be checked from time to time by comparing, for example, the pressure-time record of some suitable explosive mixture with a standard record obtained with the same mixture when the gauge is known to be working normally.

The Piezo-electric Effect

In 1880 F. and P. Curie observed that certain crystals when subjected to compressive or tensile stresses acquired an electrical charge, and they found that the magnitude of the charge was proportional to the applied force, that is,

$$Q = kP,$$

where Q is the charge in E.S. units, P is the applied force, and k is the piezo-electric constant of the crystal [16]. The effect appears to be due to an asymmetric arrangement of molecules of regular form, and all piezo-electric crystals are found to lack symmetry and to exhibit optical activity.

In 1919 Sir J. J. Thomson suggested that since the quantity of electricity liberated is proportional to the applied pressure the effect might be used to measure the variation of pressure with time in gas explosions [17], and two years later Keys described a form of gauge based upon this principle which he had successfully developed for the purpose [18]. The most suitable mineral to employ is quartz; the crystal is cut into thin disks with plain faces perpendicular to the electric axis and the disks are assembled with alternate positive and

negative faces in juxtaposition and separated by thin metal plates. The charge induced by the pressure is measured by a cathode-ray oscillograph [19].

A number of precautions have to be observed in using the gauge: the disks must be accurately ground and housed so that they are well supported and can withstand, without danger of fracture, the sudden application of high pressures, and care must be taken to keep them free from oil and moisture, both of which interfere with the action of the gauge.

BIBLIOGRAPHY

1. AMAGAT, *Ann. de Chim. et de Phys.* **19** (1880).
2. Commn. Univ. of Leiden, Nos. 44 and 70 (1898).
3. AMAGAT, *Ann. de Chim. et de Phys.* **29** (1893).
4. CAILLETET, *Ann. de Chim. et de Phys.* **19,** 386 (1880).
5. KEYES and DEWEY, *J. Opt. Soc. of America,* **14** (6), 491 (1927).
6. HOLBORN and SCHULTZE, *Ann. d. Phys.* **47,** 1095 (1915).
7. MICHELS, *Ann. d. Phys.* **72,** 285 (1923).
8. KEYES, *Proc. Amer. Acad.* **68,** 530 (1932–3).
9. BRIDGMAN, *Proc. Amer. Acad.* **47,** 321 (1912); MICHELS and LENSSEN, *Jour. Sci. Inst.* **11,** 345 (1934).
10. *Engineering,* 9 Jan. 1903, p. 31.
11. MICHELS, *Ann. d Phys.* **73,** 577 (1924).
12. BRIDGMAN, *Proc. Amer. Acad.* **44,** 201 (1909).
13. LISELL, Dissertation, Upsala, 1903.
14. PETAVEL, *Engineering,* 7 March 1903, p. 359.
15. BEALE and STANSFIELD, *The Engineer,* 26 Feb., 5 March, 1937.
16. F. and P. CURIE, *Compt. Rend.* **91** (1880).
17. J. J. THOMSON, *Engineering,* **107,** 543 (1919).
18. KEYS, *Phil. Mag.* **42,** 473 (1921).
19. E. MCFARLAND, *Ordnance and Gunnery.* J. Wiley & Sons, Inc. 1917.

PART II

THE PROPERTIES OF FLUIDS AT HIGH PRESSURES

VI

THE KINETIC THEORY AND THE IDEAL FLUID

Historical Note

THE early history of the kinetic theory is closely identified with that of the structure of matter and may be said to date from the middle of the seventeenth century. The credit of first appreciating the significance of the hypotheses or rather speculations of the ancient Indian and Grecian philosophers in regard to atomic structure properly belongs to Pierre Gassendi, who endeavoured to show that all material phenomena could be referred to the indestructible motion of rigid atoms moving in all directions through empty space [1].

About the same period (1659–82), largely owing to the inspiration of Robert Boyle, important researches upon the properties of air were in progress in England, as the result of which the relation between the pressure and volume of a gas at constant temperature was for the first time established. Boyle's earliest work on the subject appeared in 1661 and was entitled 'New Experiments, Physico-Mechanical, Touching the Spring of the Air and its Effects; made for the most part in a New Pneumatical Engine'; it is written in the form of a letter to Lord Dungarvan, dated 20 December 1659, and contains the description of a method for determining the relation of the density of air to the height of the column of mercury which it would support.

In consequence of this publication Richard Townley carried out some experiments from which he concluded that 'the pressures and expansions (of air) are in reciprocal proportions'; and in 1661 R. Hooke (2 August) and later in the same year W. Croone and Boyle (11 September) confirmed his results. It was not, however, until 1662 that Boyle, in the course of a controversy with Frances Linus, established by means of a remarkable series of experiments the law which is now known by his name. His work is described in Part II, Chap. V, of the *Defence of the Doctrine touching the Spring and Weight of the Air*, and he specifically states that up to that time

'an accurate Experiment of this nature... has not been made (that I know) by any man....' [2]

Neither Boyle nor his contemporaries appear at first to have divined the true cause of the elasticity of air; Boyle, indeed, compared air to a 'fleece of wool' or a dry sponge, and although he was aware of Descartes's suggestion that 'air is made up of innumerable flexible particles, which are so moved about by the motion of the celestial matter in which they swim, that each particle keeps those around it at a distance', he preferred to consider it as having the properties of a spring. Even as late as 1709 F. Hauksbee, one of the early Fellows of the Royal Society, compared air in respect of its elastic properties to a fine spring and endeavoured to show by some of the earliest recorded high-pressure experiments that it could 'by long and violent compression (to all appearances) be deprived of much of its Elastic Power' [3].

By the year 1678, however, Hooke had visualized the connexion between the atomic structure of a gas and its elasticity, and his statement of the elementary principles of the kinetic theory of gases is of considerable historic interest. In his own words [4]:

'The air then is a body consisting of particles so small as to be almost equal to the particles of the Heterogeneous fluid medium encompassing the earth. It is bounded but on one side, namely, towards the earth, and is indefinitely extended upward, being only hindred from flying away that way by its own gravity, (the cause of which I shall some other time explain). It consists of the same particles single and separated, of which water and other fluids do, conjoyned and compounded, and being made of particles exceeding small, its motion (to make its ballance with the rest of the earthy bodies) is exceeding swift, and its Vibrative Spaces exceeding large, comparative to the Vibrative Space of other terrestial bodies. I suppose that of the Air next the Earth in its natural state may be 8000 times greater than that of Steel, and above a thousand times greater than that of common water, and proportionably I suppose that its motion must be eight thousand times swifter than the former, and above a thousand times swifter than the latter. If therefore a quantity of this body be inclosed by a solid body, and that be so contrived as to compress it into less room, the motion thereof (supposing the heat the same) will continue the same, and consequently the Vibrations and Occursions will be increased in reciprocal proportion, that is if it be condensed into half the space the Vibrations and Occursions will be double in number. If into a quarter the Vibrations and Occursions will be quadruple, etc.

'Again, if the containing Vessel be so contrived as to leave it more space, the length of the Vibrations will be proportionally enlarged, and the number of Vibrations and Occursions will be reciprocally diminished, that is, if it be suffered to extend to twice its former dimensions, its Vibrations will be twice

as long, and the number of its Vibrations and Occursions will be fewer by half, and consequently its indeavour outward will be also weaker by half.

'The Explanations will serve *mutatis mutandis* for explaining the Spring of any other Body whatsoever.'

Some sixty years later D. Bernoulli arrived independently at very much the same conclusions in regard to the cause of the elasticity of the air, and furthermore endeavoured to modify Boyle's law so as to take into account the finite size of the molecules.

It may be said, therefore, that the kinetic theory was foreshadowed by Gassendi, Hooke, and Bernoulli, although its status as a theory had to await the discovery of the relation between heat and work. Following upon the measurement of the mechanical equivalent of heat by Joule in 1840 the foundations of the theory were laid in a series of classical papers by A. Kronig (1856), R. Clausius (1857), Clerk Maxwell (1859), and L. Boltzmann (1868).

In its present form the kinetic theory assumes the Newtonian dynamical laws to govern the transfer of energy by the translatory motion of atoms and molecules and thereby provides a mechanical analogy for the physical changes occurring in a system as the result of temperature and pressure variations; in particular it will be found adequately to explain many of the phenomena associated with matter at high pressures, and only in certain instances in which interatomic energy transfers are involved will it be necessary to introduce from the new dynamics the quantum-mechanical laws of restriction.

The Ideal Gas

In order to apply the kinetic theory to gaseous systems it is necessary to define in some detail the properties of the molecules of which the system is composed. The molecular model we adopt finally will depend, of course, upon the extent of our knowledge of the structure and behaviour of real molecules; but, in the first instance, it is best to start with the simplest possible assumptions, namely, that the molecules are hard elastic spheres of such size that they may be considered as points in comparison with the scale of intermolecular distances and that they are all alike and move freely in the space occupied by the gas in accordance with the Newtonian laws. It is also assumed that no appreciable forces of attraction or repulsion are exerted between them or by them on the walls of the containing vessel.

A gas composed of such molecules may be termed an 'ideal' or

'perfect' gas and its properties may be predicted by the kinetic theory. Thus, for example, the pressure it exerts may be calculated as follows:

Let n molecules of the gas be contained in a cubic enclosure maintained at constant temperature and let u be their mean speed and m their mass. They will move chaotically in all directions, but it may be assumed that at any instant of time one-third of them will be moving parallel to each of the three principal axes of the cube. A molecule colliding with the wall will have its direction of motion reversed and the change in its momentum will be $2mu$. If the volume of the cube is v and the unit of time is the second, a molecule will pass from side to side u/v times per second and the number of collisions it makes on one wall will be $u/2v$ per second. There will, therefore, be a total of $un/6v$ collisions per second on each wall and the change of molecular momentum per second resulting from collisions at an end wall will be $mnu^2/3v$. The rate of change of momentum of the molecules is equal to the total force exerted upon them or the total force which they exert upon the walls; that is, to the pressure p.

We may, therefore, write

$$p = \frac{mnu^2}{3v}$$

or

$$pv = \tfrac{1}{3}mnu^2; \tag{6.1}$$

and since the total kinetic energy ϵ of the gas is $\frac{1}{2}mnu^2$,

$$p = \tfrac{2}{3}n/v(\tfrac{1}{2}mu^2) = \tfrac{2}{3}\epsilon. \tag{6.2}$$

The pressure of an 'ideal' gas is therefore equal to two-thirds of the kinetic energy of translation of the molecule per unit volume.

Eqs. (6.1) and (6.2) embody all the so-called fundamental gas laws, namely:

Boyle's law: The volume of a gas at one uniform temperature varies inversely as the pressure.

Charles's law: The same temperature-rise produces in all gases the same increase in volume, provided always the pressure and mass are kept constant.

Avogadro's law: Equal volume of all gases, at the same temperature and pressure, contain the same number of molecules.

Dalton's law: The pressure exerted by a mixture of gases is equal to the sum of the pressures exerted separately by the individual components of the mixture.

It must be borne in mind that whilst these laws are always true for an 'ideal' fluid as defined above, they will only be true for 'real' fluids in circumstances in which their molecules behave substantially as ideal molecules.

The 'Ideal' Equation of State

The simple gas laws may be combined in a single equation called an 'equation of state' expressing the relation between the pressure, volume, and temperature of an 'ideal' gas. Thus if p and v are the pressure and volume of a given mass of gas maintained at a temperature of $T_1°$, and p_2 and v_2 the pressure and volume of the same mass of gas at another temperature $T_2°$, then

$$\frac{p_1 v_1}{T_1} = \frac{p_2 v_2}{T_2} = \text{a constant.} \tag{6.3}$$

At any given temperature and pressure the volume of the gas and consequently the value of the constant will be proportional to the quantity of gas taken; and since according to Avogadro's law the molecular weight in grams of all gases occupy the same volume under the same conditions of temperature and pressure, the constant for this quantity will have the same value for all gases, independent of the conditions under which they are measured; this value is usually denoted by R, and we may, therefore, write

$$pV = RT, \tag{6.4}$$

where V is the volume occupied by 1 gram-molecule of the gas at the absolute temperature T.

The Numerical Value of the Gas Constant R

The value of R depends upon the units in which the pressure and volume are measured. The volume occupied by 1 gram-molecule of an ideal gas at 0° C. and 1 atmosphere pressure is 22·410 litres, so that from (6.4)

$$R = \frac{1 \times 22{\cdot}41}{273} = 0{\cdot}08206 \text{ litre-atmospheres.}$$

If the gram and cubic centimetre are taken as units,

$$R = \frac{1033{\cdot}3 \times 22{\cdot}41}{273} = 84{,}760 \text{ gm.-cm.} \tag{6.5}$$

$$= 8{\cdot}315 \times 10^7 \text{ ergs;}$$

and since 1 gm.-cm. of mechanical energy is equivalent to 42,650 calories,

$$R = 1{\cdot}9869 \text{ calories.}$$

The Avogadro and Loschmidt Numbers

The number of molecules N_0 contained in a cubic centimetre of gas at 0° C. and 1 atmosphere pressure is independent of the chemical composition of the gas. It can be deduced from the value of the charge on the electron, from observations on the Brownian movement, from measurements of black-body radiation, and by various other methods.

The accepted value (1936) is

$$N_0 = 2{\cdot}705 \times 10^{19},$$

and for the number of molecules in 1 gram-molecule (N_1),

$$N_1 = 6{\cdot}062 \times 10^{23}.$$

The Pressure and Volume Coefficients of a Gas

The increase of pressure when a gas is heated at constant volume is given by

$$p_2 = p_1\{1+K_p(T_2-T_1)\}, \tag{6.6}$$

where K_p is the pressure coefficient of expansion of the gas over the range T_1 to T_2; and the increase of volume when a gas is heated at constant pressure is given by

$$v_2 = v_1\{1+K_v(T_2-T_1)\}, \tag{6.7}$$

where K_v is the volume coefficient of expansion for the temperature range T_1 to T_2.

For the ideal gas K_p and K_v are equal and both p and v vanish when $T_2-T_1 = -1/K$; for real gases at normal temperatures and pressure the coefficients are characteristic of the particular gas although the variations from gas to gas are comparatively small.

In Table 28 the coefficients for a number of gases over the temperature range 0–100° C. are tabulated.

TABLE 28. *The Pressure and Volume Coefficients of various Gases at Normal Pressures over the Temperature Range* 0–100° *C.*

Gas	*Pressure coefficient*	*Volume coefficient*
Ideal gas . .	0·0036617	0·0036617
Air . . .	0·003665	0·003671
Hydrogen . .	0·003663	0·003661
Carbon monoxide	0·003845	0·003669
Carbon dioxide .	0·003688	0·003728
Nitrous oxide .	0·003676	0·003719
Nitrogen . .	0·0036744	0·0036732

The magnitudes of both coefficients for real gases are found to depend upon temperature as may be seen from the following data for nitrogen:

Temperature range	K_p	K_v
0–20°	0·0036754	0·0036770
0–40°	0·0036752	0·0036750
0–100°	0·0036744	0·0036732

The pressure effect will be discussed in detail in Chapter IX.

Molecular Magnitudes

From the simple gas laws and the ideal molecular model the values of the molecular speeds, collision frequencies, molecular diameters, and certain other constants of real gases may be calculated, approximately, using the equations summarized below; for the complete derivation of these equations reference should be made to a standard treatise on the kinetic theory or to the original papers.

The Root-mean-square Speed

According to a fundamental postulate of the kinetic theory the temperature of a body is determined by the average speed of the translatory motion of its molecules (u). By combining eqs. (6.1) and (6.4),

$$RT = \tfrac{1}{3}nmu^2, \tag{6.8}$$

and since R, n, and m are constants,

$$u^2 = kT, \tag{6.9}$$

where k is a constant.

The mean molecular speed therefore depends only on the temperature, and the mean kinetic energy of the molecules of a gas is proportional to its temperature; it follows also that at the same temperature the mean kinetic energy of the molecules of all gases obeying the simple gas laws is the same.

The value of the mean molecular speed is given by (6.1):

$$u = \sqrt{\frac{3pv}{nm}},$$

or, since nm/v is the density of the gas, by

$$u = \sqrt{\frac{3p}{\rho}}. \tag{6.10}$$

The speed so calculated is that with which each of the molecules would have to move in order that their total kinetic energy would be the same as that actually possessed by the gas.

If, for example, u_1, u_2, u_3,..., u_n are the individual speeds of the molecules at any moment, then

$$\tfrac{1}{2}nmu^2 = \tfrac{1}{2}m(u_1^2+u_2^2+u_3^2+\ldots+u_n^2),$$

or

$$u^2 = \frac{1}{n}(u_1^2+u_2^2+u_3^2+\ldots+u_n^2),$$

and u will equal the square root of the arithmetic mean of the squares of the individual speeds; it is usually known as the *root-mean-square speed.*

If the average speed of the molecules is u_A it can be shown that

$$u_A = \sqrt{\frac{8u}{3\pi}} = 0{\cdot}92u.$$

The Average Number of Collisions in Unit Time between Molecules and the Mean Free Path

It is evident from the rates of gaseous diffusion and of heat conduction that the molecules of a gas cannot travel over very long distances between successive collisions; thus the mean free path (L) will depend upon the average number of collisions in unit time and will be inversely proportional to the number of molecules per unit volume of the gas.

The number of collisions Z suffered by any one molecule in unit time is given by

$$Z = \frac{4\pi n\sigma^2 u}{3v}, \tag{6.11}$$

and the mean free path L by

$$L = \frac{v}{\frac{4}{3}\pi n\sigma^2}. \tag{6.12}$$

In the derivation of these expressions the molecules are assumed to be spherical and to have an effective finite diameter σ; and a collision is said to occur whenever the centres of two molecules approach to within a distance σ of one another. In the volume v of gas there will be regions surrounding the individual molecules and the walls of the container into which the centre of a molecule is unable to penetrate; and to simplify the calculations the collisions experienced by any one molecule are considered as the collisions of

a point at its centre with one of the surfaces bounding such a region of exclusion. These regions are spheres of radius σ surrounding each of the remaining molecules and a region, negligible for most purposes, bounded by the inner surface of the container and a parallel surface situated at a distance $\frac{1}{2}\sigma$ from it. The aggregate volume of these spheres is $\frac{4}{3}\pi n\sigma^3$; but since in a binary collision between a point representing the centre of a molecule and a sphere of exclusion only that half of the sphere which is directed towards the line of relative motion of sphere and point is active in excluding the point, the effective aggregate volume of the regions of exclusion is only $\frac{2}{3}\pi n\sigma^3$. This quantity is called the *co-volume* and is usually denoted by the letter b; it is equal in magnitude to four times the aggregate sum of the volumes of the molecule.†

It is also assumed that the molecules are moving with equal speeds (the root-mean-square speed) in all directions and that the relative speed of approach of two molecules is the difference of their speeds when referred to the same reference system. It is evident, however, that as a result of collisions in a gas the speeds of the individual molecules are continually changing, and Maxwell has shown that in a system consisting of elastic spheres there will be a statistical equilibrium such that the number dn of spheres out of a total of n having speeds lying between s and $s+dv$ is given by the relation

$$dn = \frac{4n}{a^3\sqrt{\pi}} s^2\, dv\, .\, e^{-s^2/a^2}$$

where a is the most probable speed. The most probable speed, the average speed, and the root-mean-square speed are related to one another as $1 : 2/\sqrt{\pi} : \sqrt{(3/2)}$.

If the Maxwellian distribution be taken into account, the corrected expression for the number of collisions in unit time and the mean free path are

$$Z = \frac{\sqrt{2}\,\pi n\sigma^2 u}{v} \tag{6.13}$$

and

$$L = \frac{v}{\sqrt{2}\,\pi n\sigma^2}. \tag{6.14}$$

From (6.13) the total number of molecules entering into collision in unit time is $\sqrt{2}\,\pi\sigma^2 u n^2$. Eq. (6.14) shows that the mean free path

† b is the co-volume of van der Waals' equation of state; the method used in deriving it will be found in Jeans, *Dynamical Theory of Gases*, 1925, p. 126 et seq. See also Chapter VIII.

is inversely proportional to the molecular density (n/v) and to the square of the molecular diameter; and since the pressure exerted by an ideal gas at constant temperature is proportional to its molecular density (6.1) the mean free path is inversely proportional to the pressure.

BIBLIOGRAPHY

1. LASSWITZ, *Pogg. Ann.* **153**, 373 (1874).
2. G. F. RODWELL, *Chem. News*, **9**, 14, 26, 50, 242 (1864); **10**, 74 (1865); **11**, 74 (1865).
3. HAUKSBEE, *Physico-Mechanical Experiments on Various Subjects.* London, 1709. A copy of this book is in the library of the Royal Society.
4. HOOKE, *Lectures de Potentia Restitutiva, or Spring.* London, 1678.
5. BERNOULLI, *Hydronamica.* Argentoria, 1738.

VII

THE PRESSURE-VOLUME-TEMPERATURE RELATIONSHIPS OF REAL GASES. THE GENERAL FORM OF THE ISOTHERMS AND ISOCHORES OF REAL GASES

EQUATIONS of state representing the functional relationship between the pressure, volume, and temperature of a fluid may be written

$$f(p, V, T) = 0,$$

from which

$$p = f(V, T); \tag{7.1}$$

or in general forms [1]

$$p = T\psi(V) - \phi(V) - F(V, T),$$

and

$$pV = RT + \frac{1}{V}f_1(T) + \frac{1}{V^2}f_2(T) + \frac{1}{V^3}f_3(T) + \ldots, \tag{7.2}$$

pressure being expressed as an explicit function of volume and temperature. The specific forms of these functions depends upon the properties associated with the particular hypothetical molecular model used in deriving them, and their validity is assessed by the degree of accuracy with which they reproduce experimental data covering a wide range of conditions.

For an ideal gas as defined in Chapter VI, (7.2) becomes $p = RT/V$, and, employing rectangular axes, the isothermal curves showing the relation between pressure and volume consist of a system of rectangular hyperbolas. All real gases at low pressures and at temperatures sufficiently far above their respective critical temperatures approximate in behaviour to an ideal gas; but as critical conditions are approached the similarity gradually disappears, and characteristic features indicative of a more complicated relationship become prominent.

We owe to Thomas Andrews the first clear account of the sequence of events taking place when a gas undergoes compression isothermally in the neighbourhood of its critical temperature and to van der Waals the first satisfactory attempt at a quantitative interpretation of the observed phenomena. In the Bakerian Lecture delivered before the Royal Society on 17 June 1869, entitled 'On the Continuity of the Gaseous and Liquid States of Matter', Andrews

described his classical experiments with carbon dioxide and illustrated his results by the series of isothermals reproduced in Fig. 54.

The curves relate to the volume changes of a given mass of the gas compressed isothermally at various temperatures between 13·1° and 48·1° C. in a calibrated capillary glass tube so mounted as to

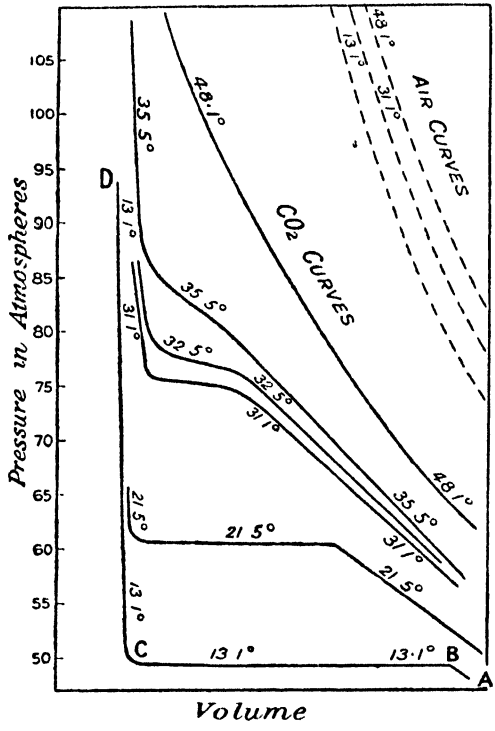

FIG. 54. Andrews's isotherms for carbon dioxide.

enable the progress of the compression to be observed visually; the results of a parallel series of observations with air contained in a second tube are included for comparison. Referring to the figure it will be seen that the isotherms differ considerably amongst themselves; at 48·1°, for example, the curve is smooth and similar in character to the air isotherms, thus indicating that at this temperature carbon dioxide behaves as a permanent gas approximately in accordance with Boyle's law. At 13·1°, on the other hand, the curve is discontinuous and is made up of three well-defined parts, namely, (i) a section AB in which the pressure varies inversely as the volume, followed by (ii) a section BC in which the pressure remains substan-

tially constant at about 49 atmospheres whilst the volume diminishes, and (iii) a section *CD* in which further increase of pressure produces only a comparatively slight diminution in volume. Andrews observed that at a certain pressure denoted by the ordinate of the point *B* liquefaction of the gas commenced and in passing from *B* to *C* the proportion of the liquid progressively increased until at *C* the process was complete. At 21·5° and 31·1° the isotherms preserve the same characteristics, albeit as the temperature increases, the horizontal section of the curve, corresponding with the coexistence of the liquid and gaseous phases, narrows until at a temperature slightly higher than 31·1° it disappears altogether; at 32·5° and upwards the system is homogeneous and gaseous at all pressures. Between 31·1° and 32·5° there is a definite temperature called the *critical temperature* at which the corresponding isotherm just ceases to show discontinuity and at which no change of state is observable no matter how high the pressure is raised. From such compressibility data a three-dimensional figure can be constructed representing the conditions of equilibrium in the solid, liquid, and gaseous phases. Thus, in Fig. 55 A, *ABC* is the isotherm at the critical temperature and all points contained in the area above this curve relate to the homogeneous gas phase. The curve *DBF* bounds the horizontal sections of the isotherms below the critical temperature and defines the conditions under which vapour and liquid coexist in equilibrium; the portion *BD* of this curve is known as the *boiling-point curve* and represents the conditions under which vaporization is first observed in gradually reducing the pressure; similarly, the portion *BF* is known as the saturated-vapour curve.

The region to the left of *CBD* corresponds with the homogeneous liquid phase and that enclosed by the curves *AB* and *BF* the vapour phase as distinct from the gas phase.

The observations of Andrews on the critical point are of considerable interest and may be given in his own words (loc. cit., pp. 575–6):

'On partially liquefying carbonic acid by pressure alone, and gradually raising at the same time the temperature to 88° Fahr., the surface of demarcation between the liquid and gas became fainter, lost its curvature, and at last disappeared. The space was then occupied by a homogeneous fluid, which exhibited, when the pressure was suddenly diminished or the temperature slightly lowered, a peculiar appearance of moving or flickering striae throughout its entire mass. At temperatures above 88° no apparent liquefaction of carbonic acid, or separation into two distinct forms of matter, could be effected, even when a pressure of 300 or 400 atmospheres was applied.'

Later observations on the critical point have shown that a blue opalescent mist appears in the tube immediately before the meniscus of the liquid takes form, when the temperature of the gas is gradually

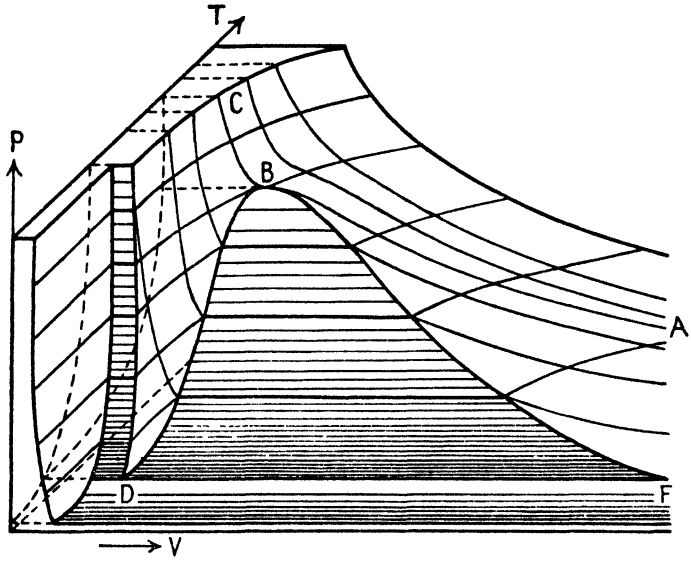

FIG. 55A. Isotherms and isochores of a typical fluid.

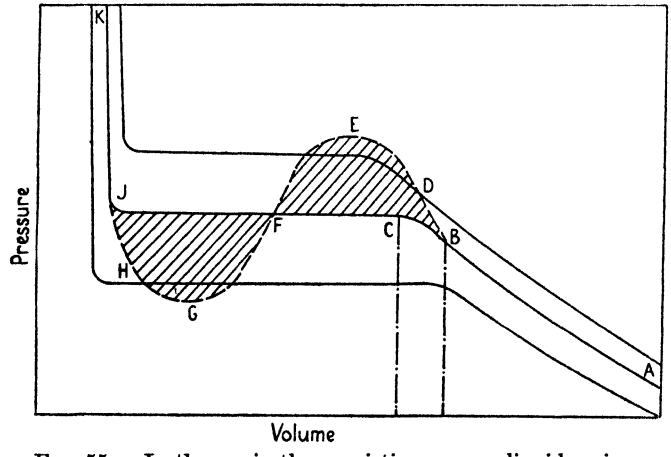

FIG. 55B. Isotherms in the coexisting vapour-liquid region.

lowered, or immediately after it disappears when the temperature is raised. According to von Smoluchowsky [2] this effect is due to inequalities in the density of the medium due to the accidental aggregation of molecules as the result of molecular collisions; the

aggregates are continually forming and disintegrating and by causing a lateral diffraction of light are responsible for the observed opalescence [3].

Traube [4] and Teichner [5] have found evidence of a density gradient in a two-phase one-component system heated slightly above the critical temperature, and Winkler and Maass [6] have shown that when liquid ethylene is heated above its critical temperature, not only is there a difference in density above and below the point where the meniscus was last seen, but there is a discontinuity in the density gradient at this point. They also find that whilst the density difference cannot be destroyed by mechanical stirring, it diminishes with further rise of temperature or diminution of pressure and eventually becomes zero. In no case was it found that the higher density in the lower part of the medium would spontaneously recur after it had once been destroyed.

According to Winkler and Maass the density difference is far greater than could be accounted for by the weight of the medium itself, and they suggest that the liquid state persists above the temperature at which the visible meniscus disappears; this would imply the existence of a critical temperature region in which the structure of the liquid is rapidly breaking down.

In determining the critical temperature by observation of the disappearance of the meniscus the thermal history of the material immediately preceding the observation must be considered. Thus one may define the critical temperature as 'the temperature at which the meniscus becomes completely invisible on increasing the temperature after the material has been previously cooled at least 1° C. below the critical temperature' [6].

The Specific Volume

The specific volume of a vapour, or its vapour density at the point of saturation, is a quantity of considerable importance in thermodynamics in connexion with the derivation of the equations of equilibrium in single-component and binary systems. It may be measured by Andrews's method, the specific volume being the volume defined by the point of intersection of the vapour isotherm (Fig. 54) with the horizontal line of constant vapour pressure, or by the method described in the next section.

Considerable care, however, is necessary in making the measure-

ments. The work of Herwig, Wüllner and Grotrian, Battelli [7], and others has shown that the pressure at which mist first appears on progressively compressing a vapour is always a little less than the maximum pressure of the saturated vapour. That is to say, there is no abrupt change in curvature of the isotherm on passing from the vapour to the coexisting vapour-liquid region. The specific volume may, therefore, be the volume corresponding with the point B or C on the isotherm (Fig. 55 B) according to the method used. Such an effect might, of course, be due to the presence of traces of impurities in the vapour; but the experiments of Battelli, in which extraordinary care was taken to eliminate all impurities, leave little doubt but that the effect is a real one. The recent work of Meyer [8] on the critical state also gives theoretical reasons for believing that the isotherms are continuous in this region.

The Densities of Coexisting Liquid and Gas—The Law of Cailletet and Mathias

The system defined by the horizontal section of the isotherm consists of liquid in contact with its saturated vapours; with increase of temperature the densities of the liquid and vapour diminish and increase, respectively, until at the critical temperature they are equal. On plotting the densities of the two phases against temperature a continuous curve (Fig. 56) having a maximum at the critical temperature is obtained; and Cailletet and Mathias [9] pointed out that the mean densities fall on a straight line which they called the 'rectilinear diameter', the equation to which may be written

$$S_t = S_0 + \alpha t, \tag{7.3}$$

where S_0 and S_t are the mean densities at 0° and $t°$, respectively, and α is a constant.

In order to test this law S. Young [10] examined some thirty substances and found that whilst (7.3) holds accurately for carbon dioxide, pentane, and probably *n*-hexane, generally speaking there is a slight curvature of the rectilinear diameter, and the experimental data are more accurately represented by the equation

$$S_t = S_0 + \alpha t + \beta t^2. \tag{7.4}$$

Recently Lowry and Erickson [11] have carried out an accurate redetermination of the densities of liquid and gaseous carbon dioxide

over the temperature range −5·8° to 22·9° C.; and since their method is similar to that used by Young (loc. cit.) and is of general applica-

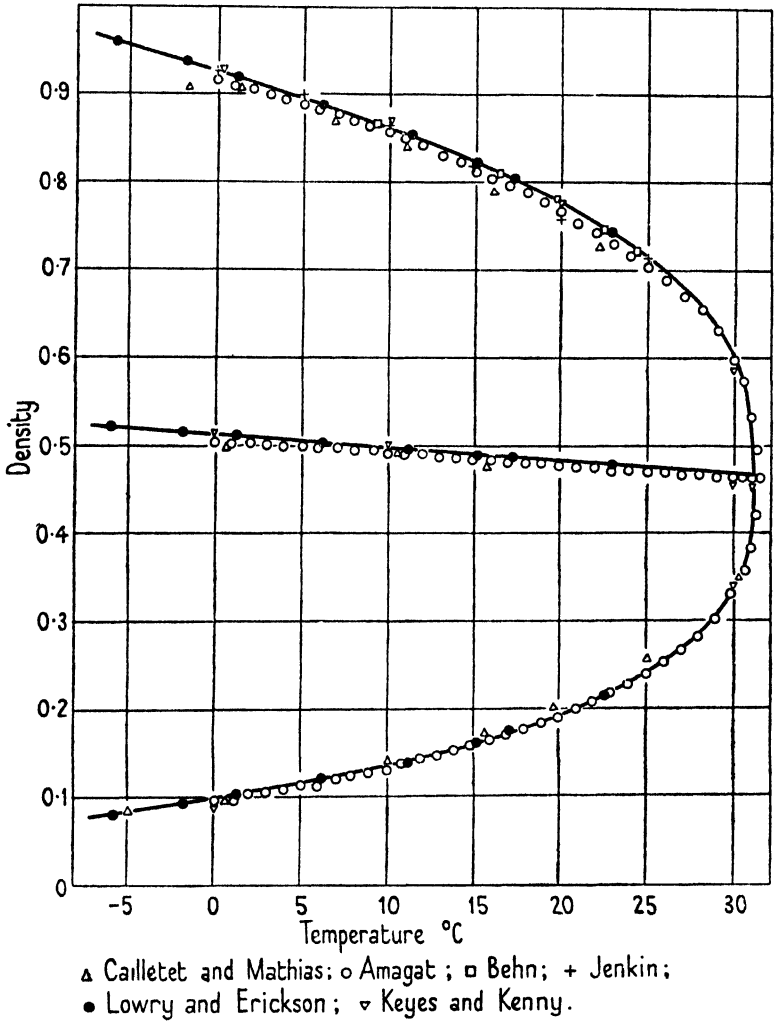

FIG. 56. Density of coexisting liquid and gaseous carbon dioxide.

tion, a brief account of the experimental details will serve to illustrate the technique employed.

The method consists in sealing up different weights of carbon dioxide in calibrated glass tubes of sufficient strength to withstand the pressures developed, and measuring the position of the line of demarcation between the two phases at constant temperature.

If W be the total weight of carbon dioxide, v_l and v_g, d_l and d_g the volumes and densities of the liquid and gaseous phases, respectively,

$$W = v_l d_l + v_g d_g. \tag{7.5}$$

Since d_l and d_g are both unknown, it is necessary to make duplicate experiments using tubes either of different total volume or containing different total weights of material; W is obtained by weighing the tubes at the end of an experiment.

The experimental error of the method is largely one of reading length. As used by Young, the lengths were read only to 0·1 mm. and the error under different conditions ranged from 0·5 to 6 per cent. In Lowry and Erickson's work they were read with a travelling microscope to 0·002 mm. and a correction was made for the volume of the liquid meniscus which otherwise would be included in the gas volume. Corrections based upon direct measurements were also applied to the volume of the tube for distortion introduced on sealing the ends. Readings were taken for both rising and falling temperatures, the lengths so measured agreeing on the average to 0·020 mm. In order to facilitate the attainment of thermal equilibrium a small rod of permalloy was sealed in the tube and stirring with it was effected by means of an electromagnet.

Calculations showed that changes in the volume of the tube due to expansion caused by (*a*) internal pressure and (*b*) temperature would amount to only about 0·02 per cent. in each case and could be neglected. Even with the above-mentioned corrections and precautions, however, analyses of the data obtained in three separate runs indicated that the average deviation of a single observation for the liquid density was $\pm 0{\cdot}1$ per cent.; and since an error in determining the liquid density introduced a larger error, opposite in sign, in the determination of the gas density, the average deviation of a single observation of gas density was greater and amounted to 0·7 per cent. It was estimated, however, that mathematical analysis of the data of this investigation permitted values of the densities of coexisting liquid and gaseous carbon dioxide to be calculated with an accuracy of $\pm 0{\cdot}1$ per cent. over the temperature range $-5{\cdot}8°$ to $22{\cdot}9°$ C.

The data obtained are given in Table 29.

The equation to the rectilinear diameter is given in the form

$$S_t = S_c + \alpha(t_c - t), \tag{7.6}$$

where S_t is the mean density at temperature t, S_c the density at the critical temperature t_c, and α is a constant. The critical density was obtained by plotting S_t (i.e. $(d_l+d_g)/2$) against t and extrapolating the straight line thus obtained to the critical temperature. Taking the critical temperature as 31·0°, S_c and α were found to be 0·4683

TABLE 29. *The Densities of Coexisting Liquid and Gaseous Carbon Dioxide*

	d_l		d_g		$(d_l+d_g)/2$	
t, °C.	*Obs.*	*Calc.*	*Obs.*	*Calc.*	*Obs.*	*Calc.*
22·9	0·7422	0·7448	0·2163	0·2152	0·4793	0·4800
17·2	0·8045	0·8044	0·1721	0·1720	0·4883	0·4882
15·2	0·8216	0·8216	0·1607	0·1606	0·4912	0·4911
11·2	0·8547	0·8535	0·1390	0·1401	0·4969	0·4968
6·2	0·8878	0·8886	0·1217	0·1196	0·5048	0·5041
1·2	0·9198	0·9201	0·1029	0·1025	0·5114	0·5113
−1·8	0·9378	0·9376	0·0940	0·0936	0·5159	0·5156
−5·8	0·9604	0·9598	0·0803	0·0828	0·5204	0·5213

and 0·001442 respectively, the equation to the rectilinear diameter being

$$S_l = 0{\cdot}4683+0{\cdot}001442(t_c-t). \qquad (7.7)$$

Since the liquid density is just as much higher as the gas density is lower than their average, the equation giving either as a function of temperature can be obtained by addition to or subtraction from (7.7) an additional term which takes the form $a\sqrt[n]{(t_c-t)}$, where $n = 3{\cdot}000$ and a is a constant the value of which is found to be $\pm 0{\cdot}1318$.

The equations for the liquid and gaseous densities are therefore

$$d_l = 0{\cdot}4683+0{\cdot}001442(t_c-t)+0{\cdot}1318\sqrt[3]{(t_c-t)} \qquad (7.8)$$

and

$$d_g = 0{\cdot}4683+0{\cdot}001442(t_c-t)-0{\cdot}1318\sqrt[3]{(t_c-t)}. \qquad (7.9)$$

The values of d_l and d_g given by these equations are included in Table 29.

The curves in Fig. 56 are also drawn to fit (7.7), (7.8), and (7.9), the points referring to the data of Amagat [12], Behn [13], and Lowry and Erickson. It may be noted that according to Amagat's data $t_c = 31{\cdot}35$ and $d_l = d_g = 0{\cdot}464$.

The Continuity of the Fluid State of Matter

Andrews's experimental results reveal an abrupt change in the slope of an isotherm corresponding with the formation of a liquid phase, and over the region where liquid and vapour coexist in equilibrium the isotherm is horizontal.

This part of the isotherm is of considerable theoretical interest. Two years after the publication of the results referred to, a paper by Professor James Thomson in the *Proceedings of the Royal Society*, entitled 'Considerations on the Abrupt Change at Boiling or Con-

densing in reference to the Continuity of the Fluid State of Matter' [14], embodied an important suggestion in regard to the continuity of the fluid state which can best be given in the author's own words.

'Now it will be my chief object in the present paper to state and support a view which has occurred to me, according to which it appears probable that, although there be a practical breach of continuity in crossing the line of boiling-points from liquid to gas or from gas to liquid, there may exist, in the nature of things, a theoretical continuity across the breach having some real and true significance. This theoretical continuity, from the ordinary liquid state to the ordinary gaseous state, must be supposed to be such as to have the various courses passing through conditions of pressure, temperature and volume in unstable equilibrium for any fluid matter theoretically conceived as homogeneously distributed while passing through the intermediate conditions. Such courses of transition, passing through unstable conditions, must be regarded as being impossible to be brought about throughout entire masses of fluids dealt with in any physical operations. Whether in an extremely thin lamina of gradual transition from a liquid to its own gas, in which it is to be noticed the substance would not be homogeneously distributed, conditions may exist in a stable state having some kind of correspondence with the unstable conditions here theoretically conceived, will be a question suggested at the close of the paper in connexion with some allied considerations.

'It is first to be observed that the ordinary liquid state does not necessarily cease abruptly at the line of boiling-points, as it is well known that liquids may, with due precautions, be heated considerably beyond the boiling temperature for the pressure to which they are exposed.'

In a footnote Thomson states: 'It has been found by Dufour (*Bib. Universelle*, Archives, 1861, Vol. XII, "Recherches sur l'ébullition des Liquides") that globules of water floating immersed in oil, so as neither to be in contact with any solid nor with any gaseous body, may, under atmospheric pressure, be raised to various temperatures far above the ordinary boiling-point, and occasionally to so high a temperature as 178° C. without boiling.' The phenomenon thus referred to would be indicated on an isothermal diagram (see Fig. 55 B) by an extension of the curve KJ representing the relation between pressure and volume of the liquid to some such point as H when the liquid would be in a 'super-heated' condition; an analogous state of 'super-cooling' would be represented by an extension of the curve AB to D, thereby crossing higher temperature isotherms, and Thomson suggested that the continuity might be preserved by joining D to H by the curve $BDEFGHJ$. Thus he says:

'The overhanging part of the curve from E to G seems to represent a state in which there would be some kind of unstable equilibrium; and so, although the curve there appears to have some important theoretical significance, yet

the states represented by its various points would be unattainable throughout any ordinary mass of the fluid. It seems to represent conditions of coexistent temperature, pressure and volume in which, if all parts of a mass of fluid were placed, it would be in equilibrium, but out of which it would be led to rush, partly into the rarer state of gas, and partly into the denser state of liquid, by the slightest inequality of temperature or of density in any part relative to other parts.'

Isochors (Isometrics)

The general equation (7.2) expressing the relation between the pressure, absolute temperature, and volume of a gaseous system may be written

$$p' = p + F(V, T) = T\psi(V) - \phi(V), \tag{7.10}$$

where p' may be defined as the 'corrected' pressure. If the volume is maintained constant the functions $\psi(V)$ and $\phi(V)$ will necessarily be constant and the equation may be written in the form originally proposed by Ramsay and Young [15], namely,

$$p = bT - a. \tag{7.11}$$

In this equation it should be noted that p is the observed pressure and b and a are constants depending upon the nature of the fluid and on the volume.† Now if from a system of isothermal curves such as those in Fig. 54 the pressures corresponding to a series of definite volumes are read off and are plotted against the absolute temperatures, a series of straight or slightly curved lines may be drawn through the points of equal volume (Fig. 57). These lines are known as isochors (ἴσος, equal, and χωρεῖν, to contain) or isometrics; for an ideal gas they would all radiate from zero pressure and would approach the vertical with diminution of volume, the tangents of the angles formed by them with the horizontal line of zero pressure would be proportional to C in the equation $p = CT$ (Gay Lussac's law), where C varies inversely as the volume. For real gases and vapours conforming to (7.11) the isochoric lines cut the vertical line representing the absolute zero of temperature at intercepts a, and are inclined to the horizontal line of zero pressure at angles whose tangents are given by b. The constant a is the negative pressure corresponding to the absolute zero of temperature.

The p, v, T relationships of ethyl ether have been examined in detail by Ramsay and Young, and in a paper 'On the Continuous

† Amagat (*Compt. Rend.* **94**, 487) has stated a similar relation for gases; his data are, however, imperfect, and he expressly states that the law does not apply to liquids.

Transitions from the Liquid to the Gaseous State of Matter at all Temperatures' [16] data are given covering a wide range of temperatures and volumes together with the isochoric diagram reproduced in Fig. 58.† In order to understand the full significance of the diagram attention may be drawn to some of the more important features embodied in it. Beginning at the largest volume (300 c.c.), it will

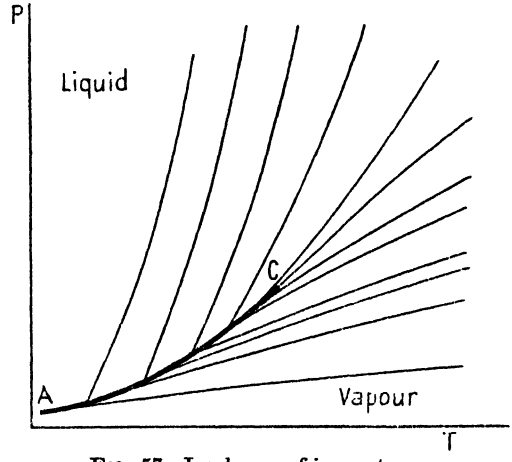

FIG. 57. Isochores of isopentane.

be noticed that two adjacent isochors intersect at a point, as regards pressure and temperature, not far above zero, but with decreasing volumes the points of intersection occur at higher and rapidly increasing temperature and slowly increasing pressure until the critical volume is reached. At volumes smaller than the critical, however, the points of intersection of adjacent isochors occur at lower and decreasing temperatures and pressures, the former decreasing slowly but the latter with great rapidity and soon extending into the region of negative pressures.

It is evident from the diagram that each isochor between the largest volume and the critical volume is the tangent of a curve *ABC* representing the relations of pressure to temperature, and each isochor below the critical volume is a tangent to another curve *CDE*, also exhibiting the like relations. Neither of these curves is identical with the vapour-pressure curve which lies in the area between them and is indicated on the diagram by the dotted curve.

† Corresponding data for methyl and ethyl alcohols, acetic and nitric peroxide are given by the same authors in *Phil. Mag.* **24**, 196 (1887).

In the area bounded by the two curves ABC and CDE and the line of zero pressure, each isochor is cut by two others at every point along its whole length, but outside this area above the line of zero pressure no two lines cut one another, and below the line of zero pressure each isochor is cut at each point by one other. It is therefore

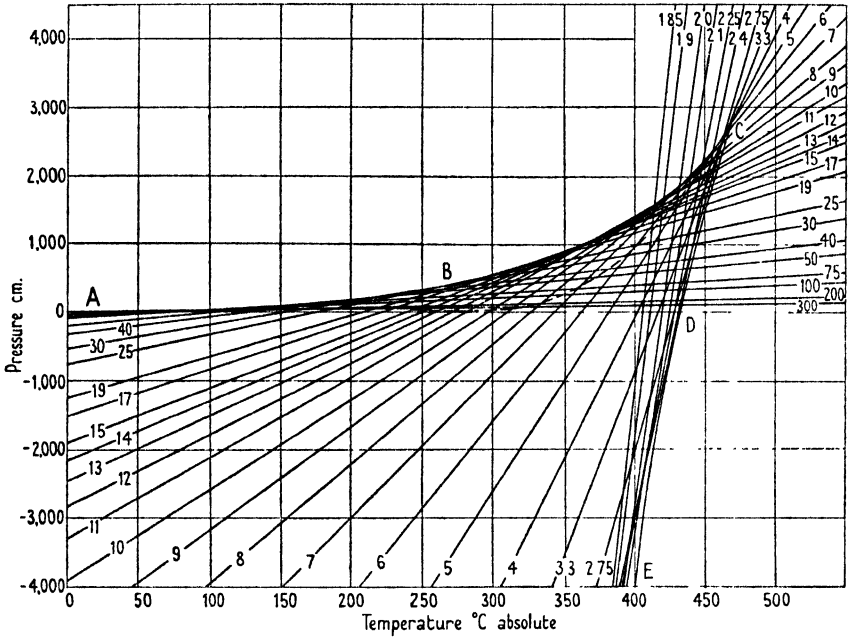

FIG. 58. Isochores of ethyl ether.

clear that in the region ACD a given mass of the substance may occupy three different volumes at the same temperature and pressure, the condition being that represented in the isothermal diagram (see Fig. 54) by the region in which a change from the vapour to the liquid phase is occurring.

From the isochoric diagram values of the constants a and b of (7.11) may be obtained for the various volumes, and, keeping T constant, the isothermals for ether may then be calculated and compared with the experimentally determined curves. The advantage of adopting this procedure is that isothermals may be drawn in the region where experimental measurements are impossible. Thus, on referring to Fig. 59, in which the calculated isothermals for ether are drawn, it will be seen that in any particular instance (at temperatures below the critical temperature) after rise of pressure and decrease

of volume have proceeded for some distance, the curves bend downwards according to the hypotheses of J. Thomson, the volume decreasing with fall of pressure. The pressure continues to fall and may reach large negative values indicative of a state of tension in the fluid. Thus Ramsay and Young note that at 0° the isothermal at a volume of 1·85 c.c. per gm. 'reaches the almost incredibly great tension of —271,700 mm.; and it has at that volume... by no means reached its limit. At still smaller volumes the tension would doubtless still increase, until the curve turned, and further decrease of volume would be represented, as it is at higher temperatures, by increase of pressure.'

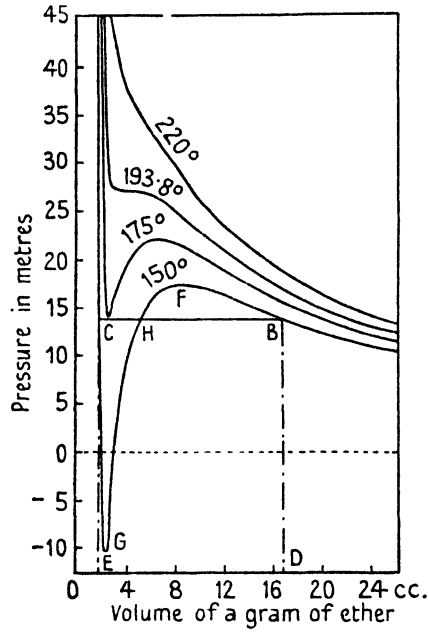

FIG. 59. Isotherms of ethyl ether.

It also follows that since under ordinary conditions the passage from vapour to liquid occurs without change of pressure, the isotherm in this region being a horizontal straight line (*BC* in Fig. 59), the area *BCDE* will represent graphically the external work performed in evaporating the liquid. If therefore the change from liquid to vapour occurs continuously as in the calculated isotherm, the area *CGH* enclosed by the isothermal line below the vapour-pressure line must be equal to the area *HFB* above the isothermal line.

As gases cannot be submitted to a negative pressure, those portions of an isothermal curve representing the truly gaseous condition of matter can never extend below the horizontal line of zero pressure. Referring again to Fig. 58, the curve *AC* represents the pressures corresponding to the apices of each isothermal line, and the curve *EDC* those corresponding to the inferior apices. These two curves and the saturated-vapour curve meet at *C*, which is the critical point, and the critical isochor forms a tangent to the vapour-pressure curve at the critical temperature.

The Measurement of the Compressibility of Gases—Historical

Although the validity of Boyle's law remained unquestioned until towards the end of the eighteenth century, several attempts were made during the intervening period to test its accuracy at high pressure [17]. Boyle himself believed that above 300 cm. of mercury pressure air was less compressible than at atmospheric pressure, but no convincing experimental evidence of any systematic deviations from the law was obtained until 1799 when M. van Marum [18] drew attention to the behaviour of ammonia. The principal difficulty encountered in such work is connected with the accurate measurement of small volumes of gas, and the results of all the early workers showed a lack of concordance which rendered it impossible to draw any definite conclusions from them. Oersted and Suensson in 1826 and Despretz [19] a year later published the results of experiments upon the comparative compressibilities of various gases, but whereas the former investigators still remained in some doubt as to whether the variations observed were real or were due to experimental errors, the latter obtained data which indicated unmistakably that deviations from the law existed and were the rule rather than the exception.

The method employed by Despretz and later by Pouillet, Amagat, and others was to compare the compressibilities of a number of gases by enclosing them in glass tubes over mercury and measuring the changes in volume (at constant temperature) on increasing the pressure. Despretz concluded that carbonic acid and ammonia were more compressible than air and that, of all gases examined, hydrogen was the least compressed at high pressures. C. Pouillet [20], using a similar method, showed that oxygen, hydrogen, and nitrogen were equally compressible up to 100 atmospheres and that carbonic acid and ammonia were far more compressible than the elementary gases.

The first direct measurements of compressibility over a comparatively wide pressure range were made by Dulong and Arago [21] in 1830, and although their results were inconclusive, it is of interest to note that they employed for the first time a long open column of mercury to produce and measure pressures of the order of 27 atmospheres. Their work was followed by that of Regnault, who introduced many refinements into the method and succeeded in measuring the compressibilities of a number of gases up to a pressure of 12 atmospheres with a considerable degree of accuracy [22].

Regnault employed a glass manometer 30 m. high mounted in an

iron vessel which also communicated with a force-pump and with a calibrated glass compressibility tube containing the gas. The tube was divided by graduation marks into two equal parts and its upper end was connected through a stopcock with a storage vessel containing the gas under pressure. In order to minimize the errors of volume measurement the tube was enclosed in a constant-temperature bath and parallel observations were made with the tube alternately half-filled and completely filled with gas; corrections were also made for the temperature of the mercury column and for variations in barometric pressure; the accuracy of the manometer readings was about 0·6 mm.

In Table 30 his data for air, nitrogen, carbon dioxide, and hydrogen are summarized.

TABLE 30. *The Compressibilities of Air, Nitrogen, Carbon Dioxide, and Hydrogen (Regnault)*

Air		*Nitrogen*		*Carbon dioxide*		*Hydrogen*	
p_0, *mm.*	$\frac{p_0 v_0}{pv}$	p_0, *mm.*	$\frac{p_0 v_0}{pv}$	p_0, *mm.*	$\frac{p_0 v_0}{pv}$	p_0, *mm.*	$\frac{p_0 v_0}{pv}$
738·72	1·001414	753·46	1·000988	764·03	1·007597	..	..
2,112·53	1·002765	4,953·92	1·002952	3,186·13	1·028698	2,211·18	0·998584
4,140·82	1·003253	8,628·54	1·004768	4,879·77	1·045625	5,845·18	0·996121
9,336·41	1·006366	10,981·42	1·006456	9,619·97	1·155865	9,176·50	0·992933

The results show clearly that the product pv diminishes as the pressure increases over the whole pressure range for all the gases except hydrogen, and in no case is Boyle's law rigorously obeyed.

We now come to a period of outstanding importance in the history of gases. Early in the nineteenth century Davy and Faraday had shown that all the common gases, with the exception of the elementary gases and methane, carbon dioxide, and nitric oxide, could be liquefied under conditions of low temperature and high pressure. In 1834 Thilorier succeeded in liquefying carbon dioxide and this was the signal for a general attack upon the so-called permanent gases. Success was not achieved, however, until 1877 when Pictet and, independently, Cailletet reported the liquefaction of oxygen; but during the intervening years a great deal of important work was done upon the measurement of compressibilities and upon improving the methods of handling gases at high pressures.

Following upon the work of Regnault, J. Natterer [23] measured

the compressibilities of oxygen, hydrogen, and air up to pressures of several hundred atmospheres and made the important observation that the value of the product pv did not continue to diminish indefinitely with increase of pressure but in the case of oxygen and air passed through a minimum and thereafter increased. He employed for the first time a primitive form of free-piston gauge to measure pressure.

Mention may also be made of the work of Cailletet [24], which like that of Natterer was directed mainly towards the problem of the liquefaction of gases but also included determinations of compressibilities. Cailletet paid great attention to the accurate measurement of pressure and in some of his earlier work employed a mercury column contained in a flexible steel tube for pressures as high as 240 atmospheres. He later adopted a free-piston gauge, of similar design to those employed at the present time, for measuring pressures up to 1,500 atmospheres.

The Researches of Amagat. By far the most comprehensive investigation into the physical properties of gases and liquids at high pressures was carried out by the famous French physicist Amagat between the years 1869 and 1893, and no treatise on the subject of high pressures would be complete without some account of his methods and results.

Amagat set out to measure the compressibility of pure, dry nitrogen with as great a degree of precision as possible, and then, employing it as a standard, to determine the compressibilities of other gases by comparison with it [25]. His apparatus, shown in section in Fig. 60, consisted of three parts, namely, a compression vessel, a pump and reservoir, and an open mercury-column manometer. The compression vessel was in the form of a glass bulb A terminating in a calibrated capillary tube 50 cm. long and approximately 1 mm. internal diameter; the actual dimensions of the capillary tubes were 10–12 mm. external diameter and 1–2 mm. internal diameter and several of them withstood successfully pressures of 500 atmospheres; the lower end A of the vessel was immersed in mercury contained in the chamber P', which communicated through capillary passages with the mercury column C and with the pump and reservoir R.

The mercury manometer consisted of a steel tube 5 mm. external and 2 mm. internal diameter, in sections about 25 m. long screwed together. It was erected in a shaft of the Verpilleux mines at Méons near Saint Étienne, a disused gallery opening into it at a depth of

327 m. serving to accommodate the main part of the apparatus. The gallery was a cul-de-sac and hence was free from currents of air and from large temperature fluctuations. In reading the manometer the steel section containing the upper part of the mercury

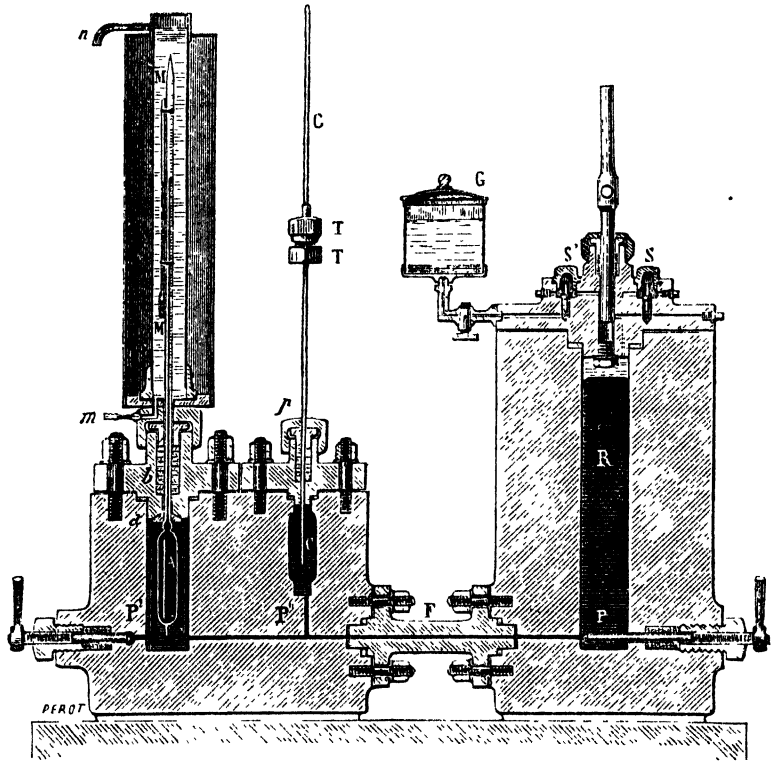

FIG. 60. Amagat's compressibility apparatus.

column was replaced by a cap containing a glass cylinder and the mercury was then raised by the pump until it entered the cylinder. Vertical heights were measured by means of a stretched steel wire subsequently compared with a reference scale 10 m. long. The temperature of the column was measured by thermometers placed at intervals of 30 m. along its whole length. The pump was of simple design, having inlet and outlet valves, S' and S, and was operated with glycerine contained in the reservoir G.

In spite of the difficulties connected with the manipulation of the apparatus and the reading of the manometer Amagat made at Verpilleux six series of experiments with nitrogen between 75 and 430

atmospheres pressure at a temperature of approximately 22° C. and a further five series at Lyon at pressures between 26 and 80 atmospheres and at a temperature of 15° C. The results are recorded in Table 31 which is taken from the original memoir.

TABLE 31. *The Compressibility of Nitrogen (Amagat)*

Pressions en mètres de mercure à 0°	*Produits*† *pv*	*Pressions en atmosphères*	*Pressions calculées*	*Différences*
20·740	50,989	27·289	27·289	0·000
35·337	50,897	46·496	46·580	+0·084
47·146	50,811	62·034	62·251	+0·217
55·481	50,857	73·001	73·181	+0·188
61·241	50,895	80·580	80·728	+0·140
69·140	50,987	90·975	90·978	+0·003
82·970	51,226	109·171	108·665	−0·506
96·441	51,602	126·896	125·388	−1·508
128·296	52,860	168·810	162·835	−5·975
158·563	54,214	208·635	196·224	−12·411
190·855	55,850	251·127	229·271	−21·855
221·103	57,796	290·934	256·669	−34·275
252·353	59,921	332·039	282·544	−49·495
283·710	62,192	373·302	306·055	−67·247
327·388	65,428	430·773	335·707	−95·066

As already stated, the compressibilities of other gases were determined by comparison with nitrogen, using the apparatus illustrated in Fig. 60 but with a second compression tube replacing the open-column manometer *C*. Amagat's data for these gases have since been superseded and need not be recorded, but the isotherms shown in Fig. 61, which is reproduced from his paper, indicate the general character of the results. In the figure the ordinates are taken as proportional to the excess of the values of pv above 1,000 (assuming $pv = 1{,}000$ at 24 m. pressure) and the abscissae the pressures in metres of mercury. All the gases, save hydrogen, show a minimum value of pv at approximately the following pressures:

Nitrogen	50 m.	Carbon monoxide	50 m.
Oxygen	100 m.	Formaldehyde	120 m.
Air	65 m.	Ethylene	65 m.

Amagat next set out to determine the influence of temperature upon the compressibility of gases, in the course of which he carried

† The product pv is expressed in arbitrary units based upon the capacity of the compression vessel; the existence of a minimum value of pv at about 65 atmospheres is clearly shown by the figures in the second column and the deviations from Boyle's law by the differences in the fifth column.

out an extensive series of experiments with nitrogen, hydrogen, ethylene, carbon dioxide, and formaldehyde at temperatures between *c.* 15° and 100° and pressures from 30 to 420 atmospheres. His results need not be considered in detail at present but attention may be

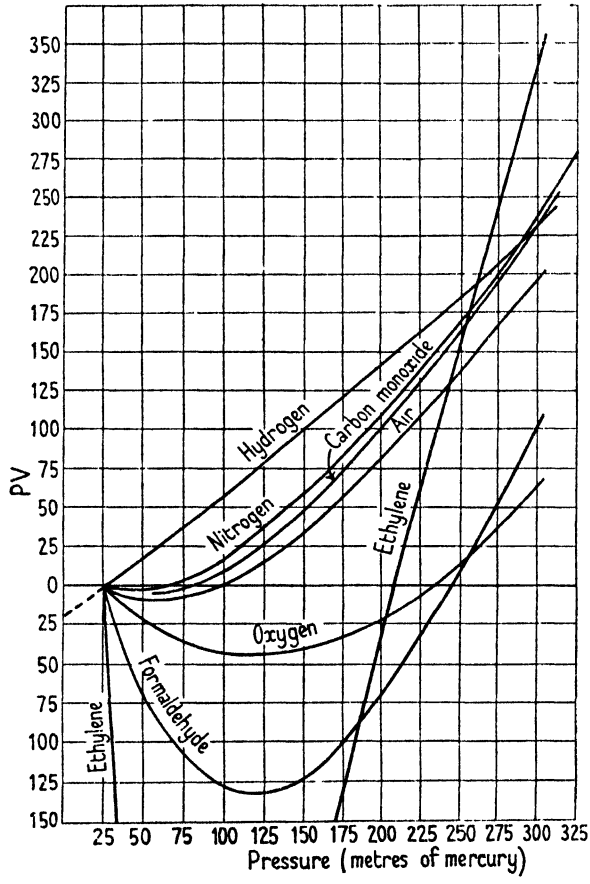

FIG. 61. Amagat's isotherms.

drawn to the following principal conclusions arrived at in regard to the temperature effect:

1. For pressures lower than the critical pressure the deviations from Boyle's law, at first positive for sufficiently low temperatures, pass through zero and become negative on increasing the temperature.

2. The pressure at which pv is a minimum at first increases with increase of temperature but eventually reaches a maximum and thereafter diminishes.

3. In general the deviation from Boyle's law diminishes with increase of temperature and above a certain temperature the law of compressibility of a

gas is represented by the relation $P(V-\alpha) = \text{constant}$, where α is the absolute volume of the matter constituting the gas; that is to say, the isotherms become straight lines.

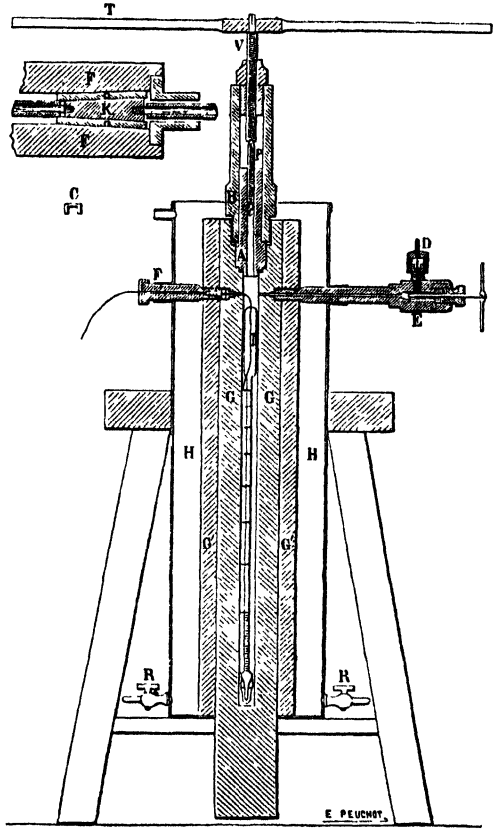

FIG. 62. Amagat's apparatus for measuring compressibilities up to 3,000 atmospheres.

In 1893 Amagat published two further important memoirs summarizing the results of his measurements of the compressibility of gases and liquids up to 3,000 atmospheres pressure and temperatures up to 200° C. [26].

In this work he employed for the first time the free-piston gauge described in Chapter V, and adopted a method of measuring volumes by electrical contacts originally suggested by Tait [27]. The glass piezometer used in his experiments with gases at temperatures between 0° and 50° and pressures up to 3,000 atmospheres is shown in Fig. 62; it consisted of a long cylindrical bulb surmounted by

a narrow section into the walls of which were fused a number of platinum wires. The piezometer was placed in a heavy steel, compound cylinder which was then completely filled with water, and pressure applied first by means of a pump through a side opening D and then by means of a screw plunger which was mounted on the upper part of the cylinder. The platinum contacts of the piezometer

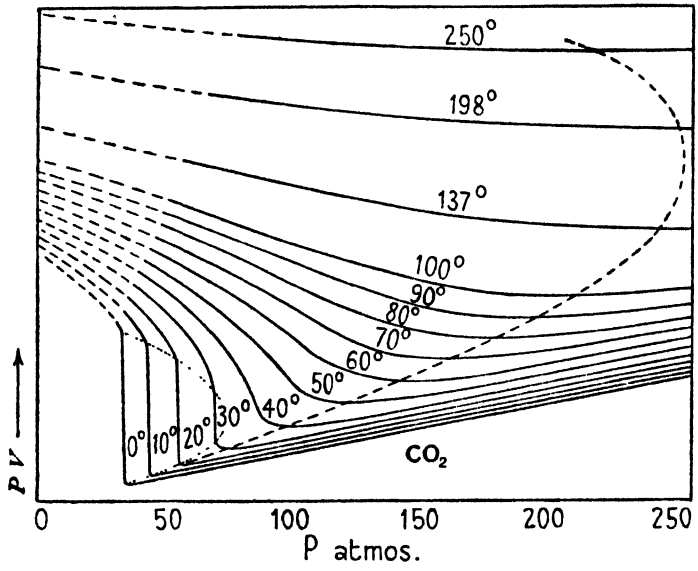

FIG. 63. Isotherms of carbon dioxide.

were connected to an insulated lead which was joined to an insulated plug F screwed into the upper part of the cylinder.

At temperatures above 50° this method of measuring volume was not found to be satisfactory, and Amagat reverted to his original method of reading visually the level of mercury in a graduated piezometer. The piezometer was enclosed in a steel cylinder fitted with an extension to accommodate its graduated stem, and the position of the mercury meniscus was observed by means of a beam of light traversing a pair of glass or quartz windows fitted into the extension.

With this apparatus the compressibilities of oxygen, hydrogen, nitrogen, and air were measured up to pressures of 1,000 atmospheres at 0°, 15°, 100°, and 200° C., and up to 3,000 atmospheres at 0°, 15°, and 45°. In addition, data were obtained for ethylene and carbon dioxide up to 1,000 atmospheres over the full temperature range.

In tabulating the results of this work Amagat employed as the unit the value of the product pv at 0° and 1 atmosphere pressure.

The isotherms for carbon dioxide reproduced in Fig. 63 are of special interest as showing the behaviour of a fluid in the neighbourhood of its critical temperature and pressure. It will be observed that the Boyle points, data for which are given in Table 32, lie on a parabolic curve which, at a sufficiently high temperature (the Boyle temperature), would cut the pv axis. Amagat also draws attention to the concavity of the isotherms at low temperatures and pressures.

TABLE 32. *Variation of the Boyle Point of Carbon Dioxide with Temperature (Amagat)*

Temp., °C.	*Pressure, atms.*	*Temp., °C.*	*Pressure, atms.*
0	35	70	162
10	45	80	179
20	57	90	196
30	76	100	211
40	101	137	247
50	124	198	255
60	143	258	218

Recent Determinations of Compressibilities

In view of the materials and equipment available at the time Amagat carried out his researches, his results are notable for the high degree of accuracy attained, and it was not until the development of high-pressure processes on an industrial scale that a redetermination of the compressibilities of the common gases was felt to be desirable. Meanwhile, improvements in the metallurgy of steels, the discovery of alloy steels of high tensile strength, and the introduction of further refinements into the methods of measuring temperatures and pressures had simplified many of the problems confronting the early workers.

When therefore a redetermination of the compressibilities was undertaken it was found possible to employ a wider range of pressures and temperatures and to aim at a higher degree of accuracy than was feasible in Amagat's day. During the past twenty years or so data have been obtained for all the more important industrial gases and their binary mixtures up to pressures of 1,000 atmospheres and even higher for temperatures from −183° to 400° C.

Of the recent investigations mention may be made of the valuable contribution by groups of workers under the direction of Holborn at the Physikalisch-Technische Reichsanstalt, Berlin; Kammerling Onnes at Leiden; F. C. Keyes at the Massachusetts Institute of Technology; E. P. Bartlett at the Fixed Nitrogen Research Laboratory (U.S.A.), and A. Michel at Amsterdam. In addition a number of

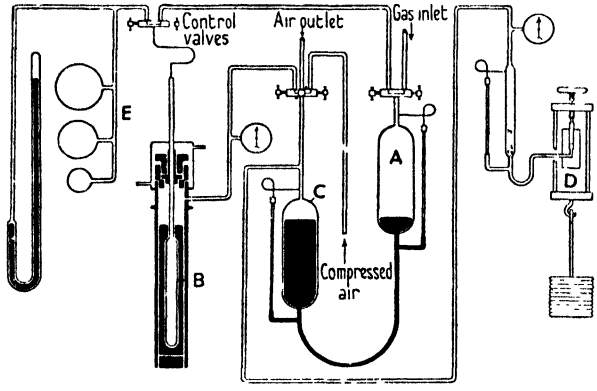

FIG. 64. Holborn's compressibility apparatus.

important papers relating to particular gases have been published by Sage and Lacey, Masson, Verschoyle, Scott and Townend, and Bhatt.

Two essentially different methods have been employed, the one depending upon the accurate measurements of the volumes occupied by a given mass of gas with variation in pressure, and the other upon the measurement of the amount of gas contained in an enclosure of known volume at various pressures; of the early workers Amagat and Cailletet employed the former whilst Regnault used a combination of the two methods.

The Berlin Isotherms. Holborn and his collaborators employ the constant-volume method up to 100 atmospheres and over a temperature range −183° to 400° C. [28]. Their apparatus, shown diagrammatically in Fig. 64, consists of a liquid-piston compressor connected to a reservoir, *A*, containing the gas, and to a steel cylinder containing the compression vessel, *B*. The reservoir, *A*, communicates directly with *B* and its gaseous contents can be transferred to it by applying compressed air to the liquid piston, *C*; it will be seen that the pressure in *B* is always balanced by an equal external pressure, and hence errors due to a change in its volume by the application of an internal pressure are eliminated.

The pressure of the gas in B is measured by a pressure balance, D, provided with a mechanism for rotating the piston, and its volume by expanding it to atmospheric pressure in the accurately calibrated capacity vessels at E.

Using this method they have measured the compressibilities of argon, helium, hydrogen, nitrogen, air, and oxygen up to 100 atmospheres with a high degree of accuracy, the errors of observation seldom exceeding 1 in 4,000.

The Leiden Isotherms. At Leiden the method used is based upon the measurement of the volumes occupied by a fixed quantity of gas at different pressures, the temperature being maintained constant [29]; the method has the disadvantage that the probable errors in the volume determinations increase with increasing pressure, but by using a sufficient quantity of gas they can, of course, be kept within any limits desired.

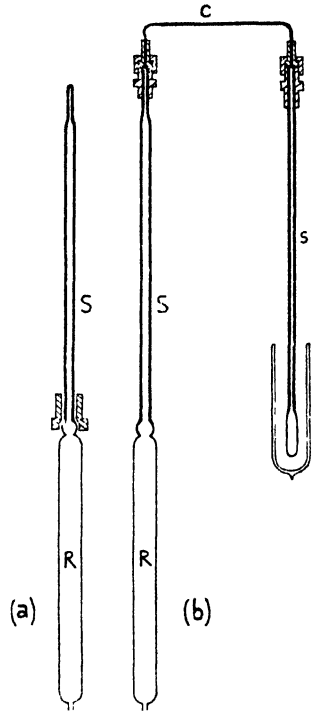

FIG. 65. The Leiden piezometers.

Two types of piezometer are employed, the 'simple' (or undivided) and the 'divided' model; the former, which is generally used in determinations at temperatures above the freezing-point of mercury, is shown in Fig. 65 (*a*). It is similar in shape to that employed by Amagat, and consists of a cylindrical stem S, the bore of which is accurately calibrated over the whole length, and a large reservoir R of known volume; the determination of an isotherm is made by compressing a known quantity of gas over mercury into successive known volumes of the stem at constant temperature and measuring the pressures by means of an open mercury manometer of reduced height.

For temperatures below the freezing-point of mercury a divided type of piezometer shown in Fig. 65 (*b*) is used. The stem S is connected by means of a flexible metal capillary tube C to a small reservoir s of known volume which is maintained at the desired

temperature. The normal volume of the gas in s can be derived from a knowledge of the total volume of the gas and the volume of the remainder of the apparatus maintained at normal temperature. The accuracy of the results therefore depends upon an accurate measurement of the volumes of the different parts of the piezometer; these are all calibrated directly with mercury. The Leiden isotherms extend only to a pressure of 100 atmospheres.

The Fixed Nitrogen Research Laboratory Isotherms. Bartlett and collaborators employ the constant-volume method [30], and as their results cover a very wide range of temperatures and pressures and are of considerable theoretical and practical interest, a detailed account of their apparatus and experimental procedure will be given.

The apparatus consists of a high-pressure system containing the compression vessel of known volume and a low-pressure system in which the volume of the expanded gas is measured; both systems are completely immersed in thermostatically controlled baths. For pressures up to 1,000 atmospheres and temperatures up to 400° C. a compression vessel of the form shown in section in Fig. 66 is employed. It consists of a massive steel body provided with a screwed cover which accommodates two valves F and G; the compressed gas enters the vessel through F and is released through G, so that any possible error due to gas trapped in the valve packings is eliminated. The vessel is immersed in the bath up to the line HH and the exposed cover is electrically heated by the coil J, a thermocouple at K registering its temperature. The upper parts of the valve spindles are water-cooled at BB.

The volume of the compression vessel, which must be known with great accuracy, is measured by connecting it in parallel with a steel vessel whose volume has previously been determined by completely filling it with pure dry mercury and weighing the contents; the two vessels are filled with hydrogen usually to 100 atmospheres and 0° and the ratio of the volumes is then equal to the ratio of the expanded volumes of gas from the two vessels.

Pressures are measured by means of a gauge of the dead-weight piston type in which the weights are supported by a scale-pan hung from a saddle which transmits the load to the bearing at the top of the oscillating piston. The piston diameter is 1·5875 cm. and the cylinder diameter 1·5883 cm., the effective diameter being taken as 1·5879 cm.; each atmosphere is therefore represented by 2·0463 kg. on the piston.

A second gauge in which the load is applied to the piston by means of a lever with a multiplying power of approximately 5 has also been used.

The bath controlling the temperature of the low-pressure system (Fig. 67) is provided with a glass front through which the manometers may be read. As the expanding gas from the compression vessel enters the bath, it passes through a capillary copper coil L, where its temperature is brought to that of the bath, and it is then saturated with water vapour in the humidifiers M and displaces an equal volume of moist gas into the burette N through the

stopcock J. The open manometer Q, filled with a heavy mineral oil, measures the differential pressure between the system and the atmosphere. The water-level gauge R is a convenience in determining the height of the water in the hydrostatic bottle S. The mercury manometer T and a 7-metre water manometer (not shown in the diagram) record the difference between the total

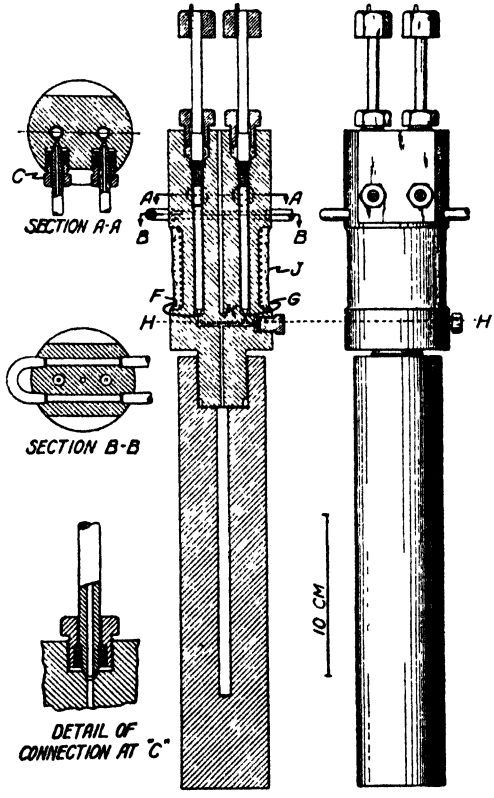

FIG. 66. Bartlett's piezometer for 1,000 atmospheres.

pressure within the hydrostatic bottle and the atmosphere; this pressure is regulated by a centrifugal vacuum-pressure pump at V.

The pressure on the expanded gas in the burette N is the algebraic sum of (1) the corrected barometric pressure in millimetres of mercury, (2) the differential pressure indicated by the mercury manometer corrected to 0° (or) the differential pressure indicated by the water manometer corrected to millimetres of mercury at 0°, and (3) the differential pressure due to the difference in height of liquid in the burette and in the water-level gauge, corrected to millimetres of mercury at 0°; capillarity at the constricted points in the measuring bulb requires a positive correction of 0·3 mm. of mercury.

When possible the quantity of gas is measured under both increased and reduced pressure, thus giving a check on the results. The value of $p_0 v_0$ is calculated from the equation

$$p_0 v_0 = \left(\frac{p}{760}\right)\left(\frac{273{\cdot}1}{T}\right) V, \tag{7.12}$$

where p is the corrected pressure in the gas in the burette, T the temperature of the bath, and V the volume of gas in the burette.

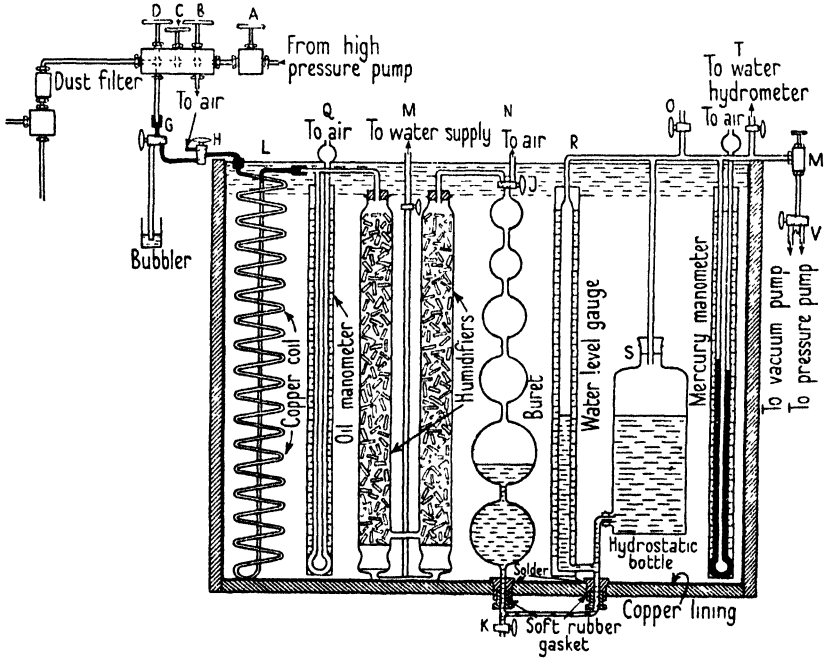

FIG. 67. Bartlett's low-pressure system.

The sources of error in the measurements will be discussed later.

After taking into account all known sources of inaccuracy Bartlett states that by this method the limit of error in the results for nitrogen to 400° should not exceed 0·3 per cent. and it is believed that the average results may be depended upon to within 0·1 to 0·2 per cent. The same limits hold for hydrogen to 200°; at 300° the error may reach 0·4 to 0·5 per cent., and at 400° the results are irregular and have no claim to a high degree of accuracy.

Bartlett and his collaborators have measured the compressibilities

of hydrogen, nitrogen, and their binary mixtures, carbon monoxide, and methane.

The Massachusetts Institute of Technology Isochores (Isometrics). Keyes and his collaborators employ the constant-volume method for measuring the isochores of gases, but their procedure differs from that of Bartlett in that the volume of gas in the compression vessel is measured before the final pressure and temperature readings are taken [31].

The compression vessel shown in section in Fig. 68 has a capacity of 13·3143 c.c. at 0° and is made in one piece from cold rolled steel, the lower end being spun shut and welded with the oxy-acetylene flame. It is filled by cooling it in boiling liquid air or other gas and connecting it to a calibrated burette containing a known volume of the gas whose isochores are to be determined; the gas condenses in the cooled vessel and when a sufficient quantity has been introduced the vessel is closed by means of a gold disk *C* held against a seating by the screw *D* which has a small hole drilled through it. The charged vessel is then placed in communication with a pressure balance and the disk is punctured by amalgamation with mercury, and the desired pressure and temperature readings are taken in the usual manner.

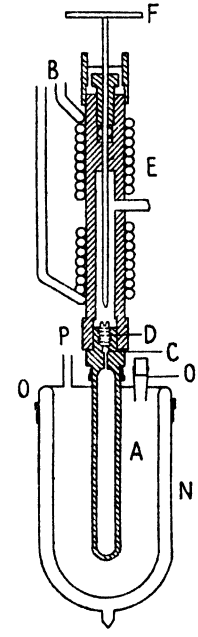

FIG. 68. Keyes's compression vessel.

The isochores of methane, nitrogen, and their binary mixtures at temperatures between 0° and 200° C. and pressures up to 200 atmospheres have been measured at Massachusetts.

The Amsterdam Isotherms. Michels and his collaborators measure the volumes occupied by a known mass of gas at constant temperature and varying pressures by a modification of Amagat's method [32]; they have, however, introduced many refinements into the apparatus and experimental procedure and have succeeded in overcoming many of the difficulties inherent in the accurate measurement of small volumes of gases at very high pressures.

The apparatus employed by them for pressures up to 250 atmospheres is shown in section in Fig. 69; it consists of a glass piezometer *A* housed in a steel vessel *C*, which contains some mercury, the remainder being filled with oil. The piezometer takes the form of a large reservoir *B* surmounted by a number of smaller bulbs connected by narrow capillaries. Through the capillaries are sealed platinum wires which make contact with a platinum lead passing out through the top of the vessel *C* by way of the insulated plug *E*;

the volumes from each of the contacts to the top of the piezometer tube are determined by weighing with mercury.

The steel vessel is placed in a thermostat and pressure is applied to its contents through the opening *D*. Mercury is forced up inside the piezometer, thus compressing the gas until the mercury surface makes contact with the platinum wires and thereby causes a drop in the electrical resistance of the main lead. The equilibrium pressure, at which contact is made, is measured with a free-piston pressure gauge; corrections must be applied for the height of the mercury column inside the piezometer and for the hydrostatic head of the oil.

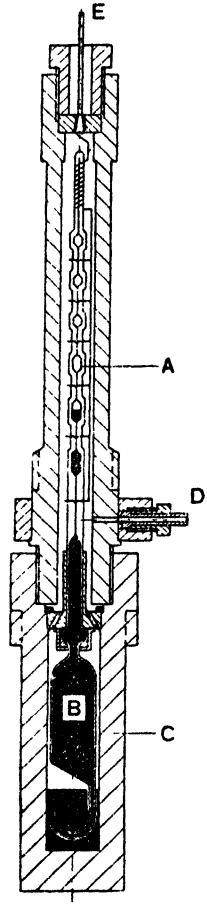

Fig. 69. Michels's piezometer for 250 atmospheres.

For pressures higher than 250 atmospheres the apparatus is modified as shown in Fig. 70 so that the piezometer can be filled initially to a pressure of between 20 and 50 atmospheres. The top half of the glass piezometer, *B* to *C*, containing the contacts is of the same shape as in the previous design; the lower half is changed to allow of it being filled under pressure through the capillary *D*, while a contact at *A* serves for the determination of the normal volume. The volume above *A* is 75 c.c., that above *B*, the first measuring contact, is 7·5 c.c., and that above the highest contact about 4·5 c.c. If, therefore, the amount of gas with which the piezometer is filled initially is chosen so that when the mercury reaches contact *A* the density is about 2·0, measurements can be carried out at densities between 200 and 340; with a second filling, giving a density of 34 at *A*, the range can be extended up to a density of 580.

The piezometer is filled with gas through the valve *E*, which is provided with a long spindle so that the packing gland *H* may be kept out of contact with the hot liquid in the thermostat.

Special precautions have to be taken to prevent mercury entering the capillary *D*, when pressure applied to the oil at *K* forces the mercury level inside the piezometer up to the contact *A*. A steel hood *L* is therefore placed over the top of the capillary, its capacity in relation to the total volume of the capillary and the passage leading to the point of the valve spindle being such that during normal operations mercury cannot be forced up to the level of the capillary outlet.

For details of filling the piezometer the original memoir should be consulted.

Michels notes that above 2,000 atmospheres the accuracy in the results obtained by the method decreases gradually owing to the increase in the viscosity of the oil; at 3,000 atmospheres it is not above 1:2,000.

A further modification of the method for measurements at and near the critical point has recently been described [33].

The Amsterdam isotherms include those of carbon dioxide, nitrogen, methane, ethane, and ethylene.

The Compressibility of Vapours

Owing to experimental difficulties very little work has been done upon the pressure-volume-temperature relationships of the vapours of high boiling-point liquids. Ramsay and Young have measured the volume changes of ethyl ether and alcohol with increase of pressure, and some account of their results has already been given. Keyes and Felsing [34] have also made some preliminary measurements with ether, and their work has been extended by Beattie, who has obtained compressibility data for the same substance up to 200 atmospheres over the temperature range 150° to 325°.

Beattie [35] employs a variable-volume method in which a known mass of ether is enclosed in a glass piezometer, kept at constant temperature, and measured quantities of mercury are injected by means of a screw plunger. The change in pressure with volume is measured by means of a pressure balance. For details of the method the original paper should be consulted.

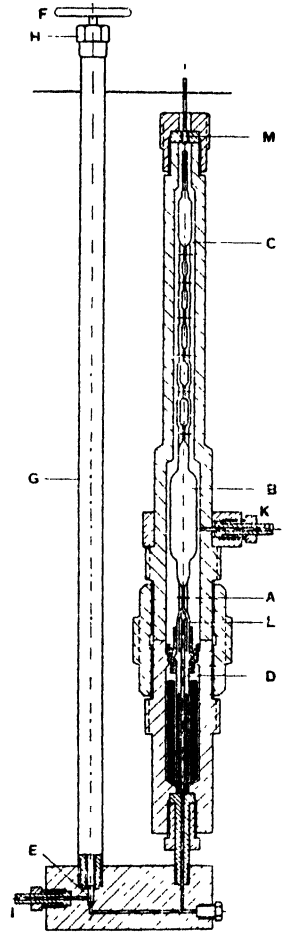

FIG. 70. Michels's piezometer for pressures above 250 atmospheres.

Newitt, Sartori, and Chow [36] have employed the constant-volume method for measuring the compressibility of ethyl ether, ethyl alcohol, and their binary mixtures up to about 250 atmospheres over the temperature range 225°–350°. Their piezometer consists of a stainless-steel cylinder fitted with a double-seating valve of the type described in Chapter IV (Fig. 38*c*); it is totally enclosed in an electrically heated thermostat the temperature of which can be maintained constant to within $\pm 0{\cdot}02°$. Liquid ether or alcohol is forced

into the vessel by means of a liquid-piston pump and, after the lapse of sufficient time for temperature equilibrium to be attained, the pressure is measured by means of a pressure balance communicating directly with the pump, and the valve is closed. The temperature of the vapour is read by a mercury-in-glass thermometer situated in a pocket traversing longitudinally the walls of the piezometer.

The piezometer is then removed from the thermostat, cooled first to room temperature and then in a solid carbon dioxide-alcohol bath. A known amount of some suitable solvent is admitted and the temperature allowed to rise to 0°. Finally, the density of the solution is determined and its composition ascertained from a reference density-composition curve.

The method is rather laborious, each point on the compressibility isotherm requiring a separate experiment, but it has the advantage of utilizing only the simplest apparatus, and is free from many of the errors associated with the use of electric contacts for measuring changes in volume.

Sources of Error in Compressibility Measurements

The Purity of the Gases. At temperatures far above the critical temperature and at high pressures the presence of traces of impurities have usually only a small influence upon the compressibility of a gas; but in the region of the critical temperature the effect of even a fraction of 1 per cent. of a foreign gas may be very considerable; it is therefore essential to take every precaution to ensure a high degree of purity and the method usually employed is to liquefy and fractionally distil the gas, and to test its purity by chemical analyses or by determining one or other of its physical constants.

Volume Measurement. The accurate measurement of the volume of a closed container is a problem of considerable difficulty and many of the earlier determinations of compressibilities are vitiated by errors introduced through the use of unreliable methods. The volume of the compression vessel at normal temperatures and pressures may be determined by filling it with mercury and weighing the contents; it is, however, necessary to make quite sure that no dead spaces exist, particularly when part of the volume includes capillary passages and soldered joints [37]. A more reliable method is to connect the compression vessel in parallel with a vessel of accurately known volume

and employ a gas of known compressibility at high pressure as the measuring fluid.

Where the compression vessel is subjected to an unbalanced internal pressure, as in Bartlett's apparatus, a correction must be applied for the change in volume due to the elastic deformation of the walls under the tensile and compressive stresses set up by the working pressure. Bartlett employs the following equation derived by Love for thin-walled cylinders in which the ratio of length to diameter is large and the uncertain end effects can be neglected [38]:

$$\Delta V = \frac{V_0}{E(r_2^2-r_1^2)}[3(1-2\sigma)(p_1 r_1^2-p_2 r_2^2)+2(1+\sigma)(p_1-p_2)r_2^2]. \tag{7.13}$$

V_0 is the inside volume of the cylinder, E the modulus of elasticity of steel ($20{\cdot}4\times10^5$ atm./cm.^{2}), r_2, r_1 the external and internal radii of the cylinder, p_1 and p_2 the external and internal pressure, and σ Poisson's ratio (0·287)

In the vessel used in Bartlett's experiments at 1,000 atmospheres r_1 is 0·2381 cm., r_2 is 1·7463 cm., and the length of the chamber is 13·41 cm.; the pressure-correction factor at 1,000 atmospheres calculated from eq. (7.13) is 1·00129. In Holborn's and Michels's apparatus the internal pressures are balanced by corresponding external pressure and this correction is unnecessary.

The temperature coefficient of the volume change for a steel vessel can be calculated from an equation due to Keyes, Joubert, and Smith [39]:

$$V_t^{\mathrm{Fe}} = V_0(1+3{\cdot}25\times10^{-5}t+2{\cdot}85\times10^{-8}t^2-1{\cdot}65\times10^{-11}t^3), \tag{7.14}$$

where V_0 is the original capacity and V_t the capacity for a change of temperature of $t°$. The numerical values of the constants are based on data obtained from the Reichsanstalt.

In addition to this correction for thermal expansion it must be borne in mind that all steels exhibit the phenomenon of 'creep', which occurs at elevated temperature under stresses far smaller than the stress at the elastic limit of the material as determined by a short time test. The rate of 'creep' for a high tensile steel at 400° C. is, however, very small, and unless the vessel is kept under pressure for an unduly long period the errors from this cause are negligible.

Errors due to Solubility, Adsorption and Diffusion of Gases. The solubility and diffusion of gases in metals are dealt with in Chapter I.

Hydrogen is the only gas for which these effects assume practical importance under the conditions of compressibility measurements; and at high temperature and pressure there is definite experimental evidence that errors of appreciable magnitude are involved.

The effect of temperature on the rate of diffusion of a gas at constant pressure may be represented by the equation

$$D = \frac{k}{d} e^{-b/T}, \tag{7.15}$$

where D is the rate of diffusion per unit area of surface, d is the thickness of the metal, k and b are constants for the gas-metal system, and T is the absolute temperature. The effect of pressure upon the rate of diffusion at constant temperature is given approximately by the equation

$$D = k\sqrt{P}, \tag{7.16}$$

where k is a constant for the gas-metal system and P is the pressure of the gas, or more accurately by

$$D = k\sqrt{P}\left(\frac{aP}{1+aP}\right), \tag{7.17}$$

where a is a second constant and the expression in brackets allows for the fraction of the surface covered by adsorbed gas.

According to Borelius [40] the solubility s of hydrogen in steel in grams per cubic centimetre of iron is given by the expression

$$s = ke^{-b/T}\sqrt{P}, \tag{7.18}$$

which is a combination of (7.15) and (7.16). At 1 atmosphere and 300° the solubility of hydrogen is $1{\cdot}2 \times 10^{-6}$ gm. per c.c. of iron [41], and hence from (7.16) the solubility at 1,000 atmospheres is $38{\cdot}6 \times 10^{-6}$ gm. per c.c. of iron, or 0·4 c.c. at N.T.P. The actual effect of this dissolved gas on the apparent volume of the compression vessel can only be estimated if the rate of diffusion be known, and unfortunately very little relevant data relating to high tensile steels is available. It seems probable, however [42], that in a vessel with walls 25·4 mm. thick in which hydrogen is contained at 300° and 1,000 atmospheres the gas would escape at the rate of about 0·025 per cent. of the total volume per minute.

Experiment shows that at 300° C. and high pressure, saturation of the metal with hydrogen takes place rapidly but diffusion through the walls is comparatively slow. As the gas in the compression vessel is released part of the dissolved hydrogen is recovered; thus whilst

there is a small loss due to diffusion there is a gain due to solution and subsequent liberation of the gas which produces the effect of an apparent increase in the volume of the vessel. Loss by diffusion might be considerable in a thin-walled vessel such as that used by Holborn, whereas in the case of Bartlett's vessel the solution effect would probably predominate. These effects possibly account for the fact that Holborn's compressibility factors for hydrogen appear too large at temperatures above 200°, whilst Bartlett's appear too small.

Errors due to Chemical Action. Under favourable conditions hydrogen, nitrogen, oxygen, and carbon monoxide combine with iron to give relatively stable compounds, and in some instances corresponding compounds are formed with nickel, chromium, molybdenum, and other constituents of high-tensile steels. There is also strong evidence that at high temperatures and pressures hydrogen will combine with the carbon in steel to give hydrocarbons (see Chap. I). The temperatures required for the rapid formation of these compounds are, however, usually higher than those at which compressibility measurements are normally made and, except in the case of carbon monoxide, no appreciable errors are liable to be introduced through this cause.

Carbon monoxide is in a metastable condition at ordinary temperature, and in the presence of a suitable catalyst tends to decompose according to the equation

$$2CO \rightleftharpoons C + CO_2 + 41{,}950 \text{ cals.};$$

at 25° and atmospheric pressure the equilibrium constant

$$K = \frac{CO_2}{CO}$$

calculated from free-energy data is $2{\cdot}65 \times 10^{21}$; the quantity of carbon monoxide in equilibrium with carbon and carbon dioxide is therefore only about 2×10^{-8} per cent. The decomposition reaction is favoured by high pressures and low temperatures and appears to be catalysed by iron or iron oxide, and Bartlett, Hetherington, Kvalnes, and Tremearne [43] report that the contents of steel cylinders containing the gas at 100 atmospheres pressure acquire a carbon dioxide content of over 1 per cent. after standing in a protected location for two or three weeks.

Carbon monoxide also readily combines with iron to give the pentacarbonyl, and steel cylinders in which the gas has been stored under

pressure for some time are always found to contain quantities of this compound. It has the undesirable property of catalysing the decomposition of carbon monoxide.

In measurements of the compressibility of carbon monoxide, therefore, it is advisable to construct or line all parts of the apparatus with which the gas comes in contact with copper or bronze and to purify the gas from the dioxide and carbonyl by scrubbing out the former with potash and condensing out the latter at $-80°$, preferably in contact with active charcoal, immediately before use.

The Measurement of Pressure. The various types of gauge employed for the measurement of high pressures are described in Chapter V. For compressibility work a high order of accuracy is essential and in nearly all recent determinations primary gauges of the free-piston type have been employed.

The Units Employed in Compressibility Measurements and the Practical Application of the Data

Compressibility data are usually expressed in Amagat units, the unit of volume (called the 'normal' volume) being the volume of gas used at 1 atmosphere and 0° C.

The compressibility factor is pv/p_0v_0, where pv is the pressure-volume product of a given mass of gas under the conditions of the experiment and p_0v_0 is the corresponding value for the same mass of gas at 0° and 1 atmosphere.

In isotherm diagrams it is customary to plot pressure against the ratio $(pv/p_0v_1)_T$, where (p_0v_1) is the pressure-volume product at 1 atmosphere and temperature T, so that all the isotherms are brought to a common origin, as shown for example in Fig. 72 (p. 186).

The volume v' occupied by a known mass of gas at any pressure p and temperature T for which the compressibility factor $(pv/p_0v_0)_{p,T}$ is known may be calculated from the expression

$$v' = \frac{v_0}{p}\left(\frac{pv}{p_0v_0}\right)_{p,T}, \tag{7.19}$$

where v_0 is the volume of the gas at 0° and atmospheric pressure.

The pressure exerted by a known mass of gas at any volume v' and temperature T is best determined by a graphical method. We may write

$$\left(\frac{pv'}{p_0v_0}\right)_T = f(p), \tag{7.20}$$

and by assuming different values of p obtain a series of values for $(pv'/p_0v_0)_T$; on plotting these values against p on a pressure-compressibility factor diagram for the gas at temperature T, the pressure exerted by the gas is given by the ordinate of the point of intersection of the two curves.

The density $\rho_{p,T}$ of any gas at a pressure p and temperature T is given by the equation

$$\rho_{p,T} = \rho_0 p\left(\frac{p_0 v_0}{pv}\right)_{p,T}, \tag{7.21}$$

where ρ_0 is the density at 1 atmosphere and 0° C.

The Normal Volume

To calculate the normal volume of gas from the volume measured at, say, 25° and about 1 atmosphere it is assumed that the value of pv is a linear function of p with sufficient accuracy in the pressure range from 0 to 1 atmosphere. Then

$$pv = (pv)_{p=0} + \beta p, \tag{7.22}$$

where β is the slope of the isotherm. If the values of β are known from the literature for 0° and 25° we may write:

$$(pv)_{p=0,\,t=25^\circ} = (pv)_{p,t=25^\circ} - \beta_{25} p,$$

$$(pv)_{p=0,\,t=0^\circ} = (pv)_{p=0,t}\frac{273{\cdot}1}{273{\cdot}1+t},$$

and

$$(pv)_{p=1,\,t=0^\circ} = (pv)_{p=0,\,t=0^\circ} + \beta_0.$$

If the values of β are unknown and pv is not a linear function of p, the following procedure due to Michels may be adopted [44].

Preliminary figures are taken for β_0 and β_{25} either from known data or by calculation from the law of corresponding states, and with these a preliminary value is calculated for the normal volume of the gas. Call this volume v_N c.c. If the volume of the piezometer (Fig. 69) above the different contacts, expressed in cubic centimetres are v_1, v_2, v_3,..., v_x, the Amagat volumes are by definition

$$v_{1A} = \frac{v_1}{v_N} \quad \text{and} \quad v_{xA} = \frac{v_x}{v_N},$$

and the Amagat densities are

$$d_{1A} = \frac{v_N}{v_1} \quad \text{and} \quad d_{xA} = \frac{v_N}{v_x}.$$

The data obtained in the isotherm measurements at 25° together with the data found at 1 atmosphere are evaluated as a series of the type

$$pv_A = A_{25} + B_{25} d_A + C_{25} d_A^2 + D_{25} d_A^4,$$

using the method of mean squares.

The values of A_{25} is identical with $(pv)_{25}$ for infinite volume; hence Charles's law can be applied and

$$A_0 = A_{25} \frac{273{\cdot}1}{273{\cdot}1 + 25},$$

where A_0 is the value of pv_A at 0° and zero density and is the first term of the corresponding series for 0° C.:

$$pv_A = A_0 + B_0 d_A + C_0 d_A^2 + D_0 d_A^4.$$

From a knowledge of A_0 and the data of the isotherm measurements at 0° the values of B_0, C_0, and D_0 are calculated by the method of mean squares. If the correct values for β_0 and β_{25} have been taken, substitution of $d_A = 1$ must lead by definition to

$$pv_{A_0} = 1 = A_0 + B_0 + C_0 + D_0.$$

If the equation, however, gives some other value, say Y, it means that the volume taken as unit was $1/Y$ times too large and the previous values must be multiplied by $1/Y$.

BIBLIOGRAPHY

1. Beattie and Bridgeman, *Proc. Am. Acad.* **63,** No. 5 (1928).
2. von Smoluchowsky, *Ann. Phys.* **25,** 205 (1908); *Bull. Acad. Cracow,* p. 1057 (1907).
3. See also Einstein, *Ann. Phys.* **33,** 1275 (1910); **36,** 1572 (1910); Onnes and Keesom, *Commn. Phys. Lab. Leiden,* No. 104 (1908).
4. Traube, *Z. anorg. Chem.* **38,** 399 (1904).
5. Teichner, *Ann. Phys.,* Leipzig, **13,** 595 (1904).
6. Winkler and Maas, *Can. J. Res.* **9,** 613 (1933).
7. Herwig, *Pogg. Ann.* **137** (1869); **141** (1870); Wüllner and Grotrian, *Wied. Ann.* **11,** 545 (1880); Battelli, *Ann. de Chim. et de Phys.* (6), **25,** 38 (1892).
8. Meyer, *J. Chem. Phys.* **5,** 67 (1937).
9. Cailletet and Mathias, *Compt. Rend.* **102,** 1202 (1886); **104,** 1563 (1887).
10. S. Young, *Trans. Chem. Soc.* **59,** 37 (1891); *Phil. Mag.* **50,** 291 (1900); *Proc. Roy. Soc.,* Dublin, **12,** 374 (1910).
11. Lowry and Erikson, *J. Am. Chem. Soc.* **49,** 2729 (1927); see also Michels, Blaisse, and Michels, *Proc. Roy. Soc.* (A), **160,** 358 (1937).
12. Amagat, *Compt. Rend.* **114,** 1093 (1892).
13. Behn, *Ann. Phys.* (4), **3,** 733 (1900).
14. Thomson, *Proc. Roy. Soc.* **20,** 1 (1871).

15. RAMSAY and YOUNG, *Phil. Mag.* **23**, 436 (1887); see also AMAGAT, *Compt. Rend.* **94**, 847 (1882).
16. —— ——, *Phil. Mag.* **24**, 1 (1887).
17. VAN MUSSCHENBROECK, 'Elementae Physicae', *Lugduni Batavorum* (1734); J. ROBINSON, *System of Mechanical Philosophy*, **3**, 637. Edinburgh, 1882.
18. VAN MARUM, *Gilbert's Ann.* **1**, 145 (1799).
19. OERSTED and SUENSON, *Edin. J. Sci.* **4**, 224 (1826); DESPRETZ, *Ann. de Chim. et de Phys.* (2), **34**, 335 and 443 (1827).
20. POUILLET, *Elements de Physique*, **1**, 327. Paris, 1884.
21. DULONG and ARAGO, *Ann. de Chim. et de Phys.* **43**, 74 (1830).
22. REGNAULT, *Mém. de l'Acad.* **21**, 1329 (1847); **26**, 229 (1862).
23. NATTERER, *Wiener Ber.*, 1850, 1851, and 1854; *Pogg. Ann.* **62**, 139; **94**, 436.
24. CAILLETET, *Compt. Rend.* **70**, 1131 (1870); **74**, 1282 (1872); **75**, 771, 1271 (1872); **88**, 61 (1879); **90**, 210 (1880).
25. AMAGAT, *Ann. de Chim. et de Phys.* **19**, 345 (1880); **22**, 353 (1881); **28**, 456, 464, 480, 500 (1883).
26. ——, *Ann. de Chim. et de Phys.* (6), **29**, 68, 505 (1893).
27. TAIT, *Proc. Edin. Roy. Soc.*, 1 Dec. 1884.
28. HOLBORN and collaborators, *Ann. Phys.* (4), **47**, 1089 (1915); *Zeit. Physik*, **23**, 77 (1924); **33**, 1 (1925).
29. ONNES, *Commn. Phys. Lab. Leiden*, Nos. 100B, 117, 127C, 169D.
30. BARTLETT and collaborators, *J. Am. Chem. Soc.* **49**, 687 (1927); **50**, 1275 (1928).
31. KEYES and collaborators, *J. Am. Chem. Soc.* **41**, 589 (1919); **45**, 2107 (1923).
32. MICHELS and collaborators, *Proc. Roy. Soc.* (A), **153**, 201 (1935); *Pub. van der Waals Fund*, Nos. 41 and 42.
33. —— ——, *Proc. Roy. Soc.* (A), **160**, 358 (1937).
34. KEYES and FELSING, *J. Am. Chem. Soc.* **41**, 589 (1919).
35. BEATTIE, *J. Am. Chem. Soc.* **46**, 342 (1924).
36. NEWITT, SARTORI, and CHOW, Private communication.
37. See, for example, PENNING, *Commn. Phys. Lab. Leiden*, No. 166.
38. LOVE, *Mathematical Theory of Elasticity*, p. 141.
39. KEYES, JOUBERT, and SMITH, *J. Math. Phys.*, Mass. Inst. Tech., **1**, 191 (1922).
40. BORELIUS, *Ann. Physik*, **83**, 121 (1927).
41. SIEVERTS, *Z. phys. Chem.* **60**, 129 (1907).
42. BARTLETT, see ref. 30.
43. BARTLETT and collaborators, *J. Am. Chem. Soc.* **52**, 1374 (1930).
44. MICHELS and collaborators, *Pub. van der Waals Fund*, No. 41.

VIII

EQUATIONS OF STATE

Compressibility Data Relating to Individual Gases and Vapours

BEFORE considering the equation of state problem it will be as well first to compare the behaviour of some typical gases and vapours at high pressures and to give a brief résumé of the results of the more recent compressibility determinations referred to in the previous chapter.

For convenience in summarizing the data and of interpolating, the product pV may be represented as a function of pressure or density by empirical series equations in which pV is developed in terms of powers of p or of ρ $(= 1/V)$, thus

$$pV = f(p) = RT(1+B'p+C'p^2+D'p^3+...), \tag{8.1}$$

$$pV = f(p) = a+bp+cp^2+dp^3+..., \tag{8.2}$$

$$pV = f(\rho) = A+B\rho+C\rho^2+D\rho^3+.... \tag{8.3}$$

There is one such equation for each isotherm, the coefficients $A, B, C,..., a, b, c,...$, and $B', C', D',...$ (usually referred to as the first, second, etc., virial coefficients) being functions of the temperature. The coefficients A and a may be associated with the product RT, and B, b, and B' with the energy of interaction of a pair of molecules. The precise theoretical significance of the remainder is not clear.

To determine the values of the coefficients in order that the functions may be true for all values of p or ρ we may proceed by the method of successive differentiation. Thus, for example, from (8.2),

$$\frac{d(pV)}{dp} = \frac{df(p)}{dp} = b+2cp+3dp^2+..., \tag{8.4}$$

$$\frac{d^2(pV)}{dp^2} = \frac{df'(p)}{dp} = 2c+2\times 3\,dp+..., \tag{8.5}$$

and since (8.2) is true for all values of p, including $p = 0$,

$$pV = f(0) = a, \tag{8.6}$$

$$\frac{d(pV)}{dp} = f'(0) = b, \tag{8.7}$$

and $$\frac{d^2(pV)}{dp^2} = f''(0) = 2c. \tag{8.8}$$

In applying series equations to compressibility data it is usually, though not invariably, the custom to conform to a suggestion of K. Onnes and omit all the odd powers of p or ρ except the first. The most probable values of the constants are then determined by, say, the method of least squares, and the validity of the resulting equation over the full range of observations tested by plotting the differences between the observed and calculated values of pV against pressure or density. The points should lie on a smooth curve, the maximum deviations from linearity being of the order of the experimental error.

As will be explained later, considerable importance attaches to the accurate evaluation of the second virial coefficient B. It is given by the slope of the tangent to the isotherm at $p = 0$ or to a near enough approximation at $p = 1$ atmosphere; and it may be obtained by graphical methods from the isotherm itself provided sufficient data are available to enable the curve to be drawn accurately in the region of low pressures. This, however, is seldom the case. Nearly all recent compressibility measurements are for pressures higher than 25 atmospheres, and the value of B obtained from the series equations (8.1), (8.2), and (8.3) fitted to observations over a wide range of high pressures are scarcely accurate enough for computations of interaction energies at low pressures.

The Leiden and Amsterdam isotherms are usually expressed in the form of (8.3) and the Berlin isotherms in the form of (8.2). At least five terms are required to cover the whole range of the experimental data, and even so it is sometimes found, as for example in the case of carbon dioxide, that at the higher concentrations the series ceases to converge and the deviations become large.

In the summary of data given below the coefficients of one or other of the series equations for a number of isotherms of the more important gases are tabulated.

Acetylene

Reference	*Temperature of isotherms, °C.*	*Maximum pressure, atms.*
1. Sameshima, *Bull. Chem. Soc. Japan*, **1**, 41 (1926)	0	12
	25	

Air

Reference	*Temperature of isotherms, °C.*	*Maximum pressure, atms.*
1. Amagat, *Ann. de Chim. et de Phys.* **19,** 345 (1880); **22,** 353 (1881); **28,** 456–500 (1883); **29,** 68 and 505 (1893)	0 15 100 200	3,000
2. Witkowski, *Phil. Mag.* **41,** 388 (1896)	0 100	130
3. Penning, *Commn. Phys. Lab. Leiden,* No. 166 (1923)	20	60
4. Holborn and Schultze, *Ann. der Physik,* **47,** 1089 (1915)	From 0 at intervals of 50 to 200	130

Argon

1. Onnes and Crommelin, *Commn. Phys. Lab. Leiden,* No. 118 B (1910); 147 D (1915)	From −150 at intervals to 20	60
2. Holborn and Schultze, *Ann. der Physik,* **47,** 1089 (1915) 3. Holborn and Otto, *Ann. der Physik,* **63,** 674 (1920); *Z. für Physik,* **10,** 367 (1922); **23,** 77 (1924); **30,** 320 (1924); **33,** 1 (1925); **38,** 359 (1926)	From −100 at intervals of 50 up to 400	125

Constants of the Series Equation for Argon

$$pV = A + Bp + Cp^2 + Dp^4.$$

Pressure range: 0–100 atmospheres.

Temp., °C.	A	$B \times 10^3$	$C \times 10^6$	$D \times 10^9$
−100	0·6346	−2·872	−10·21	−0·130
−50	0·8178	−1·687	+0·79	+0·100
0	1·0010	−0·986	2·37	..
50	1·1842	−0·492	1·79	..
100	1·3674	−0·192	1·61	..
150	1·5506	+0·052	1·24	..
200	1·7338	0·208	1·12	..
300	2·1002	0·501	0·46	..
400	2·4666	0·683	..	..

Carbon Dioxide

Reference	*Temperature of isotherms, °C.*	*Maximum pressure, atms.*
1. Amagat, *Ann. de Chim. et de Phys.* (6), **29,** 68 and 505 (1893)	0 15 100 200	1,000
2. Keesom, *Commn. Phys. Lab. Leiden,* No. 88 (1903)	Between 25 and 57	138

Reference	*Temperature of isotherms, °C.*	*Maximum pressure, atms.*
3. A. Michels and C. Michels, *Pub. van der Waals Fund*, No. 41 4. Michels, Michels, and Wouters, *Pub. van der Waals Fund*, No. 42 5. Michels, Blaisse, and Michels, *Proc. Roy. Soc.* (A), **160**, 358 (1937)	From 0 at intervals of about 15 to 150	3,000

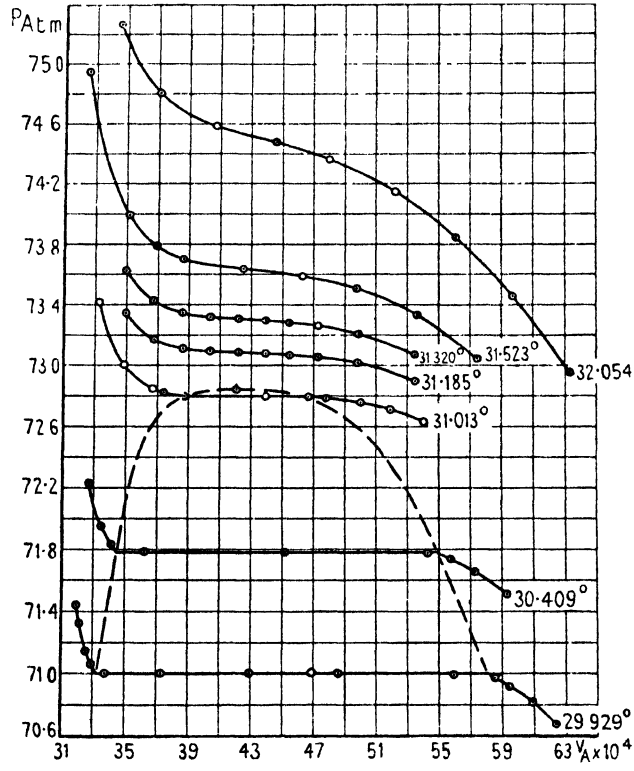

FIG. 71. (P, V) isotherms of carbon dioxide at the critical point (Michels, Blaisse, and Michels).

The (P, V) isotherms of carbon dioxide in the neighbourhood of the critical point are shown in Fig. 71.

Michels and Michels have discussed, in a recent paper [1], the whole question of the series representation of the data for carbon dioxide. They are unable to find any series that will reproduce

Series Equation for Carbon Dioxide for Pressures up to 3,000 Atmospheres (Michels and Michels)

$$pV = A + B\rho + C\rho^2 + Z\rho^3 + D\rho^4 + E\rho^6 + F\rho^8.$$

Temp., °C.	A	$B \times 10^3$	$C \times 10^6$	$Z \times 10^9$	$D \times 10^{12}$	$E \times 10^{18}$	$F \times 10^{24}$
Gas:							
40·105	1·154650	−5·691941	9·41470	17·75226	−74·64248	215·2911	−157·2770
49·712	1·190062	−5·487750	9·98347	9·76829	−53·50756	180·2757	−127·3692
75·260	1·284231	−4·972395	10·37167	−0·80821	−21·95426	128·0061	−84·1916
99·767	1·374563	−4·514801	10·24786	−5·26154	−5·16369	99·4225	−60·9761
125·007	1·467597	−4·070506	9·91486	−7·05498	5·48658	79·2425	−42·7539
150·140	1·560237	−3·661328	9·64656	−8·00258	13·42336	64·4629	−30·3258
0	1·006824	−6·837046	11·39205	..	−151·4235	..	..
25·053	1·099169	−6·099705	10·69337	14·27129	−170·3612	8,913·056	−252,457·2
29·900	1·117035	−6·029717	14·63283	−79·33782	616·6174	−15,153·460	204,050·9
31·037	1·121226	−5·958189	11·60349	−10·20406	60·7083	−965·879	6,334·6
32·075	1·125052	−5·928158	11·33589	−6·74054	46·9183	−984·129	7,614·8
Liquid:							
25·053	0·523412	−1·129210	2·72154	−13·23712	9·02762	86·36283	−51·10890
29·900	0·218806	1·555123	−4·44812	−9·14362	19·08726	62·26349	−30·95412
31·037	0·239629	1·368326	0·74904	−40·69024	80·10010	−24·54438	40·95553
32·075	0·331725	1·162219	−4·21878	−11·29488	29·06571	37·27420	−5·20579

completely the whole range of data between 1 and 3,000 atmospheres, and they therefore suggest the use of the equation

$$pV = A + B\rho + C\rho^2 + Z\rho^3 + D\rho^4 + E\rho^6 + F\rho^8,$$

employing below 40° one series for the range of gas densities and a second series for the range of liquid densities. The coefficients for the two series are given on the previous page.

Ethylene

Reference	*Temperature of isotherms, °C.*	*Maximum pressure, atms.*
Michels, de Gruyter, and Niesen, *Pub. van der Waals Fund*, No. 47 (1936)	From 0 at intervals of 25 to 150	270

The coefficients of the series equation

$$pV = A + B\rho + C\rho^2 + D\rho^4 + E\rho^6 + F\rho^8$$

as given by Michels and collaborators are as follows:

Temp., °C.	*A*	$B \times 10^3$	$C \times 10^6$	$D \times 10^9$	$E \times 10^{12}$	$F \times 10^{15}$
0	1·00734	−7·3519	3·439	7·830	−2·690	0·3570
25	1·09954	−6·7102	5·630	5·840	−1·887	0·2330
50	1·19174	−6·0873	4·410	6·465	−2·152	0·2771
75	1·28393	−5·5097	1·917	8·098	−2·853	0·3818
100	1·37613	−4·9829	0·011	9·464	−3·505	0·4925
125	1·46833	−4·5665	3·252	5·977	−1·817	0·2177
150	1·56052	−4·1786	5·771	4·741	−1·440	0·1645

Hydrogen

Reference	*Temperature of isotherms, °C.*	*Maximum pressure, atms.*
1. Kammerlingh Onnes and Braak, *Commn. Phys. Lab. Leiden*, No. 100 B	0	50
2. Kohnstamm and Walstra, *Proc. Roy. Acad. Amsterdam*, **47**, 203 (1914)	20	1,000
3. Schalkwijk, *Commn. Phys. Lab. Leiden*, No. 70	20	100
4. Onnes, Crommelin, and Smid, *Commn. Phys. Lab. Leiden*, No. 146 B	20	100
5. Holborn, *Ann. d. Physik*, **63**, 674 (1920)	−100 −50 −25 0 50 100	100
6. Verschoyle, *Proc. Roy. Soc.* (A), **111**, 552 (1926)	0 20	205

Hydrogen (cont.)

Reference	*Temperature of isotherms, °C.*	*Maximum pressure, atms.*
7. Bartlett, *J. Am. Chem. Soc.* **49**, 687 (1927).	−70	1,000
	−50	
Bartlett, Cupples, and Tremearne,	−25	
J. Am. Chem. Soc. **50**, 1275 (1928).	0	
Bartlett, Hetherington, Kvalnes,	50	
and Tremearne, *J. Am. Chem. Soc.*	100	
52, 1363 (1930)	200	
	300	
	400	

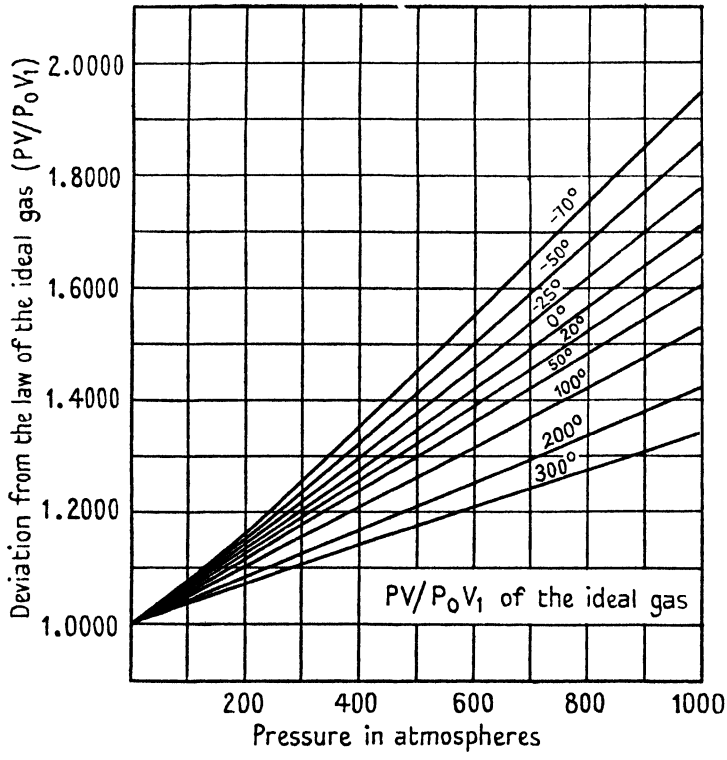

FIG. 72. Isotherms of hydrogen.

The isotherms in Fig. 72 are reproduced from the data of Bartlett, Hetherington, Kvalnes, and Tremearne.

It will be seen that above 100 atmospheres pressure the curves rapidly fan out, those at the lower temperatures showing the greatest deviations from the simple gas laws; the low-temperature isotherms

show a definite concavity upwards at the lower pressure whilst the high-temperature isotherms have a slight concavity downwards; the 0° isotherm is practically linear over the whole pressure range.

Considering the actual experimental data, the results of Verschoyle, Holborn, and Schalkwijk show satisfactory agreement where comparison is possible. At pressures from 100 to 1,000 atmospheres and temperatures up to 200° the maximum deviation between Bartlett's and Amagat's results is 0·60 per cent. and the mean deviation is 0·30 per cent.

The following series equations represent the experimental data to a close approximation over the pressure ranges indicated.

Constants of the Series Equation for Hydrogen

$pV = A + Bp + Cp^2$.

Pressure range, atms.	*Temp., °C.*	*A*	*B*	*C*	*Reference*
1–200	0	0·99937	$0·6263 \times 10^{-3}$	$0·168 \times 10^{-6}$	Verschoyle
1–100	20	1·07258	$0·6351 \times 10^{-3}$	$0·206 \times 10^{-6}$	Schalkwijk
1–200	20	1·07258	$0·6467 \times 10^{-3}$	$0·161 \times 10^{-6}$	Kohnstamm and Walstra
1–200	20	1·07257	$0·6505 \times 10^{-3}$	$0·069 \times 10^{-6}$	Verschoyle

Constants of the Series Equation for Hydrogen (Holborn)

Pressure range: 0–100 atmospheres.

Temp., °C.	*A*	$B \times 10^3$	$C \times 10^6$
−183	0·32995	−0·247	3·81
−150	0·45065	+0·132	2·00
−100	0·63360	0·408	0·90
−50	0·81650	0·540	0·50
0	0·99938	0·624	0·22
50	1·18240	0·676	..
100	1·36530	0·695	..
200	1·73100	0·701	..

Helium

Reference	*Temperature of isotherms, °C.*	*Maximum pressure, atms.*
1. Onnes, *Commn. Phys. Lab. Leiden*, Nos. 44 (1898), 102A (1907), 102 (1908). Boks and Onnes, *Commn. Phys. Lab. Leiden*, No. 170A (1924)	0 20	60
2. Holborn and collaborators, see refs. for argon	From −183 at intervals to 400	125
3. Gibby, Masson, and Tanner, *Proc. Roy. Soc.* (A), **122**, 283 (1929)	From 25 at intervals of 25 to 175	125

Constants of the Series Equation for Helium

$$pV = A + Bp + Cp^2.$$

Pressure range: 0–100 atmospheres.

Temp., °C.	*A*	$B \times 10^3$	$C \times 10^6$
−183	0·32992	0·6229	0·735
−150	0·4507	0·509	0·259
−100	0·6336	0·531	0·165
−50	0·81655	0·532	0·094
0	0·99945	0·529	..
50	1·18245	0·524	..
100	1·3654	0·508	..
200	1·7312	0·494	..
300	2·0970	0 468	..
400	2·46285	0·452	..

Krypton

Reference	*Temperature of isotherms*, °C.	*Maximum pressure, atms.*
Ramsay and Travers, *Proc. Roy. Soc.* (A), **67**, 329 (1901); *Phil. Trans.* **197**, 79 (1901)	11·2 and 237·3	100

Neon

1. Onnes and Crommelin, *Commn. Phys. Lab. Leiden*, Nos. 118 B (1910), 147 *d* (1915)	From −182·6 at intervals to 209	100
2. Holborn and collaborators, see refs. for argon	From −183 at intervals to 400	100

Nitrogen

1. Holborn and Otto, *Zeit. f. Physik*, **23**, 77 (1924)	−130	100
	−100	
	−50	
	0	
	50	
	100	
	150	
	200	
	300	
	400	
2. Onnes and van Urk, *Commn. Phys. Lab. Leiden*, No. 169 D (1924)	0	60
	20	
3. Verschoyle, *Proc. Roy. Soc.* (A), **111**, 552 (1926)	0	205
	20	
4. Bartlett, *J. Am. Chem. Soc.* **49**, 687 (1927)	−70	1,000
	−50	

Reference	Temperature of isotherms, °C.	Maximum pressure, atms.
5. Bartlett, Cupples, and Tremearne, *J. Am. Chem. Soc.* **50**, 1275 (1928)	−25	1,000
	0	
6. Bartlett, Hetherington, Kvalnes, and Tremearne, *J. Am. Chem. Soc.* **52**, 1363 (1930)	50	
	99·85	
	198·9	
	299·8	
	399·3	
7. Michels, Wouters, and de Boer, *Pub. van der Waals Fund*, Commn. No. 37 (1934); ibid., Commn. No. 51 (1936)	0	3,000
	25	
	50	
	75	
	100	
	125	
	150	

The isotherms in Fig. 73 are drawn from the data of Bartlett, Hetherington, Kvalnes, and Tremearne over the temperature range −70° to 400° C. and for pressures up to 1,000 atmospheres. They differ from the corresponding curves for hydrogen and resemble more closely those of carbon monoxide. Thus the low-temperature isotherms show a well-defined Boyle point and all the isotherms between −70° and 100° C. converge and meet at a point corresponding with a pressure of 380 atmospheres and a pv/p_0v_1 ratio of approximately 1·240. Above 400 atmospheres the isotherms at all temperatures are substantially linear.

Constants of the Series Equation for Nitrogen
(Michels, Wouters, and de Boer)

$$p(V-\alpha) = A+\beta\rho+\gamma\rho^2+\delta\rho^3+\epsilon\rho^4.$$

Pressure range: 200–3,000 atmospheres.

Temp., °C.	$\alpha\times10^3$	A	$\beta\times10^3$	$\gamma\times10^6$	$\delta\times10^9$	$\epsilon\times10^{11}$
0	0·48398	1·00045	−0·95241	3·38591	−2·22621	9·2040
25	0·59626	1·09202	−0·88854	3·18775	−0·84709	6·6287
50	0·54734	1·18358	−0·67607	3·24421	−0·58091	7·0958
75	0·51846	1·27515	−0·48391	3·29668	−0·22363	7·2360
100	0·62860	1·36671	−0·47050	3·12708	+0·69591	4·8982
125	0·65156	1·45828	−0·36509	3·17849	+0·84240	4·4999
150	0·77424	1·54985	−0·39933	2·82427	+2·03012	1·4968

Constants of the Series Equation for Nitrogen (Holborn and Otto)

$pV = A + Bp + Cp^2 + Dp^4$.
Pressure range: 1–100 atmospheres.

Temp., °C.	*A*	$B \times 10^3$	$C \times 10^6$	$D \times 10^9$
−130	0·52333	−3·56131	−14·1925	−6·7679
−100	0·63360	−2·31496	−1·7787	+0·6232
−50	0·81710	−1·17750	+3·3113	0·08167
0	1·00046	−0·46144	3·1225	..
50	1·18368	−0·01151	2·2016	..
100	1·36691	+0·27403	1·8276	..
150	1·55012	0·51465	1·2406	..
200	1·73330	0·68501	0·9151	..
300	2·09363	0·92155	0·4356	..
400	2·46591	1·04945	0·4688	..

Constants of the Series Equation for Various Nitrogen Isotherms

$pV = A + Bp + Cp^2$.

Pressure range, atms.	*Temp., °C.*	*A*	$B \times 10^3$	$C \times 10^6$	*Reference*
1–200	0	1·00049	−0·4961	3·334	Verschoyle
	20	1·07370	−0·2798	2·800	,,
1–60	0	1·00041	−0·4101	1·898	Onnes and van Urk
	20	1·07370	−0·2445	2·114	,, ,,

Carbon Monoxide. Data for the compressibility of this gas are rather scanty and only one series of measurements has been made up to 1,000 atmospheres pressure. The following list contains the principal references:

Reference	*Temperature of isotherms, °C.*	*Maximum pressure, atms.*
1. Scott, *Proc. Roy. Soc.* (A), **125**, 330 (1929)	25	170
2. Botella, *Anales. soc. espan. fis. quim.* **27**, 315 (1929)	0	130
	12·44	
	20·22	
3. Goig, *Compt. rend.* **189**, 246 (1929)	0	130
4. Bartlett, Hetherington, Kvalnes, and Tremearne, *J. Am. Chem. Soc.* **52**, 1374 (1930)	−70	1,000
	−50	
	−25	
	0	
	25	
	50	
	100	
	150	
	200	

The isotherms show a close resemblance to those for nitrogen. Carbon monoxide is slightly more compressible in the low-pressure range and slightly less so in the high-pressure range, in agreement

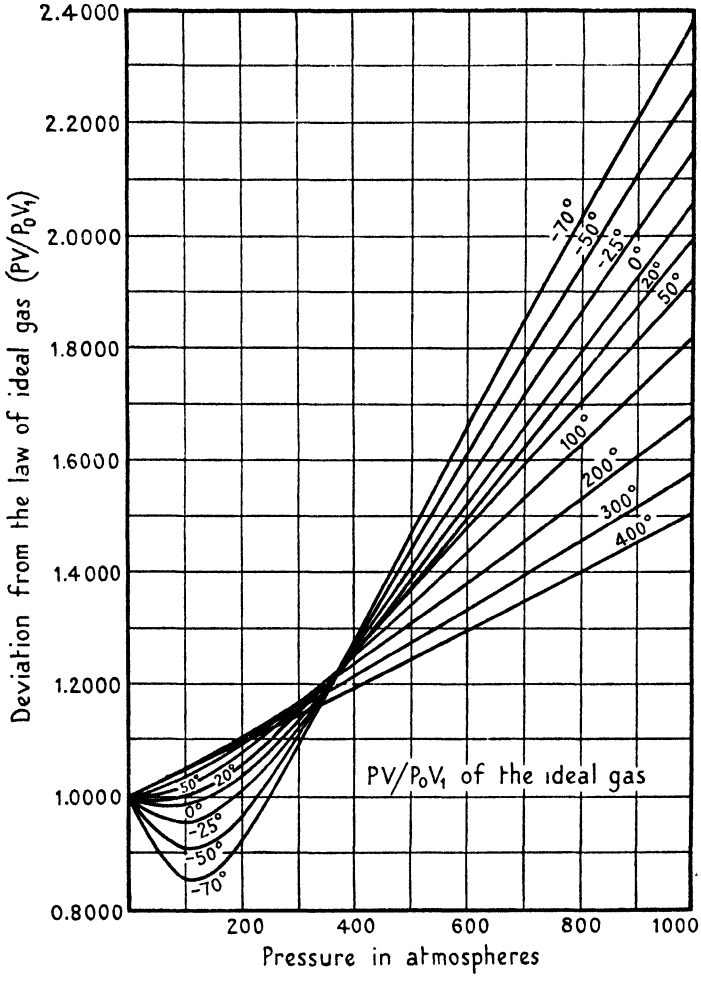

FIG. 73. Isotherms of nitrogen.

with its higher critical temperature; but the difference in compressibility tends to diminish with increasing temperature. The low-temperature isotherms show a well-defined Boyle point and all the isotherms between —70 and 200° C. converge and meet at a point

corresponding with a pressure of 375 atmospheres and a pv/p_0v_1 ratio of 1·225 approximately; above this pressure all the isotherms are linear up to 1,000 atmospheres.

Methane

Reference	*Temperature of isotherms, °C.*	*Maximum pressure, atms.*
1. Burrell and Robertson, Bur. of Mines (U.S.A.), Tech. Paper No. 158 (1917)	15	40
2. Keyes, Smith, and Joubert, *J. Math. Phys. Mass. Inst. Tech.* **1**, 191 (1922) and	0 50 100 150	300
3. Keyes and Burks, *J. Am. Chem. Soc.* **49**, 1403 (1927)	200	
4. Kvalnes and Gaddy, *J. Am. Chem. Soc.* **53**, 394 (1931)	−70 −50 −25 0 +25 +50 +100 +150 +200	1,000
5. Freeth and Verschoyle, *Proc. Roy. Soc.* (A), **130**, 453 (1931)	0 20	215
6. Michels and Nederbragt, *Pub. van der Waals Fund*, No. 48 (1936)	0 25 50 75 100 125	300

The isochores of methane shown in Fig. 74 are taken from the data of Keyes and Burks and the isotherms in Fig. 75 from that of Kvalnes and Gaddy. The critical temperature of methane is −81·0 and its critical pressure is 48 atmospheres. The −70° isotherm is, therefore, a little above the critical. All the curves show well-marked Boyle points, the minima lying on a parabolic curve. The unique point exhibited by nitrogen and carbon monoxide is not so evident in the case of methane but there is a region between 300 and 500 atmospheres in which all the isotherms cross.

Constants of the Series Equation for Methane (Michels and Nederbragt)

$$pV = A+B\rho+C\rho^2+Z\rho^3+D\rho^4.$$

Pressure range: 18–380 atmospheres. Density: Amagat units.

Temp., °C.	A	$B\times10^3$	$C\times10^6$	$Z\times10^9$	$D\times10^{12}$
0	1·00242	−2·41440	5·7541	−3·550	12·18
25	1·09416	−2·12083	5·7347	−3·928	16·36
50	1·18591	−1·83625	5·6224	−3·097	17·54
75	1·27766	−1·58436	5·9676	−4·913	24·00
100	1·36940	−1·32177	5·8711	−3·539	23·78
125	1·46115	−1·06891	5·8420	−2·266	23·20
150	1·55290	−0·80683	5·4890	+1·551	16·53

Constants of the Series Equation for Methane (Keyes and Burks)

$$pv = A+B\frac{1}{v}+C\frac{1}{v^2}+D\frac{1}{v^3}+E\frac{1}{v^4}.$$

Volumes: c.c. per gm.

Pressure range, atms.	*Temp.*, °C.	A	B	C	D	E
32–108	0	1397·7	−4485·3	7935·8	99998	−5109961
39–145	50	1653·5	−3255·2	3554·3	172063	−894859
46–182	100	1909·4	−2168·3	878·5	235365	−1253210
53–218	150	2165·3	−1194·4	1130·1	243381	−1276250
60–254	200	2421·1	−300·2	5690·7	160327	−684619

Keyes and Burks point out that the above equations represent the experimental data with considerable accuracy, except those corresponding to 10 c.c. per gm. (i.e. the highest pressure). The coefficients B of reciprocal v are given by

$$B = 14{\cdot}8413T-8207{\cdot}9+1{\cdot}74667\times10^6(1/T)-$$
$$-8{\cdot}006264\times10^8(1/T^2)+8{\cdot}16284\times10^{10}(1/T^3),$$

and similar expansions will represent the remaining coefficients. They also consider that the following equation of state is more to be relied upon for general calculations involving derivatives:

$$p_{\text{atm}} = \frac{5{\cdot}1173T(1-y/2)}{v-\delta}-\frac{9370(1-0{\cdot}586y)}{v+0{\cdot}42},$$

where y is the fraction of molecules associated to double molecules,

$$\log_{10}\delta = 0{\cdot}5611-0{\cdot}978/v,$$

$$\log_{10}(v-\delta)\frac{y}{(1-y)^2} = \frac{527}{T}-1{\cdot}25\log_{10}T+0{\cdot}813.$$

Nitric Oxide. Briner (*J. de Chimie Physique*, **4**, 476 (1906); *Compt. Rend.* **144**, 911 (1907)) has measured the compressibility of nitric

oxide at a number of temperatures between −78·6 and 9° C. and at pressures up to 160 atmospheres.

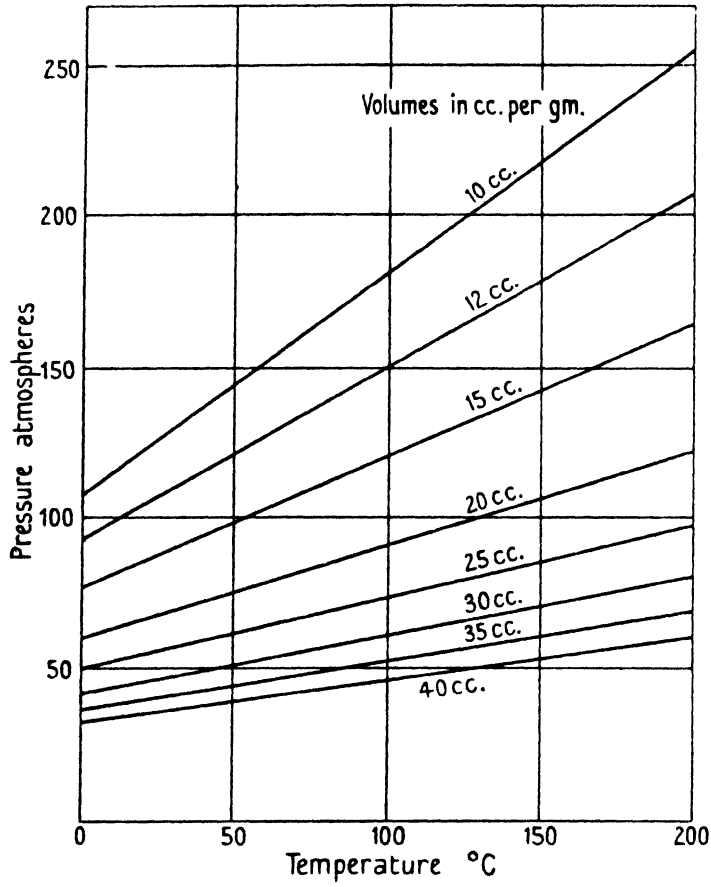

FIG. 74. Isochores of methane.

Oxygen

Reference	*Temperature of isotherms, °C.*	*Maximum pressure, atms.*
1. Onnes and collaborators, *Commn. Phys. Lab. Leiden*, Nos. 69 (1901), 78 (1902), 84 (1903), 165A (1923), 165C (1923), 169D (1924)	0	65
	15·6	
	20	
2. Holborn and Otto, see refs. for argon	0	100
	50	
	100	
3. Masson and Dolley, *Proc. Roy. Soc.* (A), **103**, 524 (1923)	25	125

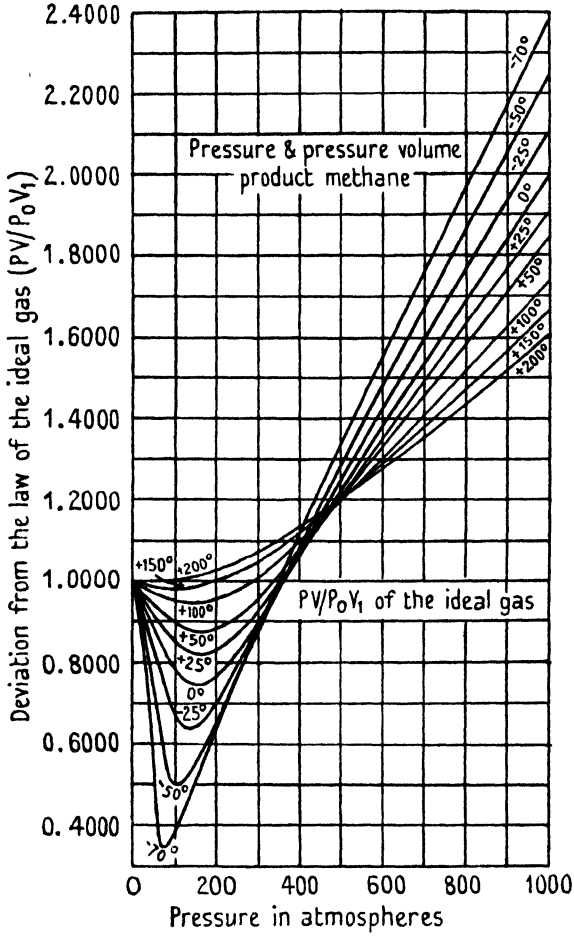

FIG. 75. Isotherms of methane.

Constants of the Series Equation for Oxygen

$pV = A+Bp+Cp^2$. Pressure range: 0–100 atmospheres.

Temp., °C.	*A*	$B\times10^3$	$C\times10^6$
0	1·0010	−0·994	2·19
50	1·1842	−0·491	1·70
100	1·3674	−0·160	1·37

$pV = A+B/V+C/V^2$. Pressure range: 0–60 atmospheres.

Temp., °C.	*A*	$B\times10^3$	$C\times10^6$
0	1·000956	−0·95803	2·0608
20	1·07426	−0·80379	2·0591

Higher Hydrocarbons

Ethane. Sage, Webster, and Lacey, *J. Ind. Eng. Chem.* **29**, 658 (1937).

Propane. Lacey and Sage, *Petroleum World*, Dec. 1934; Beattie, Poffenberger, and Hadlock, *J. Chem. Phys.* **3**, 96 (1935); Beattie, Kay, and Kaminsky, *J. Am. Chem. Soc.* **59**, 1589 (1937).

n-Butane. Sage, Webster, and Lacey, *J. Ind. Eng. Chem.* **29**, 1188 (1937).

n-Pentane. Sage, Lacey, and Schaafsma, *J. Ind. Eng. Chem.* **27**, 48 (1935).

n-Heptane. Smith, Beattie, and Kay, *J. Am. Chem. Soc.* **59**, 1587 (1937).

Equations of State

The results summarized in the preceding pages show that the variation of the product pv with pressure for real gases may usually, but not invariably, be represented satisfactorily by series equations. Five or more terms, however, are required to cover even a moderate range of pressures and the equations are, in consequence, not very convenient for thermodynamic calculations; it is doubtful, moreover, whether any definite meaning should be attached to the numerical values of any of the coefficients beyond the first and second. It remains to be seen whether any of the proposed equations of state having a theoretical or semi-theoretical basis and containing fewer constants are able to reproduce equally well the experimental data.

Theoretical equations embodying the functional relationships between the pressure, volume, and temperature of a fluid are based upon hypothetical molecular models the properties of which govern the form of the functions. Such models are, in general, endowed, *ex hypothesi*, with fields of force, but the exact nature and magnitude of the fields are not usually specified with any exactitude.

The existence of intermolecular forces was suspected long before anything was known about the intimate structure of matter. Newton, for example, in Proposition 23 of the second book of the *Principia* discussed whether the expansive properties of a gas might be explained by assuming the existence of repulsive forces between the molecules. He showed that 'if a fluid be composed of particles mutually flying each other, and the density be as the compression, the centrifugal force of the particles will be reciprocally proportional to the distance of their centres'. 'But', he added, 'whether elastic fluids do really consist of particles so repelling each other is a physical question.' Nearly a century later, Thomas Young contributed an important paper to the *Philosophical Transactions* (1805) entitled 'On the Cohesion of Fluids', in which he assumed the existence of attractive and repulsive forces and even arrived at a quantitative

estimate of the distance over which the cohesive force acts, the 'mutual distance' of the particles of vapour, and the actual magnitudes of the 'elementary atoms' of a liquid.

It was not until 1873, however, that the significance of intermolecular forces in the theory of the fluid state obtained general recognition. In that year Johannes Diderik van der Waals published an essay 'On the Continuity of the Liquid and Gaseous States' [2] in which he showed, on the basis of a comparatively simple model, how an equation of state might be derived which would take into account the cohesive forces between molecules and the space occupied by them. The status and limitations of his equation are now generally known, but the theoretical advances which have resulted from its use during the past fifty years are so important that a brief reference to its derivation and properties will not be out of place.

Van der Waals derived the cohesive-force term from considerations based upon analogy with Laplace's theory of surface tension. The average effect of the forces of attraction or cohesion in a gas is that of a permanent field of force acting upon each molecule at or near the boundary, or of an inward or negative pressure acting on the boundary molecules. This field, in the case of liquids, gives rise to surface tension. The magnitude of the inward pressure, p', is proportional to the number of molecules in the boundary layer and in the body of the gas, and hence to the square of the density, ρ. The cohesive-force term may, therefore, be written

$$p' = c\rho^2 = cN^2m^2/v^2 = a/v^2,$$

where c and a are constants independent of the pressure and temperature.

The co-volume term of the equation takes account of the regions surrounding each individual molecule into which the centres of other molecules are unable to penetrate. The aggregate volume of these regions of exclusion is $\frac{2}{3}\pi N\sigma^3$, or four times the aggregate sum of the volumes of the molecules; it is usually denoted by the letter b. The space available for the translational motion of the molecules will therefore be $(v-b)$ and will diminish with increase of the molecular density.

By adding the cohesive force and the co-volume terms to the ideal equation of state we obtain van der Waals' equation:

$$(p+a/v^2)(v-b) = NRT. \qquad (8.9)$$

It should be noted that from van der Waals' derivation the constants a and b depend only upon the nature and quantity of the gas, the former being proportional to the square and the latter to the first power of v. Actually it may be shown that both should be functions of the temperature. Jeans [3] also points out that one factor overlooked in the original derivation of the equation is that when cohesive forces are operative, some molecules which normally would have reached the walls no longer do so owing to the deflexion of their paths; these molecules therefore exert no pressure on the walls, whereas according to van der Waals they should exert a negative pressure.

The Evaluation of the Constants a and b

Van der Waals' equation is valid only at high temperatures and low or moderate densities; that is, in the region in which the deviations from the ideal gas laws are relatively small. The method of evaluating the constants from critical data is in consequence open to objection, and alternative methods based, for example, upon the measurement of the pressure and volume coefficients of thermal expansion of the gas are to be preferred [3].

The volume and pressure changes of an ideal gas with temperature are given by the equations

$$\left.\begin{aligned} v &= v_0(1+k_v t) \\ \text{and} \quad p &= p_0(1+k_p t), \end{aligned}\right\} \tag{8.10}$$

where k_p and k_v are the expansion coefficients at constant volume and constant pressure, respectively.

The Pressure Coefficient. If p_0 and p_1 are the pressures exerted by a given mass of gas at constant volume v and temperatures T_0 and T_1 respectively, then from (8.9)

$$(p_0+a/v^2)(v-b) = NRT_0, \tag{8.11}$$

and

$$(p_1+a/v^2)(v-b) = NRT_1. \tag{8.12}$$

By subtraction

$$(p_1-p_0)(v-b) = NR(T_1-T_0). \tag{8.13}$$

On combining (8.11) and (8.13) and eliminating $(v-b)$,

$$\frac{p_1-p_0}{T_1-T_0}.T_0/p_0 = 1+a/p_0v^2. \tag{8.14}$$

Now from (8.10)

$$k_p = (p_1-p_0)/p_0(T_1-T_0).$$

On substituting in (8.14),

$$k_p = (1+a/p_0v^2)/T_0. \tag{8.15}$$

Eq. (8.15) indicates that within the limits in which van der Waals' equation holds, for a given density of gas, k_p is independent of the temperature.

The Volume Coefficient. If the pressure p be kept constant whilst a given mass of gas is heated from T_0 to T_1, the volume will change from v_0 to v_1. We may write as before

$$(p+a/v_0^2)(v_0-b) = NRT_0, \tag{8.16}$$

and

$$(p+a/v_1^2)(v_1-b) = NRT_1. \tag{8.17}$$

On subtraction, neglecting the product ab,

$$(p-a/v_0 v_1)(v_1-v_0) = NR(T_1-T_0). \tag{8.18}$$

Substituting for k_v in (8.18) we obtain

$$(p-a/v_0 v_1)v_0 k_v = NR,$$

from which

$$k_v = [1+a/pv_0(1/v_0+1/v_1)-b/v_0]/T_0. \tag{8.19}$$

The volume coefficient k_v, therefore, depends both upon the volume and the pressure.

By determining k_v and k_p experimentally the values of the constants a and b may be obtained directly from (8.15) and (8.19).

If it be assumed that a and b for a particular gas are functions only of temperature, their values may be calculated from the corresponding compressibility isotherms of the gas. Michels, Wouters, and de Boer give the following values for nitrogen calculated in this way from the isotherms at temperatures between 0° and 150° C.:

Variations of the Constants a and b of the van der Waals Equation with Temperature, for Pure Nitrogen

Temp., °C.	$a \times 10^3$	$b \times 10^3$
0	2·0816	1·6296
25	1·9499	1·5769
50	1·8698	1·5639
75	1·8030	1·5571
100	1·6649	1·5069
125	1·5505	1·4770
150	1·2963	1·3732

Using these values a comparison is given in Table 33 between the calculated and observed values of pV for nitrogen at 0° and 100° C. and a number of pressures.

The agreement, particularly at the higher temperature, is good and indicates that over this range of temperatures and pressures the equation is able to reproduce satisfactorily the experimental results

provided account be taken of the variation of the constants with temperature.

TABLE 33. *A Comparison between the Calculated (van der Waals) and Observed Values of pV for Nitrogen at 0° and 100° C.*

Temp., °C.	*Pressure, atms.*	*pV, observed*	*pV, calculated*	$\Delta \times 10^5$
0	19·0215	0·99274	0·99281	−7
	23·7629	0·99122	0·99123	−1
	28·4968	0·98983	0·98976	7
	33·1101	0·98851	0·98850	1
	37·9526	0·98730	0·98729	1
	42·7435	0·98621	0·98611	10
	47·4376	0·98541	0·98541	0
	52·2160	0·98460	0·98470	−10
100	26·3546	1·37546	1·37544	2
	33·0358	1·37802	1·37802	0
	39·7519	1·38077	1·38076	1
	46·3425	1·38356	1·38359	−3
	53·3065	1·38671	1·38675	−4
	60·2424	1·38995	1·38991	4
	67·0816	1·39346	1·39346	0
	74·0947	1·39715	1·39713	2

The Dieterici Equation of State

The expression deduced by van der Waals for the cohesive force assumes the density in the boundary layer to be the same as in the body of the gas. Whilst this assumption is approximately true at low densities and high temperatures, it obviously cannot hold at the critical point, where the cohesive force is comparable with the total pressure of the gas. Dieterici has taken into account the alteration in density of the gas in the neighbourhood of the boundary and, employing the same molecular model as van der Waals, arrives at the equation [4]

$$p(v-b) = RNTe^{-a/RNTv}, \tag{8.20}$$

where b is the co-volume term and a is a constant related to the cohesion pressure. In deriving a he assumes that owing to the attractive field the number of molecules reaching the boundary in unit time will be diminished, and those molecules which do reach it will have lost part of their kinetic energy. If p' is the pressure in the body of the gas and p the actual pressure exerted at the boundary, then the work done in bringing a molecule from the interior to the boundary, a, will be

$$a = RT \log_e p'/p,$$

or

$$p = p'e^{-a/RNT}.$$

Now the magnitude of a increases with the density and it is therefore a function of the volume. By an empirical method, Dieterici found that

$$p = p'e^{-a/RNTv},$$

from which (8.20) follows.

Dieterici's equation has exactly the same range of validity as van der Waals' equation but, as will be shown later, it leads to more accurate values for some of the critical constants.

The Virial of Clausius

Clausius attempted to calculate the relation between the pressure, volume, and temperature of a real gas as follows [5]:

If X, Y, and Z are the components of a force acting upon a molecule of mass m, the equations of motion are

$$m\ddot{x} = X$$

and two similar equations.

Using the identity

$$\tfrac{1}{2}d^2/dt^2(x^2) = \dot{x}^2 + x\ddot{x}$$

we have

$$\tfrac{1}{4}md^2/dt^2(x^2) - \tfrac{1}{2}m\dot{x}^2 = \tfrac{1}{2}Xx.$$

Adding together this and the two similar equations and summing for a number of particles, we find

$$\frac{1}{4}\frac{d^2}{dt^2}(\sum mr^2) = \tfrac{1}{2}\sum mv^2 + \tfrac{1}{2}\sum (Xx+Yy+Zz),$$

where

$$r^2 = x^2+y^2+z^2 \quad \text{and} \quad v^2 = \dot{x}^2+\dot{y}^2+\dot{z}^2.$$

On integrating over a long time interval τ, and using bars to denote time averages from 0 to τ, we obtain

$$\tfrac{1}{4}\tau\left[\frac{d}{dt}(\sum mr^2)\right]_0^\tau = \tfrac{1}{2}\sum \overline{mv^2} + \tfrac{1}{2}\sum (\overline{Xx}+\overline{Yy}+\overline{Zz}).$$

In the steady motion of a gas the left-hand side of this equation can be made as small as desired by making τ sufficiently large, and it reduces to

$$\sum \tfrac{1}{2}\overline{mv^2} = -\tfrac{1}{2}\sum (\overline{Xx}+\overline{Yy}+\overline{Zz}). \qquad (8.21)$$

The quantity on the right-hand side was called by Clausius the 'virial' of the system, and the equation indicates that when a gas moves undisturbed from its steady state, the kinetic energy of its motion is equal to its virial.

It should be noted that the virial depends solely upon the forces acting on the molecules, and not upon their motion; in the case of

a gas these forces are the force exerted by the molecules upon one another and the force exerted by impact on the walls of the containing vessel.

It can be shown that the contribution of the pressure to the virial is $\frac{3}{2}pv$, where v is the volume of the vessel; and if it be assumed that the force between two molecules at a distance r is a repulsive force $\phi(r)$ and is a function of the distance r only, then that part of the pressure which arises from intermolecular forces is $-\frac{1}{2}\sum\sum r\phi(r)$. This is a co-volume term and does not take into account forces of cohesion. (8.21) may therefore be written

$$\tfrac{1}{2}\sum mc^2 = \tfrac{3}{2}pv - \tfrac{1}{2}\sum\sum r\phi(r),$$

so that the pressure is given by

$$pv = \tfrac{1}{3}\sum mc^2 + \tfrac{1}{3}\sum\sum r\phi(r). \qquad (8.22)$$

This equation shows that, theoretically, a pressure may be produced either wholly by molecular motion or wholly by intermolecular forces. The latter, however, would imply a law of force by which two molecules would repel one another with a force inversely proportional to their distance apart. Since this is obviously impossible we must conclude that the pressure of a gas must always arise in part from the motion of its molecules. If the term $\sum\sum r\phi(r)$ could be calculated for any law of intermolecular force, we should obtain at once an equation of state applicable to real gases at both high and low concentrations; this, however, is not at present possible and the best that can be done is to obtain a relation agreeing with van der Waals' equation as far as the first order of small quantities.

The More Accurate Equations of State

In recent years several semi-empirical equations have been proposed based upon an elaboration of the molecular model we have been considering. Of these mention may be made of the Beattie-Bridgeman equation [6] and the Keyes equation [7], both of which have been used extensively for interpolating compressibility data and for thermodynamic calculations.

The Beattie-Bridgeman equation rests upon the assumption that the kinetic and cohesive pressures in a gas may be treated separately, the measured pressure being the difference of two terms, one of which arises from its kinetic energy and the other from its potential energy; it also requires the assumption that the law of force (the specific

form of which need not be specified) shall be such that the force will diminish rapidly with distance.

The kinetic pressure of a gas can be measured by the time rate of transfer of momentum across an imaginary plane in the interior of the gas and, for an ideal gas, is given by the product ρRT, where ρ is the density; for a real gas in which intermolecular forces exist, the rate of transfer of momentum is greater than this quantity owing to the 'reflection' of molecules across the plane; and if r is the average value of the 'reflection' for all classes of molecules, the true rate of transfer of momentum I is given by the expression

$$I = \rho RT(1+r).$$

If the density of the gas is small so that the molecules act independently as reflectors, the fraction reflected is proportional to the density and we may write $r = \rho B$, where B is a constant, and

$$I = p_{\text{kin}} = \frac{RT}{v^2}(v+B). \tag{8.23}$$

At high densities the reflecting powers of any one molecule will be interfered with by its neighbours and B will depend upon the density approximately according to a linear relation; that is,

$$B = B_0(1-b\rho).$$

On substituting this value in (8.23),

$$p_{\text{kin}} = \frac{RT}{v^2}\{v+B_0(1-b/v)\}. \tag{8.24}$$

Another important factor entering into the calculation of the kinetic pressure is the possibility of the formation of comparatively stable aggregates or clusters of molecules, due to the loss of kinetic energy by collision with a third body, or, in the case of complex molecules, by transfer of energy to another degree of freedom of the system. The evidence for the transient existence of such aggregates in the neighbourhood of the critical temperature has already been mentioned, and Keyes has further suggested that the departure from linearity of the isochores of a gas as the temperature is lowered is explicable on the assumption of a 'quasi-association' or aggregation of the single species to double or perhaps higher-order species [8].

The formation of aggregates will increase the apparent average time of encounter between molecules and hence will affect the number of collisions, and will have the same effect as a change in the average molecular weight of the gas; and since their number will

depend upon temperature and density, the gas constant R must also be considered to depend upon these quantities.

Beattie and Bridgeman, on such assumptions, derive the following expression for the variation of R:

$$R' = R\left(1-\frac{m}{v}e^{n/T}\right), \tag{8.25}$$

where m and n are constants, R is the ideal gas constant, and R' its analogue in the equation of state of an aggregating gas. This relation is found to reproduce the experimental data in a satisfactory manner but, owing to the exponential term, is rather inconvenient to handle. They therefore suggest that, to a first approximation, the variation in the number of independent aggregates due to the effect of temperature on the average time of encounters may be taken as directly proportional to the density and inversely proportional to a power n of the absolute temperature, so that

$$R' = R\{1-f(V,T)\} = R\left(1-\frac{c}{vT^n}\right).$$

From experimental data the most probable value of the index n is found to be 3.

The cohesion pressure as derived by van der Waals is based upon the assumption that the forces between the molecules, although small, are not negligible; the average effect of these forces can be represented by a permanent field of force acting upon each molecule at or near the surface; and this field can be regarded as exerting an inward pressure (p_{coh}) per unit area upon the outer layer of molecules, the value of which is given by

$$p_{\text{coh}} = A/v^2.$$

It has been pointed out, however, that if the molecules are considered as substantially rigid electrical systems, the molecular forces which give rise to the cohesive pressure are dependent upon the dielectric constant k of the gas, so that

$$p_{\text{coh}} = A_0/kv^2;$$

and since k is related to the density by the Lorentz equation

$$\frac{k-1}{k+2} = C/v,$$

we may write $$p_{\text{coh}} = \frac{A_0}{v^2}\left(1-\frac{3C}{v}+\ldots\right),$$

in which all powers of the density higher than the first are neglected.

Putting $3C = a$, $$p_{\text{coh}} = \frac{A_0}{v^2}\left(1-\frac{a}{v}\right),$$

which is the value used in the Beattie-Bridgeman equation. The complete equation may now be written

$$p = \frac{RT(1-\epsilon)}{v^2}[v+B]-\frac{A}{v^2}, \tag{8.26}$$

where $A = A_0(1-a/v)$, $B = B_0(1-b/v)$, and $\epsilon = c/vT^3$.

The gas constant R has the same value for all gases and A_0, a, B_0, b, and c are constants whose values depend upon the gas under consideration.

Eq. (8.26) may be expressed as a series equation in powers of $1/v$:

$$pv = RT+\beta/v+\gamma/v^2+\delta/v^3, \tag{8.27}$$

where
$$\beta = RTB_0-A_0-Rc/T^2,$$
$$\gamma = -RTB_0b+A_0a-RB_0c/T^2,$$
and
$$\delta = RB_0bc/T^2;$$

for a given mass of gas β, γ, and δ are functions of temperature only.

The values of the five adjustable constants A_0, a, B_0, b, and c may be calculated from any set of pressure-volume-temperature data and with the exception of c they may be obtained as the slope or intercept of straight lines.

Thus, for example, if the generalized equation of state be written in the form

$$p' = p+F(V,T) = T\psi(V)-\phi(V),$$

p' can be designated as the 'corrected pressure' since it varies linearly with the temperature at constant density, and it can be seen that for each isochore the quantities $\psi(V)$ and $\phi(V)$ are the slope and the intercept on the p'-axis of the (p',T) line.

Since $$\psi(V) = \frac{R}{v^2}[v+B],$$

then $$B = \frac{v^2\psi(V)}{R}-v,$$

and from the known values of R, V, and the observed value of $\psi(V)$, a value of B can be calculated for each isochore. The quantities B_0 and B_0b will then be the intercept on the B-axis and the slope respectively of the straight line obtained by plotting B against $1/v$.

Also $$\phi(V) = \frac{A}{v^2},$$

and from v and the observed value of $\phi(V)$ a value of A can be calculated for each isochore.

The quantities A_0 and $A_0 a$ are the intercept on the A-axis and the slope respectively of the straight line obtained by plotting A against $1/v$.

If the form of the $F(V, T)$ function, namely

$$F(V, T) = \frac{c\psi(V)}{vT^2},$$

is accurate from the standpoint of both temperature and volume variations, there will be one value of c which will cause the 'corrected' pressure p' to vary linearly with the temperature for every isochore.

In order to evaluate p' it is necessary to know $\psi(V)$, which is the slope $(\partial p'/\partial T)_v$, and since p' is not known until the additive term $F(V, T)$ has been evaluated, several approximations are required.

Beattie and Bridgeman suggest that a provisional value for c should first be obtained from a consideration of a single isochore, which should be of sufficiently high density to depart markedly from linearity, and which should also cover as wide a temperature range as possible; a value is assumed for c and the term $F(V, T)$ evaluated at the temperatures T_2 and T_1 from the relation

$$F(V, T) = \frac{c}{vT^2}\left[\frac{p_2 - p_1}{T_2 - T_1}\right]_v = \frac{c}{vT^2}\left(\frac{\Delta p}{\Delta T}\right)_v, \tag{8.28}$$

where p_2 and p_1 are the observed pressures at the highest and lowest temperatures T_2 and T_1 on the isochore. The results are added to p_2 and p_1, giving p_2' and p_1' to the first approximation. The calculation is repeated using the slope $(\Delta p'/\Delta T)_v$ resulting from the two values of p' just obtained, and this process continued, using the extreme temperature only, until no further change appears in $(\Delta p'/\Delta T)_v$. With this slope, a set of provisional values of p' at each temperature on the isochore are computed and the slope of the straight line drawn through these points is used to give the final values of the corrected pressure; since the whole term $F(V, T)$ is usually small, several approximations are in general sufficient.

The authors have made a detailed comparison of pressures calculated from their equation with the observed pressures for ten gases up to 100 atmospheres and find an average deviation of 0·08 atmospheres, or 0·18 per cent.; they conclude that it reproduces these data within the experimental error. Other applications of the equation to compressibility measurements extending over a wider range of pressures will be referred to later.

Constants of the Beattie-Bridgeman Equation for Hydrogen. Deming and Shupe [9] have calculated the constants for hydrogen using a modification of the above method. The equation may be written

$$p + \Gamma = \psi T - \phi,$$

where $\psi = R(v+B)v^{-2}$, $\Gamma T^2 = \psi c/v$, $\phi = Av^{-2}$,

$B = B_0(1-b/v)$, and $A = A_0(1-a/v)$.

They find that on plotting A and B against the density, a straight line is obtained in the case of A, with indications of a break at a density of about 0·015 mols per c.c. (approximately the critical density); for B, two straight lines meeting at the critical density are obtained. There will consequently be one set of values for A_0 and a and two sets of values for B_0 and b, as follows:

Below the critical density:

$$B_0 = 20{\cdot}22, \qquad A_0 = 124{,}040,$$
$$b = -7{\cdot}22.$$

Above the critical density:

$$B_0 = 17{\cdot}50, \qquad a = 56{\cdot}18,$$
$$b = 19{\cdot}68, \qquad c = 20 \times 10^6.$$

Since the values of both A and B from the lowest density to the critical density lie on straight lines, the equation holds with considerable accuracy up to the critical density. Thus, over the temperature range $-70°$ to $300°$ C., it reproduces pressures with a root-mean-square error of 0·251 per cent. at a density of 0·0245 mols per c.c., the maximum error being $-0{\cdot}28$ per cent. at $-25°$ C.; and with a root-mean-square error of 1·38 per cent. at 0·0270 mols per c.c., the maximum error being 2·10 per cent. at $-70°$ C.; at lower densities the agreement is very much closer. At densities greater than 0·0270 mols per c.c. the calculated pressures are invariably too small and the errors become quite large.

It is noteworthy that the expression $\phi = Av^{-2}$, which can be identified with the cohesive pressure term of the van der Waals equation, becomes negative at the highest densities (above 0·018 mols per c.c.), a change indicating that repulsive forces are beginning to predominate as the molecules become closely packed.

Constants of the Beattie-Bridgeman Equation for Nitrogen. The values of the constants given below were calculated from data furnished by the Reichsanstalt, the Leiden laboratory, and the Massachusetts Institute of Technology [10]. On plotting values of A and B against density the points are found to lie, in the former case on the parabola $A = 1528{\cdot}6(1-0{\cdot}2748/v-0{\cdot}9084/v^2)$, and in the latter on a straight line. The effect of the parabolic relation is to introduce

an additional constant a' into the equation. The values of the six constants are

$$A_0 = 1528{\cdot}6, \qquad a = 0{\cdot}2748, \qquad a' = 0{\cdot}9084,$$
$$B_0 = 1{\cdot}643, \qquad b = -0{\cdot}9235, \qquad c = 2{\cdot}2\times 10^6.$$

With the above constants, and over the temperature range $-70°$ to 400° C., the equation reproduces pressures with a root-mean-square deviation of 0·50 per cent. at 4 c.c. per gm., the maximum being 0·95 per cent.; and with a root-mean-square deviation of 0·78 per cent. at 3 c.c. per gm., the maximum deviation being 1·41 per cent. Below 3 c.c. per gm. the calculated pressures are invariably too low, and the discrepancy becomes large at low temperatures and small volumes.

Constants of the Beattie-Bridgeman Equation for Methane (based upon Keyes and Burks's data).

$$R = 0{\cdot}08206, \qquad A_0 = 2{\cdot}2769, \qquad a = 0{\cdot}01855,$$
$$B_0 = 0{\cdot}05587, \qquad b = -0{\cdot}01587, \qquad c = 12{\cdot}83\times 10^4.$$

Constants of the Beattie-Bridgeman Equation for Propane [11].

Units: Normal atmospheres, litres per mole, °K. ($= t°+273{\cdot}13$).

$$R = 0{\cdot}08206, \qquad A_0 = 11{\cdot}9200, \qquad a = 0{\cdot}07321,$$
$$B_0 = 0{\cdot}18100, \qquad b = 0{\cdot}04293, \qquad c = 120\times 10^4.$$

Units (Amagat): Normal atmospheres, $v = 1$ at 0° and 1 atmosphere.

$$R = 3{\cdot}73059\times 10^{-3}, \qquad A_0 = 24{\cdot}6359\times 10^{-3}, \qquad a = 3{\cdot}3283\times 10^{-3},$$
$$B_0 = 8{\cdot}2286\times 10^{-3}, \qquad b = 1{\cdot}9517\times 10^{-3}, \qquad c = 54{\cdot}554\times 10^3.$$

Constants of the Beattie-Bridgeman Equation for Gaseous n-Heptane [12].

Units: Normal atmospheres, litres per mole, °K.

$$R = 0{\cdot}08206, \qquad A_0 = 54{\cdot}520, \qquad a = 0{\cdot}20066,$$
$$B_0 = 0{\cdot}70816, \qquad b = 0{\cdot}19179, \qquad c = 400\times 10^4.$$

The Keyes Equation of State

This equation, which has been applied both to single gases and to binary mixtures over a wide range of conditions [7], is written

$$p = RT/(v-\delta) - a/(v-L)^2, \tag{8.29}$$

where $\log\delta = \log\beta - \alpha/v$, and β, α, a, and L are constants charac-

teristic of the gas; R is the gas constant defined by the 'ideal' gas equation of state.

The equation is based upon similar considerations to the Beattie-Bridgeman equation and contains both a co-volume and a cohesive pressure term. These terms differ from those of the van der Waals equation in that the former is a function of the volume and the latter contains a constant L which makes the cohesion increase more rapidly than a/v^2 with diminution of volume.

For atomic gases the equation reduces to

$$p = RT/(v-\beta)-a/(v-L)^2.$$

The Second Virial Coefficient

The equations we have been considering suffer from the defects associated with an over-simplified molecular model; in their derivation the specific form of the law of force is not defined except in so far as it is assumed to be such that the force diminishes rapidly with distance; and it is assumed implicitly that binary encounters alone are involved, although at high densities it is almost certain that any one molecule or atom will permanently be under the influence of several others. It is therefore not to be expected that these equations will reproduce closely the whole of the experimental data, and in particular they will not be valid in the neighbourhood of the critical point.

To provide a sound fundamental basis for an equation of state requires a more detailed knowledge of the laws of attraction and repulsion between pairs of atoms and molecules than is at present available [13]. Keesom [14] has indeed given an exact derivation of an equation for particular forms of intermolecular force fields, and employing compressibility data has obtained numerical values for the attractive force in particular instances; but he adopts a rigid spherical model or an ellipsoid of revolution to represent the repulsive field. Eisenschitz and London [15] have progressed a step farther and, by means of quantum mechanics, have calculated the interatomic forces at large distances of separation of two hydrogen atoms. Similar calculations for hydrogen and helium atoms have been carried out by Lennard-Jones [16], Slater and Kirkwood [17], Margenau [18], and others. Approximate methods applicable to larger atoms have also been developed by London [19], Kirkwood [20], and Hellman [21].

Statistical mechanics establishes the fact that at low pressures where binary encounters alone are concerned the equation of state of a gas may be expressed as

$$p(V-B) = RT, \tag{8.30}$$

where B is a function of the temperature and the intermolecular potential and for molecules of non-polar type is given by

$$B = 2\pi N \int_0^\infty r^2(1-\exp \phi/kT)\, dr. \tag{8.31}$$

In this expression ϕ is the energy of interaction of a pair of molecules separated by a distance r and k is the Boltzmann constant.

In order to calculate the value of B from (8.31) we must know $\phi = f(r)$. The fields computed by quantum-mechanical methods are invariably complicated functions of the distance which are neither convenient nor practicable for incorporation in an equation of state. Lennard-Jones [22] has therefore suggested that for the present they be replaced by simple functions which, although not possessing the same fundamental basis, lend themselves better to mathematical analysis.

He assumes the attractive and repulsive fields to be spherically symmetrical around the centre of each molecule or atom and the two forces to have each its own distance law and force constant; the effect of the relative orientation of the molecules, which in the case of non-polar molecules is not likely to be large, is neglected.

The intermolecular energy of two like molecules is then represented by the sum of two inverse power terms, namely, an attractive term of the form $-\mu r^{-m}$ and a repulsive term of the form λr^{-n}, where r is the distance of separation, λ and μ are the repulsive and attractive force constants, and n and m are the corresponding distance-law indices. It may be mentioned at this point that whilst λr^{-n} is a valid representation of the repulsive energy over a restricted range of values of r, a more general form would be $Pe^{-r/\rho}$, where P and ρ are constants [23].

Each pure gas is assumed to have its own characteristic values of n and m and its own force constants. The complete intermolecular potential energy ϕ is then given by

$$\phi = \lambda r^{-n} - \mu r^{-m}, \tag{8.32}$$

or for the whole range of r by

$$\phi = Pe^{-r/\rho} - \mu r^{-m}.$$

The complete specification of the field thus requires a knowledge of four parameters.

From (8.32)

$$\phi = -|\phi_0| \left\{ \frac{1}{n}\left(\frac{r_0}{r}\right)^n - \frac{1}{m}\left(\frac{r_0}{r}\right)^m \right\} \Big/ \left(\frac{1}{n} - \frac{1}{m}\right), \tag{8.33}$$

where r_0 is the distance between two molecules in equilibrium under the field represented by (8.32) and $|\phi_0|$ is the energy required to separate them from this configuration.

Substituting in (8.31), the second virial coefficient B' becomes

$$B' = \tfrac{2}{3}\pi N r_0^3 f(\phi_0/kT). \tag{8.34}$$

The function f is a polynomial whose coefficients depend only on n and m, and

$$f(\phi_0/RT) = (m/n)^{3/(n-m)} F(y),$$

where

$$F(y) = y^{3/(n-m)} \left\{ \Gamma\binom{n-3}{n} - \sum_{\tau=1}^{\infty} 3\Gamma\binom{\tau m - 3}{n} \frac{y^\tau}{\tau! n} \right\}$$

and

$$y = (m/n)^{-(m/n)} (1 - m/n)^{-1+(m/n)} (\phi_0/kT)^{1-(m/n)}.$$

To determine the values of λ and μ Lennard-Jones plots $\log F(y)$ against $n \log y/(n-m)$ for various values of m and n and compares the curves so obtained with the experimental curve given by B' plotted against $\log T'$. When n and m are suitably chosen the two curves will be superposable.

A set of curves for $m = 5$ and $n = 9$, 11, $14\frac{1}{3}$, and ∞ are shown in Fig. 76.

It will be noted that all the curves save that for $n = \infty$ pass through a maximum. The curve for $n = \infty$ tends to an asymptote for infinite y and represents a rigid sphere. The left-hand side of the diagram corresponds to low temperatures and negative values of $F(y)$ and B', and the right-hand side to high temperatures and positive values of $F(y)$ and B'. The Boyle temperature T_B is the temperature at which $F(y)$ and B' are zero.

From a knowledge of the Boyle temperature the value of ϕ_0 can be determined. If the root of $F(y) = 0$ be denoted by $y_{n,m}$, then

$$\phi_0/kT_B = (m/n)^{m/(n-m)} \{1 - (m/n)\} [y_{n,m}]^{n/(n-m)}. \tag{8.35}$$

Typical values of $y_{n,m}$ together with corresponding values of kT_B/ϕ_0 are given in Table 34.

TABLE 34. *Values of* $y_{n,m}$, kT_B/ϕ_0, *and* $f_{n,m}$

n	m	$y_{n,m}$	kT_B/ϕ_0	$f_{n,m}$
9	6	1·1402	4·58	0·4469
10	6	1·1190	4·07	0·4781
11	6	1·0997	3·71	0·5049
12	6	1·0818	3·43	0·5285

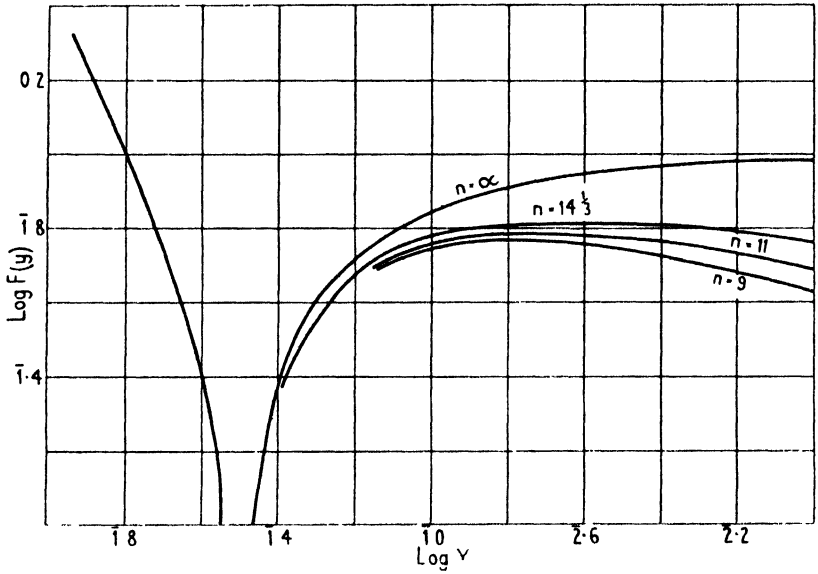

FIG. 76. Theoretical forms of the second virial coefficient.

The fifth column of the table gives maximum values of the function f from which may be calculated values of r_0 for assumed values of m and n. The observed values of the second virial coefficient B and the values of λ, μ, r_0, and ϕ_0 for a number of gases are given in Table 35 and Table 36 respectively.

The Equation of State for High Densities

The equations of state that have been considered so far take into account binary collisions between the atoms or molecules of a gas and hence are valid only when the concentration is small and the temperature sufficiently far above the critical temperature. They cease to hold in the neighbourhood of the critical point and cannot be expected to give an adequate explanation of critical phenomena.

TABLE 35. *Observed Values of the Second Virial Coefficient B in Amagat Units*

	$B \times 10^4$, *Amagat units*				
T, °*K*.	He	Ne	A	H_2	N_2
65·1	..	−9·35	..	−8·18	..
71·5	4·58†	..	..	..	..
89·9	4·81†	..	..	..	..
90·0	4·73	..	..	..	..
90·5	..	−3·65	..	−2·47	..
123	..	0·04	..	1·31	..
126·5	5·53†	..	..	..	..
143	..	..	..	..	−35·6
169·7	5·89†	..	..	..	..
173	..	2·88	−28·7	4·08	−23·1
223	..	4·06	−16·9	5·39	−11·8
273	5·29	4·75	−9·86	6·24	−4·61
323	5·23	..	−4·92	6·76	−0·11
373	5·10	5·29	−1·92	6·94	2·74
423	..	..	0·52	..	5·14
473	4·93	5·82	2·08	7·00	6·84
573	4·69	6·14	5·01	..	9·20
673	4·54	6·12	6·83	..	10·5

The above data are due to Holborn and Otto, except those marked †, which are due to Nighoff, Ilün, and Keesom (*Commn. Phys. Lab. Leiden*, No. 188c (1928)).

We have seen that at higher concentrations a more extended series than that given in (8.30) is required to express the experimental data. It is possible on certain assumptions to work out a theoretical formula for the third virial coefficient for special molecular models but not for force fields of a general type [28]. Ursell [24] has, however, developed general methods for evaluating the coefficients which correspond to the interactions of the atoms in groups of three, four, or more, but they have not been applied to particular force fields. They have been used by Mayer [25] to show that when carried far enough the equation does actually lead to critical phenomena.

Lennard-Jones and Devonshire [26] have attempted with a considerable measure of success to derive an equation of state in terms of interatomic forces that is valid at high concentrations. They assume that an atom in a dense gas may be regarded as confined for most of its time to a cell made up of its immediate neighbours in much the same way as an atom in a liquid or crystal; it is thus subject to multiple encounters. The transfer of atoms from one cell to another by diffusion is neglected as being of rare occurrence.

TABLE 36. *Intermolecular Potential Energy Constants for a number of Gases*

$$\phi = \lambda r^{-n} - \mu r^{-m} = -|\phi_0|\left\{\frac{1}{n}\left(\frac{r_0}{r}\right)^n - \frac{1}{m}\left(\frac{r_0}{r}\right)^m\right\}\Big/\left(\frac{1}{n} - \frac{1}{m}\right).$$

Gas†	n	$\mu \times 10^{10}$, *ergs* A^6	$\lambda \times 10^{10}$, *ergs* A^n	r_0, A	$-\phi_0 \times 10^{15}$, *ergs*
Helium	8	0·0370	0·304	3·31	0·701
	9	0·0237	0·510	3·18	0·755
	10	0·0173	0·948	3·09	0·792
	12	0·0108	3·56	2·95	0·827
	14	0·0076	13·9	2·84	0·823
Neon	8	0·207	1·83	3·43	3·15
	9	0·145	3·50	3·31	3·67
	10	0·114	7·32	3·22	4·13
	12	0·0832	35·45	3·08	4·88
	14	0·0678	182	2·98	5·51
Argon	8	2·37	31·4	4·20	10·8
	9	1·70	76·8	4·08	12·3
	10	1·37	204·6	3·97	13·9
	12	1·034	1,620	3·83	16·5
	14	0·867	13,660	3·72	18·7
Hydrogen	9	0·178	5·1	3·50	3·21
	10	0·142	11·6	3·41	3·58
	12	0·105	64·9	3·28	4·25
Nitrogen	9	2·27	132	4·44	9·93
	10	1·85	393	4·34	11·1
	12	1·40	3,700	4·17	13·25

† The values for the inert gases are due to Buckingham (*Proc. Roy. Soc.* (A), **168**, 264 (1938)), and for the diatomic gases are due to Lennard-Jones (*Proc. Phys. Soc.* **43**, 461 (1931)).

The total field acting upon an atom so situated is of a fluctuating kind, and to obtain the partition functions of the atoms it must be replaced by some form of statistical average; as a first approximation it is assumed that the average field in which any one atom moves is that due to its neighbours in the cell wall when each is in its equilibrium position at the centre of its own cell. The field within the cell, when averaged out, will have spherical symmetry, and the potential energy of any one atom can then be expressed as a function of the volume of the gas and of the position of the atom relative to its neighbours.

Hirschfelder and Roseveare [27] have also developed an equation applicable to high pressures based upon the observation that at high temperatures the internal energy of a gas at constant temperature is a linear function of its density and upon the assumption that at

sufficiently high temperatures the molecules behave like rigid non-attractive spheres. They make use of Happel's evaluation [28] of the third and fourth virial coefficients and add a value for the fifth virial coefficient derived on the assumption that at high pressures the molecules are packed into a body-centred lattice [29].†

TABLE 37. *Values of* b_0, ϕ_0, c (*Hirschfelder and Roseveare*)

	b_0 (*c.c. per mole*)		ϕ_0 (*ergs*)		c (*litres per degree*^{3})	
Gas	*Calculated from Beattie-Bridgeman*	*Calculated from Lennard-Jones*	*Calculated from Beattie-Bridgeman*	*Calculated from Lennard-Jones*	*Calculated*†	*Observed*
Ne	25·73	26·04	$5{\cdot}19\times10^{-15}$	$4{\cdot}881\times10^{-15}$	966	1,010
A	49·10	50·02	16·51	16·50	59,400	59,900
N_2	63·02	64·94	13·40	13·24	40,700	42,000
CO	63·02	..	13·40	13·36	40,700	42,000
H_2	26·18	31·41	4·74	4·246	749	504
O_2	57·75	..	16·22	16·97	66,200	48,000
CO_2	130·85	..	24·03	..	488,000	660,000
N_2O	130·85	..	24·03	..	488,000	660,000
CH_4	69·78	..	20·49	19·70	161,000	128,000
He	17·49	21·41	0·776	0·950	2·19	40
C_2H_4	151·8	..	25·45	..	673,000	227,000
NH_3	42·65	..	35·24	..	502,000	4,769,000
$(C_2H_5)_2O$	567·6	..	34·61	..	6,325,000	333,000

† Calculated from the relation $c = 0{\cdot}0236A_0^3/(R^3B_0^2)$, where c, A_0 and B_0 are constants of the Beattie-Bridgeman equation.

The resulting equation is

$$p = RT/V\{1+B'(T)/V+0{\cdot}625b^2/V^2+0{\cdot}2869b^3/V^3+0{\cdot}1928b^4/V^4\}, \tag{8.36}$$

where $B'(T)$ is the value of the second virial given by (8.34) and b is the co-volume term of van der Waals' equation.

The authors have tested this equation by comparing the observed and calculated values of the Joule-Thomson coefficient of argon over the temperature range 0–300° at pressures up to 200 atmospheres and find satisfactory agreement. It will be observed that the equation has only three constants, the two parameters of (8.34) and b, and it is therefore quite convenient for use in thermodynamical calculations.

† The second virial coefficient is calculated from the Lennard-Jones potential, the value agreeing with that given by the Beattie-Bridgeman equation provided the constant c of the equation has the proper value with respect to B_0 and A_0.

Equations of State and the Critical Region

A crucial test of the validity of an equation of state is the way in which it reproduces the critical isotherm; for whilst the molecules of a gas present a picture of complete disorder, those of a liquid have something of the spatial arrangement characteristic of solids; and an equation applicable to both states has to take into account the gradual introduction of molecular order as the density is increased by raising the pressure and/or lowering the temperature.† The method by which Lennard-Jones and Devonshire have attempted to overcome this difficulty has been referred to. We now propose to consider one of the simpler equations of state from the point of view of the information it affords about the critical state.

The van der Waals Critical Isotherm

Although van der Waals' equation is strictly valid only in circumstances in which the deviations from the 'ideal' gas laws are comparatively small, yet it has been applied with surprising success to critical conditions and has led to the discovery of a number of important relations to which attention may now be drawn.

The equation may be written as a cubic equation in V, thus

$$V^3-\left(b+\frac{nRT}{p}\right)V^2+\frac{a}{p}V-\frac{ab}{p}=0. \tag{8.37}$$

It has, therefore, three roots, of which all may be real or one may be real and the other two imaginary. When the roots are real and

† Onnes and Keesom (Art. V 10 of the *Encyklopädie der Mathematischen Wissenschaften*, 12 Sept. 1912, p. 793) state the problem very concisely in the following words: 'Da bei der Annäherung an den kritischen Punkt Liquid-Gas die von den Boltzmann-Gibbs'schen Prinzipien beherrschten Dichteunterschiede (Schwarmbildung), der bis α ansteigenden Zusammendrückbarkeit der Substanz wegen, besonders hervortreten, ist zu erwarten, dass bei der Entwicklung der Zustandsgleichung für die Umgebung des kritischen Punktes nach jenen Prinzipien Glieder auftreten werden, die mit der grossen Zusammendrückbarkeit in der Nähe des kritischen Punktes zusammenhängen. Diese Glieder werden wahrscheinlich durch die Art der Abweichung der Zusammendrückbarkeit in dem kritischen Gebiet (∞ im kritischen Punkt und von diesem aus, soweit sie das realisirbare homogene Gebeit betrifft, allseitig schnell abfallend) für dasselbe eine besondere Bedeutung erlangen, während sie für benachbarte Gebiete nicht mehr in Betracht kommen. Während eine allmählige Verschiebung oder Verzerrung, die sich durch das ganze Diagramm durchzieht, wie z. B. eine kontinuirliche Änderung von a_W, b_W oder R_W, sich experimentell nicht besonders zeigen würde, werden die betreffenden Glieder in der Zustandsgleichung in der Nähe des kritischen Punktes demgemäss zum Schluss führen können, dass die Eigenschaften in diesem Gebiet in beobachtbarer Weise abweichen von den Eigenschaften, die man durch Interpolation zwischen Zuständen, die um den kritischen herumliegen, aber weiter von ihm entfernt bleiben, erwarten sollte.'

unequal there will be three different values of V for given values of p and T, and the resulting isotherm will have the form suggested by Thomson for a fluid below its critical temperature. When the roots are real and equal the isotherm will correspond with the critical isotherm. Finally, when there are one real and two imaginary roots the isotherm will be that of a fluid above its critical temperature. The three types of curve are shown in Fig. 55 A.

The Calculation of the Critical Constants

Let p_c, V_c, and T_c be the critical pressure, volume, and temperature, respectively, of a fluid. The points E and G (Fig. 55 B) represent maximum and minimum points so that at E, $dp/dv = 0$ and d^2p/dv^2 is negative, and at G, $dp/dv = 0$ and d^2p/dv^2 is positive. At the critical temperature E and G coincide and $dp/dv = 0$ and $d^2p/dv^2 = 0$.

Differentiating (8.37) with respect to V,

$$\frac{dp}{dV} = -\frac{nRT}{(V-b)^2} + \frac{2a}{V^3}$$

and

$$\frac{d^2p}{dV^2} = \frac{2nRT}{(V-b)^3} - \frac{6a}{V^4}.$$

At the critical point we have

$$-\frac{nRT_c}{(V_c-b)^2} + \frac{2a}{V_c^3} = 0$$

and

$$\frac{2nRT}{(V_c-b)^3} - \frac{6a}{V_c^4} = 0;$$

from which

$$\left.\begin{aligned} V_c &= 3b, \\ p_c &= a/27b^2, \\ T_c &= 8a/27nRb, \\ \frac{nRT_c}{p_cV_c} &= \tfrac{8}{3} = 2{\cdot}67, \end{aligned}\right\} \qquad (8.38)$$

and

$$p_cV_c = \tfrac{3}{8}nRT_c.$$

On comparing the critical constants so calculated with the experimentally determined values it is found that V_c more nearly equals $4b$ and the value of nRT_c/p_cV_c is generally about 3·7 instead of 2·67. It is therefore clear that the critical point does not lie in the region within which van der Waals' equation can be regarded as a good approximation.

TABLE 38. *Values of the Ratio RT_c/p_cV_c for Various Substances*

Substance	$\frac{RT_c}{p_cVc}$
Argon	3·283
Benzene	3·755
Bromobenzene	3·809
Carbon tetrachloride	3·680
Chlorobenzene	3·776
Ethylene	3·42
Ethyl acetate	3·949
Ethyl ether	3·813
Ethyl formate	3·895
Helium	3·13
n-heptane	3·854
n-hexane	3·831
Hexa methylene	3·706
Iodobenzene	3·780
Isopentane	3·735
Methyl acetate	3·943
Methyl formate	3·922
n-octane	3·865
Oxygen	3·346
n-pentane	3·766
Xenon	3·605

The Variation of pV with Pressure according to van der Waals' Equation

Reference to Figs. 73, 63, 75 shows that the curves obtained by plotting pV against p for nitrogen, carbon dioxide, and methane pass through minima (the Boyle point); and, provided the temperature is not too high, the corresponding curves for all other gases are of similar form. The isotherms in Fig. 63 also show that the minima become less pronounced with rise of temperature and lie on a parabolic curve, known as the Boyle curve.

For any of the minima $\partial(pV)/\partial p = 0$ and the condition for a minimum point is, according to van der Waals,

$$\frac{(V-b)^2}{V^2} = \frac{b}{a}nRT. \tag{8.39}$$

The temperature of the isotherm having a Boyle point at $p = 0$ is known as the Boyle temperature. Calling this temperature T_B and substituting in (8.39),

$$V = \infty \quad \text{and} \quad nRT_B = \frac{a}{b}.$$

From (8.38)
$$\frac{a}{b} = \frac{27}{8}nRT_C$$

and hence
$$T_B = \tfrac{27}{8}T_C. \tag{8.40}$$

In Table 39 the Boyle temperatures, critical temperatures, and the ratio T_B/T_C are given for a number of gases.

TABLE 39. *The Boyle Temperatures (T_B) and Critical Temperatures (T_C) of Various Gases*

	He	H_2	Ne	N_2	*Air*	A	O_2	CO	CH_4
T_B	23	109	123	323	357	410	423	333	491
T_C	5·2	33·1	44·7	126	132·5	149·7	155	134	190·5
T_B/T_C	4·42	3·29	2·75	2·56	2·67	2·73	2·72	2·5	2·52

The Principle of Corresponding States

By expressing the pressure, volume, and temperature of a gas in terms of its critical constants the dimensionless quantities known as the reduced pressure (p_r), the reduced volume (V_r), and the reduced temperature (T_r) are obtained. Writing $p_r = p/p_c$, $V_r = V/V_c$, and $T_r = T/T_c$, and substituting for the critical constants from (8.38), we get

$$p = \frac{a}{27b^2}p_r, \qquad V = 3bV_r, \quad \text{and} \quad T = \frac{8a}{27nRb}T_r. \tag{8.41}$$

When these values are introduced into the equation of state all the constants characteristic of the particular gas disappear and we are left with the equation

$$(p_r + 3/V_r^2)(V_r - \tfrac{1}{3}) = \tfrac{8}{3}T_r, \tag{8.42}$$

which is known as a 'reduced' equation of state and should be applicable to any gas.

Gases having the same reduced pressure, volume, and temperature are said to be in 'corresponding' states. Furthermore, if the equation of state is based upon two characteristic properties of the gas, apart from the mass (in this instance the cohesive force and the co-volume), there is a relation of the form

$$p_r = f(V_r, T_r), \tag{8.43}$$

in which the coefficients in f are independent of the nature of the gas, and it is sufficient for any two of the reduced quantities to be the same for the gases to be in corresponding states. This is sometimes known as the law of corresponding states and it is a direct consequence of the assumption that the molecules of individual gases differ only in respect of their mass, size, and cohesive powers. The fact that it is not quantitatively accurate is due to the imperfection of the two-constant specification of the molecule.

Van der Waals has also pointed out that when the absolute

temperatures of two substances are proportional to their critical temperatures their vapour pressures should be proportional to their critical pressures and their orthobaric volumes,† both as liquid and vapour, to their critical volumes. This generalization may be deduced from the equation of state if that portion of the experimental isotherm where the two phases coexist (Fig. 59) is assumed to be approximately the average of the theoretical curve over the same range; that is,

$$\int_{v_l}^{v_g} p\,dv = p(v_g - v_l). \tag{8.44}$$

On substituting the value of p given by the equation of state and integrating,

$$RT \log_e \frac{(v_g - b)}{(v_l - b)} + \frac{a}{v_g} - \frac{a}{v_l} = p(v_g - v_l).$$

Dividing throughout by $p_c v_c$ and replacing the constants a, b, and R by their critical equivalents,

$$\tfrac{8}{3} T_r \log_e \frac{v_{rg} - \frac{1}{3}}{v_{rl} - \frac{1}{3}} + \frac{3}{v_{rg}} - \frac{3}{v_{rl}} = p_r(v_{rg} - v_{rl}), \tag{8.45}$$

the suffix r denoting reduced temperatures, volumes, etc.

TABLE 40. *The Ratio of the Vapour Pressures of Various Substances to their Critical Pressure at a Number of Reduced Temperatures (Young)* [30]

Reduced temperature:		*0·5170*	*0·6400*	*0·8464*	*0·9288*
Substance	*Critical pressure, mm.*	*Ratios of vapour pressure to critical pressure*			
Fluorobenzene	33,910	0·00147	0·02241	0·2949	0·5898
Chlorobenzene	33,910	0·00149	0·02252	0·2956	0·5938
Propyl acetate	25,210	0·00059	0·01404	0·2583	0·5558
Ethyl propionate	25,210	0·00059	0·01407	0·2585	0·5573
Methyl acetate	35,180	0·00093	0·01765	0·2765	0·5757
Propyl formate	30,440	0·00094	0·01799	0·2801	0·5772
Normal pentane	25,100	0·00154	0·02256	0·2960	0·5933
Normal octane	18,730	0·00060	0·01406	0·2567	0·5537
Carbon tetrachloride	34,180	0·00203	0·02681	0·3088	0·6022

It is easy to ascertain from experimental data whether the vapour pressures of two substances at corresponding temperatures are corresponding pressures. In Table 40 the ratio of the vapour pressure

† Ramsay and Young (*Phil. Trans.* **177**, pt. 1, 135 (1886)) define the orthobaric volume of a liquid as being the volume it occupies at a given temperature and under a pressure equal to its vapour pressure at that temperature.

to the critical pressure of various substances at a number of reduced temperatures are tabulated, and it will be seen that the generalization is only strictly true for closely related substances.

Young has also compared (1) the ratios of the boiling-points to the critical temperatures, T/T_C, (2) the ratios of the orthobaric volumes of liquid to the critical volumes, and (3) the ratios of the orthobaric volumes of vapour to the critical volumes, for a number of substances at the same reduced pressure, 0·08846, with results as shown in Table 41.

TABLE 41. *The Ratios of the Boiling-points and Orthobaric Volumes of Various Substances to their respective Critical Temperatures and Volumes at a Reduced Pressure of 0·08846 (Young)*

Substance	T/T_c	V_L/V_c	V_V/V_c
Hexamethylene	0·7277	0·4090	27·7
Benzene	0·7282	0·4065	28·3
Isopentane	0·7292	0·4085	27·7
Di-isopropyl	0·7329	0·4093	28·4
Normal pentane	0·7331	0·4061	28·4
„ hexane	0·7406	0·4055	29·1
„ heptane	0·7483	0·4029	29·5
Di-isobutyl	0·7498	0·4046	28·2
Normal octane	0·7544	0·4006	29·35
Carbon tetrachloride	0·7251	0·4078	27·45
Stannic chloride	0·7357	0·4031	28·15
Ether	0·7380	0·4030	28·3
Methyl formate	0·7348	0·4001	29·3
Ethyl „	0·7385	0·4003	29·6
Propyl „	0·7430	0·4008	29·4
Methyl acetate	0·7445	0·3989	30·15
„ propionate	0·7485	0·4008	29·6
„ isobutyrate	0·7502	0·4014	29·15
Ethyl acetate	0·7504	0·4001	30·25
Methyl butyrate	0·7522	0·4004	29·5
Ethyl propionate	0·7540	0·3989	30·0
Propyl acetate	0·7541	0·3985	30·35
Acetic acid	0·7624	0·4100	25·4
Methyl alcohol	0·7734	0·3973†	34·35
Propyl „	0·7736	0·4002†	30·85
Ethyl „	0·7794	0·4061†	32·15

† Values of V_c are only approximate owing to the marked curvature of the rectilinear diameter.

Considering first the ratios T/T_c it is clear that in a homologous series they tend to rise with increase in molecular weight; for iso-compounds they are also uniformly lower than for the isomeric

normal compounds, and for di-iso-compounds are lower still. The values for the alcohols and acetic acid are high compared with those for any of the other compounds included in the table.

The ratios V_L/V_c are much more constant, although among homologous hydrocarbons they show a definite diminution with increase of molecular weight. The ratios V_r/V_c follow very much the same order as the temperature ratios, although the value for methyl alcohol is unusually high and for acetic acid is very low. The abnormal values of the ratios for acetic acid are probably due to association in the vapour phase and for alcohol to association in the liquid phase.

'Reduced' Isotherms. Although the law of corresponding states is a mathematical and not a physical law it may be assumed that for any group of related substances for which the ratio RT_c/p_cV_c is a constant there will be a single reduced equation of state of the form

$$V_r = f(p_r, T_r). \tag{8.46}$$

If the deviation of a gas or vapour belonging to this group from the 'ideal' gas laws be expressed by

$$c = pV/RT,$$

where c is the compressibility factor for the pressure, volume, and temperature in question, we may write

$$c = \frac{p_rV_r}{T_r}\frac{p_cV_c}{RT_c}, \tag{8.47}$$

and c will be a unique function of p_r and T_r. This means that the compressibility isotherms, plotted on the basis of reduced pressures and temperatures, will be the same for all substances in the group. They will also be approximately the same for other substances provided the ratio RT_c/p_cV_c has the same value as in the group.

In Fig. 77 the curves showing c as a function of the reduced temperature and pressure are based upon data for carbon dioxide, nitrogen, ammonia, methane, hydrogen, propane, and pentane [31]. The value of c at 0° and zero pressure is taken as unity; at 1 atmosphere it is given by $c_1 = p_1V_1/p_0V_0$, where p_0V_0 is the extrapolated value of pV at $p = 0$. The value at 1 atmosphere may be obtained accurately from density measurements by the relation

$$c_1 = M/d_1 \times 22{\cdot}41,$$

where M is the molecular weight and d_1 is the density in grams per

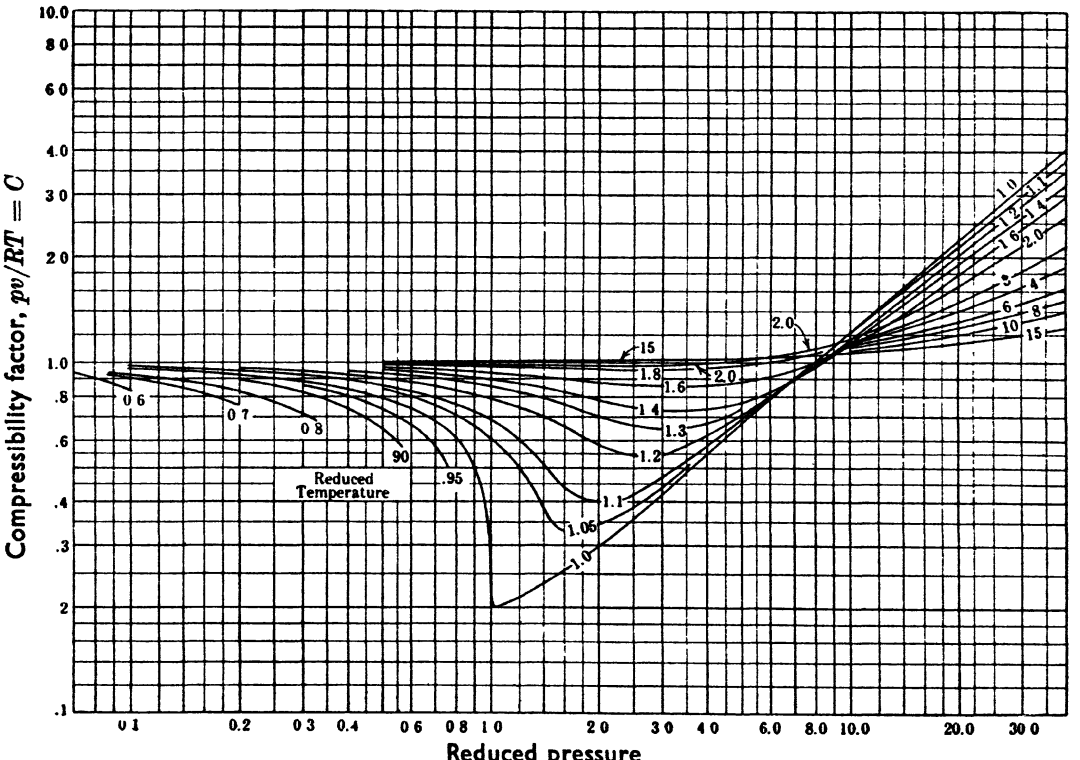

FIG. 77. 'Reduced' isotherms.

(Reprinted by permission from *Industrial Chemical Calculations*, by O. A. Hougen and K. M. Watson, published by John Wiley & Sons, Inc.)

litre at 0° and 1 atmosphere. The value at any other temperature is given by

$$c_t = \frac{c_1(pV)273}{T}.$$

It has beer. pointed out by Newton [32] that in using the above relationships for gases of low critical temperature (e.g. hydrogen, helium), better agreement is obtained by assuming $T_r = T/(T_c+8)$ and $p_r = p/(p_c+8)$.

The 'reduced' isotherms will be found useful for estimating, approximately, the compressibility of substances for which experimental data are not available. It may be noted that for reduced pressures above 10 the compressibility factor always exceeds unity.

BIBLIOGRAPHY

1. MICHELS and MICHELS, *Proc. Roy. Soc.* (A), **160**, 348 (1937).
2. VAN DER WAALS, *On the Continuity of the Liquid and Gaseous States.* Sigthoff, Leiden, 1873.
3. JEANS, *Dynamical Theory of Gases.* Cambridge University Press, 1925.
4. DIETERICI, *Ann. der Phys.* **5**, 51 (1901).
5. CLAUSIUS, *Phil. Mag.* (4), **40**, 123 (1870); the derivation given here is due to MILNE, *Phil. Mag.* **50**, 409 (1925).
6. BEATTIE and BRIDGEMAN, *Proc. Am. Acad.* **63**, 230 (1928).
7. KEYES, *Proc. Am. Acad.* **3**, 323 (1917).
8. ——, *J. Am. Chem. Soc.* **49**, 1393 (1927).
9. DEMING and SHUPE, *J. Am. Chem. Soc.* **53**, 843 (1931).
10. —— ——, *J. Am. Chem. Soc.* **52**, 1382 (1930).
11. BEATTIE, KAY, and KAMINSKY, *J. Am. Chem. Soc.* **59**, 1589 (1937).
12. SMITH, BEATTIE, and KAY, *J. Am. Chem. Soc.* **59**, 1587 (1937).
13. A full discussion of the equation of state problem is given by ONNES and KEESOM, *Enc. der Mathematischen Wissenschaften*, p. 645 (1912). See also FOWLER and GUGGENHEIM *Statistical Thermodynamics*,. Cambridge University Press, 1939.
14. KEESOM, *Commn. Phys. Lab. Leiden*, No. 24*b* (1912); *Phys. Z.* **22**, 129, 643 (1921).
15. EISENSCHITZ and LONDON, *Zeit. Phys.* **60**, 491 (1930).
16. LENNARD-JONES, *Proc. Roy. Soc.* (A), **129**, 598 (1930).
17. SLATER and KIRKWOOD, *Phys. Rev.* **37**, 686 (1931).
18. MARGENAU, *Phys. Rev.* **38**, 747 (1931).
19. LONDON, *Zeit. Phys. Chem.* (8), **11**, 222 (1930).
20. KIRKWOOD, *Phys. Z.* **33**, 57 (1932).
21. HELLMAN, *Acta Physica*, U.S.S.R., **2**, 273 (1935).
22. LENNARD-JONES, *Proc. Roy. Soc.* (A), **106**, 441 (1924).
23. BUCKINGHAM, *Proc. Roy. Soc.* (A), **168**, 264 (1938).
24. URSELL, *Proc. Cam. Phil. Soc.* **32**, 685 (1927).

25. MAYER, *J. Chem. Phys.* **5**, 67 (1937); MAYER and ACKERMANN, *J. Chem. Phys.* **5**, 74 (1937).
26. LENNARD-JONES and DEVONSHIRE, *Proc. Roy. Soc.* (A), **163**, 53 (1937); **165**, 1 (1938); LENNARD-JONES, *Physica*, **4**, No. 10, 941 (1937).
27. HIRSCHFELDER and ROSEVEARE, *J. Chem. Phys.* **43**, 15 (1939).
28. HAPPEL, *Ann. d. Physik*, **30**, 246 (1906).
29. HIRSCHFELDER, STEVENSON, and EYRING, *J. Chem. Phys.* **5**, 896 (1937).
30. YOUNG, *Phil. Mag.* (5), **33**, 153 (1892).
31. LEWIS, *Chemistry and Industry*, Feb. 14th, 1936, p. 123.
32. NEWTON, *J. Ind. Eng. Chem.* **27**, 302 (1935).

IX

THE COMPRESSIBILITY OF GASEOUS MIXTURES

For many purposes, as for example in studying the effect of pressure upon chemical reactions, we have to deal with systems containing two or more molecular species, and it is desirable to be able to calculate from the total pressure of the system and a knowledge of its composition the partial pressures of each of the reactants and products contained in it.

If the assumption is made that each constituent of the mixture completely retains its individual character, and does not by its presence influence the pressures exerted by the others, then Dalton's law may be used in the calculation of partial pressures. The law states that the pressure exerted by a mixture of gases is equal to the sum of the partial pressures of its components. If the gases behave as ideal gases, a corollary to the law is that the volume of a gaseous mixture is equal to the sum of the volumes of the individual components, all measured at the same pressure. This relation is known as Amagat's Law of Additive Volumes and is also sometimes associated with the name of Leduc.

Where real gases are concerned Dalton's and Amagat's laws are mutually incompatible and an analysis of the available experimental data for mixtures at high pressures shows that one or other of the laws, but not both, usually represents the results for a given mixture with a fair degree of accuracy; thus, for example, methane-nitrogen and oxygen-argon mixtures conform approximately to the law of additive volumes whilst argon-ethylene and oxygen-ethylene mixtures are better represented by the law of partial pressures, up to pressure of about 150 atmospheres.

It is evident, however, from the considerations set forth in the derivations of the more accurate equations of state that neither law can rigidly be obeyed except over restricted ranges of temperature and pressure, for not only must account be taken of the inter-molecular forces between molecules of the same species but similar forces operate between molecules of different species.

Amagat was the first to investigate the behaviour of mixtures and found [1] that at constant temperatures and pressures the value of the product pv for air could be calculated by linear interpolation

between the corresponding values for the pure constituents; he observed that 'les variations de l'air sont intermédiaires entre celles des gaz qui le constituent; l'oxygène et l'azote semblant, dans ce gaz, se comprimer séparément, comme s'ils étaient seuls, non pas à la pression qu'ils ont dans le mélange, mais à celle du mélange même; ce fait se vérifie même avec assez d'exactitude'.

He did not, however, pursue the matter farther and it was not until 1899 that Verschaffelt [2] again drew attention to the relation between the compressibilities of pure gases and of their binary mixtures; he noted that in the case of carbon dioxide and hydrogen, at pressures up to about 100 atmospheres, there were marked deviations from Dalton's law. Several other mixtures have since been examined and found to behave in a like manner, and the conclusion has been drawn that deviations occur for mixtures of all real gases and are greatest for those whose constituents have widely different molecular dimensions or critical constants.

One of the most valuable contributions to this part of the subject is due to I. Masson in collaboration with L. G. Dolley, C. W. Gibby, and C. C. Tanner [3], and some account of their experimental results and conclusions will serve as a fitting introduction to the equation of state problem in its relation to gaseous mixtures.

Masson and Dolley first set out to discover whether inter-atomic chemical affinities play any part in causing or increasing inter-molecular cohesion, and for this purpose they compared the compressibilities of binary mixtures of argon and oxygen, severally, with ethylene. With argon-ethylene mixtures no suspicion of chemical action could arise and, since argon and oxygen have almost identical compressibilities over the pressure range employed (5–125 atmospheres), any marked difference in the compressibilities of the two series of mixtures might be attributed to valency influences in determining cohesion.

No such difference was found as will be apparent from Table 42, in which the deviations from Amagat's law for mixtures of the three pairs of gases in question are recorded.

When oxygen is mixed with ethylene, the volume-differences which occur are seen to be slightly larger than but nearly equal to those for argon and ethylene and no effect which could be ascribed to the inter-atomic chemical affinity between carbon and oxygen is detectable.

TABLE 42. *Deviations of Various Binary Mixtures of Argon, Oxygen, and Ethylene from the Law of Additive Volumes*

$$\text{Deviation} = 100 \times \left(\frac{\text{Volume of mixture at } p \text{ atmospheres}}{\text{Sum of separate volumes at } p \text{ atmospheres}} - 1 \right).$$

The gas compositions are expressed as percentages by volume of the separate constituents at 1 atmosphere and 24·95°, i.e. approximately as molecular percentages.

Pressure, atms.	*Argon-ethylene*					*Oxygen-ethylene*			*Argon-oxygen*
	Percentage ethylene					*Percentage ethylene*			*Percentage argon*
	24·74	*49·95*	*59·86*	*70·72*	*90·06*	*25·27*	*49·91*	*59·84*	*49·99*
30	2·15	2·70	3·20	3·10	1·25	2·4	3·1	3·7	0·25
40	3·35	5·30	5·50	5·50	2·70	3·6	5·3	6·1	0·25
50	5·00	8·40	9·10	9·35	5·35	5·4	8·5	9·8	0·20
60	7·70	13·70	15·40	16·40	11·10	7·9	13·8	16·3	0·20
70	10·75	21·50	25·10	28·10	22·80	11·4	20·7	26·3	0·20
75	11·65	23·80	28·00	31·50	24·65	12·4	24·0	29·3	0·20
80	11·75	24·00	28·00	31·30	21·30	12·6	24·2	29·5	0·20
90	11·10	21·60	24·50	25·50	11·10	12·0	21·9	26·1	0·25
100	9·90	17·95	19·00	18·20	3·07	10·8	18·3	21·0	0·25
110	8·70	14·30	14·10	11·60	−0·05	9·5	14·7	16·1	0·30
120	7·50	10·90	9·70	6·40	−2·05	8·3	11·3	11·7	0·20
125	6·90	9·35	7·70	4·55	−2·65	7·7	9·7	9·6	0·25

Attention may be drawn to certain features of the results which are of interest from the point of view of the properties of binary mixtures generally, namely, (1) the volume of a mixture of argon and ethylene is usually greater than the sum of the separate volumes, all being measured at the mixture-pressure, and the extent of such differences depends upon the mixture-pressure and upon the molecular proportions of its components. With a fixed molecular ratio there is a particular value of the pressure (approx. 75 atmospheres) at which the increase is greatest, and with a fixed mixture-pressure there is a particular molecular ratio for which the difference reaches a maximum positive value. These relations are clearly indicated by the curves in Fig. 78 which show the volume change at various pressures for a full range of argon-ethylene mixtures. It will be seen that mixtures rich in ethylene and measured at the higher pressures approach the additive volume more closely, and eventually the volume-differences become negative; (2) the compressibilities of argon and oxygen are nearly identical and when argon is mixed with oxygen only a very small positive difference in total volume is found.

The deviations from Dalton's law are shown in Table 43 (p. 230).

At the highest densities, that is, with an ethylene-rich argon mixture at high pressures, the pressure exerted is greater than the sum of those of the constituents taken separately, a result which may

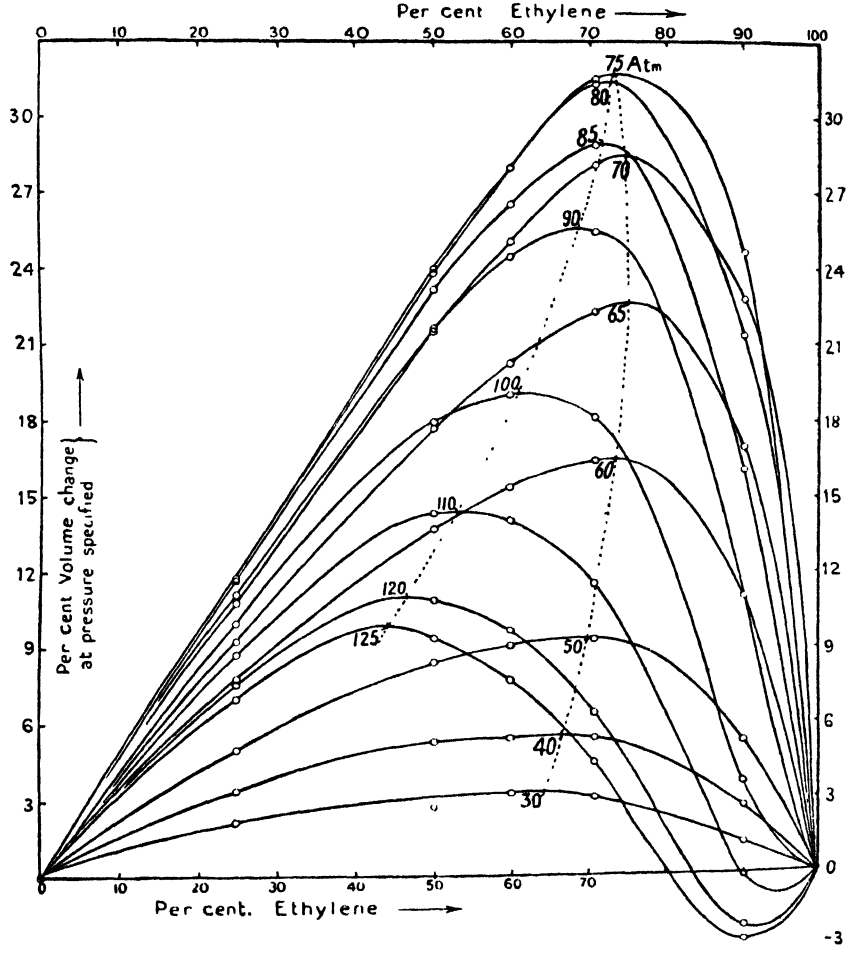

FIG. 78. Deviations of argon-ethylene mixtures from additive volume law.

be interpreted as due to the influence of the co-volume term b of the equation of state. At lower densities the pressure of the mixture is less than the additive value, and by amounts reaching 8 per cent. of the additive value. It is thus evident that a cohesive force exists between argon and ethylene sufficient in magnitude to outweigh the effect of the b term at the lower pressures.

TABLE 43. *Deviations of Binary Mixtures of Argon, Ethylene, and Oxygen from Dalton's Law*

The actual pressures of the mixtures are less than the additive pressures by:

Additive pressure, atms.	*Argon-ethylene*					*Oxygen-ethylene*			*Argon-oxygen*
	Percentage of ethylene					*Percentage of ethylene*			*Percentage of argon*
	24·74	*49·95*	*59·86*	*70·72*	*90·06*	*25·27*	*49·91*	*59·84*	*49·99*
30	0·75	0·85	0·9	0·70	0·45	..	..	..	..
40	1·05	1·60	1·6	1·40	0·70	1·0	..	..	..
50	1·70	2·70	2·7	2·25	1·20	1·6	2·5	..	..
60	2·35	3·90	4·0	3·55	1·80	2·3	3·8	3·4	0·7
70	3·35	5·45	5·7	4·85	1·95	3·1	4·5	4·2	0·9
75	3·90	6·20	6·35	5·20	1·50	3·6	5·2	5·3	..
80	4·30	6·80	6·4	5·25	0·75	4·0	6·0	5·5	1·1
85	4·75	7·30	7·0	5·20	−0·20	4·4	6·4	5·6	..
90	5·20	7·65	7·25	4·90	−1·00	4·8	6·8	5·7	1·25
100	6·05	8·00	7·1	4·00	−3·00	5·5	7·2	5·5	1·45
110	6·60	8·15	6·7	2·70	−5·25	6·1	7·5	4·5	1·6
120	..	..	..	..	−8·05	..	7·8	..	1·65
125	..	..	..	..	−9·05	..	..	..	1·7

The results in Table 43 show also that the maximum decrease from additive pressures occurs at an 'optimum' molecular composition of 50–60 per cent. ethylene, and Masson and Dolley suggest that this result may be due to the formation of molecular complexes of varying degrees of aggregation, contributing to, if not completely accounting for, the cohesion; and from the absence of valency influences in determining cohesion, they consider that on the basis of probabilities a certain number of molecules in the aggregated condition will be present as pairs, and this will be the most usual form of complex when the pressure is low.

Masson and Dolley's data for the compressibilities of argon, ethylene, and oxygen and their binary mixtures are shown graphically in Fig. 79.

Empirical Equations of State for Binary Mixtures

The compressibility isotherms of gaseous mixtures above the critical temperatures of their constituents are similar in form to those of pure gases and can be represented by empirical series equations such as

$$pV = A + Bp + Cp^2 + Dp^4 + \ldots, \qquad (9.1)$$

in which the coefficients B, C, D, etc., are functions both of the

composition and temperature of the system. The values of the coefficients cannot in general be calculated from the corresponding coefficients of the pure components but their variation with composition may be expressed by series equations

$$B = a+bx+cx^2+dx^3+..., \quad \text{etc.}, \tag{9.2}$$

where x is the mole fraction of one of the components and a, b, c, etc., are constants determined from the experimental data.

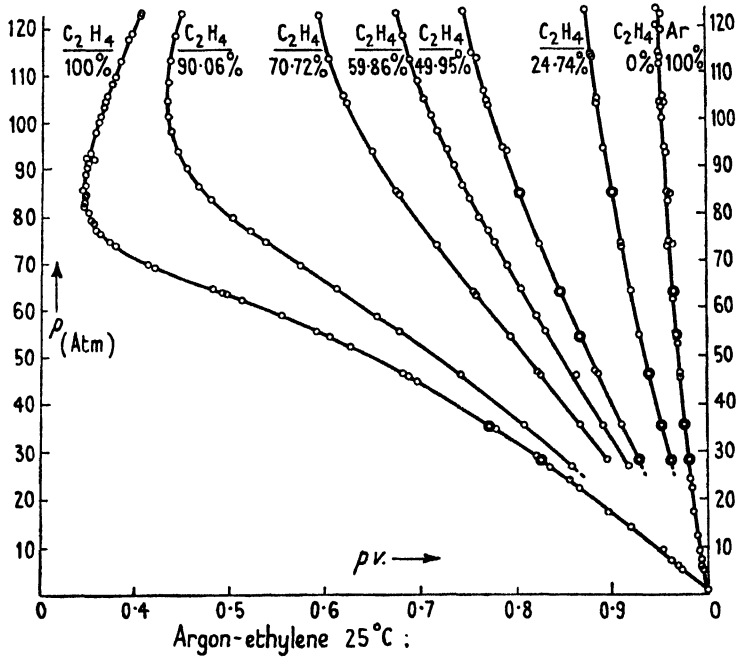

FIG. 79. Isotherms of argon-ethylene mixtures.

Theoretical Equations of State for Binary Mixtures

There is no reason to suppose that the equation of state of a gaseous mixture would differ in form from that of a pure gas. To determine the relation between the equation constants of the mixture and of its constituents, however, requires a knowledge of the intermolecular laws of force and data which are seldom available. Van der Waals [4] considered that the mixture constants could be calculated from the individual pure gas constants, and for the co-volume term he employed a relation deduced on theoretical grounds by Lorentz [5], namely,

$$b_x = b_1(1-x)^2+2b_{12}x(1-x)+b_2x^2, \tag{9.3}$$

in which $$b_{12} = (\tfrac{1}{2}\sqrt[3]{b_1}+\tfrac{1}{2}\sqrt[3]{b_2})^3$$

and x is the mole fraction of the second constituent. For the cohesive force term he used the relation

$$a_x = a_1(1-x)^2+2a_{12}x(1-x)+a_2x^2, \tag{9.4}$$

in which a_{12} is a constant which cannot be calculated from the corresponding pure gas constants without a knowledge of the laws governing the forces between the unlike molecules of the mixture. The resulting equation of state has the same form as the pure gas equation and is subject to the same limitations.

The Keyes Equation for Binary Mixtures

Keyes and Burks [6] have applied the Keyes equation to mixtures of nitrogen and methane and find that for this pair of gases the mixture constants are linear functions of the constants of the pure gases and the composition of the mixture. Thus the β, α, and L constants are given with sufficient accuracy by the expressions

$$\beta W+\beta' W', \qquad \alpha W+\alpha' W', \quad \text{and} \quad LW+L'W',$$

where β and β', etc., refer to nitrogen and methane, respectively, and W and W' to their masses. For the A constant the square roots of the constants of the pure gases are taken, thus: $(\sqrt{A}\,W+\sqrt{A'}\,W')^2$.

The constants so calculated are compared with those obtained from the experimental data for various mixtures on p. 244.

It is important to note that the linear relationship between the constants is obtained by neglecting the curvature of the isochores, which in the temperature range 0–100° is small; and, whilst it is shown to hold for two gases of approximately the same molecular diameter, it is not necessarily valid for gases of widely differing properties. With this reservation the Keyes equation may be written in a generalized form as follows:

$$p = \frac{\sum R_1 W_1 T}{v-\sum \beta_1 W_1 e^{-\epsilon\alpha_1 W_1/v}} - \frac{(\sum \sqrt{A_1}\,W_1)^2}{(v+\sum l_1 W_1)^2}. \tag{9.5}$$

The Beattie-Bridgeman Equation for Gaseous Mixtures

In calculating the constants of this equation for a mixture of gases it is assumed that those constants in which the dimension of density is contained to the first power, namely, a, B_0, b, c, and R, may be

combined linearly, whilst for the constants A_0, in which the dimension of density is contained to the second power, the square roots of the constant may be combined linearly.

The volume term V of the equation may be expressed as (*a*) the total volume of n moles of the mixture, (*b*) the volume of an average mole, or (*c*) the volume of 1 gram of the mixture.

In the first case, in which V is the volume of n moles consisting of n_1 moles of the first gas, n_2 moles of the second, etc., the constants are given by

$$\begin{aligned}
A_{0m} &= (n_1\sqrt{A_{01}}+n_2\sqrt{A_{02}}+n_3\sqrt{A_{03}}+\ldots)^2 = (\sum n_1\sqrt{A_{01}})^2,\\
a_m &= n_1 a_1+n_2 a_2+n_3 a_3+\ldots = \sum (n_1 a_1),\\
B_{0m} &= n_1 B_{01}+n_2 B_{02}+n_3 B_{03}+\ldots = \sum (n_1 B_{01}),\\
b_m &= n_1 b_1+n_2 b_2+n_3 b_3+\ldots = \sum (n_1 b_1),\\
c_m &= n_1 c_1+n_2 c_2+n_3 c_3+\ldots = \sum (n_1 c_1),\\
R_m &= n_1 R+n_2 R+n_3 R+\ldots = \sum (n_1 R),
\end{aligned}$$

where the subscript m refers to the mixture and 1, 2, etc., to the individual gases.

When V is the volume of an average molecule of the mixture, the number of moles n_1, n_2, etc., of the relations given in the preceding paragraph are replaced by the mole fractions x_1, x_2,... of the gases composing the mixture. When V is the volume of 1 gram, the mole numbers n_1, n_2,... are replaced by w_1, w_2,..., where w is the weight fraction and the values of the constants R_1, A_{01}, a_1, B_{01}, etc., are the appropriate values for 1 gram of the first pure gas.

The generalized equation for a mixture may now be written

$$p = \frac{\sum (n_1)RT(1-\epsilon)}{V^2}[V+B]-\frac{A}{V^2}, \tag{9.6}$$

where

$$A = (\sum n_1\sqrt{A_{01}})^2[1-\sum (n_1 a_1)/V],$$

$$B = \sum (n_1 B_{01})[1-\sum (n_1 b_1)/V],$$

and

$$\epsilon = \sum (n_1 c_1)/VT^3.$$

Eq. (9.6) can be rearranged into the virial form

$$pV = \sum (n_1)RT+\frac{\beta_m}{V}+\frac{\gamma_m}{V^2}+\frac{\delta_m}{V^3}, \tag{9.7}$$

where

$$\beta_m = \sum (n_1)RT \sum (n_1 B_{01}) - (\sum n_1 \sqrt{A_{01}})^2 - \left(\frac{\sum (n_1)R \sum (n_1 c_1)}{T^2}\right),$$

$$\gamma_m = -\sum (n_1)RT \sum (n_1 B_{01}) \sum (n_1 b_1) + \\ + (\sum n_1 \sqrt{A_{01}})^2 \sum (n_1 a_1) - \left(\frac{\sum (n_1)R \sum (n_1 B_{01}) \sum (n_1 c_1)}{T^2}\right),$$

$$\delta_m = \frac{\sum (n_1)R \sum (n_1 B_{01}) \sum (n_1 b_1) \sum (n_1 c_1)}{T^2}.$$

The parameters β_m, γ_m, and δ_m are algebraic functions of temperature, the mole numbers, and the values of the constants of the gases composing the mixture; for a mixture of constant composition they depend only on temperature. Eq. (9.7) therefore makes it possible to integrate in terms of elementary functions most of the usual thermodynamic relations.

The second virial coefficient β_m for a binary mixture can be written in the form given by Lennard-Jones and Cook:

$$B_x^1 = B_{11}^1(1-x)^2 + 2B_{12}^1 x(1-x) + B_{22}^1 x^2, \tag{9.8}$$

where

$$B_x^1 = \frac{\beta_m}{\sum (n_1)^2 RT}$$

and x is the mole fraction of the second constituent.

From (9.7) it can be seen that

$$B_{11}^1 = B_{01} - A_{01}/RT - c_1/T^3,$$

$$B_{22}^1 = B_{02} - A_{02}/RT - c_2/T^3,$$

and

$$2B_{12}^1 = B_{01} + B_{02} - 2\sqrt{(A_{01} A_{02})}/RT - (c_1 + c_2)T^3.$$

Thus it is possible by the method of combining the constants, to calculate the value of B_{12}^1 from the equation of state constants of the pure gases composing the mixture and also to determine its temperature variations.

Beattie has applied (9.6) to the data of Keyes and Burks for nitrogen and methane (loc. cit.) and finds satisfactory agreement between the observed and calculated pressures. Deming and Shupe [7] have also applied it to Bartlett and collaborators' data for a 3:1 hydrogen-nitrogen mixture. They combine the constants a, b, c, and A_0 linearly by mole fractions and compare three methods of combining the constant B_0.

If B_{0h} and B_{0n} are the B_0 constants for hydrogen and nitrogen, and these gases are present in a binary mixture to the extent of mole

fractions x_h and x_n, then the B_0 constant for the mixture (B_{0x}) will be formed quadratically:

$$B_{0x} = B_{0h}x_h^2 + 2B_{hn}x_h x_n + B_{0n}x_n^2.$$

The constant B_{hn} may be obtained

(i) by the linear method, $B_{hn} = \frac{1}{2}(B_{0h} + B_{0n})$;

(ii) by the Lorentz method, $B_{hn}^{\frac{1}{3}} = \frac{1}{2}(B_{0h}^{\frac{1}{3}} + B_{0n}^{\frac{1}{3}})$;

(iii) by the linear square root method, $B_{hn} = \sqrt{(B_{0h}\,B_{0n})}$.

Deming and Shupe find that the linear square root method is the most satisfactory and reproduces the (P, V, T) relations almost within the experimental error up to a density of 0·0070 mole per c.c.

Intermolecular Forces in Binary Mixtures

We have seen that the cohesion between molecules of different species does not involve any forces other than those operative between like molecules. We shall now consider the magnitudes of these intermolecular forces for various pairs of gases as calculated by means of the Lennard-Jones equation.

Gibby, Tanner, and Masson have examined in detail the system helium-hydrogen; these gases have substantially linear compressibility isotherms at temperatures of 25° and upwards, the product pv increasing with pressure according to the equation

$$pv = a + bp, \tag{9.9}$$

where v is the volume of the gas in terms of its volume at N.T.P., and a and b are constants for the particular gas at the given temperature. The coefficient b which is proportional to the second virial coefficient gives the slope of the isotherm and hence the deviation from Boyle's law, and only in the case of hydrogen at the lowest temperature employed (25°) is there a slight curvature requiring a third term cp^2.

Now if b_{11} and b_{22} are the coefficients for two pure gases and b_m is the corresponding coefficient for a mixture of the two whose compressibility is given by

$$pv = a_m + b_m p, \tag{9.10}$$

b_m will include not only encounters between like molecules but also encounters between unlike molecules; the specific effect, not directly measurable, of encounters of the latter type may be denoted by b_{12}. The experimental value of b_m will therefore be made up of contribu-

tions from the three coefficients b_{11}, b_{22}, and b_{12}, and will vary with the composition of the mixture.

Lennard-Jones has shown that if the field of force around each molecule, whatever its nature, is spherically symmetrical, then

$$b_m = b_{11}x_1^2 + 2b_{12}x_1x_2 + b_{22}x_2^2, \tag{9.11}$$

where x_1 and x_2 are the molecular proportions of the two gases in the mixture (i.e. $x_1 + x_2 = 1$).

From (9.11), by rearrangement,

$$b_{12} = \{b_m - (b_{11}x_1^2 + b_{22}x_2^2)\}/2x_1x_2, \tag{9.12}$$

in which all the terms on the right-hand side are measurable.

The values of b for a series of helium-hydrogen mixtures at 25° are given in Table 44.

TABLE 44. *Values of the Coefficient b in $pv = a + bp$ for Helium-Hydrogen Mixtures at 25°*

Per cent. helium:	*0*	*16·26*	*26·40*	*33·00*	*42·42*	*50·06*	*50·11*	*57·54*	*66·64*	*73·99*	*83·49*	*100*
$b \times 10^4$ obs.	(6·59)	6·56	6·61	6·62	6·56	6·41	6·38	6·36	5·97	5·92	5·67	5·10
calcd.	..	6·66	6·64	6·60	6·51	6·41	6·41	6·29	6·10	5·92	5·66	..

The calculated values of b in the table are obtained by assigning some fixed value to b_{12} (in this case $6{\cdot}98 \times 10^{-4}$) and substituting in (9.12). The agreement is very satisfactory, the divergence only once reaching 2 per cent., and hence the assumption made by Lennard-Jones of a spherically symmetrical field may be said to find support in the case of this pair of gases.

It is interesting to note that b reaches a maximum for mixtures containing about 20 per cent. of helium, a result indicating that certain helium-hydrogen mixtures are more incompressible than either constituent; the effect is slight but is observable also in Holborn's data for mixtures of helium and neon.

At this point it is necessary to specify in greater detail the nature of the field of force surrounding the molecules. Both attractive and repulsive encounters may occur between molecules, and according to Lennard-Jones an encounter between a pair of molecules may be treated as if it were governed by two superposed forces, the one attractive and the other repulsive. The two forces are assumed to have each its own distance law and force constant

and hence the net force of cohesion between two similar molecules is given by

$$\text{net force} = \lambda r^{-n} - \mu r^{-m}. \qquad (9.13)$$

These forces are responsible for the deviations of real gases from the simple gas laws and should be related to the coefficient b of a pure gas to which (9.9) is applicable.

The method of calculating m and n and the force constants described in Chapter VIII has been used by Gibby, Tanner, and Masson, who have computed the various functions required for plotting the theoretical curves for a number of molecular models, in which the attractive index m was put at 5, and the repulsive index n at 9, 10, 11, $14\frac{1}{3}$, 21, and ∞, respectively; and the results have been compared with the experimental curve of $\log T$ against $\log b$ (for pure gases) or $\log b_{12}$ (for mixture).

The influence of temperature upon the value of b for helium and hydrogen and of b_{12} for a 1:1 mixture of the two gases may be seen from the data in Table 45.

TABLE 45. *The Influence of Temperature upon the Coefficient b*

Values of $b \times 10^4$ ($v = 1$ at N.T.P.).

Temp., °C.:	*25·0*	*50·0*	*75·0*	*100·4*	*125·4*	*150·3*	*175·0*
Helium: observed	5·10	5·07	5·02	4·86	4·94	4·62	4·87
smoothed	5·10	5·07	5·02	4·97	4·90	4·83	4·77
Hydrogen: observed	6·59	6·71	6·86	6·93	7·02	6·93	6·87
smoothed	6·59	6·73	6·85	6·93	6·97	6·96	6·92
Mixture: observed	6·41	6·44	6·37	6·43	6·20	6·41	6·20
smoothed	6·42	6·42	6·41	6·38	6·34	6·29	6·23
b_{12} calcd. from observed points	6·98	6·99	6·80	6·97	6·42	7·04	6·53
calcd. from smoothed points	7·00	6·94	6·88	6·81	6·75	6·69	6·53

Within the temperature range 25°–175° C. the coefficient for helium diminishes with rise of temperature and that for hydrogen increases to a maximum at about 130°.

The force constants corresponding with each model and calculated by the method referred to above are tabulated on the following page. No distance-index of repulsion higher than 11 nor lower than 9 seems to be called for, and an average of $n = 10$ applies fairly well not only to hydrogen and helium but also to neon, argon, krypton, xenon, and nitrogen. It is interesting to note that the constants for the attractive component of force between 2He is only about one-quarter

Force Constants of $\lambda r^{-n} - \mu r^{-m}$ for Helium, Hydrogen, and their Binary Mixtures

Model			$2He$		$2H_2$		$He-H_2$		$He-H_2$
m	n		μ	λ	μ	λ	μ	λ	*Calcd. repulsion* μ
5	9	$10^{-44}\times$	0·67		2·26		0·98		
		$10^{-74}\times$		1·54		8·04		3·47	3·68
5	10	$10^{-44}\times$	0·51		2·08		0·74		
		$10^{-81}\times$		0·34		2·26		0·84	0·92
5	11	$10^{-44}\times$	0·405		1·66		0·57		
		$10^{-89}\times$		0·75		6·06		2·02	1·97

of that between $2H_2$ and the constants of the repulsive components bear a somewhat similar relationship.

If from the above data the attractive and repulsive force components are combined we get the net intensity of intermolecular force at any specified distance apart, and the energy involved in the encounter and the molecular diameter or distance of closest approach between molecules can also be found for each of the suitable molecules.

Thus, for example,† if two molecules acting upon each other according to (9.13) approach from infinity to a distance $r = \sigma$, the energy gained as a result of their encounter is given by

$$\frac{\lambda}{n-1}\frac{1}{\sigma^{n-1}} - \frac{\mu}{m-1}\frac{1}{\sigma^{m-1}}. \tag{9.14}$$

Substituting in this expression the values of the constants tabulated above, it is found that similar results are obtained for $n = 10$ and $n = 11$. At distances within about 10 to 15 Ångström units these molecules begin significantly to attract each other, and thus to gain kinetic energy, and as they close in upon one another, the net intensity of attraction increases and reaches a maximum at about $4\frac{1}{2}$ A. On further shortening the distance between them it rapidly falls to zero. The gain in kinetic energy due to the whole encounter up to this point may be termed the 'cohesion energy'. It is small, being less than 1 per cent. of the average kinetic energy of free thermal motion at 0° C.; it is lost again when the next 0·5 A is traversed,

† In this and the succeeding paragraphs the text of Gibby, Tanner, and Masson's paper (loc. cit.) has been followed.

for at this range (3–3½ A) the repulsive force component has begun to predominate. The intermolecular distance at this point is the closest approach of two molecules initially at rest and apart, moving together under the influence of their cohesive forces alone. The changes in the attractive, repulsive, and resultant forces with distance are shown qualitatively in Fig. 80. If the molecules are not initially

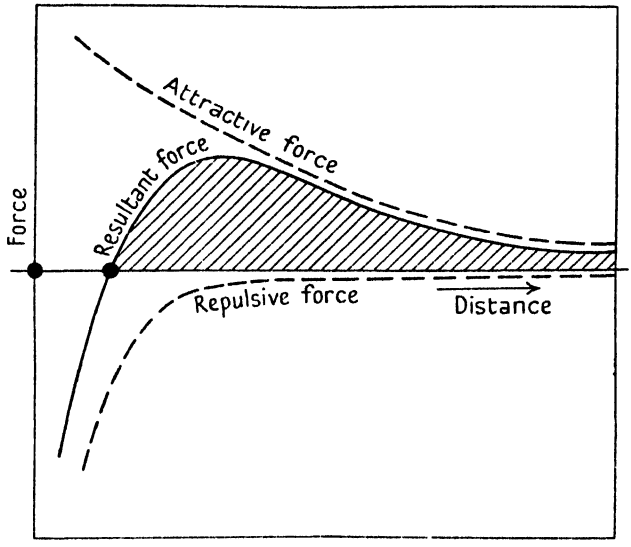

FIG. 80. Diagrammatic representation of the forces between two molecules.

at rest, but have been approaching with the kinetic energy of thermal translation as well as under their mutual influence, then they penetrate still farther into each other's repulsive core. The extent of the farther penetration in a direct encounter depends upon the amount of thermal kinetic energy to be absorbed, that is, with average molecules, upon the temperature of the gas.

The distance of closest approach, which may be termed the kinetic diameter, can thus be specified for a pair of average molecules at any given temperature at which the same law of force holds, when once the force constants have been found for these molecules.

In Table 46 the data for each of two models is summarized.

Comparing the column headed $He—H_2$ with that headed $\frac{1}{2}(\sigma_{He}+\sigma_{H_2})$ the conclusion may be drawn that when a helium atom meets a hydrogen molecule, their joint kinetic diameter is

TABLE 46. *Cohesion Energies and Kinetic Diameters (σ) for Helium, Hydrogen, and Mixtures of the two Gases*

(Energy in ergs; distance in A.U.)

	Model $n = 10$, $m = 5$				*Model* $n = 11$, $m = 5$			
	2He	$2H_2$	He—H_2	$\frac{1}{2}(\sigma_{He}+\sigma_{H_2})$	2He	$2H_2$	He—H_2	$\frac{1}{2}(\sigma_{He}+\sigma_{H_2})$
$10^{15}\times$ cohesion energy	0·39	1·08	0·38		0·40	1·05	0·37	
Gained at $r =$	3·67	4·05	4·08		3·50	3·90	3·90	
Lost at $r =$	3·12	3·44	3·46		3·01	3·37	3·35	
K.E. corresponding to T° abs. lost at σ							σ	
0 0°	3·12	3·44	3·46	3·33	3·01	3·37	3·35	3·19
$4{\cdot}12\times10^{-16}$ 1°	2·98	3·38	3·31	3·18	2·89	3·31	3·20	3·10
41·2 10°	2·58	3·07	2·85	2·82	2·55	3·02	2·82	2·88
412 100°	2·10	2·55	2·32	2·32	2·09	2·55	2·31	2·32
823 200°	1·95	2·39	2·16	2·17	1·96	2·40	2·17	2·18
1,124 273°	1·89	2·32	2·09	2·10	1·90	2·34	2·10	2·12
4,116 1,000°	1·65	2·02	1·82	1·83	1·70	2·06	1·85	1·88
Independent data:								
Diameter of electric structure from dielectric constant	1·20	1·84	..	1·52	1·20	1·84	..	1·52
Upper limit of diameter from density of solid	..	3·96	..	..	..	3·96	..	..

approximately the average of the respective kinetic diameters when each molecule meets its own kind.

If this result were generally applicable the isotherms of a mixture could be derived from those of its constituents. It must be borne in mind, however, that helium and hydrogen are by no means typical gases, for they both deviate positively from Boyle's law at all ordinary temperatures and their molecules are light, small, and 'hard'. Tanner and Masson therefore extended their work to include argon, which deviates from Boyle's law at temperatures between 25° and 75° as far in the negative sense as hydrogen and helium do

in the positive sense. Their results show that Lennard-Jones's partial pressure law holds equally well for argon-helium and argon-hydrogen mixtures as it does for helium-hydrogen mixtures, and the selection of a single value of b_{12} enables b_m to be calculated for all compositions of a given pair of gases at a given temperature.

They also calculate the force constants for encounters between pairs of argon, helium, and hydrogen molecules for different models in which $m = 5$ and n is given values of 9, 10, 11, and $14\frac{1}{2}$. The kinetic diameters given by the model $n = 11$, $m = 5$ are recorded in Table 47.

TABLE 47. *Kinetic Diameters*, 10^{-8} *cm., of Argon, Helium, Hydrogen, and their Binary Mixtures for the Model* $n = 11$, $m = 5$

Equivalent T° abs.	2A	2He	$2H_2$	A−He	½(A+He)	A−H_2	½(A+H_2)	He−H_2	½(He+H_2)
0	3·94	3·03	3·37	3·72	3·48	3·75	3·65	3·38	3·20
1	3·91	2·90	3·32	3·66	3·40	3·72	3·62	3·20	3·11
10	3·79	2·53	3·09	3·40	3·16	3·54	3·44	2·81	2·81
100	3·37	2·07	2·60	2·88	2·72	3·08	2·99	2·30	2·33
200	3·19	1·94	2·45	2·70	2·56	2·90	2·86	2·15	2·19
273	3·11	1·88	2·38	2·64	2·50	2·82	2·75	2·09	2·13
1,000	2·77	1·66	2·10	2·33	2·22	2·51	2·44	1·84	1·88

It will be seen that the kinetic diameters in encounters between unlike molecules are not such as would be expected if each molecule were to retain the same diameter as when encountering one of its own kind, and Tanner and Masson conclude that the radius of a given gaseous molecule on collision is a function not only of the kinetic energy of the invading molecule but of the nature of this molecule as well. It would seem, for example, that the argon atom is smaller when it encounters another argon atom than it is when it encounters a hydrogen molecule.

Data relating to other binary mixtures are summarized below.

The Compressibility Data for Binary Gaseous Mixtures

1. *Hydrogen and Nitrogen*

Reference	*Temperature of isotherms, °C.*	*Maximum pressure, atms.*
1. T. T. H. Verschoyle, *Proc. Roy. Soc.* (A), **111**, 552 (1926)	0 20	200
2. E. P. Bartlett, *J. Am. Chem. Soc.* **49**, 687 (1927); **49**, 1955 (1927)	0	1,000

1. *Hydrogen and Nitrogen (cont.)*

Reference	*Temperature of isotherms, °C.*	*Maximum pressure, atms.*
3. Bartlett, Cupples, and Tremearne, *J. Am. Chem. Soc.* **50**, 1275 (1928)	0	1,000
	50	
	99·85	
	198·9	
4. Bartlett, Hetherington, Kvalnes, and Tremearne, *J. Am. Chem. Soc.* **52**, 1363 (1930)	299·8	1,000
	−70	
	−50	
	−25	
	20	
5. Wiebe and Gaddy, *J. Am. Chem. Soc.* **60**, 2300 (1938)	0 to 300	1,000

The following series equations represent the experimental data to a close approximation over the pressure ranges indicated.

(i) *Verschoyle's data.*

$$pv_A = A_p + B_p p + C_p p^2.$$

The value of A_p at 0° is found from the relation

$$1 = (A_p)_0 + (B_p)_0 + (C_p)_0,$$

whilst the value of $(A_p)_{20}$ is given by

$$(A_p)_{20} = (A_p)_0 \times (1 + 20Y),$$

where $Y = 0{\cdot}0036618$. B_p and C_p are then evaluated by the method of least mean squares.

Series Equations for Hydrogen, Nitrogen, and their Mixtures (Verschoyle)

Pressure range: 1–200 atmospheres.

Gas	*Temp.*	A_p	B_p	C_p
H_2	0° C.	0·99937	$+0{\cdot}6263 \times 10^{-3}$	$0{\cdot}168 \times 10^{-6}$
$H_2 = 75$, $N_2 = 25$		0·99948	0·5229	0·516
$H_2 = 50$, $N_2 = 50$		0·99969	0·3067	1·147
$H_2 = 25$, $N_2 = 75$		1·00001	−0·0140	1·993
N_2		1·00049	−0·4961	3·334
H_2	20° C.	1·07257	+0·6505	0·069
$H_2 = 75$, $N_2 = 25$		1·07269	0·5658	0·448
$H_2 = 50$, $N_2 = 50$		1·07291	0·3979	0·933
$H_2 = 25$, $N_2 = 75$		1·07327	0·1225	1·685
N_2		1·07370	−0·2798	2·800

(ii) *Bartlett's data.* The equation $pv/p_0v_0 = A+Bp+Cp^2+Dp^3$ enables the compressibility factors of nitrogen, hydrogen, and their mixtures to be calculated with a maximum deviation of 0·5 per cent. over the pressure range 1–350 atmospheres. The constant A is the compressibility factor pv/p_0v_0 at zero pressure and differs from 1 by less than 0·06 per cent. under the given experimental conditions. The constants B, C, and D are functions of the mixture composition and are given by (9.2). The value of the constants calculated from the experimental data are as follows:

Values of the Constants of Eqs. (9.1) *and* (9.2) (*Bartlett*)

Pressure range: 1–1,000 atmospheres.
Temperature: 0° C.

Constant	*a*	*b*	*c*	*d*
B	$6{\cdot}810\times10^{-4}$	$-5{\cdot}245\times10^{-6}$	$-2{\cdot}508\times10^{-8}$	$-4{\cdot}371\times10^{-10}$
C	$-3{\cdot}487\times10^{-8}$	$+2{\cdot}914\times10^{-8}$	$-1{\cdot}488\times10^{-10}$	$+2{\cdot}885\times10^{-12}$
D	$2{\cdot}564\times10^{-10}$	$-3{\cdot}072\times10^{-11}$	$+3{\cdot}086\times10^{-13}$	$-3{\cdot}562\times10^{-15}$

Over the pressure range 350 to 1,000 atmospheres the compressibility factors may be computed from a two-constant equation

$$pv/p_0v_0 = A+B(p-400),$$

where

(*a*) for mole percentages (x) of nitrogen less than 40,

$$A = 1{\cdot}2839+(1{\cdot}2084\times10^{-4})x,$$

$$B = (7{\cdot}211\times10^{-4})+(5{\cdot}322\times10^{-6})x+(1{\cdot}0562\times10^{-8})x^2;$$

(*b*) when x equals 40 or upwards,

$$A = 1{\cdot}2585+(5{\cdot}155\times10^{-4})(100-x),$$

$$1/B = (1{\cdot}3128\times10^{3})-(7{\cdot}153)x+(1{\cdot}416\times10^{-2})x^2.$$

The Constants of the Beattie-Bridgeman Equation for a 3 : 1 *Hydrogen-Nitrogen Mixture.* The following values of the constants have been calculated by Deming and Shupe [9] from the data of Bartlett and his collaborators for a 3 : 1 hydrogen-nitrogen mixture:

Below the critical density—

$$A_0 = 3{,}000\times10^2, \qquad B_0 = 25{\cdot}03,$$

$$a = 21{\cdot}36, \qquad b = -15{\cdot}16, \qquad c = 16\times10^6.$$

Above the critical density—

$$A_0 = 3{,}489\times10^2, \qquad B_0 = 21{\cdot}42,$$

$$a = 28{\cdot}56, \qquad b = -30{\cdot}58, \qquad c = 16\times10^6.$$

They reproduce pressure almost to within the experimental error up

to 0·0270 mole per c.c., at which density the root mean square deviation is 1·8 per cent.

The constants for the mixture have also been calculated from the corresponding constants for the pure gases according to the method already described, with the following results:

For nitrogen—

$$A_{0n} = 1{,}254 \times 10^3, \qquad B_{0n} = 46{\cdot}045,$$
$$a_n = 18{\cdot}68, \qquad b_n = -25{\cdot}88, \qquad c_n = 61{\cdot}64 \times 10^4.$$

For hydrogen—

$$A_{0h} = 1{,}240 \times 10^2, \qquad B_{0h} = 19{\cdot}90,$$
$$a_h = 56{\cdot}18, \qquad b_h = -10{\cdot}72, \qquad c_h = 20 \times 10^6.$$

Combining these constants

$$A_{0m} = 2{,}889, \qquad a_m = 46{\cdot}80,$$
$$b_m = -14{\cdot}51, \quad c_m = 30{\cdot}41 \times 10^6,$$
$$B_m = \sqrt{(B_{0h} B_{0m})}$$
$$= 25{\cdot}42.$$

From these constants the pressures are reproduced with a root mean square error of 1·17 per cent. up to a density of 0·0070 mole per c.c.

2. *Methane and Nitrogen and their Mixtures* (*J.A.C.S.* **50,** 1100 (1928))

The calculated constants of the Keyes equation compared with those obtained directly from the experimental data for various methane-nitrogen mixtures are given below.

Constants of the Keyes Equation for Methane, Nitrogen, and their Mixtures

Temperature range: 0–200° C.
Pressure range: 1–300 atmospheres.
Units: c.c. per gm.; International atmospheres.
Mixtures: weight per cent. of methane.

	N_2	CH_4	$CH_4 = 70{\cdot}31\%$	$CH_4 = 68{\cdot}99\%$	$CH_4 = 30{\cdot}44\%$
A obs.	1650·5	101515·4	6803·6	6660·4	3434·9
A calcd.	..	..	6872·8	6741·8	3472·6
β obs.	1·65	3·961	3·293	3·142	2·391
β calcd.	..	..	3·275	3·245	2·354
α obs.	0·992	2·857	2·388	2·158	1·370
α calcd.	..	..	2·304	2·279	1·560
l obs.	0·313	0·536	0·400	0·511	0·209
l calcd.	..	..	0·470	0·467	0·381
R	2·9286	5·1173	4·4675	4·4383	3·5950

The Constants of the Beattie-Bridgeman Equation. The values of the constants for pure methane and nitrogen together with those calculated for the mixtures are as follows:

Values of the Constants of the Beattie-Bridgeman Equation for Methane, Nitrogen, and their Mixtures

Units: International atmospheres; c.c. per gram; degrees Kelvin ($T°$ K. $= t°$ C.$+273{\cdot}13$); compositions in weight fractions.

Gas	$\sum(w_1 R_1)$	$(\sum w_1\sqrt{A_{01}})^2$	$\sum(w_1 a_1)$	$\sum(w_1 B_{01})$	$\sum(w_1 b_1)$	$\sum(w_1 c_1)$
Nitrogen	2·92904	1457·5	0·6382	1·5398	−0·5740	$2{\cdot}00\times10^6$
$N_2 = 69{\cdot}556$ $CH_4 = 30{\cdot}444$	3·59572	3048·2	0·7961	2·1321	−0·7006	$3{\cdot}827\times10^6$
$N_2 = 31{\cdot}014$ $CH_4 = 68{\cdot}986$	4·43974	5894·4	0·9961	2·8819	−0·8610	$6{\cdot}139\times10^6$
$N_2 = 29{\cdot}69$ $CH_4 = 70{\cdot}31$	4·46873	6008·7	1·0030	2·9076	−0·8665	$6{\cdot}219\times10^6$
Methane	5·11890	8860·0	1·157	3·4852	−0·9900	$8{\cdot}00\times10^6$

Values of Constants of the Series Equation for Helium-Hydrogen Mixtures

$pv = A + Bp$.

Pressure range: 0–125 atmospheres.

Mixture—per cent. *Hydrogen*	*Helium*	*Temp., °C.*	*A*	$B\times10^6$
100	0	25	1·09085	6·56
73·60	26·40		1·0904	6·61
49·89	50·11		1·0916	6·38
26·01	73·99		1·0909	5·92
0	100		1·09085	5·10
100	0	50	1·1832	6·71
49·89	50·11		1·1836	6·44
0	100		1·1827	5·07
100	0	75	1·2748	6·86
49·89	50·11		1·2751	6·37
0	100		1·2748	5·02
100	0	100	1·3669	6·93
49·89	50·11		1·3676	6·43
0	100		1·3669	4·86
100	0	125	1·4582	7·02
49·89	50·11		1·4592	6·20
0	100		1·4605	4·94
100	0	150	1·5516	6·93
49·89	50·11		1·5494	6·41
0	100		1·5486	4·62
100	0	175	1·6420	6·87
49·89	50·11		1·6455	6·20
0	100		1·6357	4·87

3. *Other Binary Mixtures*

Masson and Dolley (*Proc. Roy. Soc.* (A), **103,** 524 (1923)) have determined the compressibility isotherms of binary mixtures of argon, ethylene, and oxygen at 25° and pressures up to 125 atmospheres, and Gibby, Masson, and Tanner (*Proc. Roy, Soc.* (A), **122,** 283 (1929)) have obtained data for helium-hydrogen mixtures at 25, 50, 100, and 175° and pressures up to 120 atmospheres.

Data are also available for the following mixtures: hydrogen and carbon monoxide (Scott, *Proc. Roy. Soc.* (A), **125,** 330 (1929); Townend and Bhatt, *Proc. Roy. Soc.* (A), **134,** 502 (1931)); nitrogen and carbon monoxide (Torocheshnikov, *Tech. Phys.*, U.S.S.R., **4,** 365 (1937)); methane and ethane (Michels and Nederbragt, *Physica,* **6,** 656 (1939)).

BIBLIOGRAPHY

1. Amagat, *Ann. de Chim. et de Phys.* **19,** 384 (1880).
2. Verschaffelt, *Commn. Phys. Lab. Leiden,* No. 47 (1899).
3. Masson, Dolley, Gibby, and Tanner, *Proc. Roy. Soc.* (A), **103,** 524 (1923); **122,** 283 (1929); **126,** 268 (1930).
4. Van der Waals, *Die Kontinuität der gasförmigen und flüssigen Zustände,* Part II. Barth, Leipzig, 1900.
5. Lorentz, *Wied. Ann.* **12,** 127, 660 (1881).
6. Keyes and Burks, *J. Am. Chem. Soc.* **50,** 1100 (1928).
7. Deming and Shupe, *J. Am. Chem. Soc.* **53,** 860 (1931).
8. Lennard-Jones, *Proc. Roy. Soc.* (A), **115,** 334 (1927).
9. Deming and Shupe, *J. Am. Chem. Soc.* **53,** 860 (1931).

X

THE THERMODYNAMIC PROPERTIES OF GASES

ALL the thermodynamic properties of a gas may conveniently be evaluated over a wide range of variables from its compressibility isotherms or from an equation of state, provided that, in addition, any one thermal property is known as a function of temperature. Whichever method is used it is necessary first to evaluate the derivatives $(dv/dp)_T$, $(dv/dT)_p$, and $(d^2v/dT^2)_p$.

At first sight it would seem that a satisfactory analytical method of obtaining $(dv/dp)_T$ over a limited pressure range would be to write pv as a power series in p along an isotherm, but in practice it is found that no set of coefficients will satisfactorily reproduce the trends of a gas such as nitrogen over the whole pressure range; one set of constants will hold fairly well to some intermediate pressure, depending on the temperature, and a second set will cover the remainder of the range; this introduces a discontinuity, and the intermediate pressure is at the end of one range and at the beginning of the other. The same difficulty exists in evaluating $(dv/dT)_p$.

The theoretically derived equations of state are also insufficiently accurate to permit of their being employed over the whole range of available data.

In these circumstances it is best to resort to graphical methods, and the treatment given below is that devised by W. E. Deming and L. E. Shupe [1], who have made a detailed study of the data for nitrogen, carbon monoxide, and hydrogen.

As we have seen, the (v, T) isobars of real gases possess only a slight curvature, and it is therefore difficult to draw accurate tangents to them; but by plotting residuals such as Δ and α against temperature, where

$$\Delta \equiv v(pv/RT-1) \tag{10.1}$$

and

$$\alpha \equiv RT/p-v, \tag{10.2}$$

the tangents to the resulting curves can easily be drawn.

The following relations hold between Δ and α and the pressure volume, temperature, and density of the gas:

$$(T/v)(dv/dT) = \frac{pv/RT+(T/v)(d\Delta/dT)_p}{1+2\Delta/v}, \tag{10.3}$$

$$(T/v)(dv/dT)_p = RT/pv-(T/v)(d\alpha/dT)_p, \tag{10.4}$$

$$(-p/v)(dv/dp)_T = 1-\rho(dpv/dp)_T, \tag{10.5}$$

$$(-p/v)(dv/dp)_T = RT/pv+(p/v)(d\alpha/dp)_T, \tag{10.6}$$

$$(-p/v)(dv/dp)_T = \frac{pv/RT-(p/v)(d\Delta/dp)_T}{1+2\Delta/v}, \tag{10.7}$$

$$(-p/v)(dv/dp)_T = -pv/RT\{2\Delta/v+1+\rho^2(d\Delta/d\rho)_T\}, \tag{10.8}$$

$$(d^2v/dT^2)_p = -(d^2\alpha/dT^2)_p, \tag{10.9}$$

$$(2\Delta/v+1)(d^2v/dT^2)_p = (d^2\Delta/dT^2)_p - \frac{2p}{RT}\frac{\{\Delta T-(d\Delta/dT)_p\}^2}{(2\Delta/v+1)^2}. \tag{10.10}$$

A 1 per cent. error in estimating the slope of a (Δ, T) or an (α, T) isobar may mean only a few hundredths per cent. error in $(dv/dT)_p$, since from (10.3) and (10.4) the slopes $(d\Delta/dT)_p$ and $(d\alpha/dT)_p$ enter as correction terms to the slope that the (v, T) isobar would have if the gas behaved as an ideal gas. Similarly, any error in the determination of $(-p/v)(dv/dp)_T$ is diminished according to (10.5)–(10.8).

The derivative $(d^2v/dT^2)_p$ is best determined by measuring the slope of the $((dv/dT)_p, T)$ isobar.

In dealing graphically with the experimental data it is assumed that, in the range under consideration, surfaces such as p, v, T; Δ, p, T; etc., have no sharp breaks; accordingly all isobars and isotherms should be smooth curves and all the curves in a given series should show these relationships one to another since they can be considered as sections all cut from the same surface. The (p, v, T) data are adjusted by first drawing smooth curves through the (Δ, p) isotherms and reading off Δ from them; then by plotting these smoothed values against T at constant pressure and smoothing the curves the final values of Δ are obtained.

In order to exhibit and interpolate (p, v, T) data a series of (Δ, ρ) isotherms and isobars such as are illustrated in Fig. 81A will be found exceedingly useful since from it any one of the (p, v, T) coordinates can quickly be estimated when the other two are known. Thus, for example, for $\rho = 0{\cdot}010$ moles per c.c. and $t = 0°$ the pressure can be roughly estimated as 240 atmospheres; when greater accuracy is required, the value of Δ, as read from the diagram corresponding to the two given coordinates, is substituted in (10.1) to give the third

coordinate. In the example given, $\Delta = 5{\cdot}0$ c.c. per mole, and taking $v = 1/\rho = 100$ c.c. per mole, $T = 273{\cdot}18°$, $R = 82{\cdot}049$ c.c. atm./mole deg., we find $p = 235{\cdot}3$ atmospheres.

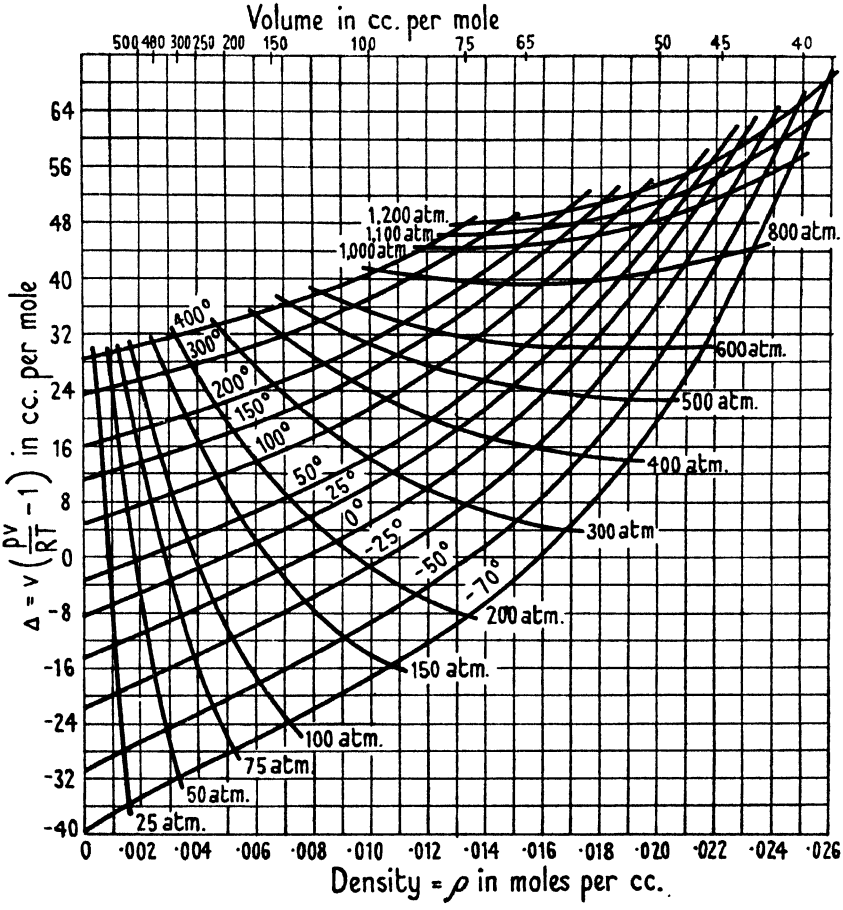

FIG. 81 A. Δ-density isotherms and isobars for carbon monoxide.

The Pressure and Temperature Coefficients of Volume Expansion

The pressure coefficient $(-1/v)(dv/dp)_T$ is calculated from (10.5)–(10.8) and the temperature coefficient $(1/v)(dv/dT)_p$ from (10.3) and (10.4); by multiplying these expressions by p and T respectively, they are converted to the dimensionless quantities $(-p/v)(dv/dp)_T$ and $(T/v)(dv/dT)_p$ which are listed in Appendix I. It should be noted

that for ideal gases these coefficients would be unity. The specific volume (v) is calculated from (10.1).

The Ideal Gas and the Thermodynamic Equations of State

In the following derivation of the thermodynamic equations of state an acquaintance with the fundamental laws of thermodynamics and the elementary theorems based upon them is assumed. A brief summary is, however, given of the more important relations employed.

In a simple process, such as the vaporization of a liquid at constant pressure, the internal energy E and the heat content or enthalpy H of the system change. If E_A is the internal energy, V_A the volume, and H_A the heat content of one mole of the liquid, and E_B, etc., the corresponding quantities for one mole of its vapour, then

$$\Delta H = H_B - H_A = (E_B + PV_B) - (E_A + PV_A) = q, \qquad (10.11)$$

where q is the heat of vaporization; and in general

$$E_B - E_A = \Delta E = q - w, \qquad (10.12)$$

where q is the heat absorbed by the surroundings and w is the work done by the system on the surroundings.

The enthalpy of the system is defined by

$$H = E + pV, \qquad (10.13)$$

or, since the absolute values of the internal energy and enthalpy are unknown,

$$\Delta H = \Delta E + \Delta(pV), \qquad (10.14)$$

where ΔH, etc., are the finite related changes in H, etc.; it will be seen from (10.11) that when heat is added to a system at constant pressure the change in enthalpy is numerically equal to the heat added.

When a system is heated at constant volume no external work is done and the heat capacity C_v is equal to the change of internal energy with temperature,

$$C_v = \left(\frac{\partial E}{\partial T}\right)_v. \qquad (10.15)$$

If the total pressure remains constant and the volume is allowed to change, heat will be absorbed both to increase the internal energy

and to supply the equivalent of the work done on expansion; the heat capacity at constant pressure C_p may therefore be written

$$C_p = \left(\frac{\partial E}{\partial T}\right)_p + p\left(\frac{\partial V}{\partial T}\right)_p = \left(\frac{\partial H}{\partial T}\right)_p, \tag{10.16}$$

and from (10.15) and (10.16)

$$C_p = C_v + \left[p + \left(\frac{\partial E}{\partial V}\right)_T\right]\left(\frac{\partial V}{\partial T}\right)_p. \tag{10.17}$$

An *ideal gas* may now be defined as one in which the internal energy E is a function of temperature alone, that is,

$$\left(\frac{\partial E}{\partial V}\right)_T = 0, \tag{10.18}$$

and in which pressure, volume, and temperature are related by the equation

$$pV = nRT. \tag{10.19}$$

When an ideal gas expands isothermally the heat absorbed must be equivalent to the work done by expansion, that is,

$$q = w = p\,dV,$$

and for a finite change

$$q = w = \int_{V_A}^{V_B} p\,dV.$$

On substituting the values of p and V given by (10.19),

$$q = w = nRT \log_e \frac{V_B}{V_A} = nRT \log_e \frac{p_A}{p_B}. \tag{10.20}$$

Entropy. In any reversible process the increase of entropy of the system (dS) is given by

$$dS = \frac{dq}{T}, \tag{10.21}$$

where dq = the heat added, and T = the absolute temperature. From (10.20) and (10.21) the increase in entropy during the free expansion of an ideal gas is given by

$$dS = nR \log_e \frac{V_B}{V_A} = \frac{q}{T} = C_p \frac{dT}{T}.$$

In a system whose pressure is in equilibrium with the external pressure

$$dE = T\,dS - p\,dV, \tag{10.22}$$

and for an isothermal process

$$p = T\left(\frac{\partial S}{\partial V}\right)_T - \left(\frac{\partial E}{\partial V}\right)_T. \tag{10.23}$$

The Thermodynamic Equations of State. From (10.22) and (10.23)

$$dH = dE + p\,dV + V\,dp = T\,dS + V\,dp,$$

and

$$V = -T\left(\frac{\partial S}{\partial p}\right)_T + \left(\frac{\partial H}{\partial p}\right)_T. \tag{10.24}$$

On substituting

$$\left(\frac{\partial S}{\partial V}\right)_T = \left(\frac{\partial p}{\partial T}\right)_V \quad \text{and} \quad \left(\frac{\partial S}{\partial p}\right)_T = -\left(\frac{\partial V}{\partial T}\right)_p$$

in (10.23) and (10.24) respectively,

$$p = T\left(\frac{\partial p}{\partial T}\right)_V - \left(\frac{\partial E}{\partial V}\right)_T, \tag{10.25}$$

and

$$V = T\left(\frac{\partial V}{\partial T}\right)_p + \left(\frac{\partial H}{\partial p}\right)_T. \tag{10.26}$$

These two equations are the thermodynamic equations of state for any fluid.

The Effect of Pressure on the Internal Energy of a Fluid

When a gas is compressed isothermally from a density 0 to a density ρ, the change in the internal energy is

$$\Delta E = {}_tE_\rho - {}_tE_0 = \int_0^\rho \left(\frac{\partial E}{\partial \rho}\right)_T d\rho, \tag{10.27}$$

where ${}_tE_0$ is the internal energy at temperature t and density 0, given by

$${}_tE_0 = E_0 + \int_0^t C_v\,dT. \tag{10.28}$$

To evaluate the integral $\int_0^t C_v\,dT$ and thus obtain the total energy, a knowledge of C_v as a function of temperature is required.

We have seen that for an ideal gas $(\partial E/\partial v)_T = 0$. For a real gas $(\partial E/\partial \rho)_T$ can be calculated from compressibility data by employing the relation

$$\left(\frac{\partial E}{\partial \rho}\right)_T = -\frac{1}{\rho^2}\left(\frac{\partial E}{\partial v}\right)_T = -\frac{1}{\rho}\left\{T\left(\frac{\partial pv}{\partial T}\right)_v - pv\right\}, \tag{10.29}$$

and ΔE can then be obtained graphically for different values of ρ and t.

If the internal energy at N.T.P. is taken as zero, then its value at any other density ρ and temperature t is given by

$$E = \int_0^t C_{v=\infty}\,dT + \int_0^\rho \left(\frac{\partial E}{\partial \rho}\right)_t d\rho - \int_0^1 \left(\frac{\partial E}{\partial \rho}\right)_{t=0} d\rho. \tag{10.30}$$

The relation between the internal energy and density can be derived from an equation of state. Thus, employing the van der Waals equation,

$$\left(\frac{\partial E}{\partial v}\right)_T = \frac{a}{v^2}, \quad \left(\frac{\partial E}{\partial \rho}\right)_T = -a, \quad \text{and} \quad E = -a\rho;$$

the internal energy is, therefore, a linear function of the density within the limits of the equation.

According to the Beattie-Bridgeman equation,

$$E = E_0(T) - \frac{1}{V}(A_0 + 3Rc/T^2) - \frac{1}{2V^2}(-aA_0 + 3RcB_0/T^2) + \frac{1}{V^3T^2}(RcbB_0), \tag{10.31}$$

an expression which at high temperatures reduces to

$$E = E_0(T) - \frac{A_0}{V}\left(1 - \frac{a}{2V}\right). \tag{10.32}$$

This is found to agree well with the experimental data when a is given the value zero.

Michels and collaborators [2] have calculated the internal energy of nitrogen and carbon dioxide from (10.30), making use of their compressibility data which extends to pressures of 3,000 atmospheres. To integrate $\int_0^t C_v\,dT$ they employ the method of Giaque and Clayton [3], in which the translational energy is taken as $\frac{3}{2}R$, while the rotational and vibrational energies are deduced from band-spectra data. Their data for carbon dioxide are shown graphically in Fig. 81 B (see also Appendix I). It will be seen that E is approximately a linear function of the density over a comparatively wide temperature range, although in the neighbourhood of the critical point there is a change in the slope of the (E, ρ) line. A similar change has been noted in the case of steam by Keenan and Keyes [4]. Hirschfelder and Roseveare [5] suggest that the deviations in the critical region are due to fluctuations in density, the denser regions giving disproportionately large contributions to the internal energy; there is also evidence based upon the behaviour of water and butane to show that the slope of the (E, ρ) line for the liquid phase differs from that of the gas phase.

The curve in Fig. 81 B is based upon values of E calculated from the Beattie-Bridgeman equation and shows that for pressures up to 100 atmospheres ($\rho = 320$ Amagat units approx.) the agreement with experiment is reasonably good.

Entropy and Pressure

The decrease of entropy of a fluid with increase of pressure is given by

$$\left(\frac{\partial S}{\partial \rho}\right)_T = -\frac{1}{\rho^2}\left(\frac{\partial p}{\partial T}\right)_v,$$

or

$$\left(\frac{\partial S}{\partial p}\right)_T = -\left(\frac{\partial v}{\partial T}\right)_p;$$

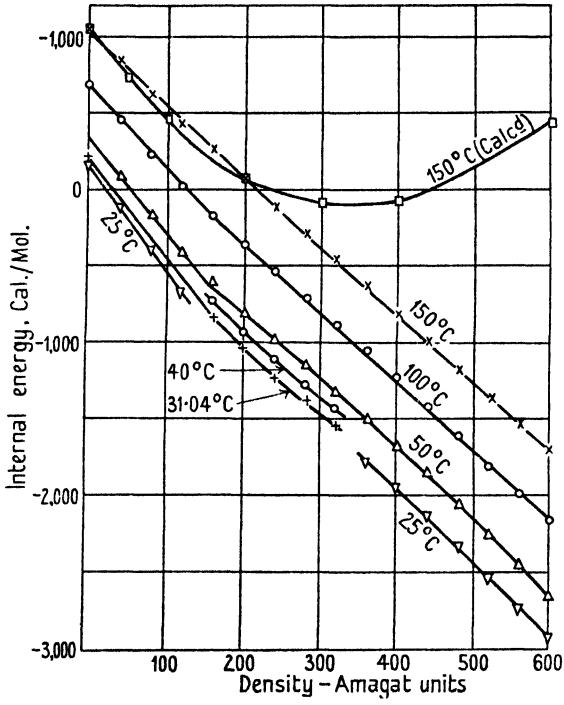

FIG. 81 B. The influence of pressure on the internal energy of carbon dioxide.

from which

$$\Delta S = -\int_1^p \left(\frac{\partial v}{\partial T}\right)_p dp = -\int_1^\rho \frac{1}{\rho^2}\left(\frac{\partial p}{\partial T}\right)_\rho d\rho. \qquad (10.33)$$

For an ideal gas the value of $-\Delta S$ is $R \log_e p$ at all temperatures.

It has been shown that the temperature coefficient of volume expansion may be derived from the compressibility isotherms of a gas, and hence it is a simple matter to evaluate (10.33) graphically along isotherms, except at pressures below about 50 atmospheres, where the steepness and curvature of the $((dv/dT)_p, p)$ curves renders the method inaccurate. At low pressures, therefore, Deming and Deming suggest the following procedure [1]: The integrand of (10.33)

can be written as the product of the two factors v/T and $(T/v)(dv/dT)_p$, each of which may be expressed as a power series in p. For nitrogen, carbon monoxide, and hydrogen the expansion coefficients can be represented, up to about 100 atmospheres, by the series

$$(T/v)(dv/dT)_p = 1+a'p+b'p^2, \tag{10.34}$$

and

$$-(p/v)(dv/dp)_T = 1+ap+bp^2. \tag{10.35}$$

The parameters of these equations depend upon the nature of the gas and the temperature.

By integrating (10.35), assuming $pv = RT$ for $p = 0$,

$$\begin{aligned} v &= (RT/p)e^{-(ap+\frac{1}{2}bp^2)} \\ &= (RT/p)[1-ap+\tfrac{1}{2}(a^2-b)p^2], \end{aligned}$$

from which

$$\begin{aligned} \Delta S &= -(1/T)\int_1^p v(T/v)(dv/dT)_p\,dp \\ &= R[\log_e p/1+(a'-a)(p-1)+\tfrac{1}{2}(b'-aa'+\tfrac{1}{2}a^2-\tfrac{1}{2}b)(p^2-1)^2]. \end{aligned}$$

To obtain absolute entropies ΔS is added to S', the entropy of the real gas at 1 atmosphere. The difference between the entropy of a real gas and that of an ideal gas is given by

$$\begin{aligned} S_{\text{real}}-S_{\text{ideal}} &= -\int_0^p \{(dv/dT)_{\text{real}}-RT/p\}\,dp \\ &= -\int_0^p \{(dv/dT)-v/T-\alpha/T\}\,dp \\ &= -(1/T)\int_0^p \mu C_p\,dp+(1/T)\int_0^p \alpha\,dp, \end{aligned}$$

where

$$\alpha = RT/p-v = -v(RT/pv-1).$$

At 1 atmosphere the difference between the entropies of a real and an ideal gas is $\mu C_p/T-\alpha T$, where μC_p and α are evaluated in the neighbourhood of zero pressure.

The values of the absolute entropy of nitrogen found by the above method are shown in Fig. 82 (see also Appendix I). The results indicate that the decrease in the entropy of a real gas with increase of pressure is always greater than that of an ideal gas ($R\log_e p$), the difference being more pronounced at low temperatures and high pressures.

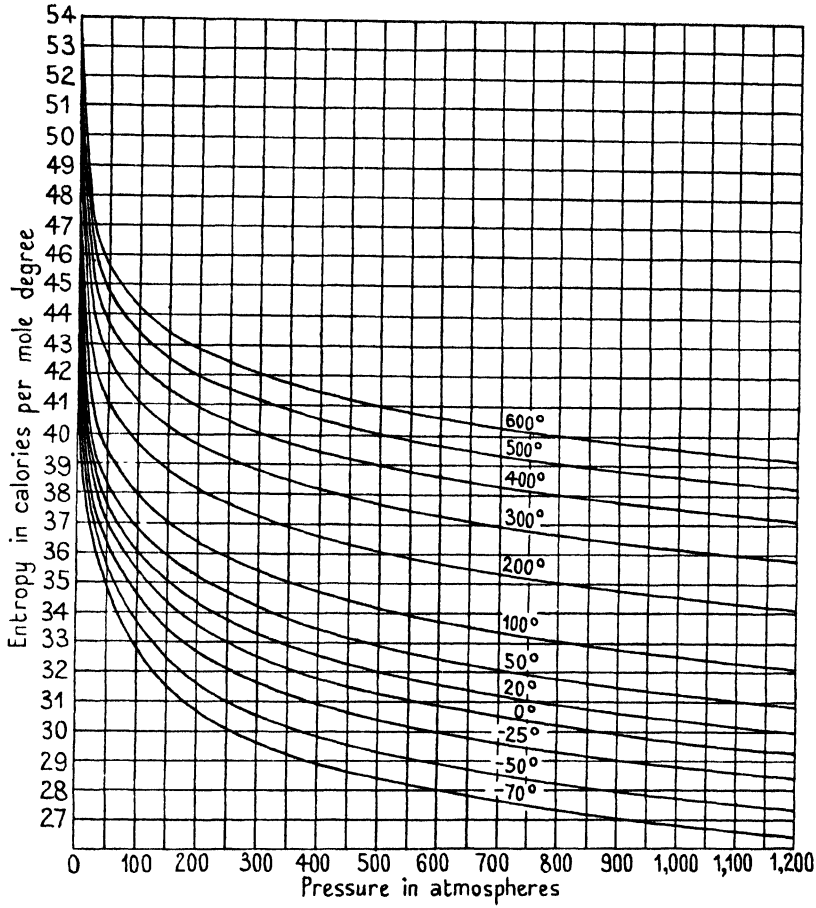

FIG. 82. The entropy of nitrogen as a function of pressure.

The Heat Capacities at Constant Pressure and Constant Volume

From (10.17)

$$C_p - C_v = \left[p + \left(\frac{\partial E}{\partial V}\right)_T\right]\left(\frac{\partial V}{\partial T}\right)_p.$$

Substituting the value of p in (10.25),

$$C_p - C_v = T\left(\frac{\partial p}{\partial T}\right)_V\left(\frac{\partial V}{\partial T}\right)_p, \tag{10.36}$$

$$= -T\left(\frac{\partial V}{\partial T}\right)_p^2 \Big/ \left(\frac{\partial V}{\partial p}\right)_T. \tag{10.37}$$

Eq. (10.37) expresses the difference between the heat capacities of a gas in terms of the temperature and pressure coefficients of volume expansion.

The temperature coefficient of volume expansion of a gas α is given by $(\partial V/\partial T)_p(1/V)$ and the pressure coefficient of volume expansion β by $-(\partial V/\partial p)_T(1/V)$. Substituting in (10.37),

$$C_p - C_v = \frac{\alpha^2 VT}{\beta}. \tag{10.38}$$

If l is the latent heat of expansion of a gas, that is, the amount of heat which must be added to the gas to maintain its temperature constant when the volume is increased by unity, then in the case of an ideal gas expanding isothermally against a pressure p,

$$l\,dV = p\,dV, \tag{10.39}$$

and no heat is required to do internal work.

The latent heat of expansion l may also be defined by

$$l = T\left(\frac{\partial p}{\partial T}\right)_v,$$

Further, since for an ideal gas

$$\left(\frac{\partial p}{\partial T}\right)_v = \frac{R}{V}, \tag{10.40}$$

and

$$\left(\frac{\partial^2 p}{\partial T^2}\right)_v = 0. \tag{10.41}$$

it may be shown that

$$\left(\frac{\partial C_v}{\partial V}\right)_T = T\left(\frac{\partial^2 p}{\partial T^2}\right)_v. \tag{10.42}$$

On combining (10.41) and (10.42),

$$\left(\frac{\partial C_v}{\partial V}\right)_T = 0. \tag{10.43}$$

The specific heat of an ideal gas at constant volume is, therefore, independent of the absolute magnitude of the volume.

In the case of real gases internal work is done on expansion against the cohesive forces of the molecules. If, for example, van der Waals' equation is differentiated with respect to temperature,

$$\left(\frac{\partial p}{\partial T}\right)_V = \frac{R}{V-b}, \tag{10.44}$$

and

$$l = \frac{RT}{V-b} = p + \frac{a}{V^2}.$$

Eq. (10.39) then becomes

$$l\,dV = p\,dV + \frac{a}{V^2}dV,$$

the term $(a/V^2)\,dV$ representing the internal work done against the cohesive force a/V^2.

On differentiating (10.44) with respect to T at constant volume

$$\left(\frac{\partial^2 p}{\partial T^2}\right)_V = \frac{\partial}{\partial T}\left(\frac{R}{V-b}\right) = 0,$$

and therefore

$$\frac{\partial C_v}{\partial V} = 0,$$

which is the same result as that arrived at for an ideal gas.

Actually the specific heats of fluids at constant volume are found to depend on volume and, in most instances, the specific heat of a substance in the liquid phase differs from that in the gas phase.

For a real gas we may calculate the partial derivatives of (10.42) from the Beattie-Bridgeman equation of state, and integrating between the limits $V = \infty$ and the variable volume V, we obtain

$$C_v = C_v^* + \frac{Rc}{T^3 V}\left(6 + \frac{3B_0}{V} - \frac{3B_0 b}{V^2}\right). \tag{10.45}$$

When the partial derivatives of (10.36) are similarly evaluated and C_v eliminated by the use of (10.45) and the relation $C_p^* - C_v^* = R$, there results

$$C_p = C_p^* - R + \frac{Rc}{T^3 V}\left[6 + \frac{3B_0}{V} - \frac{3B_0 b}{V^2}\right] + \\ + \frac{R[1+(B_0+2c/T^3)/V+(-B_0 b+2B_0 c/T^3)/V^2-2B_0 bc/T^3V^3]^2}{1+2(B_0-A_0/RT-c/T^3)/V+ \\ +3(-B_0 b+A_0 a/RT-B_0 c/T^3)/V^2+4B_0 bc/T^3V^3} \tag{10.46}$$

Here C_v^* and C_p^* are the molal heat capacities of the gas at zero pressure; for a given gas they are temperature functions which can be obtained from thermal data on C_v or C_p measured at finite values of V or p and reduced to zero pressure by use of the relations (10.45) or (10.46).

The quantities R, A_0, a, B_0, b, and c are parameters occurring in the equation of state, which may be written in the virial form

$$pV = RT + \beta/V + \gamma/V^2 + \delta/V^3,$$

where $\beta = RTB_0 - A_0 - Rc/T^2$,

$\gamma = -RTB_0 b + A_0 a - RB_0 c/T^2$,

and $\delta = RB_0 bc/T^2$.

Eqs. (10.45) and (10.46) express C_v and C_p as functions of V and T. Simple approximate relations expressing these thermal quantities as functions of p and T can be derived from (10.45) and (10.46) by dropping all terms in $1/V$ of higher order than the first and replacing $1/V$ by p/RT. There results

$$C_v = C_v^* + \frac{6cp}{T^4}, \tag{10.47}$$

$$C_p = C_p^* + \left(\frac{2A_0}{RT^2} + \frac{12c}{T^4}\right)p. \tag{10.48}$$

These relations represent the experimental data surprisingly well, particularly when the temperature is not too near the critical temperature [6]. At temperatures below the critical the deviations may amount to 5 per cent. or more, depending on the pressure.

For the determination of C_v or C_p of a gas mixture from known properties of the pure component gases by means of the Beattie-Bridgeman equation it is necessary to make the assumption that at infinitely low pressures the energy of a mixture of gases is equal to the sum of the energies of the pure component gases when each is at the temperature and occupies the total volume of the mixture, and to know C_v or C_p for all the component gases as functions of the temperature for some one pressure.

For the mixture $$C_{vm}^* = \left(\frac{\partial E_m^*}{\partial T}\right)_{V,n} \tag{10.49}$$

and $$E_m^* = \sum x_1 E_1^*, \tag{10.50}$$

where x_1 is the mole fraction of component 1 in the mixture, E_1^* its molal energy at zero pressure, and E_m^* the molal energy of the mixture at zero pressure. The summation extends over all the gases in the mixture.

Integrating (10.42) at constant temperature and composition between the limits $V = \infty$ and the variable volume V,

$$C_v = C_v^* + \int_{\infty}^{V} T\left(\frac{\partial^2 p}{\partial T^2}\right)_{V,n} dV, \tag{10.51}$$

where p, V, T, and C_v^* refer to the mixture and the subscript n

denotes differentiation at constant composition. By differentiating (10.50) with respect to temperature at constant composition and volume,

$$C_v^* = \sum x_1 C_{v_1}^*,$$

and (10.51) becomes

$$C_v = \sum x_1 C_{v_1}^* + \int_{\infty}^{V} T\left(\frac{\partial^2 p}{\partial T^2}\right)_{V,n} dV. \tag{10.52}$$

The approximate equations corresponding to (10.47) and (10.48) are

$$C_v = \sum x_1 C_{v_1}^* + \frac{6\sum x_1 c_1}{T^4} p \tag{10.53}$$

and

$$C_p = \sum x_1 C_{p_1}^* + \left[\frac{2(\sum x_1 A_{01}^{\frac{1}{2}})^2}{RT^2} + \frac{12\sum x_1 c_1}{T^4}\right] p. \tag{10.54}$$

The variations of C_p and C_v with pressure will be discussed later.

The Value of $C_p - C_v$ for Ideal and Real Gases

From the equation

$$pV = RT,$$

$$\left(\frac{\partial V}{\partial T}\right)_p = \frac{R}{p} \quad \text{and} \quad \left(\frac{\partial p}{\partial T}\right)_v = \frac{R}{V}.$$

On substituting these values in (10.36),

$$T\left(\frac{\partial V}{\partial T}\right)_p \left(\frac{\partial p}{\partial T}\right)_v = \frac{R^2 T}{pV} = R; \tag{10.55}$$

therefore, for an ideal gas, $C_p - C_v = R$.

For a real gas conforming to van der Waals' equation,

$$T\left(\frac{\partial p}{\partial T}\right)_v = \frac{RT}{V-b}.$$

$(\partial V/\partial T)_p$ is obtained by differentiating the equation of state, bearing in mind that p is constant and therefore $(\partial p/\partial T)_p = 0$:

$$0 = \frac{R}{V-b} - \frac{RT}{(V-b)^2}\left(\frac{\partial V}{\partial T}\right)_p + \frac{2a}{V^3}\left(\frac{\partial V}{\partial T}\right)_p,$$

and

$$\left(\frac{\partial V}{\partial T}\right)_p = \frac{R}{V-b} \Big/ \left(\frac{RT}{(V-b)^2} - \frac{2a}{V^3}\right).$$

Therefore

$$C_p - C_v = \frac{\{RT/(V-b)\}\{R/(V-b)\}}{RT/(V-b)^2 - (2a/V^3)}$$

$$= \frac{R}{1 - \{2a(V-b)^2/RTV^3\}}; \tag{10.56}$$

that is, $C_p - C_v$ is greater than R.

Determination of the Specific Heats from Compressibility Data

The change in the specific heat at constant pressure (C_p) is given by the equation

$$\left(\frac{dC_p}{dp}\right) = -T(d^2V/dT^2)_p, \tag{10.57}$$

which on integration becomes

$$C_p = C'_p + \int_{p'}^{p} -T(d^2V/dT^2)_p \, dp, \tag{10.58}$$

where C'_p is the heat capacity at the pressure p'.

A graphical method of evaluating the derivative $(d^2V/dT^2)_p$ has already been described and its value for a number of gases will be found in Appendix I. By plotting $(-T(d^2V/dT^2)_p, p)$ isotherms, the change in C_p with pressure is given by the area under a given isotherm between two pressures. To calculate C_p from (10.58), it is necessary to know the value of C'_p as a function of temperature.

Deming and Shupe [1] have used (10.58) to determine the variation of C_p with pressure for carbon monoxide, using the compressibility data of Bartlett and collaborators and the quantum equation

$$C'_p = 7R/2 + R(3090/T)^2 e^{3090/T}/(e^{3090/T} - 1)^2,$$

and their results are shown graphically in Fig. 83 and are tabulated in Appendix I.

The curves illustrate certain important characteristics of the pressure effect which are common to all the permanent gases, namely: (1) At temperatures below 100°, C_p increases rapidly with pressure and reaches a maximum at about 300 atmospheres; above 500 atmospheres further increase of pressure causes only a relatively small change in C_p at any temperature; (2) below 0° and at pressures above 100 atmospheres, C_p increases rapidly as the temperature is lowered, and (3) the isotherms below 50° converge with reduction of pressure and tend to a common value of C_p at some very low pressure; the last-named phenomenon is shown by nitrogen and hydrogen, although in the case of the latter gas the point of convergence for all isotherms below 100° is at a much higher pressure ($C_p = 7{\cdot}13$ at about 280 atmospheres).

To obtain $(dC_p/dp)_T$ at zero pressure van der Waals' equation may be employed, giving

$$-T(d^2v/dT^2)_p = 2a/RT^2 \quad \text{at } p = 0.$$

It is interesting to note that the general form of the (C_p, p) isotherms obtained from compressibility measurements is very similar to that of the isotherms calculated from the thermal expansion data of Witkowski [2].

The difference between the two specific heats of a gas $(C_p - C_v)$ is related to the expansion coefficients by (10.38), and hence the data

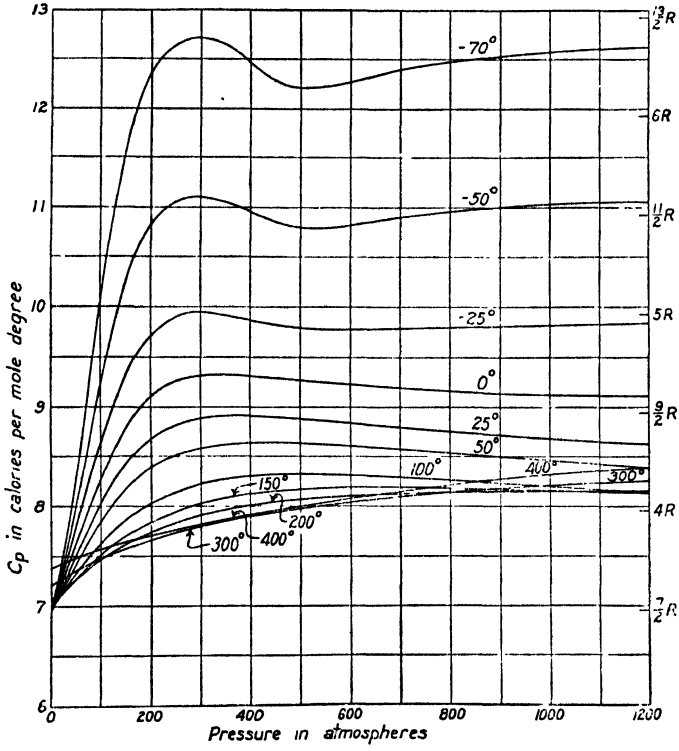

FIG. 83. The variation of C_p with pressure for carbon monoxide.

for $((C_p - C_v), p)$ isotherms can be calculated from the compressibility data. In general the value of $(C_p - C_v)$ for the permanent gases approaches R as the pressure approaches zero, at all temperatures; below 0° it increases very rapidly with rise of pressure and the isotherms show well-defined maxima at 200 atmospheres in the case of carbon monoxide and nitrogen and at 500 atmospheres in the case of hydrogen; further increase of pressure results in a progressive diminution.

A series of $((C_p - C_v), p)$ isotherms for carbon monoxide is shown in Fig. 84.

The specific heat at constant volume is given by (10.15) or by

$$\frac{1}{T}\left(\frac{\partial C_v}{\partial v}\right)_T = \left(\frac{\partial^2 p}{\partial T^2}\right)_v,$$

from which

$$\Delta C_v = -\int_1^\rho \frac{T}{\rho^2}\left(\frac{\partial^2 p}{\partial T^2}\right)_\rho d\rho. \tag{10.59}$$

In general, the values calculated from compressibility data indicate that at temperatures sufficiently far above the critical temperature

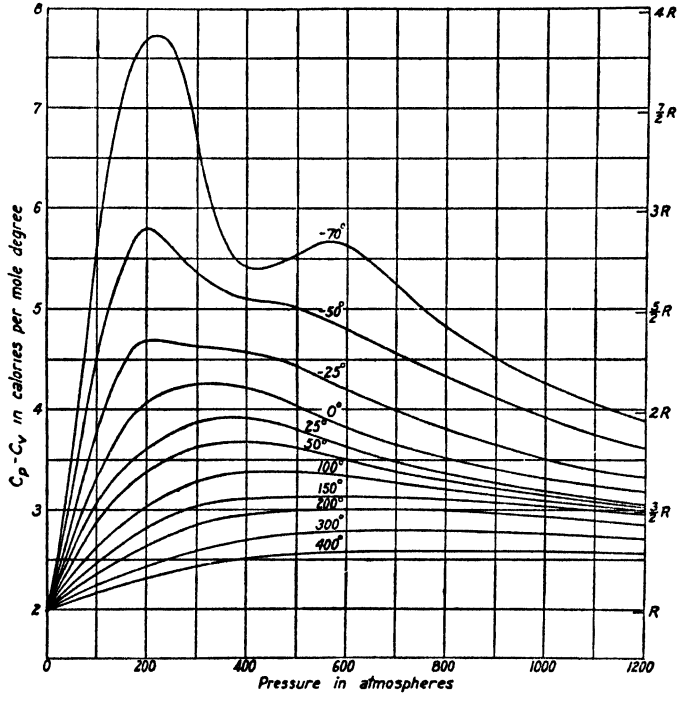

FIG. 84. $((C_p - C_v), p)$ isotherms for carbon monoxide.

C_v increases slowly and progressively with density. Near the critical temperature there is superposed on this effect a big increase of C_v with pressure, a maximum value being reached at the critical density. Thereafter it falls sharply, passes through a minimum, and then once more increases slowly. The curves in Fig. 85, taken from the data of Michels, Bijl, and Michels [2] for carbon dioxide, are typical of the behaviour of gases in the critical region.

Eucken and Seekamp [7] have suggested that the slow increase of C_v with pressure is due to the changing configurations of the

molecules. At a given temperature the configuration with the lowest potential energy has the highest probability, but with increase of temperature more molecules go over to positions of higher energy with a consequent increase in specific heat. At high densities the configurations of low potential energy are more numerous than at

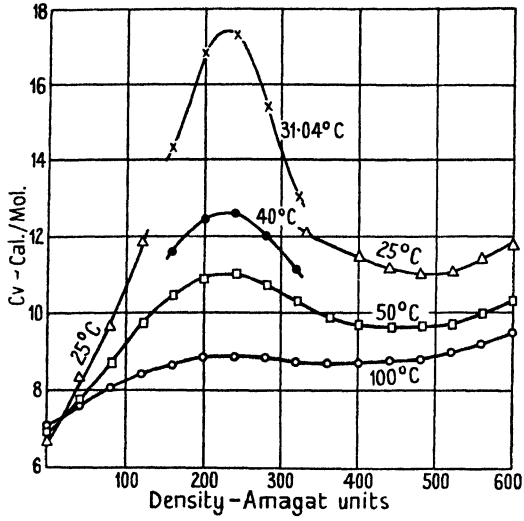

FIG. 85. The variation of C_v with pressure for carbon dioxide.

low densities and the temperature effect is therefore more pronounced.

The superposed effect in the critical region is doubtless attributable to the heat of dissociation of aggregated molecules with increase of temperature.

The Experimental Determination of Specific Heats at High Pressures

Whilst the values of the specific heats of gases calculated from compressibility and thermal expansion data serve to indicate in a general way the nature of the variations to be expected over wide ranges of temperature and pressure, the method is susceptible to large errors and it is very desirable that such data should be supplemented by direct experimental determinations of a high order of accuracy. Unfortunately very little work has been done on the subject and none that permits of a close comparison with the results we have just been considering.

The Specific Heat at Constant Volume. First in importance amongst the early experimental investigations is that of J. Joly [8], who measured the specific heats at constant volume of a number of gases up to pressures of about 30 atmospheres. He employed a differential steam-calorimeter in which two equal copper spheres, one containing the gas at a known pressure and the other empty, were suspended from the arms of a balance, in a carefully lagged steam-chamber; the water condensing on each sphere as the temperature was raised from about 10 to 100° C. was collected in a pan attached to its under side and was subsequently weighed. The general arrangement of the apparatus is shown in Fig. 86, which is self-explanatory.

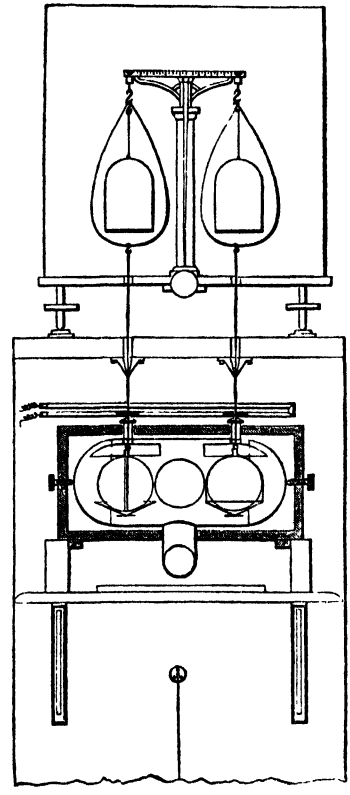

FIG. 86. Joly's apparatus for measuring the specific heat of gases (C_v)

Two pairs of spheres were used, the one designed to withstand a test pressure of 500 lb./sq. in. and a working pressure of 250 lb. /sq. in. and the other a test pressure of 1,000 lb./sq. in. and a working pressure of 500 lb./sq. in.; both pairs of spheres were about 6·7 cm. in diameter, the wall-thicknesses being 0·5 and 1 mm. respectively. According to Joly, if the stronger of the spheres (weight empty = 92·4 gm., volume = 159·8 c.c.) was filled with air to a pressure of some 22 atmospheres at about 15° its contents weighed 4·2854 gm.; on heating to 100° C. in the steam-calorimeter the total condensate weighed 1·616 gm., of which 0·116 gm. was due to the heat absorbed by the gas. In a series of six experiments the mean condensation per °C. was 0·018004 gm. The spheres were fitted with needle valves of special design, details of which will be found in Chapter IV.

The following corrections were applied to the experimental results:

(1) for the thermal expansion of the sphere. The work W done by the expansion of the gas through the increased volume of the sphere was calculated from the equation

$$W = PV\left[\alpha(t_2-t_1)+\frac{\beta-\alpha}{\beta}\log\frac{1+\beta t_2}{1+\beta t_1}\right],$$

where P and V are the initial pressure and volume of the gas, α is its

coefficient of pressure increase, and β is the coefficient of thermal expansion of copper;

(2) for the effect of the elastic distension of the vessel due to the increased pressure exerted by the gas as its temperature rises. This correction was determined experimentally;

(3) for the thermal effect of stretching the material of the sphere. The effect of the elastic distension of the metal results in a slight cooling which, however, was found to be negligibly small in magnitude;

(4) for the buoyancy, arising from the distension of the sphere when heated to $t_2°$. The amount of the correction is the product of the increase in volume of the sphere and the absolute density of steam at the temperature $t_2°$;

(5) for buoyancy arising from the distension of the sphere on filling with gas at $t°$;

(6) for unequal thermal capacities of the spheres.

The differential method eliminates any source of error common to the two spheres, and the total result of the above corrections is to reduce the direct measurement by about 0·7 per cent.

Using this apparatus and method Joly measured the mean specific heat of dry air between 10° and 100° C. at pressures of from 6·81 to 26·62 atmospheres with the results recorded in Table 48.

TABLE 48. *Mean Specific Heats of Air between* 10° *and* 100° *C. at Constant Volume and at Various Pressures (Joly)*

Pressure, atms.	*Density*	*Specific heat*
1	..	0·1689
6·81	0·00728	0·17202
9·56	0·010335	0·17111
13·56	0·01428	0·17193
14·53	0·015297	0·17192
14·58	0·015654	0·17252
23·35	0·024591	0·17223
26·62	0·027944	0·17225

From these results he concluded that 'The specific heat of air at constant volume is not constant under variation of pressure, but increases with increase of pressure, between the limits of pressure 10 to 30 atmospheres (which the experiments sufficiently cover) at the mean temperature of 50° C.'

With carbon dioxide a more pronounced increase in the specific heat with pressure was observed, as will be seen from the results in Table 49.

TABLE 49. *Mean Specific Heats of Carbon Dioxide between* 10° *and* 100° *C. at Various Pressures (Joly)*

Pressure, atms.	*Density*	*Specific heat*
1	..	0·157
7·20	0·011530	0·16841
12·10	0·019786	0·16922
12·20	0·019950	0·17054
16·87	0·028498	0·17141
20·90	0·036529	0·17305
21·66	0·037802	0·17386

Hydrogen gave rather unreliable results, but if anything the general tendency seemed to be for the specific heat to diminish with increase of pressure.

Joly's work has not been repeated or extended and no further experimental data on the variation of C_v with pressure are as yet available.

The Specific Heat at Constant Pressure. Lussana [9] carried out the first comprehensive investigation into the effect of pressure upon the specific heat at constant pressure, using a method originally employed by Delaroche and Berard [10]. In this method a known mass of gas at constant pressure was passed successively through a heater and a calorimeter and the rise in temperature of the latter was measured. A closed air-manometer was used to indicate the pressure.

As Lussana's apparatus has since been improved and greater refinements employed in measuring temperatures and pressures and in making corrections for heat losses, no detailed description of it need be given. His results, however, have still an historic interest inasmuch as they show qualitatively the nature of the pressure effect. Between 5 and 45 atmospheres he found that the mean specific heat of a gas increased linearly with pressure according to the equation

$$C_p = a+b(p-1),$$

where a and b are constants characteristic of the gas, and p is the pressure. The values of a and b over the temperature range 10–95° for a number of gases are given in Table 50.

As the result of further experiments he gave the following equation for air for the same limits of temperature:

$$C_p = 0{\cdot}23702+0{\cdot}0015504(p-1)-0{\cdot}0_519591(p-1)^2.$$

His general conclusions were that C_p increases considerably with pressure for all the gases investigated. In the case of air he observed

TABLE 50. *Mean Specific Heat at Constant Pressure (Lussana)*

Gas	*a*	*b*
Hydrogen . .	3·4025	0·013300
Methane . .	0·5915	0·003463
Carbon dioxide .	0·2013	0·0019199
Air . . .	0·23707	0·001498
Ethylene . .	0·40387	0·0016022
Nitrous oxide .	0·22480	0·0018364

that the rate of increase of pressure diminished at high pressure and tended towards a maximum, whilst in the case of carbon dioxide a maximum was reached at about 110 atmospheres, after which it diminished with further increase of pressure. At pressures below about 50 atmospheres the value of C_p for the latter gas increased with temperature but at higher pressure it diminished.

Holborn and Jacob's Determination of C_p for Air. We may next consider a very careful determination of the specific heat of air (C_p) at various pressures up to 200 atmospheres carried out by Holborn and Jacob [11] using a constant-flow method. Their calorimeter is shown in section in Fig. 87.

The gas enters the calorimeter through the lower opening and traverses a number of electrically heated narrow nickel tubes packed in the space H_1; its temperature at entry is measured by a platinum resistance thermometer at T_1. After traversing the tubes it passes round the annular space between the tubes and the wall of the calorimeter as shown by the arrows and leaves by the exit tube on the right of the diagram; the exit temperature is measured by a second thermometer at T_2.

The calorimeter itself is constructed of nickel-steel (length 45 cm., diameter 9 cm., and wall thickness 0·5 cm.), and is provided with a jacket through which oil, heated by a resistance at H_2, is caused to circulate; the whole is surrounded by a steam jacket M. In carrying out a determination the electrical energy supplied to the nickel tubes and to the oil jacket is accurately measured and the temperature of the gas at the inlet and outlet is noted. The heat-loss corrections are independent of the rate of flow of gas between the limits 10 and 39 kg. of air per hour.

Holborn and Jacob's results for dry air are given in Table 51, and, for comparison, the values obtained by Lussana, Vogel [12], and Noel [13] are also included.

The data fit the empirical equation

$$C_p \times 10^4 = 2413 + 2{\cdot}86p + 0{\cdot}0005p^2 - 0{\cdot}00001p^3,$$

as will be seen from the observed and calculated values in the table.

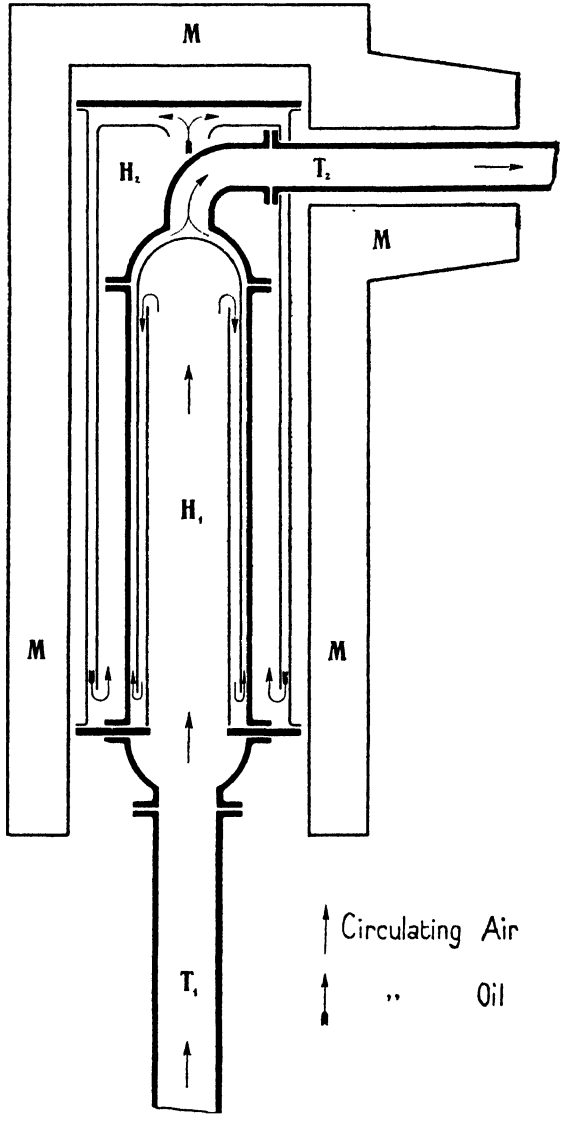

FIG. 87. Holborn and Jacob's high-pressure calorimeter.

Vogel and Noel's data are calculated from the results of porous-plug experiments using the equation

$$C_p = C_0\left(1-\frac{d\delta}{dT}\right),$$

where δ is the cooling effect.

TABLE 51. *The Effect of Pressure on the Specific Heat of Air at Constant Pressure and at 59° C.*

Pressure, kg./cm.²	$C_p \times 10^4$				
	Holborn and Jacob		*Lussana*	*Vogel*	*Noel*
	Observed	*Calculated*			
0	..	2,413	..	..	..
1	2,415	2,416	2,370	..	..
25	2,490	2,485	2,711	2,480	2,493
50	2,554	2,556	3,061	2,543	2,568
100	2,690	2,694	3,737	2,664	2,701
150	2,821	2,819	4,198	2,770	2,812
200	2,925	2,925	..	2,853	2,893

The Specific Heat of Nitrogen. Krase and Mackey [14] have measured the specific heat of nitrogen in an adiabatic constant temperature flow calorimeter designed to withstand a pressure of 1,000 atmospheres.

The general arrangement of their apparatus is shown diagrammatically in Fig. 88. Three high-pressure gas cylinders are connected through a copper deoxidizer and soda-lime scrubber to a thermostat. A long coil of steel tubing immersed in the liquid of the thermostat brings the temperature of the gas to a constant value. Passing through a short, well-insulated tube to the calorimeter, the gas flows through the coil immersed in the calorimeter liquid. Since the temperature of the calorimeter is maintained about 6° higher than that of the thermostat, the flowing gas is heated during passage. To compensate for this continuous removal of heat by the gas and for the heat losses by conduction along the steel tubing and the usual calorimeter losses, a carefully measured quantity of electrical energy is introduced into the calorimeter liquid to maintain its temperature constant. The rise in temperature of the flowing gas due to heat absorption is measured by thermojunctions placed in the gas stream. After leaving the calorimeter the gas is expanded to about atmospheric pressure, the rate of flow being indicated by a sensitive capillary flow-meter. After humidifying the gas, the rate of flow is measured in a calibrated wet-meter and the gas is then collected in a water-sealed gas-holder. As needed, the gas is recompressed by means of a three-stage gas-compressor into the first storage cylinder and, for work at 300 atmospheres or more, is further compressed above a water piston formed by the hydraulic pump.

The actual manipulation during an experiment, in addition to that just described, consists in adjusting the electrical energy input to the calorimeter so that with a constant rate of gas flow at constant pressure its temperature remains constant.

The heat of stirring and the losses due to radiation, convection, evaporation, etc., are determined by making measurements with no gas flowing but with all other conditions exactly as during a regular experiment. The heat put into the calorimeter as electrical energy plus the heat put in by the stirrer exactly equal the losses due to conduction along the steel tubing and all other losses.

The Thermostat and Calorimeter. The function of the thermostat is to deliver gas at the desired pressure and temperature to the calorimeter at a constant rate of flow. It consists of a coil 3·5 metres long of 6·5 mm. by 1·5 mm. steel tubing around which is cast a cylindrical block of copper. An electric heater is wound on the casting and a Beckmann thermometer placed in a hole drilled in it. The temperature is manually controlled to within $\pm 0{\cdot}01°$.

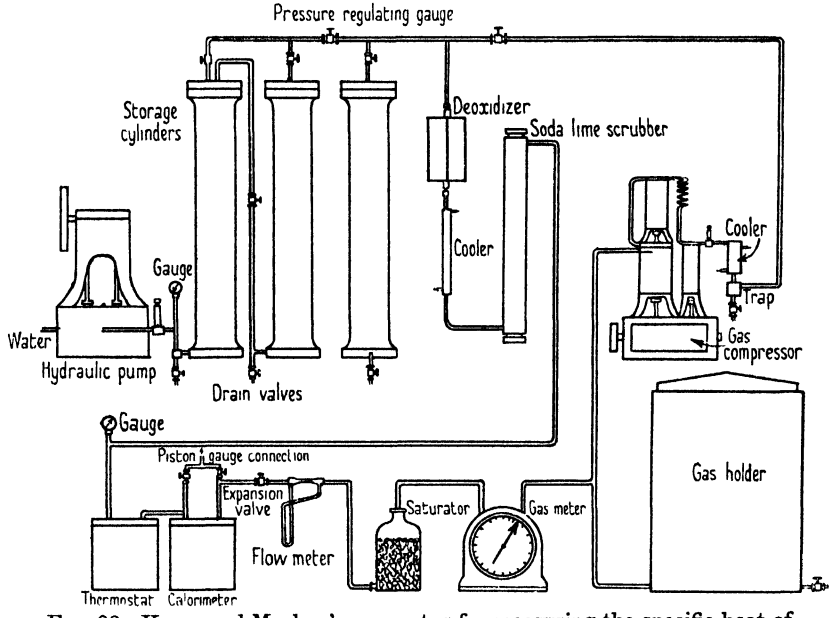

FIG. 88. Krase and Mackey's apparatus for measuring the specific heat of nitrogen (C_p).

The calorimeter is shown in Fig. 89. The gas from the thermostat enters through the horizontal side tube shown in section, passes through the coiled portion which is embedded in a copper casting 7·5 cm. long and 6·4 cm. in diameter, and leaves by the horizontal tube on the right of the diagram. The casting contains an electric heater by means of which its temperature is maintained constant at about 5 or 6° above the temperature of the thermostat. The calorimeter is enclosed in a pyrex Dewar flask contained in a heavy cylindrical copper casting closed at both ends by copper flanges. In order to operate the calorimeter adiabatically, the copper jacket is kept at the same temperature by means of an electric resistance heater wound around it, and is heavily insulated. The wires of the couples for reading the rise in temperature of the flowing gas enter at the top of the vertical steel tubes forming extensions of the calorimeter coil.

The rates of gas flow used ranged from 0·7 to 1·5 mols per minute and the results were entirely independent of rate of flow, indicating the absence of systematic errors in measurements.

The pressure regulation was accurate to about an atmosphere

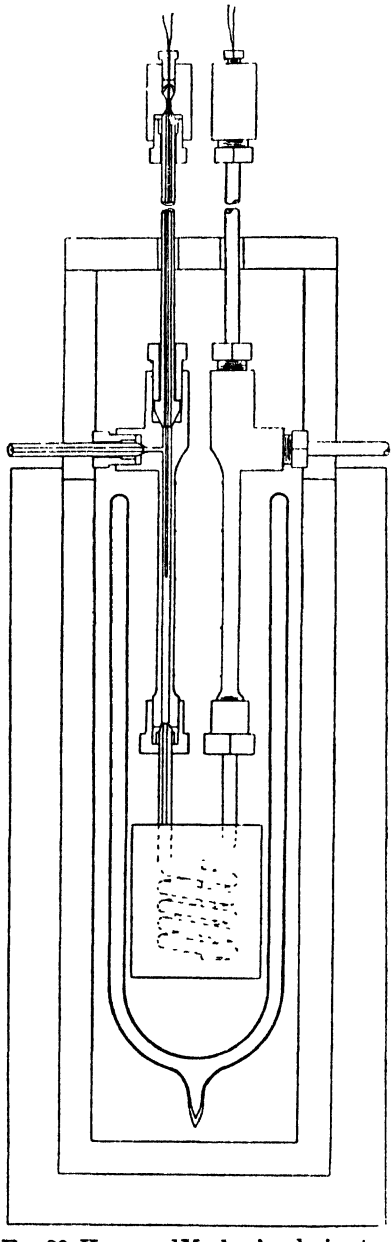

FIG. 89. Krase and Mackey's calorimeter.

during an experiment; pressures were measured by Bourdon gauges calibrated at frequent intervals against a free-piston gauge.

Krase and Mackey discuss the various sources of error in their apparatus and method and conclude that their results are reproducible and accurate to something better than 0·5 per cent.

The data for nitrogen are given in Table 52. It should be noted that the nitrogen employed was obtained from atmospheric air and, whilst otherwise pure, contained small and undetermined amounts of argon.

In Table 52A a comparison is made between the observed values of C_p and those derived from measurement of the Joule-Thomson coefficient and from compressibility data. The agreement is probably as good as can be expected in view of the differences in method. Thus Krase and Mackey's values are lower by about 0·6 per cent., with a maximum of 1·1 per cent., than those calculated by Roebuck and Osterberg from measurement of the Joule-Thomson coefficient, and are also generally lower than the values obtained from the compressibility data.

The Effect of Pressure on the Ratio (γ) of the Specific Heats

A knowledge of the variations with temperature and pressure of the ratio of the specific heats is of considerable importance in con-

TABLE 52. *Molecular Heat of Nitrogen at Constant Pressure*

Temperature, °C.	Pressure, atmospheres									
	1†	50	100	200	300	400	500	600	700	800
30	6·91	7·41	7·92	8·64	8·94	9·07	9·12	9·14	9·16	..
50	6·92	..	7·72	8·32	8·70	8·81	8·85	8·86	8·88	8·89
100	6·94	7·21	7·48	7·92	8·23	8·35	8·39	8·43	8·45	..
125	6·95	7·20	7·40	7·76	8·01	8·17	8·26	8·30	8·35	..
150	6·96	7·19	7·36	7·66	7·89	8·02	8·13	8·20	8·25	..

† Accepted values.

TABLE 52A. *C_p for Nitrogen calculated from (a) Joule-Thomson Coefficient (Roebuck and Osterberg), (b) Compressibility Data (Deming and Shupe), and (c) the Observed Values of Krase and Mackey*

T, °C. / P, atms.	−100	−50	0	50	100	150	200	300
1 (a)	0·2473	0·2466	0·2466	0·2469	0·2476	0·2484	0·2490	0·2501
(b)	..	0·2466	0·2466	0·2469	0·2476	0·2483	0·2490	0·2501
(c)	..	..	..	0·2469	0·2476	0·2483	..	..
20 (a)	0·2813	0·2636	0·2557	0·2522	0·2510	0·2507	0·2510	0·2523
(b)	..	0·2629	0·2569	0·2537	0·2519	..	0·2516	0·2519
33·5 (a)	0·3010	0·2748	0·2626	0·2569	0·2543	0·2533	0·2530	0·2538
60 (a)	0·3345	0·2967	0·2769	0·2658	0·2601	0·2573	0·2560	0·2556
(b)	..	0·2976	0·2794	0·2662	0·2601	..	0·2566	0·2551
100 (a)	..	0·3233	0·2942	0·2775	0·2680	0·2627	0·2602	0·2581
(b)	..	0·3326	0·3012	0·2776	0·2676	..	0·2608	0·2580
(c)	..	..	..	0·2755	0·2669	0·2626	..	..
140 (a)	..	0·3438	0·3071	0·2865	0·2754	0·2687	0·2648	0·2605
180 (a)	..	0·3577	0·3179	0·2943	0·2810	0·2735	0·2688	0·2629
200 (a)	..	..	0·3243	0·2986	0·2841	0·2759	0·2706	0·2690
(b)	..	0·3807	0·3301	0·2990	0·2837	..	0·2701	0·2640
(c)	..	..	..	0·2969	0·2826	0·2733	..	..

nexion with the design of plant in which adiabatic or polytropic processes are being carried out. Unfortunately, very little direct experimental data is available and it is frequently necessary to resort to the values calculated indirectly from compressibility data.

Two series of measurements for air have, however, been made by P. P. Koch [15] at temperatures of −79·3° and 0° C. respectively. He adopted Kundt's method of measuring the velocity of sound in the gas and designed an apparatus similar to that used by Kundt and Warburg, but modified so as to permit of pressures up to 200

atmospheres being employed. The two dust-figure tubes, one of which was totally enclosed in a steel vessel, were connected by a steel sounding rod clamped at a quarter of its length from each end. Pressures were read by a secondary gauge calibrated against an Amagat manometer and the temperature was maintained constant by completely immersing the tubes in a thermostat. A correction was applied for the yielding of the tube walls, but no correction was found necessary for the effect of pressure on the vibration frequency of the steel rod.

The value of γ was calculated from the relation

$$\gamma = \frac{\gamma_0(C/C_0)^2 f(p) - p\{df(p)/dp\}}{f^2(p)}, \qquad (10.60)$$

where γ and γ_0 are the values of γ at $T°$ and 0° C., C and C_0 the velocity of sound at $T°$ and 0° C., and $f(p)$ the value of the product pv for air at $T°$ and p atmospheres.

Taking the value of γ_0 as 1·4053, Koch obtained the results recorded in Table 53. Some values due to Witkowski have been included for comparison.

TABLE 53. *Values of γ for Air at Various Pressures*

Pressure, atms.	C/C_0	$f(p)$	$\frac{df(p)}{dp} \times 10^5$	γ	
				Koch	*Witkowski*
		Temperature = 0° *C.*			
25	1·008	0·9821	−51·3	1·473	1·47
50	1·022	0·9732	−27·4	1·530	1·53
75	1·041	0·9682	−15·9	1·593	1·58
100	1·064	0·9656	+ 1·6	1·646	1·64
125	1·095	0·9685	+22·3	1·690	..
150	1·132	0·9762	+37·3	1·739	..
175	1·173	0·9875	+50·3	1·783	..
200	1·220	1·0016	+62·7	1·828	..
		Temperature = −79·3° *C.*			
1	0·842	0·7092	0	1·405	..
25	0·831	0·6623	−188	1·569	1·58
50	0·830	0·6194	−162	1·767	1·79
75	0·843	0·5814	−128	2·001	2·06
100	0·885	0·5566	− 63·1	2·200	2·30
125	0·960	0·5489	− 8·1	2·402	..
150	1·047	0·5534	+ 41·8	2·469	..
175	1·140	0·5709	+ 80·3	2·413	..
200	1·239	0·5954	+106	2·333	..

It is interesting to compare these results with values calculated from compressibility data. The corresponding figures for air are not available over a sufficiently wide range, but we may take for purposes of comparison carbon monoxide, which is a gas having very similar properties to those of nitrogen. The ratio of the specific heats for this gas calculated from the data of Bartlett and collaborators for pressures up to 1,200 atmospheres are given in Table 53 A.

It will be seen that in both cases γ increases with pressure to a maximum corresponding with a pressure of about 200 atmospheres at the lower temperatures and 300 atmospheres at the higher, and with further increase of pressure diminishes progressively.

TABLE 53 A. *Values of γ for Carbon Monoxide calculated from Compressibility Data*

Pressure, atms.	γ				
	−70°	−25°	0°	50°	150°
25	1·536	1·484	1·468	1·444	1·421
50	1·713	1·579	1·543	1·493	1·444
75	1·944	1·678	1·610	1·537	1·470
100	2·215	1·763	1·670	1·573	1·489
150	2·591	1·862	1·751	1·624	1·525
200	2·660	1·934	1·802	1·665	1·559
300	2·116	1·874	1·839	1·728	1·613
400	1·769	1·864	1·825	1·740	1·623
500	1·831	1·828	1·776	1·721	1·620
600	1·852	1·743	1·712	1·669	1·629
800	1·635	1·638	1·644	1·655	1·604
1,000	1·539	1·556	1·570	1·575	1·589
1,100	1·475	1·517	1·536	1·570	1·583
1,200	1·442	1·518	1·537	1·572	1·572

The Variation with Pressure of the Mean Coefficient ('Volume Coefficient') of Expansion of a Gas at Constant Pressure

The increase in volume of an ideal gas at constant pressure when its temperature is increased is given by the relation

$$v_1 - v_0 = v_0(T_1 - T_0)k_v,$$

where v_0 is the volume at $T_0°$, v_1 is the volume at $T_1°$, and k_v is the mean 'volume coefficient' of expansion. For real gases conforming to van der Waals' equation of state we have seen that

$$k_v = 1 + \frac{a}{pv_0}\left(\frac{1}{v_0} + \frac{1}{v_1}\right) - \frac{b}{v_0}\frac{1}{T_0},$$

where p is the pressure of the gas.

This equation shows that k_v depends both upon the volume and the pressure of the gas.

In order to determine experimentally the variation with pressure of k_v, one of the most direct methods is to measure the volumes at 0° C. and 1 atmosphere of the gas at pressure p contained in two vessels of volume v_1 and v_2 respectively, maintained at temperatures of $T_1°$ and $T_2°$.

If M_1 is the mass and σ_1 the density of the gas in the vessel of volume v_1, and M_2 and σ_2 the corresponding quantities for the gas in the vessel of volume v_2, then

$$\sigma_1 = \frac{M_1}{v_1} = \frac{\sigma_0}{1+k_{v,T_1}(T_1-T_0)},$$

and

$$\sigma_2 = \frac{M_2}{v_2} = \frac{\sigma_0}{1+k_{v,T_2}(T_2-T_0)}, \tag{10.61}$$

where k_{v,T_1} and k_{v,T_2} are the values of k_v between T_0 and T_1 and T_0 and T_2 respectively, and σ_0 is the density of the gas at $T_0°$ and pressure p. From these two equations we obtain

$$k_{v,T_1} = \{1+k_{v,T_2}(T_2-T_0)\}\frac{M_2 v_1}{M_1 v_2} - \frac{1}{(T_1-T_0)}. \tag{10.62}$$

If $T_2 = T_0$, (10.62) simplifies to

$$k_{v,T_1} = \frac{1}{(T_1-T_0)}\left\{\frac{M_2 v_1}{M_1 v_2} - 1\right\}. \tag{10.63}$$

It will be remarked that the coefficient is made to depend on the two ratios M_2/M_1 and v_1/v_2, and on the temperature difference (T_1-T_0).

Witkowski [16] has employed this method to determine the thermal expansion of air at constant pressure between 1 and 130 atmospheres.

His apparatus is shown diagrammatically in Fig. 90. The air is stored under pressure and in contact with calcium chloride and caustic potash in the gas cylinder C; it passes by way of the two drying tubes S_1 and S_2, also containing calcium chloride and caustic potash, through the inlet valves R_1 and R_2 to the two piezometers W_1 and W_2 which are maintained at temperatures T_1 and T_2 respectively. The piezometers are made of glass and have a capacity of about 11 c.c. and 25 c.c. respectively. After a time-interval sufficiently long for the gas to attain thermal equilibrium the pressure is measured by means of a gas-manometer filled with nitrogen. The inlet valves are then closed and the contents of the two piezometers are immediately transferred to the eudiometers E_1 and E_2, where their volumes are measured at atmospheric pressure.

The volumes of the piezometers were determined by the weight of mercury required to fill them at 0° and +100° C. Corrections were applied for the change in volume due to temperature and pressure variations.

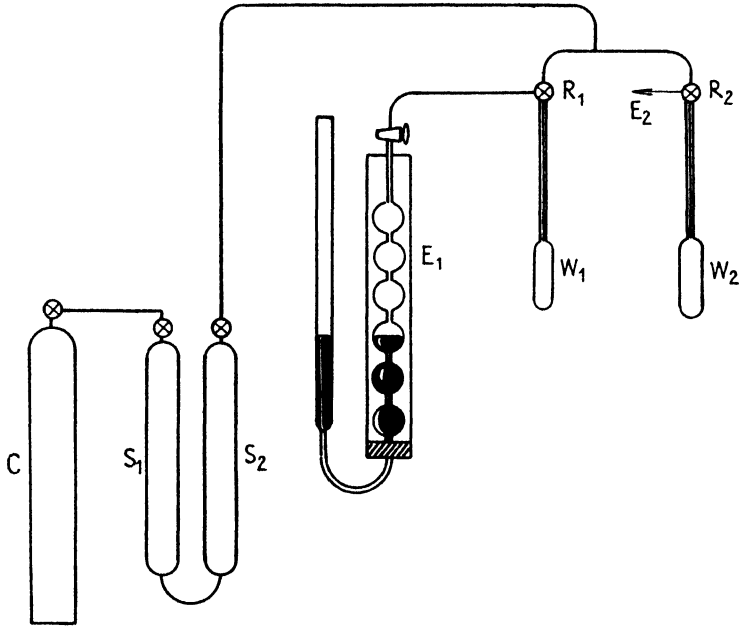

FIG. 90. Witkowski's apparatus for measuring the mean coefficient of expansion of air at high pressures.

Using this apparatus Witkowski measured the mean coefficients of expansion of atmospheric air at nine temperatures between −145 and 100° C., at pressures up to 130 atmospheres, with the results given in Table 54.

The data show very clearly the nature of the variation of k_v with pressure and temperature. At all temperatures the coefficient increases with increase of pressure, tending at the lower temperatures to reach a maximum. In the vicinity of the critical point (−141° and 39 atmospheres) the rate of increase of expansion is very great.

Witkowski showed how his results could be used to calculate the compressibility of air at low temperatures. If v_0 is the volume of a certain quantity of air at 0° and 1 atmosphere pressure and v its volume at $t°$ and p atmospheres, then, according to Boyle's and Charles's laws,

$$pv = v_0(1+\gamma t).$$

TABLE 54. *The Mean Coefficients of Expansion of Atmospheric Air between 0° C. and T_1° C. at Constant Pressure (k_v)*

$K_v \times 10^5$

Pressure, atms.	*Temperature, T_1°*								
	+100°	+16°	−35°	−78·5°	−103·5°	−130°	−135°	−140°	−145°
10	375	376	..	..	..	..	..	..	450
20	383	387	..	401	410	427	..	440	519 (29atm.)
30	392	398	..	420	434	462	477	492	..
40	402	408	..	438	461	508	544	632	..
50	410	419	430	457	487	569	619	..	..
60	418	429	442	476	512	610	622	..	..
70	425	438	454	494	536	612	..	..	..
80	431	446	467	512	557	607	..	..	..
90	437	452	479	527	572	..	..	..	..
100	441	458	489	537	579	..	..	..	..
110	445	462	497	545	580	..	..	..	..
120	449	465	501	550	577	..	..	..	..
130	..	468	..	551	571	..	..	..	..

Now since the product pv is not independent of pressure, and its dependence on temperature is not a linear one, we may write

$$pv = fv_0, \tag{10.64}$$

where f is the compressibility and is a function of pressure and temperature.

Let
$$pv = \alpha p_0 v_0. \tag{10.65}$$

Heat the volume v_0 of air at constant pressure (= 1 atmosphere) to +16°; the volume increases to $v_0(1+\gamma 16)$. At this temperature, increase its pressure to p atmospheres. Then from (10.65) its volume v will be given by

$$v = \alpha \frac{v_0(1+\gamma 16)}{p}; \tag{10.66}$$

finally, heat it at the constant pressure p to t°, when its volume will become

$$v' = \frac{v_0(1+\gamma 16)}{p} \frac{(1+tk_{p,t})}{(1+16k_{p,16})}$$
$$= fv_0/p.$$

Hence
$$f = \alpha \frac{1+16\gamma}{1+16k_{p,16}} (1+tk_{p,t}). \tag{10.67}$$

The converse of this problem, namely, the determination of the expansion coefficients from the pressure-volume-temperature relations of real gases, has already been dealt with.

Maximum Work and Free Energy

The total work performed by any process is made up of the useful work plus the work done in expansion of the system and is a maximum when the process is reversible. In a reversible isothermal process at constant pressure

$$-\Delta A = -\Delta F + p\Delta V, \tag{10.68}$$

where $-\Delta A$ is the maximum total work and $-\Delta F$ is the maximum useful work or the decrease in free energy.

The maximum total work may be defined by the relation

$$A = E - TS$$

$$= \int_0^t C_{v=\infty}\,dt - T\int_0^t \frac{C_{v=\infty}}{T}\,dt + \int^{\rho} \frac{(pv)_t}{\rho}\,d\rho - \int^{1} \frac{(pv)_{t=0}}{\rho}\,d\rho, \tag{10.69}$$

and the free energy by

$$F = (E+PV) - TS = H - TS = A + PV. \tag{10.70}$$

In a thermodynamic sense a system is stable when no change can take place in it involving a diminution in free energy. A chemical reaction, for example, can only proceed spontaneously and isothermally when the resultant free energy change is negative, and the quantity $-\Delta F$ may be taken to express the driving force of the reaction; it follows that when a condition of equilibrium is reached in a chemical reaction the free energy change is zero.

The Influence of Pressure and Temperature upon Free Energy

If the equation $F = H - TS$ is differentiated with respect to pressure,

$$\left(\frac{\partial F}{\partial p}\right)_T = \left(\frac{\partial H}{\partial p}\right)_T - T\left(\frac{\partial S}{\partial p}\right)_T,$$

and from (10.24)

$$\left(\frac{\partial F}{\partial p}\right)_T = V \quad \text{or} \quad \int dF = \int V\,dp. \tag{10.71}$$

By differentiating with respect to temperature,

$$\left(\frac{\partial F}{\partial T}\right)_p = \left(\frac{\partial H}{\partial T}\right)_p - T\left(\frac{\partial S}{\partial T}\right)_p = -S = \frac{F-H}{T} \tag{10.72}$$

To determine the effect of temperature on chemical equilibria, the

variation in the change of free energy of a reaction with change in temperature, at constant pressure, must be known.

From (10.70), $$\frac{\Delta F}{T} = \frac{\Delta H}{T} - \Delta S,$$

and $$\left(\frac{\partial(\Delta F/T)}{\partial T}\right)_p = \frac{1}{T}\left(\frac{\partial \Delta H}{\partial T}\right)_p - \frac{\Delta H}{T^2} - \left(\frac{\partial \Delta S}{\partial T}\right)_p.$$

But $$\left(\frac{\partial \Delta H}{\partial T}\right)_p = T\left(\frac{\partial \Delta S}{\partial T}\right)_p,$$

and hence $$\left(\frac{\partial(\Delta F/T)}{\partial T}\right)_p = -\frac{\Delta H}{T^2}. \tag{10.73}$$

The Escaping Tendency

Molal free energy may be used as a quantitative measure of a property of matter known as the 'escaping tendency'; for if the molal free energy of a substance is greater in one part of a system than in another, that substance will tend to migrate from the former to the latter region; it follows that the condition for equilibrium in a heterogeneous system is that the escaping tendency of each component shall be equal in all the phases.

In the case of ideal gases the escaping tendency of each constituent is measured quantitatively by its partial pressure; for real gases a corrected partial pressure known as the 'fugacity' may be employed and is partially defined in terms of the molal free energy by the equation $$F = RT\log_e f + B, \tag{10.74}$$

where f is the fugacity and B is an integration constant which is a function of temperature.

Between two isothermal states

$$F_B - F_A = RT\log_e \frac{f_B}{f_A}, \tag{10.75}$$

or $$dF = RT\, d\log_e f.$$

But $$F_B - F_A = RT\log_e \frac{p_B}{p_A},$$

and hence the fugacity of an ideal gas is proportional to its pressure.

The Fugacity of Real Gases

If the fugacity of an ideal gas is made arbitrarily equal to the pressure, it will have the same dimensions as pressure and the units of fugacity will be the same as the units of pressure.

The relation between the fugacity and pressure of a real gas may be obtained as follows:

From (10.71), $$\left(\frac{\partial F}{\partial p}\right)_T = V.$$

Combining this with (10.75),

$$\left(\frac{\partial \log_e f}{\partial p}\right)_T = \frac{V}{RT}. \tag{10.76}$$

From the equation of state of the gas, V may be expressed as a function of p and (10.76) may then be integrated to give the fugacity of the gas at any pressure.

If the pressure-volume data for a real gas are known, its fugacity may be obtained graphically by the following method due to Lewis and Randall [17]:

In Fig. 91 the curve $ABCD$ is an isotherm of the gas in question, and $EFGH$ is the corresponding isotherm for an ideal gas calculated from the equation of state $PV = RT$. Let the points K, B, F correspond to a pressure P and L, C, G to a pressure P'.

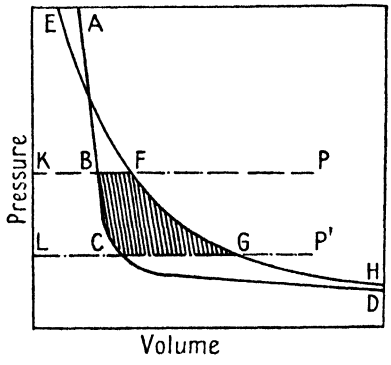

FIG. 91. Graphical determination of fugacity (first method).

On integrating (10.76),

$$RT \log_e (f/f') = \int_{P'}^{P} V\, dP = \text{area } KBCL.$$

The corresponding area $KFGL$ is equal to $RT \log_e (P/P')$. If the difference between these two areas be called A, then

$$RT \log_e \frac{f}{f'} = RT \log_e \frac{P}{P'} - A. \tag{10.77}$$

If P' is replaced by a variable pressure p, and if f'' is the corresponding fugacity, then, by definition, when $p = 0, f'' = p$.

Eq. (10.77) may therefore be written

$$RT \log_e f = RT \log_e P - A',$$

where A' is the area included between the two isotherms and the lines KBF and LCG, the latter extending to infinite volume. It is

clear from the figure that the difference between the fugacity and the pressure depends upon the degree of departure from the ideal gas equation of state, that is, upon the area A'.

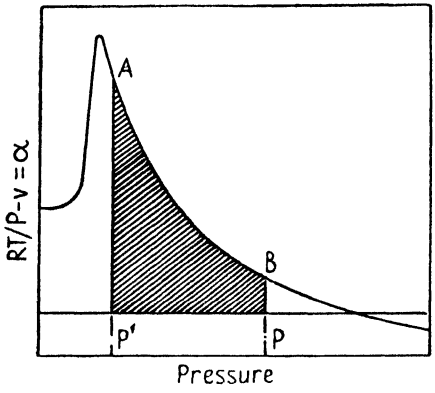

FIG. 92. Graphical determination of fugacity (second method).

A more convenient graphical method of determining the fugacity from compressibility data is to plot the deviations from the ideal gas laws against the pressure [17]. Thus, if v is the molal volume of a gas and RT/P is the molal volume calculated from the ideal equation of state, the difference, namely, $RT/P - v$, which may be denoted by α, is a function of temperature and pressure. Plotting α against P a curve similar to that shown in Fig. 92 is obtained, and

$$RT\, d\log_e f = v\, dP = RT/P\, dP - \alpha\, dP.$$

On integrating between zero pressure and a given pressure P,

$$RT \log_e f = RT \log_e P - \int_0^P \alpha\, dP. \qquad (10.78)$$

When one of the limits of pressure is zero the shaded area is equal to the last term in (10.78) and to the area A' in Fig. 91.

In the case of gaseous mixtures Lewis and Randall assume that the mixture may be regarded as a perfect solution, so that at a given temperature and total pressure the fugacity of each component is proportional to its mol fraction or to its partial pressure. The ratio of fugacity to pressure is known as the activity coefficient of the gas.

The Effect of Temperature on the Fugacity of a Gas

To determine the effect of temperature upon fugacity the molal free energy F and fugacity f of a substance in a given state is compared with the corresponding quantities F^* and f^* in the vapour phase at a pressure sufficiently low for the fugacity to equal the pressure, and at the same temperature. If H and H^* are the corresponding values of the molal enthalpy, the latter will be independent of pressure.

From (10.76),

$$F^*-F = RT\log_e(f^*/f) = RT(\log_e f^*-\log_e f). \qquad (10.79)$$

On differentiating with respect to temperature at constant pressure,

$$\left(\frac{\partial F^*}{\partial T}\right)_P-\left(\frac{\partial F}{\partial T}\right)_P = R\log_e\frac{f^*}{f}+RT\left(\frac{\partial \log_e f^*}{\partial T}\right)_P-RT\left(\frac{\partial \log_e f}{\partial T}\right)_P. \qquad (10.80)$$

Since f^* is equal to the pressure it does not change with the temperature at constant pressure; that is,

$$\left(\frac{\partial \log_e f^*}{\partial T}\right)_P = 0.$$

From (10.79) and (10.80),

$$\left(\frac{\partial F^*}{\partial T}\right)_P-\left(\frac{\partial F}{\partial T}\right)_P = \frac{F^*}{T}-\frac{F}{T}-RT\left(\frac{\partial \log_e f}{\partial T}\right)_P, \qquad (10.81)$$

and combining with (10.72),

$$\left(\frac{\partial \log_e f}{\partial T}\right)_P = \frac{H^*-H}{RT^2}. \qquad (10.82)$$

BIBLIOGRAPHY

1. Deming and Shupe, *Phys. Rev.* **34**, 527 (1929); **37**, 638 (1931); **38**, 2245 (1931); **40**, 848 (1932); Deming and Deming, ibid. **45**, 109 (1934).
2. Michels, Wouters, and de Boer, *Physica*, III, No. 7 (1936); Michels, Bijl, and Michels, *Proc. Roy. Soc.* (A), **160**, 376 (1937).
3. Giaque and Clayton, *J. Am. Chem. Soc.* **55**, 4875 (1933).
4. Keenan and Keyes, *Thermodynamic Properties of Steam.* John Wiley & Sons, Inc., New York, 1936.
5. Hirschfelder and Roseveare, *J. Phys. Chem.*, Dec. 1938.
6. Beattie, *Phys. Rev.* **34**, 1615 (1929).
7. Eucken and Seekamp, *Z. phys. Chem.* **134**, 198 (1928).
8. Joly, *Proc. Roy. Soc.* **46**, 352 (1886); **47**, 218 (1889); *Phil. Trans.* (A), **182**, 73 (1891).
9. Lussana, *Nuovo Cimento* (3), **36** (1894); ibid. 1895, 1896, 1897, 1898.
10. Delaroche and Berard, *Ann. de Chim. et de Phys.* **85**, 72 (1813).
11. Holborn and Jacob, *Sitz. Ber. der Pr. Akad. d. Wiss.*, Berlin, **1**, 213 (1914).
12. Vogel, *Zeitschrift des Vereins Deut. Ing.*, pp. 108 and 109 (1911).
13. Noel, *Sitz. d. Kgl. Bayer. Akad. d. Wiss.*, p. 218 (1913).
14. Krase and Mackey, *J. Am. Chem. Soc.* **52**, 108 (1930); **52**, 5111 (1930); *J. Ind. Eng. Chem.* **22**, 1060 (1930).
15. Koch, *Ann. Phys.* **26**, 551 (1908); **27**, 311 (1908).
16. Witkowski, *Phil. Mag.* xli, 288 (1896); xlii, 1 (1896).
17. Lewis and Randall, *Thermodynamics.* McGraw-Hill, 1923.

XI

THE THERMODYNAMIC PROPERTIES OF GASES (*continued*)

The Joule-Thomson Effect

In an endeavour to prove the existence of cohesive forces in gases Gay-Lussac and, later, Joule carried out a simple and instructive experiment in which a gas (air) was allowed to expand from a reservoir into an evacuated receiver, both vessels being immersed in a calorimeter. No measurable change in the temperature of the calorimeter could be detected and it was therefore concluded that no heat had been either given out or absorbed by the gas as a whole and no change in its internal energy had taken place. It is now known that the magnitude of any temperature change in such an experiment would be far too small to be detected by the thermometers employed.

In 1853 Joule and Thomson [1] re-examined the question, and employing a continuous method by which the gas was forced through a porous plug situated in a heat-insulated tube, the pressures on either side of the plug remaining substantially constant, were able to show that for all the gases examined, with the single exception of hydrogen, there was a definite and measurable cooling effect on the low-pressure side. Later experiments using more refined methods of measurement have confirmed this observation and have demonstrated that the extent of the cooling produced by a given pressure drop is nearly although not quite independent of the absolute value of the pressure, and increases rapidly with diminution of temperature. It has also been established that hydrogen and helium, which at ordinary temperatures are heated by free expansion, behave like other gases at low temperatures. There are, indeed, for all gases certain inversion temperatures at which no change of temperature occurs on free expansion.

The theory underlying the Joule-Thomson effect may be explained by reference to Fig. 93 which represents diagrammatically the experimental conditions.

The gas at an initial temperature T_1 is assumed to be traversing the porous plug from left to right, the two pistons A and B moving at such a rate that the pressures on either side of the plug are maintained constant at P_1 and P_2 respectively. When 1 mol of gas has traversed the plug the work done on the system will be P_1V_1 and the

work done by the system P_2V_2. Let the temperature of the expanded gas be T_2. The net work done on the gas will be $P_2V_2-P_1V_1$, and if no heat is gained or lost by the system we may write

$$E_2-E_1 = P_1V_1-P_2V_2, \tag{11.1}$$

and $\Delta H = 0$.

The ratio $(T_2-T_1)/(P_2-P_1)$ will vary with the pressure difference and its limiting value as P_2-P_1 approaches zero is known as the

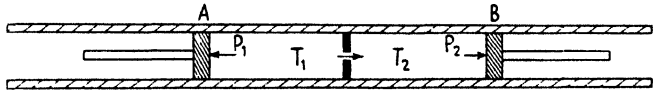

FIG. 93. Diagrammatic representation of the Joule-Thomson experiment.

Joule-Thomson coefficient and is usually denoted by μ. It is defined by the equation

$$\mu = \left(\frac{\partial T}{\partial P}\right)_H, \tag{11.2}$$

and is a constant characteristic of the fluid under examination. From (10.16) and (11.2)

$$\left(\frac{\partial H}{\partial P}\right)_T = -\mu C_p. \tag{11.3}$$

This equation gives the heat that would be absorbed per unit difference of pressure if the experiment were carried out in a conducting tube immersed in a calorimeter at constant temperature. On differentiating (11.3) with respect to temperature,

$$\left(\frac{\partial C_p}{\partial P}\right)_T = -\mu\left(\frac{\partial C_p}{\partial T}\right)_P - C_p\left(\frac{\partial \mu}{\partial T}\right)_P, \tag{11.4}$$

a relation is obtained between heat capacity and pressure.

From (11.1) $\qquad P_1V_1+E_1 = P_2V_2+E_2,$

and hence $PV+E$ is a constant irrespective of whether the simple gas laws are valid or not; if the gas obeys Boyle's law and E is a function of temperature only, there will be no Joule-Thomson effect.

The Joule-Thomson Effect in relation to the more accurate Equations of State

A thermodynamic treatment of the porous-plug experiment gives the relation [2]

$$\frac{\partial T}{\partial p} = \frac{T(\partial v/\partial T)_p - v}{C_p}, \tag{11.5}$$

and for any equation of state

$$T\left(\frac{\partial v}{\partial T}\right)_p - v = 0 \tag{11.6}$$

completely determines the inversion point and is independent of the calorimetric properties of the fluid.

On dividing (11.6) by v,

$$\frac{1}{v}\left(\frac{\partial v}{\partial T}\right)_p = \frac{1}{T},$$

and hence the inversion point may be defined as the temperature at which the coefficient of expansion of the fluid at constant pressure is equal to the reciprocal of the absolute temperature.

If we now write van der Waals' equation in the form

$$v = \frac{RT}{p} - \frac{a}{pv} + \frac{ab}{(pv)^2} + b,$$

and substitute RT for pv,

$$v = \frac{RT}{p} - \frac{a}{RT} + \frac{abp}{R^2T^2} + b.$$

Then

$$\left(\frac{\partial v}{\partial T}\right)_p = \frac{R}{p} + \frac{a}{RT^2} - \frac{2abp}{R^2T^3},$$

and

$$T\left(\frac{\partial v}{\partial T}\right)_p - v = \frac{2a}{RT} - \frac{3abp}{R^2T^3} - b.$$

From (11.5),

$$\frac{\partial T}{\partial p} = \left(\frac{2a}{RT} - \frac{3abp}{R^2T^3} - b\right)\frac{1}{C_p}. \tag{11.7}$$

Eq. (11.7) shows that for large values of pressure the Joule-Thomson coefficient should decrease with increasing pressure and should become zero when

$$\frac{2a}{RT} - \frac{3abp}{R^2T^3} - b = 0. \tag{11.8}$$

This equation is a quadratic in T, and hence at each pressure there are two inversion temperatures and the pressure-inversion temperature curve is a parabola.

For rough calculations (11.7) may be simplified by omitting the term $-3abp/R^2T^3$, when

$$\frac{dT}{dp} = \frac{T_1 - T_2}{p_1 - p_2} = \left(\frac{2a}{RT} - b\right)\frac{1}{C_p}. \tag{11.9}$$

According to this equation the difference in temperature should be directly proportional to the difference in pressure, as indeed is found to be approximately true provided the pressure ranges are not too large. The value of temperature for the reversal effect T' is given by

$$\frac{2a}{RT'} = b \quad \text{or} \quad T' = \frac{2a}{Rb}. \tag{11.10}$$

In employing (11.9) care must be taken to use consistent units; thus, if a and b are expressed in cm.$^6 \times$ atmospheres and cm.^{3} respectively, C_p in terms of the volume of gas, and $R = 1/273$, then

$$\frac{T_1 - T_2}{p_1 - p_2} = \left(\frac{2a}{T/273} - b\right) \frac{1{\cdot}013 \times 10^6}{J} \times \frac{1}{\rho C_p},$$

where C_p is the heat capacity per gram of gas, ρ is the density, and J is the mechanical equivalent of heat in ergs.

An interesting relationship may be obtained by using van der Waals' equation in its reduced form [3]:

$$(p_r + 3/v_r^2)(3v_r - 1) = 8T_r. \tag{11.11}$$

On differentiating with respect to v_r,

$$\frac{-8T_r}{3v_r - 1} + \frac{6(3v_r - 1)}{v_r^2} = 0.$$

Eq. (11.6) in its reduced form becomes

$$T_r\left(\frac{\partial v_r}{\partial T_r}\right) - v_r = 0,$$

and the reduced inversion temperature is therefore given by

$$T_r = \frac{3(3v_r - 1)^2}{4v_r^2}. \tag{11.12}$$

On eliminating T_r between (11.11) and (11.12),

$$p_r = \frac{9(2v_r - 1)}{v_r^2}. \tag{11.13}$$

This equation connects the reduced pressure and volume which correspond to an inversion point. Employing (11.12), values of T_r may be calculated from a series of assumed values of v_r, and the corresponding values of p_r may be obtained from (11.13).

The curve obtained by plotting T_r against p_r is shown in Fig. 94.

It is parabolic in shape and indicates that for all pressures from zero to nine times the critical pressure there are two inversion temperatures which range from a little below the critical temperature to about 6·7 times its value; at pressures higher than nine times the critical value there is no inversion point and the maximum pressure which gives any inversion point is that for which the volume is the critical volume.

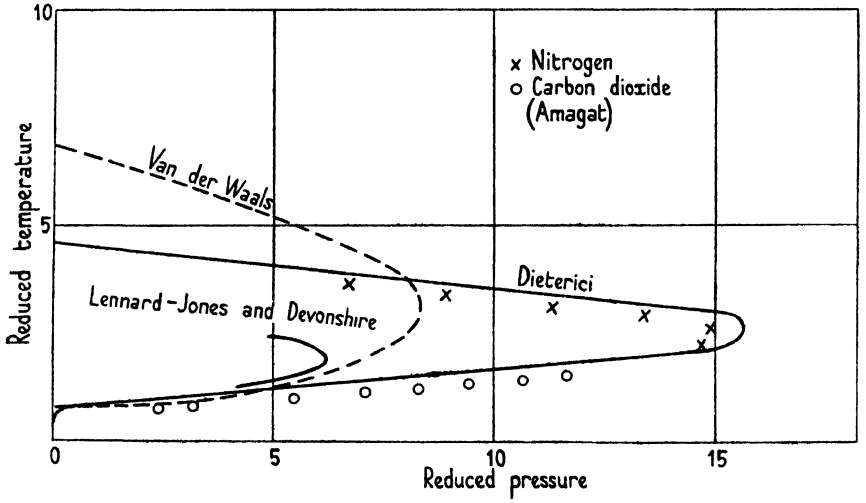

FIG. 94. Reduced inversion curves.

Dieterici's equation leads to the following relations between the reduced temperature volume and pressure of the inversion point:

$$T_r = \frac{4(2v_r - 1)}{v_r} \tag{11.14}$$

and

$$p_r = (8 - T_r)e^{(5T_r - 8)/2T_r}. \tag{11.15}$$

The curve obtained by plotting these values of p_r and T_r (see Fig. 94) is also parabolic but differs considerably from that derived from van der Waals' equation in its prediction of the upper pressure limit beyond which there is no inversion point, and of the value of the pairs of inversion points corresponding to lower pressures. The sensitiveness of the positions of these points to changes in the characteristic equation of the fluid makes a knowledge of their actual position, as determined experimentally, a valuable criterion of the validity of any proposed equation of state.

The Effect of Pressure on the Joule-Thomson Coefficient (μ) as predicted by the Beattie-Bridgeman Equation of State [4]

The Beattie-Bridgeman equation may be written in the form

$$p = \psi T - \phi - \Gamma/T^2, \tag{11.16}$$

where $\psi = \frac{R}{v^2}[v+b]$, $\phi = \frac{A}{v^2}$, and $\Gamma = \frac{\psi c}{v}$,

all three being functions of volume only. On differentiating (11.16) with respect to temperature at constant pressure,

$$\left(\frac{\partial v}{\partial T}\right)_p = \frac{\psi + 2\Gamma/T^3}{\psi' T - \phi' - \Gamma'/T^2},$$

where ψ', ϕ', and Γ' are the first derivatives with respect to volume.

Hence, from (11.5),

$$\mu C_p = T\left(\frac{\partial v}{\partial T}\right)_p - v = \frac{\psi T + 2\Gamma/T^2}{\psi' T - \phi' - \Gamma'/T^2} - v. \tag{11.17}$$

By substitution of the respective volume functions and rearrangement, (11.17) reduces at zero pressure to

$$\mu C_{p_0} = \frac{2A_0}{RT} - B_0 + \frac{4c}{T^3}. \tag{11.18}$$

From (11.16) and (11.18) values of μC_p can be calculated for a series of constant densities at various temperatures, and, provided the corresponding values of C_p are known, those of μ may be obtained directly.

Bridgeman (loc. cit.) computes C_p at high pressures from values of C_v and $C_p - C_v$; both these quantities are comparatively simple functions of v and T and may be obtained from the equation of state as follows:

$$\left(\frac{\partial C_v}{\partial v}\right)_T = T\left(\frac{\partial^2 p}{\partial T^2}\right)_v = -\frac{6\Gamma}{T^3};$$

$$\Delta C_v = C_v - C_{v_0} = -\frac{6}{T^3}\int_{\infty}^{v} \Gamma \, dv$$

$$= \frac{6Rc}{v^2 T^3}\left[v + \tfrac{1}{2}B_0 - \frac{1}{3}\frac{bB_0}{v}\right] \tag{11.19}$$

and

$$C_p - C_v = T\left(\frac{\partial v}{\partial T}\right)_p \left(\frac{\partial p}{\partial T}\right)_v = -\frac{T(\psi + 2\Gamma/T^3)^2}{\psi' T - \phi' - \Gamma'/T^2} = (\mu C_p + v)(\psi + 2\Gamma/T^3). \tag{11.20}$$

Hence $$C_p = C_{v_0} + \Delta C_v + [C_p - C_v]. \qquad (11.21)$$

The heat capacity of air at 1 atmosphere has been measured by Holborn and collaborators [5] over a wide range of temperatures and can be represented by the equation

$$C_p = 0{\cdot}2405 + 0{\cdot}000019t.$$

The C_p values are changed to C_v at zero pressure by means of (11.19) and (11.20), and the values so obtained are represented by the following equation which is valid over the range 0 to 300°:

$$C_{v_0} = 0{\cdot}1714 + 2{\cdot}3 \times 10^{-5}t - 1{\cdot}0 \times 10^{-8}t^2.$$

From the values of C_{v_0}, C_v, and $C_p - C_v$ the required values of C_p are obtained by means of (11.21).

The transformation of variables from density $(1/v)$ to pressure is effected by plotting μ along isotherms against the pressures corresponding to these densities, which are calculated by means of the equation of state. The results, summarized in Table 55, show that at all temperatures between 0 and 250° the value of μ diminishes with pressure up to 220 atmospheres.

TABLE 55. *The Variations of the Joule-Thomson Coefficient of Air with Pressure (Bridgeman)*

$\mu \times 10^3$ °C./atm.

Pressure, atms.	0°	50°	100°	200°	250°
1	266	189	133	63	40
20	249	178	124	56	35
100	178	128	89	35	16
180	113	83	58	19	3
220	81	63	45	13	−2

The inversion curve calculated from the equation of state is shown in Fig. 94A. The corresponding curves predicted by the van der Waals and Dieterici equations and that drawn through points calculated from compressibility data are also included for comparison.

The Joule-Thomson Coefficient calculated from the Keyes Equation of State

From (10.17) $$C_p = C_v + T\left(\frac{\partial v}{\partial T}\right)_p \left(\frac{\partial p}{\partial T}\right)_v.$$

On applying the Keyes equation to compute the second term on the right-hand side of this equation we obtain

$$\left(\frac{\partial p}{\partial T}\right)_v = \frac{R}{v-\delta} \quad \text{and} \quad \left(\frac{\partial v}{\partial T}\right)_p = \frac{v-\delta}{T} \times \frac{1}{1-\frac{\alpha\delta}{v^2}-\frac{2A}{RT}\frac{(v-\delta)^2}{(v-l)^3}};$$

and on substituting in (11.5),

$$\mu = \frac{\frac{2A}{RT}\frac{(v-\delta)^2}{(v-l)^3}-\delta\left(1-\frac{\alpha}{v}\right)}{C_v\left(1-\frac{\alpha\delta}{v^2}-\frac{2A}{RT}\frac{(v-\delta)^2}{(v-l)^3}\right)+R}. \tag{11.22}$$

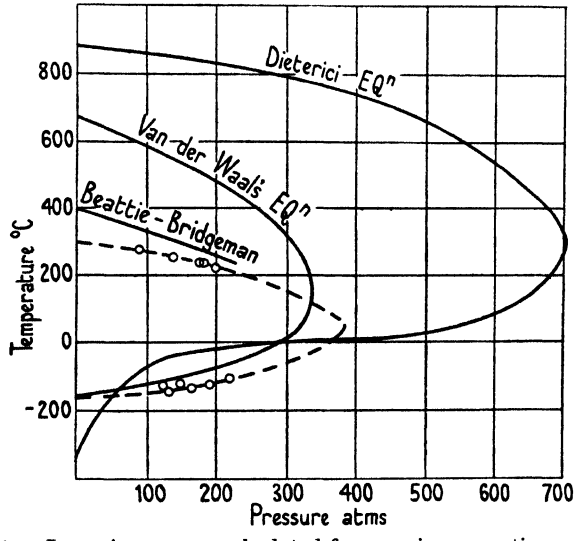

FIG. 94 A. Inversion curves calculated from various equations of state.

The Relation between the Joule-Thomson Coefficient and the Virial Coefficients

Since both the Joule-Thomson and the virial coefficients are measures of the molecular forces of attraction and repulsion a simple relation must exist between them [6].

Thus, from (11.2) and (11.3), it follows that

$$\mu = T^2[(\partial/\partial T)(V/T)]_p/C_p. \tag{11.23}$$

Both the numerator and denominator of this equation may be expressed in terms of the virial coefficients, which are here defined by the series equation

$$pV = RT(1+Bp+Cp^2+Dp^3+\ldots), \tag{11.24}$$

where p is the pressure in atmospheres, V is the molal volume in cubic centimetres, and R is the gas constant per mol (i.e. $R = 82{\cdot}07$).

From (10.71)
$$\left(\frac{\partial F}{\partial p}\right)_T = V, \tag{11.25}$$

and on integrating, using (11.24),

$$F = F^0 + RT\log p + RTBp + \tfrac{1}{2}RTCp^2 + \tfrac{1}{3}RTDp^3 + \ldots, \tag{11.26}$$

where F^0 is the constant of integration and is the value of F at zero pressure.

But since $C_p = -T(\partial^2 F/\partial T^2)_p$, it follows from (11.26) that

$$C_p = C_p^0 - RT\left[p\frac{d^2(BT)}{dT^2} + \tfrac{1}{2}p^2\frac{d^2(CT)}{dT^2} + \tfrac{1}{3}p^3\frac{d^2(DT)}{dT^2} + \ldots\right], \tag{11.27}$$

where C_p^0 is the specific heat at zero pressure.

The numerator of (11.23) is readily obtained from (11.24), so that, substituting in (11.23), we get the Joule-Thomson coefficient in terms of the virial coefficients, thus:

$$\mu = \frac{RT^2[dB/dT + p\,dC/dT + p^2\,dD/dT + \ldots]}{C_p^0 - RT\left[p\frac{d^2(BT)}{dT^2} + \tfrac{1}{2}p^2\frac{d^2(CT)}{dT^2} + \tfrac{1}{3}p^3\frac{d^2(DT)}{dT^2} + \ldots\right]}. \tag{11.28}$$

The right-hand side of (11.28) may be expanded in a Maclaurin series in powers of p, and hence

$$\mu = \mu_0 + p(\partial\mu/\partial p)_T^0 + \tfrac{1}{2}p^2(\partial^2\mu/\partial p^2)_T^0 + \ldots, \tag{11.29}$$

where μ_0 is the Joule-Thomson coefficient extrapolated to zero pressure. Here

$$\mu_0 = \frac{R}{C_p^0}T^2\frac{dB}{dT}, \tag{11.30}$$

$$\left(\frac{\partial\mu}{\partial p}\right)_T^0 = \frac{RT}{C_p^0}\left[T\frac{dC}{dT} + \mu_0\frac{d^2(BT)}{dT^2}\right], \tag{11.31}$$

and
$$\left(\frac{\partial^2\mu}{\partial p^2}\right)_T^0 = \frac{RT}{C_p^0}\left[2T\frac{dD}{dT} + \mu_0\frac{d^2(CT)}{dT^2} + 2\left(\frac{\partial\mu}{\partial p}\right)_T^0\frac{d^2(BT)}{dT^2}\right]. \tag{11.32}$$

Eq. (11.30) enables us to determine the second virial coefficient regardless of the magnitude of the remaining coefficients.

The Joule-Thomson Coefficient from Compressibility Data

From (11.5)
$$\mu\rho C_p = \frac{T}{v}\left(\frac{\partial v}{\partial T}\right)_p - 1, \tag{11.33}$$
and μ may be calculated from the values of $(\partial v/\partial T)_p$ obtained as described in Chapter X.

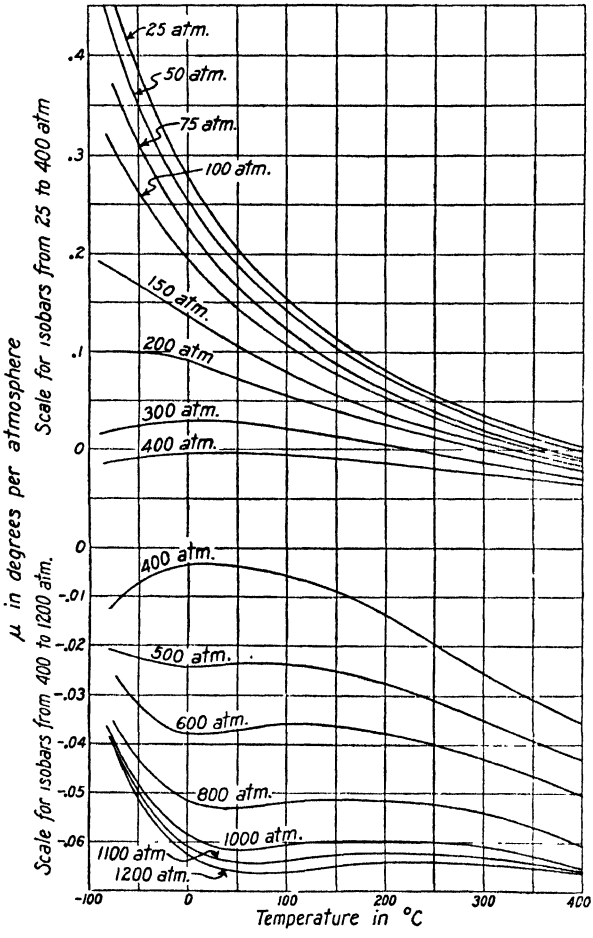

FIG. 95. (μ, t) isobars for carbon monoxide.

The (μ, t) isobars for carbon monoxide calculated from Bartlett and collaborators compressibility data are shown in Fig. 95 [7]. It will be observed that the isobars above about 300 atmospheres pass through a maximum above 0°, and at pressures higher than 390 atmospheres there is, as predicted by the various equations of state, no inversion temperature.

Experimental Determinations of the Joule-Thomson Coefficient (μ) at High Pressures

The Joule-Thomson coefficient provides data from which the enthalpy-temperature-entropy diagram of a gas may be constructed and accurate experimental values over a wide range of pressures and temperatures are, therefore, of great utility.

Roebuck's Experiments with Air, Nitrogen, Helium, and Argon. The procedure adopted by Roebuck and his collaborators [8], who have carried out a number of such measurements, is to allow the gas to expand from a known pressure and temperature through a porous partition successively to a series of lower pressures, and to measure each resulting pressure drop. Since the operation may be made substantially adiabatic, the only exchange of energy possible is through the pv relations, so that

$$E+pv = \text{a constant} = H.$$

Their apparatus is shown diagrammatically in Fig. 96. The compressed gas enters the apparatus at C, passes through the coils BB where it attains the temperature of the thermostat, and thence into the pressure vessel E which houses the diaphragm D. In order to prevent convection the space between the diaphragm and the walls of the pressure vessel is packed with cotton wool or asbestos fibre. The diaphragm† is made of porous porcelain and takes the form of an inverted thimble, $7\frac{1}{2}$ inches long and $1\frac{1}{2}$ inches outside diameter. The gas passing through the diaphragm leaves the apparatus by way of the valve E. Temperatures are measured at T_1 and T_2 by means of platinum resistance thermometers and the difference of pressure across the diaphragm by means of a free-piston gauge.

The method of carrying out an experiment is briefly as follows: With the whole apparatus assembled, the temperature is quickly raised to the desired value and the gas compression is started. By operating the valve V the gas flow is regulated, and, when conditions are steady, the pressure and temperature of the gas on the high-pressure side of the diaphragm, the values of ΔP and ΔT, and the rate of gas flow are noted. The lower pressure is then changed by operating the outlet valve and another series of readings taken. For details of the various precautions necessary to obtain concordant results the reader should consult the original papers.

The errors inherent in the method arise mainly from temperature variations due to heat conducted by the apparatus and gas. Generally speaking, the temperature inside the diaphragm is lower than that outside and the direction of heat flow and gas flow are therefore alike. Since the drop in pressure is accompanied by a proportionate

† For a full discussion of the design of diaphragms see Burnett and Roebuck, *Phys. Rev.* **30**, 529 (1910).

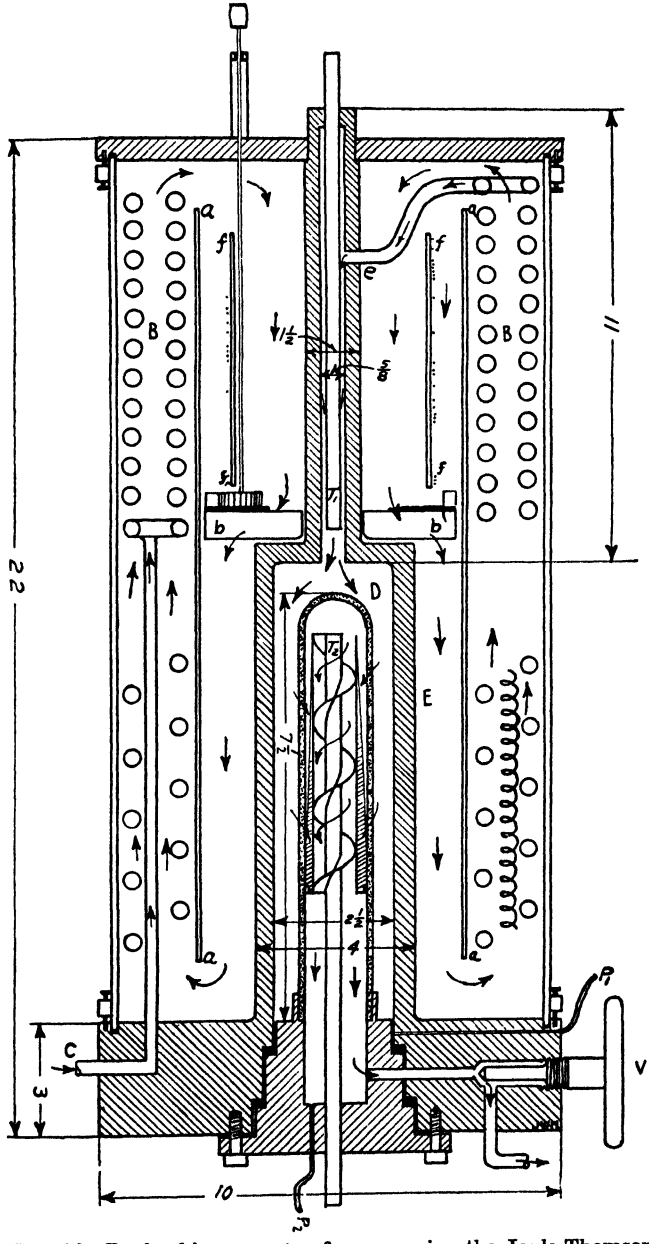

FIG. 96. Roebuck's apparatus for measuring the Joule-Thomson coefficient at high pressure.

increase in volume, and the same amount of air must pass every cross-section of the flow, it follows that the major part of the pressure drop occurs near the inner surface of the diaphragm wall. If the diaphragm and gas were both non-conductors, the temperature distribution could be determined from the properties of the gas, and the temperature gradient would be much greater near the inner surface. The effect of conductivity of the solid and gas is to move heat forward in the direction of flow, and the oncoming gas then drops in temperature faster than called for by its expansion; that is, the condition favours the leakage of heat in the region.

In the case of hydrogen and helium the temperature rises with the fall of pressure through the diaphragm walls. The temperature gradient hence requires that heat should flow against the gas stream, which is the condition for the most perfect exclusion of heat leaks.

The possibility must also be borne in mind of the existence of a temperature effect due to turbulence set up as the gas passes through the diaphragm and persisting for some little time afterwards. Experiment shows, however, that with carefully constructed diaphragms, the temperature drop is independent of the time taken for the gas to pass from the diaphragm to the thermometer and hence the error arising from this cause is probably negligibly small.

The most serious error of the method is due to heat leaks to the gas between the thermometers; its magnitude is determined by the temperature drop across the diaphragm and, for a given value of ΔT, the effect on the observed ΔT will be inversely proportional to the heat capacity in the passing gas; for a sufficiently high rate of flow the effect on ΔT may be negligible, but at low rates it may, if precautions are not taken, amount to as much as 3 or 4 per cent. A fundamental condition of accuracy is the independence of ΔT on the rate of flow.

Three typical series of observations for nitrogen are given in Table 56.

The maximum observed drop in temperature across the plug was 87° C., and the maximum value of μ, 2·32° C./atmosphere.

By plotting these values of pressure and temperature a series of isenthalpic curves is obtained (Fig. 97), the tangents to which, $(\Delta T/\Delta p)_H$, give the values of the Joule-Thomson coefficient. In the figure the curves above and below 0° C. are plotted to different scales to accommodate them on the same diagram.

TABLE 56. *Corresponding Values of Pressure and Temperature for Nitrogen traversing a Porous Diaphragm (Roebuck and Osterberg)* [9]

50° C.		−120° C.		−151° C.	
Pressure, atms.	*Temperature, °C.*	*Pressure, atms.*	*Temperature, °C.*	*Pressure, atms.*	*Temperature, °C.*
2·7	24·04	0·6	−198·24	15·2	−163·17
19·0	27·36	1·2	−193·49	21·1	−157·21
42·8	31·76	12·4	−166·50	25·9	−153·82
65·5	35·57	20·4	−157·67	32·2	−153·24
89·7	38·96	25·2	−153·52	44·5	−152·07
111·1	41·46	31·8	−148·78	68·0	−150·74
135·0	44·27	43·1	−141·86	91·3	−149·97
157·9	46·33	55·1	−136·89	114·3	−149·54
201·6†	49·78‡	78·7	−130·07	136·3	−149·52
..	..	104·3	−125·99	201·6†	−150·61‡
..	..	201·8†	−120·25‡	..	..

† Initial pressure. ‡ Temperature of bath.

It will be observed that the slopes of the isenthalps diminish with rising temperature and approach linearity at about 250° C. The saturated vapour pressure of pure nitrogen is shown by the heavy curve terminating at the critical point (33·49 atms., −147·13° C.). The situation of the various isenthalps with respect to this curve is of considerable interest. Theory requires that the isenthalp through the critical point (approximately the −120° C. isenthalp) should be tangential to the saturated vapour curve at that point. A number of isenthalps approach the upper part of the curve, meeting it at small and decreasing angles until finally a particular isenthalp grazes it at a point which corresponds to that of the maximum total heat of dry saturated vapour. The observed values of temperature and pressure below the point of intersection are at first distributed along, or very close to, the saturated vapour curve; but eventually they diverge from it, as shown, for example, by the −97° C. isenthalp.

The relations between the isenthalps and the saturated vapour curve in the neighbourhood of the critical point have been discussed by Worthing, Davis, and Burnett [10]. If the expansion of nitrogen starts from an initially superheated condition at a point sufficiently close to the upper part of the vapour curve, a part of the vapour will condense and the expanded pressure and temperature will correspond with those of equilibrium between the coexisting liquid and vapour phases. If, however, the expansion be continued sufficiently far, the condensation will gradually decrease, re-evaporation of the

liquid will take place, and eventually, at some low pressure, the isenthalp will emerge from the vapour curve.

The isenthalps of liquid nitrogen approach the saturated vapour curve with reduction of pressure, and, at the point of contact, change

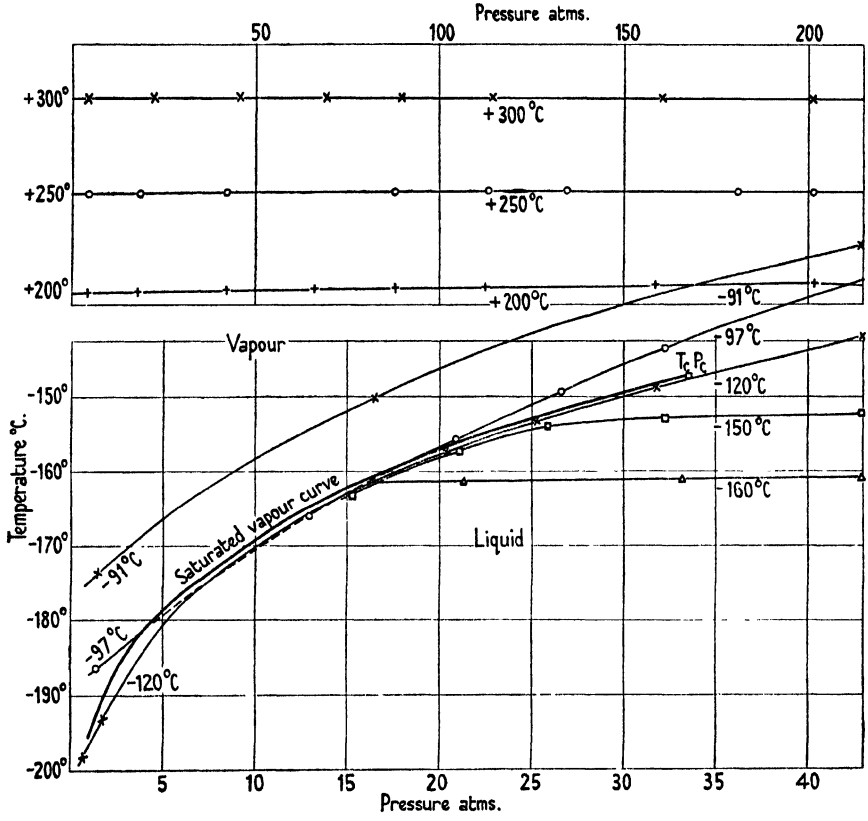

FIG. 97. Isenthalpic curves of nitrogen.

abruptly in direction so as to follow it to lower pressures. Actually the experimental points are found to lie a little below the curve, an effect which might result from some impurity having a lower critical temperature than nitrogen. A similar observation has been made by Roebuck with air and argon, and by Burnett with carbon dioxide.†

† The nitrogen contained 0·13 per cent. of argon and 0·1 to 0·2 per cent. of oxygen; the carbon dioxide employed by Burnett contained 0·025 per cent. of carbon monoxide, 0·25 to 1·5 per cent. of air, and a trace of hydrogen.

The numerical values of the Joule-Thomson coefficient are obtained with sufficient accuracy by taking the ratio of successive and corresponding differences of temperature and pressure for each experi-

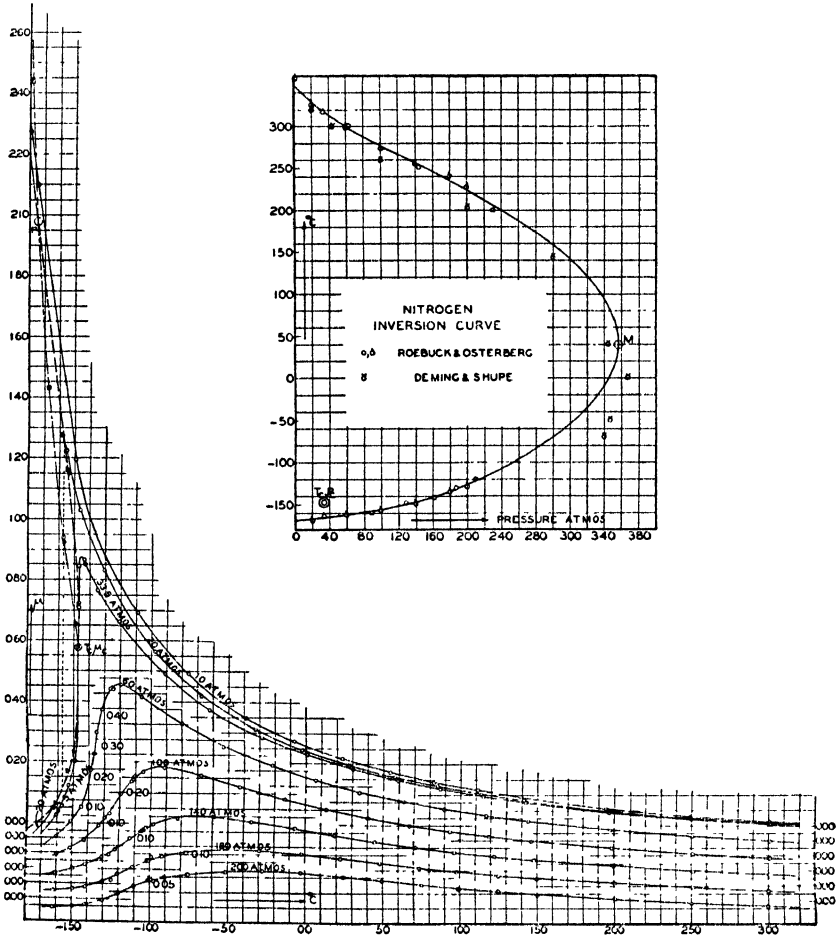

FIG. 98. The Joule-Thomson coefficient as a function of temperature. *Inset*: The inversion curve of nitrogen.

mental run. The variation of the coefficient with temperature over a wide range of pressure is shown by the series of isobaric curves in Fig. 98, which relate to nitrogen. In the figure the ordinate scale (marked on each isobar) has been shifted so as to separate the curves. It will be observed that as the temperature is lowered the coefficient at first increases rapidly, especially at the lower pressures, reaches

a maximum at a temperature somewhat higher than the critical temperature, and thereafter diminishes. As the pressure is lowered the peaks become increasingly sharp until just below the critical pressure the curve fails to turn downwards and becomes discontinuous.

The Inversion Curve ($\mu = 0$) *for Nitrogen.* The data for plotting the inversion curve are obtained from the points of zero slope of the isenthalps in Fig. 97 or from the isobars in Fig. 98, and are given below:

Data for the Inversion Curve of Nitrogen ($\mu = 0$)

Pressure, atms.	*Temperature, °C.*	
	Upper curve	*Lower curve*
1	348·0	..
20	330·0	−167·0
60	299·6	−162·4
100	277·2	−156·5
140	256·5	−148·0
180	235·0	−134·7
220	212·5	−117·2
260	187·0	−96·4
300	158·7	−68·7
340	121·3	−35·3
360	93·7	−10·0
376	40·0	+40·0

The curve plotted from these data, together with that derived by Deming and Shupe from compressibility measurements, is shown inset in Fig. 98. Generally speaking, the agreement between the two sets of data is as good as can be expected and is an example of the value of (P, V, T) data in studying the effect of pressure upon the thermodynamic properties of a fluid.

Roebuck and Osterberg have determined the values of μ for helium over the temperature range −190° to 300° C. and from 1 to 200 atmospheres pressure. In this range μ is negative and is independent of pressure except at the lowest temperature; between 0° and 200° C. it undergoes no very marked change, but at both lower and higher temperatures it diminishes rapidly; the inversion temperature is about 23·6° K.

Data for air, nitrogen, argon, and helium will be found in Appendix 2.

Burnett's Determination of the Joule-Thomson Coefficient of Carbon Dioxide. Burnett, employing the same method as Roebuck, has carried out an extensive series of measurements of the Joule-Thomson

coefficient of carbon dioxide in both the vapour and the liquid phase; the results obtained are of particular interest as showing the variations of the coefficient in the regions adjacent to the triple point and the critical point.

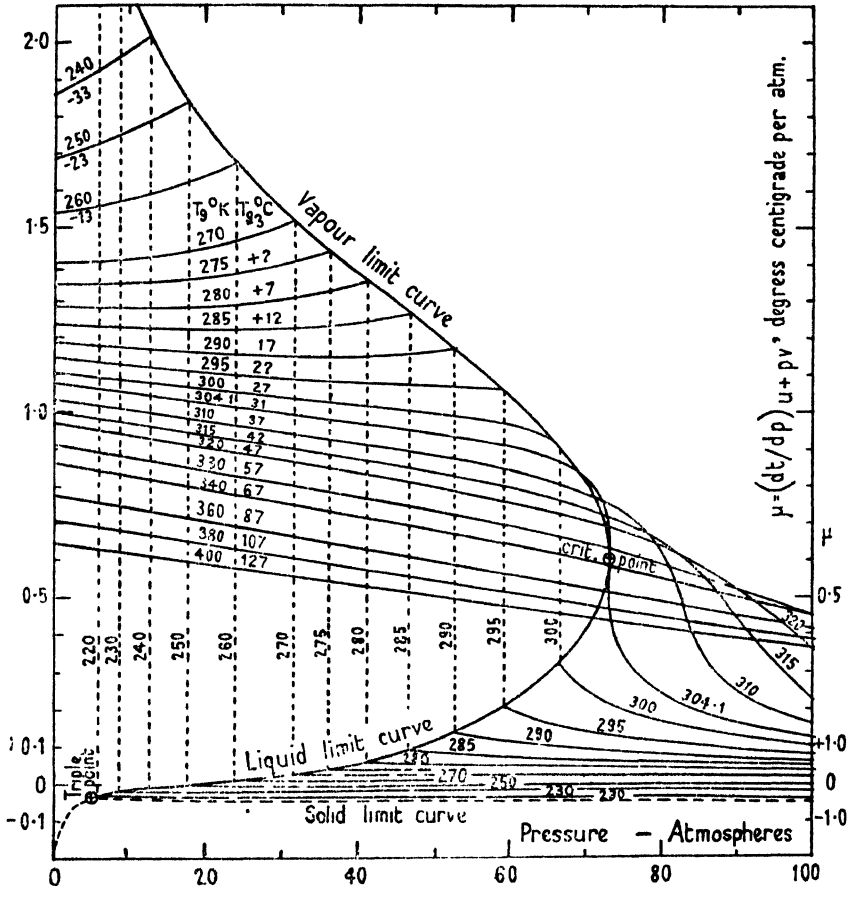

FIG. 99. The Joule-Thomson coefficient as a function of pressure.

In Fig. 99 the values of μ are plotted as an isothermal function of pressure. The curves above the critical temperature (31·1° C.) resemble those of air, argon, and nitrogen; as critical conditions are approached there is an increase in curvature corresponding with a sudden fall in the value of μ in the neighbourhood of the critical pressure (73 atmospheres). Below the critical temperature there is a definite discontinuity marking the difference between the vapour

and liquid phases. In the liquid region at $-24°$ C. μ becomes zero at all pressures above about 10 atmospheres, the isenthalp being a horizontal straight line. The lower part of the diagram is bounded by the solid limit curve terminating at the triple point.

Burnett has endeavoured to express by means of a series of empirical equations the entire experimental field for both phases, but the resulting equations are cumbersome and their field of utility is limited.

In Table 57 the isothermal and isobaric values of μ derived from the experimental data of Burnett and Jenkin and Pye [11] are recorded.

TABLE 57. *Isothermal and Isobaric Values of μ for Carbon Dioxide expressed in deg. C. per atmosphere*

Vapour phase above line; liquid phase below line.

Temp., °C.	*Pressure in atmospheres*								
	0	1	10	20	40	60	72·9	80	100
126·9	0·6475	0·6440	0·6210	0·5950	0·5375	0·4790	0·4410	0·4225	0·3635
116·9	0·6755	0·6725	0·6485	0·6200	0·5595	0·4965	0·4560	0·3850	0·3235
106·9	0·7080	0·7045	0·6780	0·6475	0·5837	0·5165	0·4742	0·4505	0·3855
96·9	0·7415	0·7335	0·7100	0·6775	0·6160	0·5405	0 4952	0·4705	0·3995
86·9	0·7790	0·7750	0·7455	0·7110	0·6420	0·5685	0·5200	0·4930	0·4155
76·9	0·8195	0·8150	0·7850	0·7500	0·6780	0·6020	0·5500	0·5210	0·4340
66·9	0·8640	0·8595	0·8290	0·7950	0·7205	0·5425	0·5872	0·5550	0·4500
56·9	0·9140	0·9095	0·8795	0·8450	0·7720	0·6925	0·6331	0·5945	0·4490
46·9	0·9710	0·9665	0·9380	0·9050	0·8360	0·7570	0·6900	0·6380	0·3570
36·9	1·0360	1·0320	1·0055	0·9765	0·9160	0·8435	0·7554	0·6100	0·1585
31·9	1·0710	1·0675	1·0445	1·0155	0·9640	0·9000	0·7468	0·2690	0·1270
31·0	1·0775	1·0740	1·0505	1·0240	0·9735	0·9100	0·6050	0·2420	0·1215
26·9	1·1070	1·1045	1·0840	1·0600	1·0175	0·9675	0·2147	0·1650	0·1005
21·9	1·1480	1·1455	1·1270	1·1090	1·0805	0·1990	0·1324	0·1134	0·0794
16·9	1·1920	1·1900	1·1750	1·1635	1·1525	0·1156	0·0999	0·0815	0·0619
11·9	1·2395	1·2385	1·2280	1·2245	1·2400	0·0761	0·06355	0·0586	0·0478
6·9	1·2900	1·2900	1·2845	1·2915	1·3470	0·0515	0·0454	0·0425	0·0364
1·9	1·3455	1·3455	1·3470	1·3645	0·0414	0·0355	0·0324	0·0309	0·0275
−3·1	1·4050	1·4060	1·4155	1·4455	0·0274	0·0246	0·0228	0·0221	0·0202
−13·1	1·5375	1·5405	1·5735	1·6375	0·0106	0·0101	0·00973	0·0096	0·0090
−23·1	1·6885	1·6954	1·7570	$0·0_3735$	$0·0_3733$	$0·0_3731$	$0·0_3730$	$0·0_3729$	$0·0_3727$
−33·1	1·860	1·870	1·974	−0·00723	−0·00742	−0·00761	−0·00774	−0·00781	−0·00801
−43·1	2·060	2·070	−0·0168	−0·0171	−0·0177	−0·0183	−0·0187	−0·0190	−0·0195
−53·1	2·2855	2·3035	−0·0294	−0·0304	−0·0323	−0·0341	−0·0353	−0·0359	−0·0375

Determination of the Isothermal Expansion Coefficient of a Gas at High Pressures

Whilst a knowledge of the Joule-Thomson coefficient enables the enthalpy and entropy diagrams of a gas to be drawn, its evaluation requires comparatively large quantities of gas at high pressures, and

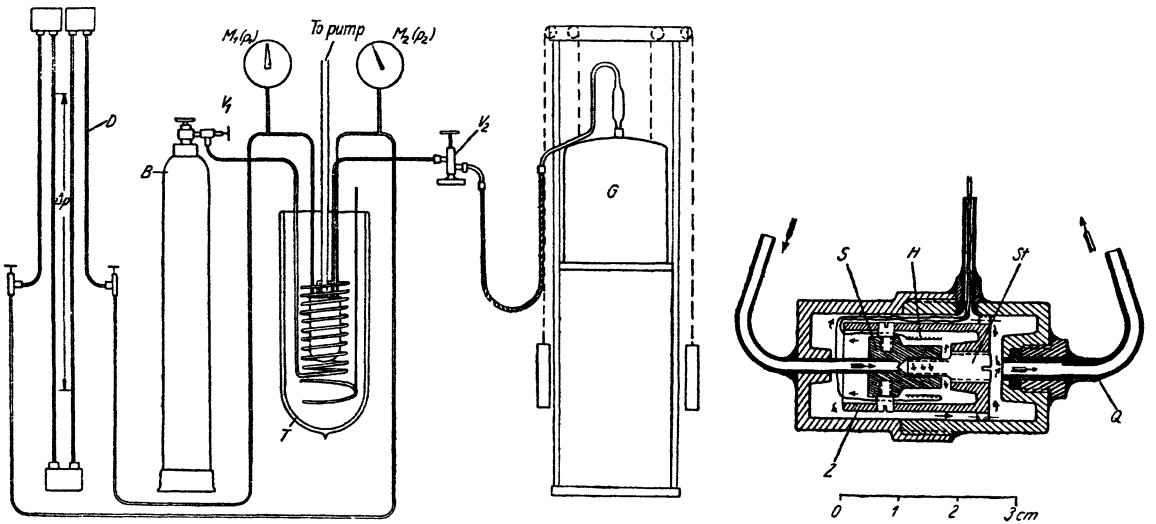

FIG. 100. Eucken's apparatus for measuring the isothermal expansion coefficient of a gas.
Inset: Details of the throttle valve.

the necessary apparatus is rather cumbersome. Eucken, Clusius, and Berger [12] have, therefore, suggested an alternative by which the isothermal expansion coefficient $(\partial H/\partial p)_T$ is measured over a range of pressures and temperatures. The method is, of course, applicable only to regions in which the coefficient is negative, but the apparatus is comparatively simple and compact and the quantity of gas required for a determination is small. Furthermore, with the same apparatus measurements may be made in the critical region and the latent heat of evaporation determined. A minor disadvantage is that three experimental values must be quantitatively determined, namely, a pressure difference, a quantity of heat, and a velocity of flow, whereas in the Joule-Thomson method only a pressure and a temperature difference need be measured.

The apparatus is shown in section in Fig. 100 with (inset) a diagram of the adjustable throttle valve. The gas flows from a storage cylinder B through the needle valve V_1 and a spiral coil contained in the thermostat T. From the coil it enters the throttle valve which is enclosed in a highly evacuated jacket. Connexions from the two sides of the valve lead to gauges M_1 and M_2 for indicating the pressures p_1 and p_2, and to a mercury differential gauge D for determining the pressure difference Δp. The gas passes from the throttle valve, through a second needle valve V_2, to a calibrated gasometer G of about 275 litres capacity.

The accuracy of the determination depends largely upon the careful design and construction of the throttle valve. The details of the valve are shown in the diagram. The spindle St is made of steel and seats on the brass plug S. The heating wires are mounted on a mica cylinder placed in the stream of expanded gas so that heat is communicated directly to the gas without loss. The remaining parts of the valve are constructed of copper and the whole is totally enclosed so as to avoid the use of non-metallic packing. The inlet and outlet temperatures are measured by eightfold copper-constantan thermopiles, a number of thermocouples also being included in the system for checking purposes.

Employing this apparatus and method Eucken and Berger [13] have determined $(\partial H/\partial p)_T$ for methane up to 60 atmospheres and have constructed the (H, T) diagram reproduced in Fig. 101; Gusak [14] has also employed it for extending the enthalpy diagram of nitrogen from 60 to 200 atmospheres. These diagrams and the method of using them will be discussed in Chapters XII and XV.

Collins and Keyes [15] have modified the method in such a way that heat is supplied to the fluid during the course of the pressure drop through a fine capillary, which is partially plugged by the heating element.

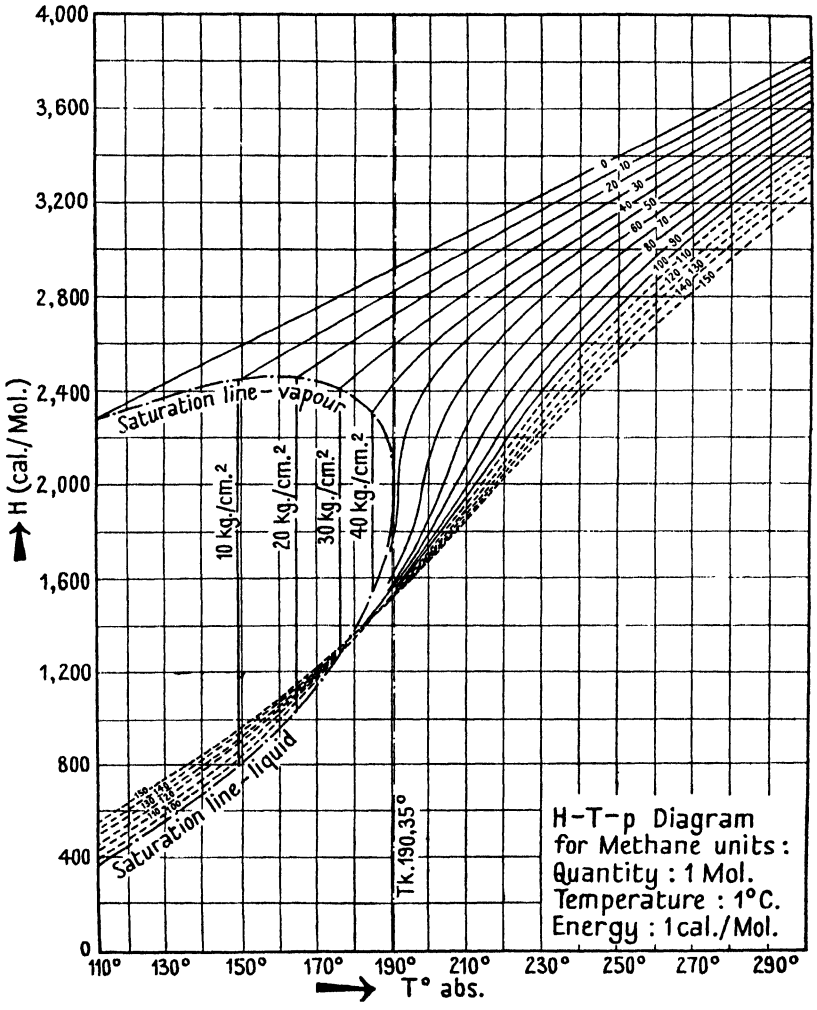

FIG. 101. The enthalpy-temperature diagram of methane.

REFERENCES

1. JOULE and THOMSON, *Proc. Roy. Soc.* **143**, 357 (1853).
2. JELLINEK, *Lehrbuch der physikalischen Chemie*, **1** (1914).
3. PORTER, *Phil. Mag.* [6], **11**, 554 (1906); **19**, 888 (1910).
4. BRIDGEMAN, *Phys. Rev.* **34**, 527 (1929).
5. HOLBORN and collaborators, *Wiss. Abh.* **4**, 131 (1905); *Ann. d. Phys.* **18**, 739 (1905); **23**, 810 (1907).
6. HIRSCHFELDER, EWELL, and ROEBUCK, *J. Chem. Phys.* **6**, 205 (1938).
7. DEMING and SHUPE, *Phys. Rev.* **34**, 527 (1929).

8. ROEBUCK, *Proc. Am. Acad. Arts and Sci.* **60**, 537 (1925).
9. ROEBUCK and OSTERBERG, *Phys. Rev.* **48**, 450 (1935).
10. WORTHING, *Phys. Rev.* **33**, 256 (1911); DAVIS, *Proc. Am. Acad. Arts and Sci.* **45**, 241 (1910); BURNETT, *Phys. Rev.* [2], **22**, 590 (1923).
11. JENKIN and PYE, *Phil. Trans.* (A), **213**, 67 (1914); **215**, 353 (1915).
12. EUCKEN, CLUSIUS, and BERGER, *Zeit. f. tech. Phys.* **13**, 267 (1932); **15**, 1 (1934).
13. EUCKEN and BERGER, *Zeit. fur Kälte-Ind.* **9**, 145 (1934).
14. GUSAK, *Phys. Zeit. Soujet.* **11**, 60 (1937).
15. COLLINS and KEYES, *J. Phys. Chem.* **43**, 5 (1939).

XII

THE COEXISTING LIQUID AND VAPOUR PHASES OF BINARY AND TERNARY MIXTURES

THE behaviour of gaseous mixtures in the neighbourhood of their critical temperatures and pressures presents phenomena of considerable theoretical and practical interest and has formed the subject of a number of important researches. The changes concerned are usually associated with a two-phase system in which two or more liquids are in contact with their vapours under conditions such that evaporation or condensation is taking place, the experimental arrangements being such that each phase is substantially homogeneous.

It will be recalled that the vapour pressure, boiling-point, and composition of the vapour from two or more non-miscible liquids are independent of the relative proportions of the components, provided they are all present in sufficient quantity, and that evaporation can take place freely. The vapour pressure of such a mixture is the sum of the vapour pressures of its components when heated separately to the same temperature, and the boiling-point is that temperature at which the sum of the vapour pressures of the components is equal to the atmospheric pressure.

In the case of liquids which are miscible in all proportions the state of affairs is more complex. For binary mixtures of closely related liquids the composition of the vapour is given, approximately, by the relation

$$M'_a/M'_b = C \times M_a/M_b,$$

where M' and M are the quantities of vapour and liquid respectively, and C is a constant which may be identified with the ratio of the vapour pressures of the two liquids at the boiling-point of the mixture. If such a mixture be distilled at constant pressure, the boiling-point will rise progressively until one component only is left, or if the distillation be at constant temperature, the vapour pressure will fall until it reaches that of the less volatile component.

For binary mixtures which are not closely related, the above expression does not hold; and account must be taken of the shape of the boiling-point–composition curves, which may have a maximum

or minimum (*a* or *b*, Fig. 102) or may increase progressively with increase in the proportion of one of the constituents (*c* or *d*).

In the case of a mixture whose boiling-point–composition curves have the characteristics of curves *a* or *b* there will be mixtures of maximum or minimum boiling-point which will distil unchanged like a pure liquid at constant temperature, and complete separation of the components of the mixture by simple distillation cannot be effected. With curves having the characteristics of *c* and *d* there is no constant boiling-point mixture, and by fractional distillation a separation of one of the constituents is usually possible.

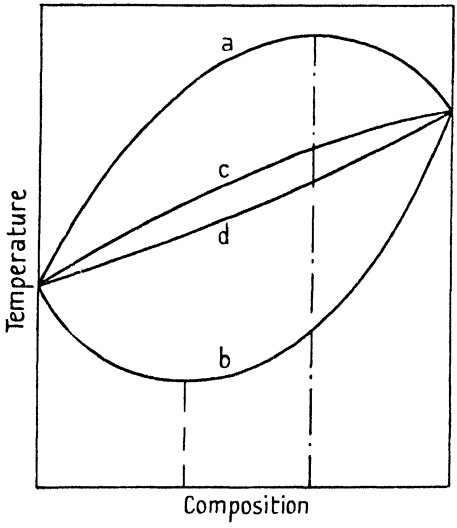

FIG. 102. Boiling-point–composition curves of binary mixtures.

Now consider two miscible liquids whose vapour-pressure curves are represented by the two curves 1 and 10 (Fig. 103), the terminal points C_1 and C_2 denoting their respective critical points. For a mixture of the two liquids the vapour-pressure curve will take the form of a loop such as $XPRY$ enclosing an area in which both liquid and vapour are present in equilibrium, and there will be one such curve, known as a border curve, for every mixture. This group of curves may, in general, be enclosed within an area bounded by the vapour-pressure curves of the two pure liquids and a third curve, $C_1 WC_2$, known as the plait-point curve, tangential to the border curves. The temperature T_c defined by the point of contact P between a border curve and the plait-point curve is known as the plait point or the critical temperature of the mixture. A second temperature T_r characteristic of the mixture is that defined by the isothermal line tangential to the border curve at R, and known as the critical point of contact, the critical condensation temperature, or the cricondentherm.

At temperatures above T_r the mixture behaves like a pure substance above its critical point; below T_p vaporization and condensa-

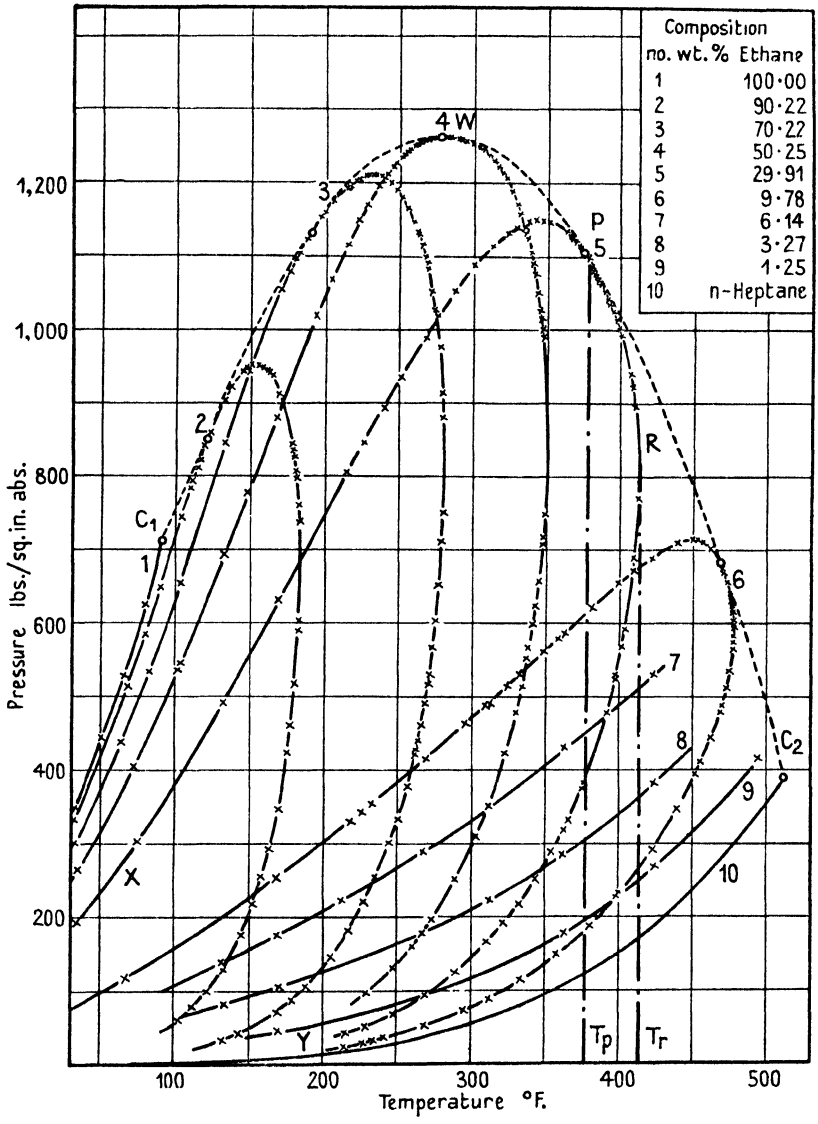

FIG. 103. Vapour pressure and boundary curves and the plait-point curve of ethane–*n*-heptane mixtures.

tion take place in the ordinary manner. At intermediate temperatures an interesting change, first observed by Andrews and later by Cailletet [1], takes place.

According to Cailletet:

'Lorsqu'on enferme dans l'appareil qui m'a servi à la liquéfaction des gaz (*Ann. de Chim. et de Phys.*, 5e série, t. XV, p. 132) un mélange d'air et d'acide carbonique, on remarque, ainsi que M. Andrews et plusieurs autres savants l'avaient déjà observé, que la liquéfaction de l'acide carbonique subit un retard souvent très grand ; il est même possible de comprimer à zéro jusqu'au delà de 400 atm. 1 vol. d'air et 1 vol. d'acide carbonique mélangés sans obtenir de changement d'aspect dans le tube.

'En comprimant dans l'appareil 5 vol. d'acide carbonique et 1 vol. d'air l'acide carbonique se liquéfie facilement. Si l'on porte alors la pression jusqu'à 150 atm. ou 200 atm., le ménisque de l'acide liquéfié, qui jusque-là était concave et d'une netteté parfaite, devient plan, perd sa netteté, puis s'efface progressivement ; enfin le liquide disparaît entièrement. Le tube paraît lors rempli d'une matière homogène qui, désormais, résiste à toute pression, comme le ferait un liquide.

'Si maintenant on diminue la pression avec lenteur, on observe qu'à une pression constante pour des températures déterminées le liquide reparaît subitement ; il se produit un brouillard épais qui se développe, s'évanouit en un instant, et marque le niveau du liquide qui vient de reparaître.'

Referring again to Fig. 103, the phenomenon described by Cailletet, and now known as retrograde condensation, is seen to be associated with a change in direction of the boundary curve between the two temperatures T_p and T_r; thus, for example, on increasing the pressure of a 29·91 per cent. ethane mixture along the 400° isothermal line, condensation will begin at the point of intersection of the isothermal with the boundary curve and the liquid phase will first increase in amount with further rise of pressure to a maximum, and will then diminish and finally disappear at the second point of intersection.

Kuenen [2], Caubet [3], and others have examined a large number of binary liquid mixtures and find that retrograde condensation may be observed in nearly all cases. Kuenen has also drawn attention to a second kind of retrograde condensation which will occur when the plait-point curve is tangential to the border-line curve in such a position that the point P corresponds to a lower pressure than the point R. Referring to Fig. 104, in which such a condition is represented, the process of condensation between T_p and T_r differs from that described above in that by compression a vapour phase appears which reaches a maximum and then diminishes and disappears. Near the plait-point temperature the liquid surface is very flat and indistinct, whilst below T_p the condensation is normal.

The realization of retrograde condensation of the second kind depends upon whether the plait-point curve or a part of it rises

whilst the border curves are situated on its left side. This may occur (*a*) if the critical points of some of the mixtures be outside the critical temperatures of the two pure components, or (*b*) if the substance having the higher critical temperature has at the same time higher vapour pressure than the substance of lower critical temperature.

There are only a few pairs of substances that comply with these conditions; substances of low critical temperatures mostly have high critical pressures and high vapour pressures. When this is not the case the differences are often too small to exhibit the phenomenon in a distinctive way.

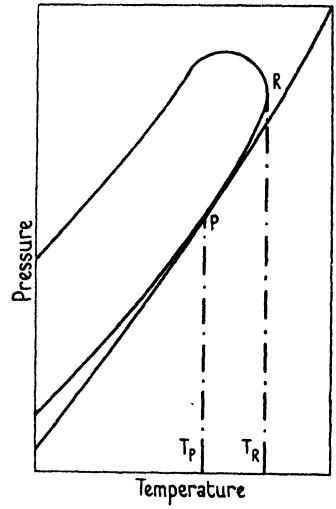

FIG. 104. Retrograde condensation of the second kind.

Kuenen [2] has examined binary mixtures of ethane with carbon dioxide, acetylene, and nitrous oxide, all of which afford evidence of the existence of retrograde condensation of the second kind. For the ethane-nitrous oxide mixture he found the critical temperature for ethane to be 32·2° C. (P_c = 48·8 atmospheres) and that for nitrous oxide 36·1° C. He employed five mixtures of composition x = 0·18, 0·25, 0·43, 0·55, and 0·76, where x is the number of parts of ethane in the volume in the gaseous state at 1 atmosphere, and embodied his results in the diagram reproduced in Fig. 105.

In the figure C_1 and C_2 are the critical points for ethane and nitrous oxide respectively and C_1ABC_2 is the plait-point curve; the border-line curves are shown by the dotted loops. It will be observed that the critical temperatures of a number of the mixtures lie below those of the pure gases. By adding ethane to nitrous oxide the critical temperature is lowered to a disproportionate extent; thus, for example, for a mixture containing x = 0·1 of ethane the critical temperature is as low as 32°, and all mixtures containing a greater quantity of ethane than this have critical temperatures below that of pure ethane; addition of nitrous oxide to ethane therefore makes the critical temperature decrease instead of increase; the lowest critical temperature (25·8°) belongs to a mixture containing 0·5 of ethane.

Dewar [4] has observed one instance, namely, that of carbon

dioxide and acetylene, in which the critical temperature of a mixture lies above that of its pure components, but in general the critical temperature of mixtures occupy an intermediate position, as shown in Fig. 103.

Referring again to Fig. 105, some of the border curves lie outside and above the vapour-pressure curves of ethane and nitrous oxide,

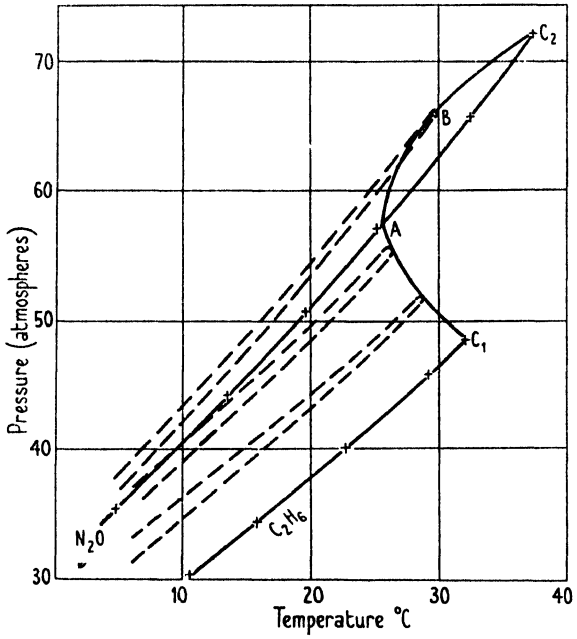

FIG. 105. Vapour pressure, boundary and plait-point curves of ethane-nitrous oxide mixtures.

and at every temperature there is therefore a maximum of pressure for one mixture, in the present instance the one having a composition of approximately $x = 8{\cdot}2$. The border curves in this region are relatively narrow, showing that only a very small change of pressure (i.e. about 0·2–0·3 atmosphere) is necessary to ensure complete condensation. The mixtures between 0·2 and 0·5 ethane exhibit retrograde condensation of the second kind, whilst all other mixtures belong to the first category.

In dealing with the condensation of pure gases attention was drawn to certain phenomena indicating that molecular association might occur in the neighbourhood of the critical point. Kuenen finds similar evidence of association with mixtures and suggests that [2]

'an association of that kind one would feel inclined to identify with what is called the formation of molecular compounds. This would'—he continues—'have a great influence on the vapour pressure, and it is not unlikely that rules like those . . . deduced from van der Waals' formula would fail entirely in those cases.'

A number of important generalizations have resulted from the work of Kuenen [5], of which the following may be mentioned:

(1) Certain pairs of substances, as, for example, ethane, with nitrous oxide, acetylene, or carbon dioxide, form mixtures of minimum critical temperature, whilst others, as, for example, methyl ether and hydrogen chloride [6], form mixtures of maximum critical point; such substances which form mixtures of minimum or maximum critical temperature form also mixtures of minimum or maximum boiling-point at lower pressures. (2) Any two substances which at a low temperature form a mixture of maximum or minimum vapour pressure form a similar mixture at high temperatures up to the critical point. If the composition of the mixture of minimum or maximum vapour pressure remained unchanged at all temperatures the pressure-temperature diagram for the binary system would include a third vapour-pressure curve for the mixture in question. In fact the composition does change with temperature, and for mixtures which have a maximum vapour pressure for a given composition at a low temperature, the maximum shifts towards the component with the higher vapour pressure, and may either disappear or remain up to the critical condition. In the neighbourhood of the curves of maximum pressure, and also of the vapour-pressure curves for the pure substances, the border curves are very narrow and the phenomenon of retrograde condensations is difficult to observe. (3) If the mixtures are abnormal owing to, for example, the mutual association of the two kinds of molecules, a maximum vapour pressure may be due not to the low mutual attraction of the two substances, which is the cause of a maximum with normal mixtures, but to the association at low temperature of the molecules of the component which has the higher vapour pressure at high temperatures, and the abnormally low vapour pressure exerted by this substance in consequence. This abnormality naturally makes the vapour pressure of the mixture appear relatively high, and may even produce a maximum.

Liquid- and Vapour-phase Equilibria

The fundamental thermodynamic equations which have up to the present been applied to pure substances in one phase only are valid for systems of all kinds and, in particular, for binary and ternary systems in which solid, liquid, and vapour phases are in equilibrium one with another.

The condition for equilibrium in any process occurring at constant temperature and pressure is defined by the equation $dF = 0$. Let us consider first the equilibrium between two phases of a pure substance.

If P_1, V_1, and F_1, and P_2, V_2, and F_2 are the pressures, molal volumes, and molal free energies of the two phases, respectively, at equilibrium at constant temperature, then on increasing the pressure in one phase by an amount dP_1 there will be a corresponding change in pressure dP_2 in the other, and from (10.71) we can write $dP_1 = dF_1/V_1$ and $dP_2 = dF_2/V_2$. But for equilibrium dF_1 must equal dF_2, and hence

$$dP_1/dP_2 = V_2/V_1. \tag{12.1}$$

This relation was first worked out for the specific case of a pure liquid and its vapour by Poynting and for the general case by Le Chatelier [7]. It is sometimes known as Poynting's law.

The equilibrium conditions for a binary system are more complex since there is an additional variable, namely, the composition. If A and B are the two components of such a system in equilibrium in the phases 1 and 2, then the total free energy of the system, F, is given by (10.70), namely

$$F = E - TS + PV;$$

and if there be n_A molecules of component A and n_B molecules of component B in the system, then

$$F' = (n_A + n_B)F, \tag{12.2}$$

where F is the free energy per mole.

The condition for equilibrium is, as before, $dF' = 0$, and hence we may write

$$\left(\frac{\partial F'}{\partial n_A}\right)_1 = \left(\frac{\partial F'}{\partial n_A}\right)_2. \tag{12.3}$$

Alternatively, the partial molal free energies, $\bar{F}_{A_1}$ and $\bar{F}_{A_2}$ of either component in the two phases (defined by $\bar{F}_{A_1} = \partial F_1'/\partial n_{A_1}$, where F_1' = the total free energy in phase 1) must be equal.

Writing $\quad x = \dfrac{n_B}{n_A + n_B}$ and $(1-x) = \dfrac{n_A}{n_A + n_B}$

we obtain

$$\frac{\partial F'}{\partial n_A} = F - x\frac{\partial F}{\partial x}$$

and

$$\frac{\partial F'}{\partial n_B} = F + (1-x)\frac{\partial F}{\partial x}.$$

From (12.3),

$$F_1 - x_1\frac{\partial F_1}{\partial x_1} = F_2 - x_2\frac{\partial F_2}{\partial x_2} \tag{12.4}$$

and

$$F_1 + (1-x_1)\frac{\partial F_1}{\partial x_1} = F_2 + (1-x_2)\frac{\partial F_2}{\partial x_2}. \tag{12.5}$$

By subtraction,
$$\frac{\partial F_1}{\partial x_1} = \frac{\partial F_2}{\partial x_2}. \tag{12.6}$$

But
$$dF = V\,dP - S\,dT + \frac{\partial F}{\partial x}dx \tag{12.7}$$

and
$$dF = d\left(x\frac{\partial F}{\partial x}\right).$$

From (12.7),
$$v_1\,dP - S_1\,dT - x_1\,d\frac{\partial F}{\partial x_1} = v_2\,dP - S_2\,dT - x_2\,d\frac{\partial F}{\partial x_1}.$$

Hence
$$(v_2-v_1)\,dP - (S_2-S_1)\,dT - (x_2-x_1)\left(d\frac{\partial F}{\partial x}\right) = 0. \tag{12.8}$$

But
$$d\frac{\partial F}{\partial x} = \frac{\partial^2 F}{\partial x^2}dx + \frac{\partial^2 F}{\partial x \partial P}dP + \frac{\partial^2 F}{\partial x \partial T}dT, \tag{12.9}$$

and
$$\left(\frac{\partial F}{\partial P}\right)_T = v; \qquad \left(\frac{\partial F}{\partial T}\right)_p = -S;$$

hence, for one phase,
$$\left\{(v_2-v_1)-(x_2-x_1)\frac{\partial v_1}{\partial x_1}\right\}dP - \left\{(S_2-S_1)-(x_2-x_1)\frac{\partial S_1}{\partial x_1}\right\}dT - \\ -(x_2-x_1)\frac{\partial^2 F_1}{\partial x_1^2}dx_1 = 0, \tag{12.10}$$

and for the other phase
$$\left\{(v_1-v_2)-(x_1-x_2)\frac{\partial v_2}{\partial x_2}\right\}dP - \left\{(S_1-S_2)-(x_1-x_2)\frac{\partial S_2}{\partial x_2}\right\}dT - \\ -(x_1-x_2)\frac{\partial^2 F_2}{\partial x_2^2}dx_2 = 0. \tag{12.11}$$

These are the general equations for equilibrium. For an isothermal change (12.10) becomes
$$\left\{(v_2-v_1)-(x_2-x_1)\frac{\partial v_1}{\partial x_1}\right\}dP = (x_2-x_1)\frac{\partial \mu_1}{\partial x_1}dx_1, \tag{12.12}$$

where $\mu = \partial F/\partial x$, a quantity which is sometimes known as the chemical potential, or
$$\left(\frac{dP}{dx_1}\right)_T = \frac{(x_2-x_1)(\partial \mu_1/\partial x_1)}{(v_2-v_1)-(x_2-x_1)(\partial v_1/\partial x_1)}. \tag{12.13}$$

It can be shown that

$$\frac{\partial^2 F}{\partial x^2} = \frac{\partial \mu}{\partial x} = \int \frac{\partial^2 v}{\partial x^2} dP + \frac{RT}{x(1-x)} \tag{12.14}$$

and, on substituting in (12.13),

$$\left(\frac{dP}{dx_1}\right)_T = \frac{(x_2-x_1)\left\{\int \frac{\partial^2 v_1}{\partial x_1^2} dP + \frac{RT}{x_1(1-x_1)}\right\}}{(v_2-v_1)-(x_2-x_1)\frac{\partial v_1}{\partial x_1}}. \tag{12.15}$$

It is evident from (12.15) that to calculate $(dP/dx_1)_T$ for a given value of x_1 at temperature T, we must know (1) the corresponding value of x_2, (2) the specific volumes of both phases, (3) the partial molal volume $(\partial v_1/\partial x_1)_{P,T}$ of the gas phase as an explicit function of P, and (4) the pressure at which x_1 is a saturated vapour. From a knowledge of one point on the vapour curve we can then construct the whole curve from the liquid curve.

For the special case when the vapour is a perfect gas and $v_2 \ll v_1$, we have $\partial v_1/\partial x_1 \equiv 0$, and (12.15) becomes

$$\frac{RT}{P} dP = \frac{(x_1-x_2)RT}{x_1(1-x_1)} dx_1 \tag{12.16}$$

or

$$dx_1 = \frac{x_1(1-x_1)\,dP}{(x_1-x_2)P}.$$

This is identical with the Duhem-Margules equation, which is usually written in the form

$$x_2\, d\log_e p_A + (1-x_2)\, d\log_e (p-p_A) = 0, \tag{12.17}$$

where $p_A = x_1 p$ and p and p_A are the partial pressures of the two components in the vapour phase.

In recent years a considerable amount of work has been done upon the coexisting liquid and vapour phases of binary mixtures of hydrocarbons and other industrial gases, and in one instance of a ternary mixture. The following references relate to important papers on the subject.

Oxygen and Nitrogen

Baly, *Phil. Mag.* (V), **49**, 517 (1900).
Inglis, *Phil. Mag.* (VI), **11**, 640 (1906).
Kuenen and collaborators, *Commn. Phys. Lab. Leiden*, Nos. 150B and 161.
Dodge and Dunbar, *J. Am. Chem. Soc.* **49**, 591 (1927).

Oxygen and Argon

Inglis, loc. cit.
Bourbo and Ischkin, *Phys. Zeit. Sow.* **10**, 271 (1936).

Argon and Nitrogen
Holst and Hamburger, *Z. phys. Chem.* **91**, 513 (1916).

Carbon Monoxide, Nitrogen, and Hydrogen (Binary and Ternary Mixtures)
Verschoyle, *Phil. Trans.* (A), **230**, 189 (1931).
Steckel, *Sow. Phys.* **8** (1935).
Torotscheschnikow, *J. Tech. Phys., U.S.S.R.*, **4**, 365 (1937).
Ruhemann and Zinn, *Phys. Zeit. Sow.*, **12**, 389 (1937).

Helium and Nitrogen
Fedoritenko and Ruhemann, *J. Tech. Phys., U.S.S.R.*, **4**, 1 (1937).

Methane and Hydrogen
Freeth and Verschoyle, *Proc. Roy. Soc.* (A), **130**, 453 (1931).

Methane and Propane
Sage and Lacey, *J. Ind. Eng. Chem.* **26**, 214 (1934).

Ethane and n-Heptane
Kay, *J. Ind. Eng. Chem.* **30**, 459 (1938).

Methane and Ethane
Ruhemann, *Proc. Roy. Soc.* (A), **171**, 121 (1939).

The method usually employed in these investigations is to isolate the two-phase system in a suitable equilibrium vessel maintained at constant temperature and simultaneously to withdraw and analyse liquid- and vapour-phase samples. In order to ensure the attainment of equilibrium, arrangements must be made for intimate contact between the two phases in the equilibrium vessel. The details by which this is done vary somewhat. Freeth and Verschoyle, for example, employ a modification of the Leiden method, in which the two phases in contact in a closed vessel are mechanically stirred, whilst Dodge and Dunbar employ a dynamic method in which the vapour distilled from the liquid is recirculated, by means of a mercury pump, back through the liquid by way of a heat-interchange system. Both the static and dynamic methods yield accurate results in skilled hands, but the latter has the advantage of permitting comparatively large samples of each phase to be removed from the system without disturbing equilibrium.

A brief description of the cryostat and equilibrium vessel used by Dodge and Dunbar in their classical investigation of the oxygen-nitrogen system at temperatures between 90° and 125° K. will serve to indicate the precautions necessary to arrive at and maintain equilibrium conditions. The essential parts of the apparatus are shown in Fig. 106. The equilibrium vessel holding the mixture is made up of a brass tube *G* closed at the upper end by the plug *H* and at the

lower end by a copper cup I on the outside surface of which is cut a triple screw thread. Gas enters the vessel through the pipe L, branching at J into three small tubes which lead to the screw threads on I. The vapour is thus forced to take a helical path through the liquid, and small holes drilled through the walls of I at the base of the threads ensure effective stirring of the liquid and intimate contact with the vapour.

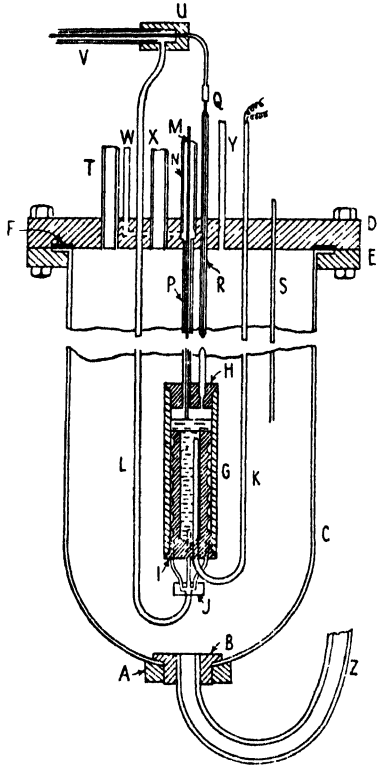

FIG. 106. Dodge and Dunbar's apparatus for measuring equilibrium in the system oxygen-nitrogen.

The equilibrium vessel is enclosed in a copper container C which is well lagged and is filled with liquid oxygen or other liquid suitable for maintaining the desired temperature. The container is fitted with a gas-tight cover D. Vapour leaves the equilibrium vessel through the capillary tube Q which is protected from contact with the thermostat liquid by means of the jacket R. Liquid samples are withdrawn through the capillary copper tube M. The temperature and pressure of the system are measured by a copper-constantan thermo-couple passing into the vessel through the tube K, and by a free-piston balance, respectively.

The Flow Method. A modification of the above method, due to Steckel and Zinn, has been used at the Imperial College of Science by Ruhemann in a study of the equilibrium conditions of various binary and ternary mixtures of hydrocarbons. The apparatus and experimental procedure are simple and may be briefly described.

The general arrangement of the apparatus is shown in Fig. 107. The mixtures are made up in the copper cylinder M (capacity *c.* 100 c.c.) by cooling it in liquid air and condensing each component into it separately. On allowing the temperature to rise until the contents are completely gaseous, the pressure of the mixture can be

read off from the Bourdon gauge P_1. It is not necessary to know accurately the composition of the mixture in M. The fine-adjustment valve V_1 allows gas to be introduced from M into the equilibrium vessel E which is completely immersed in a liquid of known temperature contained in a Dewar vessel. The mixture separates into a liquid and vapour phase, the former being removed continuously

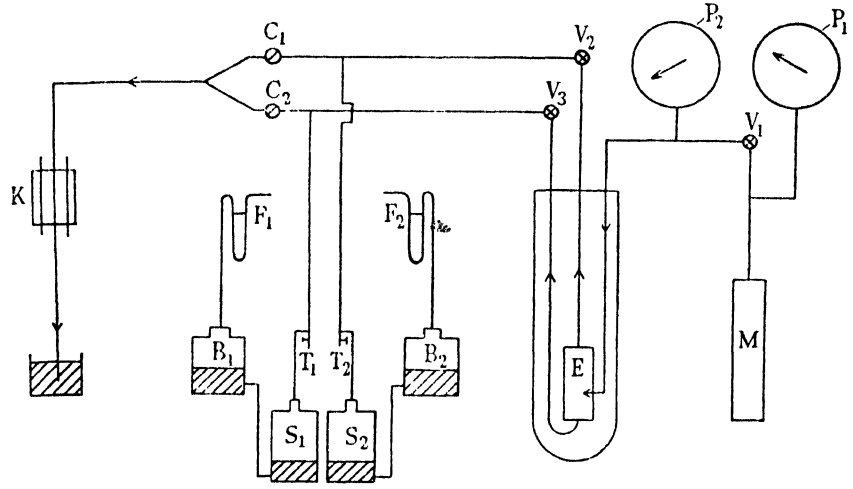

FIG. 107. Ruhemann's apparatus for measuring equilibrium in the system methane-ethane.

through the valve V_3 and the latter through the valve V_2. The two mixtures which emerge as gases at room temperature and atmospheric pressure can, by manipulating the stopcocks C_1 and C_2, be passed either to the storage vessels S_1 and S_2, or through the catharometer K in which their composition is determined by thermal conductivity measurement. The vessels S_1 and S_2 are connected through the glass bottles B_1 and B_2 to the flow-meters F_1 and F_2 which enable the rate of flow of both phases to be observed while an experiment is in progress.

During the course of an experiment the valves V_1, V_2, and V_3 are so adjusted that the pressure in E, as indicated by the Bourdon gauge P_2, remains constant to within 0·1 atmosphere for periods of about 20 minutes, during which the catharometer is read every minute. When the reading becomes constant it is assumed that equilibrium has been reached.

The equilibrium vessel is shown in detail in Fig. 108. It consists

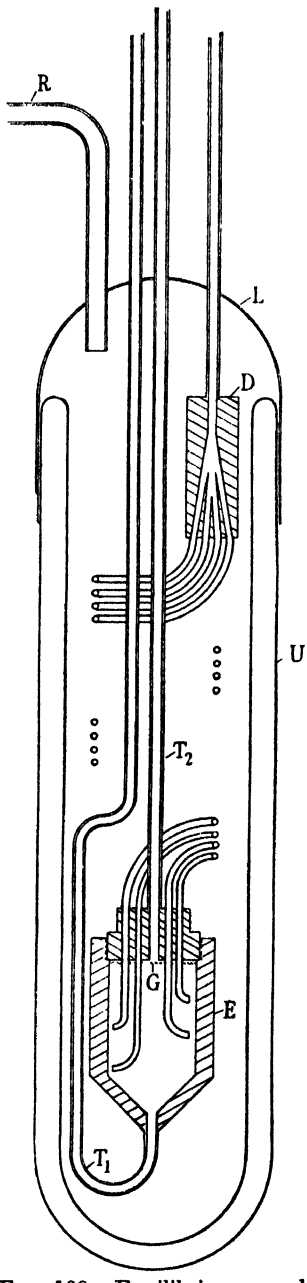

FIG. 108. Equilibrium vessel used by Steckel and Zinn and Ruhemann.

of a thick-walled copper vessel of about 10 c.c. capacity, tapering at the lower end, and fitted at the upper end with a screwed cap, soft-soldered in position. The incoming gas is distributed in the manifold D into eight narrow copper capillary tubes, 0·5 mm. internal diameter, of which only four are shown in the figure. The tubes are wound in a spiral of four turns and are soldered through the cap of the equilibrium vessel; within the vessel their ends are bent, as shown, to face the walls. The liquid phase leaves E through the tube T_1 and the gas phase through T_2; both tubes are soldered to and pass through a spun-brass cap L which fits closely the Dewar vessel and is made gas-tight by means of a rubber band. The vapour of the thermostat liquid passes out through the tube R to a gas-holder.

When the binary mixture passes slowly through the apparatus, a liquid-vapour equilibrium is established in the capillary coils and the two phases spurt against the walls of the equilibrium vessel and separate by gravity. To prevent entrainment of the liquid phase, two layers of fine copper gauze are inserted below the vapour exit tube at G. Details of the catharometer will be found in Ruhemann's paper.

The Dew- and Boiling-point Method. In this method a gas of known composition is introduced into an equilibrium vessel at constant temperature, and corresponding points on the border curves are obtained by determining the boiling-point of the liquid phase and the dew-point of the vapour phase, respectively, by visual observation.

It has been employed by Kuenen and collaborators at Leiden [9], by Steckel, Holst and Hamburger, Sage and Lacey, and Kay. The apparatus required is comparatively simple. Kay, for example, employs Pyrex capillary tubing to construct the equilibrium vessel which is connected to a liquid-piston mercury pump, and effects mixing by an electro-magnetic stirrer.

Experimental Data. In a binary system in two phases there are two degrees of freedom, and if the temperature of the system is fixed the compositions of the vapour and liquid phases in equilibrium may be determined as a function of the pressure. The equilibrium data may conveniently be represented by border curves showing the relation between pressure and temperature for mixtures of constant composition, by pressure-composition isotherms ((P,x) curves), or by temperature-composition isopiestics ((T,x) curves). A set of such curves for ethane–*n*-heptane, determined by Kay, are shown in Figs. 109 and 110, and give a fairly complete picture of the properties of the system. The critical constants of the two hydrocarbons are:

	Critical temperature, °C.	*Critical pressure, atms.*
Ethane . .	32·3	48·78
n-Heptane . .	266·9	26·87

and Kay's data extend from 0° to 270° C. and from 3·4 to 85 atmospheres pressure.

The composition and physical constants of the mixtures studied are given in Table 58.

TABLE 58. *Composition and Physical Constants of Ethane–n-Heptane Mixtures*

Composition, mole %			*Critical point*			*Point of max. temp.*			*Point of max. pressure*		
Ethane	*n-Heptane*	*Average mol. wt.*	T_c, °C.	P_c, atms.	d_c, gm./c.c.	T_t, °C.	P_t, atms.	d_t, gm./c.c.	T_p, °C.	P_p, atms.	d_p, gm./c.c.
0	100	100·17	267·4	26·95	0·234	..	..	..	..	..	..
4·04	95·96	97·34	..	..	..	..	..	..	..	..	..
10·13	89·87	93·07	..	..	..	..	..	..	..	..	..
17·89	82·11	87·63	..	..	..	..	..	..	..	..	..
26·54	73·46	81·56	242·3	46·40	0·260	247·9	40·10	0·168	233·3	48·60	0·330
58·71	41·29	59·01	189·9	75·25	0·266	211·8	54·45	0·130	173·9	78·25	0·331
77·09	22·91	46·12	136·0	85·95	0·279	177·1	57·90	0·104	136·1	85·95	0·279
88·71	11·29	37·98	87·7	77·05	0·272	138·3	55·20	0·083	111·1	82·40	0·203
96·83	3·15	32·27	49·1	57·85	0·248	83·9	46·25	0·069	68·3	64·70	0·157
100·0	0	30·06	32·3	48·45	0·220	..	..	..	..	..	..

Referring to the border curves (Fig. 103) it will be seen that the maximum pressure for the existence of two phases occurs at a higher temperature than the critical temperature for mixtures containing upwards of 50 per cent. ethane and at a lower temperature for

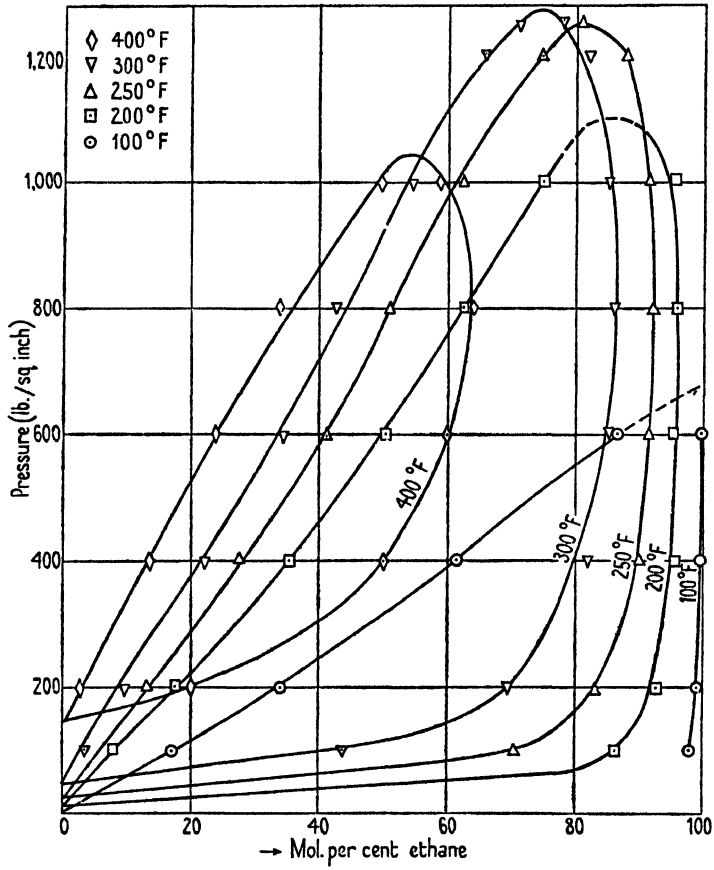

FIG. 109. Pressure-composition curves for ethane–*n*-heptane (Kay).

mixtures containing less than 50 per cent. ethane. There is also a comparatively large region in which retrograde condensation of the first kind takes place. The (P,x) and (T,x) curves in Figs. 109 and 110 show that as the pressure increases the liquid-vapour phase region diminishes. Below 26·95 atmospheres (396 lb. sq. inch), the critical pressure of *n*-heptane, this region is limited only by the temperature; above 26·95 atmospheres it is limited by both temperature and composition. At 40 atmospheres (600 lb. sq. inch), for

example, the (T, x) curve terminates with a mixture containing 17·5 mole per cent. of ethane, whilst at 54·4 atmospheres (800 lb. sq. inch), which is above the critical pressure of ethane, the liquid and vapour phases can coexist only in mixtures containing between 33·0 and 99·0 mole per cent. of ethane. At 85·9 atmospheres (1,263 lb. sq.

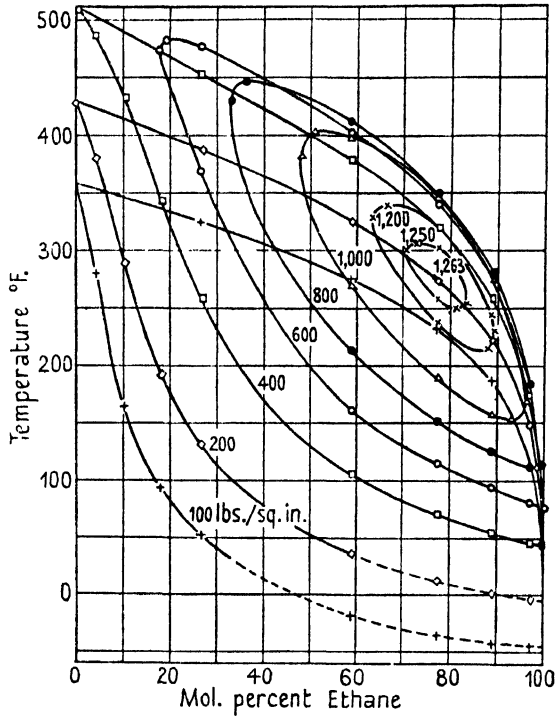

FIG. 110. Temperature-composition curves for ethane–*n*-heptane (Kay).

inch) the two phases can coexist only for a mixture containing 77·1 mole per cent. of ethane, and at higher pressures the whole range of mixtures is completely homogeneous at all temperatures.

Similar data have been obtained for the system methane-propane by Sage, Lacey, and Schaafsma (loc. cit.), although their measurements do not extend as low as the critical temperature of methane. Their critical and cricondentherm data are summarized in Table 59.

Ternary Systems. In a ternary system in two phases there are three degrees of freedom, and in determining the equilibrium conditions it is usual to fix the temperature and pressure, leaving one degree of freedom to be satisfied.

TABLE 59. *Critical and Cricondentherm Data for Methane-Propane*

Composition, mole % CH_4	*Critical constants*			*Cricondentherm constants*		
	T_c, °C.	P_c, *atms.*	d_c, *gm. c.c.*	T_p, °C.	P_p, *atms.*	d_p, *gm. c.c.*
Propane	100·1	43·77	0·232	..	..	..
10·0	91·0	52·1	0·232	93·7	48·6	0·199
20·0	81·2	60·6	0·232	86·5	53·8	0·171
30·0	70·9	69·3	0·232	78·5	58·8	0·149
40·0	59·3	78·8	0·231	69·2	63·4	0·133
50·0	46·3	87·9	0·231	57·9	67·2	0·121
60·0	31·1	95·7	0·229	43·5	70·8	0·115
70·0	10·4†	99·9	0·225†	26·8	73·8	0·113
100·0	−95·5	50·0	..	..	..	..

† Extrapolated.

Consider a system in which x_A, x_B, and x_C are the mole fractions of the three components A, B, and C and the subscripts L and V refer to the liquid and vapour phases respectively. Then $x_{AL}+x_{BL}+x_{CL} = x_{AV}+x_{BV}+x_{CV} = 1$. If, now, some particular value of the mole fraction of A in the liquid phase is selected, say x'_{AL}, then at constant temperature and pressure x'_{BL}, x'_{CL}, x'_{AV}, x'_{BV}, and x'_{CV} will be fixed; and employing the conventional triangular diagram, a pair of nodes on the liquid and vapour equilibrium curves will be obtained. By varying x_{AL} progressively a whole series of nodes can be determined and the equilibrium curves drawn. The area enclosed by the two curves gives the range of composition within which separation into two phases can take place.

It can easily be shown that if the components of the system obey Raoult's law the equilibrium curves are straight lines. Thus, if p_A is the partial pressure of component A and π_A its vapour pressure in the pure state, then, according to the law,

$$p_A = x_{AL}\pi_A, \qquad p_B = x_{BL}\pi_B, \quad \text{and} \quad p_C = x_{CL}\pi_C.$$

The total pressure of the system is given by $p_A+p_B+p_C = P$. If the mole fraction of component A in the liquid phase is fixed, then

$$P = x_{AL}\pi_A+x_{BL}\pi_B+(1-x_{AL}-x_{BL})\pi_C,$$

$$x_{BL} = \frac{P-\pi_C}{\pi_B-\pi_C} - \frac{x_{AL}(\pi_A-\pi_C)}{\pi_B-\pi_C},$$

and

$$x_{CL} = \frac{P-\pi_B}{\pi_C-\pi_B} - x_{AL}\left(\frac{\pi_A-\pi_C}{\pi_C-\pi_B}\right).$$

Equations for the vapour phase in which the mole fractions of each

component are expressed in terms of the vapour pressures of the pure components and the total pressure may be derived in a similar manner.

Verschoyle and Ruhemann and Zinn have examined the ternary system CO–N_2–H_2, the former at 30, 90, and 150 atmospheres and

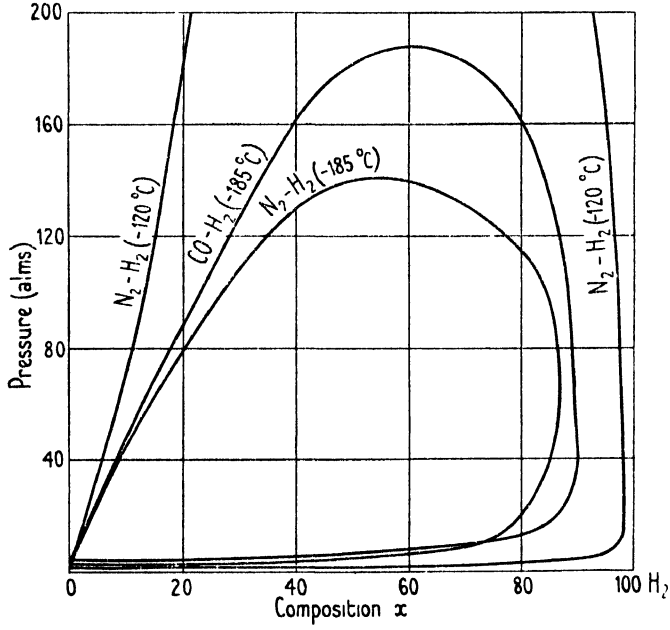

FIG. 111. Pressure-composition curves for nitrogen-hydrogen and carbon monoxide-hydrogen mixtures (Verschoyle).

at temperatures of −185°, −195°, and −205° C., and the latter at 12, 20, 26, 35, and 50 atmospheres and at temperatures of −183°, −190°, and −195° C. The critical constants of the three components of the system are:

	T_c	P_c
H_2 . .	−234·5	12·8
N_2 . .	−146·0	33
CO . .	−141·1	35·9

Verschoyle's data therefore relate for the most part to pressures above, and Ruhemann and Zinn's data to pressures below the critical pressures of the pure gases.

In order to assist in the interpretation of the ternary diagram, Verschoyle's (p,x) data for binary mixtures of N_2–H_2 and CO–H_2

at −185° and for N_2–H_2 at −210° are reproduced in Fig. 111. The critical constants for these mixtures are:

Mixture	Temp., °C.	Plait point		Critical point of contact	
		Pressure, atms.	% H_2	Pressure, atms.	% H_2
CO–H_2	−185	187	58	54	90
	−190	228	60	48	93
	−200	(325)	(64)	34	97·5
	−205	(380)	(66)	30	99·5
N_2–H_2	−185	138	53	60	87
	−195	191	58	50	93·5
	−205	(340)	..	35	98
	−210	..	..	25	98·5

The figures in parentheses are estimated.

The ternary system may be represented graphically by the usual triangular diagram, and in Fig. 112 Verschoyle's data at 150 atmo-

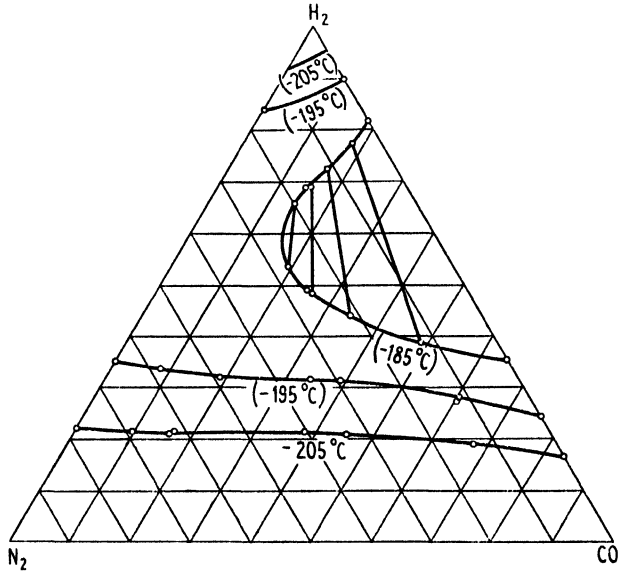

FIG. 112. Equilibrium curves for the ternary system nitrogen-hydrogen-carbon monoxide at 150 atmospheres (Verschoyle).

spheres and −185° to −205°, and in Fig. 113 Ruhemann and Zinn's data at −183° for pressures of 12, 26, and 50 atmospheres, are shown. Referring to Fig. 112, it will be seen that at −185° and 150 atmospheres there is a plait point corresponding to the mixture

CO = 15, N_2 = 25, H_2 = 60 per cent., whilst for all other conditions included in Verschoyle's experiments two phases are present throughout.

Ruhemann and Zinn discuss their results in relation to the Linde-Bronn method of separating carbon monoxide from coke-oven gas

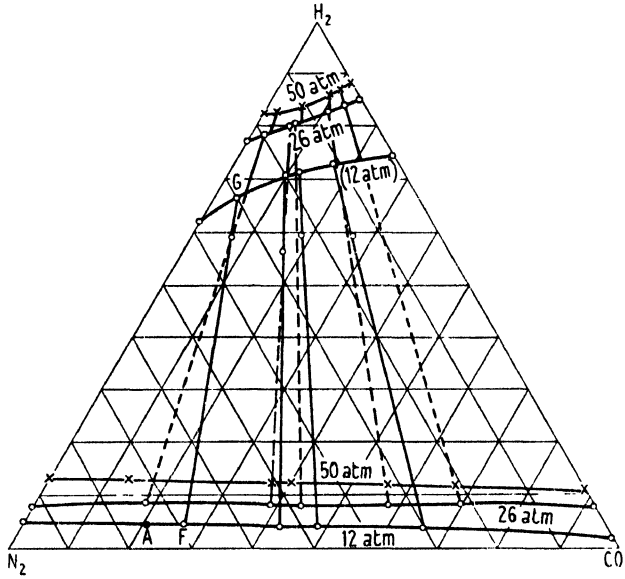

FIG. 113. Equilibrium curves for the ternary system nitrogen-hydrogen-carbon monoxide at −183° C. (Ruhemann).

by means of liquid nitrogen; this problem affords a useful illustration of the use of such data and the considerations involved may now be summarized briefly.

The coke-oven gas which after removal of methane and ethylene contains about 6 per cent. of CO enters a fractionating column (Fig. 114) at *G* and meets a descending stream of liquid nitrogen entering at *L*. The scrubbed gas, consisting mainly of nitrogen and hydrogen, leaves at *D* and the scrubber liquid containing the greater part of the carbon monoxide at *A*.

The difference between the boiling-point of nitrogen and carbon monoxide at atmospheric pressure is 4°, and since the quantity of the latter compared with that of the former is comparatively small, the temperature differences in the column may be neglected. Actually it is found to be of the order of $1\frac{1}{2}$°. The difference in the heats of vaporization of the two gases is also small (1,336 and 1,414 cals./mole

respectively), so that the quantities of fluid and vapour on successive plates of the column may be assumed to be approximately equal.

If M and x with subscripts L, D, A, G represent quantities of liquid or vapour and the percentage content of carbon monoxide in the liquid and gas phase, then for equilibrium in the column we may write

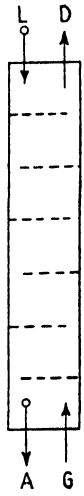

FIG. 114. Diagrammatic representation of column for separation of carbon monoxide from coke-oven gas.

$$x_A M_A - x_L M_L = x_G M_G - x_D M_D;$$

or, since

$$M_A = M_L, \qquad M_G = M_D, \quad \text{and} \quad x_L = 0,$$

$$x_A = (x_G - x_D) M_G / M_L. \tag{12.18}$$

Now the carbon monoxide content of the scrubber liquid leaving at A cannot exceed the quantity at equilibrium with the gas at G. That is, referring to Fig. 113, the maximum carbon monoxide concentration at A ($= x_A$) will be given by the point F on the liquid curve which is obtained by drawing a connodal through the point G on the vapour curve.

Since x_D is very small compared with x_G, (12.18) may be written

$$x_A = x_G M_G / M_L \tag{12.19}$$

and the value of x_A may be calculated from the known value of x_g and M_g and an arbitrarily selected value of M_L (the quantity of scrubber liquid).

If the point so calculated comes to the left of F, say at A, the column will function. It is also evident that the efficiency of the process depends to some extent on the degree of asymmetry of the connodals.

BIBLIOGRAPHY

1. CAILLETET, *Compt. Rend.* **90**, 210 (1880).
2. KUENEN, *Phil. Mag.* **40**, 176 (1895); **44**, 174 (1897).
3. CAUBET, *Z. physik. Chem.* **40**, 257 (1902); **43**, 115 (1903); **49**, 101 (1904).
4. DEWAR, *Proc. Roy. Soc.* (A), **30**, 543 (1879).
5. KUENEN, *Phil. Mag.* **4**, 116 (1902).
6. ——, *Phil. Mag.* **1**, 597 (1900).
7. POYNTING, *Phil. Mag.* (4), **12**, 32 (1881); LE CHATELIER, *Z. physik. Chem.* **9**, 335 (1892).
8. KAY, *J. Ind. Eng. Chem.* **30**, 461 (1938).
9. KUENEN and CLARK, *Commn. Phys. Lab. Leiden*, No. 150B (1917); KUENEN, VERSCHOYLE, and VAN URK, *Commn. Phys. Lab. Leiden*, No. 161 (1922).

XIII

THE LIQUEFACTION OF GASES

Liquefaction, Refrigeration, and Pressure

AFTER the discovery of critical phenomena by Andrews and Cagniard de la Tour, it became clear that the liquefaction of the so-called permanent gases could be effected only after they had been cooled below the temperature of the environment. It was in this way that the problem of refrigeration, with respect to gases, was first realized.

The thermodynamics of refrigeration may be stated briefly as follows:

A system is to be cooled from a temperature T_1 to a temperature T_0, which is below that of the surroundings. For this the enthalpy of the system must be reduced from H_1 to H_0, a quantity of heat Q_1 must be removed from the system at room temperature, and a quantity of work W must be done on the system, also at room temperature. The pressure before and after the operation is assumed to be the same, though nothing is specified regarding intermediate pressures. Then the first law gives the equation

$$H_1 - H_0 = Q_1 - W. \tag{13.1}$$

According to the second law, the change in entropy of the system and the surroundings together must be greater than or equal to zero. If we assume that Q_1 is given off reversibly, the change in entropy of the surroundings will be

$$\Delta S' = Q_1/T_1,$$

and the change of entropy of the system

$$\Delta S = S_0 - S_1,$$

where S_0 and S_1 are the entropy of the system at the low temperature and at room temperature respectively.

Therefore
$$S_0 - S_1 \geqslant -Q_1/T_1. \tag{13.2}$$

Substituting Q_1 from equation (13.1), we have

$$S_0 - S_1 \geqslant -\frac{W + H_1 - H_0}{T_1}$$

or
$$W \geqslant T_1(S_1 - S_0) - (H_1 - H_0). \tag{13.3}$$

If the process of refrigeration involves first cooling and then liquefying a gas, the expression on the right of (13.3) is known as the

theoretical work of liquefaction and gives the minimum amount of work needed to liquefy a gas, starting from a temperature T_1.

Using this equation, we find, for example, that the minimum amount of work needed to produce one gallon of liquid air, starting from room temperature, is 0·74 kWh., and to produce one gallon of liquid methane requires 0·575 kWh. In practice the power consumption is considerably greater.

We have shown that work must be expended to liquefy a gas, but we have yet to see how this is to be effected. We merely know that the enthalpy and entropy of the gas must be lowered, and this must evidently be done by changing the values of one or other of the variables on which enthalpy and entropy depend. These variables are temperature and pressure. To bring about a fall of temperature without altering the pressure we might bring our system into thermal contact with another system at a lower temperature; but since the temperature we are seeking to attain is lower than that of the surroundings, this possibility is ruled out.

We thus come to the conclusion that it is only by altering the pressure that we can effect a change in enthalpy and entropy of the gas that is to be liquefied.

Since
$$\left(\frac{\partial S}{\partial p}\right)_T = -\left(\frac{\partial v}{\partial T}\right)_p \tag{13.4}$$
and since $(\partial v/\partial T)_p$ is essentially greater than zero, isothermal compression must always lead to a decrease of entropy.

Since
$$\left(\frac{\partial H}{\partial p}\right)_T = -\mu C_p, \tag{13.5}$$
where μ is the Joule-Thomson coefficient, which may, as we have seen, be positive or negative, compression of a gas may or may not lead to a decrease in enthalpy.

On the other hand,
$$\left(\frac{\partial H}{\partial T}\right)_p = C_p \tag{13.6}$$
and
$$\left(\frac{\partial S}{\partial T}\right)_p = C_p/T \tag{13.7}$$
are essentially positive quantities.

Now compression is the only way in which work may be done on a gas. Therefore, in any process for liquefying gases, one of the steps must always consist in compressing the gas. This shows the connexion between refrigeration and pressure. We have still to find

how the work done in compressing the gas may be so utilized as to bring about the reduction in enthalpy, entropy, and temperature necessary for liquefaction.

Thermodynamic Diagrams

To understand the processes of gas liquefaction, and to evolve and develop these processes, it is essential that the thermal properties of the gases be available in an easily accessible form. Equations of state and thermodynamic formulae involve too cumbersome numerical operations to present a rapid survey of the behaviour of a gas under various conditions of temperature and pressure, and for this purpose it is more expedient to make use of geometrical representation.

The three properties of a gas that should be known as functions of temperature and pressure for purposes of liquefaction are enthalpy H, entropy S, and specific volume v. In principle all these quantities may be determined from a sufficiently accurate equation of state together with a few calorimetric measurements; for, as we have seen, all the thermodynamic functions are connected with the derivatives of pressure, volume, and temperature by well-known equations. But the (p, v, T) relations of gases near the critical point are generally not known with sufficient accuracy and are difficult to determine.

In a thermodynamic diagram, any two of the variables p, T, H, S, v may be taken as coordinates, and the curves plotted are those along which the other properties remain constant. Which pair of variables are singled out as coordinates is a matter of expediency, and varies according to the use to which the diagram is to be put. In principle all complete diagrams are equivalent. Those in general use are the (H, T) diagram, in which enthalpy is plotted as a function of temperature, the $(\log p, H)$ diagram, in which ordinates are $\log p$ and abscissae H, the (T, S) diagram, and the (H, S) or Mollier diagram.

There are many ways of constructing these diagrams on the basis of experimental results. Most methods start by determining $H(p, T)$ and then evaluating S and, occasionally, v with the help of thermodynamic formulae involving H. Thus the (H, T) diagram with isobaric curves or the $(\log p, H)$ diagram with isothermal curves are usually obtained first.

To construct either of these, we must know the vapour-pressure curve and the latent heats of evaporation. The latter may either be determined directly, or may be calculated from specific-volume measurements with the help of the Clausius-Clapeyron equation. Apart from these a few isolated data must be known and one other thermal property must be determined experimentally over the entire field of temperatures and pressures. This may be

1. The specific heat at constant pressure, $C_p = (\partial H/\partial T)_p$.
2. The Joule-Thomson coefficient, $\mu = (\partial T/\partial p)_H$.
3. The isothermal expansion coefficient, $\alpha = (\partial H/\partial p)_T$.

Though μ is probably more difficult to determine than any of the other properties, the technique described in the last chapter has been so well developed that the Joule-Thomson coefficient has come to be considered as the natural basis of operations. As an example of how μ may be utilized for constructing thermodynamic diagrams, we may refer to Hausen's work on air [1].

Hausen determined μ for air as a function of temperature and pressure in a very wide interval of these variables. He then constructed an (H, T) diagram as follows:

$$\text{For } p = 0, \qquad H_0 = H_c + \int_{p=0} C_{p_0}\, dT, \tag{13.8}$$

the index 0 referring to zero pressure. H_c is an arbitrary constant, which was chosen as 50 cals. per gm. C_{p_0}, the specific heat at infinitely low pressure, is given the value corresponding to a perfect diatomic gas:

$$C_{p_0} = 7/2 . R/M = \frac{7 \times 1{\cdot}986}{2 \times 28{\cdot}84} = 0{\cdot}241.$$

Therefore $$H_0 = 50 + 0{\cdot}241T.$$

The isobaric curve for $P = 0$ is therefore a straight line (Fig. 115).

The other isobaric curves in the superheated region are then obtained from the relation

$$T_2 - T_1 = \Delta T = \int_1^2 \mu\, dp \tag{13.9}$$

by marking off the corresponding length horizontally from the line for $p = 0$. The vapour branch of the boundary line from A to the point B with a horizontal tangent is built up in the same way with the help of the experimental values of μ. The liquid branch from A' to B' is obtained from the known latent heats of evaporation.

Isobaric curves to the right of $A'B'$ are constructed by integrating μ from the high pressure in question to the liquid boundary curve.

To obtain the part of the boundary curve to the right of BB' Hausen makes use of the fact that, for a given pressure before expansion and for a given temperature of saturation, a group of four points $DCC'D'$ are known except for the absolute height of the group as a whole. A series of such four-point groups must be so distributed along known vertical straight lines that the isobaric line DD' as well as the boundary line $BCC'B'$ may give smooth curves. The distribution was found to be unique with a negligible error. Thus all the isobaric curves and the whole boundary line can be constructed.

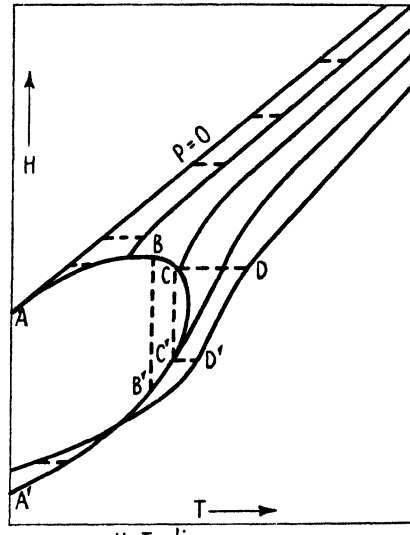

FIG. 115. Enthalpy-temperature diagram.

From this (H, T) diagram Hausen obtained $C_p = (\partial H/\partial T)_p$ by measuring the slopes of the isobaric curves at various points. To calculate the entropy we now have the equation

$$dS = C_p\, dT/T - \left(\frac{\partial v}{\partial T}\right)_p dp. \tag{13.10}$$

Thus, for a given temperature, $S = S_c - \int (\partial v/\partial T)_p\, dp$, where S_c is an arbitrary constant, which is so chosen that, for $p = 1$ atmosphere, the entropy of liquid air at the boiling-point is zero. Hausen uses the isothermal curve for air at room temperature, which is known very accurately. The integral $\int (\partial v/\partial T)_p\, dp$ can thus be computed for the entire pressure interval at this temperature.

At constant pressure $dS = C_p\, dT/T = dH/T$, so that the entropy can now be determined for all temperatures and pressures from the (H, T) diagram with the relation

$$S = S_0 + \int_{T_0}^{T} dH/T. \tag{13.11}$$

This enables us to insert the curves of constant entropy in the (H, T) diagram and to construct a (T, S) diagram, in which the isenthalpic curves may be traced.

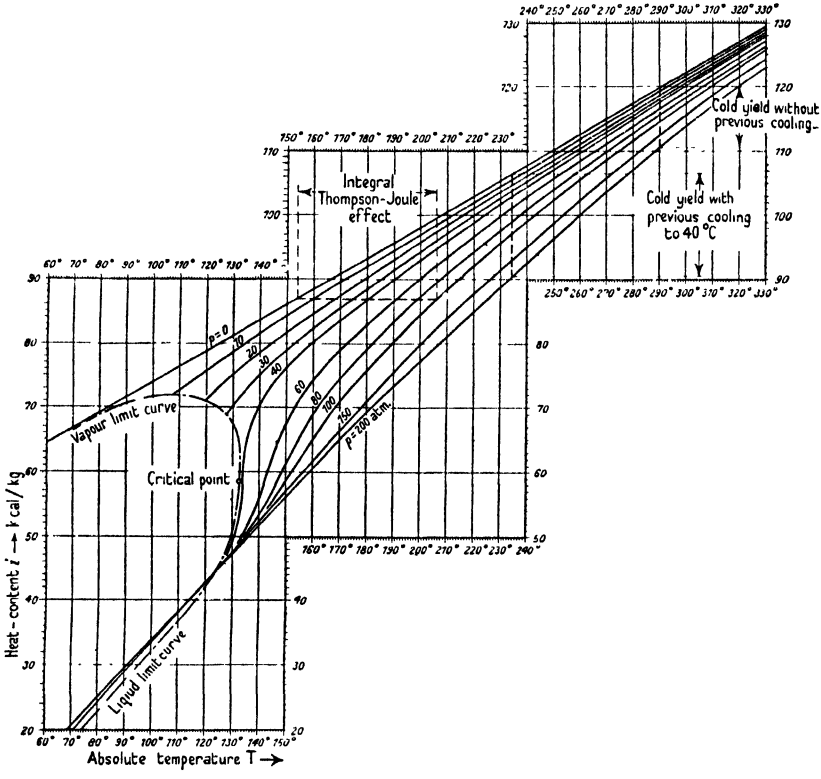

FIG. 116. Enthalpy-temperature diagram for air (Hausen).

The specific volume is calculated from the Joule-Thomson coefficient μ with the help of the equation

$$\mu = \left(\frac{\partial T}{\partial p}\right)_H = \frac{T(\partial v/\partial T)_p - v}{C_p} = \frac{T^2}{C_p}\left(\frac{\partial (v/T)}{\partial T}\right)_p. \qquad (13.12)$$

For constant pressure this gives

$$d(v/T) = \frac{\mu C_p}{T^2}\,dT = \frac{\mu}{T^2}\,dH, \qquad (13.13)$$

and

$$v/T = v_0/T_0 + \int_{T_0}^{T} \frac{\mu}{T^2}\,dH. \qquad (13.14)$$

In this way all the thermodynamic properties needed can be determined and the diagrams built up. Figs. 116, 117, and 118 show the (H, T), (T, S), and (H, S) diagrams for air, as constructed by Hausen.

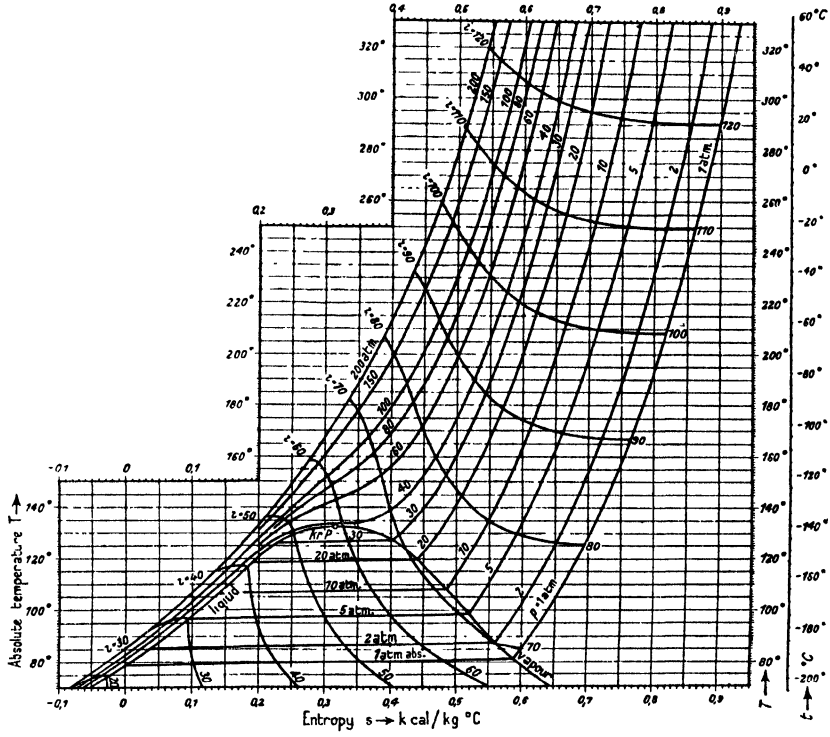

FIG. 117. Temperature-entropy diagram for air (Hausen).

The (H, T) diagram of methane was recently constructed by Eucken and Berger [2] with the help of the isothermal expansion coefficient a (Fig. 101). The diagrams of oxygen were built up by F. Schmidt on the basis of compressibility data. Numerous diagrams for most of the existing gases have been evolved by various authors from miscellaneous data collected from the literature.

Liquefaction Cycles

Suppose that we have compressed a gas at room temperature and suppose that its Joule-Thomson coefficient μ is positive at room temperature throughout the entire interval of pressure. Then the enthalpy and entropy have been decreased as a result of the compression. This may be verified by referring to one of the diagrams

on Figs. 116, 117, or 118. We may then carry out one of the two following operations:

(*a*) expand the gas at constant enthalpy,

(*b*) expand it at constant entropy.

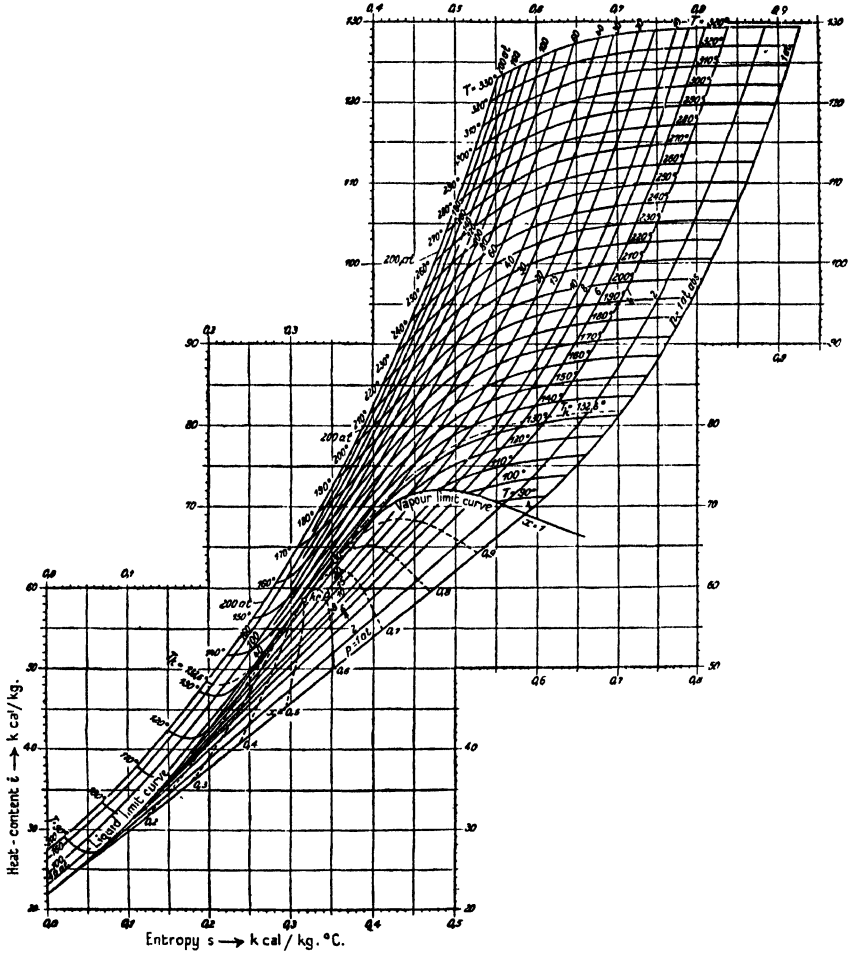

FIG. 118. Enthalpy-entropy diagram for air (Hausen).

(*a*) From Chapter XI we know that this can be effected in a Joule-Thomson expansion, letting the gas lose pressure by passing it through a porous plug or a reducing valve. In this case the work done by the gas is reduced to the work against the intermolecular forces and is much smaller than the work that it might do by driving

a turbine or a piston in a reciprocating engine. The process is therefore irreversible and so the entropy increases. On the other hand, since $\mu = (\partial T/\partial p)_H > 0$, the temperature will decrease when the pressure is lowered. So when we have expanded the gas to normal pressure, its enthalpy will be smaller than before compression and its temperature will be lower. Moreover, since entropy decreases with decreasing temperature at constant pressure, the entropy of the gas after expansion will be less than before the compression. That is to say, the increase in entropy during the expansion is less than its decrease during compression.

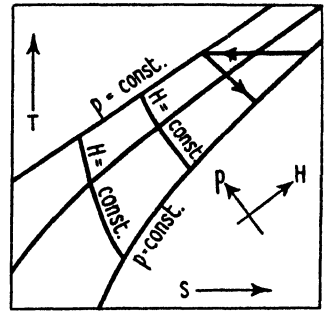

FIG. 119. Refrigeration cycle (*a*); temperature-entropy diagram.

Thus, by compressing at room temperature and expanding at constant enthalpy, we have lowered enthalpy, entropy, and temperature of the gas and so brought it nearer to liquefaction. The gas has, in fact, passed through a refrigeration cycle, which is shown on the schematical (T, S) diagram on Fig. 119.

(*b*) If the gas is expanded reversibly its entropy will remain constant. This can be achieved approximately by allowing the gas to press back a piston in a cylinder in such a way that the pressure behind the cylinder is the same as, or very slightly less than, the pressure of the gas at every point of the stroke. The same effect can be brought about with a turbine. In this way the entire decrease in entropy created by compressing the gas may be retained after the expansion. The entropy after isentropic expansion will therefore be less than after isenthalpic expansion. The temperature will therefore likewise be lower, and so will the enthalpy. The refrigerating cycle (*b*) (see Fig. 120) is therefore more effective than (*a*), since, by doing the same amount of work, we have brought the gas nearer to liquefaction.

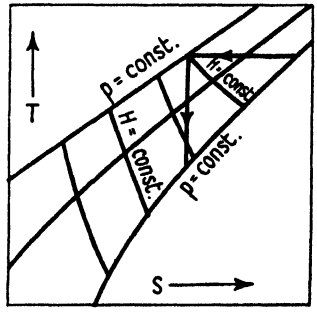

FIG. 120. Refrigeration cycle (*b*).

If μ is negative at room temperature for all pressures, the operation (*a*), carried out after compressing the gas, does not constitute

a refrigerating cycle at all, since the temperature of the gas will rise on expansion.

Neither of the cycles (*a*) and (*b*) is sufficiently potent to liquefy a permanent gas in a single operation. The thermal data of these gases, as shown by the diagrams, are such that, with pressures attainable in practice, a single cycle will not lower the temperature as far as the boiling-point, much less liquefy the gas. To ensure ultimate liquefaction, the cycle must be repeated in a way that will make its effect cumulative. This can be brought about by means of heat exchangers.

If the cold expanded gas be returned through a heat exchanger in counter-current with compressed gas, it will exchange heat with the latter. By a suitable design the expanded gas can be made to leave the exchanger almost at room temperature. It will thus have given up practically all its cold, $H_1 - H_0$, to the compressed gas. The latter will therefore leave the exchanger at a temperature lower than that of the surroundings, and its entropy and enthalpy will have been decreased, not merely by compression, but also by heat exchange. At the end of the expansion it will therefore be still colder than the first portion of the gas was at the same point of the apparatus. Since the expanded gas leaves the exchanger with almost its full original enthalpy H_1, the entire refrigerating effect of the cycle, which is equal to $H_1 - H_0$, will have been left inside the apparatus. The heat exchanger thus serves to accumulate the refrigerating effect of the cycle.

In the course of time the temperature behind the expansion valve or cylinder will fall, and with it the enthalpy and entropy of every cubic foot of gas as it passes this point. Finally, a state will be reached in which part of the gas will be liquefied. The liquid will collect at the bottom of the apparatus, and the amount of expanded gas returning through the heat exchanger per unit of time will gradually decrease. Simultaneously, its refrigerating capacity will decrease and it will no longer be able to absorb so much heat from the incoming compressed gas. The temperature of the latter behind the heat exchanger will therefore fall more slowly, and finally, as less and less expanded gas meets it, it will cease to fall altogether. From this moment on, a stationary state is reached; the temperature at all points of the apparatus will no longer vary with time; a certain portion out of every cubic foot of gas compressed will be liquefied and the rest will return through the heat exchanger.

In the stationary state the laws of conservation of mass and energy may be applied to the apparatus as a whole in the following way, if we assume that the liquid formed is continuously drained and removed from the plant.

Suppose the apparatus as a whole, consisting of heat exchanger and valve or expansion cylinder, is thermally insulated from the surroundings. Then

$$\sum E + \sum pv + W = \sum H + W = 0, \tag{13.15}$$

where $\sum$ denotes the sum of everything entering minus the sum of everything leaving the apparatus. Similarly, if m denotes the amount of gas or liquid,

$$\sum m = 0. \tag{13.16}$$

(*a*) If there is no expansion cylinder, $W = 0$. Suppose, in a specified time, 1 cubic foot of gas enters the apparatus (state 1), and suppose a fraction ϵ is liquefied (state 0). Then $(1-\epsilon)$ cubic feet leave the apparatus through the heat exchanger (state 2). Then

$$H_1 = \epsilon H_0 + (1-\epsilon)H_2$$

or

$$\epsilon = \frac{H_2 - H_1}{H_2 - H_0}. \tag{13.17}$$

But $H_2 - H_0 = Q_2$ is the total amount of enthalpy that must be removed from the gas to liquefy it entirely, starting from room-temperature and 1 atm. And $H_2 - H_1 = q$ is the amount of enthalpy withdrawn from the gas when 1 cubic foot is compressed isothermally. (This is, of course, less than the amount of heat which is actually taken up by the water cooling the compressor. In fact, neither Q_2 nor q appears as 'visible' heat and it is best to consider these expressions merely as abbreviations for the difference of two enthalpies.)

Thus $$\epsilon = q/Q_2 \quad \text{or} \quad q = \epsilon Q_2.$$

Since Q_2 is a characteristic constant of the gas and does not depend on the cycle employed, the efficiency of the cycle is determined by $H_2 - H_1 = q$.

(*b*) If an expansion engine is used, which may be a cylinder or a turbine, the latter performs an amount of work w. Then

$$H_1 = \epsilon H_0 + (1-\epsilon)H_2 + w,$$

and

$$\epsilon = \frac{H_2 - H_1 + w}{H_2 - H_0} = \frac{q + w}{Q_2}. \tag{13.18}$$

The 'liquefaction coefficient' ϵ is increased by w/Q_2 and the efficiency of the liquefier is determined by q and w.

The isenthalpic expansion of a compressed gas in a valve with a view to attaining its ultimate liquefaction is known as the Linde principle. It was used by Carl Linde when he first liquefied air on a commercial scale in 1895.

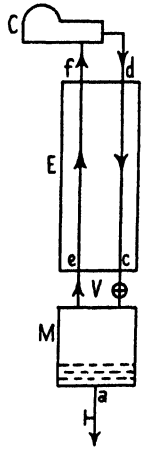

FIG. 121. Simple Linde liquefier.

The use of an expansion engine to lower the temperature of and finally liquefy a gas is known as the Claude principle. It was first used successfully by Georges Claude to liquefy air in 1902.

Linde Air Liquefiers

The simple Linde liquefier, which is shown schematically in Fig. 121, consists of a multi-stage compressor C, a heat exchanger E, the expansion valve V, and a container M for the liquid. The compressed air enters the heat exchanger at d and leaves it at c. In V it is expanded to atmospheric pressure and partially liquefied. The liquid may be drained off at a. The cold, uncondensed vapour re-enters the heat exchanger at e and is emitted to the atmosphere or back to the compressor at f. The entropy changes occurring in the process are shown in diagrammatic form in Fig. 122.

The efficiency of an air liquefier may be judged by the ratio of the theoretical to the practical work of liquefaction. We have seen that the former is 0·74 kWh. for a gallon of liquid air. The practical work of liquefaction is equal to the work of compressing to the pressure needed a quantity of air equivalent to 1 gallon of liquid, divided by the coefficient of liquefaction ϵ. For in order to obtain 1 gallon of liquid, we must pass an amount equivalent to $1/\epsilon$ gallons through the compressor. However, the practical work of liquefaction may be defined in two ways. It may be fixed as the work needed to liquefy a gallon of air in a plant of given type, assuming that the cycle is perfectly designed and constructed, or it may be taken as the work actually needed in practice. In most cases these two figures differ by a factor of approximately 2, for even the best liquefiers do not work without considerable losses. In practice the power consumption of a compressor is about 1·7 times as great as the work of isothermal compression which it is supposed to carry out, owing

partly to frictional losses and partly to the fact that compression is not really isothermal but takes place in a series of almost adiabatic stages. Moreover, the lagging of a low-temperature plant is never perfect, and this leads to the coefficient of liquefaction being smaller than it should be. In large plants, the heat losses due to imperfect lagging are approximately 0·3–0·4 B.Th.U. per cubic foot of gas

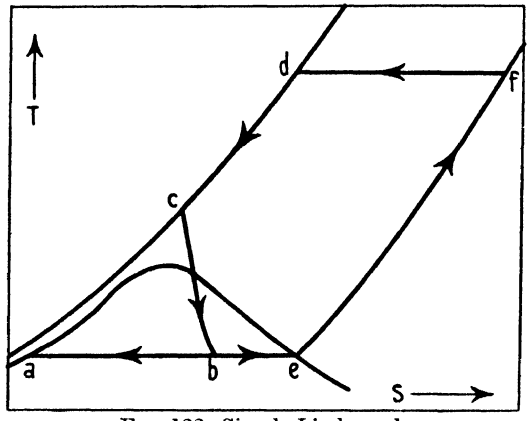

FIG. 122. Simple Linde cycle.

traversing the plant, and in small pieces of apparatus they may be considerably greater. Further losses will occur through imperfect heat exchange, since the expanded gas will leave the exchanger at a slightly lower temperature than that at which the compressed gas enters. In well-constructed heat exchangers this temperature head is about 2–3° C.

We have seen that the coefficient of liquefaction ϵ depends on the difference in enthalpy $H_f - H_d$ of outgoing and incoming gas. As may be seen from the diagram, this is the greater the higher the pressure of the latter. On the other hand, a higher pressure involves a greater work of compression. That the efficiency is nevertheless increased by raising the pressure is shown in Table 60, in which figures are given for working pressures of 50, 100, and 200 atmospheres.

TABLE 60. *Simple Linde Liquefier*

Working pressure, p, in atmospheres	50	100	200
Coefficient of liquefaction, ϵ	0·029	0·056	0·098
Theoretical power consumption, w', for ideal Linde plant, kWh./gallon	12·0	7·5	4·8
Practical power consumption, w	..	..	10·3
Theoretical power consumption for reversible process, w_0	0·74	0·74	0·74
Efficiency, w_0/w	..	..	7·2%

We see that the simple Linde cycle is a very inefficient process, even at 200 atmospheres. It has not been found expedient to increase the pressure still further, though it may be shown that an optimum should exist at about 450 atmospheres.

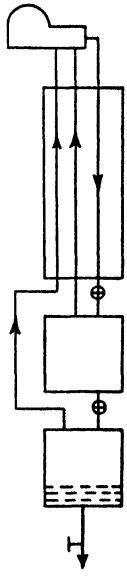

FIG. 123. Linde high-pressure cycle.

The efficiency of the Linde liquefier has been increased by two devices. One of these is the so-called high-pressure cycle. Only a part of the air is expanded to atmospheric pressure. The rest is brought to an intermediate pressure of from 30 to 50 atmospheres and is returned to the last stage of the compressor. Thus only a small part of the gas has to be compressed from 1 atmosphere to the intermediate pressure and the total amount need be raised only from the intermediate to the high pressure. Since the work of compression is roughly proportional to $\log p_1/p_2$, the first stages of compression are relatively the most costly. Thus the high-pressure cycle brings about a considerable reduction in the power consumption, which outweighs the disadvantage of a smaller refrigerating capacity $H_2 - H_1$.

The cycle is shown schematically on Fig. 123. Its efficiency depends on the choice of high and intermediate pressure and of the fraction ψ of air expanded to atmospheric pressure. It may be shown that the latter must be at least 20 per cent. Fig. 124 shows a series of curves which give the power consumption in kWh. per kg. of liquid air for a high pressure of 200 atmospheres as a function of the intermediate pressure for various values of ψ. The lowest value is 1·31 kWh. per kg. or 5·24 kWh. per gallon for $\psi = 20$ per cent. and an intermediate pressure of 60 atmospheres. In these curves heat losses have been neglected, and the lowest practical figure is 6·0 kWh. per gallon, or 58 per cent. of the power consumption for the simple cycle. The efficiency of this plant is 12·3 per cent.

The second device for increasing the efficiency of the Linde liquefier consists in pre-cooling the compressed air with liquid ammonia boiling under reduced pressure at about $-50°$ C. As may be seen from Fig. 117, the curves of constant enthalpy become much steeper as the temperature falls. The difference in enthalpy between expanded and compressed gas is much greater at $-50°$ than at room

temperature. Thus a greater refrigerating effect is produced with the same power consumption. The additional power consumption

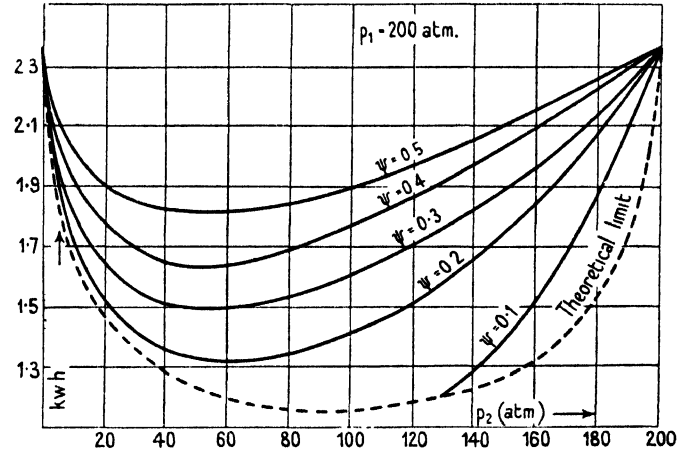

FIG. 124. Power consumption of Linde high-pressure cycle in kWh. per kg. of liquid air.

of the ammonia cycle is small as compared with the economy obtained through the increase in ϵ. A combination of the high-pressure and ammonia cycles brings the practical power consumption per gallon of liquid air down to 3·49 kWh. and raises the efficiency to 21 per cent. Table 61 summarizes the data for Linde liquefiers.

TABLE 61. *Linde Air Liquefiers*

Type	*Simple*	*High-pressure*	*High-pressure and ammonia*
ϵ	0·10	0·07	0·20
w', theoretical .	4·81	2·72	1·60
w, practical . .	10·3	6·0	3·49
Efficiency . .	7·2	12·3	21

Claude and Heylandt Liquefiers

In these liquefiers use is made of isentropic expansion of compressed air in a cylinder. When Georges Claude began his experiments in 1899 he intended to use this principle alone and to liquefy the air in the expansion cylinder. However, this was soon found to be impracticable. At pressures and temperatures near the critical point, expansion in a cylinder is very inefficient. Thus, though it is quite possible to lower the temperature in this way, the coefficient

of liquefaction remains very small. Moreover, great difficulties were experienced with regard to lubrication of the expansion engine. Ordinary lubricating oils are solid at these low temperatures, and so Claude lubricated his cylinders with petroleum ether, which, at temperatures slightly above the boiling-point of air, has fair lubricating properties. At the lowest temperatures, liquid air itself was used as a lubricant, but not very successfully.

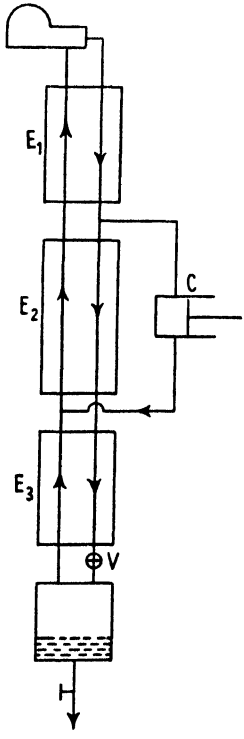

FIG. 125. Claude liquefier.

The advantages of the Claude liquefier did not become apparent until, in 1902, the idea of liquefying air in the cylinder was abandoned. Thereafter isentropic expansion was employed only to cool the air. Actual liquefaction was brought about by expanding a separate circuit of compressed air in a valve, as in the case of the Linde plant. The Claude liquefier thus assumes the rather complicated form depicted in Fig. 125.

After passing through the heat exchanger E_1, the compressed air separates into two branches. One continues through the exchangers E_2 and E_3, is expanded to atmospheric pressure in the valve V, and is partially liquefied. The uncondensed, expanded air returns through all three exchangers. The other, major, portion of compressed air is expanded and cooled in the expansion engine C, after which it joins the outgoing air between E_2 and E_3.

In the Claude plant the air is compressed to 40 atmospheres; it enters the expansion cylinder at $-80°$ C. and leaves it at about $-160°$. Eighty per cent. of the air passes through the cylinder and only 20 per cent. through the valve. Thus the engine carries the weight of the process, the valve being an additional device to improve the efficiency.

The efficiency of this type of plant depends in rather a complicated way on a number of factors: the amount of air M expanded in the valve, the temperature T_2 at which the air enters the cylinder, and the working pressure p_1. A theoretical computation is difficult, as the practical efficiency of the expansion engine itself depends on the

temperature and pressure of the ingoing gas. In Fig. 126 the process is shown on the (T, S) diagram. The line 2–5, giving the isentropic expansion, should in theory be vertical. In actual fact it is not vertical, since the expansion is not truly isentropic. Heat is transferred to the air from the walls of the cylinder during the expansion and the heat transfer itself depends on temperature and pressure of the gas. The shape of the line 2–5 can be determined only by experiment.

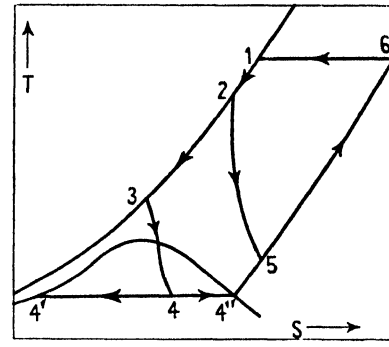

FIG. 126. Claude cycle.

It can be shown that for every value of M and p_1 a most favourable temperature T_2 exists at which the air should enter the cylinder. If this condition is fulfilled, we obtain empirical curves giving the power consumption per kg. of liquid air as a function of M for various pressures. These curves are shown in Fig. 127. We see that at 40 atmospheres and $M = 0{\cdot}2$, which are Claude's conditions, 3·4 kWh. are needed to produce a gallon of liquid air (0·89 kWh. per kg.), which is about the same as in the case of Linde liquefiers. For these conditions $T_2 = -80°$ C. On the other hand, it is apparent that by raising p_1 and M, greater efficiency can be obtained. This was the line taken by Heylandt, whose liquefiers operate at 200 atmospheres with $M = 0{\cdot}45$. The power consumption is reduced to 2·9 kWh. per gallon (0·76 kWh. per kg.), but this is not the only advantage. It could be shown that the optimum temperature T_2, at which the air should enter the cylinder, is room temperature under these conditions. In the Heylandt plant the air is therefore conducted straight from the compressor to the expansion cylinder without any intermediate heat exchanger, so that E_1 in Fig. 125 vanishes. The expanded air leaves the engine at about $-130°$ C., at which lubrication is still fairly simple. Heylandt's system is thus a very finely balanced synthesis of the Claude and Linde processes.

Cascades

It has been shown that Linde succeeded in raising the efficiency of his liquefier by pre-cooling the compressed air with liquid ammonia. This is only one example of a very general principle, well known in

refrigeration engineering, that it is profitable to let the refrigerant absorb as much heat as possible at the highest possible temperature.

In the case of the Linde liquefier, the ammonia absorbs heat at $-50°$ C. and above, which would otherwise have to be transferred to the expanded air at a lower temperature. The ammonia is itself

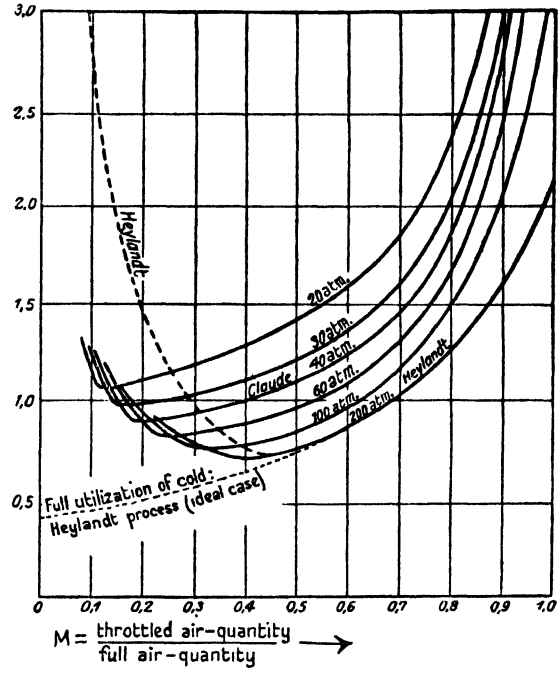

FIG. 127. Power consumption in kWh. per kg. of liquid air as a function of M.

liquefied at room temperature at about 10 atmospheres pressure and the liquid ammonia then expanded.

This effect can be enhanced by employing a whole series of intermediate refrigerants, each of which can be liquefied under pressure in the liquid of the one with the next higher boiling-point. This so-called 'cascade principle', which goes back as far as Pictet's experiments of 1877, was developed by Olszewski at Krakov in the eighties and perfected by Kamerlingh Onnes at Leiden, and was for many years the basis of the Dutch low-temperature school. The Leiden cascade consisted of four cycles, methyl chloride, ethylene, oxygen, and nitrogen [3].

In recent years, largely as a result of Keesom's calculations [4],

there has been much talk of employing cascades for commercial purposes. The four-cycle cascade suggested by Keesom for liquefying nitrogen, consists of ammonia, ethylene, methane, and nitrogen cycles. It is shown schematically in Fig. 128, and, according to Keesom's very lucid computation, requires only 2·05 kWh. per gallon of liquid nitrogen. This figure includes all thermal and frictional losses that may be expected to occur in practice.

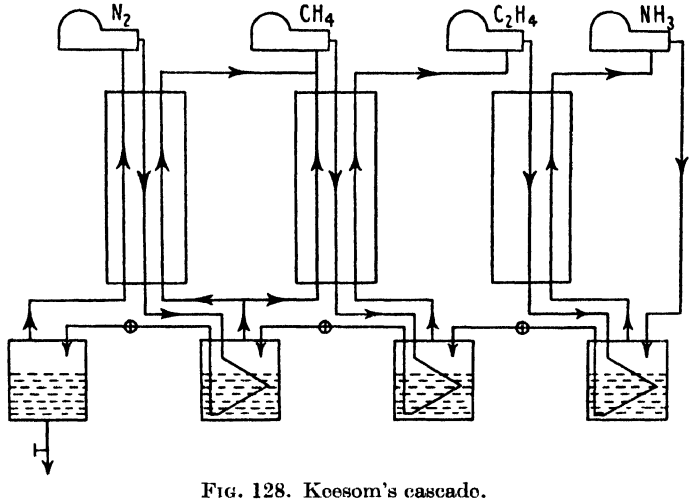

FIG. 128. Keesom's cascade.

From Keesom's detailed analysis of the liquefaction process the particular advantage of the cascade may be understood rather better than from the general remarks at the beginning of this paragraph. If we disregard for the moment the losses in the compressor, and concentrate on those in the liquefier itself, we can see that the increased power consumption, as compared with the theoretical work of liquefaction, is due to irreversible changes occurring within the apparatus. Such irreversible changes take place every time a compressed gas or liquid is expanded in a valve, or when two substances are brought into thermal contact at different temperatures, or when a gas is expanded in a cylinder under incompletely adiabatic conditions. It can be shown quite generally that every such occurrence, connected with an increase of entropy ΔS, entails the expenditure of an additional amount of work equal to $T_1 \Delta S$, where T_1 is room temperature, or, more generally, the temperature at which the work is to be performed.

Now the advantage of a cascade over a Linde liquefier is to be found in the fact that only liquids are expanded in valves, but no gases. The increase in entropy undergone by a liquid boiling at any pressure, when it is expanded to a lower pressure in a valve, is less than the corresponding entropy increase of an expanding gas. For example, when air at 25° C. is expanded at constant enthalpy from 40 to 1 atmosphere, its entropy increases by 0·25 kcal. per kg. and degree, whereas when liquid air is similarly expanded the corresponding increase is only 0·15 kcal. Actually the discrepancy is still greater, since the Linde method requires pressures up to 200 atmospheres, which entail entropy losses of 0·34 unit, while the cascade needs only 25 atmospheres, which gives $\Delta S = 0{\cdot}13$ unit. Since the losses incurred through expansions in valves are by far the greatest losses in these plants, this makes the advantages of the cascade particularly plain.

Application of the Linde Principle to the Liquefaction of Hydrogen and Helium

We have seen that the Linde principle of isenthalpic expansion is applicable only if the isothermal expansion coefficient

$$\alpha = (\partial H/\partial p)_T < 0,$$

or, which comes to the same thing, the Joule-Thomson coefficient $\mu = (\partial T/\partial p)_H > 0$. We have seen that, in the case of air, this condition is fulfilled at all available pressures from room temperature downwards. On the other hand, it is evident from an inspection of the (T, S) diagram in Fig. 117 that the lines of constant enthalpy become less and less steep as the temperature rises, and we may surmise that, at still higher temperatures, the slope of these curves will change its sign. We shall, in fact, approach the inversion curve of the Joule-Thomson coefficient, which was discussed in Chapter XI.

This typical behaviour of the lines of constant enthalpy is illustrated much more clearly in Fig. 129, which shows the (T, S) diagram for helium. It is evident that, at about 40° abs., these curves change their direction. The curves below 40° slope downwards from left to right. While those marked 55 and 60 display flat maxima in the pressure interval covered, those from 65 on slope upwards from left to right. We have passed through the region of the inversion curve. As the temperature increases, the curves become steeper and steeper;

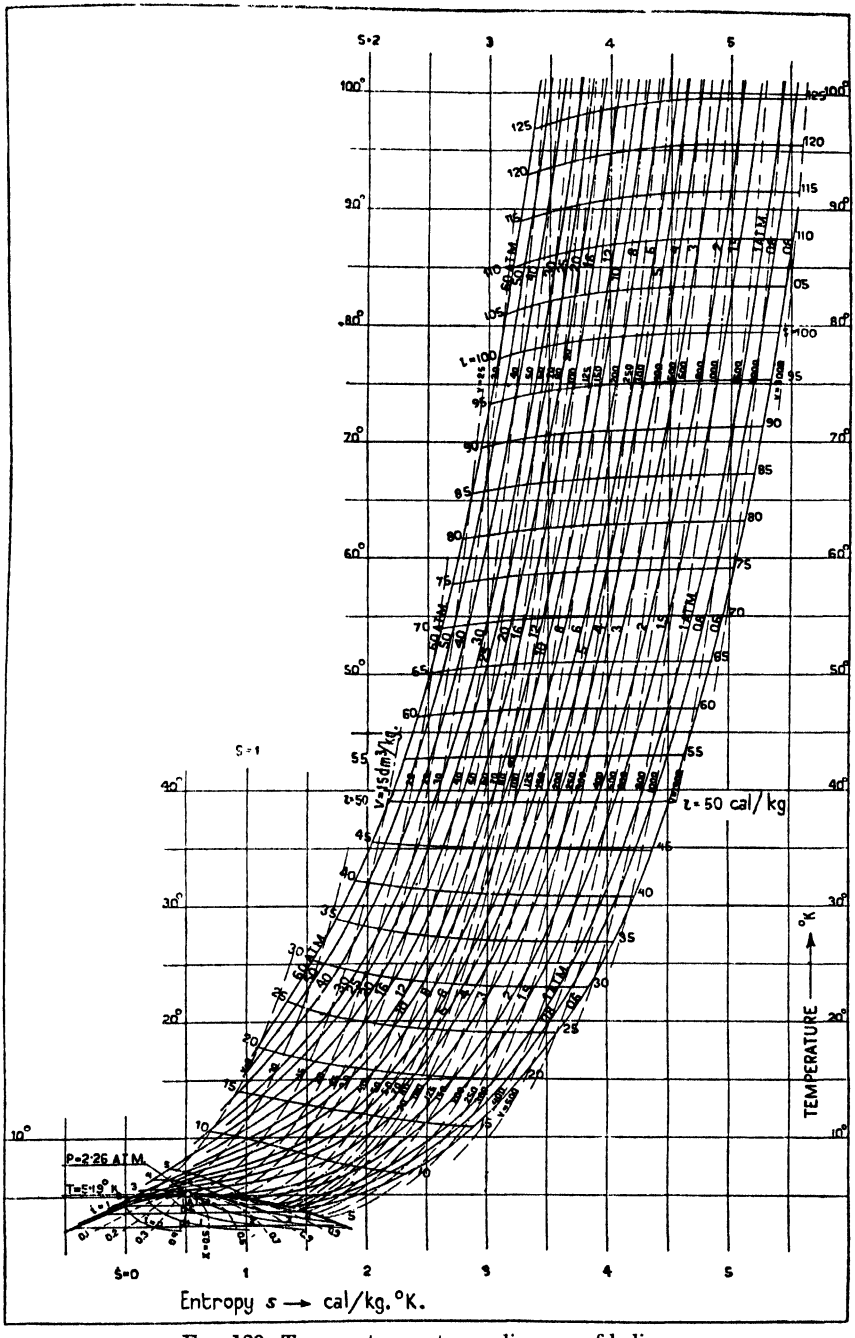

FIG. 129. Temperature-entropy diagram of helium.

μ becomes more and more negative and α assumes greater and greater positive values. The same phenomena are exhibited by hydrogen round about 170° K. As was to be expected from the law of corresponding states, and as was explained in Chapter XII, hydrogen and helium are the only two gases whose inversion curves lie wholly below room temperature.

It is therefore clear that these two gases cannot be liquefied by the Linde method if we start from room temperature. Hydrogen will have to be pre-cooled at least to 170° K. and helium at least to 40° K. before the method will be applicable. Moreover, since the isenthalpic curves become steeper the farther we proceed away from the inversion region, it will be advisable to pre-cool the gases well below the temperatures mentioned.

In spite of this difficulty, the Linde method was until recently the only method by which these gases could be liquefied, since it was not possible to design an expansion engine that would function at such low temperatures. This problem was solved in 1934 by Kapitza in Cambridge [5]. In liquefiers of the Linde type hydrogen is pre-cooled with liquid nitrogen and helium with liquid hydrogen, both refrigerants boiling under greatly reduced pressures.

The question soon arose as to which pressures were the most advantageous for the liquefaction of hydrogen and helium. Since the apparatus was designed for laboratory use and not primarily for industrial purposes, the power consumption was less important than the coefficient of liquefaction. It was desirable to liquefy a few litres quickly and not very important how many kilowatt-hours were needed. We have seen on p. 341 that the liquefaction coefficient for air rose from 0·029 at 50 atmospheres to 0·098 at 200 atmospheres, and this was also incidentally the essential factor influencing the power consumption. However, it would be wrong to conclude that, in the general case, the higher the pressure the greater ϵ. It would be very unwise to attempt to liquefy helium at 200 atmospheres.

Assuming that we have fixed the starting temperature, which must, of course, be below the upper limit of the inversion curve, the most advantageous pressure, from the point of view of the liquefaction coefficient, can be deduced as follows:

Our condition is that ϵ shall be a maximum, and so we may write

$$\left(\frac{\partial \epsilon}{\partial p}\right)_T = 0. \tag{13.19}$$

Now we have seen that, in the Linde process,

$$\epsilon = \frac{H_2 - H_1}{H_2 - H_0},$$

where 0, 1, and 2 refer to the liquid, the compressed gas, and the expanded gas respectively, the last two at the starting temperature. Of these three quantities, only H_1 is a variable, as it may be altered by varying the pressure, and we may write

$$\epsilon = \frac{H_2 - H}{Q} = -\frac{1}{Q}\int_2^p \left(\frac{\partial H}{\partial p}\right)_T dp. \tag{13.20}$$

But according to equation (13.5),

$$\left(\frac{\partial H}{\partial p}\right)_T = -\mu C_p.$$

Therefore

$$\epsilon = \frac{1}{Q}\int_2^p \mu C_p \, dp. \tag{13.21}$$

Then our condition is that

$$\left(\frac{\partial \epsilon}{\partial p}\right)_T = \frac{1}{Q}\frac{\partial}{\partial p}\int_2^p \mu C_p \, dp = \frac{\mu C_p}{Q} = 0. \tag{13.22}$$

Since C_p and Q are essentially positive, our condition for a maximum liquefaction coefficient reduces to $\mu = 0$. That is to say, at a given temperature below the upper limit of the inversion curve, p must be so chosen that the point from which liquefaction starts lies on the inversion curve.

To make sure that, on the inversion curve, ϵ is indeed a maximum and not a minimum, we must form the second derivative of ϵ by the pressure.

From equation (13.22),

$$\left(\frac{\partial^2 \epsilon}{\partial p^2}\right)_{TT} = \frac{1}{Q}\left[\left(\frac{\partial \mu}{\partial p}\right)_T C_p + \mu\left(\frac{\partial C_p}{\partial p}\right)_T\right]. \tag{13.23}$$

For $\mu = 0$ this reduces to

$$\left(\frac{\partial^2 \epsilon}{\partial p^2}\right)_{TT} = \frac{C_p}{Q}\left(\frac{\partial \mu}{\partial p}\right)_T. \tag{13.24}$$

If ϵ is to be a maximum, the expression on the right-hand side must be negative. Now C_p and Q are essentially positive, and $(\partial\mu/\partial p)_T$ is

negative along the inversion curve, since, by definition, on passing through the curve from lower to higher values of p, μ changes from a positive to a negative quantity. So ϵ is indeed a maximum when $\mu = 0$.

In the case of air at room temperature, the optimum pressure is about 450 atmospheres. For hydrogen at 70° K. (temperature of liquid nitrogen boiling under reduced pressure) p should be chosen at 160 atmospheres. For helium at 17° K. (liquid hydrogen at reduced pressure) p should be 35 atmospheres. These are the pressures at which hydrogen and helium liquefiers are actually run [6].

The Significance of Gas Liquefaction

The large-scale air liquefiers, designed by Linde, Claude, Heylandt, and others, were developed with a view to producing commercial oxygen. The separation of air into its two principal components can be effected by the same methods of fractionation as are employed for the purification of alcohol and the refining of petroleum, but in order to bring about the necessary two-phase equilibrium the air must first be liquefied. In this way liquefaction became a preliminary step in the separation of gaseous mixtures.

Well into the beginning of the present century oxygen was the only valuable constituent of atmospheric air; but since then the development of the synthetic ammonia industry has created a demand for pure nitrogen, the importance of argon has been realized as a medium for filling incandescent lamps, and considerable quantities of neon are required mainly for advertising purposes. In recent times attempts have been made to replace argon in lamps by a mixture of krypton and xenon, and the krypton discharge lamp is considered as a possible innovation in street lighting.

Moreover, apart from air, other natural and industrial gases are separated by low-temperature methods into fractions and pure components. Natural gases have been made to yield helium, hydrogen is obtained from coke-oven gas, and the mixtures formed in petroleum-cracking have become valuable sources of ethylene and propylene. The inventions of Linde and Claude have thus led to the development of a large low-temperature industry, which is now widely distributed in Europe and America.

But quite apart from its industrial objects, the liquefaction of gases has had far-reaching scientific consequences, in that it has

brought low temperatures within the sphere of physical and physico-chemical research. An entirely new field has been opened up in which scientists have approached nearer and nearer to the absolute zero of temperature and studied the properties of matter under these conditions. Yet the relations between gas liquefaction and the attainment of low temperatures are by no means as clear as is often imagined.

We have seen that low temperatures are essential for the liquefaction of the so-called permanent gases, and it is frequently supposed that, conversely, gas liquefaction is essential for the production of yet lower temperatures. But this is only partly true. The existence of liquid air as a comparatively cheap commodity does indeed supply us with an unlimited reservoir of cold as a starting-point for low-temperature research, and the possibility of obtaining liquid hydrogen and liquid helium in the laboratory extends these facilities to yet lower temperatures. And yet, from another point of view, many low-temperature research workers would be glad if these gases did not become liquid at all.

The value of gases as refrigerating agents for the production of low temperatures is due to their high compressibility, as a result of which it is possible to perform a large amount of work on a gas and, conversely, for the gas to perform work, without involving very high pressures. We have seen that refrigeration requires the expenditure of work, and the gases are necessary to take up this work. Now when a gas is liquefied, though it constitutes a valuable reservoir of cold, its capacity as a refrigerant for obtaining lower temperatures is exhausted. As a practically incompressible liquid it can no longer have work performed upon it. Thus the lowest temperatures that can be produced by means of a given gas are those at which it can be made to boil at the smallest pressures available. Fortunately a series of gases exist with widely different boiling-points, which cover a great part of the temperature scale. But for many purposes it would be exceedingly useful if air did not become liquid at $-190°$ C. and if we could continue to cool it with Joule-Thomson expansions to the vicinity of absolute zero. The fact that air is useless for obtaining temperatures below $-200°$ and that we must have recourse first to hydrogen and then to helium has vastly complicated low-temperature technique.

Helium, the gas with the lowest boiling-point (4·2° abs.), deter-

mines the lowest temperatures which can be attained by the methods outlined above. All attempts to produce yet lower temperatures by reducing the vapour pressure over liquid helium have not been able to go far beyond 1° abs. The recent developments in low-temperature physics, in which results of great interest have been obtained at temperatures only a few thousandths of a degree above absolute zero, have been achieved by very different methods, which have nothing to do with the compression and expansion of gases and which are therefore beyond the scope of our subject.

BIBLIOGRAPHY

1. H. Hausen, *Forschung auf dem Gebiet des Ingenieurwesens*, p. 274 (1924).
2. A. Eucken and W. Berger. See Chapter XII.
3. H. Kamerlingh Onnes, *Leiden Communications*, 158 (1926).
4. W. H. Keesom, *Leiden Communications*, Suppl. 76A.
5. P. Kapitza, *Proc. Roy. Soc.* (A), **147**, 189 (1934).
6. W. Meissner, *Handbuch der Physik*, **11** (1926).

XIV

THE INFLUENCE OF PRESSURE UPON THE SOLUBILITIES OF GASES AND UPON THE VAPOUR PRESSURE OF LIQUIDS

THE equations for equilibrium developed in Chapter XII may be applied to binary gas-liquid systems. Thus, for example, in (12.12),

$$\left\{(v_2-v_1)-(x_2-x_1)\frac{\partial v_1}{\partial x_1}\right\}dp = (x_2-x_1)\frac{\partial \mu_1}{\partial x_1}dx_1,$$

subscripts 1 and 2 may be taken as referring to the liquid and gas phases respectively, x is the mol fraction of gas, $(1-x)$ that of the liquid, v is the specific volume, and $\partial\mu/\partial x = \partial^2 F/\partial x^2$, where F is the free energy. Employing this equation, the effect of change of pressure on the compositions of the two phases may be determined by the following method [1].

The Composition of the Liquid Phase

Since the concentration of gas in the solvent is usually small, both x_1 and $(1-x_2)$ are small and (12.12) therefore reduces to

$$v_2-v_1-\left(\frac{\partial v_1}{\partial x_1}\right)_{p,T} = \frac{\partial^2 F_1}{\partial x_1^2}\frac{dx_1}{dp}. \tag{14.1}$$

The specific volume of the gas phase, v_2, is approximately equal to the specific volume of the pure gas, V, at the same temperature and pressure. Also $\partial v_1/\partial x_1$ is the change in the volume of the liquid when 1 mol of solvent is replaced by 1 mol of gas, and, putting $v_1+\partial v_1/\partial x_1 = \Delta v$, (14.1) becomes

$$V-\Delta v = \frac{\partial^2 F_1}{\partial x_1^2}\frac{dx_1}{dp}. \tag{14.2}$$

For small values of x_1 we may write

$$\frac{\partial^2 F_1}{\partial x_1^2} = \frac{RT}{x_1(1-x_1)} = \frac{RT}{x_1},$$

and substituting in (14.2),

$$V-\Delta v = RT\frac{d\log_e x_1}{dp}. \tag{14.3}$$

In order to take into account the deviation of the gas from the ideal state we put $\alpha = pv/RT - 1$ and substitute in (14.3), which then becomes

$$\frac{d\log_e x_1}{dp} = \frac{1}{p}\frac{pV}{RT} - \frac{\Delta v}{RT} = \frac{1+\alpha}{p} - \frac{\Delta v}{RT}. \tag{14.4}$$

On integrating,

$$\log_e \frac{x_1}{p} = \int \frac{\alpha}{p}\,dp - \frac{1}{RT}\int \Delta v\,dp + A'. \tag{14.5}$$

When (14.5) is written in practical units and Δv is expressed in c.c. per mol,

$$\log_{10} \frac{x_1}{p} = 0{\cdot}4343 \int \frac{\alpha}{p}\,dp - 0{\cdot}0052936 \int \frac{\Delta v}{T}\,dp + A. \tag{14.6}$$

If it be assumed that Δv is constant, then

$$\log_e \frac{x}{p} - \int_0^p \frac{\alpha}{p}\,dp = A' - p\frac{\Delta v}{RT}, \tag{14.7}$$

and, by plotting the left-hand side as a function of p, the slope of the resultant line gives Δv and the intersection with $p = 0$ gives A'.

Composition of the Gas Phase

In dealing with the gas phase it is more convenient to employ (12.13):

$$\left\{(v_1 - v_2) - (x_1 - x_2)\frac{\partial v_2}{\partial x_2}\right\} dp = (x_1 - x_2)\frac{\partial^2 F_2}{\partial x_2^2}\,dx.$$

We may simplify this equation by putting $x_1 = 0$, $x_2 = 1$, and

$$\frac{\partial^2 F_2}{\partial x_2^2} = \frac{RT}{x_2(1-x_2)},$$

which gives

$$v_1 - v_2 - \frac{\partial v_2}{\partial(1-x_2)} = \frac{RT}{1-x_2}\frac{d(1-x_2)}{dp},$$

or

$$v_1 - V - \frac{\partial V}{\partial(1-x_2)} = \frac{RT\,d\log_e(1-x_2)}{dp}. \tag{14.8}$$

In order to calculate the quantity of solvent vapour, β, per unit volume of the gas phase, it is assumed that

$$\beta = \frac{1-x_2}{v_2} \sim \frac{1-x_2}{V}$$

and hence $$\frac{d\log_e\beta}{dp} = \frac{d\log_e(1-x_2)}{dp} - \frac{1}{\bar{V}}\left(\frac{\partial V}{\partial p}\right)_T, \tag{14.9}$$

or $$RT\frac{d\log_e\beta}{dp} = v_1 - V - \frac{\partial V}{\partial(1-x_2)} - \frac{RT}{V}\left(\frac{\partial V}{\partial p}\right)_T, \tag{14.10}$$

which is the equation for the change in composition of the gas phase with pressure. It will be noted that according to (14.10) the number of molecules of solvent vapour in the gas phase increases with the pressure.

Units

The experimental data for solubilities are usually expressed in one or other of the following units:

1. *The Bunsen Absorption Coefficient* (ϕ) is the volume of gas, reduced to 0° C. and 760 mm. pressure, which at the temperature of the experiment is dissolved in 1 volume of the solvent when the partial pressure of the gas is 760 mm.

2. *The Ostwald Absorption Coefficient* (χ) is the ratio of the concentrations of the gas in the liquid and gas phases respectively.

3. *The Kuenen Absorption Coefficient* (ψ) is the volume of gas reduced to 0° C. and 760 mm. pressure which at the temperature of the experiment is dissolved in 1 gm. of the solvent when the partial pressure of the gas is 760 mm.

The following relationships hold between the three coefficients:

$$\phi = \frac{273{\cdot}1}{T}\chi, \tag{14.11}$$

$$\psi = \frac{\chi}{\left(1+\frac{t}{273{\cdot}1}\right)}\rho, \tag{14.12}$$

where ρ is the density of the solvent.

Definition of Partial Molal Volume. One mol of solution consisting of n_1, n_2, etc., mols of components A, B, etc., is that quantity in which $n_1+n_2+\ldots = 1$. Its volume v, called the molal volume, is given by $v = V/(n_1+n_2+\ldots)$, where V is the total volume of the solution. The partial molal volume of any one of the constituents, A, is $\partial V/\partial n_1 = \overline{v_1}$, and may be defined as the increase in volume produced by the addition of 1 mol of A to such an amount of the solution that no appreciable change in composition results; it may be either positive or negative in sign.

If the volumes, V, of a solution, containing a constant amount of solvent and varying quantities of one of the components B, are

measured, then on plotting V against n_2 the slope of the tangent to the resulting curve at any point gives the partial molal volume $\overline{v_2}$ of the solute. Alternatively, by plotting values of the molal volume v of the solution against the mol fraction N_2 of component B, the slope of the tangent to the curve at any point is dv/dN_2, and it can be shown that

$$v - N_2 dv/dN_2 = \overline{v_1}, \tag{14.13}$$

and

$$v + N_1 dv/dN_2 = \overline{v_2}. \tag{14.14}$$

Henry's law states that the volume of gas measured at S.T.P., dissolved in a liquid, is directly proportional to its partial pressure, provided no combination takes place between solvent and solute.

If N_2 is the mol fraction of the gas in solution and p_A is its partial pressure, then, according to the law,

$$p_A/N_2 = k, \tag{14.15}$$

where k is known as Henry's law constant.

Eq. (14.7) indicates that Henry's law (x proportional to p) can only hold when α and Δv are negligible, or in the special case when the sum of the two integrals happens to be zero; the former condition is realized at low pressures and the latter when the gas is above the Boyle temperature and α is positive. The variation of k with pressure for nitrogen dissolved in water is as follows:

TABLE 62. *Henry's Law Constant for Nitrogen (Saddington and Krase)*

Temperature, °C.	*Pressure (atmospheres)*			
	1	*100*	*200*	*300*
50	86·8	104·2	110·0	117·2
80	101·9	110·4	114·8	124·6
100	..	108·6	109·4	117·8
200	..	49·2	54·7	54·5

The Experimental Determination of the Influence of Pressure on the Equilibrium of a Liquid-Gas System

It will be evident from the considerations outlined above that the determination of the equilibrium conditions in a liquid-gas system involves the measurement of the composition of the two phases, the partial molal volumes of the two components in each phase, and the compressibilities of the two phases over sufficiently wide ranges of temperature and pressure. These measurements are not easy to carry out at high pressures, and although the effect of pressure on

the solubilities of gases and on the composition of the gaseous phase have been determined separately, the complete data for any one system is seldom available.

There are two methods in general use for determining solubilities at high pressures, the one depending upon the direct measurement of the amount of gas required to saturate a known volume of solvent,

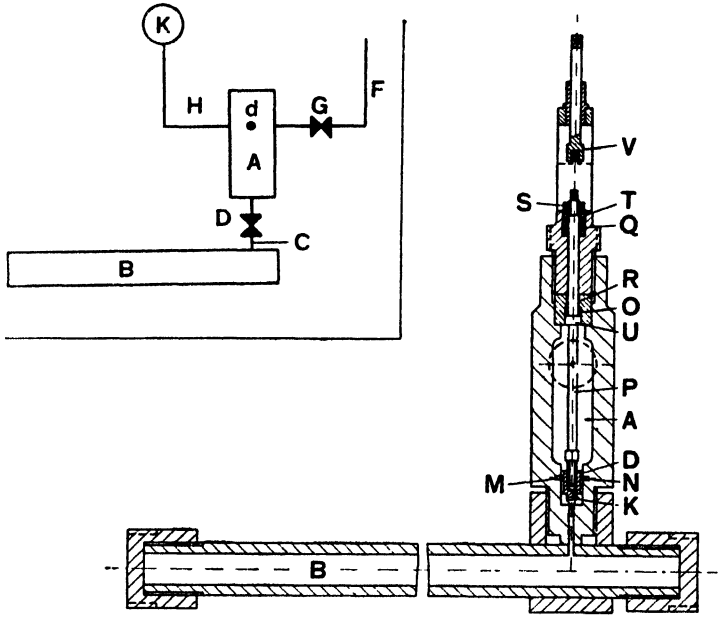

FIG. 130. Apparatus used by Michels, Gerver, and Bijl to determine the solubility of methane.

and the other upon the analysis of a known amount of the saturated solution. The first method has been used by Wiebe and Tremearne [2] and by Michels, Gerver, and Bijl [1]. It is suitable for sparingly soluble gases at temperatures far removed from the critical temperature of the solvent. The second method, which is more flexible, has been employed by Frolich and collaborators [3], Goodman and Krase [4], and Wiebe and collaborators [5]. It has also been adapted by Saddington and Krase [6] to give complete data for the equilibrium of the system nitrogen-water in both phases.

The apparatus employed by Michels, Gerver, and Bijl is illustrated in Fig. 130. The tube *B* has a capacity of about 300 c.c. and is filled with the solvent leaving a free space of about 10 c.c. The vessel *A* (capacity *circa*

10 c.c.) is filled with the gas under pressure. The two vessels communicate by a capillary channel, closed by the valve D which is operated from above. Gas is supplied to A through the valve G and its pressure is indicated by means of the gauge K. The apparatus is suspended on the axis d, about which it can be rocked in either direction through about 40°. The whole system, with the exception of the gauge, is placed in a thermostat which can be maintained constant to within 0·001°; the gauge is placed in a separate case maintained at the same temperature as the rest of the apparatus. The whole apparatus as far as it comes in contact with the solvent is made of stainless steel.

In carrying out a determination a measured volume of solvent is first introduced into B. With the valve D shut, the vessel A is then filled with gas and the pressure noted. The valve is then opened, and the immediate drop in pressure gives a check on the free volume above the liquid in B. The apparatus is rocked for several hours, and from the pressure drop and the known volumes of gas and solvent the solubility is calculated. The accuracy of the measurements is limited by the accuracy of the pressure gauges; three gauges reading to 50, 250, and 1,000 atmospheres were employed, and by means of frequent calibrations the readings could be made to 0·02, 0·1, and 0·5 atmosphere respectively.

Wiebe and Tremearne have employed a similar form of apparatus with the addition of a device for measuring the variation in the volume of solution with composition. This consists of a tube of known volume, fitted with a valve at each end, and connected with the lower part of the vessel B. By operating the valves a sample of the saturated solution may be withdrawn and subsequently analysed. Samples may also be obtained at concentrations intermediate between the pure solvent and the saturated solution; thus, for example, a sample may be taken of a 400-atmosphere equilibrium mixture and before closing the valve the pressure in B may be raised to, say, 600 atmospheres by gas pressure. The new pressure is transmitted instantly to the sample without any immediate increase in its gas content.

The apparatus used by Saddington and Krase is shown schematically in Fig. 131. The solute gas is compressed from a large gas-holder C, through a drying tower E containing calcium chloride, to three 1 cub. ft. capacity cylinders. These provide sufficient gas to ensure constant pressure conditions in the apparatus during the course of an experiment. From these cylinders the gas passes through a charcoal absorption trap to the pre-saturating bottles 1 and 2 which have a capacity of 150 c.c. and are constructed of stainless steel; they are kept half-full of solvent and are maintained at a temperature 10° higher than that of the solubility apparatus proper. The saturated gas then passes into the equilibrium bottle 3 and through one or both of the bottles 4 and 5 to the gasometer B. When so desired additional solvent can

be introduced into bottles 4 and 5 under pressure by means of the Cailletet hand-pump *G*. The bottles 3–5 are contained in a thermostat *J* maintained at the experimental temperature, and all connexions and valves through which the saturated gas passes are kept at a temperature sufficiently above this to ensure that no condensation takes place. Pressures are measured by means of a dead-weight pressure balance and temperatures by means of a number of thermocouples, the positions of which are indicated in the figure.

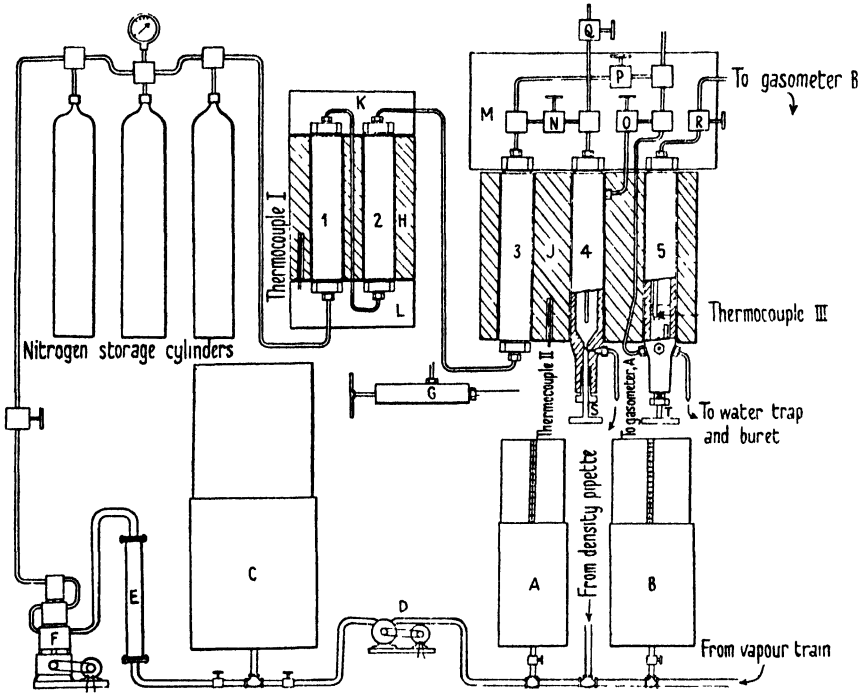

FIG. 131. Apparatus used by Saddington and Krase to determine the equilibrium of a gas-liquid system at high pressures.

Analysis of the Liquid Phase. Gas is allowed to bubble through the solvent for about 15 hours and 5 to 10 gm. of the solution are then withdrawn through the valve *T* into a combined trap, condenser, and anhydrone drying train which is cooled in an ice bath. The expanded gas from the sample is led into a gas burette of capacity 30 c.c., graduated in 0·05 c.c. divisions. The expanded solvent is allowed to stand for 15 minutes or more to allow of complete separation of the dissolved gas. After measuring the expanded gas volume, dry nitrogen is passed through the exit tubing of the sampling line to carry over any deposited solvent to the trap.

Analysis of the Gas Phase. The upper part of bottle 5 houses a spray trap which consists of a roll of tightly wound copper gauze. The gas-phase samples are expanded through the valve *R* which is kept at a temperature 25–50°

above the solubility temperature. The expanded gases are passed through a heated tube to the analytical train consisting of three U-tubes, the first of which is packed with anhydrone and absorbs at least 95 per cent. of the solvent; the remaining two are packed with copper wool and are immersed in liquid air.

The Density of the Liquid Phase. The volume of bottle 4 is accurately measured and liquid from bottle 3 is then allowed to enter through the valve N until the experimental pressure is reached. The contents of the bottle are then analysed as described for the gas phase.

Errors and Corrections

Apart from the usual experimental errors associated with the measurement of temperature, pressure, and volume, errors may arise from the imperfect attainment of equilibrium and from the neglect of certain corrections which, at high pressures, may be of importance. Of these mention may be made of (*a*) the change in the partial pressure of the vapour of the solvent due to a change in the total pressure, and (*b*) the change in the volume of the solvent due to its compressibility and to the solution of the gas.

The correction for the change in the partial pressure may be calculated from (12.1) and for the compressibility from available data, by the use of the equation

$$v' = v(1-kP), \tag{14.16}$$

where k is the coefficient of compressibility.

The change in the volume of the solvent due to solution of the gas is not so easy to determine. It has been measured for a number of solvents and solutes at atmospheric pressure by Ångström [7] and by Horiuti [8], and at high pressures, in one specific instance, by Wiebe and Tremearne [9].

Ångström measured the increase in volume of solvent ΔV due to the solution of a volume of gas ΔV_g at constant temperature and pressure and found that δ in the equation

$$\Delta V/\Delta V_g = \delta \tag{14.17}$$

was constant with varying V_g. This observation has been confirmed by Horiuti for a large number of gases and solvents and only one exception, namely, in the case of sulphur dioxide in various organic liquids, has been found.

Wiebe and Tremearne have measured, by the method already described, the partial molal volumes of ammonia and hydrogen in

TABLE 63. *Partial Molal Volumes of Ammonia and Hydrogen in Liquid Ammonia at* 100° *C.*†

Mole fraction of ammonia, N_1	*Partial molal volume of ammonia,* $\bar{v}_1$	*Partial molal volume of hydrogen,* $\bar{v}_2$	*Mole fraction of ammonia,* N_1	*Molal volume of mixture,* $v = V/(n_1+n_2)$
		100 atms.		
1·000	35·46	190·2	1·000	35·456
0·99	35·46	190·2	0·9888	37·189
0·9888	35·46	190·2		
		200 atms.		
1·000	34·02	95·16	1·000	34·017
0·99	34·02	94·20	0·9888	34·695
0·9888	34·03	93·88	0·9612	36·276
0·96	34·10	90·92	0·9589	36·343
0·9586	34·11	90·77	0·9584	36·577
		400 atms.		
1·000	31·74	62·13	1·000	31·739
0·99	31·73	63·23	0·9588	33·118
0·96	31·65	66·45	0·9582	33·071
0·9585	31·64	66·65	0·9094	34·963
0·91	31·29	71·60	0·9036	35·221
0·9020	31·22	72·62	0·9026	35·244
..	..	..	0·9024	35·172
		600 atms.		
1·000	30·40	50·66	1·000	30·399
0·99	30·40	51·13	0·9591	30·147
0·96	30·36	52·50	0·9025	32·597
0·9591	30·36	52·54	0·8527	33·891
0·91	30·21	54·68	..	..
0·9025	30·18	55·00	..	..
0·86	29·94	56·75	..	..
0·8527	29·89	57·04	..	..
		800 atms.		
1·000	29·42	41·91	1·000	29·419
0·99	29·42	42·39	0·8529	31·779
0·96	29·38	43·80	0·8083	32·701
0·91	29·22	46·06	..	..
0·86	28·95	48·20	..	..
0·8529	28·42	48·49	..	..
0·8083	28·53	50·28	..	..

† The molal volumes for pure liquid ammonia were calculated from the results of Keyes (*J. Am. Chem. Soc.* **53**, 965 (1931)).

liquid ammonia-hydrogen solutions at 100° C. and pressures up to 800 atmospheres with the results summarized in Table 63 and shown by means of curves in Fig. 133 (inset). Referring to the table, it is

clear that at the higher pressures there is an increase in volume of the solvent sufficient to necessitate a correction to the solubility data. Michels, Gerver, and Bijl point out that the molecular volume of the dissolved gas, although not constant, is of the same order of magnitude as the co-volume term of the van der Waals equation; and in the case of methane they show that when plotted as a function of temperature it passes through a minimum in the neighbourhood of 50°.

Experimental Data. The following lists of references include the more recent determinations of solubilities at high pressures:

Helium.

Reference	*Temp., °C.*	*Pressure, atms.*	*Solvent*
1. Wiebe and Gaddy, *J. Am. Chem. Soc.* **57**, 847 (1935)	0 25 50 75	1,000	water

TABLE 64. *Absorption Coefficients of Helium in Water (Wiebe and Gaddy). Solubility in c.c. at S.T.P. per gram of water*

Partial pressure of helium, atms.	*Temperature, °C.*			
	0	*25*	*50*	*75*
25	0·2322	0·2156	0·225†	0·2442
50	0·4674	0·4332	0·445	0·4892
75	0·6973†	0·641†	0·6645†	0·7308†
100	0·9240	0·8491	0·8827	0·9699
150	1·371†	1·270†	1·301	1·443†
200	1·807	1·688	1·734	1·907
300	2·643†	2·479†	2·552†	2·805†
400	3·436	3·241	3·358	3·666
500	4·196†	3·975†	4·114†	4·489†
600	4·916	4·681	4·844	5·277†
700	5·591†	5·361†	5·559†	6·038†
800	6·228	6·015	6·248	6·787
900	6·838†	6·645†	6·907†	7·519†
1,000	7·421	7·263	7·536	8·251

† Interpolated values from an equation of the type

$$S = ap + bp^2 + cp^3,$$

where S = absorption coefficient, a, b, and c are constants, and p = partial pressure of helium.

Hydrogen.

Reference	*Temp., °C.*	*Pressure, atms.*	*Solvent*
1. Larson and Black, *J. Ind. Eng. Chem.* **17**, 715 (1925)	−25 to 22	150	ammonia
2. Frolich, Tauch, Hogan, and Peer, *J. Ind. Eng. Chem.* **23**, 548 (1931)	25	200	water methanol hydrocarbons
3. Wiebe, Gaddy, and Heins, *J. Ind. Eng. Chem.* **24**, 823 (1932)	25	25–1,000	water
4. Wiebe and Tremearne, *J. Am. Chem. Soc.* **55**, 975 (1933); **56**, 2357 (1934); **57**, 2601 (1935)	25 50 75 100	1,000	ammonia
5. Wiebe and Gaddy, *J. Am. Chem. Soc.* **59**, 1984 (1937)	0	1,000	ammonia

Wiebe, Gaddy, and Heins's results for the solubility of hydrogen in water are recorded in Table 64 A.

The data between 50 and 1,000 atmospheres are reproduced within the estimated experimental error by the equation

$$S = 0{\cdot}0244 + 0{\cdot}01712p - 0{\cdot}00000196p^2, \qquad (14.18)$$

where S is the absorption coefficient and p is the partial pressure of hydrogen; below 50 atmospheres the equation gives impossibly high values.

TABLE 64 A. *Absorption Coefficients for Hydrogen in Water at* $25 \pm 0{\cdot}1°$ *C. (see Fig.* 132). *(In c.c. of gas at S.T.P. per gram of water)*

Pressure, atms.	*Absorption coefficient*	*Calculated from* (14.18)
25	0·436	..
50	0·867	0·876
100	1·728	1·717
200	3·39	3·37
400	6·57	6·56
600	9·58	9·59
800	12·46	12·47
1,000	15·20	15·19

Wiebe and Tremearne have also measured the solubility of hydrogen in liquid ammonia and find that at high pressures it increases with increase of temperature as shown by the results in Table 65.

TABLE 65. *Absorption Coefficients for Hydrogen in Liquid Ammonia (c.c. of hydrogen at S.T.P. per gram of ammonia)*

Total pressure, atms.	*Temperature, °C.*				
	0	*25*	*50*	*75*	*100*
25	..	1·695†	0·85†	..	..
50	3·28†	4·47	5·10	3·49†	..
75	..	7·20†	9·33†	9·95†	5·80†
100	6·70	9·88	13·49	16·35	15·67
150	..	15·08	21·60	29·00	36·65
180	..	..	26·35	..	..
200	13·11	20·08	29·39	41·41	57·10
300	18·96†	29·45†	44·42	65·40	98·74
400	24·33	38·13	58·33	88·34	140·6
500	29·27†	46·18†	71·33†	110·22†	182·4†
600	33·99	53·71	83·48	131·0	224·0
700	38·25†	60·77†	94·82†	150·6†	264·3†
800	42·33	67·63	105·4	169·2	305·2
900	46·20†	73·74†	115·3†	186·8†	346·5†
1,000	49·77	79·25	124·9	203·3	388·2

The values marked † were interpolated by means of the equation

$$S = a(p-p_v)+b(p-p_v)^2+c(p-p_v)^3,$$

where S = absorption coefficient of hydrogen, p = total pressure, and p_v = the vapour pressure of pure liquid ammonia.

Nitrogen.

Reference	*Temp., °C.*	*Pressure, atms.*	*Solvent*
1. Goodman and Krase, *J. Ind. Eng. Chem.* **23**, 401 (1931)	..	100–300	water
2. Frolich and collaborators, *J. Ind. Eng. Chem.* **23**, 548 (1931)	25	200	water
3. Wiebe, Gaddy, and Heins, *J. Ind. Eng. Chem.* **24**, 927 (1932); *J. Am. Chem. Soc.* **55**, 947 (1933)	25 50 75 100	25–1,000	water
4. Saddington and Krase, *J. Am. Chem. Soc.* **56**, 353 (1934)	50 80 150 200 250	100–300	water
5. Wiebe and Gaddy, *J. Am. Chem. Soc.* **59**, 1984 (1937)	0 50 75 90 100	50–1,000	ammonia

TABLE 66. *Absorption Coefficients of Nitrogen in Water (Wiebe, Gaddy, and Heins) (c.c. of nitrogen at S.T.P. per gram of water)*

Pressure, atms.	*Temperature, °C.*			
	25	*50*	*75*	*100*
25	0·348	0·273	0·254	0·266
50	0·674	0·533	0·494	0·516
100	1·264	1·011	0·946	0·986
200	2·257	1·830	1·732	1·822
300	3·061	2·534	2·413	2·546
500	4·441	3·720	3·583	3·799
800	6·134	5·221	5·062	5·365
1,000	7·15	6·123	5·934	6·256

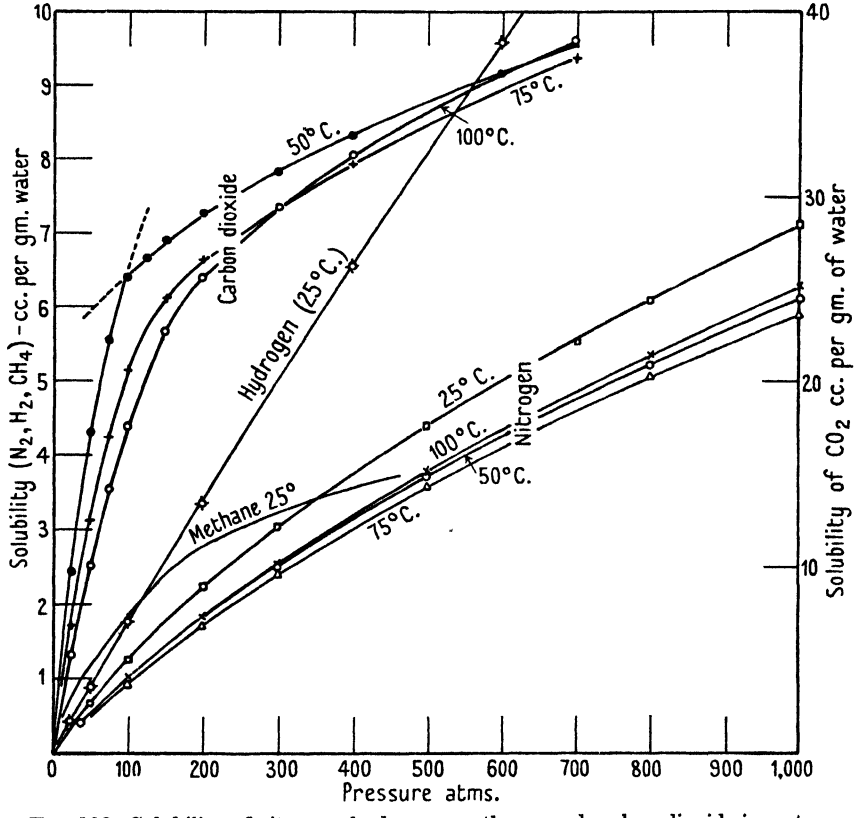

FIG. 132. Solubility of nitrogen, hydrogen, methane, and carbon dioxide in water.

The data of Wiebe, Gaddy, and Heins are summarized in Table 66 and are shown by means of curves in Fig. 132. In all cases equilibrium was approached from both sides and a correction was made

for the change of the partial pressure of the water due to the change in the total pressure.

It will be noted that at the higher pressures the solubility isobars pass through minima at about 70°. In view of the general behaviour of mixtures the occurrence of such minima is not unexpected, and Kuenen has suggested [10] that all gases should exhibit a similar phenomenon and that for sparingly soluble gases the minima should occur at relatively low temperatures. In this connexion it may be mentioned that Bohr and Bock [11] and Ipatiew [12] have detected minima in the solubility curves for hydrogen, Goodman and Krase [4] in those for nitrogen, and Wiebe and Gaddy in those for carbon dioxide. Methane up to 200 atmospheres does not exhibit the effect.

The work of Wiebe and Gaddy on the solubility of nitrogen in liquid ammonia is of particular interest in that it shows the changes in solubility in the neighbourhood of the critical point of the solvent. Their experimental data are given in Table 67 and are shown graphically in Fig. 133. In the figure the dotted line indicates the probable

TABLE 67. *Absorption Coefficients of Nitrogen in Liquid Ammonia (c.c. of nitrogen at S.T.P. per gram of ammonia). (Partly interpolated from data of Wiebe and Gaddy)*

Total pressure, atms.	*Temperature, °C.*										
	0	*10*	*20*	*30*	*40*	*50*	*60*	*70*	*80*	*90*	*100*
50	4·10	4·55	5·45	5·85	6·30	6·63	6·35	5·20	2·7	..	..
100	7·90	9·40	11·11	13·02	15·09	17·19	19·14	20·51	21·10	21·0	20·50
200	13·73	16·77	20·42	24·81	30·16	36·24	43·02	50·93	60·67	72·7	86·32
300	17·70	22·30	27·60	34·30	42·50	51·90	63·87	79·0	99·8	134·9	193·16
400	20·76	26·42	33·11	41·45	52·10	65·35	82·22	105·6	137·5	218·8	..
500	23·00	29·50	37·20	46·85	59·45	76·07	98·05	129·4	197·0	310·6	..
600	24·95	31·84	40·43	51·17	65·31	84·78	110·8	149·3	..	..	..
700	26·60	33·87	43·07	54·75	70·35	91·70	120·4	165·1	..	..	..
800	28·06	35·52	45·19	57·68	74·39	97·20	127·8	177·6	..	..	..
900	29·00	36·75	46·95	59·95	77·35	101·25	133·6	186·7	..	..	..
1,000	29·69	37·93	48·53	62·02	79·89	104·59	138·8	194·3	..	..	..

trend of the critical curve of the mixture; it will be observed that the critical pressure of the system ammonia-nitrogen at 90° C. is close to 600 atmospheres, whilst at 100° it has dropped to below 400 atmospheres. The critical point of pure liquid ammonia is $P_c = 112{\cdot}3$ atms. and $t_c = 132{\cdot}9°$ C., and of nitrogen is $P_c = 33{\cdot}5$ atms. and $t_c = -147{\cdot}1°$ C.

It would be of considerable interest if the complete plait-point curve and the conditions for retrograde condensation for the

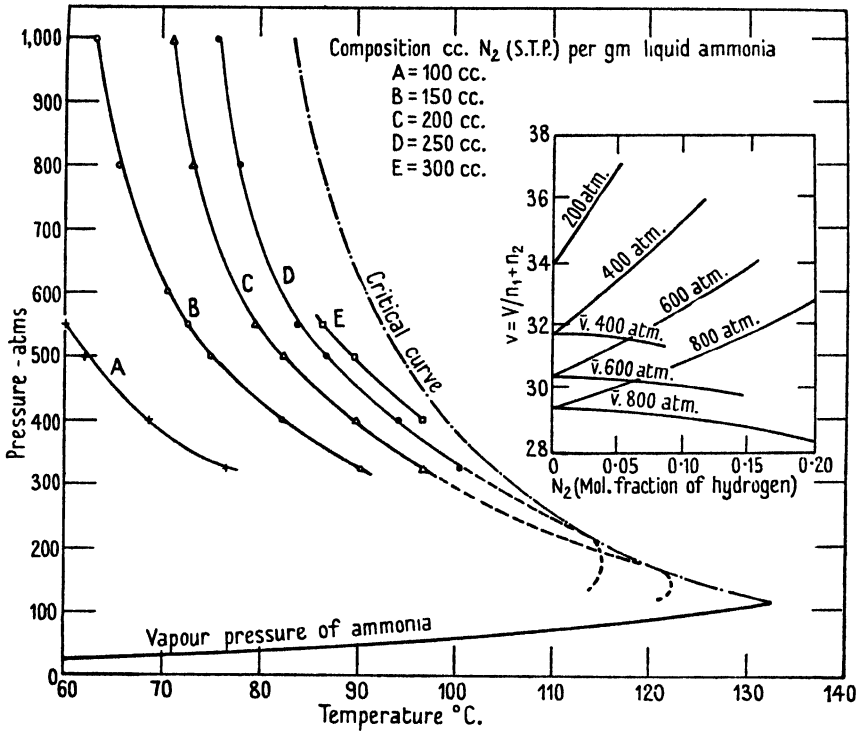

FIG. 133. Constant composition curves and critical curve for nitrogen-ammonia mixtures. *Inset.*—Partial molal volumes of liquid ammonia and hydrogen mixtures and of liquid ammonia.

ammonia-nitrogen system were known, for the above data indicate that it would pass through a maximum at some very high pressure and that a very small quantity of ammonia in solution in liquid nitrogen might exert a comparatively large effect upon the critical temperature.

Methane.

References	*Temp., °C.*	*Pressure, atms.*	*Solvent*
1. Fischer and Zerbe, *Brennstoffchemie*, **4**, 17 (1923)	..	20	water and organic liquids
2. Frolich and collaborators, *J. Ind. Eng. Chem.* **23**, 548 (1931)	25	200	water and organic liquids
3. Michels, Gerver, and Bijl, *Physica*, **3**, 797 (1936)	25 50 75 100 125 150	200	water and aqueous solutions of inorganic salts and organic substances

Data for the solubility of methane are given in Tables 68 and 71 and are shown graphically in Figs. 132 and 134.

TABLE 68. *Solubility of Methane in Water* (*mol* CH_4/*mol* $H_2O \times 10^3$ *and c.c. at S.T.P. per gram of water*)

Temperature, °C.	*Pressure, atms.*	*Solubility*	
		(*a*) $\frac{mol\ CH_4}{mol\ H_2O \times 10^3}$	(*b*) *c.c. at S.T.P. per gram* H_2O
25	40·1	0·81	1·008
	45·4	0·90	1·119
	80·2	1·28	1·592
	110·5	1·58	1·965
	144·0	1 87	2·326
	174·2	2·10	2·612
	202·2	2·29	2·848
	326·5	2·69	3·347
	463·0	2·98	3·707
50	49·0	0·72	0·896
	81·2	1·12	1·393
	111·6	1·42	1·766
	143·7	1·69	2·002
	174·2	1·90	2·363
	205·5	2·07	2·575
75	43·7	0·61	0·759
	78·2	1·01	1·256
	113·0	1·33	1·655
	146·2	1·57	1·953
	173·9	1·74	2·164
	205·3	1·93	2·401
100	48·4	0·66	0·821
	81·1	1·01	1·256
	111·5	1·27	1·580
	146·4	1·52	1·891
	178·1	1·71	2·127
	206·5	1·84	2·289
125	48·4	0·64	0·796
	81·0	0·98	1·219
	111·5	1·24	1·543
	148·0	1·50	1·866
	178·7	1·66	2·065
	209·5	1·79	2·227
150	46·5	0·62	0·771
	80·6	0·93	1·157
	109·4	1·19	1·480
	143·5	1·42	1·766
	175·5	1·60	1·990
	203·4	1·73	2·152

Carbon Dioxide.

Reference	*Temp., °C.*	*Pressure, atms.*	*Solvent*
1. Sander, *Z. physik. Chem.* **78**, 513 (1912)	35 100	100	water
2. Zelvinskii, *J. Chem. Ind.* (U.S.S.R.), **14**, 1250 (1937)	50–100	90	water
3. Wiebe and Gaddy, *J. Am. Chem. Soc.* **61**, 315 (1939)	50 75 100	700	water

The effect of pressure on the solubility of carbon dioxide is made use of in a number of processes for the purification of gases by scrubbing, and accurate data covering wide ranges of pressure and temperature are, therefore, of some practical importance.

From the results of Wiebe and Gaddy, summarized in Table 69 (Fig. 132), it will be seen that at moderate pressures the solubility diminishes with rise of temperature, but above about 400 atmospheres the solubility isobars show a minimum at approximately 75° C. It has also been pointed out by Sander, and confirmed by Wiebe and Gaddy, that at temperatures between 0 and 50° C. there is an abrupt change in slope of the solubility isotherms at 100 atmospheres almost amounting to a discontinuity.

TABLE 69. *The Absorption Coefficient of Carbon Dioxide in Water (c.c. gas at S.T.P. per gram of water)*

Total pressure, atms.	*Temperature, °C.*		
	50	*75*	*100*
25	9·71	6·815	5·365
50	17·246	12·590	10·179
75	22·534	17·044	14·289
100	25·628	20·61	17·67
125	26·77	..	..
150	27·643	24·58	22·725
200	29·143	26·66	25·694
300	31·34	29·51	29·53
400	33·29	31·88	32·39
600	36·73	..	..
700	38·34	37·59	38·50

The Variation of the Surface Tension of a Liquid-Gas System with Pressure and the Relation between Surface Tension and Solubility

The surface tension of a liquid is associated with the properties of the boundary between two phases, one of which may consist of

the vapour of the liquid or of a mixture of the vapour and a gas, and the other of the pure liquid or the liquid saturated with gas at its partial pressure in the gas phase.

In the single-component system the total pressure is fixed by the temperature, and the surface tension is therefore a function of temperature and of the nature of the liquid. In the binary system the boundary between the two phases may be assumed to consist of a film of finite thickness, the properties of which show a progressive variation from the properties in the interior of one phase to those in the interior of the other. The total pressure of such a system, at constant temperature, may be varied by adding or withdrawing gas, but in so doing the compositions of both phases and of the boundary film will be altered. Any change of surface tension will then be a composite effect due to changes in pressure and composition.

If the gas is assumed to be completely insoluble in and inert with respect to the liquid, thermodynamics predicts that the surface tension will vary with the density of the surface film according to the relation

$$\left(\frac{\partial \gamma}{\partial P}\right)_{\sigma} = \left(\frac{\partial V}{\partial \sigma}\right)_{P}, \tag{14.19}$$

where γ is the surface tension and σ is the surface area.

The validity of this expression cannot be tested by direct experiment, but some scanty data are available for the surface-tension changes of liquid-gas systems over comparatively wide ranges of pressure. Kundt has measured the surface tensions of a number of organic liquids with respect to air, hydrogen, and oxygen, at 21° C. and pressures up to about 150 atmospheres, by the capillary-tube method [13]. His results, summarized in Table 70, show that in all the cases examined the surface tension diminishes with increase in pressure and that $\Delta\gamma$ bears some relation to the solubility of the gas by means of which the pressure is imposed. Thus, for example, in the ether series there is a diminution of surface tension of 7·7 per cent. for a pressure rise of 50 atmospheres with hydrogen, which is the least soluble of the three gases, whereas for carbon dioxide there is a diminution of 31 per cent. for a pressure rise of only 23 atmospheres. The experimental method does not enable the pressure and composition effects to be disentangled, but it is evident that the magnitude of the former is small compared with that of the latter.

TABLE 70. *The Variation of the Surface Tension of certain Liquid-Gas Systems with Pressure, at circa 21° C. (Kundt)*

Pressure, atms.	*γ, dynes/cm.*	*Pressure, atms.*	*γ, dynes/cm.*
CS_2–air		$(C_2H_5)_2O$–air	
1	32·2	1	16·9
49	28·8	32	14·1
56	22·3	141	8·3
C_2H_5OH–air		$(C_2H_5)_2O$–H_2	
1	22·2	1	17·0
24	20·6	51	15·7
212	12·1	152	13·4
C_2H_5OH–H_2		$(C_2H_5)_2O$–CO_2	
1	21·3	1	17·0
51	20·1	24	11·0
155	18·0		

A fairly simple relationship between the solubility of a gas and the surface tension of the solvent at low pressure can be worked out on certain reasonable assumptions [14]. The procedure adopted by Uhlig is to separate the energy of solution into two terms: the first represents the energy associated with the surface produced by the introduction of a gas molecule into the solvent, and is proportional to $4\pi r^2\gamma$, where r is the radius of the gas molecule and γ is the surface tension of the solvent; the second is a molecular solvent-solute interaction term which may be denoted by E.

The energy change ΔU on transferring a molecule from the liquid phase to a low-pressure gas phase will be given by

$$\Delta U = 4\pi r^2\gamma - E, \tag{14.20}$$

and the equilibrium concentration of solute molecules in the two phases can then be calculated from the Maxwell-Boltzmann distribution theorem, which leads to the relation

$$\lambda = \frac{c'}{c} = e^{-\Delta U/kT}, \tag{14.21}$$

where λ is the Ostwald coefficient of solubility, c' and c are the concentrations of gas molecules in the solvent and gas phase respectively, and k is Boltzmann's constant.

From (14.20) and (14.21),

$$\log_e\lambda = \frac{-4\pi r^2\gamma + E}{kT},$$

and a straight-line relationship should exist between $\log\gamma$ and the

solubility provided the conditions are such that E and its variation from one liquid to another are small.

Data for the solubilities of methane, oxygen, nitrogen, and hydrogen in ethyl ether, acetone, methyl chloride, carbon tetrachloride, benzene, and chlorobenzene at atmospheric pressure confirm the linear relationship and suggest that, in general, the smaller the surface tension of the solvent the greater is its capacity to dissolve gas [8], [15]. Furthermore, for any particular gas the slope of the line gives a value of the molecular radius in fair agreement with accepted values. The magnitude of E may be calculated from the intercept of the line and is found, in most instances, to be approximately constant for any one gas in a variety of solvents; if the solubility is small it approaches zero and is usually negative.

No comparable data are available at high pressures, but Michels, Gerver, and Bijl have carried out measurements of the solubility of methane in aqueous solutions of inorganic salts, cane sugar, glucose, and formaldehyde. Some of their results are shown graphically in Fig. 134. The data for the solubility of methane in sodium chloride solutions up to 5 N relate to a ternary two-phase system the surface tension of which is a function of the solubility of the methane and the strength of the solution; the two effects tend to counteract one another, for the surface tension increases with the concentration of the salt, whilst with rise of pressure the solubility of the methane increases and brings about a lowering of the surface tension.

In the case of salts both anion and cation have a marked influence on the solubility, particularly at the higher pressures; thus, if the solubility of methane, at 200 atmospheres pressure, in a 2·7 N sodium chloride solution is taken as a standard of comparison, the following values are found for other salts possessing a common anion or cation:

TABLE 71

2·7 *N*	*c.c. of gas at S.T.P. per gram of water*	2·7 *N*	*c.c. of gas at S.T.P. per gram of water*
NaCl	1·41	NaCl	1·41
NaBr	1·37	KCl	1·73
NaI	1·87	LiCl	1·83
		$CaCl_2$	0·98

The values of the quantities Δv and A' of (14.7) for the various solvents are given in Table 72. It will be noted that Δv as a function

of temperature passes through a minimum in the neighbourhood of 50° C. for all the solvents, and that the values of Δv and A' for solutions are smaller than the corresponding values for pure water, formaldehyde being an exception.

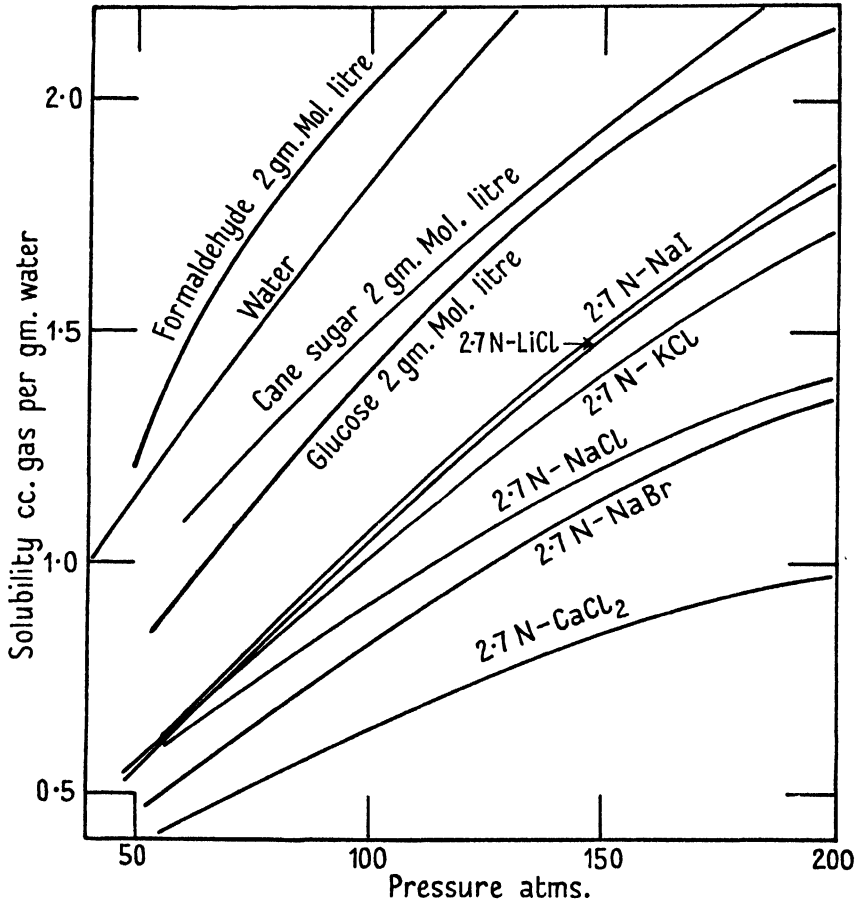

FIG. 134. The solubility of methane in aqueous solutions of inorganic salts, cane sugar, glucose, and formaldehyde.

The Gas Phase

The concentration of water vapour in compressed gases in equilibrium with liquid water has been determined experimentally by Pollitzer and Strebel [16] and by Bartlett [17], whilst Sander [18] has investigated the system ether–carbon dioxide. The method

TABLE 72. *Values of the Constants Δv and A' of* (14.7) *for Methane in various Solvents*

Solvent	*Temperature, °C.*	Δv	A'
Water	25	50·0	1·376
	50	44·2	1·245
	75	58·0	1·209
	100	69·5	1·195
	125	77·3	1·190
	150	83·5	1·183
Sodium chloride, 2·5 N	25	42·0	1·082
	50	38·0	0·975
	75	45·6	0·940
	100	55·5	0·921
	125	58·8	0·893
	150	70·4	0·866
Lithium chloride, 2·7 N	25	0·0	1·000
Potassium chloride, 2·7 N	25	9·6	1·005
Sodium bromide, 2·7 N	25	13·7	0·915
Sodium iodide, 2·7 N	25	−2·9	0·993
Calcium chloride, 2·7 N	25	43·1	0·867
Glucose, 2 N	25	30·8	0·963
Cane sugar, 2 N	25	34·6	1·228
Formaldehyde, 2 N	25	56·8	1·390

employed by Bartlett is to pass the compressed gas at constant pressure and temperature through a series of humidifiers in which the gas bubbles through columns of the liquid. Equilibrium is approached from both sides by maintaining the first humidifier of the series at a temperature 5° above or below the final saturation temperature. The saturated gas then passes through a spray-catcher and an expansion valve to a train of absorption vessels, the first two vessels being immersed in liquid air. Pressures are measured by a free-piston gauge and the final expanded volume of vapour-free gas by means of a wet gas-meter or by a large calibrated gas-holder. About 500 litres of expanded gas are used in each experiment which occupies some 10 hours.

Bartlett's data for hydrogen and nitrogen at 50° are given in Table 73.

The mg. per litre of gas expanded after contact with liquid water at high pressure, W_E, is calculated from the equation

$$(W_E)_T = \left\{\frac{W_c}{P}\left(\frac{pv}{p_0 v_0}\right)_P\right\}_T, \quad \text{or} \quad \frac{W_E}{W_c} = \frac{v}{v_0}, \tag{14.22}$$

where W_c is the mg. per litre of compressed gas, P the total pressure,

TABLE 73. *The Weight of Water Vapour per litre of Compressed Gas, per litre of Gas expanded from High-pressure Contact with Liquid Water, and the volume per cent. of Water Vapour in the Expanded Gas at 50° C. (Bartlett)*

	Hydrogen			*Nitrogen*		
Pressure, atms.	*Mg./litre compressed gas*	*Mg./litre expanded gas*	*Vol. % water vapour*	*Mg./litre compressed gas*	*Mg./litre expanded gas*	*Vol. % water vapour*
Saturation pressure .	82·94	82·94	..	82·94	82·94	..
100	89·2	0·9455	0·1391	106·5	1·0713	0·1576
200	95·6	0·5339	0·0785	128·7	0·6808	0·1001
300	100·0	0·3957	0·0582	141·0	0·5415	0·0796
400	103·0	0·3218	0·0473	148·7	0·4651	0·0684
500	105·8	0·2776	0·0408	155·6	0·4238	0·0623
600	108·5	0·2477	0·0364	161·5	0·3973	0·0584
700	111·2	0·2273	0·0334	165·0	0·3748	0·0551
800	113·5	0·2118	0·0312	167·7	0·3580	0·0527
900	116·0	0·2001	0·0294	169·5	0·3435	0·0505
1,000	118·7	0·1917	0·0282	170·3	0·3304	0·0486

and pv/p_0v_0 the compressibility factor at pressure P and temperature T.

The data indicate that the water-vapour content of a saturated compressed gas is a function of the properties of the gas and of the pressure; thus, for example, at 1,000 atmospheres and at 50° C. nitrogen will hold 44 per cent. more water vapour than will hydrogen, volume for volume; furthermore, the difference in water-vapour content of the gases is not explained by a difference in 'free space' and there is no apparent relationship between the observed results and those calculated by Poynting's relation. Bartlett has shown that in the case of a 3 : 1 hydrogen-nitrogen mixture at 50° C. the water-vapour content at pressures up to 1,000 atmospheres can be calculated within the experimental limits of accuracy, as a linear function of gas composition from the water content of the pure components.

Saddington and Krase (loc. cit.) employed a similar method to Bartlett, but their apparatus, which has been described on p. 360, was so arranged that liquid-phase samples could also be taken; they draw particular attention to the need for heating the expansion valve to a temperature 25 to 50° above the temperature of saturation, to avoid condensation during the passage of the gas and vapour, and

they attribute the difference between their results and those of Bartlett at 50° to the probable condensation of water in the expansion valve of his apparatus. Their results for the vapour-phase composition together with its density and compressibility are given in Table 74. In calculating the weight of water per litre of compressed gas (W_c) below 100° the volume of the compressed gas was found from Bartlett's compressibility data for pure nitrogen; above 100° it was calculated from the relation

$$D_V = a + W_c,$$

where D_V is the density of the gas phase in grams per litre and a is the weight in grams of nitrogen per litre of compressed gas; the ratio W_c/a is readily determined from the analysis of the gas phase.

TABLE 74. *Vapour-phase Composition, Density, and Compressibility of Nitrogen-Water System (Saddington and Krase)*

Temp., °C.	*Pressure, atms.*	*Gm. water per litre compressed gas (W_c)*	*Gm. water per gm. of gas phase*	*Gm. of N_2 per gm. of gas phase (a)*	*Density of gas-phase mixture, gm./litre (D_v)*	*Compressibility of mixture (C_m), obs.*	*C_m, calc.*
50	100	0·1236	0·00118	0·9988	..	..	..
80	100	0·3817	0·00403	0·9960	94·2	1·320	1·328
100	100	0·6474	0·00726	0·9927	88·0	1·417	1·411
150	100	2·710	0·0341	0·9659	76·8	1·620	1·607
190	100	5·880	0·0828	0·9172	..	..	..
210	..	..	..	..	68·5	1·755	1·799
230	100	13·300	0·1958	0·8042	67·7	1·773	1·814
50	200	0·1463	0·00085	0·9992	196·8	1·272	1·273
80	..	..	..	..	176·7	1·411	1·406
85	200	0·5116	0·00290	0·9971	..	..	..
100	..	..	..	..	169·3	1·470	1·495
150	200	2·960	0·0203	0·9797	145·8	1·695	1·695
190	200	7·550	0·0564	0·9436	..	..	..
200	..	..	..	..	132·6	1·822	1·878
225	200	14·840	0·1180	0·8820	..	..	..
240	..	..	..	..	122·0	..	..
50	300	0·1975	0·00073	0·9993	273·1	1·376	1·368
70	..	..	..	..	256·3	1·438	1·460
75	300	0·4607	0·00262	0·9974	..	..	..
100	300	0·9126	0·00372	0·9963	237·2	1·586	1·596
115	300	1·450	0·00629	0·9937	225·0	1·656	1·658
140	..	..	..	..	212·1	1·761	1·760
145	300	3·240	0·0155	0·9835	..	..	..
165	300	5·320	0·0259	0·9741	..	..	..
170	..	..	..	..	198·3	1·863	1·877
230	300	16·400	0·0932	0·9067	176·4	2·007	2·0593
240	300	..	..	..	173·0	1·980	2·0773

The compressibility factor C_m (obs.) was found from the values of the density of the gas phase D_V by the equation

$$C_m = \frac{pv}{p_0 v_0},$$

where v_0 is the volume in c.c. of the expanded gas at p_0 (= 1 atm.) and 0° C., p is the total pressure in atmospheres, and v is the volume of the compressed gas in c.c.

C_m (calc.) is obtained by taking the weighted mean of the known specific volume of saturated steam and Bartlett's values for nitrogen.

Generally speaking, the results accord with the assumption, implied in the thermodynamic treatment, that the compressed gas acts as a solvent of the vapour; there is in effect a two-component, liquid-gas, system in which the solubility of each phase in the other increases with pressure until at the 'critical pressure' the two phases become indistinguishable; the water content of the compressed gases exceeds the values predicted by the Poynting relation at all temperatures.

The effect of pressure upon the water content of a given volume of the gas phase becomes more marked as the temperature is raised whilst the vapour-phase density decreases with rising temperature at constant pressure. At temperatures above 150° C., where the concentration of water vapour reaches fairly large values, an additive rule for the calculation of the compressibility does not hold.

BIBLIOGRAPHY

1. Michels, Gerver, and Bijl, *Physica*, **3**, 797 (1936).
2. Wiebe and Tremearne, *J. Am. Chem. Soc.* **55**, 975 (1933).
3. Frolich and collaborators, *J. Ind. Eng. Chem.* **23**, 548 (1931).
4. Goodman and Krase, *J. Ind. Eng. Chem.* **23**, 401 (1931).
5. Wiebe, Gaddy, and Heins, *J. Ind. Eng. Chem.* **24**, 823 (1932).
6. Saddington and Krase, *J. Am. Chem. Soc.* **56**, 353 (1934).
7. Ångström, *Wied. Ann.* **15**, 297 (1882); **33**, 223 (1888).
8. Horiuti, *Sci. Papers*, Inst. Phys. and Chem. Research (Tokyo), **17**, 125 (1931).
9. Wiebe and Tremearne, *J. Am. Chem. Soc.* **57**, 2601 (1935).
0. Kuenen, *Verdampfung und Verflüssigung von Gemischen*, p. 82. J. A. Barth, Leipzig, 1906.
11. Bohr and Bock, *Wied. Ann.* **44**, 318 (1891).
12. Ipatiev and collaborators, *Ber.* **65**, 568 (1932).
13. Kundt, *Ann. d. Physik*, **12**, 538 (1881).

14. SKIRROW, *Z. physik. Chem.* **41**, 139 (1902); SISSKIND and KASARNOWSKY, *Z. anorg. allgem. Chem.* **214**, 385 (1933); UHLIG, *J. Phys. Chem.* **41**, 1215 (1937).
15. HORIUTI, *Sci. Papers*, Inst. Phys. and Chem. Research (Tokyo), **17**, 222 (1931).
16. POLLITZER and STREBEL, *Z. physik. Chem.* **110**, 768 (1924).
17. BARTLETT, *J. Am. Chem. Soc.* **49**, 65 (1927).
18. SANDER, *Z. physik. Chem.* **513** (1912).

XV

THE COMPRESSION AND CIRCULATION OF GASES. THE INFLUENCE OF PRESSURE ON THE VISCOSITY OF GASES

THE general principles involved in the compression and circulation of gases are comparatively simple, but the problem, in practice, is complicated by extraneous factors connected with the design and construction of the compressors and circulating pumps employed to effect the change. The functions of the two machines differ in some important respects. A compressor has to supply, by suitable mechanical means, the work required to bring about a change of state in a fixed weight of gas, allowance being made for frictional and other losses in its various parts. A circulating pump, on the other hand, has to provide the kinetic energy needed to move a gas of known density at some predetermined rate around a closed circuit, and to make up losses of momentum due to bends, changes of section, and to the frictional resistance of pipe-lines. In both cases an accurate estimate, based upon thermodynamic and hydrodynamic considerations, has to be made of the energy requirements of the process.

The most convenient procedure in dealing with problems involving the handling of gases is to equate the total energy entering and leaving some suitable section of the system under consideration according to the method first employed by Bernoulli. The equation may be written in the general form

$$(E_A+P_AV_A)+X_A+u^2/2g+(W+w) = (E_B+P_BV_B)+X_B+u^2/2g, \quad (15.1)$$

where E is the internal energy of the gas, X and $u^2/2g$ the gravity and velocity heads respectively, W the energy given to the gas during its passage through the section, and w the loss of energy due to bends, friction, etc.

The Enthalpy of the System

The change in the internal energy of a gas compressed isothermally from zero density to density ρ is given by

$$E' = \int_0^\rho \frac{\partial E}{\partial \rho} d\rho. \quad (15.2)$$

The value of $(\partial E/\partial \rho)_T$ is obtained from the relation

$$\left(\frac{\partial E}{\partial \rho}\right)_T = -\frac{1}{\rho^2}\left(\frac{\partial E}{\partial v}\right)_T = -\frac{1}{\rho}\left\{T\left(\frac{\partial pv}{\partial T}\right)_v - pv\right\}, \tag{15.3}$$

from which E' may be evaluated for different values of ρ and T, according to the method described in Chapter X.

The change in the enthalpy of the system is then given by

$$\Delta H = (E_A + P_A V_A) - (E_B + P_B V_B). \tag{15.4}$$

The Evaluation of the Term W

By definition the term W includes all the energy, whether in the form of heat or work, given to the gas during its passage through the section. In particular it includes the work of compression and the kinetic energy required to circulate the gas. The work of compression is

$$W = \int_{V_A}^{V_B} P\, dV. \tag{15.5}$$

To integrate this equation we may employ the relationship

$$PV = nRT, \tag{15.6}$$

which is strictly valid only for an ideal gas and an isothermal process, whence

$$W = nRT \log_e (V_B/V_A) = nRT \log_e (P_A/P_B), \tag{15.7}$$

or we may employ the relationship

$$PV^\gamma = \text{a constant},$$

which applies to an adiabatic process and an ideal gas, whence

$$W = \frac{P_A V_A - P_B V_B}{1-\gamma} \tag{15.8}$$

$$= \frac{R(T_A - T_B)}{1-\gamma} \tag{15.9}$$

$$= \frac{P_A V_A}{\gamma - 1}\left\{\left(\frac{V_A}{V_B}\right)^{\gamma-1} - 1\right\} \tag{15.10}$$

$$= \frac{P_A V_A}{\gamma - 1}\left\{\left(\frac{P_B}{P_A}\right)^{(\gamma-1)/\gamma} - 1\right\}. \tag{15.11}$$

γ is the ratio of the specific heats at constant pressure and constant volume respectively, and, for an ideal gas, is independent of pressure and temperature.

In practice neither isothermal nor adiabatic compression can be achieved and the law takes the form

$$PV^m = \text{a constant}, \tag{15.12}$$

where m usually has a value between 1 and γ, or may be greater than γ, according to circumstances; it may also change progressively during the actual compression cycle. Provided m remains constant the work done in a polytropic compression may be calculated from any of the equations (15.8–11), γ being replaced by the appropriate value of m.

The (P, V) relationships used in integrating (15.5) imply that the internal energy and enthalpy of the gas are independent of the volume and hence that the two specific heats are independent of pressure and temperature. These assumptions are only valid under certain limiting conditions and cannot be applied to the case of a gas undergoing compression over a wide range of pressure.

Equations of general application can be derived by employing one of the more accurate equations of state to integrate (15.5), but a more convenient procedure in dealing with gas compressors is to construct an enthalpy-temperature-entropy (H, T, S) chart for the gas and to evaluate the work terms by graphical methods. If such a chart for one of the permanent gases be examined (e.g. Fig. 117), it will be noted that the temperature and enthalpy lines are parallel at low pressures, but as the pressure is raised they begin to separate and at high pressures the divergence is considerable. The use of the (H, T, S) chart is best explained by showing how various changes of state are represented on it and comparing the resulting diagrams with the conventional (P, V) diagrams for the same changes.

Consider, for example, a volume V_1 of gas at pressure P_1 and temperature T_1. It would be indicated on the (P, V) and the (H, T, S) diagrams by the point A_1 (Fig. 135 *a* and *b*). On heating the gas at constant volume to a higher temperature T_2, the pressure increases to P_2 and the change is represented on the (P, V) diagram by the vertical line A_1A_2 and on the (H, T, S) diagram by the curve A_1A_2. The former gives no indication of the temperature and internal energy changes of the gas; the latter gives directly the temperature and entropy changes. The enthalpy change may be determined by measuring on the temperature-entropy scales the area bounded by the curve A_1A_2 and the two entropy lines S_1 and S_2.†

† Unless otherwise stated all areas on the (H, T, S) diagram are measured on the temperature-entropy scales.

If the gas be further heated, at constant pressure P_2, from T_2 to T_3, the volume will increase to V_2, there will be a change in the internal energy, and external work will be done by the system. The operation is represented on the (P, V) diagram by the horizontal line A_2A_3, the area $P_2 \times A_2A_3$ $(= P_2(V_2 - V_1))$ giving the external work performed. On the (H, T, S) diagram the area below the curve A_2A_3 represents

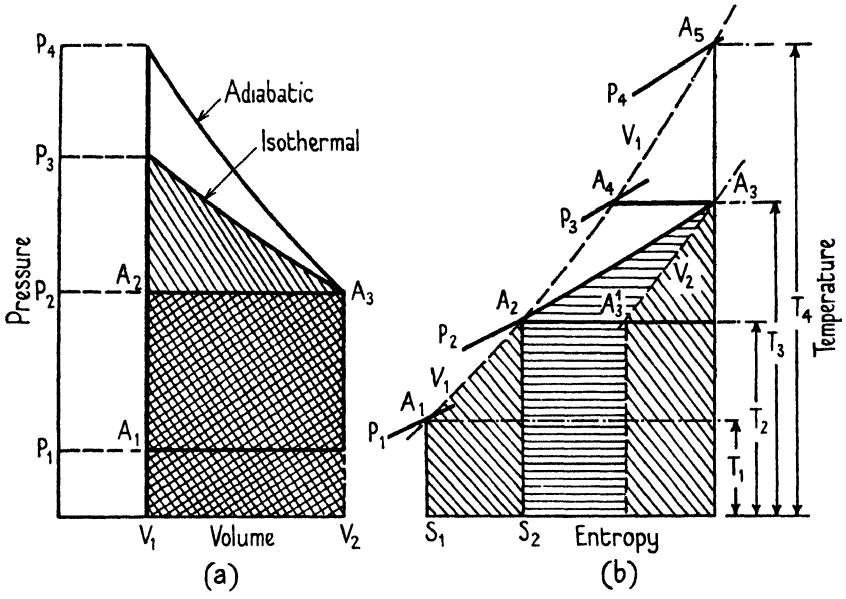

FIG. 135 *a* and *b*. The (P, V) and (H, T, S) diagrams of various changes of state of a gas.

the total heat involved in the process $(= c_p(T_3 - T_2))$, and the area beneath the constant-volume curve A_3A_3' gives the internal energy change $(= c_v(T_3 - T_2))$.

Finally, suppose the gas be now recompressed isothermally to its original volume V_1. In the case of an ideal gas there will be no change in the internal energy and the work of compression will be given by (15.7). On the (P, V) diagram the compression is represented by the isothermal curve through A_3, the area beneath the curve giving the external work required. On the (H, T, S) diagram the horizontal line A_3A_4 represents the isothermal change and the area beneath the heat equivalent of the work done. Had the gas been compressed adiabatically a greater pressure (P_4) would have been required to reduce the volume to V_1 and the temperature of the gas would have increased

to T_4. The adiabatic change is represented on the (P, V) diagram by the adiabatic curve through A_3 and on the (H, T, S) diagram by the vertical, constant entropy, line A_3A_5; the work involved $(= c_v(T_4-T_3))$ is given, on the former, by the area below the adiabatic curve, and its heat equivalent on the latter by the area below the constant volume curve A_4A_5.

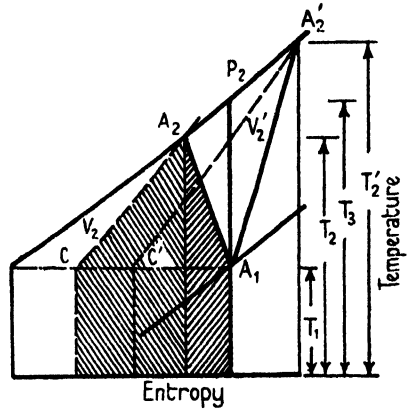

FIG. 136. The (H, T, S) diagram of a polytropic compression.

Polytropic Compression

In a polytropic compression cycle part of the heat of compression may be abstracted $(m > 1, < \gamma)$ or no heat may be removed but additional heat added $(m > \gamma)$. The value of m will depend upon the sign and magnitude of the heat transfer. On the (P, V) diagram the operation will be represented by a curve situated either between the adiabatic and isothermal curves or above the former. The heat transferred is the difference between the work done and the increase in internal energy and is given by

$$h = \kappa W - c_v(T_2-T_1), \tag{15.13}$$

where κ is the reciprocal of Joule's equivalent. Substituting the value of W from (15.9),

$$h = \left(\frac{\kappa R}{m-1} - c_v\right)(T_2-T_1) \tag{15.14}$$

$$= c_v\left(\frac{\gamma-m}{m-1}\right)(T_2-T_1). \tag{15.15}$$

From (15.15) the entropy change may be calculated:

$$S_2-S_1 = c_v\left(\frac{\gamma-m}{m-1}\right)\log_e\frac{T_2}{T_1} \tag{15.16}$$

$$= c_v\left(\frac{\gamma-m}{m-1}\right)\left(\frac{\gamma-1}{\gamma}\right)\log_e\frac{P_2}{P_1}. \tag{15.17}$$

A polytropic compression is represented on the (H, T, S) diagram (Fig. 136) by the line A_1A_2 or A_1A_2', the area beneath the line giving the heat transferred during the operation. The increase of internal energy is given by the area below the constant volume curve CA_2.

The utility of the (H, T, S) diagram will now be apparent, for by its aid all the pressure, volume, temperature, entropy, and enthalpy changes involved in a succession of expansions and compressions can be obtained without any calculations whatsoever.

The Representation of a Complete Compression Cycle on the (H, T, S) Diagram

For the sake of simplicity we shall start with what may be termed an 'ideal' compressor, that is, a single-stage frictionless machine in

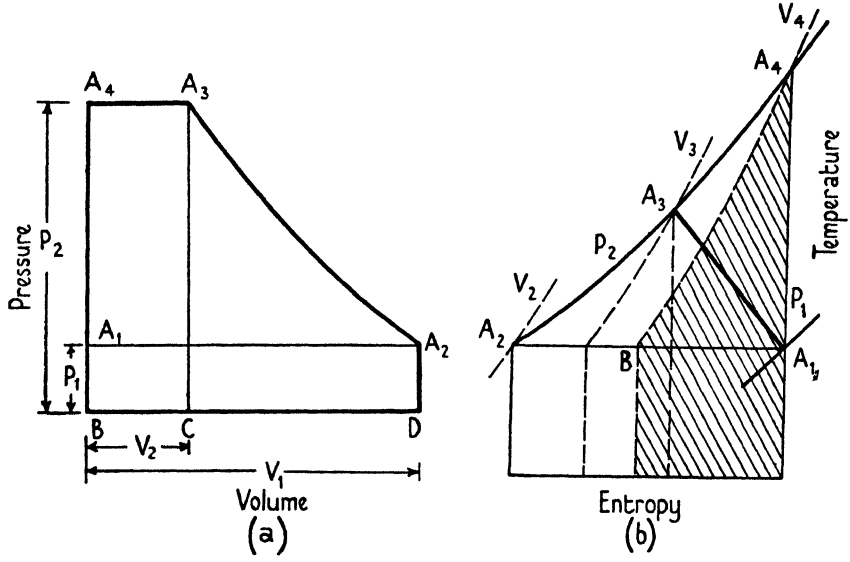

FIG. 137 *a* and *b*. The (P, V) and (H, T, S) diagrams for an 'ideal' compressor cycle.

which the clearance space and valve-loading are negligibly small and in which the compression may be conducted either isothermally or adiabatically. The (P, V) and (H, T, S) diagrams for the complete cycle of the compressor are shown in Fig. 137 *a* and *b*. During the suction stroke, A_1A_2, a volume V_1 of gas at a pressure P_1 is drawn into the cylinder, the area A_1A_2DB on the (P, V) diagram representing the work done on the piston. The compression stroke is indicated by the curve A_2A_3, the work required being given by the area A_2A_3CD. The gas which now occupies a volume V_2 is discharged through the delivery valve at constant pressure P_2, the area A_3A_4BC giving the work expended during this part of the cycle. The net

work W required to receive, compress, and deliver the gas is thus given by the area $A_1A_2A_3A_4$, or in terms of pressures and volumes by

$$W = P_1V_1\log_e P_2/P_1 + P_2V_2 - P_1V_1; \tag{15.18}$$

for isothermal compression this equation reduces to

$$W = P_1V_1\log_e P_2/P_1. \tag{15.19}$$

For adiabatic compression, from (15.8),

$$W = \frac{P_1V_1 - P_2V_2}{1-\gamma} + P_2V_2 - P_1V_1 \tag{15.20}$$

$$= \frac{\gamma}{1-\gamma}(P_1V_1 - P_2V_2). \tag{15.21}$$

From (15.21) is obtained the heat equivalent of the work of adiabatic compression $h = c_p(T_2 - T_1)$. Comparing (15.8) and (15.21) it will be seen that γ times the theoretical compression work is required to compress the gas adiabatically and deliver it; similarly, in polytropic compression m times the theoretical work is required.

Referring to the (H, T, S) diagram and bearing in mind that we are still considering an ideal gas, A_1A_2 represents the isothermal, A_1A_3 the polytropic, and A_1A_4 the adiabatic compression. The heat equivalent of the work of the isothermal compression is given by the area below the line A_1A_2, that of the work of adiabatic compression by the area under the constant volume line through A_4 (i.e. A_4B), and that of the work of delivery at constant pressure by the area below the constant pressure line (P_2) through A_4 (i.e. A_4A_2). For the polytropic cycle the heat transferred (abstracted) during the compression stroke is given by the area under the line A_1A_3, whilst the heat equivalent of the work of the whole cycle is given by the area beneath $A_1A_3A_2$, that is, by

$$h = c_p(T_2 - T_1) + (S_1 - S_2)\tfrac{1}{2}(T_1 + T_2). \tag{15.22}$$

The 'isothermal efficiency' of any given cycle may now be defined as the ratio of the work required for isothermal compression and that for the cycle in question, i.e.

$$\epsilon_i = \frac{P_1V_1\log_e P_2/P_1}{\frac{m}{m-1}P_1V_1\left(\left[\frac{P_2}{P_1}\right]^{(m-1)/m} - 1\right)}, \tag{15.23}$$

it being assumed that the exponent m remains constant during the compression stroke.

From (15.23) the isothermal efficiency is seen to depend upon the compression ratio P_2/P_1 and upon the value of m.

The Clearance Volume

The term 'clearance' includes the space between the cylinder and piston heads at their distance of nearest approach together with any other dead spaces such as valve pockets not swept out by the piston.

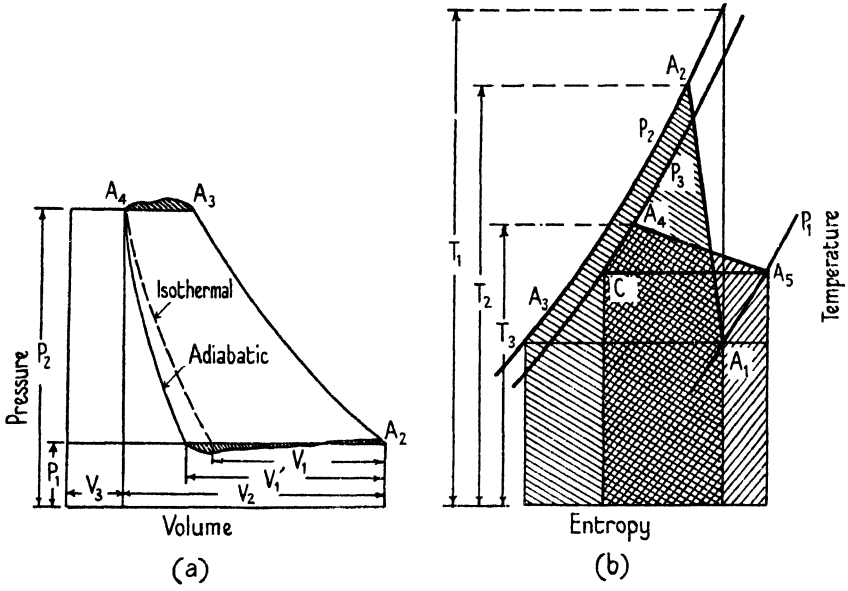

FIG. 138 *a* and *b*. (P, V) and (H, T, S) diagrams showing the effect of clearance and re-expansion.

In spite of the implication contained in the German equivalent of the term—*schädlicher Raum*—it is not entirely without its uses: for example, in balancing the work in multi-stage compressors. The effect of clearance on the (P, V) diagram is shown in Fig. 138*a*. Referring to the figure—after the discharge stroke A_3A_4 the cylinder still contains a volume V_3 (the clearance volume) of gas at a pressure P_2, which re-expands isothermally to the suction pressure along the isothermal curve through A_4, or polytropically. The volumetric efficiency of the cycle ϵ_v is defined as the ratio of the volume of gas passing the suction valve during the suction stroke (i.e. V_1 or V_1') and the volume swept out by the piston (i.e. V_2). The clearance volume at P_1 is $V_2+V_3-V_1$ and the clearance ratio is V_3/V_2.

For a polytropic cycle

$$(P_2V_3)^m = P_1(V_2+V_3-V_1)^m,$$

$$V_1 = V_3\{1-(P_2/P_1)^{1/m}\}+V_2,$$

and hence

$$\epsilon_v = \frac{V_3}{V_2}\{1-(P_2/P_1)^{1/m}\}+1. \qquad (15.24)$$

Eq. (15.24) shows that the volumetric efficiency increases with m and diminishes with increase in the compression ratio.

In practice compressors always work with a polytropic cycle, and although, for reasons which will be explained later, the value of the exponent m varies continuously at all parts of the cycle, it may be taken as a general rule that the compression part of the cycle approximates to adiabatic conditions whilst the re-expansion part is nearer to an isothermal process.

If the exponent m be assumed to have a constant, but not necessarily the same, value for compression and re-expansion, then, for unit weight of gas, the cycle between pressures P_1 and P_2 will be represented on the (H, T, S) diagram (Fig. 138*b*) by the two lines A_1A_2 (compression) and A_4A_5 (re-expansion). The heat equivalent of the work of compression is given by the area below $A_1A_2A_3$ and equals, approximately, $(S_2-S_1)T_c$, where T_c is the mean absolute temperature of the gas during compression. The equivalent of the work given to the piston during re-expansion per unit weight of clearance gas is similarly given by the area below A_5A_4C, or by $(S_2-S_1)T_e$, where T_e is the mean absolute temperature during re-expansion. It will be noted that owing to cooling during the delivery stroke re-expansion starts at a lower temperature and pressure than those corresponding with final compression conditions. The gain or loss of work, per unit weight of gas, due to re-expansion is $(S_2-S_1)(T_c-T_e)$, and hence the effect of clearance will depend to a large extent upon the temperature distribution in the compressor.

The Cooling Characteristics of the Compressor

It will be clear from the foregoing considerations that it is desirable to obtain, as nearly as is possible or practicable, isothermal compression and adiabatic re-expansion. Both changes of state, however, take place in the same cylinder in rapid succession, and the problem of designing a container that will alternately abstract heat at a constant rate and be perfectly insulating, presents insuperable difficulties.

At this point it will be instructive to consider an actual example based upon the indicator diagram of a single-stage compressor having the following characteristics [1]:

Cylinder diameter . . .	45·0 cm.
Stroke	50·0 cm.
R.P.M.	145
Clearance volume . . .	3 per cent. (= 0·03)

The data in Table 75 is obtained directly from the indicator diagram.

TABLE 75. *Pressure, Volume, and Temperature Variations in the Cycle of a Single-stage Compressor*

	Compression				*Re-expansion*			
P, kg./cm.²	x, mm.	V, m.³/kg.	T, °C. abs.	t, °C.	x, mm.	V, m.³/kg.	T, °C. abs.	t, °C.
0·94	61·4	0·975	313	40	9·5	1·28	410	137
1·0	60·0	0·950	322·5	49·5	9·0	1·175	401	128
1·5	45·4	0·720	369·5	96·5	5·4	0·720	369·5	96·5
2·0	36·8	0·585	400	127	4·0	0·535	365·5	92·5
2·5	31·0	0·495	422	149	3·2	0·431	368	95
3·0	27·0	0·430	440	167	2·7	0·364	373	100
3·5	23·2	0·369	456·5	183·5	2·4	0·320	383	110
4·0	21·7	0·344	470	197	2·1	0·289	395	122
4·5	19·5	0·310	477	204	2·0	0·266	408	135
5·0	17·7	0·282	481	208	1·8	0·248	423	150
5·4	16·5	0·262	482	210	..	..	..	..

The volumetric efficiency is given by

$$\frac{61{\cdot}4-9{\cdot}5}{61{\cdot}4-1{\cdot}8} = 0{\cdot}871.$$

It may also be calculated from the clearance and the specific volumes at the beginning and end of the expansion stroke:

$$1-0{\cdot}03(1{\cdot}28/0{\cdot}248-1) = 0{\cdot}875.$$

By transferring the data in Table 75 to an (H, T, S) diagram (Fig. 139) the compression is represented by the curve A_1A_2 and the expansion by A_3A_4, the value of m changing continuously in both cases. The heat equivalent of the work of adiabatic compression between the pressures p_1 and p_2 is

$$h = 0{\cdot}242(240-40) = 48{\cdot}4 \text{ k.cals./kg.}$$

The equivalent of the actual work of compression is given by the

area below $E_1 A_2 A_1$ plus the area $A_1 A_2 B$, or approximately by $\Delta S \times T_m = 0{\cdot}12 \times 409 = 49$ k.cals./kg.

During the delivery period the temperature falls from 210° to 150° C. and the pressure from 5·4 to 5·0 atmospheres. The equivalent

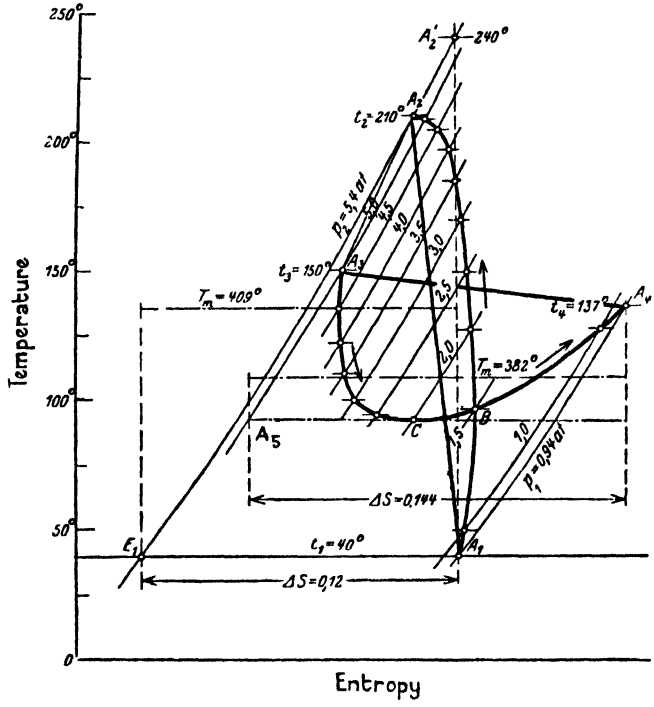

FIG. 139. The (H, T, S) diagram of one cycle of a single-stage compressor.

of the work regained on expansion is given by the area beneath $A_3 A_4$ less the area enclosed by $A_3 C A_4$, or by

$$\Delta S \times T_m = 0{\cdot}144 \times 382 = 55 \text{ k.cals./kg.}$$

Referring again to the compression stroke, the curve $A_1 A_2$ lies first to the right of the adiabatic line, showing that initially the gas is receiving heat from the hot cylinder walls. Towards the end of the stroke the curve bends over and heat is abstracted from the gas by the walls. Since the curve cuts the adiabatic line at a point corresponding with a temperature of 183·5° C., we may assume this to be approximately the mean temperature of the walls in contact with the gas at that point.

Re-expansion starts at a temperature of 150° C. which is not far

removed from the temperature of the cylinder head, and hence $m = \gamma$. At a later stage heat is given to the gas from the cylinder walls, and the temperature, having fallen to 92·5°, again rises to 137° C. Now we have seen that the work gained on re-expansion per kg. (55 k.cals./kg.) is greater than the work of compression (49 k.cals./kg); the equivalent of the net work of compression is therefore

$$\begin{aligned} 49-\left(\frac{0{\cdot}03\times 0{\cdot}0975}{0{\cdot}87\times 0{\cdot}248}\right)(55-49) \\ = 49-0{\cdot}1356\times 6 \\ = 48{\cdot}2 \text{ k.cals./kg.,} \end{aligned}$$

which agrees very closely with the figure for true adiabatic compression. For this reason it is customary in designing high-pressure compressors to assume the compression to be adiabatic.

It should be noted that although the effect of the heat gained during re-expansion is to diminish the work required by 0·8 k.cals./kg., or 1·6 per cent., it has an adverse effect on the volumetric efficiency. The gas entering during the suction stroke at 20° C. encounters and mixes with the re-expanded gas at 137° C., the resultant temperature t_m being given by

$$t_m = \frac{20+0{\cdot}1356\times 137}{1{\cdot}1356} = 34^\circ \text{C.}$$

This temperature is further increased to 40° C. by heat from the suction valve and cylinder walls.

The temperature changes indicated on the (H, T, S) diagram are typical of what happens during the compression cycle of a reasonably well-designed single-stage machine and illustrate the difficulty of arranging for adequate cooling of the piston, cylinder head, and valves. It will be evident that the volumetric efficiency, which takes no account of temperature, is not a good measure of the performance of the machine. For practical purposes, what is required is the ratio of the weight of gas delivered per stroke to the weight of gas at suction conditions corresponding to the piston displacement, i.e. the delivery efficiency.

The losses of energy due to valve-loading and friction in the various delivery pipes and inter-coolers cannot conveniently be shown on the (H, T, S) diagram since a variable quantity of gas is concerned. They are, however, indicated on the (P, V) diagram (Fig. 138*a*) by the shaded areas above and below the delivery and suction lines.

Multi-stage Compression

Since it is impossible to approach isothermal conditions with practicable compression ratios, all high-pressure compressors employ the multi-stage principle whereby the process is carried out in steps with intervening cooling periods. In calculating the work involved the same procedure as for single-stage compression may be employed and the complete compression cycles may be worked out on the (P, V) and (H, T, S) diagrams.

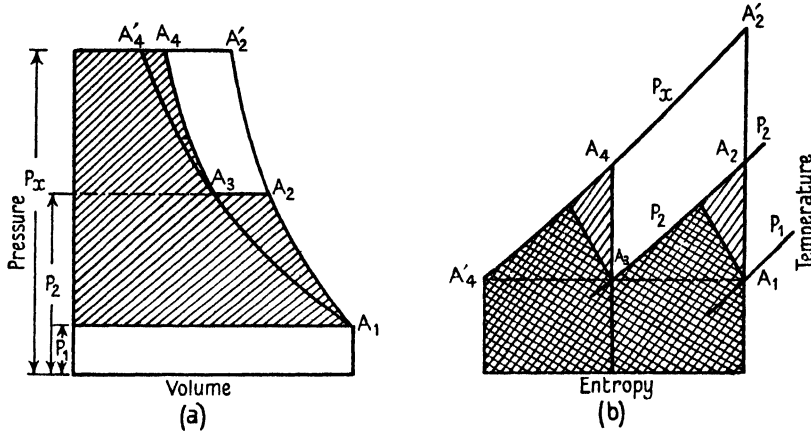

FIG. 140 *a* and *b*. The (P, V) and (H, T, S) diagrams of a two-stage compression process.

In the (P, V) diagram (Fig. 140*a*) the operations of isothermal and adiabatic compression from a pressure P_1 to P_x are represented by the two curves A_1A_4' and A_1A_2'. If at some intermediate pressure P_2 during the adiabatic compression the gas is cooled down to the initial suction temperature and the compression is then continued to P_x, the dual process will be represented by $A_1A_2A_3A_4$ and the saving in work over that required for the single-stage compression will be given by the area $A_2A_3A_4A_2'$. Fig. 140*b* shows the same operation on the (H, T, S) diagram with additional graphs for polytropic compression in two stages.

For unit weight of gas the work of the two-stage adiabatic compression is given by

$$W = RT_1\frac{\gamma}{\gamma-1}\left\{\left(\frac{P_2}{P_1}\right)^{(\gamma-1)/\gamma} + \left(\frac{P_x}{P_2}\right)^{(\gamma-1)/\gamma} - 2\right\}. \qquad (15.25)$$

If this expression is differentiated with respect to P_2 and equated

to zero the greatest value of the area $A_2A_3A_4A_2'$ or the optimum value of P_2 is obtained:

$$\left(\frac{1}{P_2^{1/\gamma}}\right)\left(\frac{P_1^{1/\gamma}}{P_1}\right) = P_x^{(\gamma-1)/\gamma}P_2^{(1-2\gamma)/\gamma}. \tag{15.26}$$

From (15.26), $$P_2/P_1 = P_x/P_2. \tag{15.27}$$

Similarly, for compression in n stages

$$P_2/P_1 = P_3/P_2 = \ldots = P_n/P_{n-1} = P_x/P_n, \tag{15.28}$$

and each individual compression ratio will be $\sqrt[n]{(P_x/P_1)}$.

In an n-stage compressor the work of any individual stage, per unit weight of gas, is

$$W = RT_1\frac{\gamma}{\gamma-1}\left\{\left(\frac{P_x}{P_1}\right)^{(\gamma-1)/n\gamma} - 1\right\}, \tag{15.29}$$

and for the n stages

$$W = RT_2\frac{n\gamma}{\gamma-1}\left\{\left(\frac{P_x}{P_1}\right)^{(\gamma-1)/n\gamma} - 1\right\}. \tag{15.30}$$

The temperature attained at the end of the first stage will be

$$T_2 = T_1\left(\frac{P_2}{P_1}\right)^{(\gamma-1)/\gamma}, \tag{15.31}$$

and with adiabatic compression in n stages the minimum temperature attainable will be

$$T_x = T_1\left(\frac{P_x}{P_1}\right)^{(\gamma-1)/n\gamma}. \tag{15.32}$$

For polytropic compression with $m < \gamma$ the above equations hold provided γ is replaced by the appropriate value of m.

The above equations, which are applicable to an 'ideal' gas or to real gases at low and medium pressure, show that theoretically the lowest temperatures and the minimum work of compression are associated with an equal division of the work between the stages. This does not imply, necessarily, that the compression ratios for all the stages should be equal, since the effects of piston leakage, imperfect intercooling, etc., must be taken into account. If, for example, there is insufficient intercooling, resulting in a progressive increase in suction temperature from stage to stage, the result will be that the maximum temperature attained in the successive stages will increase considerably, as shown in the (H, T, S) diagram—Fig. 141—

and extra work (the shaded area) will have to be done. To counteract this effect and to maintain approximate constancy of maximum temperature the distribution of work may be altered as indicated on the diagram by the dotted lines [1].

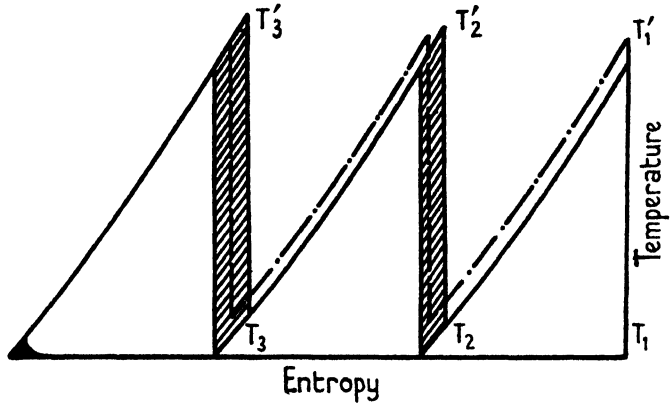

FIG. 141. An (H, T, S) diagram showing the effect of imperfect intercooling.

Notes on the Design of Multi-stage Compressors

(1) *A Compressor for Medium Pressures.* A compressor has to apply by suitable mechanical means the work required (*a*) to bring about a change of state in a definite weight of gas and (*b*) to make up the frictional and other losses in its various parts. An estimate of the work of compression can be made as already explained, although the calculations are complicated by transfers of energy taking place at all parts of the compression cycle. The frictional losses are more difficult to compute with accuracy and an estimate of their probable magnitude usually has to be made on the basis of the laws of fluid flow supplemented by the results of experience with similar types of machine.

In working out the details of a multi-stage compressor the first step is to determine the pressure and temperature distributions in the various stages, bearing in mind the desirability of dividing the work of compression fairly equally between the stages and ensuring that there will be no great maximum temperature variation. The procedure may best be illustrated by an example [1]:

Let it be required to compress 1,500 cubic metres of air hourly from atmospheric to 300 atmospheres pressure, in five stages. In the preliminary calculations the temperature at the beginning of the

compression stroke is assumed to be the same for all stages and somewhat higher than that of the suction air, say $t_0 = 25°$ C. The pressure in the fifth stage must also be some 10 atmospheres higher than the specified final pressure to allow for losses due to the valve loading and pressure drop in the delivery pipe-line. On the (H, T, S) diagram (Fig. 142) the intercept on the 25° isothermal line cut off

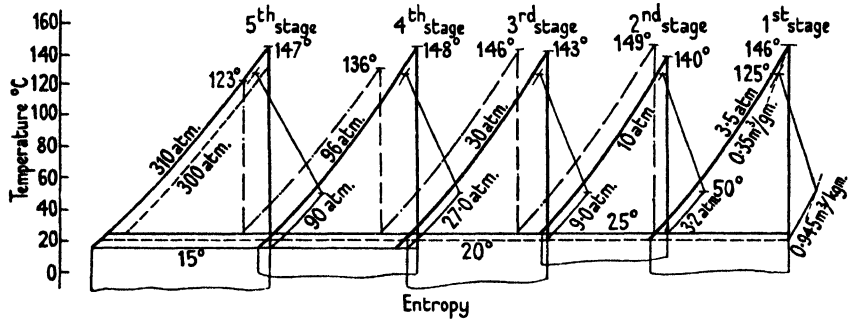

FIG. 142. The pressure and temperature distributions in a five-stage compressor.

by the $p = 1$ and $p = 310$ isobars is divided into equal parts corresponding with the number of stages, and the constant pressure line through each division then gives the pressure at that stage. Assuming adiabatic compression, the maximum temperatures for each stage may be read off directly from the diagram. In the figure the dotted curves represent the preliminary (T, S) diagrams for each of the five stages. From the diagram the following data are obtained:

	1st stage	*2nd stage*	*3rd stage*	*4th stage*	*5th stage*
H_1, k.cals./kg.	46·5	46·5	46·0	44·0	41·0
H_2 ,,	77·5	76·0	75·0	70·0	66·0
H_3 ,,	46·5	46·0	44·0	41·0	..
V_1, m.³/kg.	0·88	0·25	0·072	0·022	0·0075
V_2 ,,	0·36	0·105	0·032	0·011	0·0043
V_3 ,,	0·25	0·072	0·022	0·0075	0·0031
P_1, atms.	1	3·5	12	38	118
P_2 ,,	3·5	12	38	118	310
T_1, °C.	25	25	25	25	25
T_2 ,,	151	149	146	136	123
dS	0·087	0·087	0·087	0·087	0·087
P_2/P_1	3·50	3·43	3·16	3·10	2·62
$T\,dS$, k.cals./kg.	31·40	31·36	31·18	30·74	30·18
$H_2 - H_1$,,	31·0	29·5	29·0	26·0	25·0

Note: The subscripts 1, 2, 3 refer to the beginning and end of the compression stroke and the end of the delivery stroke.

It will be seen that on proceeding from the first to the fifth stage there is a progressive drop in the maximum temperature (T_2) and in the compression ratio. The heat equivalent of the work done in each stage as given by ($H_2 - H_1$) also falls from 31·0 k.cals./kg. in the first stage to 25·0 k.cals./kg. in the fifth stage.

By displacements of the pressure lines on the diagram the maximum temperature variations can be reduced to within 5° C. and a more even distribution of the work obtained. At this point corrections may also be applied for variations in the initial temperature due to imperfect intercooling between the stages.

The full-line curves in the figure show the (H, T, S) diagrams of the five stages after these adjustments have been made; the re-expansion lines for each stage are also included, the assumption being made that re-expansion is polytropic, starts at 125°, and terminates at 50° C.

The specific volumes at the beginning of the first stage of re-expansion (0·35 m.^{3}/kg.) and at the end (0·945 m.^{3}/kg.) are read off from the diagram and the volumetric efficiency ϵ_v is then given by

$$\epsilon_v = 1 - 0{\cdot}05\left(\frac{0{\cdot}945}{0{\cdot}35} - 1\right) = 0{\cdot}915,$$

where 0·05 is the clearance volume of the first stage.

If the compressor runs at 100 r.p.m. and the mean piston velocity is 2 m./sec., the length of the stroke will be 0·6 m.

The effective surface area of the first-stage piston (f_1) is

$$f_1 = \frac{1{,}500}{60 \times 0{\cdot}9 \times 0{\cdot}6 \times 100} = 0{\cdot}464 \text{ m.}^2$$

For the remaining stages, provided the volumetric efficiencies are constant, the effective areas will be proportional to the specific volumes at the beginning of the stroke.

The specific volume at the beginning of the first-stage compression, as read off from the diagram, is 0·86 m.^{3}/kg., and the weight of gas transmitted per hour is 1,500/0·86 = 1,745 kg.

The power requirements may be read off directly from the (H, T, S) diagram or may be calculated as already explained.

The data for the five stages are summarized in Table 76.

The diameters of the pistons are determined by the general arrangement of the compressor. If, for example, the pistons are

TABLE 76

Stage	I	II	III	IV	V
Initial pressure, atms.	1·0	3·2	9·0	27·0	90·0
Final pressure, atms.	3·5	10·0	30·0	96·0	310
Pressure ratio	3·5	3·13	3·3	3·56	3·44
Initial temperature, °C.	20	25	20	15	15
Final temperature, °C.	146	140	143	148	147
Specific heat (mean)	0·241	0·242	0·244	0·245	0·252
Work of compression (adiabatic), k.cals./kg.	30·3	31·0	30·0	31·8	32·2
Specific volume, m.³/kg.	0·86	0·273	0·098	0·0312	0·0093
Effective piston area, cm.²	4,640	1,470	528	168	50·1

alined as shown in Fig. 143 and the first stage is double, the diameters will be: $D_1 = 66{\cdot}5$, $D_2 = 51{\cdot}4$, $D_3 = 27{\cdot}8$, $D_4 = 16{\cdot}7$, and $D_5 = 8{\cdot}0$ cm. The diameter of the shaft $D_0 = 10{\cdot}0$ cm.

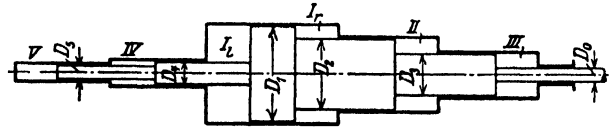

FIG. 143. The arrangement of cylinders in a five-stage compressor.

(2) *Compressors for High Pressures or for Gases near the Critical Point.* In the example worked out in the previous section the gas is far above its critical temperature and the conditions are such that no considerable changes in the specific heat occur, the enthalpy and temperature lines on the (H, T, S) diagram being nearly parallel. Even so, it has been noted that the procedure of taking equal entropy intervals does not lead to a satisfactory distribution of work in the final stages and an arbitrary method of smoothing out the inequalities had to be adopted; had the final pressure been 1,000 instead of 300 atmospheres the method would have broken down completely.

The reason for this limitation lies in the assumption that the gas obeys the law PV = a constant. In deriving an expression for the work of compression, valid over a wide pressure range, we might, as already pointed out, make use of one of the more accurate equations of state to integrate (15.5). The resulting calculations, however, would be laborious and the expression would not hold for compression near the critical point. A more satisfactory procedure is to employ the (H, T, S) diagram in the manner now to be described [2].

In Fig. 144 the adiabatic compression and constant pressure

delivery strokes of one stage of a multi-stage compressor are shown on an (H, T, S) diagram. At the beginning of the compression stroke A_1 the gas occupies a volume V_1 at a temperature and pressure of T_1 and P_1 respectively. Compression occurs at constant entropy and is represented on the diagram by the line A_1A_2; the final state of the gas is P_2, V_2, T_2. At A_2 the delivery valve opens and the gas is cooled to its original temperature at constant pressure P_2, the final volume being V_3. It is to be noted that P_1V_1 and P_2V_3 are not necessarily equal.

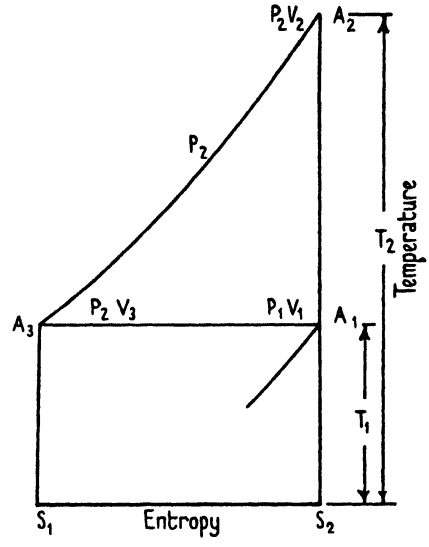

FIG. 144. The (H, T, S) diagram for one stage of a high-pressure compressor.

The work done during the compression stroke A_1A_2 is given by

$$W_{12} = \int_{V_1}^{V_2} P\,dV = E_2 - E_1 = E_{21}$$
$$= H_{21} - (PV)_{21} \qquad (15.33)$$

since no heat is received by or lost to the system. All the quantities on the right-hand side of this equation may be obtained directly from the (H, T, S) diagram.

The work of the delivery stroke A_2A_3 is given by

$$W_{23} = -\int_{V_2}^{V_3} P\,dV = -P_2 \int_{V_2}^{V_3} dV = -P_2(V_3 - V_2). \qquad (15.34)$$

By summing (15.33) and (15.34) we get the total work of compression and delivery:

$$W = W_{12} + W_{23} = \Delta H_{21} - \Delta(PV)_{31}. \qquad (15.35)$$

For an ideal gas, since the initial and final temperatures are the same, $P_1V_1 = P_2V_3$, $\Delta(PV)_{31} = 0$, and hence

$$W = \Delta H_{21}. \qquad (15.36)$$

The work of the delivery stroke may be expressed in terms of the change of entropy, as follows:

During delivery a quantity of heat Q_{32} is lost to the system and

$$W_{23} = \Delta E_{32} - Q_{32}$$

$$= \Delta E_{32} - \int_2^3 T\,dS. \tag{15.37}$$

Therefore $$W_{23} = \Delta H_{32} - \int_2^3 T\,dS - P_2(V_3 - V_2), \tag{15.38}$$

and, from (15.33) and (15.38),

$$W = \Delta H_{31} - \Delta(PV)_{31} - \int_2^3 T\,dS. \tag{15.39}$$

For an ideal gas $\Delta H_{31} = 0$ and $\Delta(PV)_{31} = 0$, so that (15.39) simplifies to

$$W = -\int_2^3 T\,dS = \Delta H_{21}, \tag{15.40}$$

which is the relation employed in the previous section.

From (15.35) and (15.39),

$$\Delta H_{32} = \int_2^3 T\,dS. \tag{15.41}$$

Eqs. (15.35) and (15.39) enable the work of compression and delivery to be calculated for any temperatures and pressures included on the (H, T, S) diagram. An interesting application is to the case of a gas undergoing compression at a temperature several degrees above its critical temperature. A practical example is carbon dioxide which has a critical temperature of 31·1° and a critical pressure of 73 atmospheres.

It will be seen from Fig. 145 that in the neighbourhood of the critical point the pressure lines have a point of inflexion above the critical temperature and are horizontal in the region of coexisting vapour and liquid; the enthalpy lines also curve sharply upwards and approach the vertical. The quantities $T\,dS$ and ΔH_{21} will, therefore, differ by a considerable amount.

Let it be required to compress carbon dioxide at 40° C., from 1 to 120 atmospheres. The first step is to fix the number of stages and the inter-stage pressures. For the purpose of comparison with the previous example we will employ five stages and determine the pressures by taking equal entropy intervals along the 40° isotherm between 1 and 120 atmospheres. The compression and delivery

TABLE 77. *Characteristics of a Five-stage Compressor for Carbon Dioxide at 40° C. (see (15.35) and (15.39) and Fig. 145)*

	1st stage	*2nd stage*	*3rd stage*	*4th stage*	*5th stage*
H_1, k.cals./kg.	177·2	176·5	173·3	163·0	145·0
H_2 ,,	204·0	198·0	188·3	168·0	147·3
H_3 ,,	176·5	173·3	163·0	145·0	123·0
V_1, litres/kg.	600	125	30	7·6	3·1
V_2 ,,	190	42	13	5·7	2·6
V_3 ,,	125	30	7·6	3·1	1·0
P_1, atmospheres	1	4·8	18·0	56	85
P_2 ,,	4·8	18	56	85	120
T_1, °C.	40	40	40	40	40
T_2 ,,	162	142	120	72	61
$T\,dS$, k.cals./kg.	26·1	25·5	24·7	23·0	22·6
ΔH_{21} ,,	26·8	21·5	15·0	5·0	2·3
ΔH_{31} ,,	0·7	3·2	10·3	18·0	22·0
$\Delta(PV)_{31}$,,	0	1·44	2·75	3·89	3·44
W (eq. 15.35), k.cals./kg.	26·8	22·94	17·75	8·89	5·74
W (eq. 15.39) ,,	25·4	23·74	17·15	8·89	4·04

TABLE 78. *Characteristics of a Three-stage Compressor for Carbon Dioxide at 40° C. (see (15.35) and (15.39) and Fig. 145)*

	1st stage	*2nd stage*	*3rd stage*
H_1, k.cals./kg.	177·2	176·5	171·7
H_2 ,,	204·0	202·3	196·0
H_3 ,,	176·5	171·7	123·0
V_1, litres/kg.	600	125	23
V_2 ,,	190	32	6
V_3 ,,	125	23	1
P_1, atmospheres	1	4·93	24·3
P_2 ,,	4·93	24·3	120.0
T_1, °C.	40	40	40
T_2 ,,	162	160	162
$T\,dS$, k.cals./kg.	26·2	31·7	74·8
ΔH_{21} ,,	26·8	25·8	24·3
ΔH_{31} ,,	0·7	4·8	48·7
$\Delta(PV)_{31}$,,	0	1·38	10·53
W (eq. 15.35), k.cals./kg.	26·8	27·18	34·83
W (eq. 15.39) ,,	25·5	28·28	36·6

strokes are shown by the dotted lines in Fig. 145 and the data required to solve (15.35) and (15.39), as read off from the figure, are summarized in Table 77.

Referring to the table, the pressure ratio (P_2/P_1) diminishes progressively from 4·8 at the first stage to 1·41 at the fifth stage;

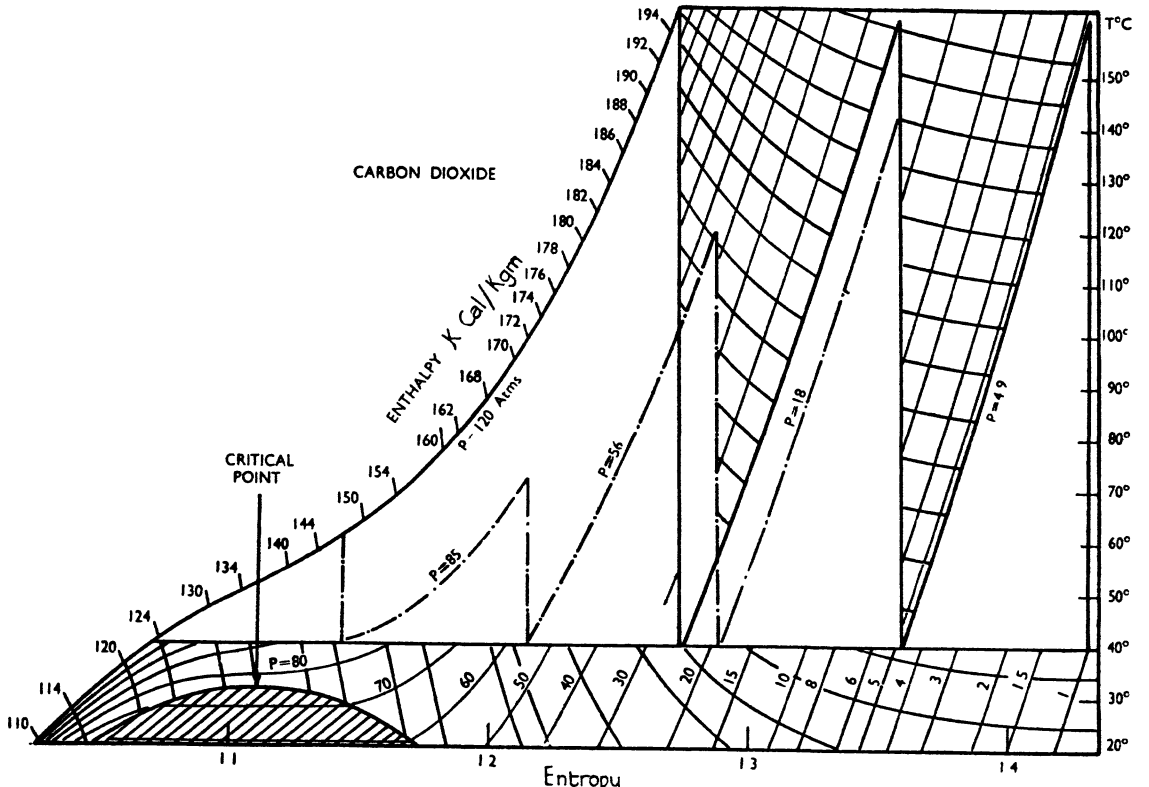

FIG. 145. The (H, T, S) diagram of a carbon dioxide compressor.

the optimum value calculated from (15.28) is 2·6. The maximum temperature (T_2) also diminishes throughout. Comparing the values of $T\,dS$ and ΔH_{21} it will be seen that they are approximately equal at the first stage, but the latter diminishes at a much greater rate than the former with increase of pressure. The work required for compression and delivery (W) also diminishes progressively from the first to the fifth stage. The result from the point of view of equal work distribution and equal maximum temperatures is unsatisfactory.

Now let the compression be carried out in three stages and let the inter-stage pressures be obtained by using (15.28). The compression and delivery strokes are shown in Fig. 145 and the data for calculating the work of compression are summarized in Table 78. As in the previous example, $T\,dS$ and ΔH_{21} are nearly equal in the first stage but differ considerably in the third stage. The maximum temperature is the same in all three stages, but the work of compression and delivery vary somewhat. It is possible, however, by small displacements of the pressure lines to equalize the work without introducing any large variations in T_2, and one or two attempts should be sufficient to arrive at the optimum conditions.

The (H, T, S) diagrams of all the common gases are available over wide ranges of temperature and pressure, and, provided they are drawn to a sufficiently large scale, enable the work of compression to be estimated with sufficient accuracy for most engineering purposes. It will be evident from the law of corresponding states, however, that the distribution of work in the various stages of a particular compressor is governed by the properties of the gas undergoing compression, and a machine designed for one gas will not be equally efficient for any other gas save at the same reduced temperature.

The Evaluation of the Terms w and $u^2/2g$

The kinetic energy required to circulate a gas in a closed system may be provided by means of a single-stage compressor of conventional design or, in special circumstances, as in the synthesis of ammonia, by sharing the energy of additional gas introduced continuously to the system through an injection nozzle. It may be evaluated with the aid of Reynolds's resistance law which embodies all the factors governing the flow of fluids in pipes under normal conditions.

In applying the resistance law the velocity of the gas is usually expressed in terms of the quantity $\eta/\rho d$, which also has the dimensions of a velocity; η is the viscosity, ρ the density of the gas, and d the diameter of the pipe. The resultant ratio (the Reynolds number) is dimensionless and it has been shown that for all fluids the change from stream-line to turbulent flow takes place at a value of the number not far removed from 2,300 [3].

In dealing with gases it is usual to assume the viscosity to be independent of and the density to be directly proportional to the pressure [4]. Neither of these assumptions is valid near the critical point of the gas or at high pressures, and to evaluate the Reynolds number, values based upon experimental data must be employed. When this procedure is followed it has been shown by Newitt and Sircar that the resistance law holds for compressed gases up to velocities corresponding with numbers as high as 536,000 [5].

The Viscosity of Gases at High Pressures

Viscosity is an irreversible phenomenon by means of which transfer of momentum takes place; the process is conditioned by the second law of thermodynamics, and its time-rate, on the basis of a classical molecular model, may be calculated by means of the kinetic theory.

The coefficient of viscosity (η) in C.G.S. units is defined as the force in dynes per square centimetre acting on a plane in the gas when the velocity gradient per centimetre normal to the plane is 1 cm. per second.

Maxwell has shown that for an ideal gas

$$\eta = \tfrac{1}{3} N m \bar{c} L; \tag{15.42}$$

and since for the same molecular model

$$L = \frac{1}{\sqrt{2}\,\pi\sigma^2 \bar{N}}, \tag{15.43}$$

we may write

$$\eta = \frac{m\bar{c}}{3\sqrt{2}\,\pi\sigma^2}. \tag{15.44}$$

If, on the other hand, the molecules behave as elastic spheres repelling one another according to the distance law μr^{-s}, Chapman [6] and Enskog [7] have derived a more accurate expression for the coefficient

$$\eta = \frac{0{\cdot}499 m\bar{c}}{\sqrt{2}\,\pi\sigma^2}. \tag{15.45}$$

In (15.45) the value $\bar{c}$ is given by

$$\bar{c} = \sqrt{\frac{8RT}{\pi Nm}} \tag{15.46}$$

and hence the viscosity should vary as the square root of the temperature; actually it is found to vary more rapidly than this owing to the dependence of the molecular diameter σ on temperature. The term σ is defined as the average distance of nearest approach of the centres of two molecules in collision; and if they are assumed to be elastic spheres surrounded by symmetrical fields of force, their apparent diameters will decrease as the mean molecular velocity increases and therefore as the temperature rises.

If the law is μr^{-s}, the force of repulsion between two molecules at a distance σ is

$$\frac{\mu}{\sigma^s} = -R\frac{dT}{d\sigma}, \tag{15.47}$$

which on integration gives

$$\sigma = \left[\frac{\mu}{RT(s-1)}\right]^{1/(s-1)}. \tag{15.48}$$

From this equation it follows that $1/\sigma^2$ will vary as $T^{2/(s-1)}$ and η as T^n, where

$$n = \frac{1}{2} + \frac{2}{s-1}.$$

Values of n and s for various gases are given in Table 79.

TABLE 79. *Values of n, s, and C*

Gas	*n observed*	*s calculated*	*C*
Air	0·754	8·87	111·3
Argon	0·815	7·36	169·7
Carbon dioxide	0·980	5·20	239·7
Carbon monoxide	0·740	9·30	100·0
Helium	0·681	12·05	80·3
Hydrogen	0·700	11·00	83·0
Nitrogen	0·740	9·30	118·0
Oxygen	0·800	7·70	138·0

It is found that η is given with reasonable accuracy over a not too wide temperature range by the equation

$$\eta = \eta_0\left(\frac{T}{273{\cdot}1}\right)^n, \tag{15.49}$$

where η_0 is the value of the coefficient at 0° C. Eq. (15.48), however,

would require σ to vanish at a sufficiently high temperature; in the light of modern views of molecular structure it is more probable that it would reach a minimum value, and Sutherland has proposed, on the basis of a van der Waals molecule, the relation

$$\sigma^2 = \sigma_\infty^2\left(1+\frac{C}{T}\right), \tag{15.50}$$

where σ_∞ is the value of σ for $T = \infty$, and C, known as Sutherland's constant, is the temperature at which $\sigma^2 = 2\sigma_\infty^2$.

From (15.50), $$\eta = \eta_0\left(\frac{T}{273{\cdot}1}\right)^{\frac{3}{2}}\frac{C+273{\cdot}1}{C+T}. \tag{15.51}$$

The values of C for a number of gases are given in Table 79.

Eq. (15.51) reproduces with considerable accuracy the variation of viscosity with temperature at normal and high temperatures, but for a number of gases it is not valid at low temperatures, and in the case of helium it fails at all temperatures.

Since for an ideal gas the quantities m, $\bar{c}$, and σ are independent of pressure, the coefficient of viscosity should also be independent except at very low pressures when the mean free path of the molecules becomes comparable with the dimensions of the containing vessel. For real gases the cohesive forces of the molecules must play an important part and, in the neighbourhood of the critical point, the viscosity should vary with temperature in much the same way as does the viscosity of a liquid. This prediction has been confirmed by Phillips, who has measured the variation with pressure of the viscosity of carbon dioxide at temperatures between 20 and 40° C.

The theory of the pressure effect has been worked out by Enskog [8] and leads to the prediction that the kinematic viscosity (η/ρ) should diminish at first with rise of pressure, pass through a minimum, and thereafter increase [8]. On the basis of his equation of state, namely,

$$p+a\rho^2 = \frac{RT}{M}\rho(1+b\rho k), \tag{15.52}$$

he concludes that the kinematic viscosity plotted against density should satisfy the equation

$$\eta/\rho = \frac{1}{2{\cdot}545}(\eta/\rho)_{\min}\left[\frac{1}{b\rho k}+0{\cdot}80+0{\cdot}7614b\rho k\right]. \tag{15.53}$$

It will be shown later that experimental determinations over a wide pressure range support his conclusions.

The Viscosity of Carbon Dioxide as a Function of Pressure

In 1912 P. Phillips published an account of a determination of the viscosity of carbon dioxide over pressure and temperature ranges

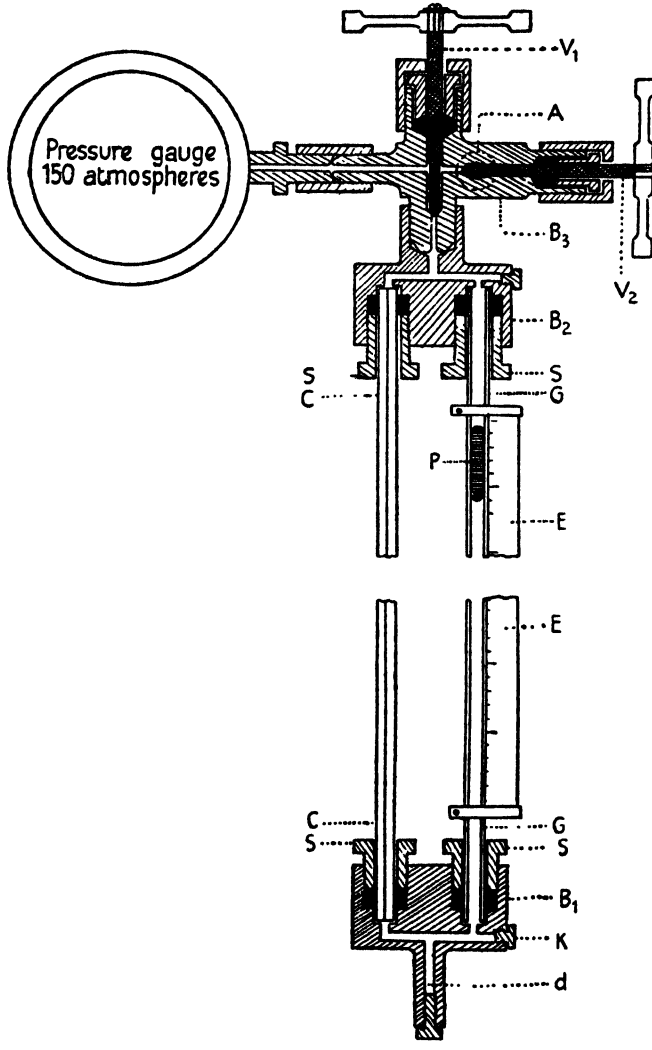

FIG. 146. Phillips's apparatus for measuring the viscosity of carbon dioxide.

including the critical point of the gas [9]. The method employed was to measure the rate of flow of the gas through a narrow capillary tube using the apparatus devised by A. O. Rankine [10], suitably modified to withstand high pressures (Fig. 146). In this method the

pressure head required to drive the gas through the capillary tube C is provided by a pellet of mercury P contained in the wide-bore tube G. The two tubes are housed in mild steel end blocks B_1 and B_2 and are obturated by soft rubber rings contained in the stuffing boxes S, S.

In Phillips's experiments the capillary tube was calibrated by a slight variation of the method of W. J. Fisher [11], the value of R^4 for the equivalent uniform tube being $1{\cdot}956 \times 10^{-8}$. Its length was 58·4 cm.

The whole apparatus was immersed in a thermostat provided with a window through which the movement of the mercury pellet could be observed and timed.

The relation used for the calculation of the viscosity is

$$\eta = \frac{\pi R^4 p t}{8 l v}, \tag{15.54}$$

where η is the coefficient of viscosity, R the radius of the capillary tube, p the difference of pressure on the two sides of the mercury pellet, l the length of the capillary tube, v the volume swept out by the pellet, and t the time of fall between two marks on the tube G. Since at high pressures p is only a very small fraction of the total pressure, the equation holds approximately whatever the law relating the volume and pressure.

The data for the viscosity and kinematic viscosity isotherms at 20, 30, 32, 35, and 40° C. for pressures up to 120 atmospheres are shown graphically in Figs. 147 and 148.

Referring to Fig. 147, it will be seen that below the critical temperature (30·29° C.) there are abrupt breaks in the viscosity isotherms, whilst at the critical point there is a point of inflexion; by analogy with the (P, V) isotherms of a gas one may assume a continuity of viscosity by joining the two points A and D marking the limits of the discontinuous region by the curve $ABCD$. The section AB of this curve would represent the viscosity of the superheated liquid and CD that of the supercooled vapour. The isotherms in the neighbourhood of the critical temperature cross before the gas is liquefied, a result indicating that in this region the gas is beginning to assume some of the characteristics of a liquid. The isotherms must necessarily cross since the viscosity of a gas increases with rise of temperature, whilst that of a liquid diminishes.

The kinematic viscosity isotherms at 30, 32, and 35° C. pass through minima at a constant value of $0{\cdot}69 \times 10^{-3}$ C.G.S. units, which is also the critical value of the kinematic viscosity (Fig. 148). Taking the critical density of carbon dioxide as 0·464 gm. per c.c., the critical viscosity will therefore be $0{\cdot}321 \times 10^{-3}$ C.G.S. units.

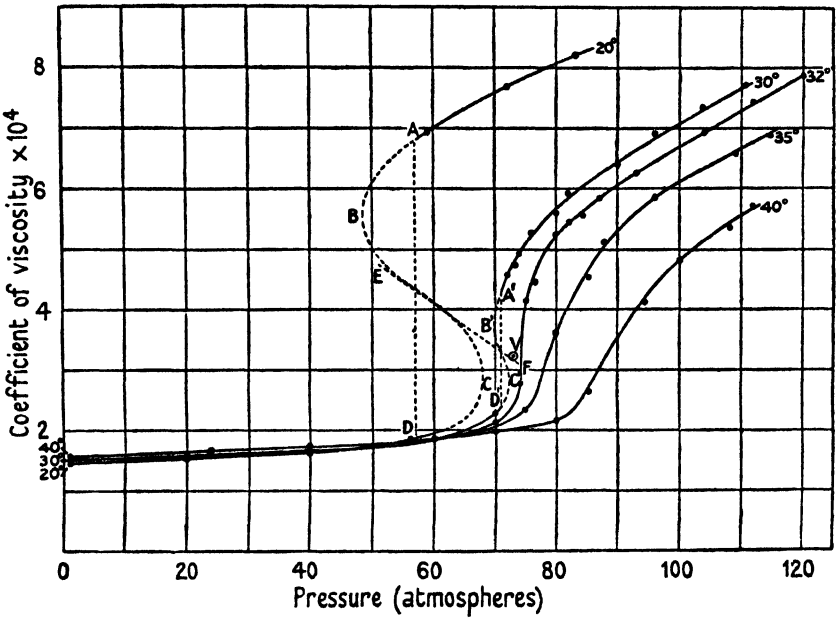

FIG. 147. The viscosity of carbon dioxide as a function of pressure.

Michels and Gibson's Determination of the Viscosity of Nitrogen [12]

The method employed by these investigators is based on the transpiration of the gas through a narrow glass capillary tube. The rate of stream-line flow of a fluid through a capillary is given by the equation

$$W = -\frac{\pi r^4}{8\eta}\rho\frac{dp}{dl}, \tag{15.55}$$

where W is the mass of fluid flowing in unit time through a tube of radius r under a pressure gradient dp/dl, ρ is its density, and η its viscosity.

The density will vary over the length of the capillary, but the

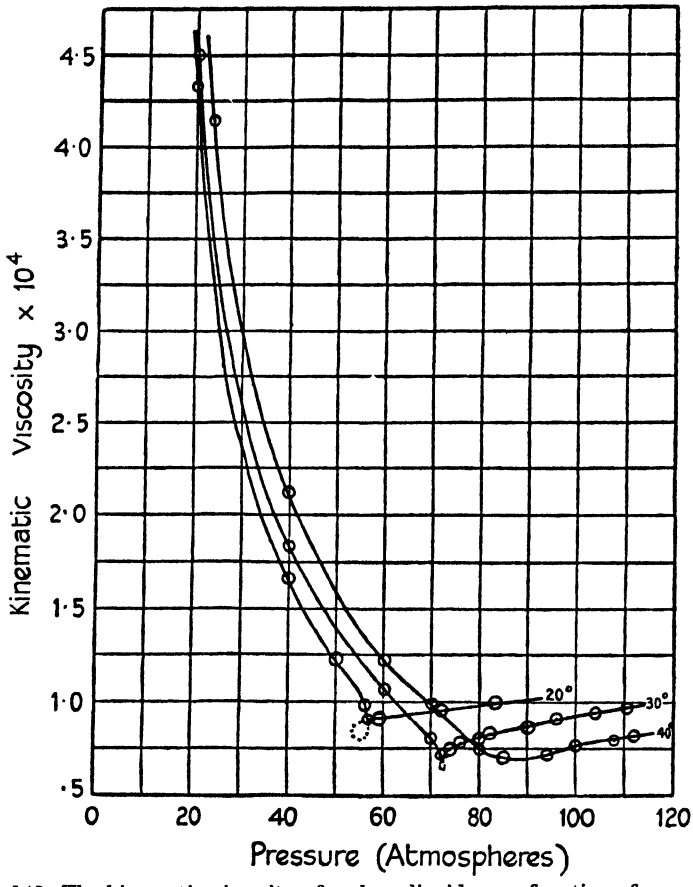

FIG. 148. The kinematic viscosity of carbon dioxide as a function of pressure.

viscosity and the weight W may be assumed to be constant. We may therefore write

$$-\frac{\pi}{8\eta}\int_{p_1}^{p_2}\rho\,dp = W\int_0^l \frac{dl}{r^4} \tag{15.56}$$

and

$$W = -\frac{\pi}{8\eta}\frac{\int_{p_1}^{p_2}\rho\,dp}{\int_0^l \frac{dl}{r^4}}. \tag{15.57}$$

To avoid turbulent flow in a capillary tube of the dimensions employed by Michels and Gibson (80 cm. long × 0·1 mm. diameter), the

pressure difference in the case of nitrogen must not exceed about 1 atmosphere. The density ρ of the gas at pressure p is calculated from the relation

$$\rho = \rho_0 \frac{p}{f(p)},$$

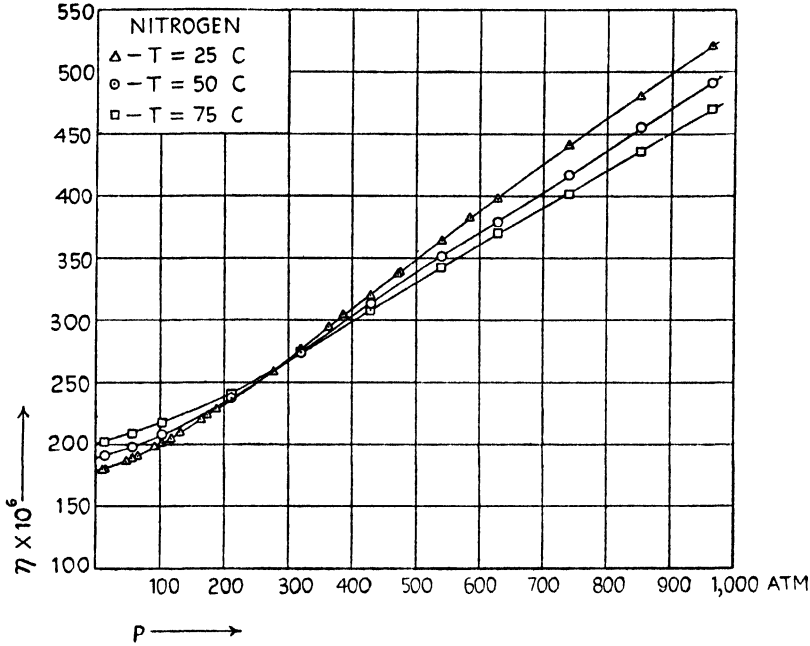

FIG. 149. The viscosity of nitrogen as a function of pressure.

where $f(p)$ is the experimental value of the product pV of the gas in Amagat units and ρ_0 is the density at 1 atmosphere. Substituting in (15.57),

$$W = -\frac{\pi}{8\eta}\rho_0 \frac{\int_{p_1}^{p_2} \frac{p\,dp}{f(p)}}{\int_0^l \frac{dl}{r^4}}; \tag{15.58}$$

or, if it be assumed that within the desired limits of accuracy $f(p)$ is constant over the pressure range $(p_1 - p_2)$,

$$W = -\frac{\pi}{8\eta}\frac{\rho_0}{f(p)\int_0^l \frac{dl}{r^4}} \tfrac{1}{2}(p_2^2 - p_1^2). \tag{15.59}$$

Corrections are necessary for the hydrostatic head of gas and for that part of the effective pressure difference utilized in accelerating the gas on entering the capillary and along its length on account of expansion.

For details of the experimental method the original paper should be consulted. The results of the measurements at 25, 50, and 75° C. for pressures up to 1,000 atmospheres are shown graphically in Fig. 149. It should be noted that at low pressures the viscosity has a positive temperature coefficient $(\partial\eta/\partial T)_p > 0$; at about 290 atmospheres the coefficient is zero whilst at higher pressures it is negative. If the viscosity is plotted against the density, then, within the limits of the experimental accuracy, $(\partial\eta/\partial T)_v$ is positive and remains substantially constant over the whole density range.

The kinematic viscosity when plotted against density exhibits well-defined minima as predicted by Enskog.

BIBLIOGRAPHY

1. P. Ostertag, *Die Entropietafel fur Luft.* J. Springer (Berlin), 1930; J. Ford, *Compressor Theory and Practice.* Constable & Co., Ltd. (London), 1923.
2. Newitt, *Trans. Inst. Chem. Eng.* (1939).
3. Stanton and Pannell, *Phil. Trans.* (A), p. 199 (1914).
4. Wildhagen, *Z. angew. Math. Mech.* **3**, 181 (1923).
5. Newitt and Sircar, *Trans. Inst. Chem. Eng.* **10**, 22 (1932).
6. Chapman, *Phil. Trans.* **211** A, 433 (1911); **216** A, 279 (1915).
7. Enskog, Inaug. Diss., Upsala (1917).
8. —— *K. Svenska Veten. Hand.* **63**, No. 4 (1922).
9. Phillips, *Proc. Roy. Soc.* (A), **87**, 48 (1912).
10. Rankine, *Proc. Roy. Soc.* (A), **83**, 265 (1908).
11. Fisher, *Phys. Rev.*, Feb. 1909.
12. Michels and Gibson, *Proc. Roy. Soc.* (A), **134**, 288 (1931).

XVI

THE INFLUENCE OF PRESSURE ON THE DIELECTRIC STRENGTH AND REFRACTIVITY OF GASES

In discussing the equation of state problem account has been taken of the forces originating with the positive and negative charges of the nucleus and electrons which constitute the framework of atoms and molecules. Further information about these forces may be obtained from a study of the dielectric strength and refractivity of gases; the two properties are related, the dielectric constant being the limit of refractivity for long wave-lengths.

As far back as 1858 the relation between the refractivity of a gas and its density was investigated by Gladstone and Dale [1], who found that the refractive index diminished by unity and divided by the density gave a constant characteristic of the substance in a particular state of aggregation; the relation when applied to the atoms of a compound was found to be additive, but it was not valid for mixtures nor for changes of state. Some ten years later Clausius [2] showed that the dielectric constant, D, of a gas is related to its density, ρ, by the expression

$$\frac{D-1}{D+2}\frac{1}{\rho} = \text{a constant}, \tag{16.1}$$

and, in 1860, Lorenz and Lorentz [3] simultaneously arrived at a similar relation for the refractive index, n, namely,

$$\frac{n^2-1}{n^2+2}\frac{1}{\rho} = \text{a constant}. \tag{16.2}$$

The assumption made in deriving these relationships is that the molecules behave as spherical electrical conductors, so that when placed in an electric field the centres of electrical action of the positive and negative charges in each molecule are separated and an induced polarity is created.

The constant of (16.1) is proportional to the polarizability of the molecules and has a value $\frac{4}{3}\pi z\alpha$, where z is the number of molecules in unit mass of the substance and α is the polarizability of a single molecule. Eq. (16.1) may, therefore, be written in the form

$$\frac{D-1}{D+2}\frac{M}{\rho} = \tfrac{4}{3}\pi\alpha N = P_0, \tag{16.3}$$

where M is the molecular weight of the substance and N is the Avogadro number; (16.3) is usually known as the Clausius-Mosotti equation.

Furthermore, since the index of refraction for long wave-lengths is equal to the square root of the dielectric constant,

$$\frac{n^2-1}{n^2+2}\frac{M}{\rho} = \tfrac{4}{3}\pi\alpha N = P \text{ (Lorenz-Lorentz relation).} \qquad (16.4)$$

The constant P of (16.4) gives a measure of the specific refraction of the substance; it is independent of the temperature and of the state of aggregation and is additive in respect of a molecule and its constituent atoms. Since $D = n^2$, one might expect P_0 to have similar properties. It is found, however, that for certain substances P_0 varies both with temperature and with the state of aggregation, and the additive rule does not hold. A satisfactory explanation of this difference between the two constants is given by Debye's theory [4].

Debye first pointed out that molecules composed of positive nuclei and negative orbital electrons would react in a similar way to conducting spheres when placed in an electric field, provided a proportionality between the induced polarization and the field strength is assumed. If some of the molecules possess permanent electrical dipoles due to the segregation of their charges, they will try to orientate themselves in the field with the axis of the natural moment in the direction of the field; this tendency will be opposed by the motion of the molecules due to their kinetic (thermal) energy, and, consequently, only a fraction of the permanent dipole moment will be effective. The contribution of the permanent dipole to the dielectric constant will diminish with increase of temperature and hence for this type of molecule P_0 will be dependent on temperature.

Debye has shown that for molecules having displaceable charges and permanent dipoles the polarizability is given by

$$\alpha = \alpha' + \frac{1}{3}\frac{\mu^2}{kT}, \qquad (16.5)$$

where α' is the polarizability due to the induced dipoles, μ is the permanent electric moment, and k is Boltzmann's constant. The corrected value for P_0 is, therefore,

$$P_0 = \tfrac{4}{3}\pi N\left\{\alpha' + \frac{\mu^2}{3kT}\right\}. \qquad (16.6)$$

This may be written in the form

$$P_0 T = a + bT, \tag{16.7}$$

where $a = \frac{4}{9}\pi N \frac{\mu^2}{k}$ and $b = \frac{4}{3}\pi N \alpha'$.

On plotting $P_0 T$ against temperature a straight line is obtained, the intersection of which with the axis of ordinates gives a and the slope of which gives b. From the values of a obtained from experimental data μ can be calculated and its magnitude for a number of substances is given below:

Substance	*Dipole moment*
Ammonia	$1{\cdot}44 \times 10^{-18}$
Carbon dioxide	0·06
Ethyl ether	0·84
Hydrochloric acid	1·034
Methyl alcohol	1·64
Propyl alcohol	1·66
Sulphur dioxide	1·62

It will be seen that the high values of μ are associated with those substances known as 'polar' compounds.

Since b represents the contribution made by the induced polarity it should have a value approximately equal to the constant P of (16.4) calculated for optical frequencies. Thus, for example, in the case of ammonia P has a value of 6·13 c.c. as compared with 5·45 c.c. for b. From the relative magnitudes of a/T and b the contributions of the displacement dipoles to the polarization can be ascertained. Thus, for ammonia, $a/T = 50{\cdot}8$ and $b = 5{\cdot}45$; hence the polarizability of the ammonia molecule is due largely to its permanent dipole moment.

Both P_0 and P have the dimensions of a volume and, according to the earlier Clausius-Mosotti theory,

$$P_0 = \frac{4\pi}{3} N r^3,$$

where r is the radius of the molecule, assumed to be a conducting sphere. P_0, therefore, represents the total volume of the spherical molecules contained in 1 gram-molecule, and should equal one-quarter of the co-volume term b of the van der Waals equation. A comparison of the values of P_0 obtained, on the one hand, from measurements of the dielectric constant, and, on the other, from critical data, show agreement only in the case of non-polar molecules.

Debye's theory has found ample support from numerous investigations into the dielectric properties both of gases at low pressures and of polar substances in dilute solution in non-polar solvents; but, as pointed out by the author, it embodies certain assumptions in regard to intermolecular forces which may not be valid for liquids or for gases at high pressures. In order to test whether the polarizability of a molecule is affected by changes of density, and, in the case of polar substances, whether the dipole moment is dependent on pressure, it is necessary to have data of a high order of accuracy both for the densities and the dielectric constants of the substances in question.

Until recently the methods available for the measurement of the dielectric constants of gases were not sufficiently refined to admit of any definite conclusions being drawn as to the existence of a pressure effect. The earliest recorded measurements are those of Occhialini and collaborators [5] (for air up to 350 atmospheres at room temperature), and Tangl [6] (for air, hydrogen, and nitrogen up to 100 atmospheres at 20° C.); they concluded that, apart from fluctuations in the measurements amounting to 1 per cent., the Clausius-Mosotti function is independent of the pressure. Of the more recent investigations those of Keyes and Michels and their collaborators have established beyond question the existence and nature of the pressure effect and have provided accurate data for many of the more important permanent gases.

The method and apparatus used for the determination of the constant at high pressure may be illustrated by reference to Michels and Michels's work upon carbon dioxide [7].

Michels and Michels's Determination of the Dielectric Constant of Carbon Dioxide. The dielectric constant was obtained by measuring the change in capacity of a condenser containing the gas by the standard heterodyne-beat method. One high-frequency circuit included the pressure condenser and a calibrated variable condenser, and the other was stabilized by means of piezo-electric quartz. The beat note from these circuits, after detection and amplification, was observed with a loud-speaker together with the note from a tuning-fork. During measurements the variable condenser was set so that the audible beat between the heterodyne note and the tuning-fork disappeared. For details of the circuits the original paper should be consulted.

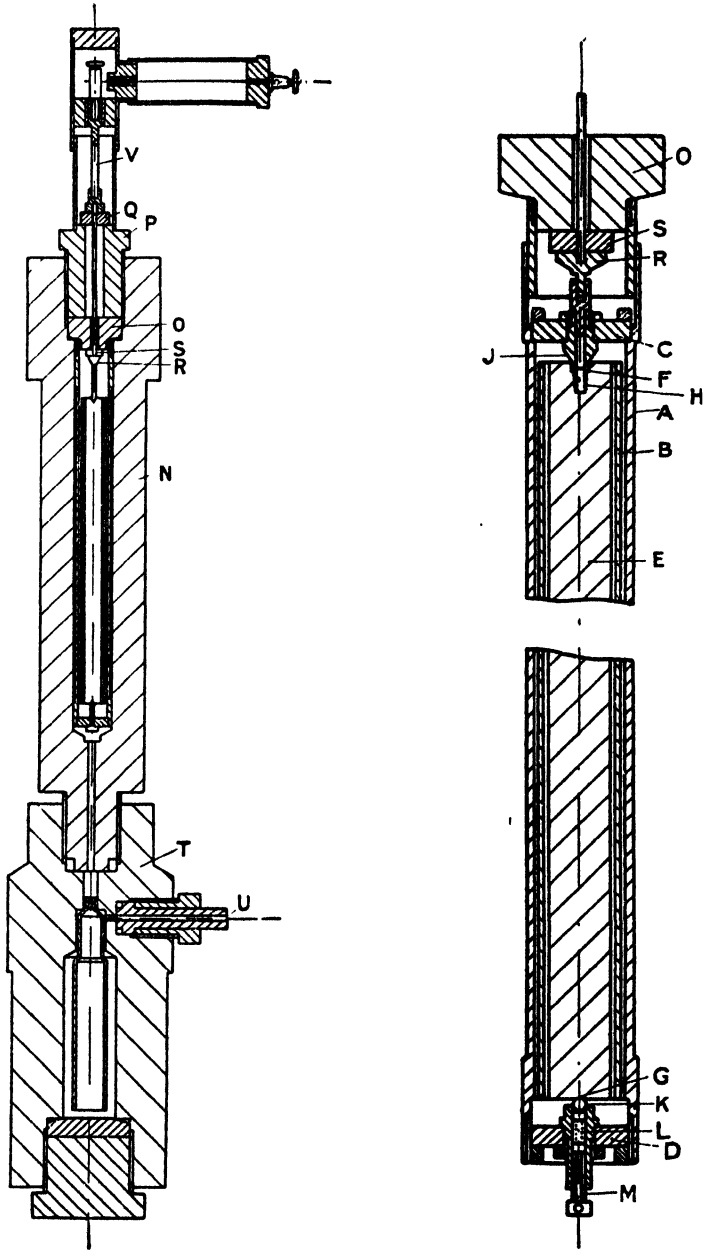

FIG. 150. Apparatus for measuring the dielectric constant of a gas at high pressure.

The high-pressure system comprises a high-pressure condenser, a gas compressor, a hydraulic press, a pressure balance, and auxiliary pipe-lines and valves. The high-pressure condenser shown in section, to scale, in Fig. 150 consists of two coaxial brass cylinders A and B, insulated from one another by two silica disks C and D. In order to decrease the dead space of the apparatus, and at the same time provide means for adjusting the inner tube inside the outer, a brass rod E was placed inside the inner tube. By means of the screw H the rod E was pulled against the steel cone J, its lower end being kept in position by the steel ball K. The condenser was contained in the steel cylinder N, the lead from the inner tube through the steel end plug P being insulated by means of the two silica disks Q and S. To make a gas-tight joint the two sides of the disk S were ground optically flat and rested against the optically smooth surfaces of the plug R and the lens-ring O. The cylinder N was screwed into the container T, which served as a mercury trap in the event of mercury coming over from the gas compressor. The gas was admitted to the condenser through the tube U. The connexion from the lead V to the high-frequency set was shielded from induction effects by a brass tube about 5 cm. in diameter.

The zero-capacity of the condenser was calculated from the change in the capacity when the condenser was evacuated and filled with benzene.

The condenser and its containing vessel were placed in a thermostat kept constant to within 0·01° C. The change of the zero-capacity due to the deformation of the material by the hydrostatic pressure and to temperature changes was calculated from the linear compressibility and the expansion coefficient of the material respectively.

The accuracy of the dielectric constants measured by this method is estimated to be $\pm 0{\cdot}0007$. Determinations were carried out at twelve temperatures between 25 and 150° C., thus including values through the critical region; the pressure range was from 30 to 1,000 atmospheres.

The results show that above the critical temperature the dielectric constant increases progressively with increase of pressure, the effect diminishing as the temperature is increased; below the critical temperature there is evidence of a very abrupt increase or discontinuity at the critical pressure (Fig. 151). The Clausius-Mosotti function decreases with increase of pressure above a density of 200 Amagat,

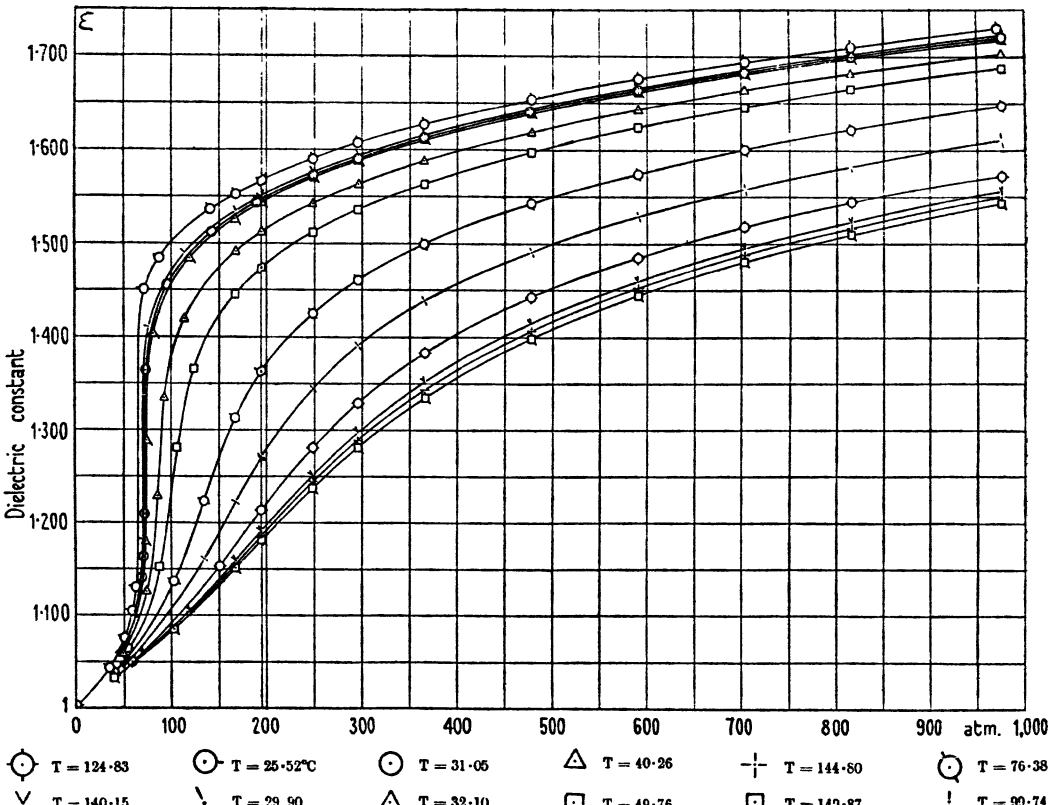

FIG. 151. The dielectric constant of carbon dioxide as a function of pressure.

but below this density any change in its value with pressure is comparable with the errors of the experiment. Later and more accurate determinations show that the function passes through a maximum at a density of about 300 Amagat.

The following include the more important recent determinations of the dielectric constants of gases at high pressures:

Helium and Hydrogen

Keyes, *Z. physik. Chem.*, Cohen Festschrift, p. 709 (1927).
Keyes, *Chem. Rev.* **6**, 175 (1929).
Michels, Sanders, and Schipper, *Physica*, **2**, 753 (1935).

The Clausius-Mosotti (C-M) function shows no definite trend with density or temperature. Michels and collaborators' results for hydrogen extend to 1,425 atmospheres at 25 and 100° C.

Nitrogen

Keyes and Kirkwood, *Phys. Rev.* **37**, 202 (1931).
Michels and Michels, *Phil. Mag.* **13**, 1192 (1932).
Michels, Jaspers, and Sanders, *Physica*, **1**, 627 (1934).

The data extend to pressures of 1,000 atmospheres and temperatures up to 150° C. The higher density data appear to show a faint positive trend with density, although there is some doubt as to whether the magnitude of the effect exceeds the experimental error.

Air

Waibel, *Ann. Physik*, **72**, 161 (1923).
Broxton, *Phys. Rev.* **37**, 1338 (1931).
Jordan, Broxton, and Walz, *Phys. Rev.* **46**, 66 (1934).
McNabney, Wills Moulton, and Beuschlein, *Phys. Rev.* **47**, 695 (1935).

The data which extend to pressures of 335 atmospheres are similar to those for nitrogen.

Methane and Propane

Keyes and Oncley, *Chem. Rev.* **19**, 195 (1936).

The C-M function for methane is independent of density up to 6·01 moles per litre. In the case of propane there is a positive drift with density.

Carbon Dioxide

Keyes and Kirkwood, *Phys. Rev.* **36**, 754, 1570 (1930).
Uhlig, Kirkwood, and Keyes, *J. Chem. Phys.* **1**, 155 (1933).
Michels and Michels, *Phil. Trans.* **231**, 409 (1933).
Michels, Michels-Veraart, and Bijl, *Nature*, **138**, 509 (1936).
Michels and Kleerekoper, *Physica*, **6**, 586 (1939).

The data both for the density and dielectric constants of carbon dioxide are known with a considerable degree of accuracy over a wide pressure range and the theoretical significance of the variation of the C-M function has been discussed critically by Keyes and Oncley (loc. cit.) and by Michels, de Boer, and Bijl [8].

Keyes and Oncley point out that whilst the molar polarization (the C-M function) for carbon dioxide at approaching zero density is very close to 7·35 c.c., neither their results nor those of Michels and Michels extrapolate

closely to this value, but instead show a widening spread as lower densities are approached. On plotting the expression $(D-1)/(D+2)$ against density the data do not in general lie on a line passing through the zero of the co-

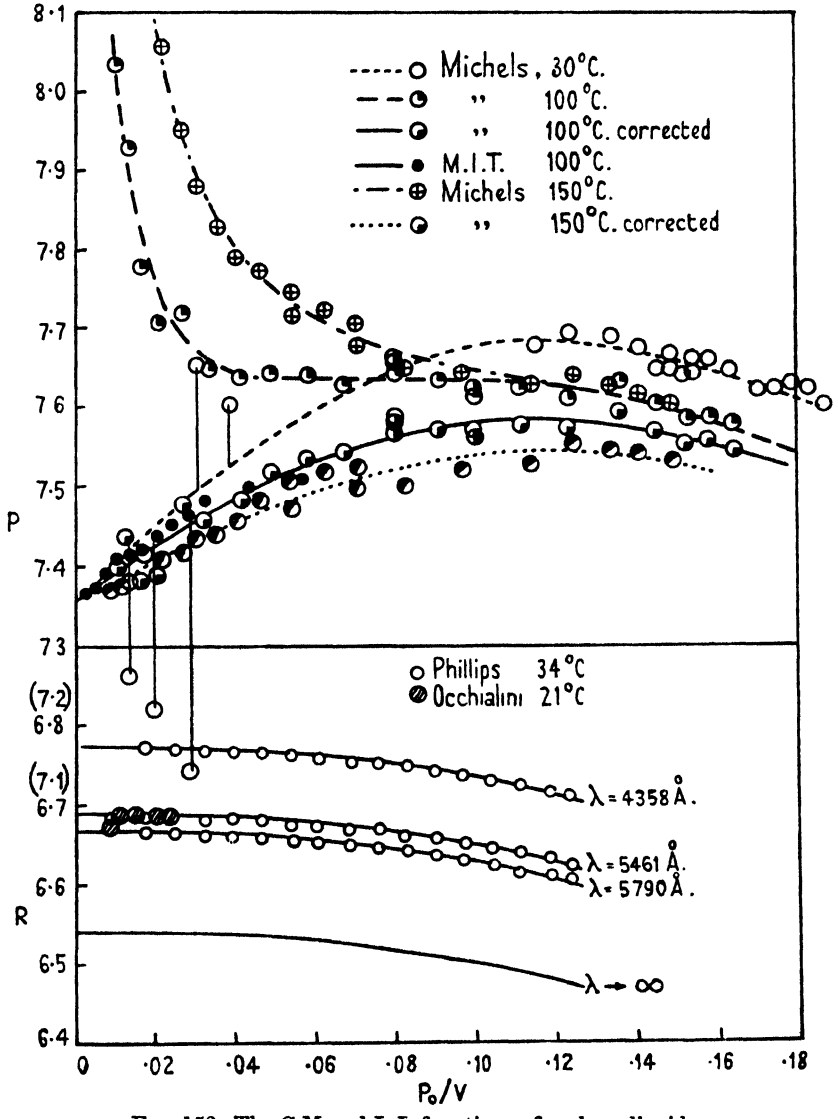

FIG. 152. The C-M and L-L functions of carbon dioxide.

ordinates, but when a correction equal in amount to the 'origin failure' is applied to all the values of $(D-1)/(D+2)$ the systematic trend in the low-pressure values of the C-M function is eliminated. The data shown graphically in Fig. 152 have been treated in this way and indicate that the C-M function

(1) at higher densities exceeds the value 7·35, (2) exhibits a maximum at about 16·3 moles per litre ($p_0/v = 0{\cdot}12$), and (3) has a rate of increase at low densities diminishing with increase in temperature. The magnitude of the initial variation of the function is about 2 per cent. for 100 atmospheres increase in pressure in the gaseous phase.

These conclusions are confirmed by a redetermination of the dielectric constant of carbon dioxide at 50 and 100° C. up to 1,700 atmospheres, by Michels and Kleerekoper (loc. cit.). They find that the C-M function as a

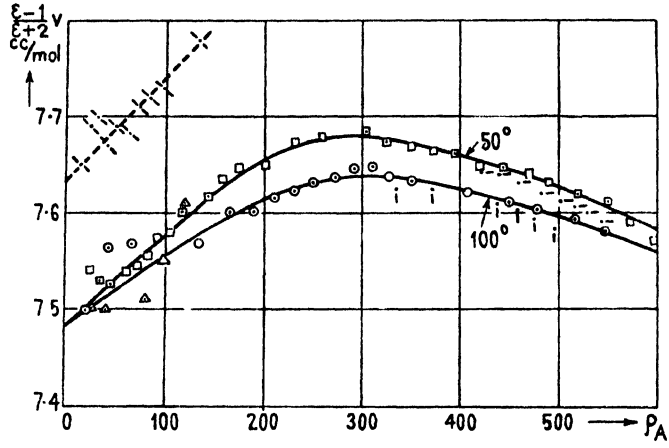

FIG. 153. Clausius-Mosotti function of carbon dioxide as a function of density. The experimental error in ϵ leads to an inaccuracy in the value of the C-M function of 0·045 cm.³ at 40 Am. and of 0·008 cm.³ at 200 Am. \ refers to data of Uhlig, Kirkwood, and Keyes.

function of the density passes through a maximum at about 300 Amagat and the extrapolated value at density 1 (7·48) is in fair agreement with accepted values at atmospheric pressure. Their results are shown graphically in Fig. 153.

It may be noted that the polarization (P) calculated from the Lorenz-Lorentz function has the same value as that given by the C-M function: its trend with density is, however, of opposite sign.

Ammonia

Keyes and Kirkwood, *Phys. Rev.* **36**, 754, 1570 (1930).

This is the only polar gas for which the dielectric constant has been measured over a wide range of pressures. The C-M function increases with pressure by approximately the same amount at all temperatures up to 200° C., the initial increase being about 5 per cent. per 100 atmospheres. The value of the dipole moment appears to be independent of the density.

There seems to be little doubt from the data given above that the polarizability of gaseous molecules is changed by pressure. Such a result might be brought about (a) as a result of intramolecular changes, e.g. by an alteration of the electronic levels of the molecules

with pressure, and (*b*) by intermolecular changes, e.g. the mutual orientation effect of non-spherical anisotropic molecules, or the occurrence of 'association' or 'aggregation' of the molecules.

At present insufficient data are available to enable any conclusions to be formed as to the reason for the dependence of the C-M function on pressure, and various attempts to develop a molecular statistical theory of the dielectric properties of non-polar molecules have not been successful [9].

The Effect of Pressure on the Refractive Indices of Gases

The earlier measurements of the refractive index by Siertsema [10] and Occhialini [11] were made with a Jamin refractometer and involved errors due to the pressure distortion of the apparatus, of such magnitude as to render uncertain the existence of any real fluctuation in the Lorenz-Lorentz function.

Phillips [12] overcame this difficulty by employing a Fabry and Perot étalon completely enclosed in the high-pressure container of his apparatus; his results for carbon dioxide at 34° C., densities between 58 and 360 Amagat units, and wave-lengths $\lambda = 5{,}790$, 5,461, and 4,358 A show a non-linear decrease of the L-L function with increase of density.

A similar method has been used by Michels and Hamers [13], who have obtained data for carbon dioxide up to 2,400 atmospheres at 25, 32, 50, and 100° C. and $\lambda = 6{,}678$, 5,876, 5,016, 4,922, 4,713, and 4,471 A. The essential parts of their apparatus are shown in Fig. 154. The étalon *C*, consisting of two silica disks separated by three minute silica plates, is contained in a high-pressure reservoir provided with a flat window *B*; it is mounted in a brass holder *D*, the conical end of which fits into a brass cup. The axis of the conical holder deviates by about $\frac{1}{6}$ degree from the central axis of the pressure reservoir so that the front plate of the étalon makes the same angle with the window; this arrangement is designed to prevent light, reflected from the window, obscuring the interference pattern. The light from a helium discharge tube is used to give a reference spectrum.

In carrying out a series of measurements the apparatus is first evacuated and a photograph taken of the interference and the reference spectra, the light source for the former being given by a carbon arc. The camera is then removed and a reading telescope focused

on the spectrum, the cross-wires coinciding with the yellow line (λ = 5,876 A) of the reference spectrum. Gas is then slowly admitted and the number of fringes passing the cross-wires up to the attainment of the desired pressure is counted. When the gas has attained thermal equilibrium a second photograph of the spectrum is taken.

In two regions special precautions have to be taken. For the runs at 32° C. in the neighbourhood of the critical point of carbon

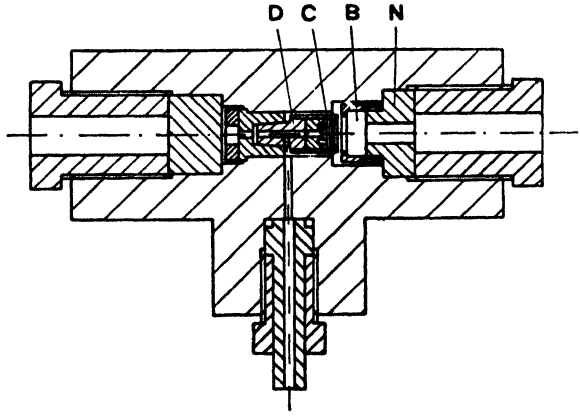

FIG. 154. Apparatus for determining the refractive index of a gas at high pressures.

dioxide, the density changes so rapidly for small variations in pressure that it is hardly possible to count the fringes if the pressure is raised by hand. In this region, therefore, the compression is carried out by first balancing the pressure against the pressure balance and increasing the weight on the balance by about 2 gm. (2·5 gm. = 0·001 atm.).

A second difficulty lies in correlating directly the measurements at 25° in the liquid region with those in the gaseous state at the same temperature. This is best effected by measuring the refractive index at 50° up to liquid densities and cooling to 25° while counting the fringes passing.

Michels and Hamers's results are given in Appendix 3. In Fig. 155 their data at 25° and 32°, together with Phillips's data at 34°, are shown graphically.

The results indicate that the refractive index increases and the L-L function decreases with increase of pressure, the magnitude of the effect being of the same order as that found for the Clausius-

Mosotti function. There are also indications of a decrease in the dispersion of the L-L function with respect to its value for $\lambda = 5{,}876$ A as obtained from the measurements at the highest densities with values derived from experimental data at atmospheric pressure.

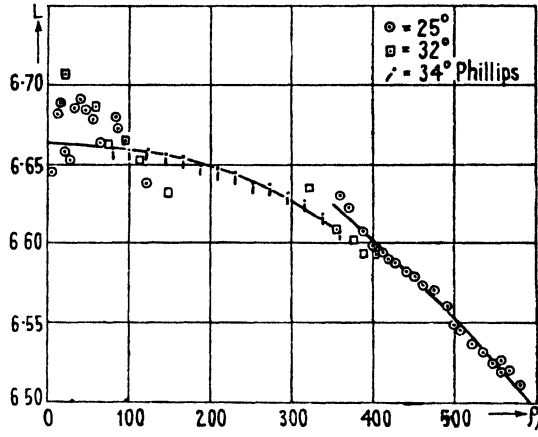

FIG. 155. The Lorenz-Lorentz function of carbon dioxide as a function of density.

The dispersion formula of Fuchs for carbon dioxide at low pressures indicates that the polarization calculated from the L-L function (7·28 c.c.) has the same value as that given by the C-M function (7·35 c.c.).

BIBLIOGRAPHY

1. GLADSTONE and DALE, *Phil. Trans.*, p. 8 (1858) and p. 523 (1863).
2. CLAUSIUS, *Collected Papers*, **2**, 135 (1876).
3. LORENZ, *Wied. Ann.* **11**, 70 (1880); LORENTZ, ibid. **9**, 641 (1880).
4. DEBYE, *Phys. Zeit.* **13**, 97 (1912).
5. OCCHIALINI, *Phys. Zeit.* **6**, 669 (1905); *Ann. d. Physik*, **42**, 67 (1913).
6. TANGL, *Ann. Phys.* **10**, 748 (1903); **23**, 559 (1907); **26**, 59 (1908).
7. MICHELS and MICHELS, *Phil. Trans.* **231**, 409 (1933).
8. MICHELS, DE BOER, and BIJL, *Physica*, **4**, 981 (1937).
9. See, for example, KEYES and KIRKWOOD, *Phys. Rev.* **37**, 202 (1931); KIRKWOOD, *J. Chem. Phys.* **4**, 592 (1936); MICHELS, DE BOER, and BIJL, *Physica*, **4**, 981 (1937).
10. SIERTSEMA, *Phys. Zeit.* **14**, 574 (1913).
11. OCCHIALINI, *Nuovo Cimento*, **8**, 123 (1914).
12. PHILLIPS, *Proc. Roy. Soc.* (A), **97**, 225 (1920).
13. MICHELS and HAMERS, *Physica*, **4**, 995 (1937).

XVII

THE EFFECT OF PRESSURE ON THE VISCOSITY AND REFRACTIVITY OF LIQUIDS

Introductory

In describing the phenomena associated with a fluid at and near its critical point, reference has been made to the principle of the continuity of state and a general resemblance has been shown to exist between the pressure-volume-temperature relationships of gases and liquids in this region. The analogy, however, must not be pressed too far; recent studies of the internal configuration of liquids based upon X-ray diffraction and optical analysis (infra-red and Raman spectra) suggest that even optically isotropic liquids may possess, in some degree, the spatial orderly arrangements characteristic of solids. The classification of liquids according to the variation of such properties as viscosity, surface tension, and compressibility with temperature and pressure can thus be shown to have a physical basis and a more precise meaning can be given to the term 'association', which hitherto has been used rather loosely.

A normal liquid may be defined as one composed of relatively simple molecules in which there are only undirected and unlocalized forces of the van der Waals type; such a liquid will exhibit no large fluctuations in density and no extensive regions of quasi-crystalline structure at temperatures and pressures above the critical point, and the probability of finding a molecule at a given distance from another molecule will be independent of the position of either in the liquid [1]. With the aid of this definition it is possible to present a rough picture of the behaviour of a hypothetical liquid and to derive approximate expressions for the collision number of the molecules in a pure liquid and of the solute molecules in a dilute solution.

A medium containing molecules of two species dissolved in an inert solvent affords a useful example of the mechanism by which collisions may occur in the liquid phase. The molecules of the liquids as a whole may be assumed to be each in thermal agitation so that any centre of mass is confined to an approximately spherical cage which, adopting the nomenclature proposed by Rabinowitch [2], may be designated the 'first coordination sphere'; the cage has a radius equal to the diameter of the molecule and is formed by adja-

cent solvent molecules which are themselves contained in cages of the same size. Each cage may be surrounded by a second one, but the regularity of arrangement is lost at a distance of a few molecular diameters. If attention be fixed on a particular solute molecule A and a second solute molecule B approaching it, then it is evident that whilst still several diameters apart B will enter a region in which an orderly arrangement prevails and its further movement will be affected by the presence of A; its path will no longer be independent in the sense that it would be in similar circumstances in a gas.

A collision in a gaseous medium is a unique event and a second collision between two specific molecules hardly ever occurs immediately. The actual values of the collision intervals are distributed according to the usual statistical law, the probability of an interval θ being proportional to $e^{-\theta}$. The mean number of collisions Z at normal temperatures and pressures is of the order of 10^{10} per second, and the average duration t of a collision is between 10^{-13} and 10^{-12} sec. In a solution such as has been postulated, if the diffusion rate is slow one pair of molecules, once having become coordinated, will in general make a large number of collisions before separating; the collisions occur in sets and a distinction may be made between the coordination frequency (Z_{coor}), indicating how often a molecule B comes into the coordination sphere of A, and the collision frequency (Z_{coll}), giving the number of vibrations of A–B during their coordination. According to Rabinowitch Z_{coll} is roughly twenty times larger and Z_{coor} about thirty times smaller than the corresponding value for a gas. The coordinations of A and B are brought about by diffusion, the diffusion coefficient D being given by

$$D = Ae^{-E_d/RT}, \tag{17.1}$$

where E_d is the activation energy of diffusion.

Jowett has pointed out [3] that an increase in viscosity at constant temperature increases the number of collisions, for although the diffusion rate is thereby diminished, the mean free paths of the molecules are also diminished whilst their speeds remain unchanged. According to this view the number of collisions taking place in unit time between a single molecule of species A and all molecules of species B in a liquid medium may be represented by the equation

$${}_AZ_B = \frac{1}{v_{f_{AB}}}\sigma_{AB}^2 n_A n_B \sqrt{\left\{8\pi RT\left(\frac{1}{M_A}+\frac{1}{M_B}\right)\right\}}, \tag{17.2}$$

which relates the collision rate in a liquid with that in a gas by means of a free space term v_f.

In dealing with a pure liquid Jowett assumes the validity of the Sutherland-Einstein equation for evaluating the diffusion coefficient in terms of the viscosity and derives the relation

$$Z = \frac{9\pi\eta r N}{M}. \tag{17.3}$$

Hence in any one liquid there is a linear relation between the collision rate and the viscosity. For a pure liquid (17.2) becomes

$$Z = \frac{16Nr^2}{Mvv_f}\sqrt{\left(\frac{\pi RT}{M}\right)}, \tag{17.4}$$

where v is the volume of 1 gm. of the liquid.

The value of v_f may now be obtained by combining (17.3) and (17.4):

$$v_f = \frac{16r}{9\eta v}\sqrt{\left(\frac{RT}{\pi M}\right)}. \tag{17.5}$$

For a number of organic liquids v_f is found to vary between 0·06 and 0·15, and hence the collision number would be about ten times greater than in a gas. The temperature coefficient of the collision rate is negative and approximately equal to that of the viscosity.

This and other methods of calculating the collision number suggest that instances in which the numbers in the gaseous and liquid phases are equal are fortuitous [4].

Associated Liquids

A liquid ceases to be 'normal' when the molecules are or can be linked by forces which are directed in space and localized on a definite part of the molecule, and a further classification of associated liquids is possible based upon the number of effective links that can be formed by each molecule [1]. In the case of water, for example, a maximum of four effective links or bonds is found in the solid phase and from two to three in the liquid phase between 0 and 100° C., and at room temperature association extends throughout the whole liquid. This condition accounts for the anomalous thermal expansion and high viscosity characteristic of water and other liquids of the same type.

A single link gives rise to bimolecular association such as is found in monohydric alcohols, whilst a double link may produce either

association in closed rings or in open chains according to the temperature; the open-chain association is usually characterized by high viscosity. For substances liquid at ordinary temperatures the links are usually H or OH bonds.

It will be evident that in associated liquids the conditions governing molecular collisions are complex, and attempts to calculate collision numbers by the methods applicable to gases will be fruitless.

Reduced Temperatures of Liquids

In studying the static properties of liquids and their variation as a function of temperature it is convenient to use a reduced temperature θ defined by the relation [13]:

$$\theta = \frac{T-T_f}{T_c-T_f}, \tag{17.6}$$

where T is the Kelvin temperature, T_f the melting-point or, more correctly, the triple-point temperature, and T_c the critical temperature. This variable may assume all values between 0 and 1 as the liquid passes from T_f to T_c; at the critical point it equals the van der Waals reduced temperature.

The use of reduced temperatures leads to some far-reaching generalizations which suggest the possibility of deriving a simple equation of state for liquids analogous to the reduced van der Waals equation; it has not yet been possible, however, to find a suitable reduced pressure, although this is not of importance since the properties of liquids are not very sensitive to changes of pressure except near the critical point. As an example of their application we may consider the case of molecular volumes. If the ratio of the molecular volumes of a series of liquids of widely differing properties at temperature T to their molecular volumes at temperature T_f be plotted against the reduced temperature θ, a mean curve may be drawn through the points, the deviations being less than 2 per cent. for values of θ up to 0·99. The mean curve may be fitted by an empirical equation containing only two arbitrary constants, namely,

$$V_T/V_f - 1 = 3{\cdot}36[1-(1-\theta)^{1/10}]. \tag{17.7}$$

A similar curve may be drawn for compressibilities, the ratio β_T/β_f being plotted against the reduced temperature. The results for ten liquids are shown in Fig. 156. The values of β used were those

obtained by extrapolating the experimental data to zero pressure. An empirical equation

$$\frac{\beta_T}{\beta_f} = \frac{1-\theta^4}{(1-\theta)^2} \tag{17.8}$$

represents closely the results for values of θ varying from 0 to 0·7.

As already pointed out, the method is not applicable to dynamic properties such as the viscosity.

The Influence of Temperature and Pressure on the Viscosity of Liquids

The temperature effect on the viscosity of liquids may satisfactorily be reproduced by two types of semi-empirical equations, in the first of which temperature is only responsible for the change in viscosity in so far as liquids generally expand on heating at constant pressure, and in the second of which it exerts a direct influence by activating the molecules [5].

The simplest form of the first type of equation is that due to Macleod, namely,

$$\eta = \frac{C}{(v-b)^n}, \tag{17.9}$$

where v is the specific volume, b the constant volume occupied by the molecules, and C is a constant containing the molecular weight as a factor. For non-associated liquids n approximates to unity and for associated liquids is greater than unity. The equation applies essentially to non-configurational liquids and indicates that for such liquids the viscosity is mainly a function of the volume or free space.

For liquids having a quasi-crystalline structure the application of a shearing stress will tend to produce changes in the configuration that will relieve the stresses; work will therefore be done by the shearing forces and a certain amount of energy B will be expended. The number of molecules or ions with energy exceeding this amount is proportional to $e^{-B/RT}$ and the viscosity will be inversely proportional to this number. For this class of liquid we therefore obtain the second type of semi-empirical equation

$$\eta = Ae^{B/RT}. \tag{17.10}$$

On the basis of the classification of liquids according to the types

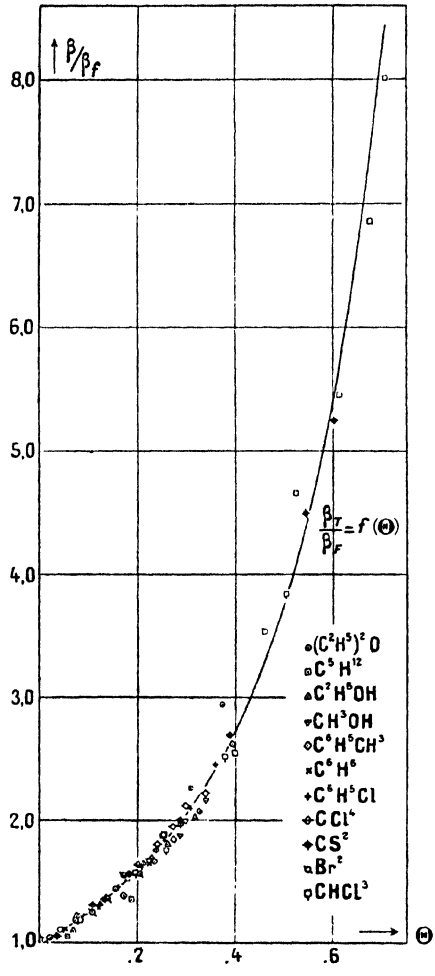

FIG. 156. 'Reduced' compressibilities of liquids.

of force between the particles of which they are composed, namely, (1) the presence or absence of permanent groups (molecules or complex ions) which cannot be treated as spherically symmetrical, (2) the presence or absence of directional forces, and (3) the magnitude, and change of magnitude with distance of separation, of the forces between the particles, it can be shown that the value of B in (17.10) depends on the coordination of the molecules and/or ions in the liquid, and if the mean coordination remains unchanged B will, to a first approximation, be independent of T; furthermore, for liquids of the same structural type when no change of coordination occurs on melting, the ratio B/L_f (where L_f is the latent heat of fusion) is approximately constant [6].

As an example of the modern approach to the problem of viscosity reference may be made to the reaction-rate theory recently proposed by Eyring [7] and worked out in some detail by him in collaboration with Hirschfelder [8]. The theory leads to an equation of state for liquids and an equation for the viscosity in terms of the energy of vaporization and the molal volume.

Eyring defines the free volume (V_f) of a liquid as the effective volume in which a particular molecule can move and obey the perfect gas law. If V_l is the molal volume of the liquid, d the incompressible diameter of a molecule, and b a 'packing' factor, then

$$V_f = b^3(V_l^{\frac{1}{3}}-d)^3. \tag{17.11}$$

For cubical packing, in which one molecule oscillates about the origin and the six nearest neighbours are assumed to be fixed at their mean positions along the three axes, each molecule is at a distance $V_l^{\frac{1}{3}}$ from the origin and $2V_l^{\frac{1}{3}}-2d$ is the distance that the central molecule is free to move along each axis; hence in this instance $b = 2$.

The external pressure (P_{ext}) acting on a liquid may be expressed in terms of the total and free volumes, thus:

$$P_{\text{ext}} = RT\frac{\partial}{\partial V_l}\log V_f + \frac{\partial \Delta E}{\partial V_l}, \tag{17.12}$$

where ΔE is the energy of vaporization. Combining (17.11) and (17.12) gives an equation of state for the liquid:

$$\left[P_{\text{ext}} - \frac{\partial \Delta E}{\partial V_l}\right] V_l^{\frac{1}{3}} V_f^{\frac{1}{3}} = bRT. \tag{17.13}$$

On solving (17.10) for V_f,

$$V_f = \left[\frac{bRT}{P_{\text{ext}} - (\partial \Delta E/\partial V_l)}\right]^3 \frac{1}{V_l^2}. \tag{17.14}$$

The change of configuration of the molecules may be supposed normally to occur equally in all directions and to be in energy equilibrium with the thermal vibrations; but when the liquid is subjected

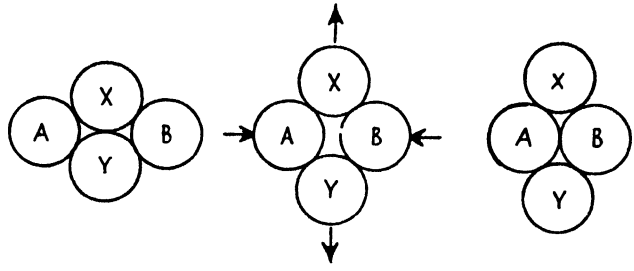

FIG. 157. Interchange between pairs of molecules.

to shearing stresses, those changes which tend to relieve the stresses will be favoured. The simplest type of change may be considered to be the interchange of neighbours between pairs of molecules, as shown in Fig. 157, there being an intermediate state in which the molecules are farther apart than in either stable configuration. Such a process requires a certain activation energy, and from this point of view viscosity is essentially a problem in chemical kinetics.

The activation energy for viscous flow ΔE_v will be some fraction of the energy of vaporization (i.e. of the energy required to make a hole in the liquid of the size of a molecule), and we may write

$$\Delta E_v = \Delta E/n,$$

where n has a value of 3 for molecules possessing spherical symmetry.

The Effect of Pressure on the Viscosity of Liquids

From the above considerations the following expression [9] for the viscosity η of a liquid may be derived:

$$\eta = \frac{1{\cdot}090 \times 10^{-3} M^{\frac{1}{2}} T^{\frac{1}{2}}}{V_l^{\frac{2}{3}} \Delta E} e^{\Delta E/nRT}. \tag{17.15}$$

The energy required to make a hole in the liquid at any pressure is given by $v(P_{\text{int}} + P_{\text{ext}})$, that is, by the work done in expanding a volume v against the combined internal and external pressures, v being the volume occupied by a molecule at P_{ext}. At low pressures

$vP_{\text{int}} = \Delta E$ and vP_{ext} is negligible; at high pressures, on the other hand, the two pressures are of the same order, and hence the equation for viscosity must be written

$$\eta = 1{\cdot}090 \times 10^{-3} \frac{M^{\frac{1}{2}} T^{\frac{1}{2}}}{V^{\frac{1}{2}}(P_{\text{int}} + P_{\text{ext}})} e^{V(P_{\text{int}}+P_{\text{ext}})/nRT}, \qquad (17.16)$$

where n is independent of pressure at least up to pressures of several thousand atmospheres.

If the internal pressure can be ascertained, (17.16) can be used to calculate the variation of viscosity with pressure.

The Internal Pressure or Cohesion of Liquids

The idea that liquids possess cohesive strength is by no means new and as far back as 1805 Thomas Young [10] published an account of his views 'On the Cohesion of Fluids', in which he states:

'We may suppose the particles of liquids, and probably those of solids also, to possess that power of repulsion, which has been demonstrably shown by Newton to exist in aeriform fluids, and which varies in the inverse ratio of the distance of the particles from each other. In air and vapour this force appears to act uncontrolled; but in liquids it is overcome by a cohesive force, while the particles still retain a power of moving freely in all directions. . . . It is simplest to suppose the force of cohesion nearly or perfectly constant in its magnitude, throughout the minute distance to which it extends, and owing its apparent diversity to the contrary action of the repulsive force which varies with the distance.'

Dupré (*Théorie mécanique de la chaleur*, 1869) identified the internal pressure of a liquid with the mechanical equivalent of the heat rendered latent in the evaporation of the liquid and considered that evaporation could be regarded as a process of disaggregation in which the cohesive forces have to be overcome. Thus he says: 'Le travail de désagrégation totale d'un kilogramme d'un corps quelconque égale le produit de l'attraction au contact par le volume, ou, ce qui équivaut, le travail de désagrégation totale de l'unité de volume égale l'attraction au contact.'

Air-free water possesses considerable tensile strength, and Berthelot has demonstrated that it can sustain a stress equivalent to about 50 atmospheres applied directly [11]. Worthington [12] has also studied the mechanical stretching of liquids and concludes that 'The unequivocal proof that a liquid can exist in stable equilibrium, in a state of isotropic tensile strain, has a bearing on the theory of

surface forces in fluids. For it can be shown to be necessary for equilibrium that a compressible liquid shall be, close to the free surface, less dense than in the interior; in other words, the surface layers are in a condition to which interior liquid could be brought by stretching it, and are, therefore, a seat of energy in precisely the same way that stretched liquid is a seat of energy.'

An estimate of the internal pressure can best be obtained from an equation of state representing accurately the behaviour of the liquid. If, for example, we consider the thermodynamic equation of state

$$P+\left(\frac{\partial E}{\partial V}\right)_T = T\left(\frac{\partial P}{\partial T}\right)_V, \tag{17.17}$$

$(\partial E/\partial V)_T$ represents the internal pressure, that is, the energy absorbed in overcoming the forces of molecular attraction when the liquid expands at constant temperature, and $T(\partial P/\partial T)_V$ represents the increase of pressure of a liquid at constant volume due to a rise in temperature, and is sometimes known as the thermal pressure.

The thermal pressure may be measured directly or obtained from the coefficients of expansion α and compressibility β by the relation

$$T\left(\frac{\partial P}{\partial T}\right)_V = -T\frac{\alpha}{\beta} \tag{17.18}$$

and the internal energy then calculated from the equation of state.

It should be noted that $(\partial E/\partial V)_T$ gives the slope of the potential energy-volume curve of the liquid and the point where P_{int} is a maximum (i.e. $(\partial P_{\text{int}}/\partial V)_T = (\partial^2 E/\partial V^2) = 0$) corresponds with the inflexion point of the potential energy curve where the repulsive forces are just beginning to become effective.

The Experimental Determination of the Viscosity of Liquids at High Pressures

Apart from the extensive measurements of Bridgman comparatively few data upon the effect of pressure on viscosity are available. Mention may be made, however, of the pioneer work of Roentgen [14] in 1884, of the work of R. Cohen [15] on the viscosity of water and sodium chloride solutions up to pressures of 900 kg./cm.^{2}, of Faust's [16] measurements of the viscosity of ether, ethyl alcohol, and carbon disulphide up to 3,000 kg./cm.^{2}, and of E. Cohen and Bruin's [17] work on mercury up to 1,500 kg./cm.^{2} Capillary flow

methods were employed by all the earlier experimenters and in no instance did the data obtained cover the range where the external pressure exceeds the internal pressure of the liquid.

Bridgman [18] employed for most of his work a falling weight method and carried his measurements up to pressures of 12,000 kg./cm.^{2}

The apparatus, shown in section in Fig. 158, consists of a steel cylinder of 6 mm. internal diameter so mounted that it can be rotated through 180° and observations carried out with the weight falling through a vertical column of the liquid from either end of the cylinder. The weight, which is made from pure nickel, is hollow and is provided with three projecting lugs which act as guides and which also serve to make electrical contact with the sides of the cylinder. At each end of its path the weight comes in contact with the insulated terminals *D* and the time of fall is determined electrically by making the current flowing through the circuit between walls of the cylinder and the terminals operate a suitable timing device. In order to keep the time of fall within reasonable limits, different weights are used according to the absolute viscosity of the liquid under investigation; the annular space between the weight and the cylinder may also be varied.

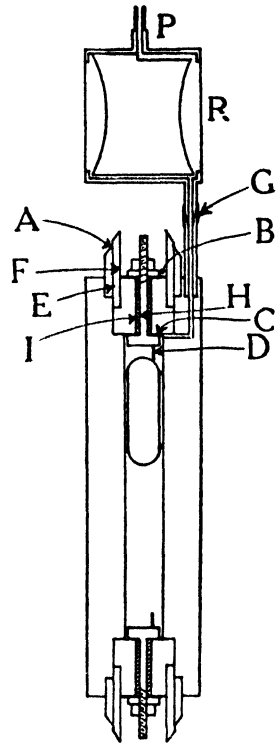

FIG. 158. Apparatus for measuring the viscosity of a liquid at high pressure.

The liquid whose viscosity is to be determined is kept from contact with the pressure transmitting fluid by means of a collapsible reservoir *R* made of pure tin. The reservoir and cylinder are filled through the opening *P* which is then closed by means of a soldered plug. The whole apparatus is then placed in a large pressure vessel and completely surrounded by the pressure-transmitting liquid. The reservoir *R* is 0·75 in. in diameter, the cylindrical tin wall being soldered at top and bottom to end disks of brass. It contains a metal core of such size that when the walls are entirely collapsed against the core, there is a diminution in volume of perhaps twice the compression volume of the liquid under the maximum pressure.

The insulated plugs *D* at the two ends of the cylinder require some description. The function of these plugs is not only to provide insulated leads but also to prevent the contamination of the liquid inside with the pressure-transmitting liquid. The central stem of the plug *H* is of brass, with a projecting needle of platinum. It is insulated by a sleeve of pipestone *I* and flat washers of mica *B* and *C*. The actual obturation of the plug is effected by the washer *C*. The seats on which the mica washers rest are ground flat

and the joint is made as tight as possible initially by means of the nut on the stem; it becomes still tighter under pressure owing to the differential compressibility of the brass stem and the steel housing.

Corrections are necessary for the inertia of the weight, for the change in buoyancy as the density of the liquid changes, and for variations in the dimensions of the apparatus with changes in pressure. The error in determining the time interval does not exceed 1/120 sec. For details of the timing apparatus the original paper should be consulted.

Versluys, Michels, and Gerver [19] have employed a similar method for determining the viscosity of oil at high pressures, with the addition of a capacity method for timing the fall of the weight. The method cannot be used with conducting liquids, and Bridgman [20] has therefore reverted to the capillary flow method for determining the viscosity of mercury.

The General Character of the Results

The results show that viscosity is a very distinctive property depending not only upon the molecular complexity but also upon the molecular structure. Generally speaking it increases with pressure, there being an approximately linear relationship between P and η over the first few thousand atmospheres. The largest pressure effects are associated with liquids composed of complicated molecules, and there is a marked constitutive effect, iso-compounds, for example, having a larger coefficient than the corresponding normal compound. It has also been observed that liquids composed of molecules containing OH or NH groups in which association occurs have greater viscosities than would be expected from the size and internal structure of the molecules. It is evident that in such cases the shearing forces required to produce flow have to overcome not only the van der Waals forces and dipole bonds but also the hydrogen bonds. Water (Table 80) differs from organic liquids in that the viscosity at 0° and 10° at first diminishes with increase of pressure, passes through a minimum at about 1,000 kg./cm.^{2}, and then increases.

Very little is known as to the effect of pressure on the viscosity of binary mixtures. R. B. Dow has examined six mixtures over the entire composition range at two temperatures, 30° and 75° C., and at pressures up to 12,000 kg./cm.^{2} [22], and finds occasional variations which cannot be explained by the thermodynamic properties

TABLE 80. *Relative Viscosity of Water at High Pressures (Bridgman)*

Pressure, kg./cm.²	*Relative viscosity*			
	0°	*10·3°*	*30°*	*75°*
1	1·000	0·779	0·488	0·222
500	0·938	0·755	0·500	0·230
1,000	0·921	0·743	0·514	0·239
1,500	0·932	0·745	0·530	0·247
2,000	0·957	0·754	0·550	0·258
3,000	1·024	0·791	0·599	0·278
4,000	1·111	0·842	0·658	0·302
5,000	1·218	0·908	0·720	0·333
6,000	1·347	0·981	0·786	0·367
7,000	..	1·064	0·854	0·404
8,000	..	1·152	0·923	0·445
9,000	..	..	0·989	0·494
10,000	Freezes	..	1·058	..
11,000	..	..	1·126	..

of the components. Thus, for example, whilst the isobaric curves on the viscosity-composition diagram for *n*-hexane-*n*-decane and for *n*-hexane-carbon disulphide are linear at both temperatures, the corresponding curves for *n*-hexane-chlorobenzene and *n*-hexane-diethyl ether are complex and show unexpected irregularities in certain regions of composition.

Unlike most other temperature effects the temperature coefficient of viscosity increases with pressure, the ratio η_{30}/η_{75} changing by as much as 4 over a pressure range of 12,000 kg./cm.², and Bridgman concludes from his results that the viscosity of liquids is not a function of the volume.

On applying (17.9) to viscosity data it must be borne in mind that the term b is dependent both on temperature and pressure, and if its value at any pressure can be calculated, as, for example, in the case of simple substances from the compressibility in the solid state, then the equation is found to hold with reasonable accuracy over the full pressure range of Bridgman's data. In the case of mercury Bernal [21] has calculated in this way the values of $(V-b)\eta$ over the range 1–12,000 kg./cm.² and find them to be reasonably constant (see Table 81).

It will also be evident that the term B of (17.10), the viscosity activation energy, increases with pressure; by extrapolating to negative pressures B, in the case of mercury, would vanish at a pressure of the order of −50,000 kg./cm.², which is approximately

TABLE 81. *The Variation of the Viscosity of Mercury with Pressure at 30° C.*

Pressure, kg./cm.²	b	V_{30}	$V_{30}-b$	η_{30}	$(V_{30}-b)\eta_{30}$
1	1·0000	1·0555	0·0555	0·0152	843
2,000	0·9950	1·0478	0·0528	0·0159	840
4,000	0·9906	1·0407	0·0501	0·0166	833
6,000	0·9864	1·0341	0·0477	0·0174	829
8,000	0·9826	1·0280	0·0454	0·0182	826
10,000	0·9791	1·0225	0·0434	0·0191	828
12,000	0·9761	1·0175	0·0414	0·0200	828

the internal pressure of mercury. Furthermore, since the viscosity of a liquid may be represented by the relations of (17.9) and (17.10), simultaneously, there is obviously a dependence on the configurational change in the liquid such as would lead to an expression

$$V = b + Ae^{-B/RT} \tag{17.19}$$

for the temperature dependence of volume.

Viscosity provides perhaps the best method at present available for measuring the free space in a liquid, and further data upon its variation with temperature and pressure would therefore be very desirable.

The Influence of Pressure on the Refractive Index of a Pure Liquid

It was pointed out in Chapter XVI that, although the specific refraction of a non-polar fluid (the Lorentz-Lorenz function) should depend only on its specific volume, a slight but definite drift in its value with pressure had been observed in the case of nitrogen. Very little comparable data is available for the liquid phase, the most complete series of observations being those of Gibson and Kincaid [23]. These workers have measured the refractive index of pure benzene at 25°, 35°, and 45° up to pressures of about 1,000 atmospheres by a method which consists in adjusting the pressure of the liquid at constant temperature until it has the same refractive index as a piece of optical glass immersed in it.

The benzene is contained in a small glass vessel provided with plane parallel windows, which also holds fragments of an optical glass whose refractive index is higher than that of the liquid at atmospheric pressure. Monochromatic light enters through one window, and through the other, the boundaries between the glass and liquid are observed by means of a microscope. The glass vessel

is contained in a steel pressure bomb which is also fitted with glass windows and is immersed in an oil bath the temperature of which is maintained constant to within 0·05° C.

With a good source of monochromatic light it is easily possible to reproduce within 1 bar the pressure at which the indices match, a precision corresponding with a change of approximately 0·00004 in the index of the liquid. Measurements were made with the sodium doublet $\lambda = 589$ mμ and the mercury lines 546 and 436 mμ. The compression of the benzene was also measured in the same apparatus according to the method already described. Corrections have to be applied for the effect of pressure and temperature on the refractive index of the glass; it was assumed that within the limits of the experiments the refractive index is a function of the volume only and the corrections could, therefore, be calculated from the compressibility and thermal expansibility by one of the well-known refraction formulae. For a given change in pressure the index of the glass was found to change about 0·025 times that of the liquid.

The results for two wave-lengths are given in Table 82.

It will be seen that whilst the Lorentz-Lorenz function diminishes with increase of pressure, the Eykman function $v(n^2-1)/n+0{\cdot}4$, which, however, is purely empirical, is constant.

From the data in Table 82 and the results of Hubbard [24] and of Timmermans and Martin [25] the dispersion of benzene is found to increase by approximately 7 per cent. per 1,000 bars rise in pressure.

TABLE 82. *The Refractive Index of Benzene as a Function of Pressure*

$\lambda = 589\,m\mu$

Temp., °C.	*Pressure bars*	n	*v*, c.c.	*Specific refraction*	
				Eykman	*Lorentz-Lorenz*
25	1	1·4983	1·14461	0·7506	0·3357
	272	1·5108	1·11819	0·7505	0·3349
	617	1·5240	1·09184	0·7506	0·3341
	868	1·5323	1·07611	0·7507	0·3336
35	1	1·4918	1·15878	0·7507	0·3361
	411	1·5108	1·11798	0·7504	0·3348
	767	1·5241	1·09185	0·7507	0·3341
	1,030	1·5324	1·07594	0·7507	0·3336
45	1	1·4851	1·17343	0·7504	0·3364
	547	1·5108	1·11782	0·7503	0·3348
	919	1·5242	1·09149	0·7505	0·3340
	1,188	1·5324	1·07574	0·7505	0·3335

TABLE 82 (*cont.*)

$\lambda = 436 m\mu$

Temp., °C.	*Pressure* bars	*n*	*v*, c.c.	*Specific refraction*	
				Eykman	*Lorentz-Lorenz*
25	1	1·5201	1·14461	0·7813	0·3480
	26	1·5212	1·14186	0·7810	0·3478
	343	1·5365	1·11221	0·7816	0·3471
	561	1·5449	1·09572	0·7812	0·3464
35	1	1·5134	1·15878	0·7815	0·3485
	154	1·5213	1·14171	0·7810	0·3478
	486	1·5365	1·11192	0·7814	0·3470
	713	1·5449	1·09545	0·7810	0·3463
45	1	1·5065	1·17243	0·7814	0·3489
	280	1·5214	1·14158	0·7811	0·3478
	629	1·5366	1·11144	0·7812	0·3469
	867	1·5450	1·09479	0·7807	0·3461

BIBLIOGRAPHY

1. BERNAL, *Trans. Far. Soc.* **33**, 27 (1937); Chem. Soc. Discussion, Feb. 1938.
2. RABINOWITCH, *Trans. Far. Soc.* **33**, 1225 (1937).
3. JOWETT, *Phil. Mag.* **8**, 1059 (1929).
4. EVANS and POLANYI, *Trans. Far. Soc.* **32**, 1350 (1936); BRADLEY, *Trans. Far. Soc.* **33**, 1185 (1937).
5. WIJK and SEIDER, *Physica*, **4**, 1073 (1937).
6. WARD, *Trans. Far. Soc.* **33**, 88 (1937).
7. EYRING, *J. Chem. Phys.* **4**, 283 (1936).
8. EYRING and HIRSCHFELDER, *J. Phys. Chem.* **41**, 249 (1937).
9. EWELL and EYRING, *J. Chem. Phys.* **5**, 726 (1937).
10. YOUNG, *Phil. Trans.* (1805).
11. BERTHELOT, *Ann. de Chim. et de Phys.* **30**, 232 (1850).
12. WORTHINGTON, *Phil. Trans.* (A), **183**, 355 (1892).
13. BAUER, MAGET, and SURDEN, *Trans. Far. Soc.* **33**, 81 (1937).
14. ROENTGEN, *Wied. Ann.* **22**, 578 (1884).
15. R. COHEN, *Wied. Ann.* **45**, 666 (1892).
16. FAUST, *Z. physik. Chem.* **86**, 479 (1914).
17. E. COHEN and BRUIN, *Z. physik. Chem.* **114**, 441 (1925).
18. BRIDGMAN, *Proc. Nat. Acad.* **11**, 603 (1925); **61**, 57 (1926).
19. VERSLUYS, MICHELS, and GERVER, *Physica*, **3**, 1093 (1936).
20. BRIDGMAN, *Proc. Am. Acad.* **62**, 187 (1927).
21. BERNAL, *Proc. Roy. Soc.* (A), **163**, 319 (1937).
22. DOW, *Phys. Rev.* **43**, 502 (1933).
23. GIBSON and KINCAID, *J. Am. Chem. Soc.* **60**, 511 (1938).
24. HUBBARD, *Phys. Rev.* **30**, 740 (1910).
25. TIMMERMANS and MARTIN, *J. Chim. Phys.* **23**, 747 (1926).

XVIII

THE PRESSURE-VOLUME-TEMPERATURE RELATIONSHIPS OF LIQUIDS

THE earliest extensive measurements of the compressibilities of liquids were carried out by Amagat, and his results for water and some ten organic liquids, including several normal aliphatic alcohols, ether, acetone and ethyl chloride, bromide, and iodide, are to be found in a paper published in the *Ann. de Chim. et de Phys.* (**29**, 68, 1893). The data cover the pressure range 1–3,000 atmospheres at temperatures between 0 and 40° C. and are of a high order of accuracy. The method and apparatus employed were similar to those already described for gases. The liquid was enclosed in a glass piezometer over mercury, and the change in volume with pressure was measured by visual observation of the mercury meniscus through a glass window in the steel containing vessel (Fig. 62, p. 161), or electrically by contact of the mercury surface with a series of platinum points fused into the capillary wall of the piezometer.

In 1903 T. W. Richards published the first of a series of papers on the compressibility of liquids and solids up to pressures of 500 kg./cm.^{2} at 25° C. [1]. In his earlier experiments the liquid was hermetically sealed in a very thin flat-sided flexible glass bulb, and the decrease in volume of the bulb upon compression was determined as if it were a homogeneous solid, by compressing it under mercury in a suitable containing vessel. Allowance was made for the change in volume of the mercury and glass by carrying out blank experiments with the containing vessel full of mercury. The glass bulbs when empty would collapse under an unbalanced pressure of 0·25 atmosphere, so that substantial equality of the inside and outside pressure could be assumed.

The compressibilities of water, mercury, and a number of pure organic liquids up to a pressure of 12,000 kg./cm.^{2}, at temperatures between 0 and 100° C., have been determined by P. W. Bridgman [2] who has tested several alternative methods of measuring small volume changes; in most of his work he uses one which consists essentially in observing the displacement of the piston by which the pressure is increased. The advantage of this method is that it enables a series of observations to be made at progressively increasing pressures with

one setting of the apparatus. The design of the pressure vessel and piston is similar to that illustrated in Fig. 44 (p. 102). The liquid is confined over mercury in a thin-walled cylindrical tube contained in a steel pressure vessel, which also houses the manganin resistance gauge used for measuring the pressure; the piston displacement is measured with an accuracy of 0·0001 inch on a total movement of 3 inches. The volume swept out by the piston includes the change in volume of the liquid, its container, the mercury, and the pressure-transmitting fluid; allowance has also to be made for the distortion of the whole cylinder. The various extraneous effects can be measured by replacing part of the liquid by a piece of steel or other solid of known compressibility; the change of cross-section of the cylinder with pressure cannot be measured directly but may be estimated to a near enough degree of accuracy by the theory of elasticity; the correction is at most 1 per cent. at 12,000 kg./cm.^{2}

A simple and convenient modification of the above method, suitable for measuring the compressibilities of liquids up to about 500 atmospheres pressure and at temperatures as high as 460° C., has been described by J. Keyes [3]. The apparatus is shown diagrammatically in Fig. 159. The liquid is contained in the vessel J, which in Keyes's experiments was made of pure nickel, and is in communication through a capillary tube with one of the risers of the volumenometer A. The latter consists of a plunger fitting closely into a steel cylinder containing mercury, and so designed that the volume swept out by the plunger is accurately known. Details of the screw operating the piston will be found on p. 104. The left-hand riser H of the volumenometer is connected to a pressure balance and is provided with an insulated lead for indicating the mercury-level. An injection pump fitted to the pressure balance enables the level to be kept constant.

Even with the most careful construction the volume displacement of the piston for successive turns of the screw will not be uniform and calibration over the whole range of the screw is necessary. Before doing this, however, the apparatus should be seasoned by subjecting it to a pressure considerably in excess of the highest working pressure, for several hours. The volumenometer and all accessory parts containing pressure-transmitting fluid are enclosed in a thermostat and maintained at constant temperature.

The compressibilities of a number of pure liquids and binary systems have been measured up to pressures of 12,000 bars by L. H.

Adams and R. E. Gibson of the Geophysical Laboratory of the Carnegie Institution of Washington. For the pressure range 1–1,000 bars they employ a piezometer of the form shown in Fig. 160 [4], constructed of pyrex glass. The volume of the piezometer is 8·5 c.c. and the diameter of the capillary at the base and at the tip is 0·5 mm.

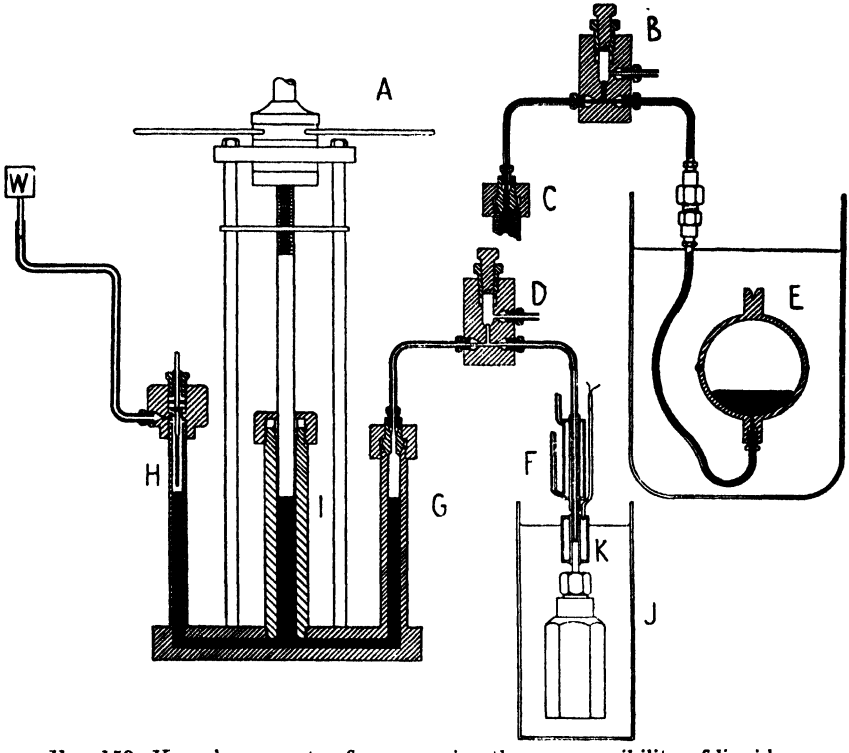

FIG. 159. Keyes's apparatus for measuring the compressibility of liquids.

It is filled with the liquid, including the capillary tube, and is placed in a thin-walled cup containing mercury which serves to transmit the pressure. On increasing the pressure the liquid diminishes in volume and mercury rises in the capillary tube and enters the vessel where it is trapped on release of pressure.

The piezometer is enclosed in a steel pressure vessel contained in a thermostat and pressure is applied by a hand-pump. The pressure is measured by a manganin resistance gauge, calibrated against a dead-weight piston gauge. In some later work a steel pressure vessel fitted with glass windows, through which the capillary tube of the piezometer could be viewed, was employed [10]. This enabled the

mercury-level to be adjusted flush with the tip of the capillary at the highest pressure and thus removed all uncertainty as to the

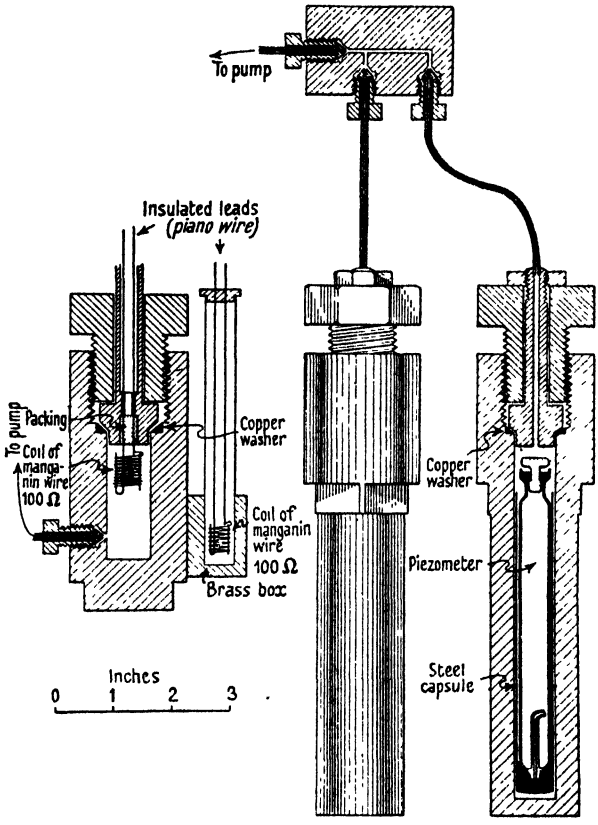

FIG. 160. Adams's apparatus for measuring the compressibility of liquids.

magnitude of the last drop. In this method corrections are necessary for the volume changes of the pyrex glass and of the mercury.

For pressures above 1,000 bars Adams and Gibson employ a piston-displacement method similar to that developed by Bridgman.

Corrections and Errors in the Experimental Determination of Compressibility

All the above methods measure the apparent volume change of a known amount of liquid when subjected to a given pressure, at constant temperature. Corrections are necessary for any accompanying changes in the volume of the pressure-transmitting liquids

(usually oil and mercury) and of the containing vessels. In those methods employing a glass piezometer, in which the change in volume is measured by the the weight of mercury occupying the compression space, the volume corrections are for the compressibility of the mercury and of the piezometer. By replacing a part of the liquid by a piece of steel, or other material whose compressibility is known, and again measuring the volume change, the absolute change in the volume of the liquid can be determined.

The total volume change ΔV divided by the initial volume of the liquid at atmospheric pressure V_0 is known as the compression or bulk compression of the liquid. If the compression of mercury k_m and of glass k_g are known, then the compression of the liquid k may be calculated from the apparent volume change in Adams and Gibson's apparatus by the equation

$$k = \frac{(V_m)_0(1-k_m)+(V_l)_0(1-k_g)}{V_0}+k_g, \qquad (18.1)$$

where V_0, $(V_m)_0$, and $(V_l)_0$ denote the volumes of liquid, of mercury remaining in the piezometer, and of the inside of the piezometer including the central capillary; the subscript 0 refers to atmospheric pressure.

In using glass vessels subjected to a uniform hydrostatic pressure hysteresis effects are of considerable importance; thus Bridgman has found that the elastic deformation of glass at a pressure of 6,000 kg./cm.^{2} may have irregularities of as much as 4 per cent. Adams and Gibson also conclude from their experiments that the apparent compressibility of pyrex glass depends on its thermal history, and they recommend an annealing treatment in which the piezometer is heated slowly to 550°, held at this temperature for some 15 minutes, cooled at the rate of 1° per minute for 20 minutes, and then cooled fairly rapidly in the furnace to room temperature. In using steel piezometers and in the piston-displacement method the steel containing vessels should always undergo a preliminary pressure 'seasoning' process in which they are subjected to a pressure in excess of the maximum working pressure for several hours.

In the piston-displacement method corrections are necessary for the change in volume of the whole of the pressure-transmitting liquids and of the outer steel pressure vessel. The method of calculating the latter correction has been given in Chapter VII.

It is important to avoid temperature fluctuations during the measurement of changes in volume, and the whole of the compression apparatus should be contained in some form of thermostat and maintained constant to at least 0·02°. Pressure should also be increased slowly and with frequent halts to permit of the heat of compression being dissipated before the final measurement is made.

The compression (k) at 25° for various materials used in connexion with compressibility measurements are given in Table 83.

TABLE 83. *The Compression* (k) *at* 25° *C. of Various Materials* (*Adams*)

$$k = -\frac{\Delta V}{V_0}.$$

Pressure in bars	*Water*	*Sodium chloride*	*Bessemer steel*	*Pyrex glass*	*Mercury*	*n-butyl ether*
1	0·0000	0·0000	0·0000	0·0000	0·0000	0·0000
500	0·0212	0·00205	0·00030	0·00151	0·00201	0·0439
1,000	0·0393	0·00409	0·00060	0·00303	0·00399	0·0747
1,500	0·0555	0·00611	0·00090	0·00456	0·00594	0·0964
2,000	0·0699	0·00812	0·00119	0·00608	0·00786	0·1156
3,000	0·0945	0·01208	0·00178	0·00915	0·01157	0·1441
4,000	0·1152	0·01598	0·00236	0·01224	0·01518	0·1665
5,000	0·1330	0·01982	0·00294	0·01534	0·01861	0·1843
6,000	0·1485	0·02360	0·00352	0·01846	0·02191	0·1998
7,000	0·1622	0·02731	0·00409	0·02159	0·02507	0·2132
8,000	0·1746	0·03095	0·00465	0·02475	0·02807	0·2246
9,000	0·1858	0·03454	0·00521	0·02792	0·03090	0·2353
10,000	0·1964	0·03806	0·00579	0·03111	0·03360	0·2448
11,000	(0·2059)	0·04151	0·00632	0·03432	0·03615	0·2532
12,000	(0·2147)	0·04492	0·00687	0·03754	0·03856	0·2608

Experimental Data

The volume change of a liquid with pressure (called the compression) is defined as

$$k = \frac{\Delta V}{V_0} = \frac{V_0 - V}{V_0}, \tag{18.2}$$

where V_0 and V are the total volumes at 1 atmosphere and P atmospheres respectively. The compressibility β is a derived quantity given by

$$\beta = -\frac{1}{V_0}\frac{dV}{dP} = \frac{dk}{dP} \tag{18.3}$$

and the specific compressibility β' by

$$\beta' = -\frac{dv}{dP} = v_0\frac{dk}{dP} = v_0\beta, \tag{18.4}$$

where v is the specific volume (volume per gram of liquid). The compressibility may be determined graphically from the pressure-volume isotherms or by differentiating the equation representing k as a function of the pressure.

The experiments of P. Bridgman provide the most complete data yet available of the changes of volume with pressure for a large number of pure liquids;† the pressure range covered is from 1 to 12,000 kg./cm.^{2} and the temperature range from 0 to 95° C.

Of the liquids tested the greater number diminish in volume by 20 to 30 per cent. when the pressure is raised from 1 to 12,000 kg./cm.^{2} at room temperature, *n*-pentane, ether, and ethyl chloride being the most compressible and chlor- and brom-benzene the least so. Glycerine is an exception in that it diminishes in volume by only 13·4 per cent. in similar circumstances. Of inorganic liquids carbon disulphide loses 24 per cent., phosphorus trichloride 22·4 per cent., and mercury only 4 per cent. in similar circumstances. The pressure-volume isotherms show a general resemblance one to another, and indicate that the compressibilities decrease with increasing pressure; in most instances indeed the value has decreased by about one-half over the first 1,000 kg./cm.^{2} (see Table 84). It is also noteworthy that the variations both in compressibility and in thermal expansion from liquid to liquid are much greater in the lower pressure range [2].

According to Bridgman, the results as a whole suggest that the volume change is determined by two factors, namely, the free space of the liquid and the compressibility of the molecules themselves. In the light of recent work on the liquid state, however, it would probably be more correct to say that the volume change is due to changes in molecular configuration, the closer packing of individual molecules, and to some extent the deformation or compression of the molecules themselves.

From the pressure-volume isotherms a number of important thermodynamic quantities may be derived using methods similar to those described for gases.

From the point of view of the mechanism of liquid-phase reactions an important derivative is the pressure coefficient $(dP/dT)_v$. It is

† The liquids employed were mercury water, phosphorus trichloride, carbon disulphide, methyl alcohol, ethyl alcohol, propyl alcohol, isobutyl alcohol, amyl alcohol, ether, acetone, ethyl chloride, ethyl bromide, ethyl iodide, glycerine, chlorbenzene, brombenzene.

TABLE 84. *The Compressibilities and Thermal Expansions of Fourteen Liquids (Bridgman)*

Liquid	*Compressibility, K*				*Thermal expansion,* $\delta = \left(\frac{dv}{dt}\right)_p$			
	$\frac{K_1}{K_{12,000}}$	$\frac{K_{1,000}}{K_{12,000}}$	$\frac{K_{6,000}}{K_{12,000}}$	$K_{12,000}$	$\frac{\delta_1}{\delta_{12,000}}$	$\frac{\delta_{1,000}}{\delta_{12,000}}$	$\frac{\delta_{6,000}}{\delta_{12,000}}$	$\delta_{12,000}$
Water	4·9	3·7	1·64	$0{\cdot}0_5 89$	1·00	1·00	1·00	$0{\cdot}0_3 400$
Methyl alcohol	18·4	8·2	2·20	$0{\cdot}0_5 74$	4·29	2·76	1·23	$0{\cdot}0_3 298$
Ethyl ,,	13·7	7·4	2·02	$0{\cdot}0_5 81$	4·50	2·73	1·30	$0{\cdot}0_3 268$
Propyl ,,	15·8	7·8	1·94	$0{\cdot}0_5 70$	4·80	3·06	1·33	$0{\cdot}0_3 237$
Isobutyl ,,	16·6	6·3	1·68	$0{\cdot}0_5 86$	4·15	2·62	1·17	$0{\cdot}0_3 275$
Amyl ,,	14·4	7·1	1·88	$0{\cdot}0_5 74$	4·40	2·84	1·30	$0{\cdot}0_3 240$
Ethyl ether	..	7·7	1·62	$0{\cdot}0_5 96$	..	3·65	1·32	$0{\cdot}0_3 248$
Acetone	..	7·3	1·85	$0{\cdot}0_5 87$	..	3·27	1·35	$0{\cdot}0_3 282$
Carbon disulphide	13·8	6·3	1·82	$0{\cdot}0_5 87$	5·47	3·16	1·31	$0{\cdot}0_3 262$
Phosphorus trichloride	14·2	7·1	1·81	$0{\cdot}0_5 80$	4·84	2·83	1·31	$0{\cdot}0_3 278$
Ethyl chloride	..	8·4	1·78	$0{\cdot}0_5 90$	..	3·44	1·37	$0{\cdot}0_3 267$
,, bromide	14·9	8·3	1·87	$0{\cdot}0_5 82$	..	3·46	1·33	$0{\cdot}0_3 260$
,, iodide	14·9	7·2	1·89	$0{\cdot}0_5 81$	4·86	3·15	1·22	$0{\cdot}0_3 248$
Kerosene	..	..	1·82	$0{\cdot}0_5 87$	..	..	1·14	$0{\cdot}0_3 280$

mathematically equivalent to the ratio of the dilatation to the compressibility:

$$(dP/dT)_v = -(dV/dT)_p/(dV/dP)_T. \qquad (18.5)$$

At low pressures experiment tends to show that the pressure coefficient is a function of the volume only, but at high pressures temperature also appears to exert an appreciable influence. Thus, in the case of carbon disulphide, the isothermal curves (Fig. 161), showing the changes in the coefficient with volume at 20, 40, and 80° C., indicate clearly the progressive influence of rising temperature, and similar results are obtained for a large number of organic liquids [2].

The thermal expansion or dilatation $(dV/dT)_p$ decreases with increasing pressure up to about 4,000 atmospheres, after which the pressure effect becomes irregular and in some instances the dilatation may increase with rising pressure over a range of several thousand atmospheres, and then again decrease. To mention an example, the dilatation of carbon disulphide at 20° C. at first decreases rapidly as the pressure is raised from 1 to 5,000 atmospheres and thereafter increases up to about 9,000 atmospheres, after which it again

decreases; at 80° C. similar though less pronounced effects are observable.

As regards the variation of dilatation with respect to temperature it is noteworthy that whereas at atmospheric pressure the dilatation

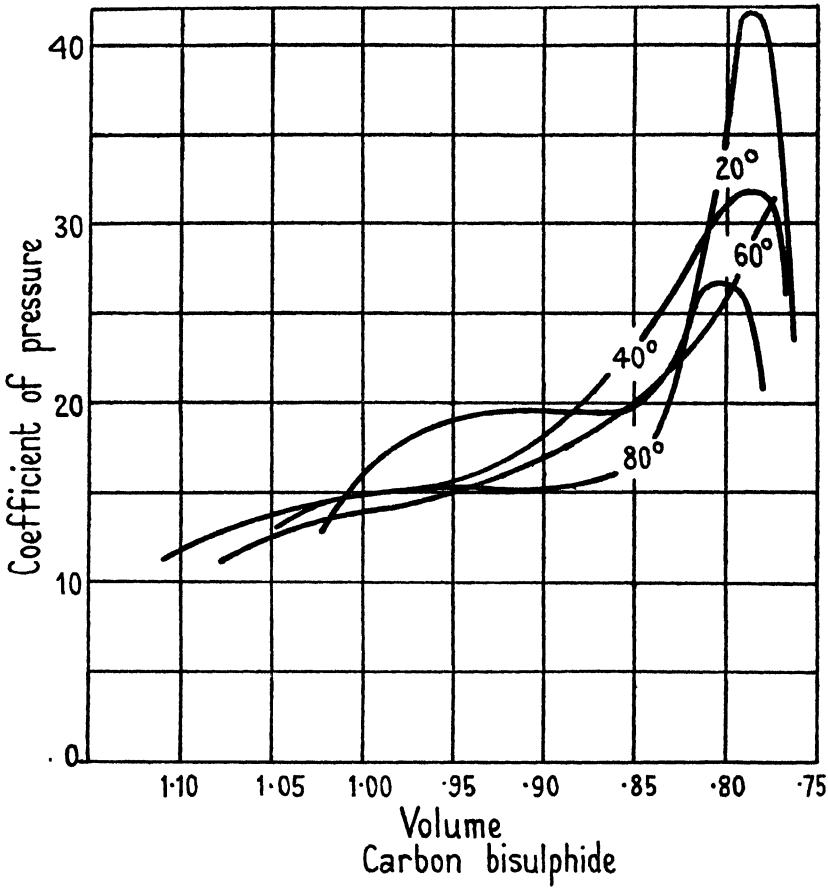

FIG. 161. The pressure coefficient of carbon disulphide as a function of volume.

increases with temperature, at pressures above about 3,000 atmospheres it diminishes; the reversal of the effect in almost all cases takes place sharply at a definite pressure, the same for all temperatures between 20 and 80° C.

It will be seen from Table 84 that both for compressibility and dilatation there is a tendency for most liquids at high pressures to

lose the individual differences which ordinarily characterize them; thus the ratio of the dilatation of ether to that of amyl alcohol at low pressures is 1·5, whilst at 12,000 kg./cm.^{2} it has dropped to 1·03; furthermore, the effect of pressure in decreasing the compressibility is much greater than its effect in decreasing the dilatation.

The quantity $-V^2(dE/dV)_T$ usually tends to decrease with rising temperature and rising pressure, an increase of 1,000 bars, in the case of benzene, causing a reduction of approximately 10 per cent.

The data for work and heat of compression, change of internal energy, and specific heats at constant pressure and volume are derived from the compressibility and thermal dilatation measurement and require little comment.

The mechanical work of compression is given by

$$(dw/dp)_T = -p(dv/dp)_T. \tag{18.6}$$

The curve showing the relation between the work of compression and the pressure is practically linear above about 1,000 atmospheres, and it may be noted that the maximum amount of work stored at 10,000 atmospheres is approximately the same for all liquids.

The heat of compression is given by the formula

$$(dQ/dp)_T = T(dv/dT)_p; \tag{18.7}$$

it is always positive and increases with pressure. The difference between the work received and the heat given out gives the change of internal energy on compression. Generally for liquids the internal energy, after decreasing over an initial pressure range of several thousand atmospheres, passes through a minimum and then increases with further increase of pressure; methyl and propyl alcohols are exceptions in that their internal energies diminish continuously over the whole pressure range from 1 to 12,000 kg./cm.^{2}

The Volumetric Behaviour of Binary Systems

The pressure-volume relationships of binary systems and, in particular, of aqueous solutions of inorganic substances present phenomena of considerable theoretical and practical interest. The properties that can conveniently be measured are the compressions and specific volumes of the systems as functions of composition, pressure, and temperature. From these data can be derived the partial molal volumes and partial compressibilities of the com-

ponents in solutions of varying concentration, the solubility of the solute as a function of pressure, and certain other thermodynamic quantities requisite for the determination of equilibrium conditions in the system.

The most comprehensive work on this subject has been carried out by L. H. Adams and R. E. Gibson, and a brief account will now be given of some of the principal conclusions resulting from their work [6].

In the case of aqueous solutions of salts it is found that the solution, in general, is very much less compressible than pure water at medium pressures but that the difference tends to disappear at high pressures. As an example, a 25 per cent. solution of sodium chloride at atmospheric pressure has a compressibility of $27{\cdot}4 \times 10^6$ compared with $44{\cdot}9 \times 10^6$ for water, but at 10,000 bars the corresponding values are $8{\cdot}3 \times 10^6$ and $9{\cdot}46 \times 10^6$ respectively. For the sulphates of sodium, magnesium, lithium, potassium, zinc, copper, cadmium, caesium, beryllium, cerium, ammonia, and hydrogen it is found that the compressions of solutions of the same molality, for those which are not greatly hydrolysed in solution, are approximately the same.

The molal lowering of the specific compression of water by the solute has been shown to be approximately the same for the sulphates of sodium, magnesium, lithium, potassium, zinc, copper, cadmium, and caesium; the effect is not so great for beryllium, cerium, and ammonia, and it is surprisingly small for sulphuric acid, 2·7 moles of acid being required to produce the same lowering of compression as 0·5 mole of sodium sulphate. Carbonates and hydroxides, in general, exert the greatest effect.

Richards and Chadwell suggest that the physico-chemical factors leading to the change of compressibility of water by the addition of a solute are depolymerization, changes in intermolecular forces, and the compressibility of the solute itself [7]. From their measurements of the compressibilities of aqueous solutions of ether, methyl acetate, and urethane they conclude that in dilute solutions depolymerization is the most important factor, the extent of the effect being approximately proportional to the number of moles of solute added. In order to obtain further information upon this aspect of the subject it would be desirable to have experimental data upon the changes of the viscosity of aqueous solutions with pressure, from which the free space and internal pressures could be calculated, as already described.

The anion portion of a salt appears to be most effective in changing the degree of association of the water; in dilute solutions, for example, equal numbers of moles of sulphate reduce the polymerization by the same amount; the cation portion of the solute also exerts a small but specific influence. From the results of an extensive series of compressibility measurements of the halide salts of potassium, lithium, sodium, caesium, barium, and cerium and various nitrates, chlorates, ferrocyanides, carbonates, and acetic acid it is found that on plotting the bulk compression k against the concentration function $\frac{1}{2}C_2(v_c z_c + v_a z_a^2)$, where C_2 is the number of moles of solute per litre of solution, v_c and v_a are the number of cations and anions into which a molecule dissociates, and z_c and z_a are the valencies of cations and anions respectively, the points for all the above compounds fall within a relatively narrow band (Fig. 162).

Tait and Tammann have each put forward a semi-empirical expression for the specific compressibility of water as a function of pressure [8]. Tait's equation is written

$$dv/dP = C/(B+P), \tag{18.8}$$

where C and B are constants. In the integrated form this becomes

$$-\Delta_p v = C\log(B+P)+\text{constant},$$

or

$$k = C\log\frac{B+P}{B}. \tag{18.9}$$

Adams's data for water and Gibson's data for methanol and glycol are represented fairly well by this equation with the following values of the constants:

Water at 25° C., over the pressure range 1–10,000 bars:

$$-\Delta_p v = 0{\cdot}3071\log(2{\cdot}923+P)-0{\cdot}1430; \tag{18.10}$$

Methanol at 25° C., over the pressure range 1–1,000 bars:

$$-\Delta_p v = 0{\cdot}2807\log(0{\cdot}764+P)-\log 0{\cdot}765; \tag{18.11}$$

Glycol at 25° C., over the pressure range 1–1,000 bars:

$$-\Delta_p v = 0{\cdot}2054\log(2{\cdot}706+P)-0{\cdot}08879; \tag{18.12}$$

where P is measured in kilobars, and $-\Delta_p v$ is the specific compression of the pure liquid. The subscript p after Δ signifies that the change in the quantity under consideration pertains to two different pressures at the same concentration.

It has been shown by Carl [9] that the constant C of the Tait equation is independent of temperature, and it has been suggested

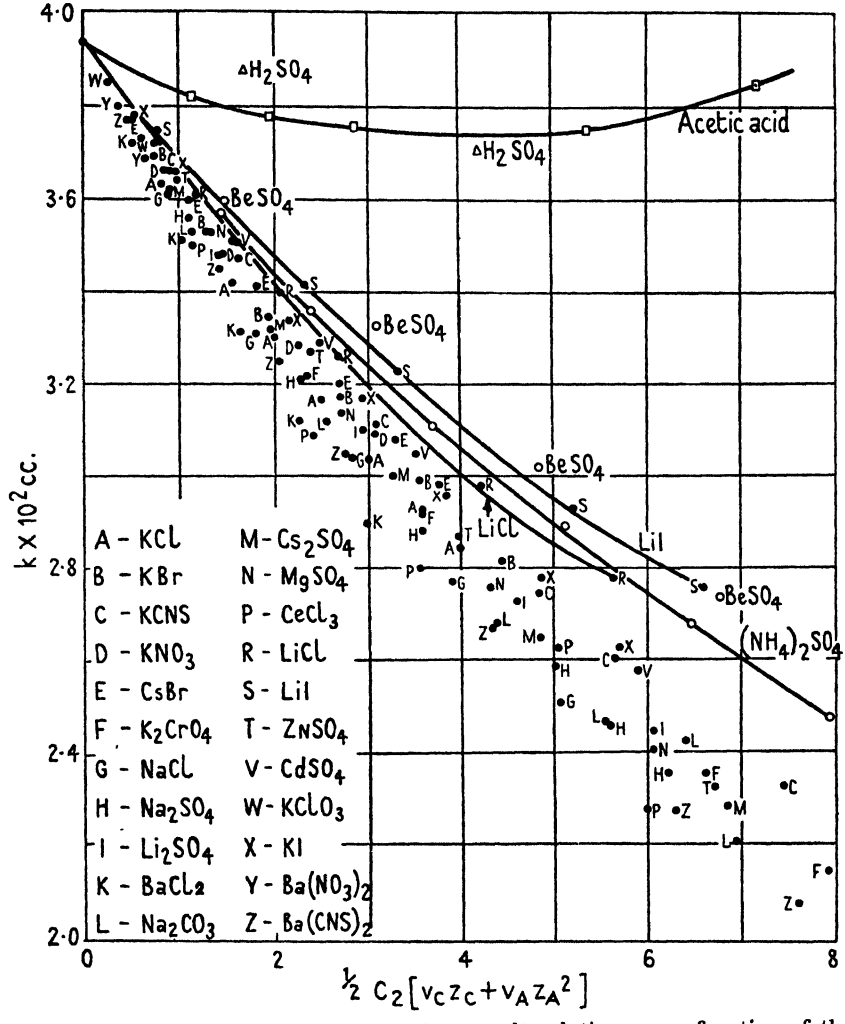

FIG. 162. The bulk compression of different salt solutions as a function of the 'modified ionic strength'.

that it depends upon the repulsive forces between the molecules themselves. From an analysis of the results of compressibility measurements of benzene Gibson and Kincaid have also tried to identify the constant B with the net internal pressure of the liquid, that is, with the difference between the cohesive pressure set up by

the attractive forces between the molecules and the expansive pressure due to their thermal energy [10].

The values of the constants for benzene and some of its derivatives at different temperatures are given in Table 85.

TABLE 85. *Constants of the Tait Equation for Benzene and some of its Derivatives*

For all the liquids at all temperatures $C = 0{\cdot}21591$.

Substance	*v at* 25° *C.*	*B in kilobars*			
		25°	45°	65°	85° *C.*
Benzene . .	1·14461	0·970	0·829	0·701	..
Chlorobenzene .	0·90817	1·248	1·0978	0·9609	..
Bromobenzene .	0·67177	1·4044	1·2473	1·1033	..
Nitrobenzene .	0·83451	1·8652	1·6794	1·5035	..
Aniline . .	0·98291	2·009	1·7983	1·6056	1·4304

From the derivation of the equation, however, it is doubtful whether there is any justification for giving a precise physical meaning to the constants.

Tammann assumes that a given amount of water in a solution behaves as the same amount of pure water under a constant but greater pressure P_e. This amounts to the same thing as assuming that there is an appreciable difference between the internal pressure of pure water and water in solutions, and there is evidence that this difference is a linear function of the product of the concentration of salt and water in the solution.

If, then, Tait's equation is modified by the introduction of a constant representing the change of the internal pressure of the water by the addition of the solute, and a small term which gives an approximation to the compression of the salt in the solution, the resulting equation is found to represent the pressure-volume relations in salt solutions up to 10,000 bars with an error of less than 4 per cent.

The equation takes the form

$$-\Delta_p v/x_1 = 0{\cdot}3071 \log \frac{2{\cdot}923+P_e+P}{2{\cdot}923+P_e} - (x_2/x_1)\Delta_p v_s, \quad (18.13)$$

where $\Delta_p v$ is the increase in volume of 1 gm. of solution when its pressure is raised P kilobars above atmospheric, x_2 and x_1 the weight fractions of solute and solvent, and $-\Delta_p v_s$ the specific compression

of the pure solute. The quantity P_e may be treated either as a constant to be determined empirically from the compression data or as the increase in the internal pressure of water consequent on the addition of the solute, and determinable from specific volume data at ordinary pressures. Except at high pressures and concentrations the quantity $-(x_2/x_1)\Delta_p v_s$ is negligible.

On the assumption that the water in a given solution occupies the same volume as it would in the pure state under an external pressure P_e, one may calculate the volume ψ_2 which 1 gm. of the salt appears to occupy in the solution

$$v = x_1\psi_1 + x_2\psi_2, \tag{18.14}$$

where ψ_1 is the volume of 1 gm. of water under a pressure of P_e kilobars.

It is found that for many salts ψ_2 is practically independent of the concentration and is of the same order of magnitude as would be expected for the pure liquefied salt.

The Partial Molal Volumes and Apparent Molal Volumes of Solutions

The partial molal volume of the solute in a solution ($\bar{v}_2$) is the increase in the volume of a large amount of solution when 1 mol of the solute is added, and is given by

$$\bar{v}_2 = \frac{\partial V}{\partial n_2}. \tag{18.15}$$

It may be either positive or negative in sign; if the formation of a solution is accompanied by a contraction in volume, and if the compressibility of the solvent decreases with pressure, Δv_2 must be positive, at least in dilute solutions.

The apparent molal volume of the solute ϕ is defined by

$$\phi = \frac{V - n_1 v_1}{n_2}, \tag{18.16}$$

where $V - n_1 v_1$ is the difference between the volume of the solution and the volume of the pure solvent. The partial molal volume and the apparent molal volume will approach identity for infinite dilution.

The partial molal volume of the solute is related to the molal volume of the solution by the expression

$$\bar{v}_2 = V - N_1 \frac{dV}{dN_1}, \tag{18.17}$$

where N_1 is the mol fraction of the solvent ($= n_1/(n_1+n_2)$).

There are several methods available for determining the partial molal quantities which depend upon a knowledge of the volume of the solution as a function of composition and of pressure at constant temperature.† Gibson and Adams proceed as follows: Instead of employing partial molal volumes they use partial volumes defined by

$$v_2 = \left(\frac{\partial V}{\partial m_2}\right)_{m_1} \quad \text{and} \quad v_1 = \left(\frac{\partial V}{\partial m_1}\right)_{m_2}, \tag{18.18}$$

where m_1 and m_2 are the total weights of solvent and solute respectively. The partial volume of the solute may also be obtained from

$$v_2 = v + x_1\left(\frac{\partial v}{\partial x_2}\right)_{P,t}, \tag{18.19}$$

where v is the specific volume of the solution and x_1 and x_2 are the weight fractions of the solvent and solute. Since this expression holds at all pressures,

$$\Delta_p v_2 \equiv v_2 - (v_2)_0 = \Delta v + x_1\left(\frac{\partial \Delta v}{\partial x_2}\right)_{P,t}, \tag{18.20}$$

where $(v_2)_0$ is the value of v_2 at atmospheric pressure, and Δv is the increase in the specific volume with pressure.

At any pressure and concentration Δv is readily obtained from the compression k,

$$\Delta v = -v_0 k. \tag{18.21}$$

Now Δv may be represented as a function of pressure at constant composition by a series equation

$$\Delta v = BP + CP^2 + DP^3 + \ldots, \tag{18.22}$$

from which

$$\Delta v_2 \equiv v_2 - (v_2)_0 = \left(B + x_1\frac{\partial B}{\partial x_2}\right)P + \left(C + x_1\frac{\partial C}{\partial x_2}\right)P^2 + \ldots, \tag{18.23}$$

or, alternatively,

$$k = BP + CP^2 + DP^3 + \ldots, \tag{18.24}$$

† See, for example, Lewis and Randall, *Thermodynamics*, p. 36. McGraw-Hill (1923).

from which

$$\Delta v_2 \equiv v_2 - (v_2)_0 = -kv_0 - kx_1 \frac{\partial v_0}{\partial x_2} - x_1 v_0 \left(P \frac{\partial B}{\partial x_2} + P^2 \frac{\partial C}{\partial x_2} + \ldots \right). \tag{18.25}$$

Several alternative methods are described by Lewis and Randall and by Adams (loc. cit.).

It may be noted that by the substitution of thermal expansion for diminution in volume under pressure, the above equations may also be used for the calculation of partial volumes at various temperatures [13].

Employing the above relations to the case of aqueous solutions of sodium chloride, it is found that as the pressure is increased, v_1 in solutions of any concentration decreases by an amount not very different from the decrease in the specific volume of pure water at the same pressure. The quantity v_2 (the partial volume of sodium chloride), on the other hand, increases with increasing pressure except at the highest pressures and in the most concentrated solutions. At high pressures v_1 is much less affected by changes of concentration than at low pressures [6].

The data relating to sodium chloride are summarized in Table 86.

From a knowledge of the partial volumes of the solute its partial compressibility at constant temperature β_2' may be calculated from

$$\beta_2' = -\left(\frac{\partial v_2}{\partial P}\right)_x = \beta' + x_1 \left(\frac{\partial \beta'}{\partial x_2}\right)_P, \tag{18.26}$$

where β' is the specific compressibility of the solution, defined by

$$\beta' = -\frac{dv}{dP} = v_0 \frac{dk}{dP}. \tag{18.27}$$

β_2' may be determined by differentiating any of the equations used to calculate v_2 from Δv. The increase of v_2 with pressure is now seen to indicate that β_2' is negative. In dilute solutions it has a large negative value comparable in magnitude with the compressibility of water, but of opposite sign; in concentrated solutions at pressures above about 8,000 bars it changes in sign and acquires a slowly increasing positive value. The partial compressibility of pure water in sodium chloride solutions at 25° C. does not differ much from the compressibility of pure water.

TABLE 86. *The Compression, k, for Sodium Chloride at 25° C. (Adams)*

(Δk is the difference between the compression of the solution and that of pure water.)

Pressure in bars	$x_2 = 0$		$x_2 = 0{\cdot}05$		$x_2 = 0{\cdot}10$		$x_2 = 0{\cdot}15$		$x_2 = 0{\cdot}20$		$x_2 = 0{\cdot}25$	
	k	$-10^4\Delta k$	k	$-10^4\Delta k$	k	$-10^4\Delta k$	k	$-10^4\Delta k$	k	$-10^4\Delta k$	k	$-10^4\Delta k$
1	0·0000	0	0·0000	0	0·0000	0	0·0000	0	0·0000	0	0·0000	0
500	0·0212	0	0·0192	20	0·0176	36	0·0161	51	0·0147	65	0·0133	79
1,000	0·0393	0	0·0361	32	0·0331	62	0·0304	89	0·0277	116	0·0251	142
1,500	0·0555	0	0·0513	42	0·0472	83	0·0433	122	0·0396	159	0·0361	194
2,000	0·0699	0	0·0647	52	0·0597	102	0·0551	148	0·0507	192	0·0462	237
3,000	0·0945	0	0·0880	65	0·0817	128	0·0756	189	0·0699	246	0·0644	301
4,000	0·1152	0	0·1076	76	0·1000	152	0·0933	219	0·0864	288	0·0799	353
5,000	0·1330	0	0·1248	82	0·1166	164	0·1089	241	0·1015	315	0·0941	389
6,000	0·1485	0	0·1397	88	0·1312	173	0·1228	257	0·1147	338	0·1070	415
7,000	0·1622	0	0·1530	92	0·1442	180	0·1353	269	0·1267	355	0·1183	439
8,000	0·1746	0	0·1647	99	0·1555	191	0·1462	284	0·1375	371	0·1289	457
9,000	0·1858	0	0·1759	99	0·1662	196	0·1567	291	0·1479	379	0·1388	470
10,000	0·1964	0	0·1860	104	0·1762	202	0·1668	296	0·1574	390	0·1481	483
11,000	(0·2059)	0	0·1953	106	0·1853	206	0·1757	302	0·1661	398	0·1564	495
12,000	(0·2147)	0	..	..	..	..	..	..	0·1740	407	0·1643	504

The results for aqueous solutions of potassium sulphate are very similar to those for sodium chloride. Ammonium nitrate, on the other hand, shows some notable differences. Thus, for example, the partial volumes of ammonium nitrate decrease as the pressure is increased (for solutions below 15 per cent. there is at first a slight

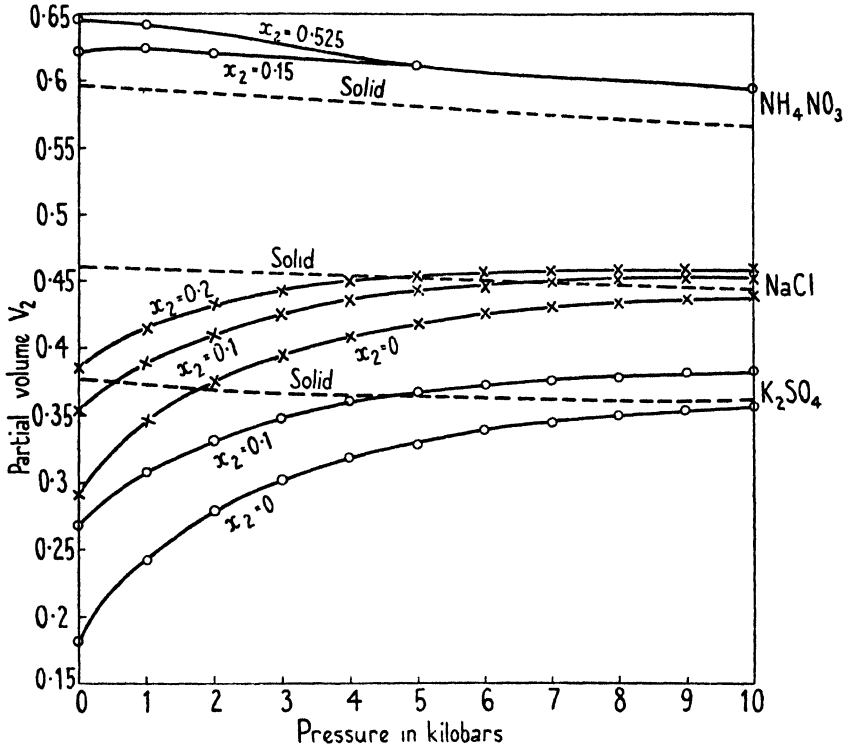

FIG. 163. The partial volumes of sodium chloride, potassium sulphate, and ammonium nitrate as a function of pressure.

increase), and at a pressure of about 6,000 bars the value of v_2 tends to become independent of the concentration.

In Fig. 163 the partial volumes of the three salts as functions of pressure are shown graphically. The corresponding curves for the solid salts are included for comparison.

In non-aqueous solutions it is found that the partial volumes of the salts also increase with pressure, the more compressible the solvent the larger being the initial value of $\Delta_p v_2$ and the more rapid its diminution with concentration [11].

Determination of Equilibrium in the System Solvent–Solute

The equilibrium in a binary system may be determined by the methods described in Chapters XII and XIV. In a saturated solution in the presence of an excess of the solute it is a condition for equilibrium that if an infinitesimal quantity of the solid phase passes into solution the change of free energy, dF, is zero; or, if $F_2(S)$ denotes the molal free energy of the solid solute and $\bar{F}_2$ its partial molal free energy in the solution,

$$\bar{F}_2 = F_2(S). \tag{18.28}$$

Now the changes of free energy with pressure and temperature are given by

$$\left(\frac{\partial F}{\partial P}\right)_T = V \quad \text{and} \quad \left(\frac{\partial F}{\partial T}\right)_P = \frac{F-H}{T} = -S.$$

On differentiating with respect to the number of molecules of one of the constituents of the system

$$\left(\frac{\partial \bar{F}_1}{\partial P}\right)_{T,N} = \bar{v}_1, \tag{18.29}$$

$$\left(\frac{\partial \bar{F}_1}{\partial T}\right)_{P,N} = \frac{\bar{F}_1-\bar{H}_1}{T} = -\bar{S}_1, \tag{18.30}$$

and

$$N_1\left(\frac{\partial \bar{F}_1}{\partial N_1}\right)_{P,T} + N_2\left(\frac{\partial \bar{F}_2}{\partial N_1}\right)_{P,T} = 0. \tag{18.31}$$

The fugacity of one of the constituents of the system (f_1) may partially be defined by

$$\left(\frac{\partial \log_e f_1}{\partial \bar{F}_1}\right)_T = \frac{1}{RT} \quad \text{or} \quad \bar{F}_1 = RT \log_e f_1 + B \tag{18.32}$$

and the system will be in equilibrium when the fugacities of each constituent are constant throughout; the fugacity of any constituent may be obtained from its fugacity in the vapour phase over the solution. On replacing free energy by fugacity in (18.31),

$$N_1\left(\frac{\partial \log_e f_1}{\partial N_1}\right)_{P,T} + N_2\left(\frac{\partial \log_e f_2}{\partial N_1}\right)_{P,T} = 0. \tag{18.33}$$

When the vapours behave as an ideal gas, fugacity may be measured by the vapour pressure, and

$$N_1\left(\frac{\partial \log_e p_1}{\partial N_1}\right)_{P,T} = N_2\left(\frac{\partial \log_e p_2}{\partial N_2}\right)_{P,T}, \tag{18.34}$$

which is the Duhem equation.

In dealing with aqueous solutions of salts Adams employs the chemical potential μ, which is defined by

$$\mu_1 = \left(\frac{\partial F}{\partial m_1}\right)_{P,T,m}, \tag{18.35}$$

where m_1 is the mass of component 1. From (18.29)

$$\left(\frac{\partial \mu_1}{\partial P}\right)_{T,m} = v_1 \text{ (the partial volume of component 1).} \tag{18.36}$$

Now since v_1 may be either positive or negative the escaping tendency of a pure substance may increase or decrease with pressure. Since the chemical potential is determined by the partial volume, it is evident that a knowledge of the latter will enable the equilibrium diagram of the system to be constructed provided, in addition, the identity of the phases concerned and their equilibrium proportions at any one pressure are known.

In determining the equilibrium of the system sodium chloride–water over a wide range of pressures at constant temperature, the experimental method consists in measuring the densities at atmospheric pressure and the compressions of the various solid phases and of the solutions at several concentrations as already described. The partial volumes in solution of each component and the chemical potentials are then calculated (18.36), and finally the pressure at which, for each concentration, the respective chemical potentials of the several components in the two phases become equal is determined. In this way a series of points on the equilibrium curve is established.

It is found, in practice, to be more convenient to deal with the differences between the chemical potentials of the various solutions and the corresponding values in some reference state. Thus, for example, in determining the freezing-point of a liquid component as a function of pressure, the condition for equilibrium may be written

$$\mu_s - \mu_l = \mu_1 - \mu_l, \tag{18.37}$$

or, by integrating (18.36),

$$\int_{P_f}^{P} (v_s - v_l)\, dP = (\mu_1 - \mu_l)_0 + \int_{0}^{P} (v_1 - v_l)\, dP. \tag{18.38}$$

In these equations P_f refers to the freezing-point of the pure com-

ponent 1, the subscripts l and s to pure liquid 1 and pure solid 1 respectively, and subscript 0 to atmospheric pressure. The values of the left- and right-hand members of (18.38) are determined by graphical or tabular integration.

Points on the freezing-point curve may now be determined by first plotting the values of the left-hand member for various pressures and then, on the same chart, plotting a series of curves expressing the numerical values of the right-hand member as a function of pressure for various concentrations. The points of intersection of this series of curves with the first curve will give pairs of values of pressure and concentration for which there is equilibrium between solid and liquid [12].

The solubility curve of a solid component of the system may be determined by a similar procedure.

The system sodium chloride–water at 25° C. and over a sufficiently wide pressure range includes, besides the pure solute and the aqueous solution, ice_{vl}, which melts at a pressure of 9,630 bars, and a dihydrate $NaCl.2H_2O$ which separates as a solid phase. The incongruent melting-point of the dihydrate is raised by pressure, reaches a maximum temperature at about 10,000 bars, and then diminishes [14].

From the partial-volume data and the chemical potentials the complete equilibrium diagram of the system can be obtained and is reproduced in Fig. 164. It includes the freezing-pressure curve for ice_{vl} and the solubility curve for sodium chloride. Adams draws attention to the following features of the diagram:

'The solubility of sodium chloride, which at atmospheric pressure is 26·42%, is increased at first by pressure and a maximum is reached at 4000 bars, the solubility at this point being 27·6%. A further increase of pressure causes the solubility to diminish steadily, but, at pressures between 8000 and 11,800 bars, $NaCl.2H_2O$ not sodium chloride is the solid phase that is stable in contact with the liquid. In other words, increase of pressure causes the system to pass through two transformation points at the pressures indicated. Although for this pressure range the equilibrium line is the solubility curve of the dihydrate, the rate of reaction in the direction of the formation of $NaCl.2H_2O$ is practically nil, and it is easy to realize experimentally the unstable portion of the sodium chloride solubility curve, which in the diagram is shown by the dotted line. Above 11,800 bars sodium chloride is again the stable solid phase and its solubility diminishes steadily until at 16,700 bars the curve intersects the freezing pressure curve for ice_{vl}, at which point the solubility has fallen to 25·4%. The freezing pressure line starts on the left at 9630 bars

(the freezing pressure of pure water) and for increasing concentration curves upward with rapidly increasing slope. At the place where the freezing pressure and solubility curves meet three phases are present; the intersection is therefore an invariant point (at constant temperature).'

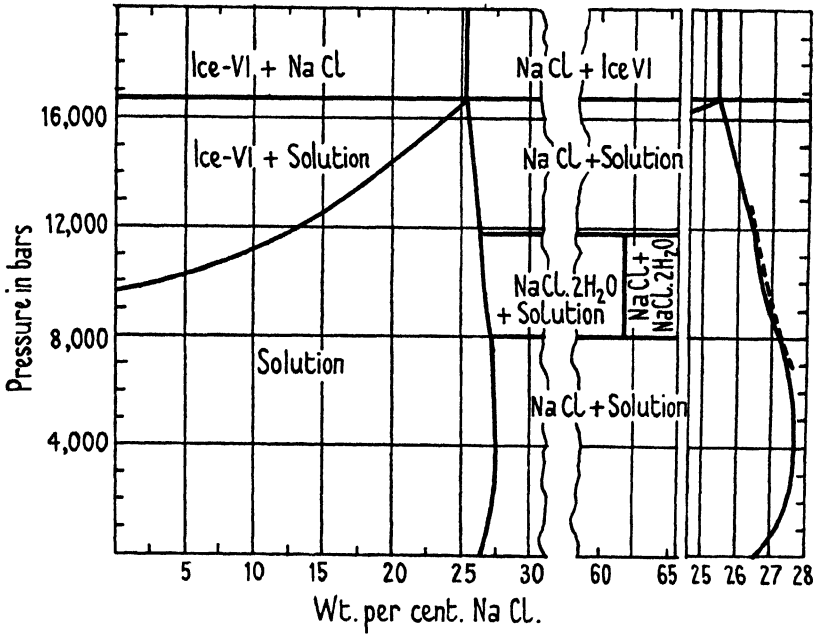

FIG. 164. Equilibrium diagram of the system sodium chloride–water at 25° C.

Parts of the freezing-pressure and solubility curves were checked by direct measurements and showed agreement within the probable experimental errors.

The Direct Determination of the Influence of Pressure on the Solubility of a Solid

In dealing with a solid solute-solvent system (9.1) may be rearranged and simplified to give solubility as a function of pressure:

$$\frac{dx_2}{dP} = -\frac{v_2 - v_2^s}{(\partial\mu_2/\partial x_2)_{P,T}}, \tag{18.39}$$

where x_2 is the concentration of the solute in the saturated solution, v_2 is the partial volume of the solute in the solution, v_2^s its specific volume in the solid phase, and $(\partial\mu_2/\partial x_2)_{P,T}$ is the rate of change of the chemical potential of the solute with concentration at constant temperature and pressure. Since the last term must always be

positive, the solubility will increase with pressure if the difference between the partial volume of the solute in the saturated solution and its specific volume in the solid phase is negative. As we have seen, the value of $(v_2 - v_2^s)$ depends on the concentration of the solution, the compressibility of the solvent, and the chemical nature of the solute.

In dealing with an ideal solution the partial molal volume of the dissolved solute is equal to the molal volume of supercooled liquid solute; $(v_2 - v_2^s)$ is, in fact, a composite expression since, when a solid dissolves in a liquid, two separate processes may be said to occur—the solute melts with a given volume change and the liquid solute subsequently mixes with the solvent with another volume change [15]. Expressed algebraically, if v_2' is the volume of the supercooled liquid solute, then

$$(v_2 - v_2^s) \equiv (v_2 - v_2') + (v_2' - v_2^s). \tag{18.40}$$

Most substances expand on melting, and $(v_2' - v_2^s)$ is, therefore, usually positive; and although the liquid phase is more compressible than the corresponding solid phase, the difference does not produce a change in sign in the volume change on melting, even at very high pressures. For sparingly soluble salts, such as the sulphates, sulphides, and carbonates of the alkaline earth metals, $(v_2 - v_2')$ is large and negative and the pressure effect on their solubility will be large. Thus, for example, Gibson has made the following rough estimate of the percentage change in the solubility in water of a number of calcium salts by an increase of pressure from 1 to 1,000 bars:

Salt	*Percentage increase in solubility for a pressure increase of* 1,000 *bars*
$CaCO_3$	75
$Ca(OH)_2$	44
$CaSO_4$ (anhydrite)	77
$CaSO_4.2H_2O$	57
CaF_2	33
CaS	57

In the experimental determination of the solubility of a solid at high pressures it is necessary to ensure that equilibrium between the two phases is reached whilst the system is still under pressure, and to make provision for analysing the saturated solution *in situ* or for isolating a part of it from the solid phase under pressure.

A method, first described by Sill [16] and later developed and

refined by Cohen and Moesveld [17], consists in the use of a double pipette of the form shown in Fig. 165 (*b*). The saturated solution together with a quantity of the solid solute is placed in the lower pipette (capacity, 15 c.c.), and is confined over mercury; the upper pipette (capacity, 9·5 c.c.) is filled with some suitable liquid non-miscible with the system under investigation, and the intermediate bulb is filled with cotton wool or other filtering medium. The whole apparatus is placed in a pressure bomb, the upper end being connected directly to a fine adjustment valve contained in the screwed plug closing the bomb. The vessel is rocked for a time sufficient to ensure the attainment of equilibrium, and a portion of the saturated solution is then filtered into the upper pipette by cautiously opening the control valve. The pressure is then released and the sample subsequently analysed.

A second method, developed by Adams and Hall [18] and applicable only to electrolytes, depends upon the measurement of the electrical resistance of the saturated solution under pressure. The conductivity cell (Fig. 165 (*a*)) is made of glass and is fitted with platinum electrodes, coated with platinum black, and bent into circular loops about 3 mm. in outside diameter. Outside the cell the wires are fused to gold leads in order to reduce the external resistance. The upper and lower enlarged portions of the cell contain crystals of the salt and the cell is filled to within 1·5 cm. of the top with saturated solution; it is housed in a steel bomb and is surrounded by sulphur-free oil which serves to transmit the pressure. To avoid appreciable heating during the conductivity measurements the maximum current employed should not exceed 0·5 milliamperes.

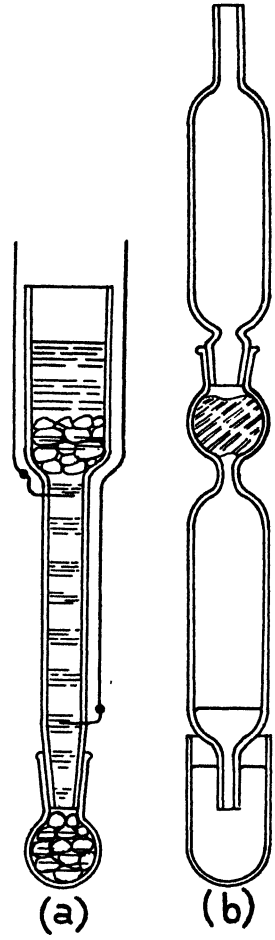

FIG. 165 (*a*). Adams and Hall's apparatus for measuring the electrical conductivity of solutions at high pressures.

FIG. 165 (*b*). Cohen and Moesveld's apparatus for measuring the solubility of solids at high pressures.

In order accurately to interpret the results it is necessary to ascertain by preliminary experiments the conductivity of the solution over a range of concentrations in the vicinity of saturation, as a function of pressure.

This method has not yet been tested extensively, but determinations of the solubility of sodium chloride in water at 30° C. and at pressures up to about 3,600 bars give results in good agreement with those obtained by other direct methods and with those derived from thermodynamic data.

BIBLIOGRAPHY

1. RICHARDS and STULL, *J. Am. Chem. Soc.* **26**, 399 (1904); RICHARDS, STULL, MATHEWS, and SPEYERS, ibid. **34**, 971 (1912); RICHARDS and SHIPLEY, ibid. **38**, 989 (1916); RICHARDS, BARTLETT, and HODGES, ibid. **43**, 1538 (1921).
2. BRIDGMAN, *Proc. Am. Acad. Arts and Sci.* **47**, 347 (1911) (mercury); **47**, 441 (1912) (water); **48**, 309 (1912) (water); **49**, 3 (1913) (organic liquids).
3. KEYES, *Proc. Am. Acad. Arts and Sci.* **68**, 505 (1933).
4. GIBSON, *J. Am. Chem. Soc.* **56**, 4 (1934).
5. MACLEOD, *Trans. Faraday Soc.* **33**, 694 (1937).
6. ADAMS, *J. Am. Chem. Soc.* **53**, 3769 (1931) (sodium chloride); **54**, 2229 (1932) (sodium sulphate); ADAMS and GIBSON, ibid. **54**, 4520 (1932) (ammonium nitrate); GIBSON, ibid. **56**, 4 (1934) (sulphates); **57**, 284 (1935); **57**, 1551 (1935); **59**, 1521 (1937); GIBSON and LOEFFLER, *J. Phys. Chem.* **43**, 207 (1939); *J. Am. Chem. Soc.* **61**, 2515 (1939).
7. RICHARDS and CHADWELL, *J. Am. Chem. Soc.* **47**, 2299 (1925); GUCKER, ibid. **55**, 2709 (1933).
8. TAMMANN, *Über die Beziehungen zwischen den inneren Kräften und Eigenschaften der Lösungen.* Leipzig, 1907.
9. WOHL, *Z. physik. Chem.* **99**, 234 (1921); CARL, ibid. **101**, 238 (1922).
10. GIBSON and KINCAID, *J. Am. Chem. Soc.* **60**, 511 (1938) (benzene).
11. GIBSON, *J. Am. Chem. Soc.* **59**, 1521 (1937).
12. ADAMS, *Am. J. Sci.* **35**, 1 (1938).
13. GIBSON, *J. Phys. Chem.* **31**, 496 (1927).
14. ADAMS and GIBSON, *J. Am. Chem. Soc.* **52**, 4252 (1930).
15. GIBSON, *Am. J. Sci.* **35A**, 49 (1938).
16. SILL, *J. Am. Chem. Soc.* **38**, 2632 (1916).
17. COHEN and MOESVELD, *Z. physik. Chem.* **93**, 385 (1919).
18. ADAMS and HALL, *J. Wash. Acad. Sci.* **21**, 183 (1931).

APPENDIX I

THERMODYNAMIC PROPERTIES OF HYDROGEN, NITROGEN, CARBON MONOXIDE, CARBON DIOXIDE, AND METHANE

(SEE CHAPTER X)

Thermodynamic Properties of Hydrogen (Deming and Shupe)

Pressure p, *atmospheres*	v, *c.c./mol*	*Density* ρ, *gm./litre*	*Fugacity* f, *atmospheres*	$\frac{-p}{v}\left(\frac{dv}{dp}\right)_T$	$\frac{T}{v}\left(\frac{dv}{dT}\right)_p$	C_p, *cal./mol deg.*	C_v, *cal./mol deg.*
			$t = -50°$ C., $C_p^* = 6{\cdot}660$, $C_v^* = 4{\cdot}674$				
25	744·7	2·707	25·41	0·983	0·9956	6·72	4·68
50	378·8	5·321	51·69	0·965	0·9889	6·78	4·69
75	257·1	7·841	78·90	0·946	0·9802	6·83	4·70
100	196·3	10·27	107·1	0·927	0·9695	6·88	4·72
150	135·8	14·84	166·6	0·890	0·9455	6·96	4·74
200	105·6	19·08	230·8	0·854	0·9183	7·04	4·77
300	75·67	26·64	374·5	0·788	0·8619	7·14	4·82
400	60·80	33·15	541·4	0·732	0·8074	7·21	4·87
500	51·91	38·83	735·1	0·684	0·7571	7·26	4·90
600	46·00	43·82	959·4	0·643	0·7102	7·29	4·94
800	38·57	52·26	1,517·0	0·579	0·6277	7·34	5·07
1,000	34·10	59·11	2,252·0	0·524	0·5592	7·38	5·18
			$t = 0°$ C., $C_p^* = 6{\cdot}841$, $C_v^* = 4{\cdot}855$				
25	910·3	2·214	25·38	0·985	0·9917	6·88	4·86
50	462·3	4·360	51·55	0·969	0·9825	6·91	4·87
75	313·1	6·437	78·56	0·952	0·9724	6·94	4·88
100	238·6	8·447	106·4	0·936	0·9617	6·97	4·88
150	164·2	12·27	165·0	0·905	0·9391	7·03	4·90
200	127·1	15·86	227·4	0·875	0·9156	7·07	4·91
300	90·12	22·37	365·1	0·820	0·8678	7·14	4·94
400	71·62	28·14	521·6	0·774	0·8211	7·19	4·98
500	60·56	33·28	699·2	0·730	0·7771	7·22	5·00
600	53·19	37·90	900·2	0·693	0·7355	7·24	5·04
800	43·95	45·86	1,383·0	0·634	0·6644	7·28	5·11
1,000	38·35	52·56	1,993·0	0·586	0·6026	7·31	5·20

Thermodynamic Properties of Hydrogen (Deming and Shupe) (cont.)

Pressure p, *atmospheres*	v, *c.c./mol*	*Density* ρ, *gm./litre*	*Fugacity* f, *atmospheres*	$\frac{-p}{v}\left(\frac{dv}{dp}\right)_T$	$\frac{T}{v}\left(\frac{dv}{dT}\right)_p$	C_p, *cal./mol deg.*	C_v, *cal./mol deg.*
			$t = 25°$ C., $C_p^* = 6{\cdot}892$, $C_v^* = 4{\cdot}906$				
25	992·8	2·030	25·36	0·985	0·9910	6·92	4·91
50	503·8	4·001	51·48	0·970	0·9814	6·95	4·92
75	340·9	5·912	78·37	0·955	0·9712	6·98	4·92
100	259·6	7·765	106·1	0·940	0·9606	7·00	4·93
150	178·3	11·30	164·1	0·911	0·9389	7·04	4·94
200	137·7	14·63	225·8	0·882	0·9165	7·08	4·95
300	97·26	20·72	360·9	0·832	0·8719	7·14	4·97
400	76·97	26·18	513·2	0·789	0·8280	7·18	5·00
500	64·85	31·08	684·6	0·749	0·7864	7·20	5·03
600	56·75	35·52	876·8	0·713	0·7480	7·22	5·06
800	46·61	43·24	1,332·0	0·656	0·6799	7·26	5·12
1,000	40·46	49·82	1,899·0	0·611	0·6211	7·28	5·21
			$t = 50°$ C., $C_p^* = 6{\cdot}927$, $C_v^* = 4{\cdot}941$				
25	1,075·0	1·874	25·34	0·986	0·9906	6·95	4·95
50	545·2	3·697	51·40	0·972	0·9809	6·97	4·95
75	368·6	5·468	78·19	0·958	0·9708	7·00	4·96
100	280·4	7·187	105·8	0·943	0·9605	7·02	4·96
150	192·3	10·48	163·3	0·916	0·9394	7·05	4·97
200	148·3	13·59	224·3	0·890	0·9181	7·08	4·98
300	104·3	19·32	357·1	0·843	0·8762	7·13	5·00
400	82·30	24·49	505·7	0·802	0·8349	7·16	5·02
500	69·12	29·16	671·6	0·765	0·7960	7·19	5·05
600	60·30	33·43	856·4	0·731	0·7595	7·21	5·07
800	49·26	40·92	1,289·0	0·676	0·6941	7·24	5·13
1,000	42·56	47·36	1,820·0	0·634	0·6379	7·26	5·21
			$t = 100°$ C., $C_p^* = 6{\cdot}969$, $C_v^* = 4{\cdot}983$				
25	1,240·0	1·625	25·31	0·988	0·9905	6·99	4·99
50	627·8	3·210	51·26	0·975	0·9809	7·00	4·99
75	423·9	4·755	77·88	0·962	0·9712	7·02	5·00
100	322·0	6·259	105·2	0·949	0·9614	7·03	5·00
150	220·2	9·155	161·9	0·924	0·9419	7·06	5·01
200	169·3	11·91	221·6	0·901	0·9225	7·09	5·01
300	118·4	17·02	350·6	0·861	0·8846	7·12	5·03
400	92·90	21·70	493·2	0·824	0·8481	7·15	5·05
500	77·59	25·98	650·3	0·791	0·8130	7·17	5·07
600	67·35	29·92	823·1	0·760	0·7795	7·19	5·09
800	54·53	36·96	1,221·0	0·709	0·7192	7·21	5·14
1,000	46·75	43·12	1,696·0	0·671	0·6676	7·23	5·21

Thermodynamic Properties of Hydrogen (Deming and Shupe) (cont.)

Pressure p, *atmospheres*	v, *c.c./mol*	*Density* ρ, *gm./litre*	*Fugacity* f, *atmospheres*	$-\frac{p}{v}\left(\frac{dv}{dp}\right)_T$	$\frac{T}{v}\left(\frac{dv}{dT}\right)_p$	C_p, *cal./mol deg.*	C_v, *cal./mol deg.*
			$t = 200°$ C., $C_p^* = 6{\cdot}993$, $C_v^* = 5{\cdot}007$				
25	1,569·0	1·285	25·26	0·990	0·9914	7·00	5·01
50	792·6	2·543	51·04	0·979	0·9827	7·01	5·01
75	534·0	3·775	77·36	0·969	0·9740	7·02	5·01
100	404·7	4·980	104·2	0·958	0·9653	7·03	5·01
150	275·5	7·316	159·7	0·937	0·9483	7·04	5·01
200	211·0	9·554	217·6	0·918	0·9316	7·05	5·01
300	146·4	13·77	341·0	0·885	0·8996	7·08	5·02
400	113·9	17·70	474·9	0·855	0·8690	7·09	5·04
500	94·42	21·35	619·9	0·827	0·8395	7·11	5·05
600	81·36	24·77	776·6	0·803	0·8114	7·12	5·07
800	65·00	31·01	1,128·0	0·757	0·7594	7·14	5·11
1,000	55·08	36·59	1,534·0	0·724	0·7142	7·15	5·16
			$t = 300°$ C., $C_p^* = 7{\cdot}006$, $C_v^* = 5{\cdot}020$				
25	1,898·0	1·069	25·22	0·991	0·9923	7·01	5·02
50	957·1	2·106	50·88	0·982	0·9846	7·02	5·02
75	643·8	3·131	76·99	0·973	0·9769	7·02	5·02
100	487·2	4·137	103·6	0·964	0·9692	7·03	5·02
150	330·6	6·096	158·2	0·947	0·9542	7·04	5·02
200	252·4	7·986	214·8	0·930	0·9395	7·05	5·02
300	174·1	11·58	334·3	0·902	0·9115	7·06	5·03
400	134·8	14·96	462·4	0·877	0·8849	7·08	5·04
500	111·1	18·14	599·5	0·853	0·8595	7·09	5·06
600	95·28	21·15	745·8	0·832	0·8352	7·10	5·07
800	75·40	26·73	1,068·0	0·794	0·7899	7·11	5·11
1,000	63·38	31·80	1,432·0	0·761	0·7494	7·12	5·14
			$t = 400°$ C., $C_p^* = 7{\cdot}029$, $C_v^* = 5{\cdot}043$				
25	2,226·0	0·9054	25·19	0·992	0·9932	7·03	5·04
50	1,122·0	1·797	50·76	0·985	0·9863	7·04	5·04
75	753·4	2·675	76·72	0·977	0·9794	7·04	5·05
100	569·5	3·539	103·1	0·969	0·9726	7·04	5·04
150	385·6	5·227	157·1	0·953	0·9591	7·05	5·04
200	293·7	6·862	212·8	0·939	0·9461	7·06	5·04
300	201·7	9·992	329·5	0·914	0·9213	7·07	5·05
400	155·5	12·96	453·5	0·892	0·8977	7·08	5·06
500	127·8	15·78	585·0	0·872	0·8750	7·09	5·08
600	109·1	18·47	724·1	0·854	0·8534	7·10	5·09
800	85·77	23·50	1,026·0	0·820	0·8130	7·11	5·12
1,000	71·65	28·13	1,362·0	0·790	0·7767	7·12	5·15

Thermodynamic Properties of Nitrogen (Michels, Wouters, and de Boer)

Density ρ, Amagat units	*Maximum total work A, cal./mol*	*Entropy S, cal. T^{-1}/mol*	*Total energy E, cal./mol*	C_v, *cal./mol*	*Maximum total work A, cal./mol*	*Entropy S, cal. T^{-1}/mol*	*Total energy E, cal./mol*	C_v, *cal./mol*
	0°				25°			
0	$-\infty$	$+\infty$	+1·6	4·97	$-\infty$	$+\infty$	125·8	4·97
1	0	0	0	..	−3·9	+0·435	124·3	..
40	1,993·2	−7·526	−62·5	5·12	2,176·2	−7·080	65·3	5·08
80	2,365·7	−9·106	−123·6	5·23	2,580·6	−8·652	6·4	5·16
120	2,580·5	−10·118	−183·2	5·28	2,827·9	−9·659	−51·9	5·21
160	2,736·4	−10·904	−242·0	5·32	3,003·4	−10·441	−109·6	5·26
200	2,860·6	−11·572	−300·3	5·37	3,144·2	−11·105	−166·8	5·31
240	2,966·2	−12·171	−358·3	5·42	3,264·4	−11·699	−223·7	5·37
280	3,060·6	−12·728	−416·1	5·46	3,372·5	−12·251	−280·1	5·42
320	3,148·2	−13·259	−473·5	5·53	3,473·3	−12·776	−335·9	5·49
360	3,232·5	−13·776	−530·4	5·60	3,570·6	−13·287	−390·9	5·56
400	3,316·3	−14·287	−586·2	5·68	3,666·8	−13·790	−444·7	5·64
440	3,402·2	−14·799	−640·1	5·78	3,765·1	−14·293	−496·4	5·73
480	3,491·8	−15·314	−691·2	5·88	3,867·6	−14·800	−545·0	5·84
520	3,587·3	−15·836	−738·3	5·98	3,976·0	−15·313	−589·6	5·94
560	3,691·1	−16·369	−780·1	6·10	4,092·8	−15·836	−628·7	6·06
600	3,803·5	−16·913	−816·3	6·20	4,218·9	−16·371	−662·1	6·16
	50°				75°			
0	$-\infty$	$+\infty$	250·0	4·97	$-\infty$	$+\infty$	374·3	4·98
1	−20·2	+0·836	248·5	..	−45·9	+1·207	372·9	..
40	2,347·7	−6·672	191·6	5·03	2,509·5	−6·297	317·2	5·03
80	2,796·8	−8·239	134·4	5·09	2,997·3	−7·860	260·8	5·06
120	3,064·1	−9·242	77·5	5·14	3,290·2	−8·859	205·9	5·09
160	3,259·1	−10·020	21·1	5·19	3,503·5	−9·633	149·8	5·14
200	3,416·4	−10·680	−34·8	5·24	3,677·7	−10·290	95·2	5·17
240	3,551·3	−11·269	−90·2	5·30	3,827·0	−10·875	40·9	5·22
280	3,673·2	−11·816	−145·1	5·35	3,962·4	−11·418	−12·8	5·27
320	3,787·1	−12·336	−199·3	5·42	4,090·1	−11·935	−65·1	5·33
360	3,897·3	−12·842	−252·6	5·48	4,212·7	−12·436	−116·9	5·39
400	4,006·2	−13·339	−304·3	5·57	4,333·5	−12·926	−166·7	5·48
440	4,116·9	−13·834	−353·6	5·65	4,456·8	−13·416	−214·0	5·56
480	4,231·8	−14·332	−399·6	5·75	4,584·9	−13·907	−256·8	5·65
520	4,353·0	−14·836	−441·3	5·85	4,717·6	−14·403	−296·8	5·75
560	4,482·8	−15·350	−477·6	5·98	4,860·0	−14·908	−330·2	5·85
600	4,622·3	−15·877	−508·4	6·07	5,012·8	−15·429	−358·8	5·93

Thermodynamic Properties of Nitrogen (Michels, Wouters, and de Boer) (cont.)

Density ρ, Amagat units	*Maximum total work A, cal./mol*	*Entropy S, cal. T^{-1}/ mol*	*Total energy E, cal./mol*	*C_v, cal./ mol*	*Maximum total work A, cal./mol*	*Entropy S, cal. T^{-1}/ mol*	*Total energy E, cal./mol*	*C_v, cal./ mol*
	100°				125°			
0	$-\infty$	$+\infty$	498·8	4·99	$-\infty$	$+\infty$	624·5	5·00
1	−80·7	+1·553	497·4	..	−122·8	+1·877	623·1	..
40	2,661·9	−5·949	442·0	5·02	2,807·9	−5·623	569·1	5·03
80	3,189·1	−7·509	387·1	5·05	3,373·1	−7·181	514·0	5·04
120	3,505·9	−8·506	331·9	5·07	3,715·0	−8·177	459·3	5·05
160	3,739·9	−9·279	277·4	5·10	3,968·0	−8·948	405·4	5·07
200	3,929·6	−9·932	223·5	5·12	4,174·3	−9·600	352·1	5·10
240	4,094·1	−10·515	170·4	5·17	4,353·0	−10·180	299·8	5·13
280	4,242·9	−11·054	118·1	5·22	4,515·7	−10·717	248·7	5·17
320	4,381·3	−11·565	65·8	5·26	4,667·6	−11·225	198·4	5·21
360	4,517·8	−12·062	16·9	5·32	4,815·8	−11·719	149·9	5·26
400	4,651·0	−12·547	−30·9	5·40	4,961·5	−12·201	103·7	5·32
440	4,786·9	−13·032	−76·0	5·48	5,109·4	−12·681	60·5	5·38
480	4,926·0	−13·516	−117·5	5·56	5,260·7	−13·160	21·0	5·45
520	5,071·8	−14·005	−154·4	5·65	5,419·7	−13·643	−13·8	5·54
560	5,227·3	−14·506	−185·6	5·74	5,585·8	−14·137	−42·8	5·62
600	5,392·3	−15·018	−211·7	5·82	6,161·8	−14·644	−66·9	5·71
	150°							
0	$-\infty$	$+\infty$	747·5	5·02				
1	−175·4	+2·181	746·1	..				
40	2,942·5	−5·317	692·6	5·04				
80	3,546·5	−6·874	637·8	5·05				
120	3,913·3	−7·869	583·5	5·05				
160	4,184·7	−8·637	530·0	5·06				
200	4,507·5	−9·288	477·3	5·08				
240	4,610·5	−9·866	435·7	5·09				
280	4,776·5	−10·401	375·3	5·12				
320	4,941·3	−10·907	326·0	5·16				
360	5,101·6	−11·398	278·5	5·19				
400	5,249·0	−11·876	233·7	5·24				
440	5,417·8	−12·350	191·9	5·30				
480	5,581·3	−12·826	154·0	5·35				
520	5,751·4	−13·306	121·0	5·42				
560	5,931·4	−13·795	94·0	5·50				
600	6,120·0	−14·296	70·6	5·59				

Thermodynamic Properties of Carbon Monoxide (Deming and Shupe)

p, atms.	v, c.c./mol	Density ρ, gm./c.c.	Fugacity f, atms.	$-\frac{p}{v}\left(\frac{dv}{dp}\right)_T$	$\frac{T}{v}\left(\frac{dv}{dT}\right)_p$	C_p, cal./mol deg.	C_v, cal./mol deg.
			$t = -50°$ C., $C_p^* = 6{\cdot}953$, $C_v^* = 4{\cdot}967$ cal./mol deg.				
25	703·6	0·3980	24·00	1·038	1·168	7·46	4·95
50	339·9	0·08239	46·22	1·062	1·352	8·02	4·85
75	220·6	0·1269	67·00	1·064	1·500	8·63	4·83
100	162·9	0·1719	86·70	1·037	1·619	9·23	4·77
150	109·3	0·2561	124·3	0·909	1·655	10·23	4·87
200	86·02	0·3256	161·7	0·751	1·528	10·82	5·02
300	66·20	0·4231	242·9	0·551	1·172	11·11	5·74
400	57·44	0·4876	339·4	0·433	0·942	10·96	5·86
500	52·60	0·5325	457·9	0·374	0·810	10·81	5·80
600	49·36	0·5674	604·6	0·337	0·710	10·83	6·02
800	45·00	0·6224	1,010·0	0·291	0·569	10·97	6·63
1,000	42·16	0·6643	1,624·0	0·271	0·484	11·03	7·08
			$t = 0°$ C., $C_p^* = 6{\cdot}956$, $C_v^* = 4{\cdot}970$ cal./mol deg.				
25	884·0	0·03168	24·62	1·012	1·094	7·28	4·96
50	437·6	0·06400	48·60	1·015	1·183	7·62	4·94
75	290·3	0·09649	72·13	1·008	1·255	7·95	4·94
100	217·8	0·1286	95·38	0·989	1·305	8·27	4·95
150	147·4	0·1900	141·7	0·926	1·334	8·79	5·02
200	114·2	0·2453	189·0	0·843	1·299	9·10	5·05
300	83·71	0·3346	290·8	0·674	1·135	9·32	5·07
400	69·96	0·4003	408·3	0·566	0·980	9·31	5·10
500	62·19	0·4504	547·6	0·493	0·851	9·27	5·22
600	57·13	0·4902	714·1	0·443	0·748	9·23	5·39
800	50·72	0·5521	1,152·0	0·380	0·616	9·16	5·57
1,000	46·72	0·5995	1,778·0	0·352	0·531	9·12	5·81
			$t = 25°$ C., $C_p^* = 6{\cdot}959$, $C_v^* = 4{\cdot}973$ cal./mol deg.				
25	971·8	0·02882	24·80	1·005	1·073	7·23	4·97
50	484·2	0·05784	49·31	1·003	1·140	7·50	4·96
75	322·8	0·08675	73·64	0·994	1·193	7·77	4·96
100	243·1	0·1152	97·94	0·977	1·229	8·02	4·98
150	165·1	0·1696	147·0	0·926	1·248	8·43	5·04
200	127·6	0·2195	197·5	0·851	1·229	8·68	5·08
300	92·40	0·3031	306·2	0·724	1·116	8·89	5·02
400	76·25	0·3673	430·8	0·612	0·984	8·91	4·99
500	67·04	0·4177	576·4	0·540	0·869	8·89	5·08
600	60·94	0·4596	748·1	0·488	0·772	8·84	5·22
800	53·55	0·5230	1,191·0	0·417	0·644	8·76	5·30
1,000	48·97	0·5719	1,808·0	0·387	0·555	8·69	5·52

Thermodynamic Properties of Carbon Monoxide (Deming and Shupe) (cont.)

p, atms.	v, c.c./mol	Density ρ, gm./c.c.	Fugacity f, atms.	$-\frac{p}{v}\left(\frac{dv}{dp}\right)_T$	$\frac{T}{v}\left(\frac{dv}{dT}\right)_p$	C_p, cal./mol deg.	C_v, cal./mol deg.
			$t = 50°$ C., $C_p^* = 6{\cdot}965$, $C_v^* = 4{\cdot}979$ *cal./mol deg.*				
25	1,059·0	0·02645	24·94	1·000	1·058	7·19	4·98
50	529·8	0·05286	49·82	0·995	1·109	7·42	4·97
75	354·5	0·07899	74·74	0·985	1·149	7·64	4·97
100	267·7	0·1046	99·81	0·969	1·176	7·85	4·99
150	182·2	0·1537	150·8	0·925	1·193	8·17	5·03
200	140·6	0·1992	203·7	0·871	1·177	8·39	5·04
300	101·0	0·2773	317·8	0·755	1·097	8·59	4·97
400	82·47	0·3396	447·5	0·650	0·984	8·65	4·97
500	71·87	0·3896	597·7	0·580	0·883	8·64	5·02
600	64·92	0·4314	772·9	0·527	0·796	8·61	5·11
800	56·53	0·4955	1,218·0	0·454	0·673	8·54	5·16
1,000	51·27	0·5462	1,826·0	0·418	0·580	8·46	5·37
			$t = 100°$ C., $C_p^* = 6{\cdot}987$, $C_v^* = 5{\cdot}001$ *cal./mol deg.*				
25	1,231·0	0·02276	25·11	0·994	1·037	7·16	5·00
50	619·3	0·04522	50·48	0·986	1·069	7·33	5·00
75	416·2	0·06730	76·18	0·974	1·092	7·49	5·00
100	315·1	0·08889	102·3	0·959	1·108	7·63	5·01
150	215·0	0·1303	155·9	0·924	1·119	7·86	5·02
200	165·7	0·1690	211·9	0·881	1·112	8·02	5·01
300	117·9	0·2375	333·1	0·792	1·064	8·22	4·94
400	95·04	0·2947	469·8	0·705	0·980	8·31	4·95
500	81·70	0·3428	625·9	0·643	0·898	8·33	5·00
600	73·04	0·3835	805·1	0·588	0·831	8·32	4·98
800	62·44	0·4485	1,249·0	0·514	0·715	8·26	5·04
1,000	55·91	0·5009	1,835·0	0·470	0·635	8·20	5·08
			$t = 200°$ C., $C_p^* = 7{\cdot}076$, $C_v^* = 5{\cdot}090$ *cal./mol deg.*				
25	1,569·0	0·01784	25·26	0·989	1·015	7·18	5·09
50	793·5	0·03529	51·08	0·977	1·028	7·28	5·09
75	535·2	0·05233	77·48	0·964	1·035	7·38	5·10
100	406·3	0·06893	104·5	0·951	1·040	7·47	5·10
150	277·7	0·1008	160·5	0·923	1·045	7·62	5·09
200	213·9	0·1309	219·4	0·892	1·038	7·74	5·09
300	150·7	0·1858	347·1	0·830	1·014	7·91	5·04
400	119·7	0·2340	489·8	0·769	0·962	8·02	5·07
500	101·4	0·2763	649·9	0·718	0·908	8·07	5·09
600	89·28	0·3137	830·1	0·671	0·859	8·10	5·09
800	73·39	0·3765	1,261·0	0·600	0·767	8·14	5·15
1,000	65·50	0·4276	1,805·0	0·550	0·692	8·15	5·24

Thermodynamic Properties of Carbon Monoxide (Deming and Shupe) (cont.)

p, *atms.*	*v*, *c c./mol*	*Density* *ρ*, *gm./c.c.*	*Fugacity* *f*, *atms.*	$\frac{-p}{v}\left(\frac{dv}{dp}\right)_T$	$\frac{T}{v}\left(\frac{dv}{dT}\right)_p$	C_p, *cal./mol deg.*	C_v, *cal./mol deg.*
			$t = 300°$ C., $C_p^* = 7{\cdot}218$, $C_v^* = 5{\cdot}232$ *cal./mol deg.*				
25	1,905·0	0·01470	25·31	0·988	1·006	7·29	5·23
50	964·3	0·02905	51·27	0·975	1·009	7·36	5·23
75	651·0	0·04302	77·88	0·962	1·010	7·42	5·24
100	494·5	0·05664	105·2	0·950	1·010	7·48	5·24
150	338·0	0·08285	161·9	0·924	1·010	7·58	5·21
200	257·8	0·1086	221·6	0·900	1·000	7·66	5·22
300	182·2	0·1537	350·8	0·850	0·976	7·80	5·21
400	143·6	0·1951	494·1	0·803	0·946	7·90	5·20
500	120·6	0·2322	653·2	0·763	0·904	7·98	5·25
600	105·3	0·2659	829·7	0·722	0·864	8·04	5·28
800	86·42	0·3241	1,243·0	0·655	0·792	8·14	5·34
1,000	75·02	0·3733	1,749·0	0·606	0·721	8·21	5·49
			$t = 400°$ C., $C_p^* = 7{\cdot}386$, $C_v^* = 5{\cdot}400$ *cal./mol deg.*				
25	2,238·0	0·01252	25·32	0·987	1·000	7·44	5·40
50	1,133·0	0·02472	51·31	0·975	0·999	7·49	5·40
75	765·0	0·03661	77·96	0·962	0·997	7·54	5·41
100	581·0	0·04821	105·3	0·950	0·996	7·58	5·40
150	396·9	0·07057	162·1	0·927	0·987	7·65	5·40
200	304·9	0·09186	221·8	0·905	0·978	7·71	5·40
300	212·9	0·1316	350·6	0·864	0·954	7·82	5·40
400	166·9	0·1678	492·4	0·823	0·931	7·92	5·39
500	139·4	0·2009	648·6	0·790	0·897	8·00	5·45
600	121·0	0·2314	820·3	0·758	0·861	8·08	5·52
800	98·18	0·2852	1,215·0	0·696	0·793	8·21	5·66
1,000	84·41	0·3318	1,688·0	0·649	0·733	8·32	5·81

Thermodynamic Properties of Carbon Dioxide (Michels, Bijl, and Michels)

Density, ρ, Amagat units	*Maximum total work A,† cal./mol*	*Entropy S,† cal. T^{-1}/mol*	*Total energy E,† cal./mol*	C_v, *cal./mol*	*Maximum total work A, cal./mol*	*Entropy S, cal. T^{-1}/mol*	*Total energy E, cal./mol*	C_v, *cal./mol*
	25°				31·04°			
1	−7·5	+0·590	+168·5	6·79	−11·5	+0·727	+209·6	6·82
40	+2,052·9	−7·270	−114·5	8·30	..	..	..	..
80	2,346·1	−9·198	−396·3	9·65	..	..	..	..
120	2,478·4	−10·559	−669·9	11·85	..	..	..	..
160	..	..	..	..	+2,620·3	−11·354	−833·5	14·3
200	..	..	..	..	2,668·9	−12·219	−1,047·9	16·8
240	..	..	..	..	2,701·4	−12·928	−1,231·1	17·3
280	..	..	..	..	2,724·7	−13·520	−1,387·8	15·4
320	..	..	..	..	2,742·2	−14·072	−1,538·3	13·0
360	2,667·3	−14·913	..	12·05	..	..	..	..
400	2,677·8	−15·509	..	11·50	..	..	..	..
440	2,690·7	−16·160	..	11·20	..	..	..	..
480	2,709·8	−16·872	..	11·15	..	..	..	..
520	2,739·7	−17·648	..	11·20	..	..	..	..
560	2,786·2	−18·486	..	11·45	..	..	..	..
600	2,855·0	−19·389	..	11·80	..	..	..	..
	40°				50°			
1	−18·9	+0·925	+270·9	6·86	−31·2	+1·148	+339·7	6·90
40	..	..	..	..	+2,226·8	−6·641	+80·7	7·75
80	..	..	..	..	2,566·9	−8·474	−171·6	8·75
120	..	..	..	..	2,731·5	−9·712	−406·9	9·70
160	+2,720·5	−11·004	−725·5	14·3	2,828·1	−10·678	−622·5	10·45
200	2,776·7	−11·828	−927·1	16·8	2,893·4	−11·487	−818·6	10·90
240	2,815·6	−12·530	−1,108·1	17·3	2,939·3	−12·187	−999·0	11·00
280	2,844·2	−13·153	−1,274·6	15·4	2,974·2	−12·821	−1,168·8	10·75
320	2,866·8	−13·744	−1,437·1	13·0	3,002·8	−13·426	−1,335·8	10·35
360	..	..	..	..	3,028·4	−14·033	−1,506·2	9·95
400	..	..	..	..	3,054·2	−14·661	−1,683·4	9·70
440	..	..	..	..	3,083·6	−15·326	−1,868·9	9·65
480	..	..	..	..	3,120·5	−16·039	−2,062·6	9·65
520	..	..	..	..	3,169·8	−16·805	−2,260·6	9·75
560	..	..	..	..	3,236·8	−17·626	−2,459·1	10·00
600	..	..	..	..	3,327·9	−18·503	−2,651·5	10·30

† The values of *A*, *S*, and *E* at N.T.P. have been taken as zero.

Thermodynamic Properties of Carbon Dioxide (Michels, Bijl, and Michels) (cont.)

Density, ρ, Amagat units	Maximum total work A, cal./mol	Entropy S, cal. T^{-1}/mol	Total energy E, cal./mol	C_v, cal./mol	Maximum total work A, cal./mol	Entropy S, cal. T^{-1}/mol	Total energy E, cal./mol	C_v, cal./mol
	75°				100°			
1	−64·3	+1·659	+513·4	7·00	−111·9	+2·148	+689·7	7·11
40	+2,385·6	−6·077	+269·8	7·60	+2,530·9	−5·550	+459·9	7·60
80	2,770·8	−7·857	+35·5	8·20	2,960·1	−7·181	+237·2	8·05
120	2,965·5	−9·046	−183·7	8·70	3,184·2	−8·400	+28·5	8·40
160	3,086·8	−9·978	−387·0	9·10	3,328·5	−9·357	−167·3	8·65
200	3,171·1	−10·766	−577·2	9·25	3,432·3	−10·176	−353·0	8·85
240	3,244·4	−11·492	−756·5	9·30	3,513·1	−10·838	−531·4	8·85
280	3,285·5	−12·109	−930·2	9·25	3,580·2	−11·486	−705·8	8·85
320	3,329·4	−12·730	−1,102·6	9·15	3,639·8	−12·112	−888·0	8·75
360	3,370·3	−13·351	−1,277·7	9·05	3,696·8	−12·739	−1,056·9	8·70
400	3,412·0	−13·988	−1,458·0	9·00	3,754·0	−13·377	−1,237·6	8·70
440	3,458·1	−14·656	−1,644·4	9·00	3,816·8	−14·043	−1,423·5	8·75
480	3,512·8	−15·364	−1,836·1	9·10	3,889·1	−14·746	−1,613·7	8·80
520	3,581·0	−16·118	−2,030·5	9·25	3,976·0	−15·489	−1,803·8	9·00
560	3,668·4	−16·921	−2,222·6	9·45	4,083·2	−16·275	−1,989·8	9·20
600	3,781·1	−17·774	−2,406·8	9·75	4,217·0	−17·107	−2,166·5	9·50
	125°				150°			
1	−171·5	+2·612	+868·6	7·21	−242·4	+3·054	+1,050·1	
40	+2,663·5	−5·059	+650·1	7·60	+2,774·2	−4·570	+840·4	
80	3,136·0	−6·780	+436·4	7·91	3,299·5	−6·299	+634·2	
120	3,388·8	−7·921	+235·0	8·20	3,580·7	−7·425	+438·8	
160	3,555·8	−8·820	−44·2	8·40	3,769·9	−8·309	+253·9	
200	3,678·9	−9·588	−138·4	8·50	3,912·1	−9·069	+74·4	
240	3,777·0	−10·279	−315·6	8·55	4,027·4	−9·759	−102·3	
280	3,860·3	−10·927	−490·4	8·55	4,127·0	−10·409	−277·6	
320	3,935·6	−11·564	−668·5	8·50	4,218·5	−11·041	−453·7	
360	4,007·8	−12·407	−832·0	8·50	4,306·1	−11·672	−632·9	
400	4,081·4	−12·825	−1,025·0	8·50	4,395·7	−12·312	−814·2	
440	4,160·9	−13·490	−1,210·0	8·50	4,511·6	−13·020	−997·6	
480	4,250·6	−14·183	−1,396·5	8·61	4,598·8	−13·660	−1,181·5	
520	4,356·0	−14·915	−1,582·2	8·75	4,722·2	−14·383	−1,364·0	
560	4,482·6	−15·686	−1,762·6	8·95	4,868·0	−15·146	−1,541·1	
600	4,637·0	−16·530	−1,944·6	9·20	5,042·6	−15·948	−1,705·8	

Thermodynamic Properties of Methane (Michels and Nederbragt)

Density ρ, Amagat units	*Maximum total work A, cal./mol*	*Entropy S, cal. T^{-1}/ mol*	*Total energy E, cal./mol*	*Maximum total work A, cal./mol*	*Entropy S, cal. T^{-1}/ mol*	*Total energy E, cal./mol*
	0° C.			25° C.		
0	$-\infty$	∞	3	$-\infty$	∞	164
1	0	0	0	−7	0·56	161
25	1,716	−6·55	−74	1,873	−5·98	90
50	2,062	−8·09	−148	2,257	−7·51	18
75	2,254	−9·06	−220	2,473	−8·47	−52
100	2,384	−9·79	−290	2,622	−9·20	−121
125	2,481	−10·40	−359	2,733	−9·80	−187
150	2,557	−10·92	−425	2,823	−10·32	−253
175	2,620	−11·39	−490	2,898	−10·79	−317
200	2,674	−11·82	−554	2,962	−11·22	−381
225	2,721	−12·22	−618	3,019	−11·62	−443
	50° C.			75° C.		
0	$-\infty$	∞	331	$-\infty$	∞	504
1	−28	1·10	328	−62	1·62	501
25	2,015	−5·43	260	2,145	−4·91	435
50	2,438	−6·96	190	2,605	−6·43	367
75	2,678	−7·91	122	2,869	−7·38	300
100	2,845	−8·64	55	3,053	−8·09	235
125	2,971	−9·23	−10	3,195	−8·68	171
150	3,074	−9·74	−74	3,310	−9·19	108
175	3,160	−10·20	−137	3,408	−9·66	45
200	3,235	−10·63	−200	3,494	−10·08	−16
225	3,303	−11·03	−262	3,571	−10·48	−78
	100° C.			125° C.		
0	$-\infty$	∞	684	$-\infty$	∞	873
1	−108	2·12	681	623	2·60	870
25	2,261	−4·41	615	3,143	−3·93	804
50	2,760	−5·93	548	3,672	−5·44	738
75	3,047	−6·87	483	3,978	−6·39	673
100	3,249	−7·58	419	4,197	−7·10	610
125	3,406	−8·17	356	4,372	−7·68	548
150	3,534	−8·68	294	4,522	−8·19	486
175	3,643	−9·14	232	4,656	−8·65	425
200	3,740	−9·56	171	4,784	−9·07	365
225	3,827	−9·96	111	4,909	−9·46	305

Thermodynamic Properties of Methane (Michels and Nederbragt) (cont.)

Density ρ, Amagat units	*Maximum total work A, cal./mol*	*Entropy S, cal. T^{-1}/ mol*	*Total energy E, cal./mol*
	150° C.		
0	$-\infty$	∞	1,069
1	−238	3·08	1,066
25	2,458	−3·45	1,000
50	3,032	−4·96	934
75	3,367	−5·90	870
100	3,604	−6·61	807
125	3,790	−7·20	745
150	3,943	−7·71	684
175	4,076	−8·16	624
200	4,193	−8·58	564
225	4,300	−8·97	504

Thermodynamic Properties of Methane (Michels and Nederbragt)

Specific Heats

Density ρ, Amagat units	$C_v - C_{v=\infty}$, *cal./mol*						
	37·5° C.	50° C.	62·5° C.	75° C.	87·5° C.	100° C.	112·5° C.
25	0·12	0·09	0·06	0·04	0·02	0·01	0·00
50	0·21	0·17	0·13	0·09	0·06	0·04	0·02
75	0·30	0·25	0·20	0·15	0·11	0·08	0·05
100	0·36	0·31	0·26	0·21	0·16	0·12	0·08
125	0·42	0·37	0·32	0·26	0·20	0·15	0·10
150	0·47	0·41	0·36	0·30	0·24	0·19	0·13
175	0·51	0·45	0·39	0·33	0·27	0·21	0·16
200	0·54	0·49	0·43	0·36	0·30	0·24	0·18
225	0·57	0·52	0·46	0·39	0·33	0·26	0·20

APPENDIX II

Values of Joule-Thomson Coefficient for Nitrogen (Roebuck and Osterberg)

P_{atms} / $T\,°C.$	1	20	33·5	60	100	140	180	200
300	0·0135	0·0095	0·0050	−0·0010	−0·0070	−0·0120	−0·0150	−0·0160
250	0·0320	0·0250	0·0225	+0·0160	+0·0075	+0·0015	−0·0030	−0·0050
200	0·0540	0·0460	0·0420	0·0365	0·0260	0·0170	+0·0100	+0·0075
150	0·0840	0·0755	0·0715	0·0615	0·0480	0·0350	0·0250	0·0225
125	0·1035	0·0945	0·0880	0·0770	0·0615	0·0460	0·0345	0·0320
100	0·1250	0·1140	0·1070	0·0955	0·0760	0·0580	0·0460	0·0415
75	0·1505	0·1380	0·1300	0·1165	0·0930	0·0735	0·0580	0·0535
50	0·1795	0·1660	0·1575	0·1415	0·1150	0·0910	0·0730	0·0660
25	0·2145	0·2000	0·1905	0·1690	0·1380	0·1100	0·0875	0·0780
0	0·2570	0·2420	0·2310	0·2040	0·1660	0·1310	0·1020	0·0900
−25	0·3120	0·2925	0·2775	0·2475	0·1975	0·1510	0·1120	0·0950
−50	0·3840	0·3625	0·3370	0·2995	0·2315	0·1695	0·1155	0·0940
−75	0·4870	0·4535	0·4200	0·3640	0·2680	0·1770	0·1090	0·0840
−87·5	0·5525	0·5095	0·4730	0·4020	0·2825	0·1675	0·0980	0·0760
−100	0·6280	0·5785	0·5355	0·4430	0·2810	0·1425	0·0800	0·0620
−112·5	0·7190	0·6645	0·6050	0·4880	0·2375	0·0980	0·0515	0·0375
−125	0·8280	0·7725	0·6870	0·4945	0·1475	0·0530	0·0200	0·0070
−137·5	0·9650	0·9100	0·7910	0·2500	0·0685	0·0210	−0·0040	−0·0140
−150	1·2250	1·0970	0·1775	0·0620	0·0215	−0·0025	−0·0180	−0·0255
−160	1·5800	0·0730	0·0330	0·0075	−0·0075	−0·0160	−0·0235	−0·0295
−170	1·9400	−0·0075	−0·0360	..	..	..	..	..
−180	2·3150	..	..	..	..	..	..	..

Values of Joule-Thomson Coefficient for Air (Roebuck)

P_{atms} / $T\,°C.$	1	20	60	100	140	180	220
280	0·0297	0·0246	0·0161	0·0078	0·0011	−0·0054	−0·0110
250	0·0402	0·0346	0·0251	0·0164	0·0093	0·0027	−0·0054
200	0·0625	0·0564	0·0447	0·0347	0·0258	0·0185	0·0127
150	0·0927	0·0856	0·0708	0·0587	0·0467	0·0366	0·0286
100	0·1327	0·1244	0·1057	0·0890	0·0723	0·0578	0·0452
75	0·1581	0·1490	0·1275	0·1073	0·0875	0·0800	0·0542
50	0·1887	0·1777	0·1527	0·1283	0·1047	0·0833	0·0627
25	0·2269	0·2116	0·1815	0·1517	0·1237	0·0974	0·0718
0	0·2663	0·2494	0·2143	0·1782	0·1445	0·1125	0·0812
−25	0·3160	0·2965	0·2540	0·2115	0·1640	0·1250	0·0975
−50	0·3755	0·3565	0·3080	0·2470	0·1815	0 1305	0·0935
−75	0·4620	0·4380	0·3765	0·2870	0·1960	0·1165	0·0685
−100	0·5750	0·5535	0·4700	0·2845	0·1415	0·0745	0·0310
−120	0·7070	0·7050	0·5220	0·1650	0·0845	0·0285	−0·0150
−150	..	..	0·0440	0·0190	−0·0030	−0·0215	−0·0385

Values of μ for Air (Hausen)†

T °C. / P_{atms}	*150°*	*120°*	*−100°*	*−50°*	*−25°*	*0°*	*25°*
0	..	0·796	0·642	0·399	0·327	0·269	0·224
100	−0·006	0·164	0·244	0·168	0·127	0·086	0·055
200	−0·035	−0·007	0·028	0·100	0·110	0·095	0·088

† Hausen, *Zeit. f. tech. Phys.*, pp. 371 and 445 (1926).

Values of Joule-Thomson Coefficient for Helium (Roebuck and Osterberg)

Temp., °C.	$-\mu$	*Temp.*, °C.	$-\mu$
300	0·0578	25	0·0604
250	0·0609	0	0·0596
200	0·0621	−50	0·0586
150	0·0624	−100	0·0565
100	0·0618	−155	0·0487
75	0·0615	−180	0·0399
50	0·0611	−190	0·0368

Values of Joule-Thomson Coefficient for Argon (Roebuck and Osterberg)

T °C. / P_{atms}	*1*	*20*	*60*	*100*	*140*	*180*	*200*
300	0·0620	0·0580	0·0522	0·0445	0·0375	0·0319	0·0280
250	0·0948	0·0884	0·0770	0·0649	0·0552	0·0477	0·0475
200	0·1330	0·1235	0·1080	0·0935	0·0802	0·0714	0·0680
150	0·1777	0·1655	0·1458	0·1275	0·1115	0·0975	0·0965
125	0·2035	0·1905	0·1677	0·1478	0·1290	0·1126	0·1100
100	0·2340	0·2180	0·1927	0·1715	0·1480	0·1312	0·1260
75	0·2690	0·2530	0·2235	0·1975	0·1678	0·1515	0·1417
50	0·3115	0·2935	0·2597	0·2265	0·1920	0·1704	0·1575
25	0·3590	0·3392	0·3000	0·2585	0·2177	0·1886	0·1728
0	0·4170	0·3440	0·3498	0·2995	0·2475	0·2048	0·1871
−25	0·4890	0·4630	0·4120	0·3460	0·2750	0·2155	0·1967
−50	0·5765	0·5450	0·4878	0·3934	0·2900	0·2110	0·1877
−75	0·6847	0·6450	0·5767	0·4285	0·2528	0·1577	0·1312
−100	0·8335	0·7780	0·6840	0·3970	0·1227	0·0592	0·0425
−125	1·0765	1·0155	0·1277	0·0430	0·0077	−0·0058	−0·0110
−150	1·7503	..	−0·0040	−0·0238	−0·0390	−0·0540	−0·0550
−160	2·315	..	..	..	..	..	..
−170	3·015	..	..	..	..	..	..

APPENDIX III

Refractive Index of Carbon Dioxide (Michels and Hamers)

ρ, *Am. units*	p, *int. atms.*	n						$\frac{n^2-1}{n^2+2}\frac{1}{\rho}$ ρ (*mols/c.c.*) $\lambda = 5{,}876$ Å
		6,678 Å	*5,876 Å*	*5,016 Å*	*4,922 Å*	*4,713 Å*	*4,471 Å*	
$t = 25{\cdot}053°$								
0·914	1·00	..	..	..	..	..	..	6·6628†
0·91	0·99	1·0004	1·0005	1·0004	1·0004	1·0004	1·0004	7·054
7·03	7·43	1·0031	1·0032	1·0032	1·0032	1·0032	1·0032	6·644
12·76	13·05	1·0058	1·0057	1·0058	1·0058	1·0058	1·0058	6·681
16·76	16·76	1·0075	1·0076	1·0076	1·0076	1·0076	1·0076	6·688
22·03	21·37	1·0098	1·0100	1·0101	1·0101	1·0101	1·0101	6·700
22·14	21·46	1·0099	1·0100	1·0101	1·0101	1·0101	1·0101	6·678
22·14	21·47	1·0098	1·0098	1·0099	1·0100	1·0099	1·0100	6·592
27·84	26·11	1·0124	1·0124	1·0125	1·0126	1·0126	1·0126	6·627
27·87	26·14	1·0125	1·0126	1·0127	1·0127	1·0127	1·0127	6·678
34·08	30·81	1·0153	1·0154	1·0155	1·0155	1·0155	1·0156	6·684
40·90	35·51	1·0184	1·0185	1·0186	1·0187	1·0187	1·0188	6·690
48·43	40·18	1·0218	1·0219	1·0221	1·0221	1·0221	1·0222	6·683
56·85	44·80	1·0256	1·0257	1·0258	1·0259	1·0260	1·0260	6·671
56·93	44·84	1·0256	1·0258	1·0259	1·0259	1·0260	1·0261	6·682
66·25	49·26	1·0297	1·0298	1·0301	1·0302	1·0302	1·0304	6·661
66·25	49·26	1·0297	1·0298	1·0301	1·0301	1·0302	1·0303	6·657
66·42	49·33	1·0299	1·0300	1·0302	1·0302	1·0303	1·0305	6·671
85·10	56·18	1·0384	1·0386	1·0388	1·0389	1·0390	1·0391	6·681
85·10	56·18	1·0383	1·0385	1·0388	1·0389	1·0390	1·0390	6·676
86·89	56·70	1·0391	1·0393	1·0396	1·0397	1·0397	1·0399	6·671
122·53	63·44	1·0551	1·0553	1·0557	1·0558	1·0559	1·0561	6·637
360·05	63·84	1·1655	1·1662	1·1674	1·1676	1·1680	1·1686	6·626
360·80	64·03	1·1660	1·1666	1·1679	1·1680	1·1685	1·1690	6·629
361·52	64·21	1·1664	1·1670	1·1683	1·1686	1·1689	1·1694	6·633
372·18	67·65	1·1712	1·1718	1·1732	1·1734	1·1738	1·1744	6·621
372·20	67·65	1·1711	1·1718	1·1732	1·1734	1·1738	1·1744	6·621
389·21	76·42	1·1789	1·1797	1·1811	1·1812	1·1816	1·1823	6·606
401·77	86·17	1·1846	1·1855	1·1869	1·1871	1·1876	1·1882	6·597
412·47	97·18	1·1896	1·1906	1·1920	1·1922	1·1927	1·1933	6·593
420·01	106·72	1·1931	1·1941	1·1955	1·1958	1·1962	1·1969	6·588
420·02	106·74	1·1933	1·1941	1·1956	1·1958	1·1962	1·1969	6·590
429·92	121·75	1·1979	1·1988	1·2003	1·2005	1·2010	1·2017	6·586
442·70	146·02	1·2039	1·2048	1·2064	1·2066	1·2071	1·2078	6·581
452·70	169·40	1·2087	1·2097	1·2112	1·2115	1·2119	1·2126	6·578
461·55	193·74	1·2128	1·2137	1·2154	1·2156	1·2161	1·2169	6·573
461·59	193·87	1·2126	1·2137	1·2154	1·2157	1·2162	1·2169	6·571
476·07	242·19	1·2196	1·2206	1·2223	1·2225	1·2231	1·2239	6·566
476·07	242·21	1·2197	1·2209	1·2225	1·2227	1·2233	1·2241	6·571
492·36	311·06	1·2272	1·2284	1·2302	1·2304	1·2310	1·2318	6·560
498·74	342·71	1·2302	1·2311	1·2328	1·2331	1·2336	1·2345	6·548

† Figures marked thus are derived from measurements of Stoll.

Refractive Index of Carbon Dioxide (cont.)

ρ, *Am. units*	p, *int. atms.*	n 6,678 Å	5,876 Å	5,016 Å	4,922 Å	4,713 Å	4,471 Å	$\frac{n^2-1}{n^2+2}\frac{1}{\rho}$ ρ (*mols/c.c.*) $\lambda = 5{,}876$ Å
$t = 25{\cdot}053°$ (*cont.*)								
506·76	386·73	1·2340	1·2350	1·2367	1·2370	1·2374	1·2384	6·544
522·18	485·90	1·2412	1·2422	1·2440	1·2443	1·2449	1·2457	6·535
535·16	586·55	1·2473	1·2485	1·2503	1·2506	1·2512	1·2521	6·530
546·60	688·38	1·2528	1·2538	1·2558	1·2561	1·2566	1·2575	6·524
556·64	790·27	1·2575	1·2587	1·2605	1·2609	1·2615	1·2624	6·518
556·76	791·55	1·2580	1·2590	1·2609	1·2612	1·2617	1·2628	6·525
565·85	894·58	1·2622	1·2633	1·2652	1·2654	1·2661	1·2670	6·519
580·27	1080·38	1·2690	1·2701	1·2721	1·2724	1·2730	1·2740	6·510
594·09	1286·86	1·2753	1·2764	1·2784	1·2787	1·2794	1·2804	6·496
$t = 32{\cdot}075°$								
0·893	1·00	..	..	..	..	..	..	6·6628†
21·27	21·35	1·0094	1·0097	1·0097	1·0097	1·0097	1·0098	6·707
61·29	49·24	1·0276	1·0278	1·0279	1·0280	1·0280	1·0281	6·685
76·33	56·25	1·0344	1·0345	1·0347	1·0347	1·0348	1·0349	6·663
96·74	63·35	1·0435	1·0438	1·0441	1·0442	1·0443	1·0444	6·665
113·29	67·41	1·0509	1·0512	1·0517	1·0517	1·0517	1·0521	6·653
149·46	72·35	1·0673	1·0676	1·0681	1·0682	1·0683	1·0686	6·633
322·24	77·92	1·1474	1·1482	1·1495	1·1497	1·1500	1·1506	6·635
356·88	86·45	1·1633	1·1642	1·1655	1·1657	1·1660	1·1668	6·609
376·58	96·74	1·1725	1·1735	1·1749	1·1750	1·1754	1·1761	6·602
389·20	106·46	1·1782	1·1794	1·1807	1·1809	1·1814	1·1819	6·594
403·85	121·60	1·1855	1·1864	1·1878	1·1880	1·1884	1·1892	6·594
$t = 49{\cdot}712°$								
0·844	1·00	..	..	..	..	..	..	6·6628†
0·91	1·08	1·0003	1·0003	1·0003	1·0004	1·0004	1·0004	5·794
6·35	7·34	1·0028	1·0028	1·0029	1·0028	1·0029	1·0029	6·572
11·50	12·97	1·0050	1·0051	1·0051	1·0051	1·0052	1·0052	6·547
15·04	16·68	1·0066	1·0066	1·0067	1·0068	1·0066	1·0068	6·547
19·70	21·39	1·0086	1·0087	1·0088	1·0088	1·0089	1·0089	6·581
19·76	21·45	1·0088	1·0089	1·0089	1·0089	1·0089	1·0090	6·631
24·58	26·08	1·0109	1·0109	1·0110	1·0111	1·0110	1·0111	6·602
29·66	30·73	1·0132	1·0133	1·0133	1·0134	1·0134	1·0135	6·628
35·03	35·40	1·0156	1·0157	1·0158	1·0158	1·0159	1·0159	6·639
40·67	40·02	1·0182	1·0182	1·0183	1·0184	1·0184	1·0185	6·632
46·72	44·68	1·0209	1·0210	1·0212	1·0212	1·0212	1·0212	6·645
52·79	49·06	1·0236	1·0237	1·0239	1·0239	1·0240	1·0241	6·643
52·82	49·09	1·0237	1·0237	1·0239	1·0239	1·0240	1·0241	6·648
85·79	68·32	1·0384	1·0386	1·0390	1·0390	1·0391	1·0392	6·642
85·80	68·32	1·0384	1·0386	1·0389	1·0389	1·0391	1·0391	6·634
106·34	77·05	1·0478	1·0480	1·0484	1·0485	1·0485	1·0487	6·647
132·44	85·46	1·0596	1·0599	1·0603	1·0604	1·0605	1·0607	6·640
180·87	95·93	1·0817	1·0820	1·0826	1·0827	1·0829	1·0832	6·631
244·28	106·12	1·1113	1·1118	1·1127	1·1128	1·1131	1·1136	6·654
244·29	106·12	1·1111	1·1115	1·1123	1·1125	1·1127	1·1131	6·635
244·32	106·12	1·1113	1·1118	1·1126	1·1128	1·1130	1·1135	6·650

Refractive Index of Carbon Dioxide (cont.)

p, *Am. units*	p, *int. atms.*	n 6,678 Å	5,876 Å	5,016 Å	4,922 Å	4,713 Å	4,471 Å	$\frac{n^2-1}{n^2+2}\frac{1}{\rho}$ ρ (*mols/c.c.*) $\lambda = 5{,}876$ Å
$t = 49{\cdot}712°$ (*cont.*)								
307·69	121·44	1·1406	1·1412	1·1423	1·1425	1·1428	1·1433	6·627
307·70	121·44	1·1406	1·1412	1·1422	1·1424	1·1427	1·1432	6·625
336·38	134·69	1·1539	1·1547	1·1560	1·1562	1·1565	1·1571	6·623
350·72	144·14	1·1608	1·1614	1·1626	1·1628	1·1632	1·1638	6·616
376·67	168·34	1·1729	1·1737	1·1750	1·1752	1·1756	1·1762	6·607
395·48	193·55	1·1817	1·1825	1·1839	1·1842	1·1846	1·1852	6·601
408·67	216·31	1·1879	1·1887	1·1902	1·1904	1·1909	1·1915	6·595
420·86	241·80	1·1937	1·1945	1·1961	1·1962	1·1967	1·1974	6·591
420·88	241·83	1·1937	1·1947	1·1962	1·1963	1·1969	1·1976	6·595
420·89	241·86	1·1937	1·1945	1·1961	1·1963	1·1968	1·1975	6·593
420·97	242·05	1·1939	1·1948	1·1962	1·1964	1·1968	1·1975	6·595
438·71	288·53	1·2022	1·2032	1·2047	1·2050	1·2054	1·2061	6·590
454·56	341·10	1·2097	1·2106	1·2122	1·2125	1·2129	1·2137	6·581
465·59	384·99	1·2149	1·2158	1·2175	1·2178	1·2183	1·2190	6·577
485·85	483·98	1·2245	1·2255	1·2271	1·2272	1·2279	1·2287	6·565
502·22	584·42	1·2321	1·2332	1·2350	1·2352	1·2358	1·2366	6·557
516·04	686·04	1·2387	1·2398	1·2416	1·2419	1·2425	1·2433	6·551
528·00	787·92	1·2442	1·2453	1·2472	1·2475	1·2481	1·2489	6·541
536·57	869·65	1·2482	1·2493	1·2511	1·2515	1·2521	1·2530	6·534
546·17	970·69	1·2529	1·2540	1·2559	1·2561	1·2567	1·2576	6·532
546·17	970·72	1·2527	1·2540	1·2559	1·2561	1·2567	1·2576	6·530
555·36	1077·62	1·2573	1·2584	1·2602	1·2605	1·2611	1·2621	6·527
570·95	1283·99	1·2647	1·2659	1·2678	1·2681	1·2687	1·2697	6·520
582·02	1451·36	1·2700	1·2712	1·2732	1·2735	1·2742	1·2752	6·515
582·02	1451·36	1·2698	1·2712	1·2731	1·2734	1·2740	1·2750	6·512
594·90	1669·59	1·2760	1·2773	1·2794	1·2797	1·2804	1·2813	6·507
$t = 99{\cdot}767°$								
0·729	1·00	..	..	..	..	..	..	6·6628†
0·71	0·98	1·0003	1·0003	1·0002	1·0002	1·0002	1·0002	5·213
8·99	12·00	1·0039	1·0039	1·0039	1·0039	1·0039	1·0039	6·416
16·47	21·45	1·0074	1·0074	1·0074	1·0073	1·0074	1·0074	6·586
24·22	30·78	1·0109	1·0108	1·0108	1·0109	1·0108	1·0109	6·596
32·46	40·21	1·0146	1·0145	1·0146	1·0146	1·0146	1·0147	6·616
40·33	48·76	1·0182	1·0182	1·0184	1·0184	1·0185	1·0184	6·693
48·09	56·78	1·0217	1·0217	1·0218	1·0200	1·0220	1·0220	6·678
48·14	56·83	1·0217	1·0217	1·0219	1·0219	1·0219	1·0220	6·673
66·33	74·21	1·0299	1·0300	1·0302	1·0302	1·0302	1·0304	6·675
88·89	93·37	1·0400	1·0401	1·0405	1·0405	1·0406	1·0408	6·664
110·93	110·05	1·0502	1·0503	1·0506	1·0507	1·0508	1·0510	6·668
140·75	130·33	1·0638	1·0640	1·0645	1·0645	1·0647	1·0649	6·671
175·80	152·37	1·0800	1·0802	1·0808	1·0809	1·0810	1·0813	6·674
200·58	167·82	1·0916	1·0920	1·0925	1·0927	1·0928	1·0932	6·685
225·01	183·83	1·1028	1·1032	1·1040	1·1041	1·1043	1·1046	6·677
241·14	195·22	1·1102	1·1107	1·1115	1·1116	1·1119	1·1123	6·671
254·18	205·15	1·1164	1·1168	1·1177	1·1178	1·1180	1·1185	6·671
268·94	217·41	1·1231	1·1237	1·1246	1·1247	1·1250	1·1254	6·663

Refractive Index of Carbon Dioxide (cont.)

ρ, *Am. units*	ρ, *int. atms.*	n						$\frac{n^2-1}{n^2+2}\frac{1}{\rho}$ ρ (*mols/c.c.*) $\lambda = 5{,}876$ Å
		6,678 Å	*5,876 Å*	*5,016 Å*	*4,922 Å*	*4,713 Å*	*4,471 Å*	
$t = 99{\cdot}767°$ (*cont.*)								
290·08	237·46	1·1330	1·1335	1·1345	1·1346	1·1349	1·1354	6·656
329·06	285·73	1·1514	1·1519	1·1529	1·1531	1·1534	1·1539	6·645
377·71	379·94	1·1741	1·1747	1·1759	1·1761	1·1764	1·1771	6·624
424·04	529·56	1·1953	1·1962	1·1977	1·1979	1·1983	1·1990	6·594
454·45	677·12	1·2097	1·2106	1·2122	1·2124	1·2129	1·2137	6·581
476·71	819·33	1·2202	1·2211	1·2227	1·2230	1·2234	1·2243	6·568
476·71	819·33	1·2204	1·2213	1·2229	1·2231	1·2235	1·2243	6·572
493·95	953·93	1·2284	1·2295	1·2312	1·2315	1·2321	1·2329	6·568
494·12	955·38	1·2285	1·2295	1·2312	1·2314	1·2319	1·2327	6·564
507·47	1076·96	1·2348	1·2359	1·2377	1·2380	1·2386	1·2394	6·561
526·78	1283·26	1·2441	1·2452	1·2470	1·2472	1·2478	1·2487	6·551
540·19	1450·56	1·2503	1·2515	1·2533	1·2535	1·2542	1·2551	6·542
555·50	1668·63	1·2575	1·2587	1·2606	1·2609	1·2615	1·2624	6·533
572·05	1940·62	1·2655	1·2667	1·2686	1·2689	1·2695	1·2705	6·525
572·05	1940·66	1·2654	1·2665	1·2685	1·2688	1·2694	1·2704	6·522
583·76	2158·32	1·2710	1·2723	1·2744	1·2747	1·2753	1·2763	6·521
594·84	2385·20	1·2761	1·2775	1·2797	1·2799	1·2806	1·2816	6·512

AUTHOR INDEX

SUBJECT INDEX

PRINTED IN
GREAT BRITAIN
AT THE
UNIVERSITY PRESS
OXFORD
BY
JOHN JOHNSON
PRINTER
TO THE
UNIVERSITY

PHARMACEUTICS